Wojskowa Akademia Techniczna

PROGRAM „KATEDRA AD HOC”

Wydział Mechaniczny

Cykl wykładów:

„Mechanics of Random Media”

PROF. MARTIN OSTOJA-STARZEWSKI

Wojskowa Akademia Techniczna
Wydział Mechaniczny

Warszawa, 26-30 czerwca 2017 r.

Planar and Spatial Random Processes and Models of Material Microstructures

Martin Ostoja-Starzewski

Department of Mechanical Science & Engineering

also Institute for Condensed Matter Theory, and Beckman Institute

University of Illinois at Urbana-Champaign

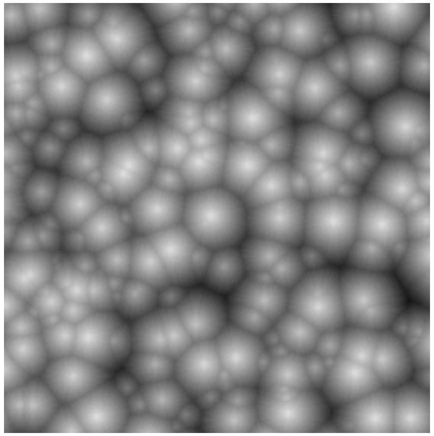

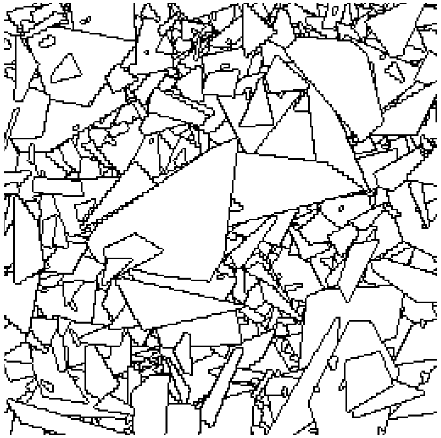

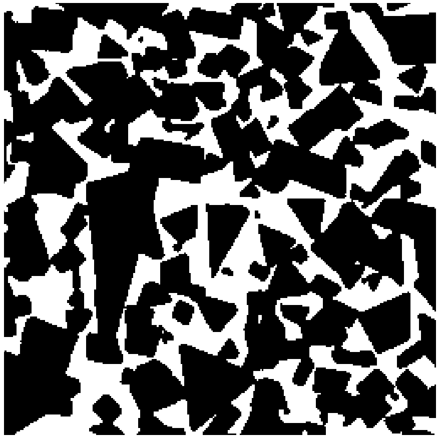

[Support: NSF, DOE, DTRA, LANL, ARDEC]

three scales:

microscale: average size of grain d
(microstructure)

mesoscale: L
if not RVE, then
inhomogeneous continuum

macroscale: L_{macro}

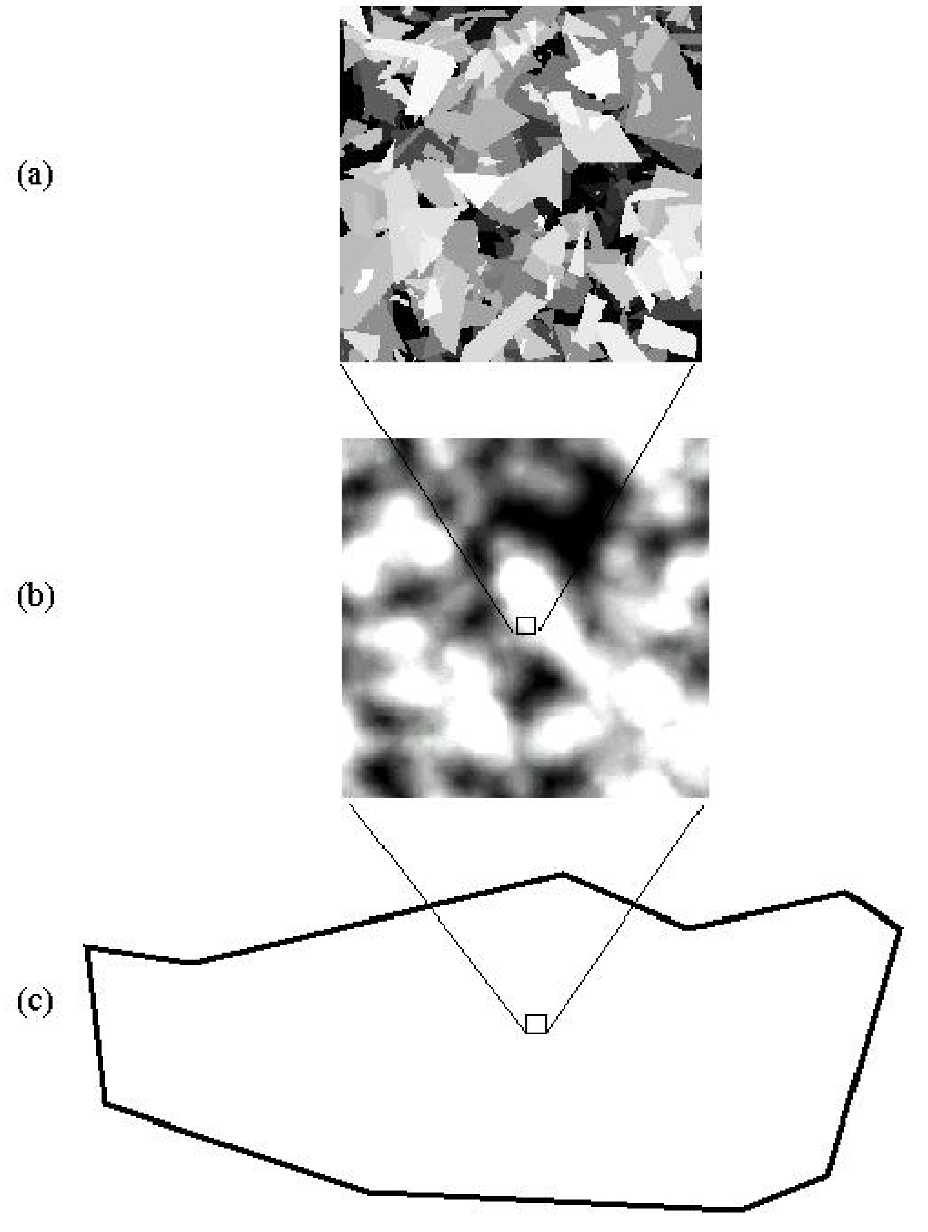

three scales:

microscale: average size of grain d
(microstructure)

mesoscale: L
if not RVE, then
inhomogeneous continuum

macroscale: L_{macro}

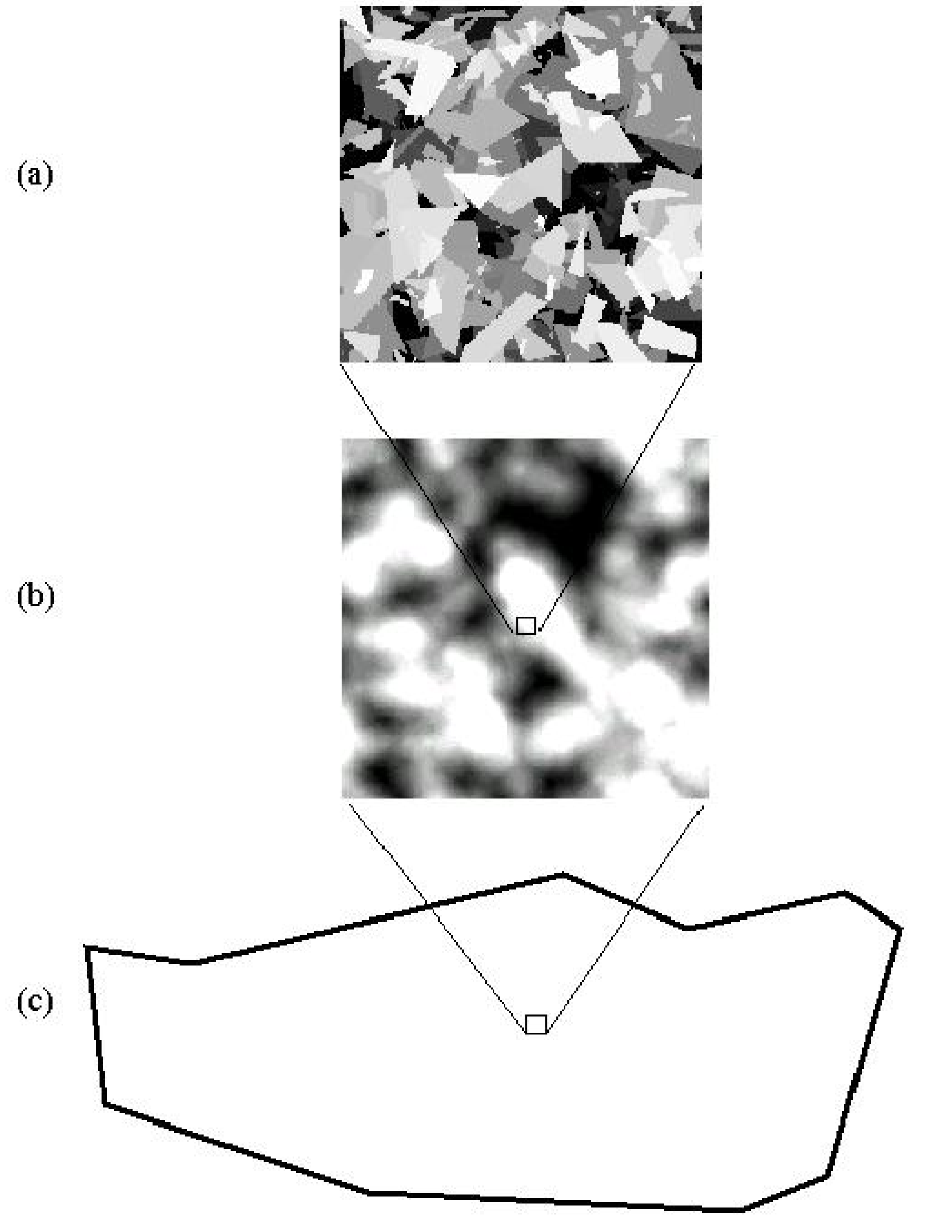

separation of scales $d << L << L_{macro}$
does not always hold!

three scales:

microscale: average size of grain d
(microstructure, non-fractal)

mesoscale: L
if not RVE, then
inhomogeneous continuum

macroscale: L_{macro}

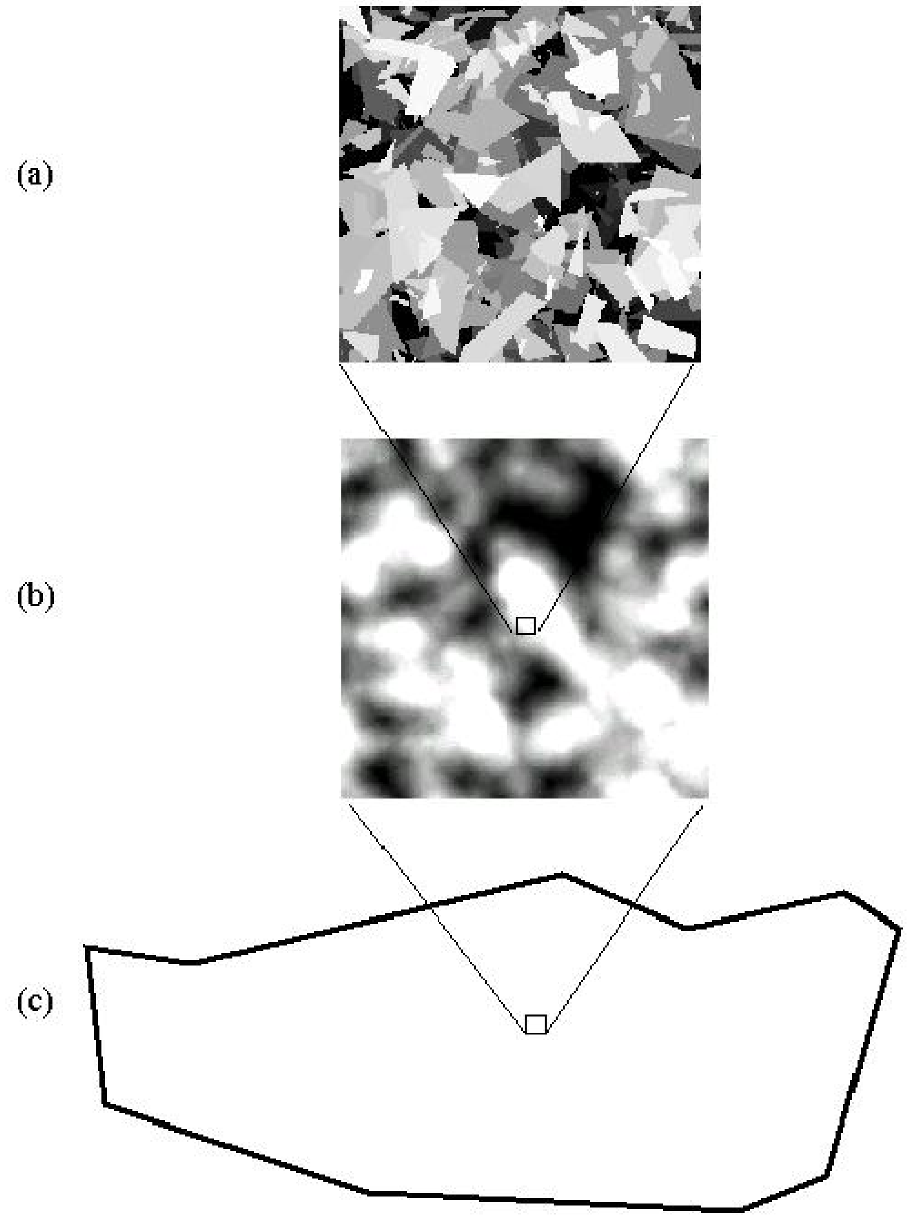

separation of scales $d << L << L_{macro}$
does not always hold!

random checkerboard (chessboard) model

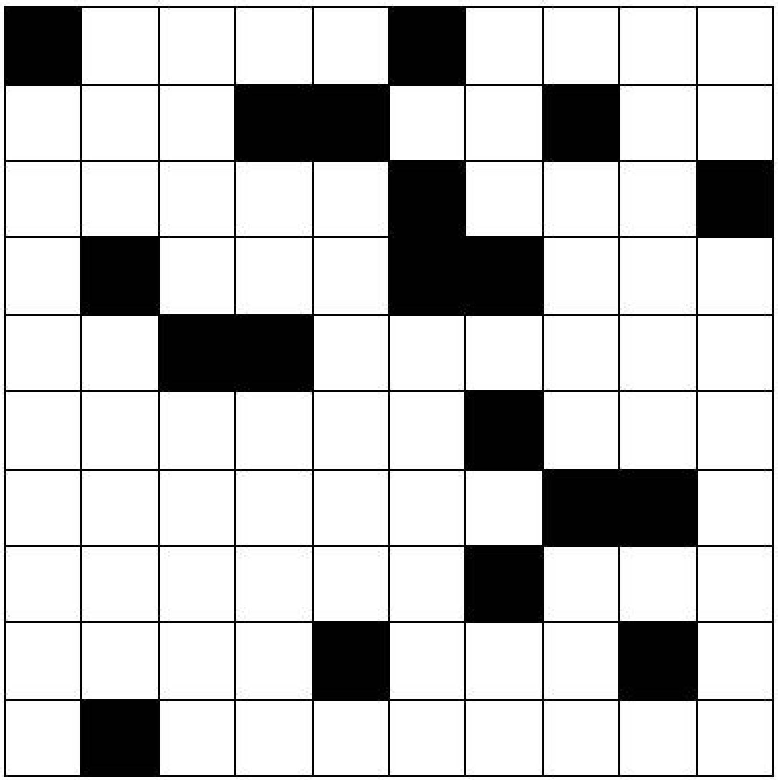

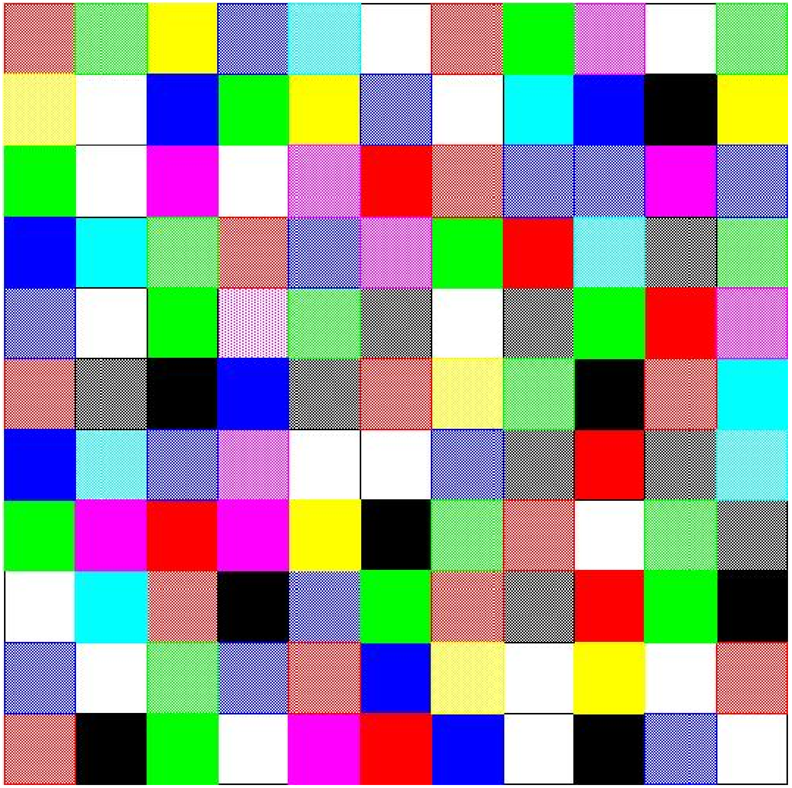

16 phases

probabilities of black/white phases

size of space Ω of all (elementary) events ω

probability of each ω

Bertrand paradox:

Consider an equilateral triangle inscribed in a circle. Suppose a chord of the circle is chosen at random.
What is the probability that the chord is longer than a side of the triangle?

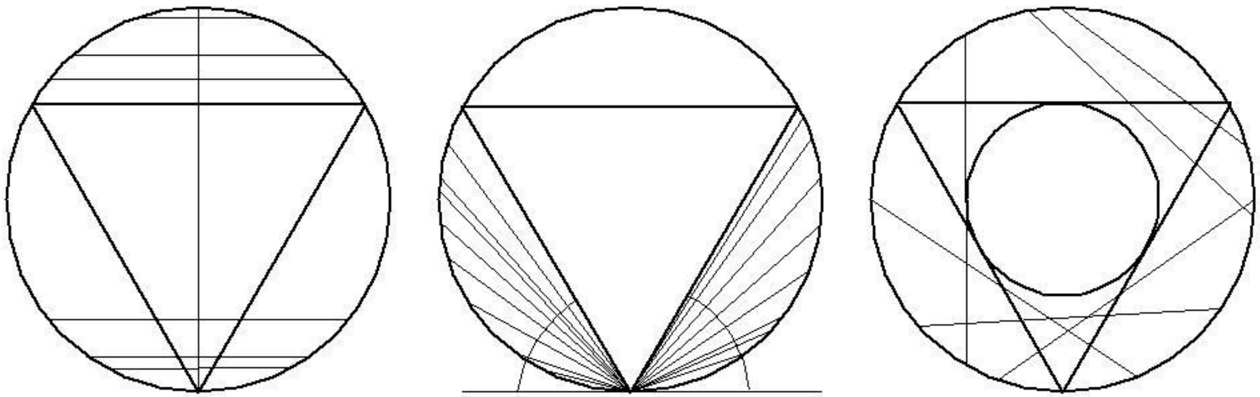

(a) (b) (c)

Three different solutions of Bertrand's problem, showing cords which are too short.

(a) The "random radius" method: ½

(b) The "random endpoints" method: 1/3

(c) The "random midpoint" method: ¼

Bertrand paradox:

Consider an equilateral triangle inscribed in a circle. Suppose a chord of the circle is chosen at random.
What is the probability that the chord is longer than a side of the triangle?

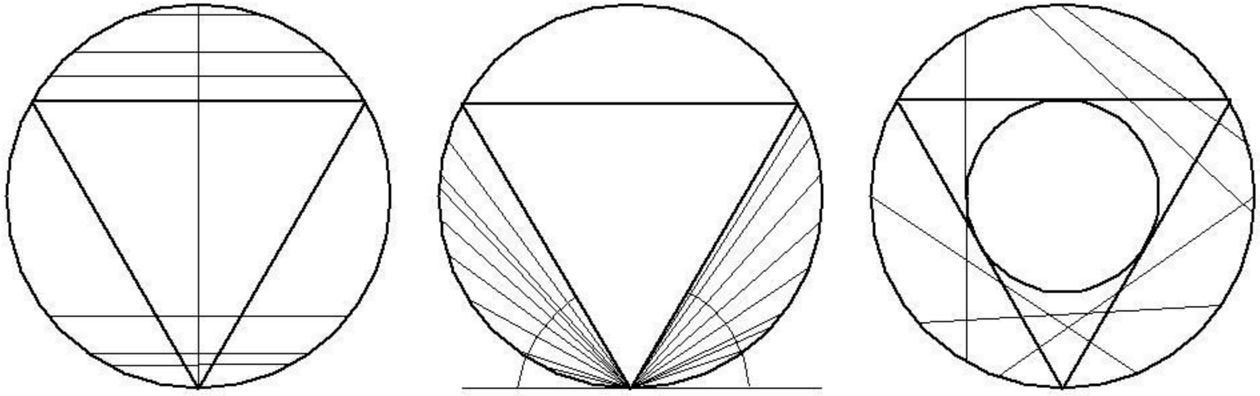

(a) (b) (c)

The problem's classical solution hinges on the method by which a chord is chosen "at random". It turns out that if, and only if, the method of random selection is specified, does the problem have a well-defined solution. There is no unique selection method, so there cannot be a unique solution. The three solutions presented by Bertrand correspond to different selection methods, and in the absence of further information there is no reason to prefer one over another.

Bertrand paradox:

Consider an equilateral triangle inscribed in a circle. Suppose a chord of the circle is chosen at random.
What is the probability that the chord is longer than a side of the triangle?

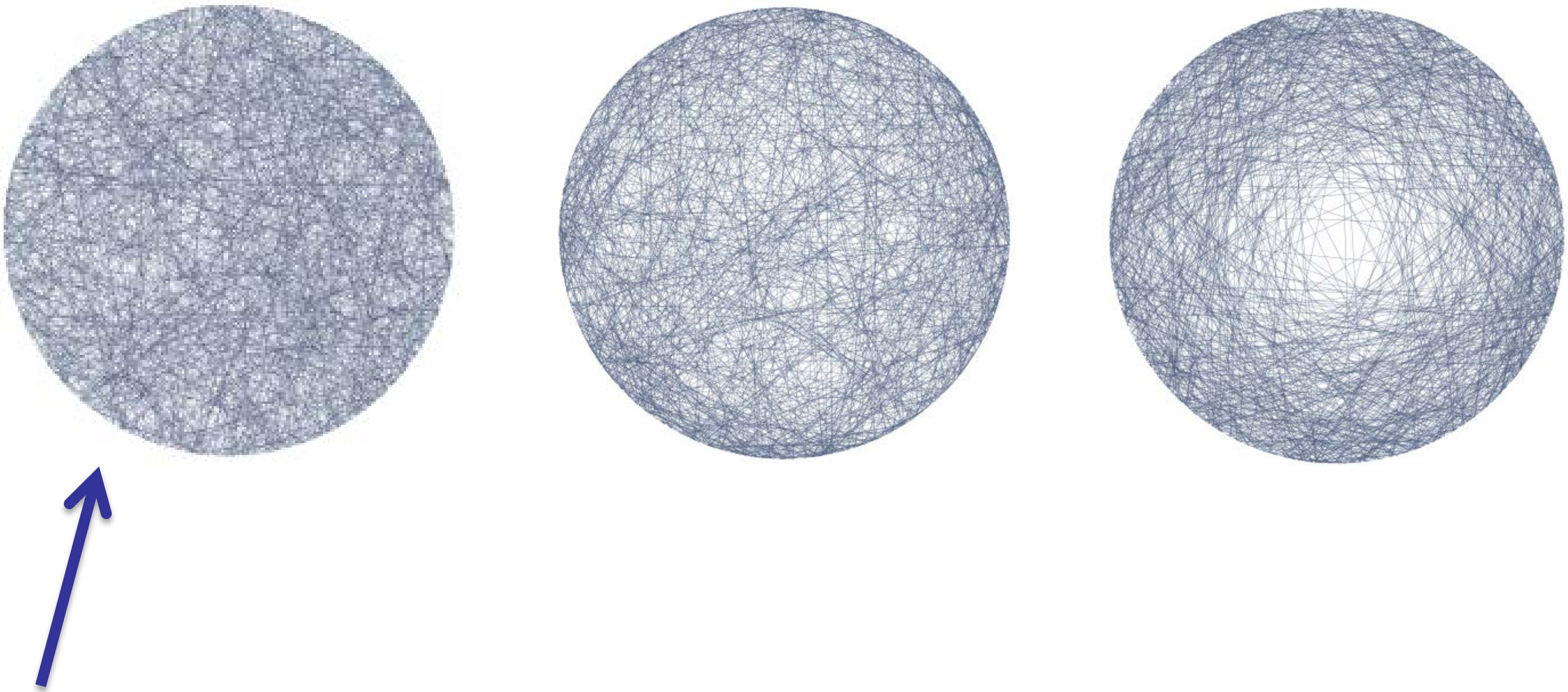

this solution is both **scale** and **translation invariant**

Basic Random Media Models

Poisson line field

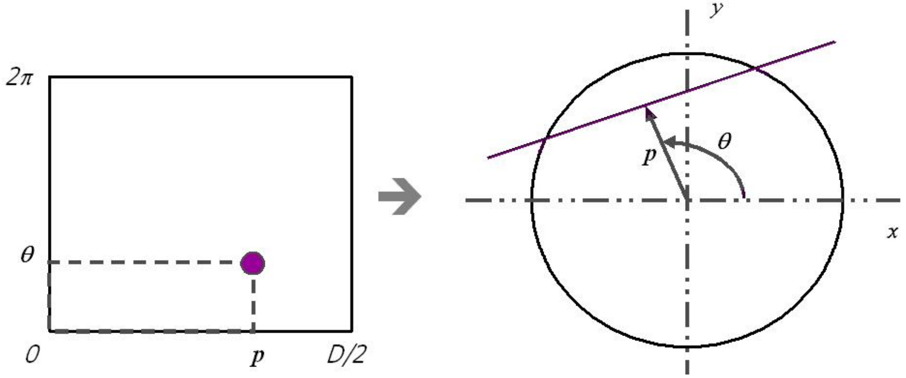

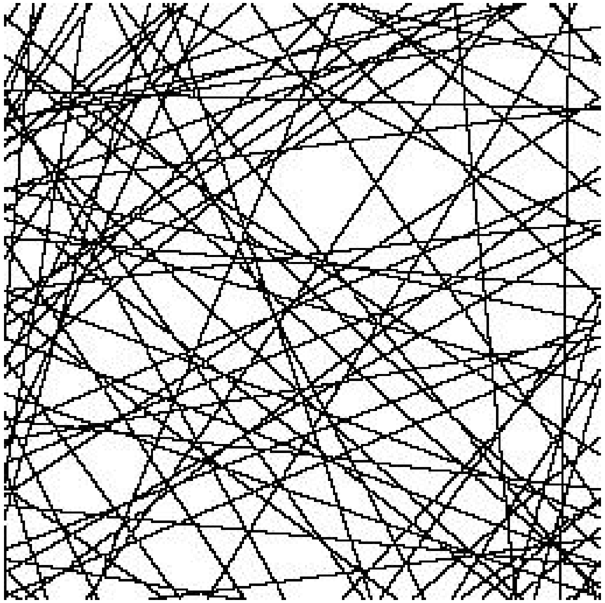

Basic Random Media Models

Poisson line field

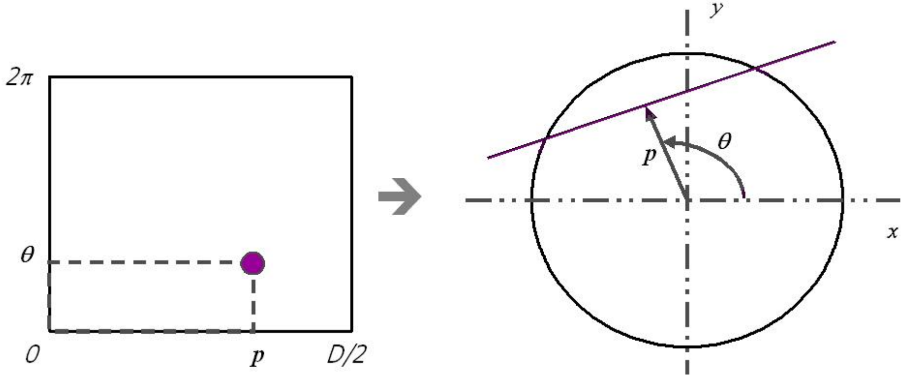

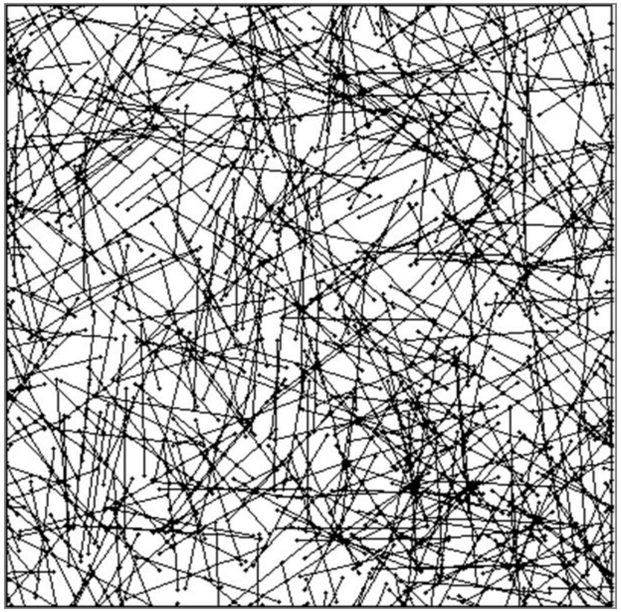

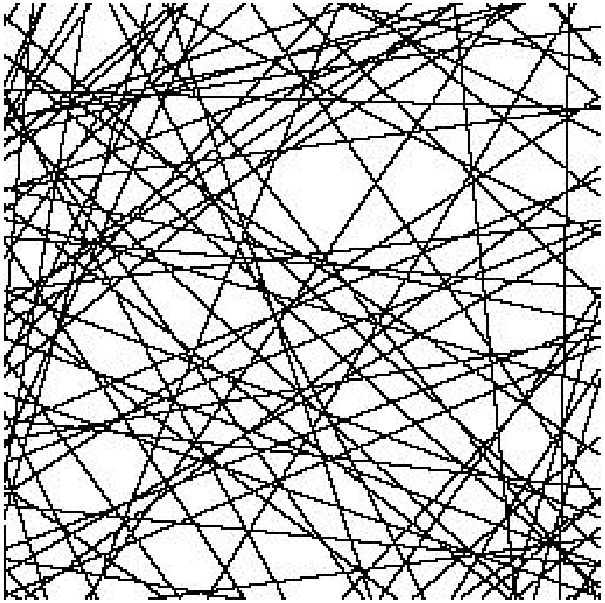

Basic Random Media Models

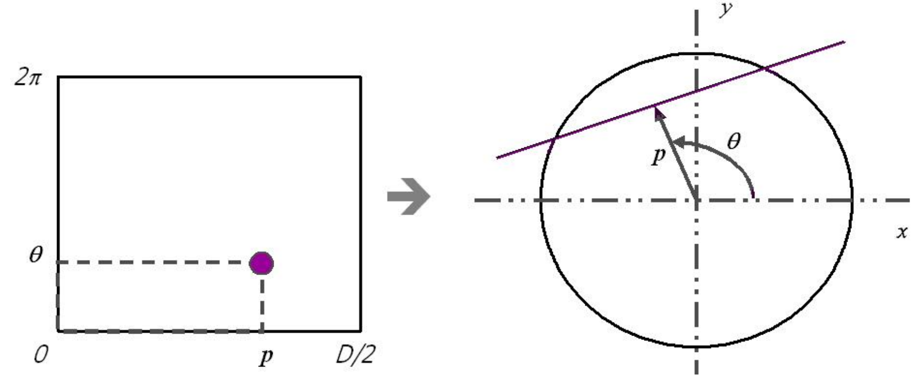

Poisson line field
is not a random fiber field

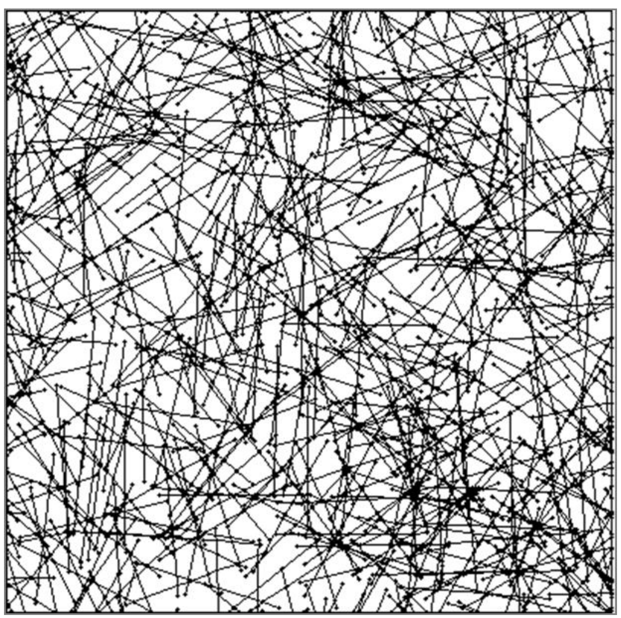

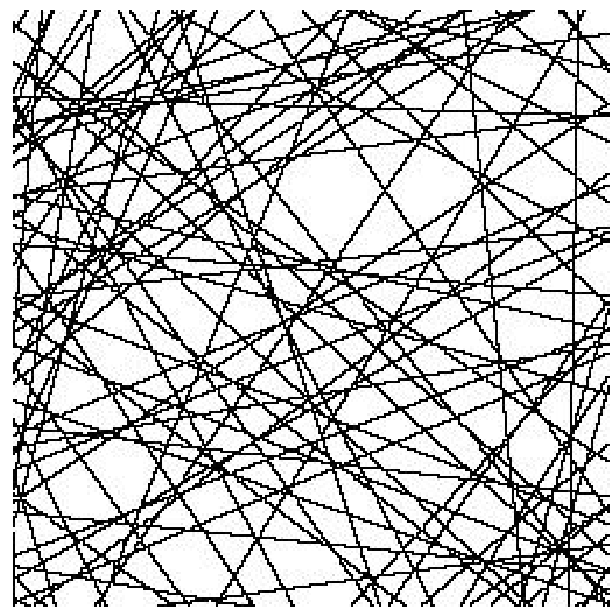

Basic Random Media Models

two-phase mosaic generated from a Poisson line field with 100 lines

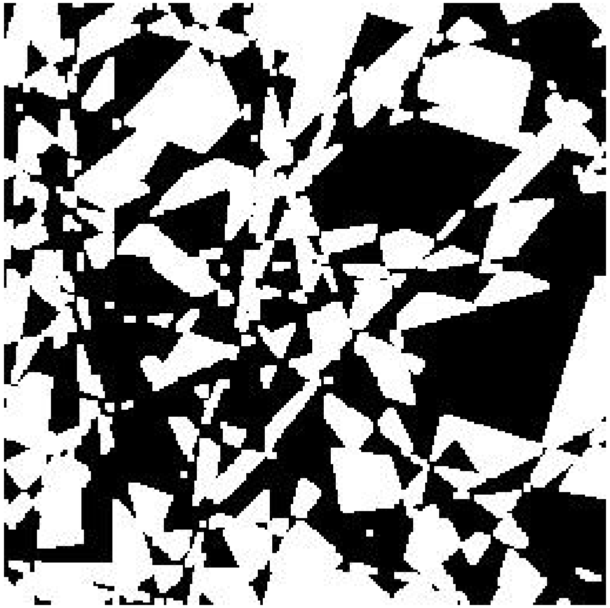

Basic Random Media Models

random finite fiber field

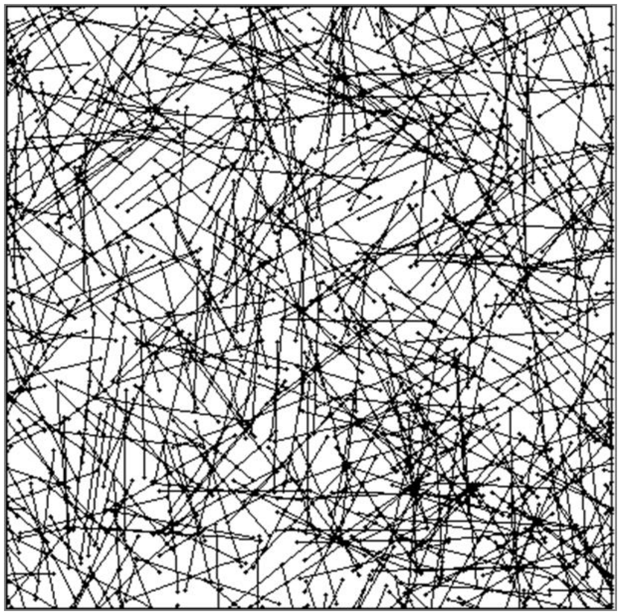

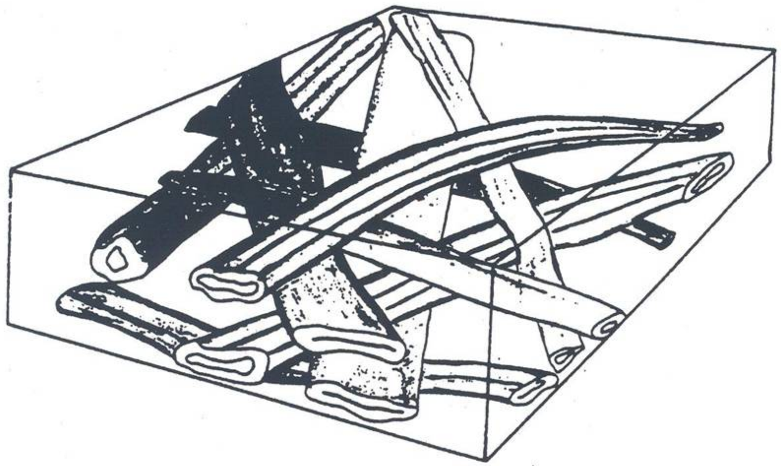

“anatomy” of paper

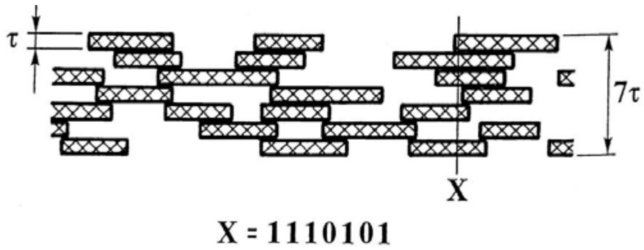

Multiscale Anatomy of Paper

paper manufacture

up to 10 *m* wide
at 100 *km*/h

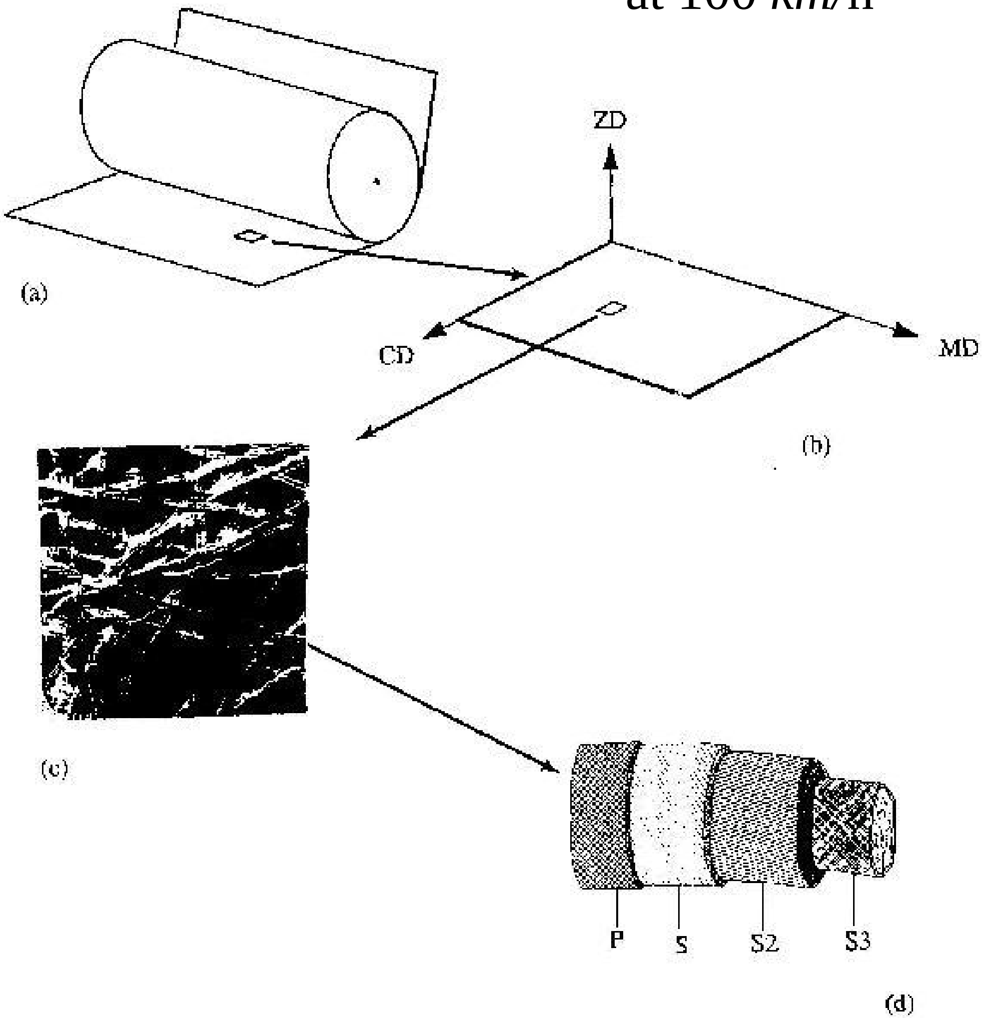

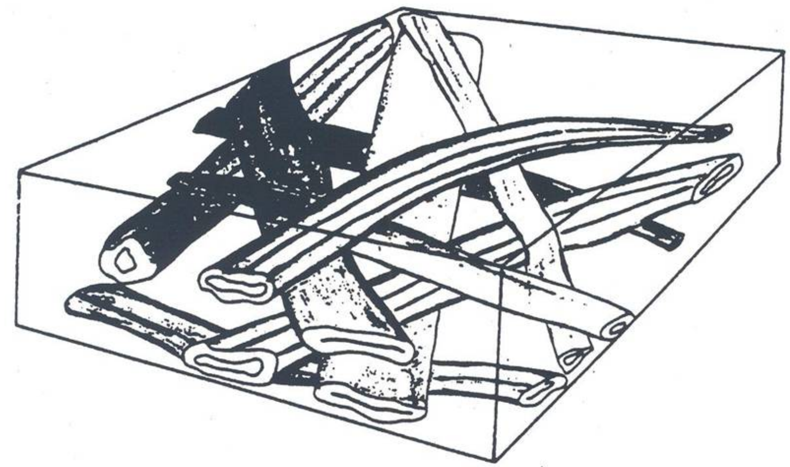

sequential inhibition process

(100 points)

binomial point process

$\Longrightarrow$ *Poisson point process*

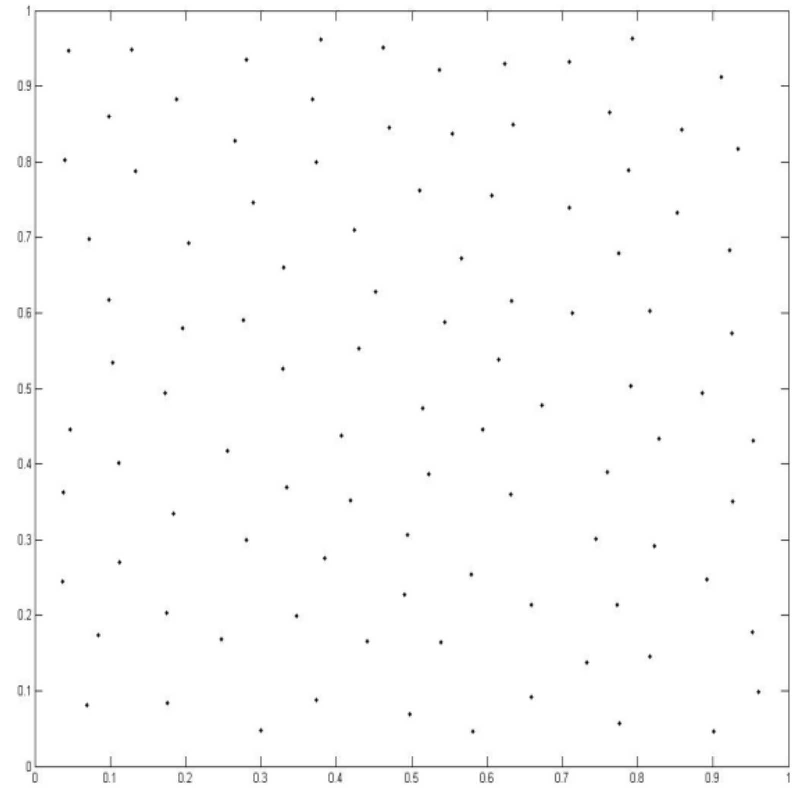

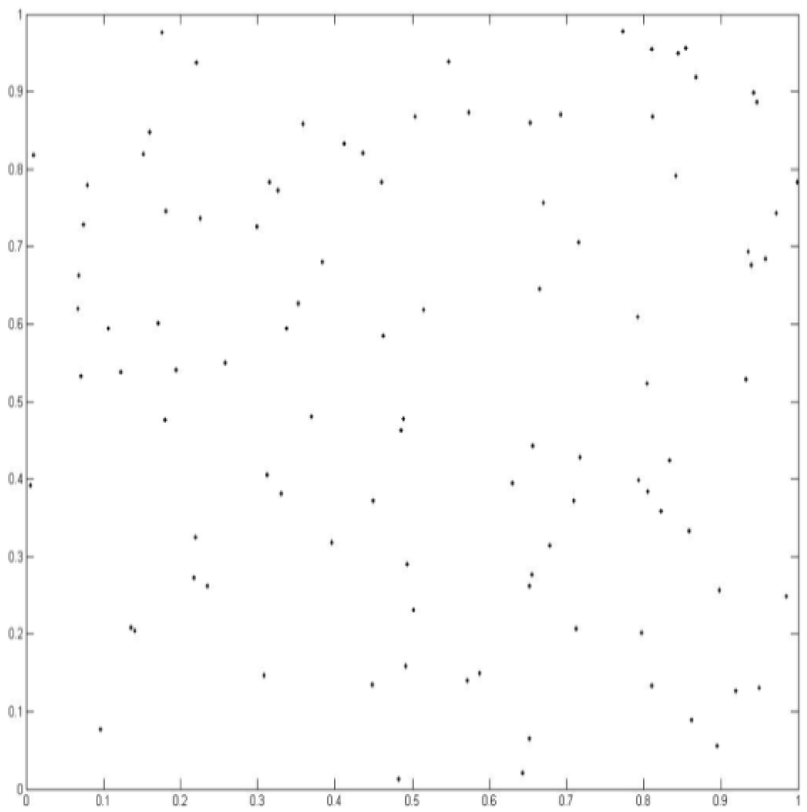

sequential inhibition process

(100 points)

binomial point process

$\Longrightarrow$ *Poisson point process* $\Longrightarrow$ (*tessellation*)
Poisson-Voronoi mosaic
Delaunay triangulation

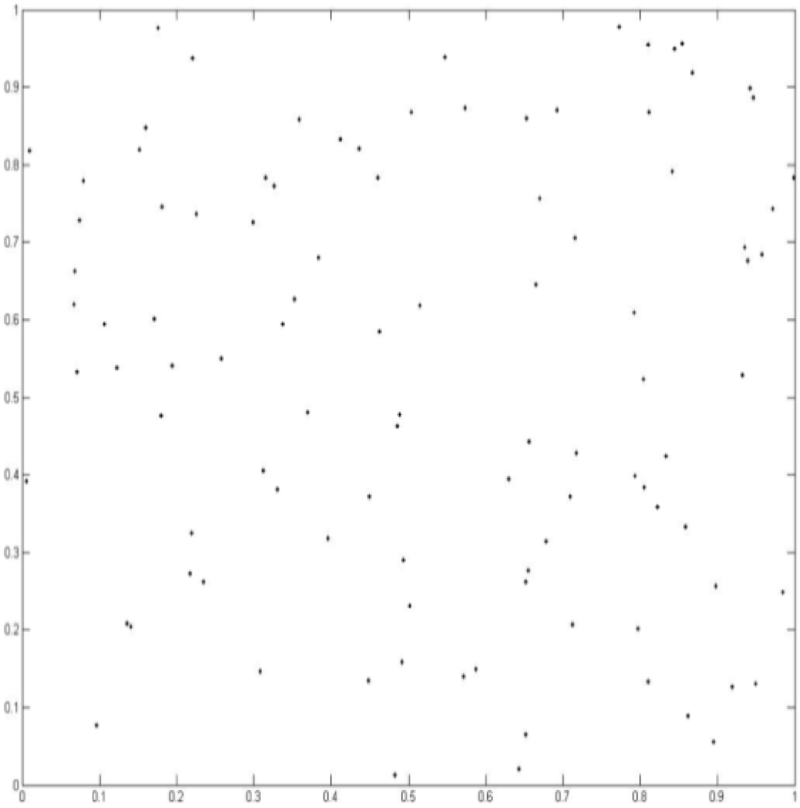

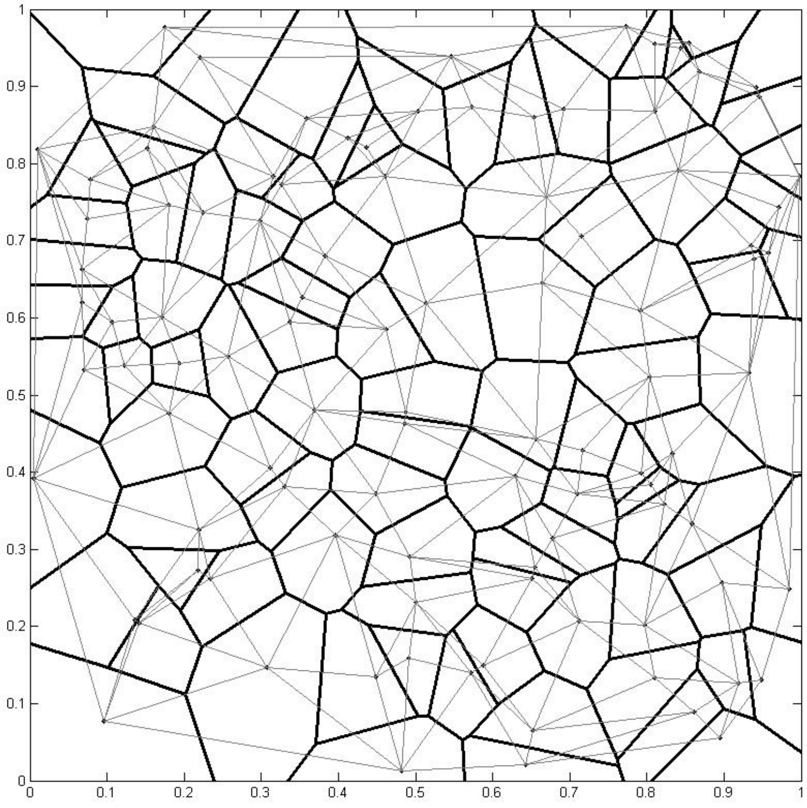

(100 points)

in Euclidean metric d_2

in non-Euclidean metric

(*tessellation*)

Poisson-Voronoi mosaic

Delaunay triangulation

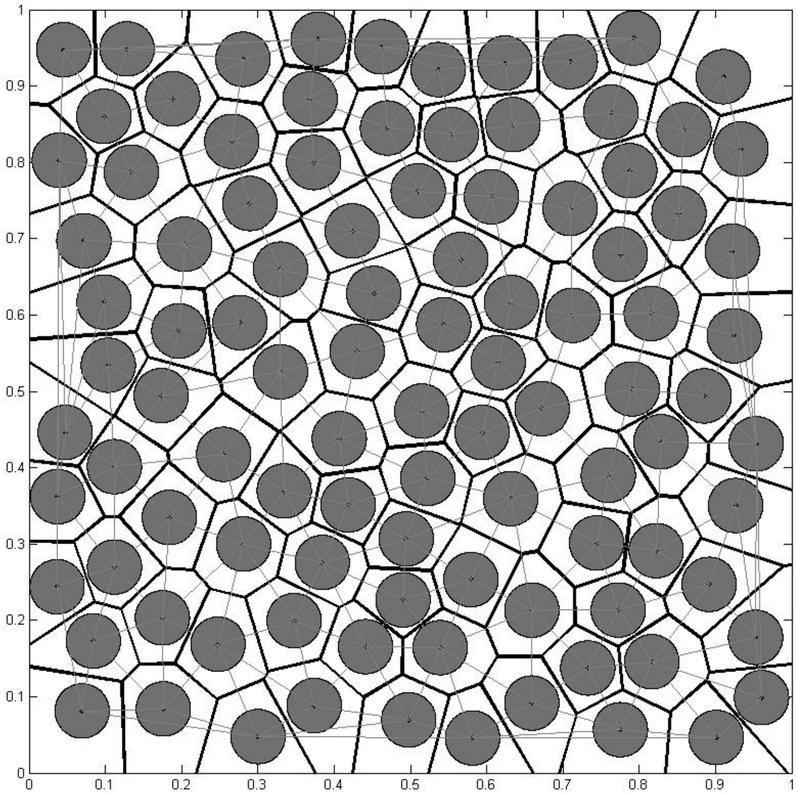

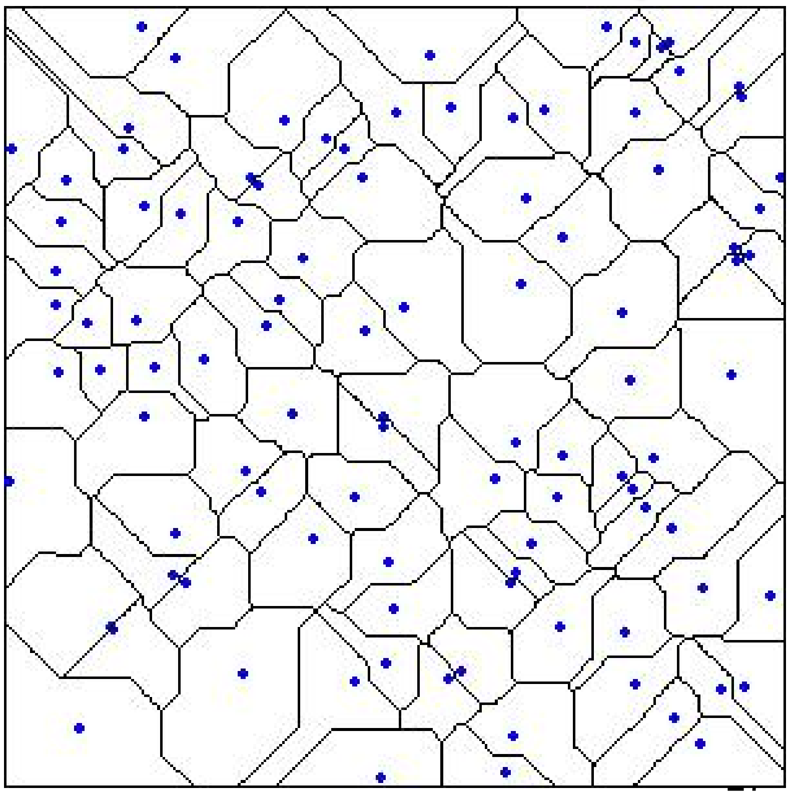

(100 points)

non-Euclidean metrics

$$d_p(\mathbf{y},\mathbf{x}) = \left(\sum_i^n |y_i - x_i|^p \right)^{1/p} \qquad 1 \le p \le \infty,$$

(*tessellation*)

Poisson-Voronoi mosaic

d_1

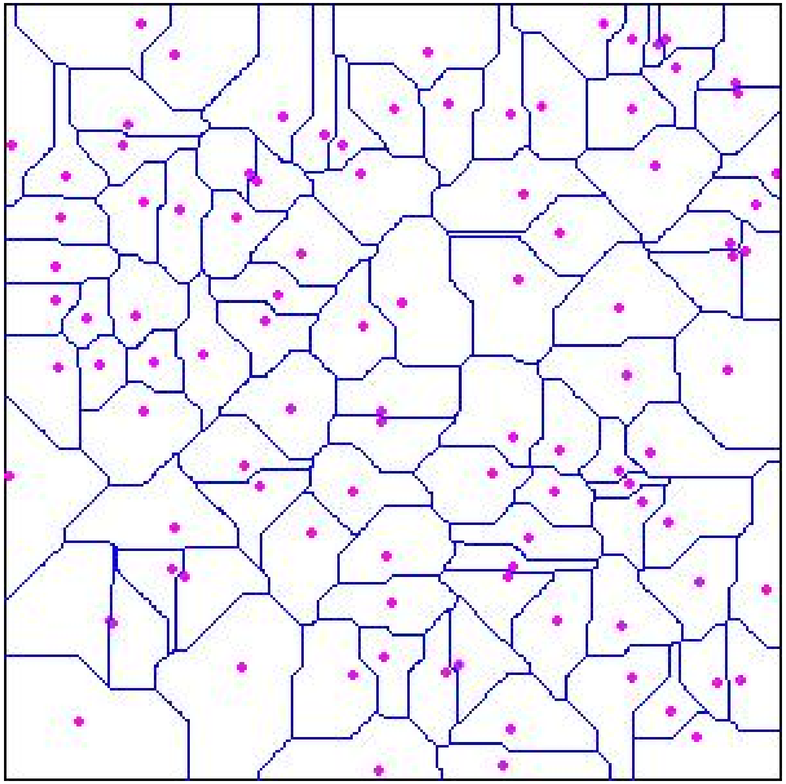

d_∞

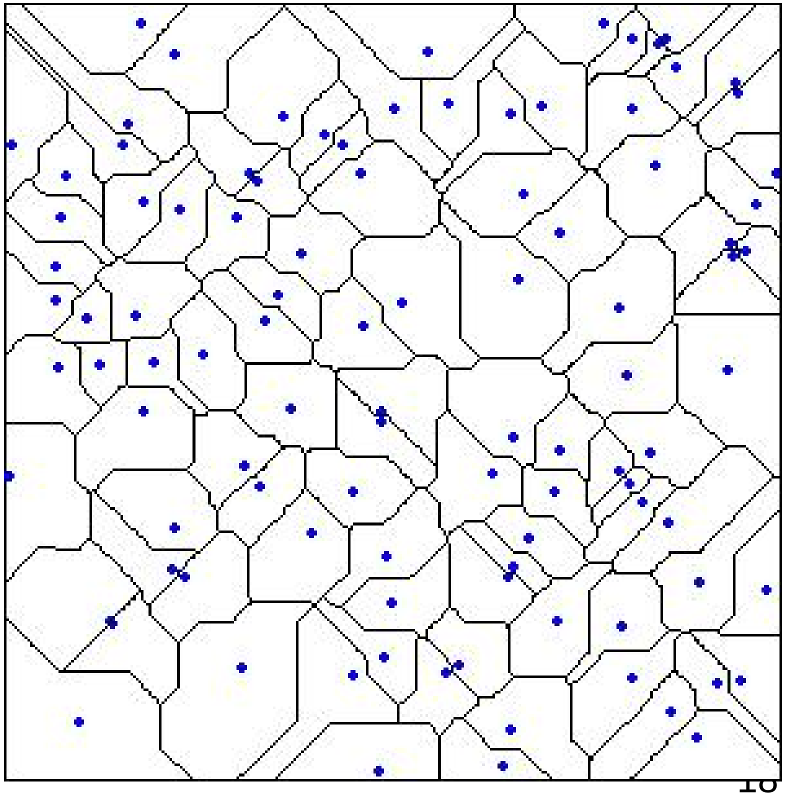

random crack model

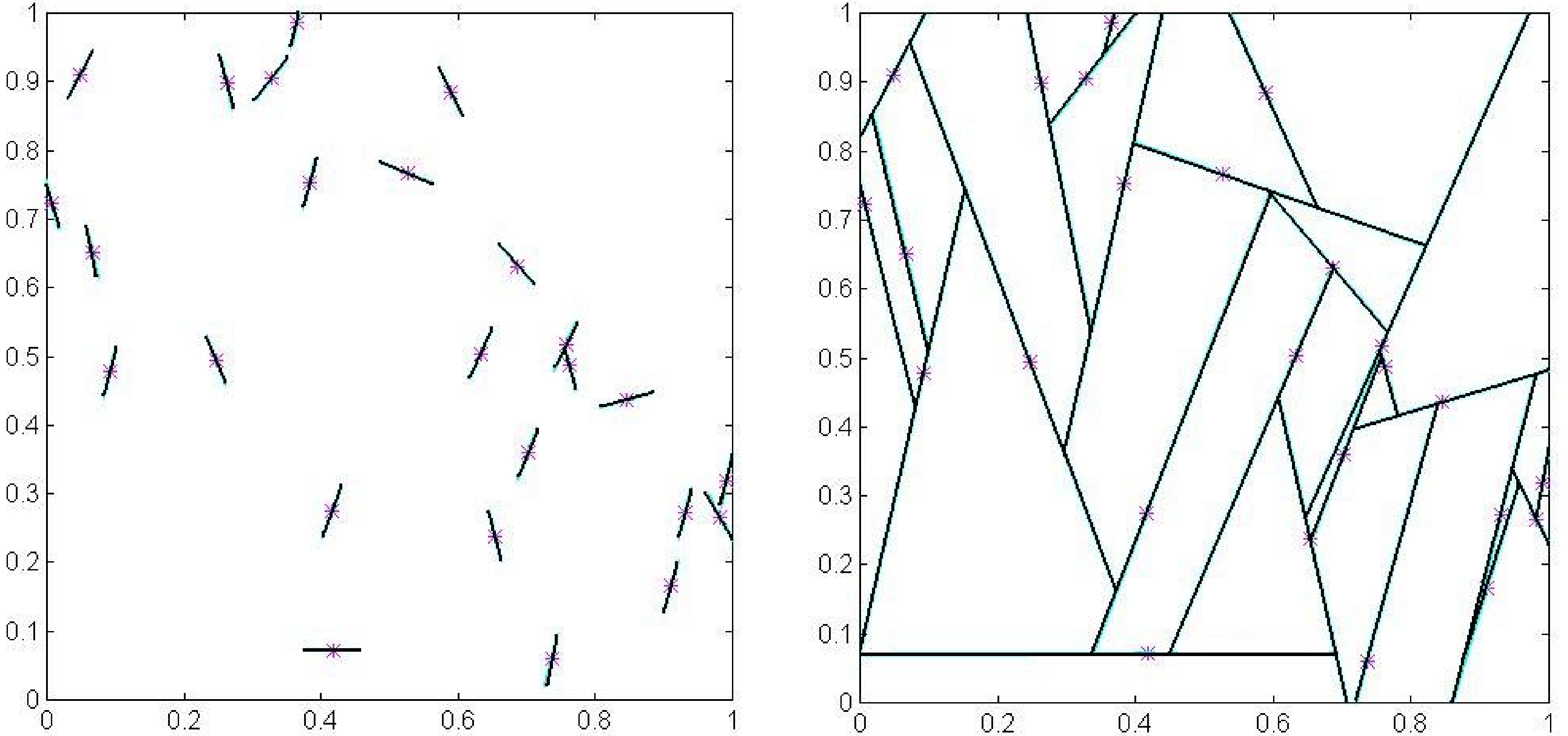

Many complex microstructures may be modeled via mathematical morphology

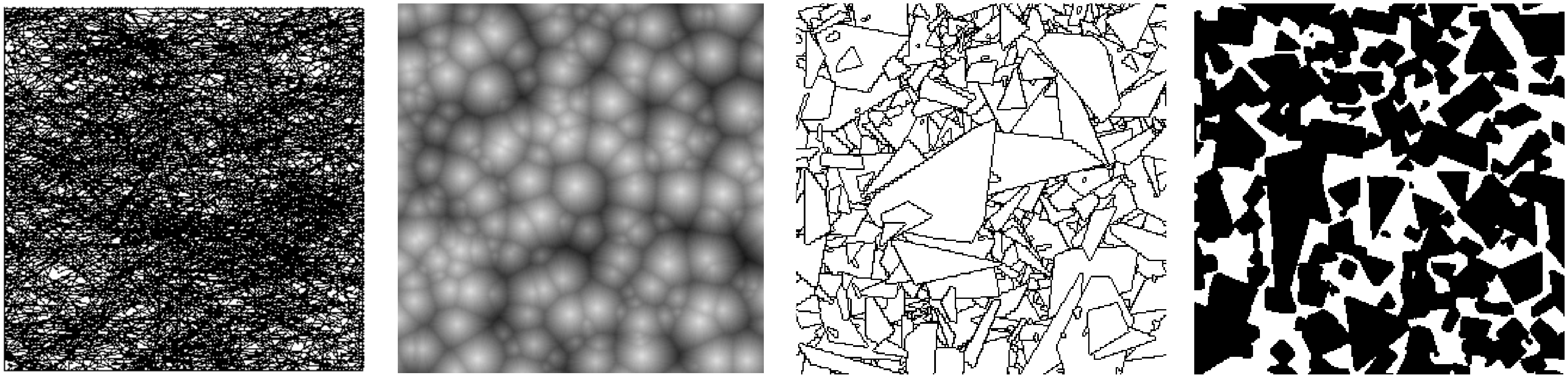

(a) (b) (c) (d)

(a) germ-grain fiber model (… fiber structures)

(b) hard-core Boolean random function (… cellular/biological tissues)

(c) dead leaves random tessellation of Poisson polygons

(… randomly micro-layered systems)

(d) Boolean model of Poisson polygons

(… tungsten-carbide [black] and cobalt [white])

Boolean model

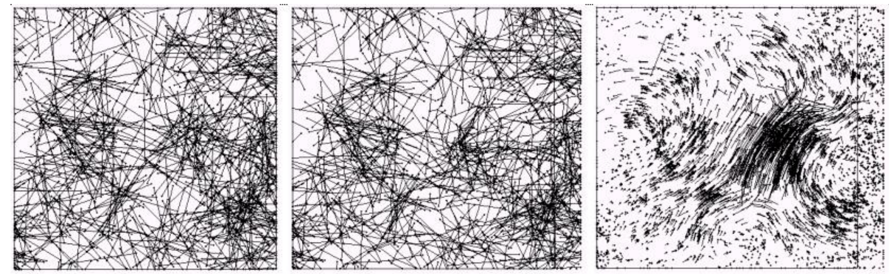

a) floc parameter b = 2.0

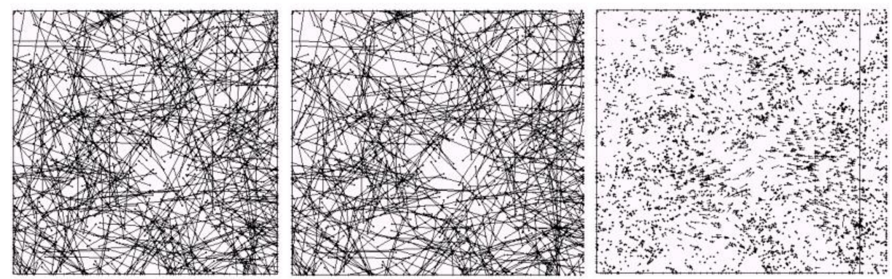

b) floc parameter b = 0.4

Generate a Poisson point field
Place grains at those points

If non-Poisson point field,
a **germ-grain model**

Boolean models

Generate a Poisson point field
Place grains at those points

If non-Poisson point field,
a **germ-grain model**

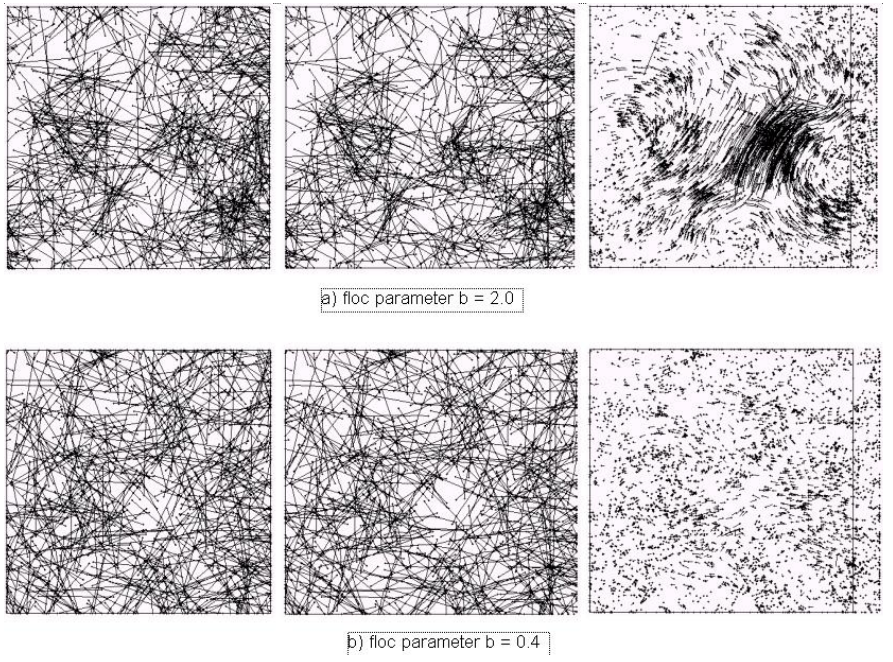

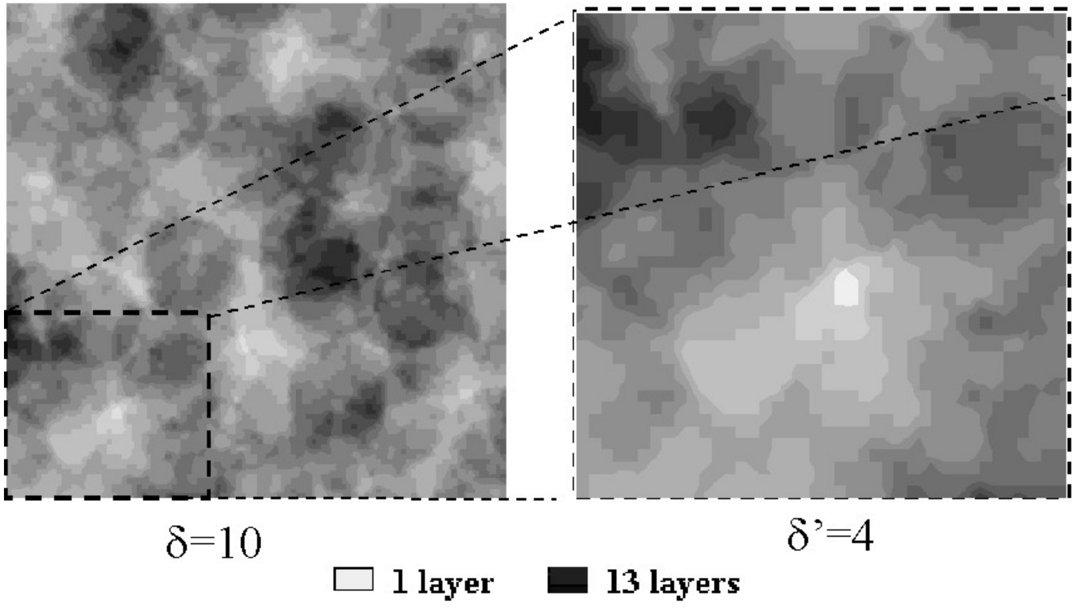

Boolean models

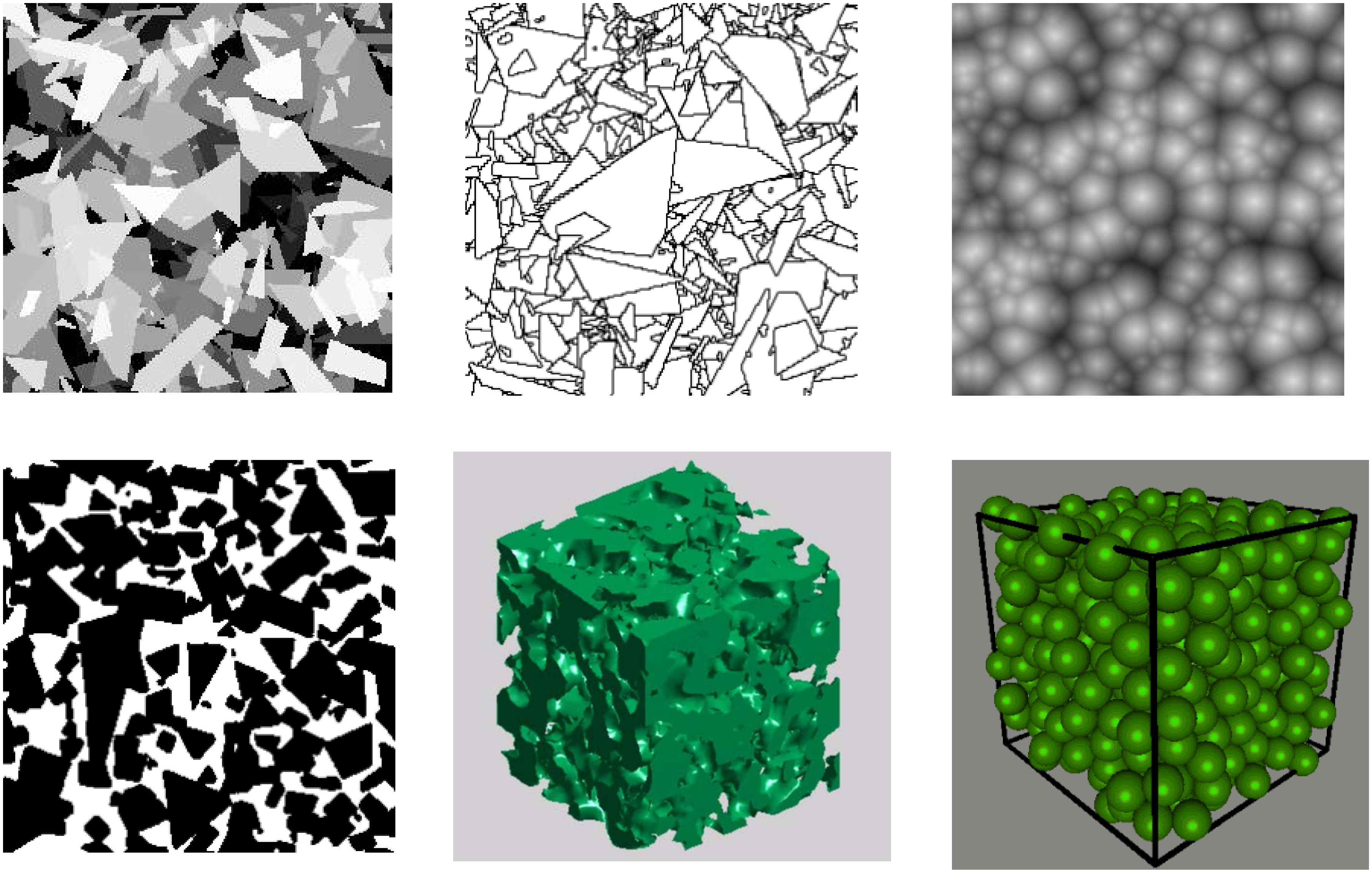

3-d model of a porous medium:
percolation of pores

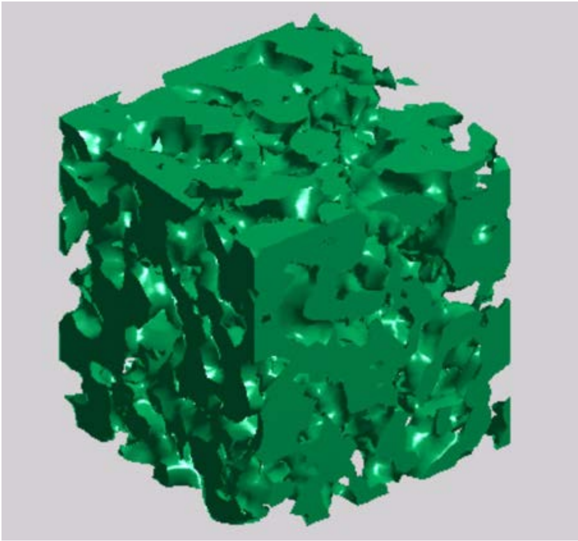

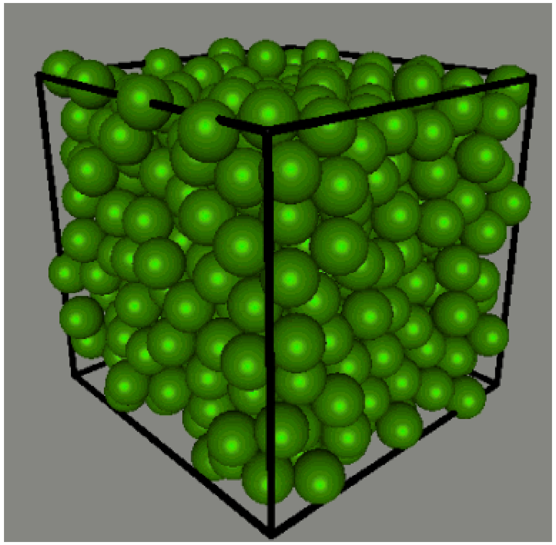

Gaussian correlated microstructures

- Two-phase isotropic correlated microstructures constructed using the Fourier Filtering based algorithm proposed by Makse *et al. (1996).*

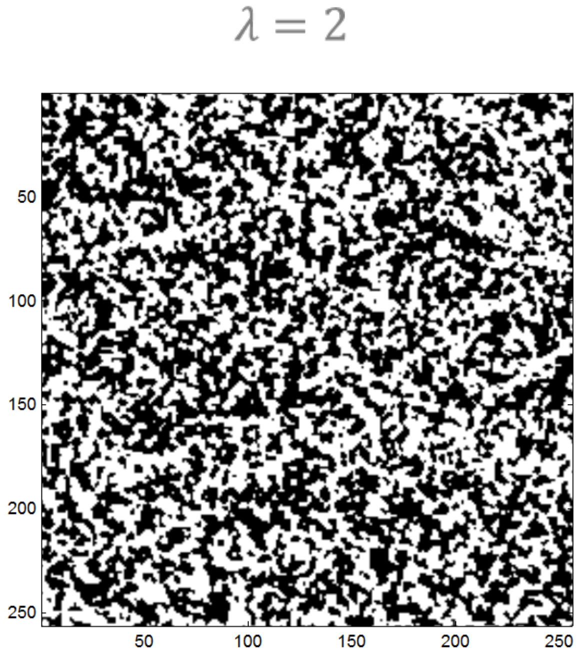

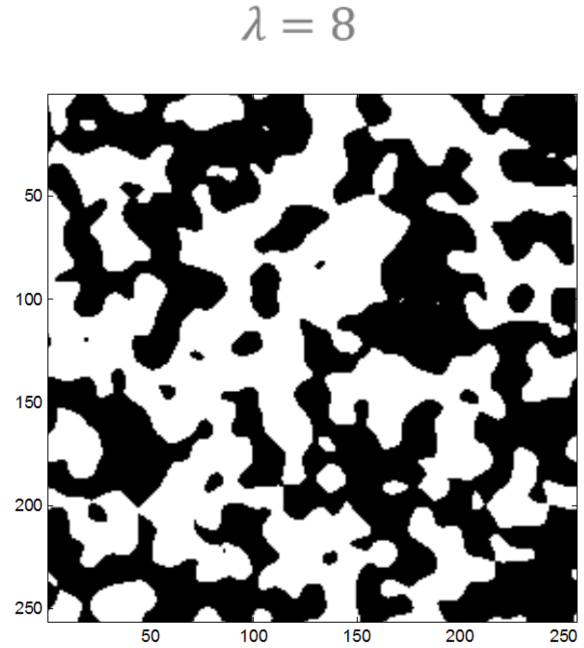

Mesoscale = 256 at 50 % volume fraction

[Makse, Hernán A., *et al*. "Method for generating long-range correlations for large systems." *Physical Review E* 53.5 (1996): 5445]

Gaussian correlated microstructures

SEM generated micrographs of Al2O3/Ni

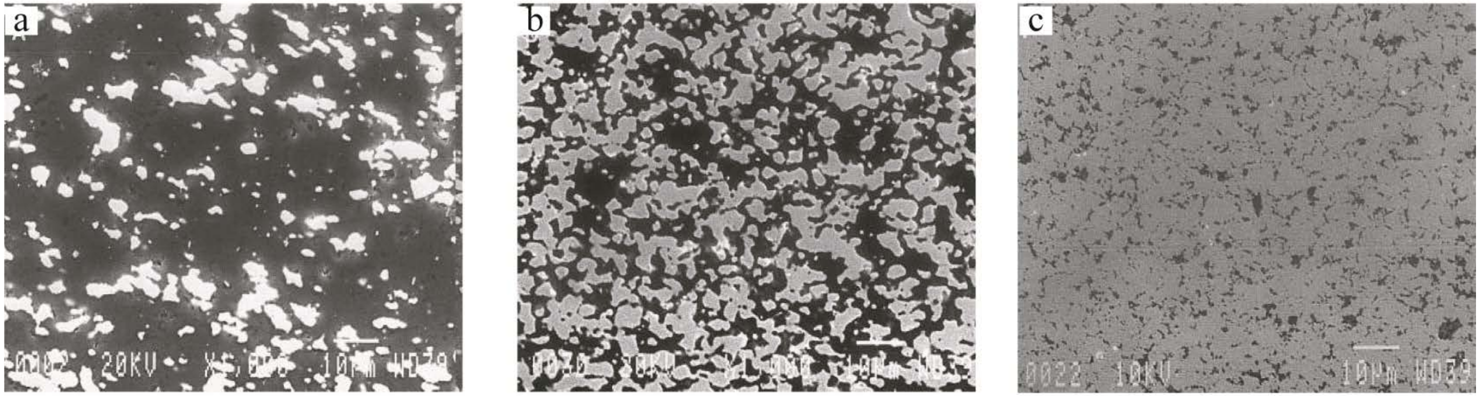

15% Ni 50% Ni 85% Ni

Aldrich, D. E., Z. Fan, and P. Mummery. "Processing, microstructure, and physical properties of interpenetrating Al2O3/Ni composites." *Materials science and technology* 16.7-8 (2000): 747-752.

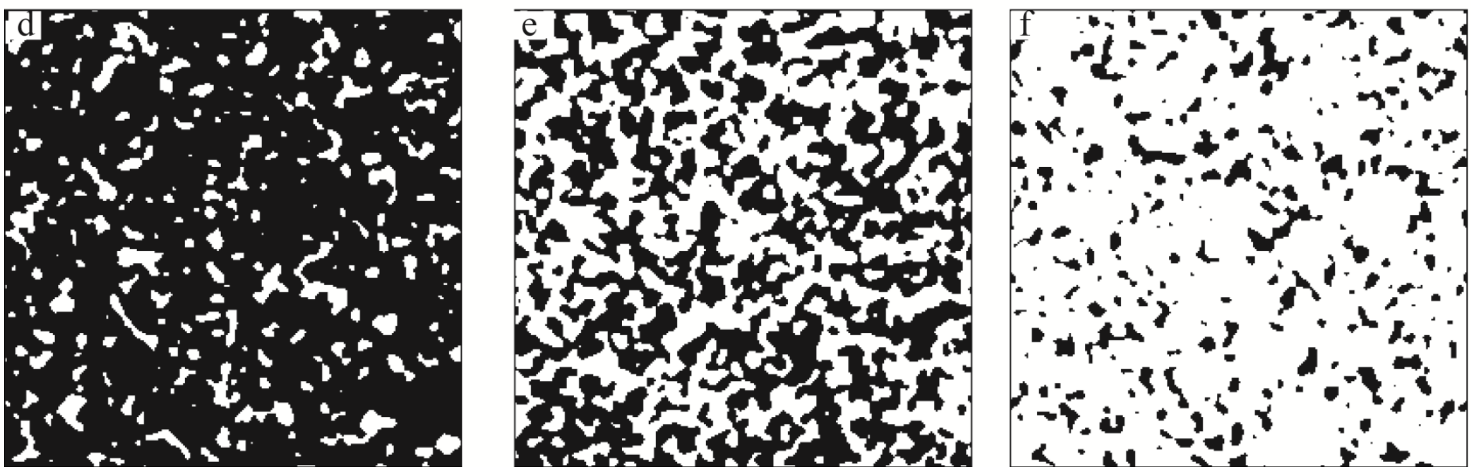

Numerically generated microstructures

Comparison with experiments*

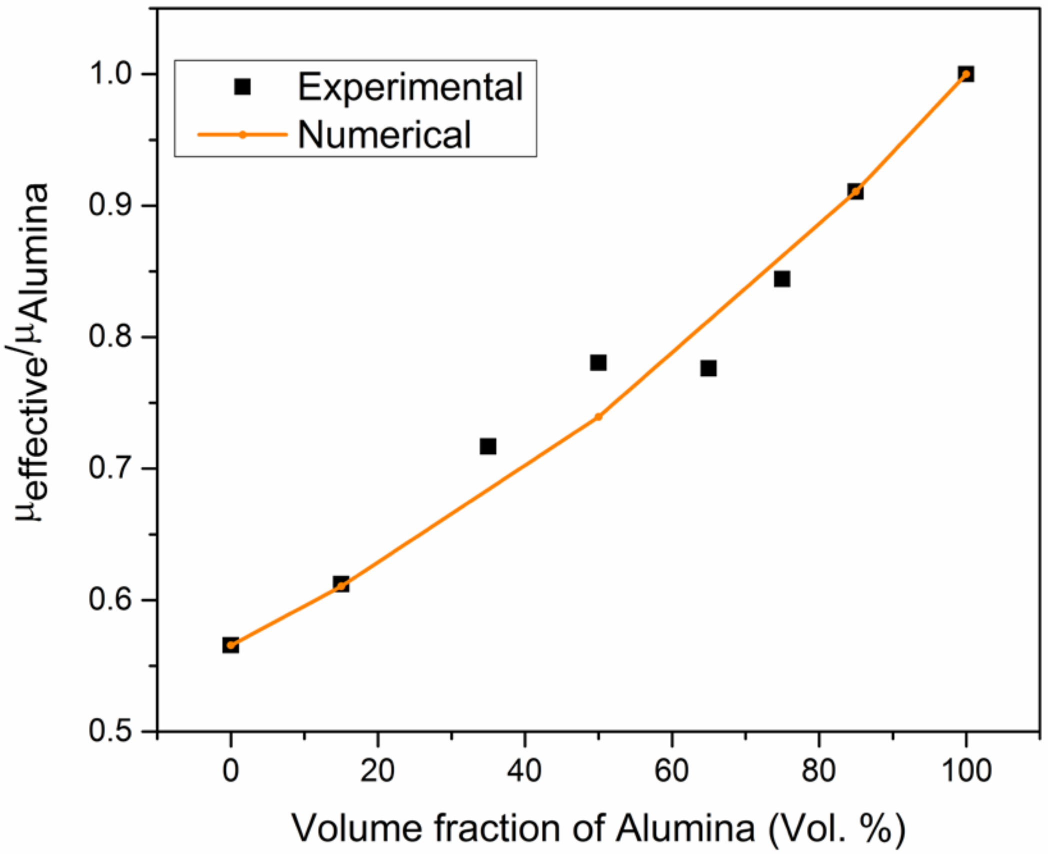

*[Aldrich, D. E., Z. Fan, and P. Mummery. "Processing, microstructure, and physical properties of interpenetrating Al2O3/Ni composites." *Materials Science and Technology* 16.7-8 (2000): 747-752]

Gaussian correlated microstructures

- Gaussian correlation function, $\rho(x,y) = e^{-\gamma_1 x^2 - \gamma_2 y^2}$
- Correlation length is defined as $\lambda = \int_0^\infty \int_0^\infty \rho(x,y)\,dx\,dy$
- For the isotropic correlations considered, $\gamma_1 = \gamma_2 = \gamma = \pi/4\lambda^2$

$\lambda = 8$

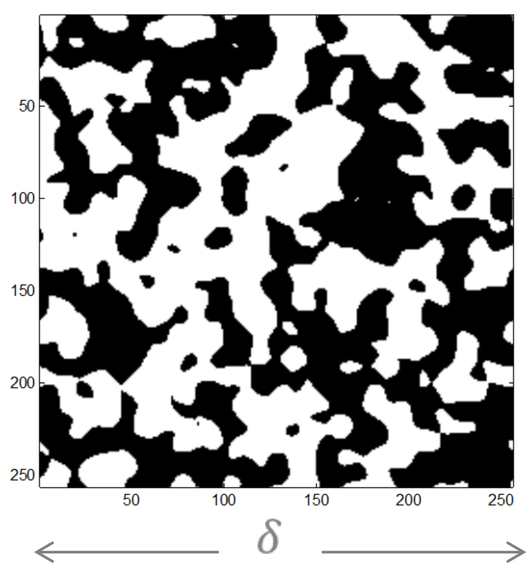

- What is the effect of these two length scales, δ and λ, on the scale dependent bounds?

Functionally Graded Materials (FGM)

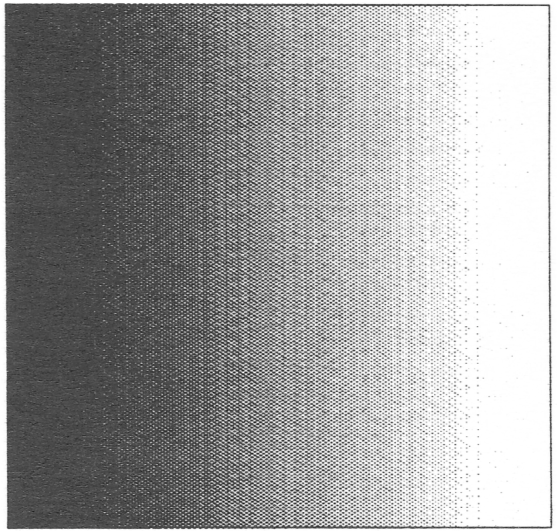

Random medium

$$\mathrm{B} = \{B(\omega); \omega \in \Omega\}$$

Functionally graded materials

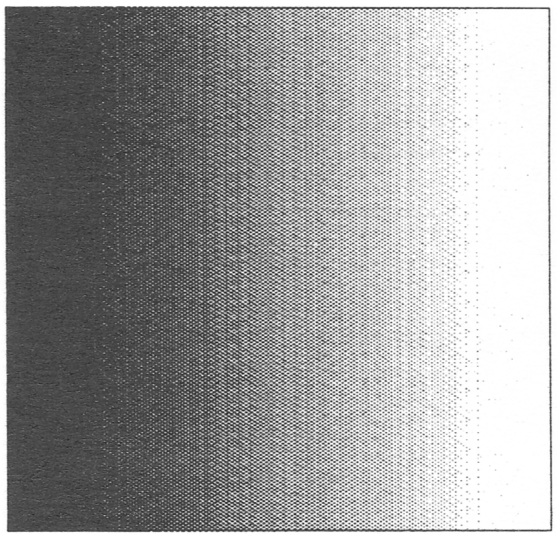

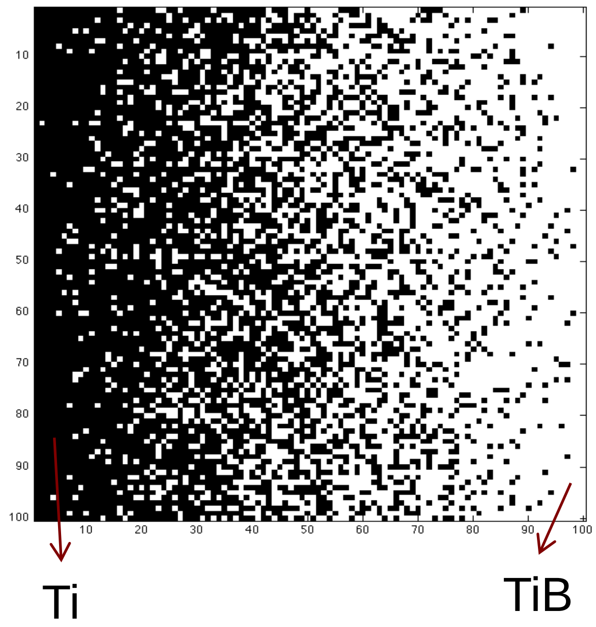

Random medium

$$\mathrm{B} = \{B(\omega); \omega \in \Omega\}$$

Functionally graded materials

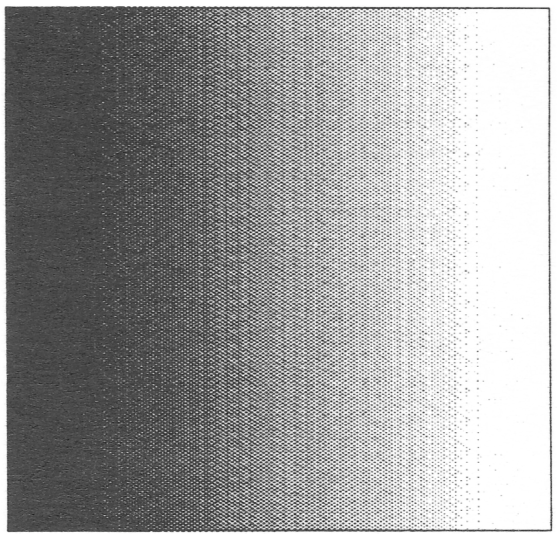

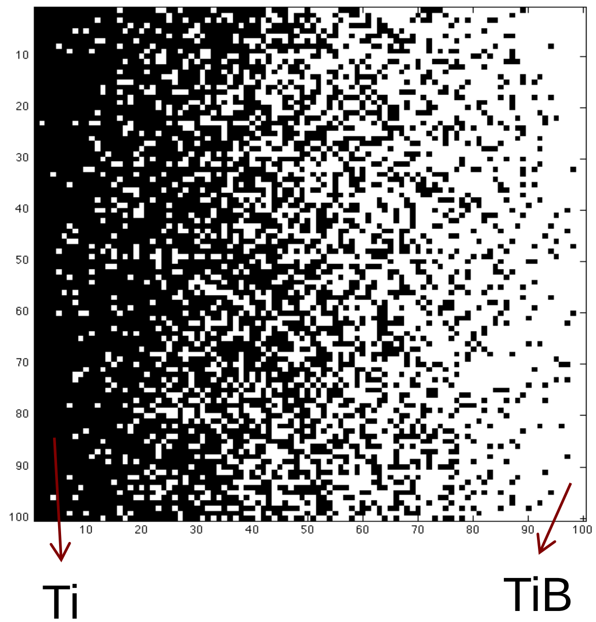

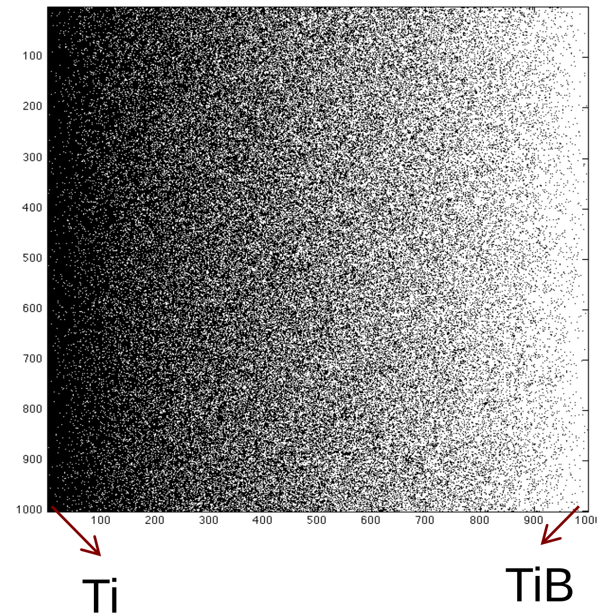

Random medium

$$\mathrm{B} = \{B(\omega); \omega \in \Omega\}$$

[A. Saharan *et al.*, "Fractal geometric characterization of functionally graded materials," *ASCE J. Nanomech. Micromech.*, 2013]

Edge Plots

Fineness: 100

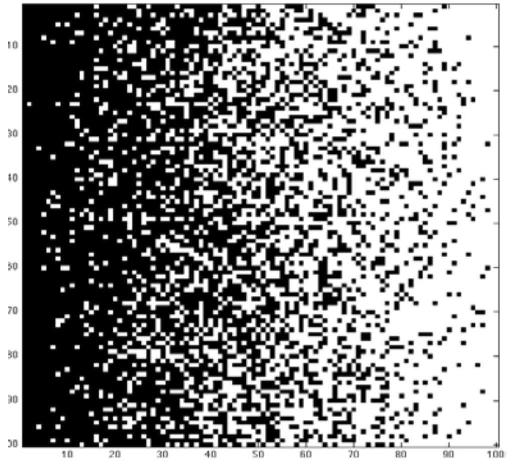

Edge Plots

Fineness: 100

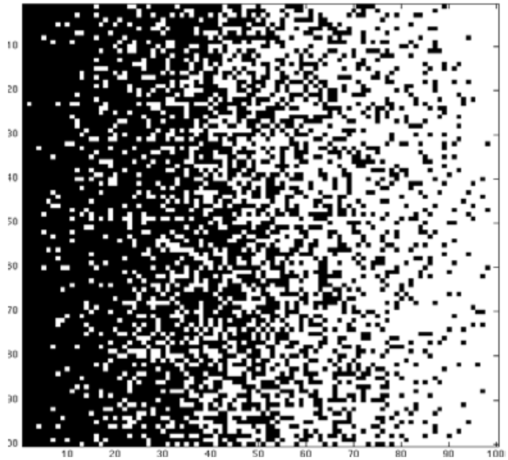

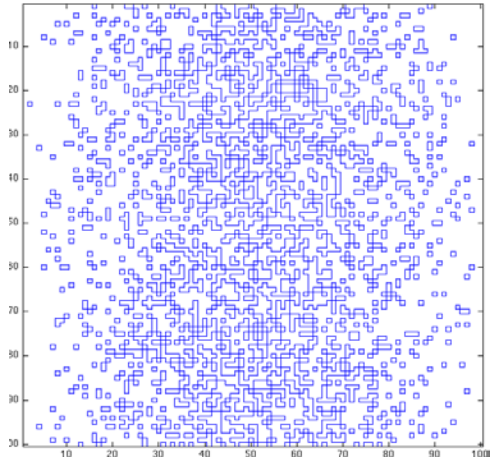

Edge Plots

Fineness: 100

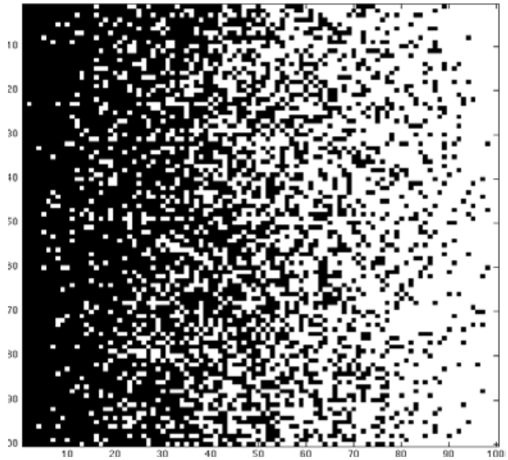

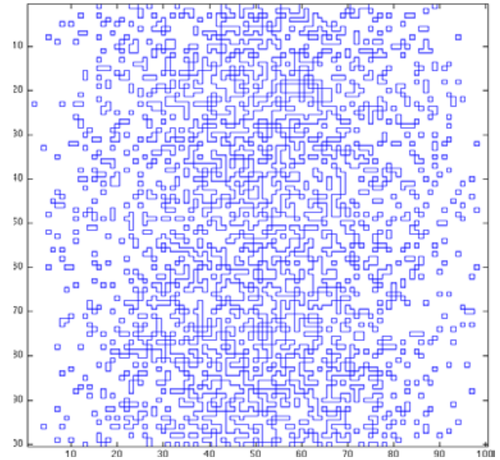

Fineness: 1000

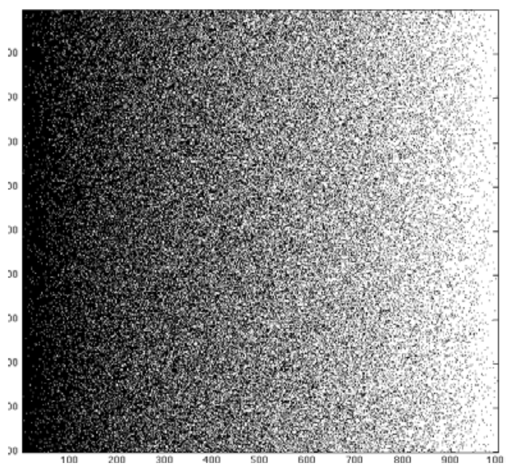

Edge Plots

Fineness: 100

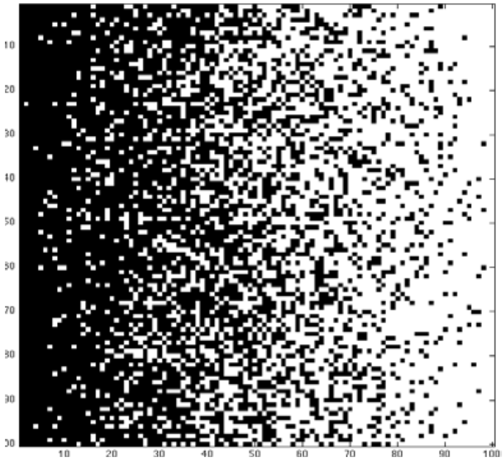

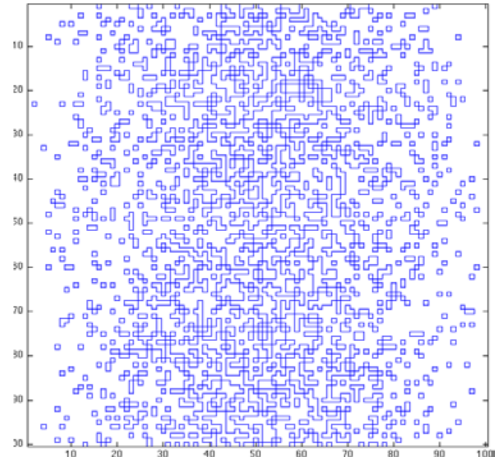

D ~ 1.7–1.8

Fineness: 1000

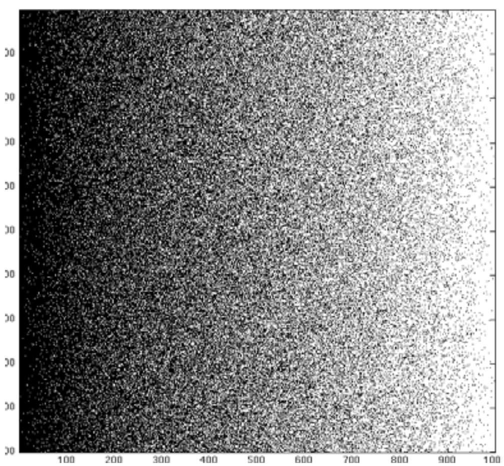

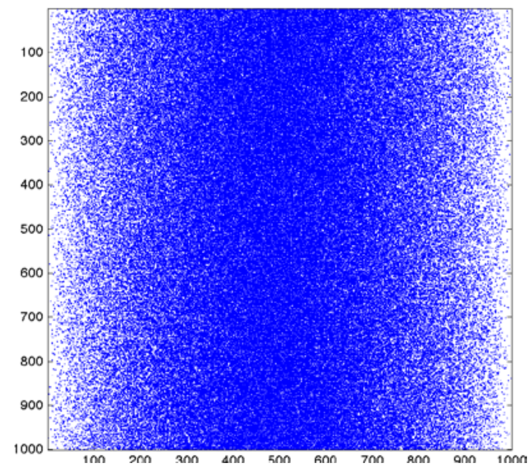

Functionally graded materials

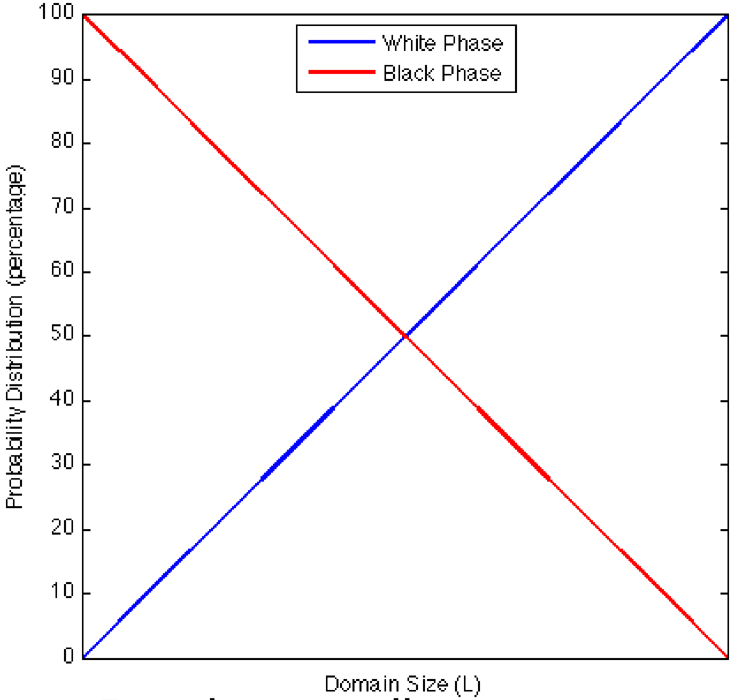

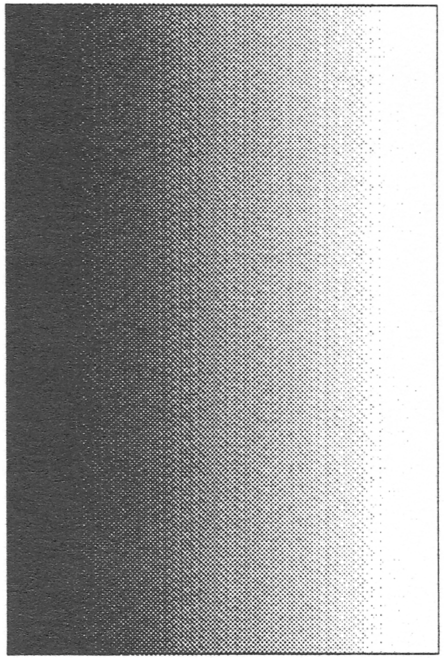

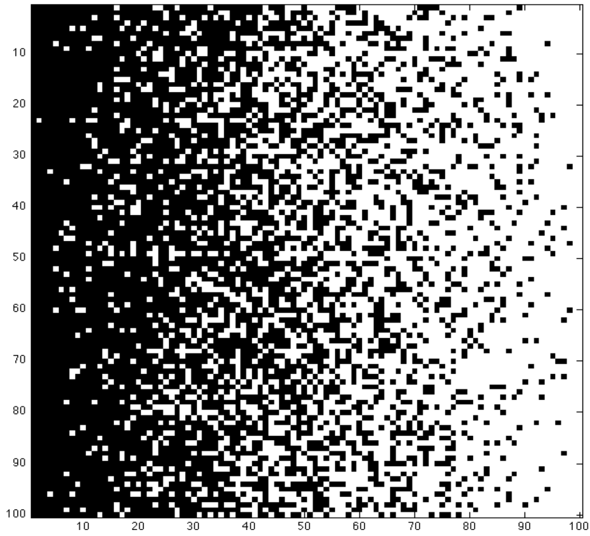

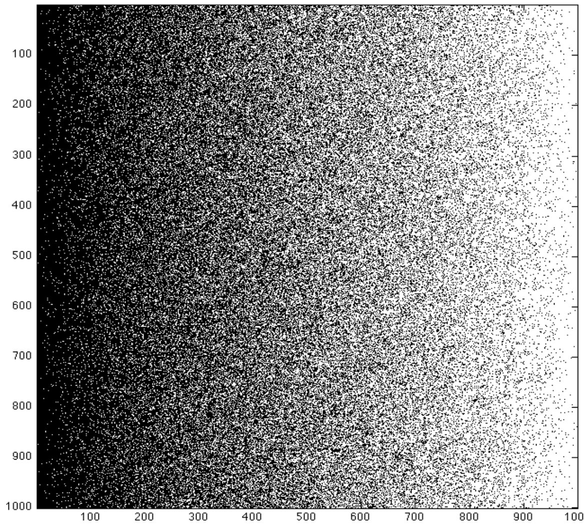

Random medium

$$\mathrm{B} = \{B(\omega); \omega \in \Omega\}$$

P(black, white) = {0.5,0.5}

Curve fit for local fractal dimension D(x)

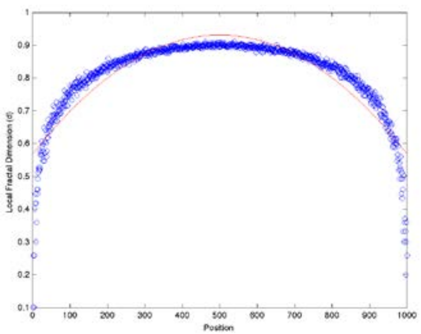

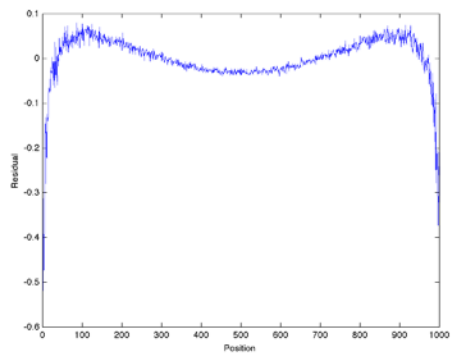

$$f(x) = 0.5676 + 0.0015x - 1.4505e^{-6}x^2$$

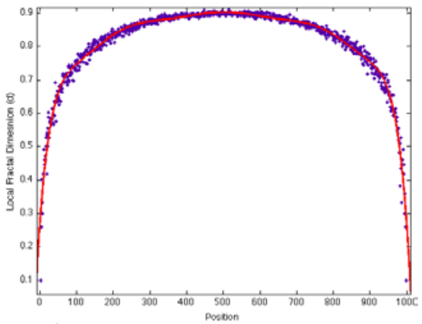

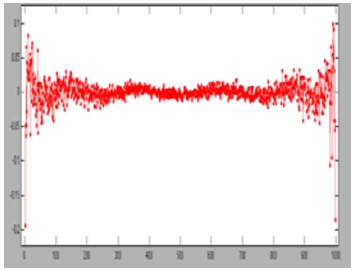

$$f(x) = a_0 + a_1\cos(\omega x) + b_1\sin(\omega x) + a_2\cos(2\omega x) + b_2\sin(2\omega x) + a_3\cos(3\omega x) + b_3\sin(3\omega x) + a_4\cos(4\omega x) + b_4\sin(4\omega x) + a_5\cos(5\omega x) + b_5\sin(5\omega x)$$

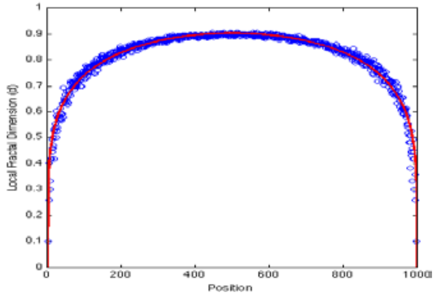

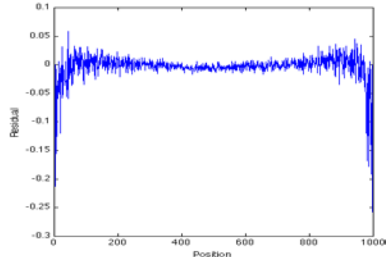

$$f(x) = \frac{x^{\alpha-1}(1-x)^{\beta-1}}{B(\alpha,\beta)}C$$

Curve fit for local fractal dimension D(x)

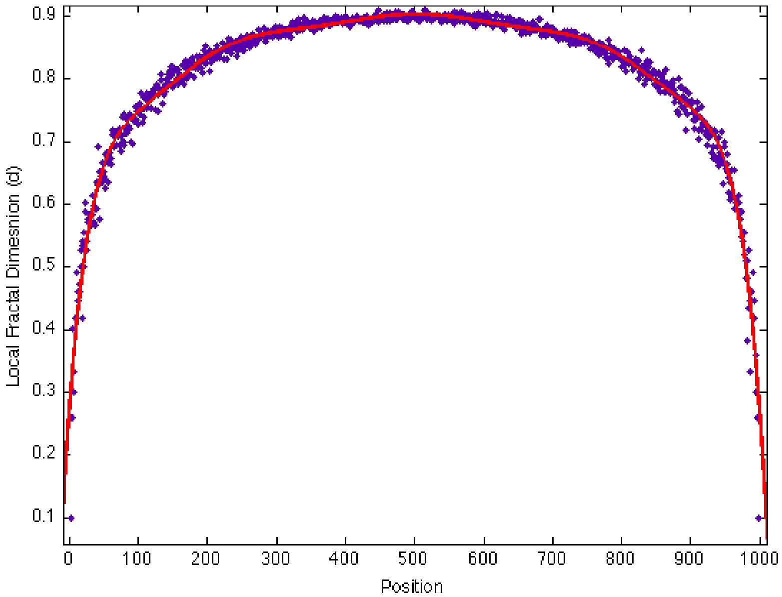

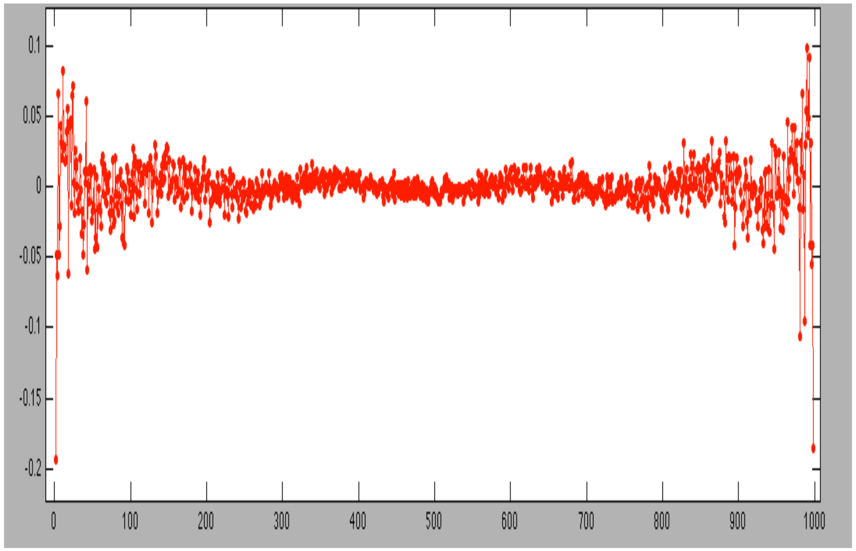

$$f(x) = a_0 + a_1 \cos(\omega x) + b_1 \sin(\omega x) + a_2 \cos(2\omega x) + b_2 \sin(2\omega x) + a_3 \cos(3\omega x) + b_3 \sin(3\omega x) + a_4 \cos(4\omega x) + b_4 \sin(4\omega x) + a_5 \cos(5\omega x) + b_5 \sin(5\omega x)$$

$$a_0 = -3.897e+06; \omega = 0.2666$$
$$a_1 = 6.525e+06; b_1 = -1833$$
$$a_2 = -3.781e+06; b_2 = 2098$$
$$a_3 = 1.451e+06; b_3 = -1182$$
$$a_4 = -3.331e+05; b_4 = 350.5$$
$$a_5 = 3.473e+04; b_5 = -43.7$$

Curve fit for local fractal dimension D(x)

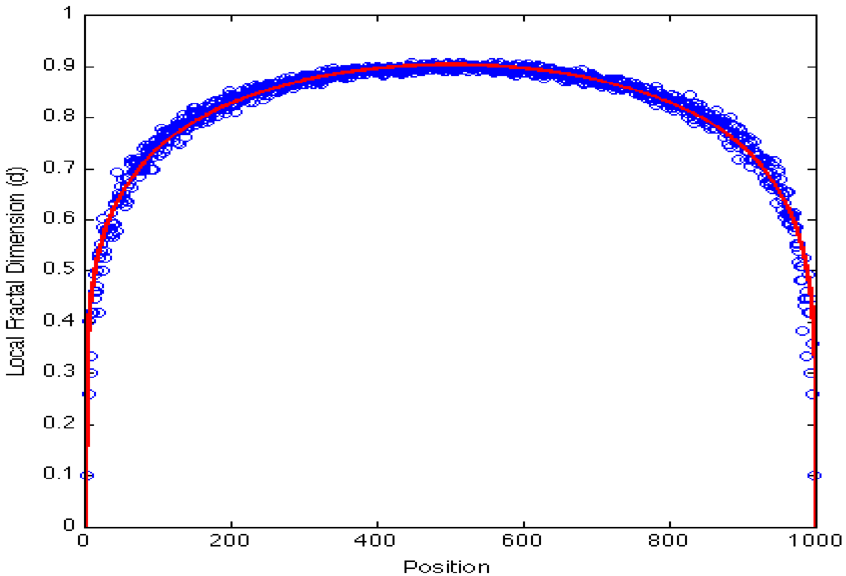

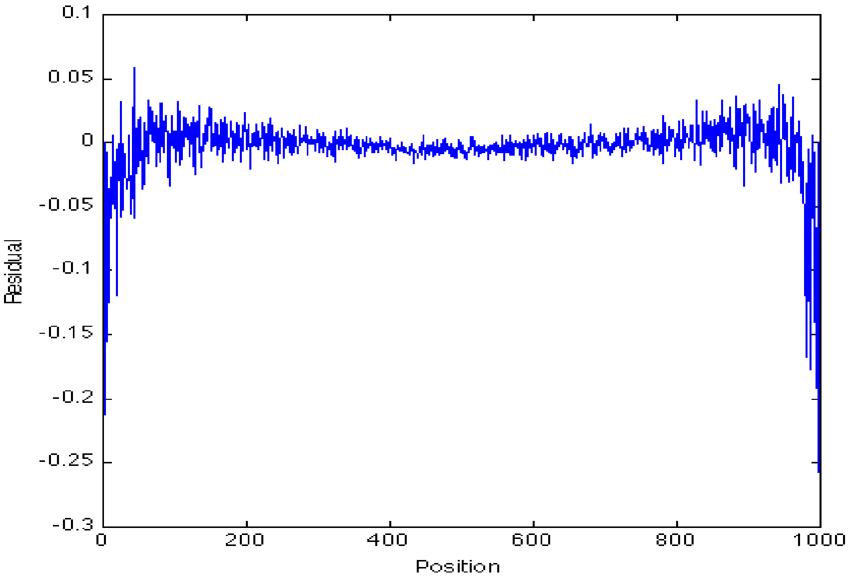

$$f(x) = \frac{x^{\alpha-1}(1-x)^{\beta-1}}{B(\alpha,\beta)}C$$

$$B(x,y) = \frac{\Gamma(x)\Gamma(y)}{\Gamma(x+y)} = \int_0^1 t^{x-1}(1-t)^{y-1}\,dt$$

$\alpha = 1.692$;$\beta = 1.692$

$$\Gamma(z) = \int_0^\infty t^{z-1}e^{-t}\,dt$$

$C = 0.8129$

Interfacial Fractal Dimension

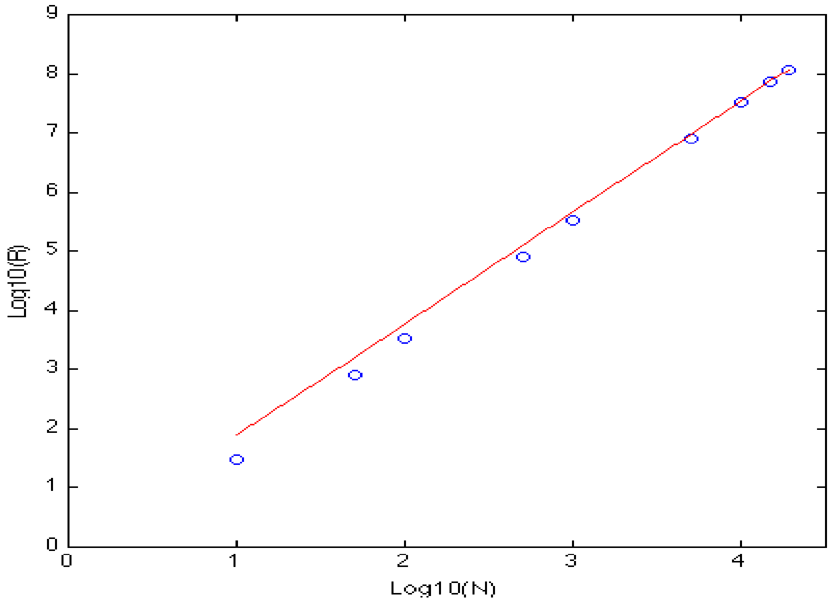

Fineness of FGM	Interfacial Fractal Dimension
10	1.459328817
50	1.710635642
100	1.757886781
500	1.822756529
1000	1.840748953
5000	1.870978452
10000	1.880705808
15001	1.88573187
19001	1.888491704

System fineness and corresponding "interfacial fractal dimension"

Edge Plots

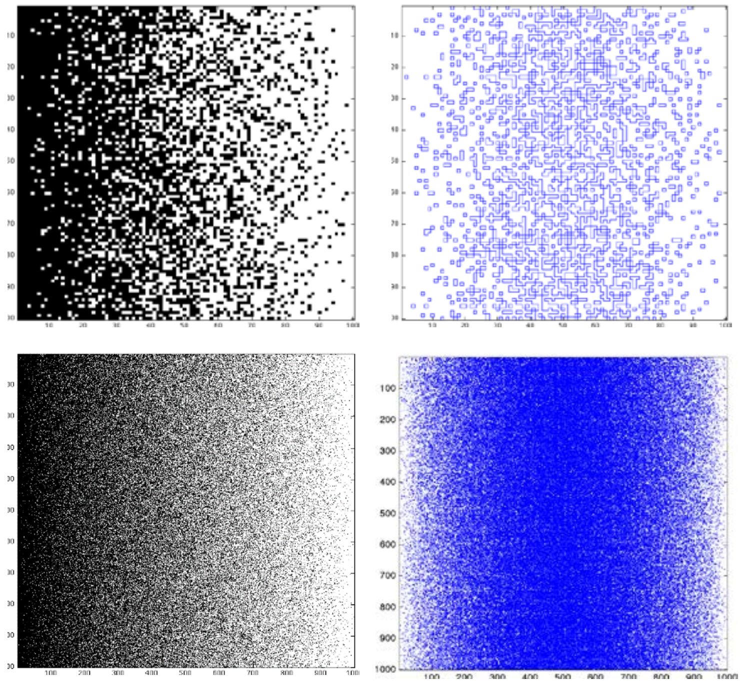

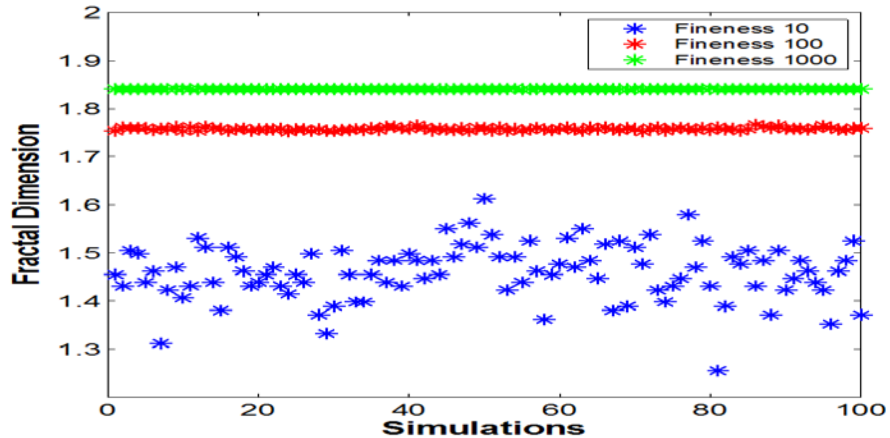

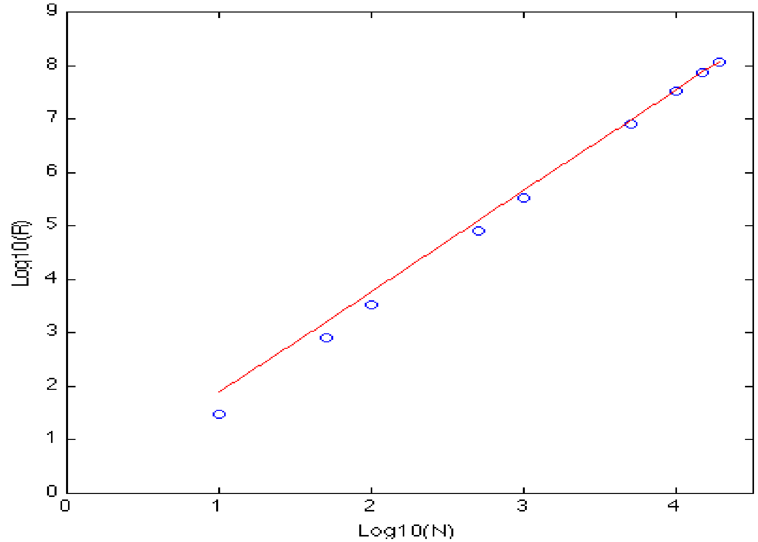

D~1.88

$$D = \frac{log(R)}{log(N)}$$

3d Functionally graded materials (FGM)

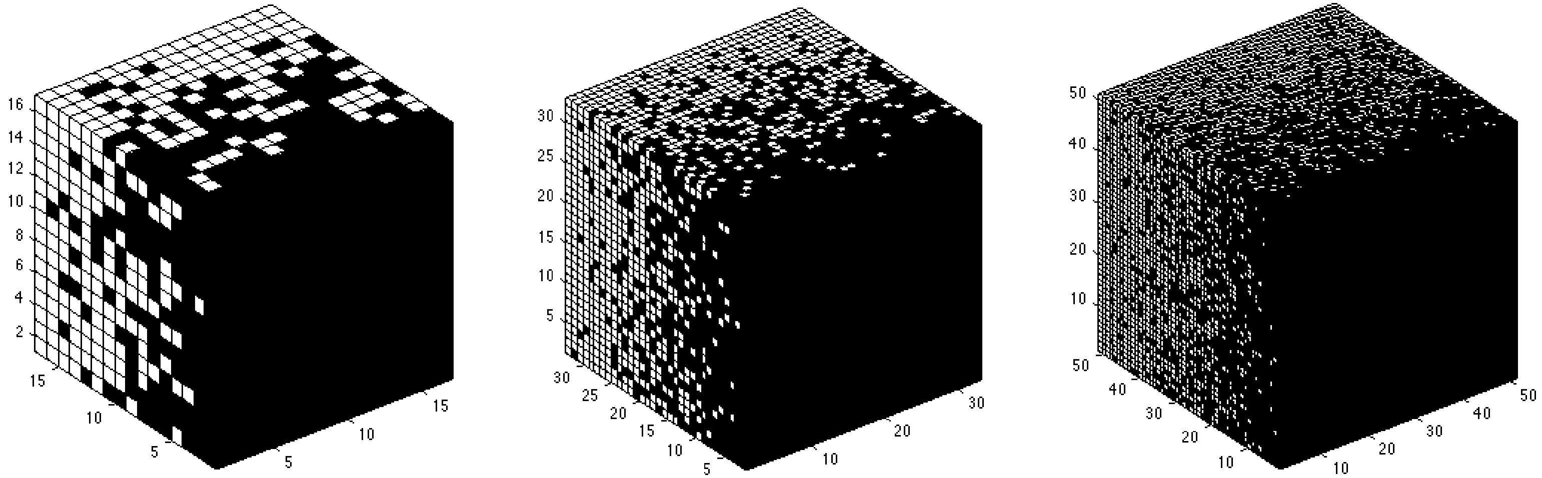

$\delta = 16$ $\delta = 32$ $\delta = 50$

Future work – Experimental study

OBJET Eden 350 3D printer in MEL, UIUC

- A preliminary experimental study was carried out on FGM samples printed using additive manufacturing technology.
- The printer reads the sample geometry through a *'STL file format'* (STereoLithography).

3D printed FGM samples

A 3D printed FGM sample

Property	ASTM	Value
Young's modulus	D-638-04	2740 MPa
Tensile strength	D-638-03	55 MPa

Material properties of VeroBlue material

- The blue material on the right is the hard material called *'VeroBlueFullCure®840'*.
- The white material on the left is a soft *'gel'* like material called *'SupportFullCure®705'.*
- These materials are polymers provided by OBJET.
- The properties of the white phase have not been released by the manufacturer.
- The mean dimensions of the sample were: $19.35mm \times 6.35mm \times 2.37mm$

Towards simulations of fractals…

Topological Dimension	**Object**
0	Point
1	Line
2	Plane
3	Space

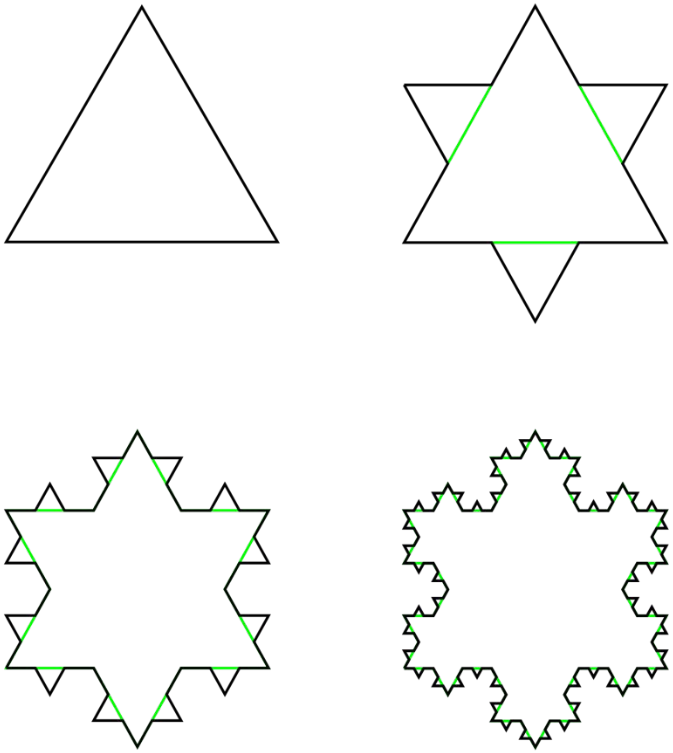

URL: http://davidprice.files.wordpress.com/2013/07/2000px-kochflake.png

In between?

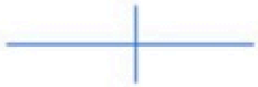

1-D N parts, scaled by ratio r = 1/ N

$$N\,r^1 = 1$$

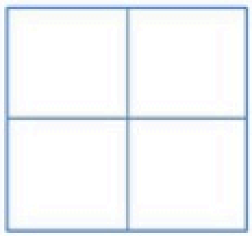

2-D N parts, scaled by ratio r = 1/ $N^{1/2}$

$$N\,r^2 = 1$$

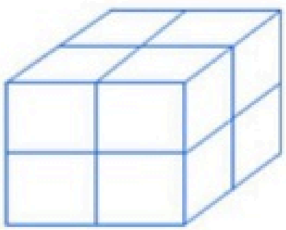

3-D N parts, scaled by ratio r = 1/ $N^{1/3}$

$$N\,r^3 = 1$$

Generalize

For an object of N parts, each scaled down by a ratio r from the whole:

$$N\,r^D = 1$$

$$D = \frac{\log N}{\log 1/r}$$

Generating Different Dimensions

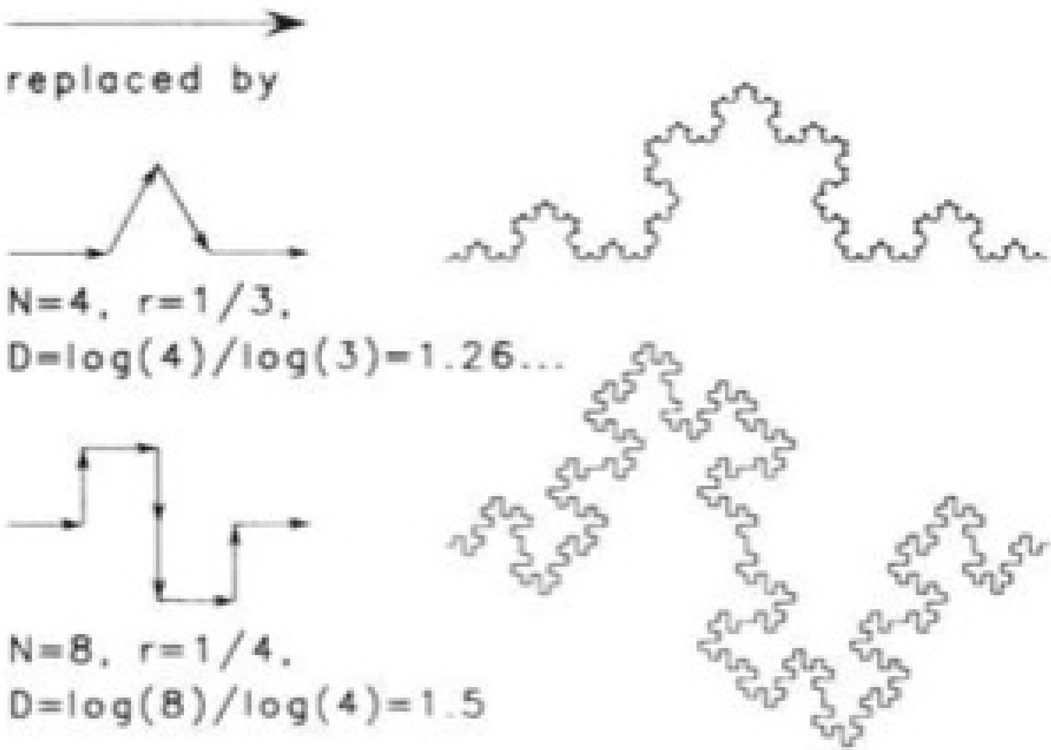

Curve F:
D≈1.051

Curve G:
D≈1.293

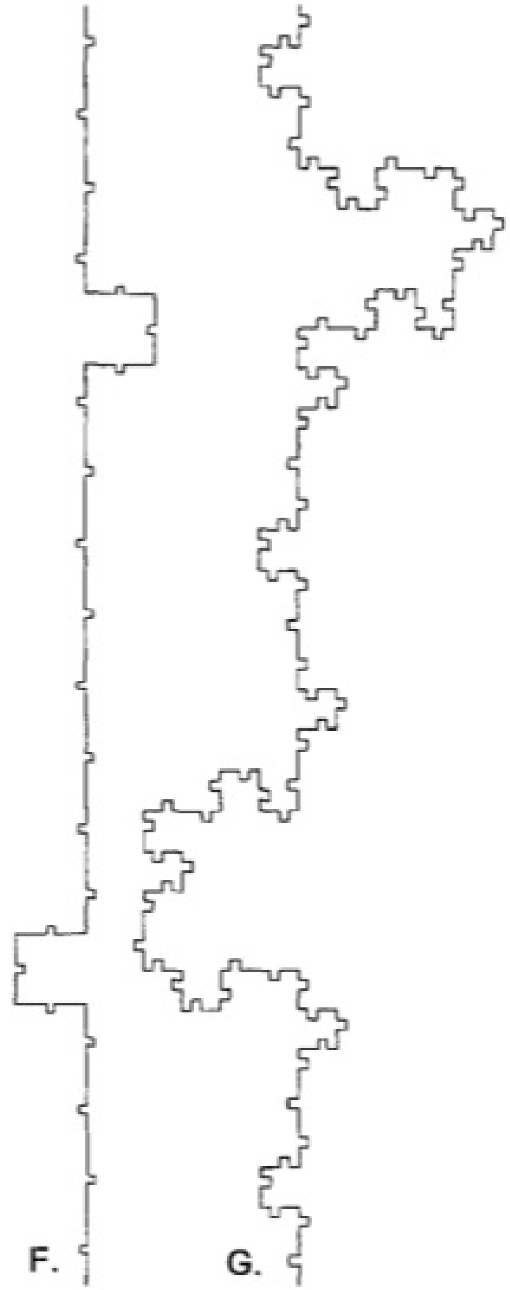

What is the length of coast of Britain?

What is the length of coast of Britain?

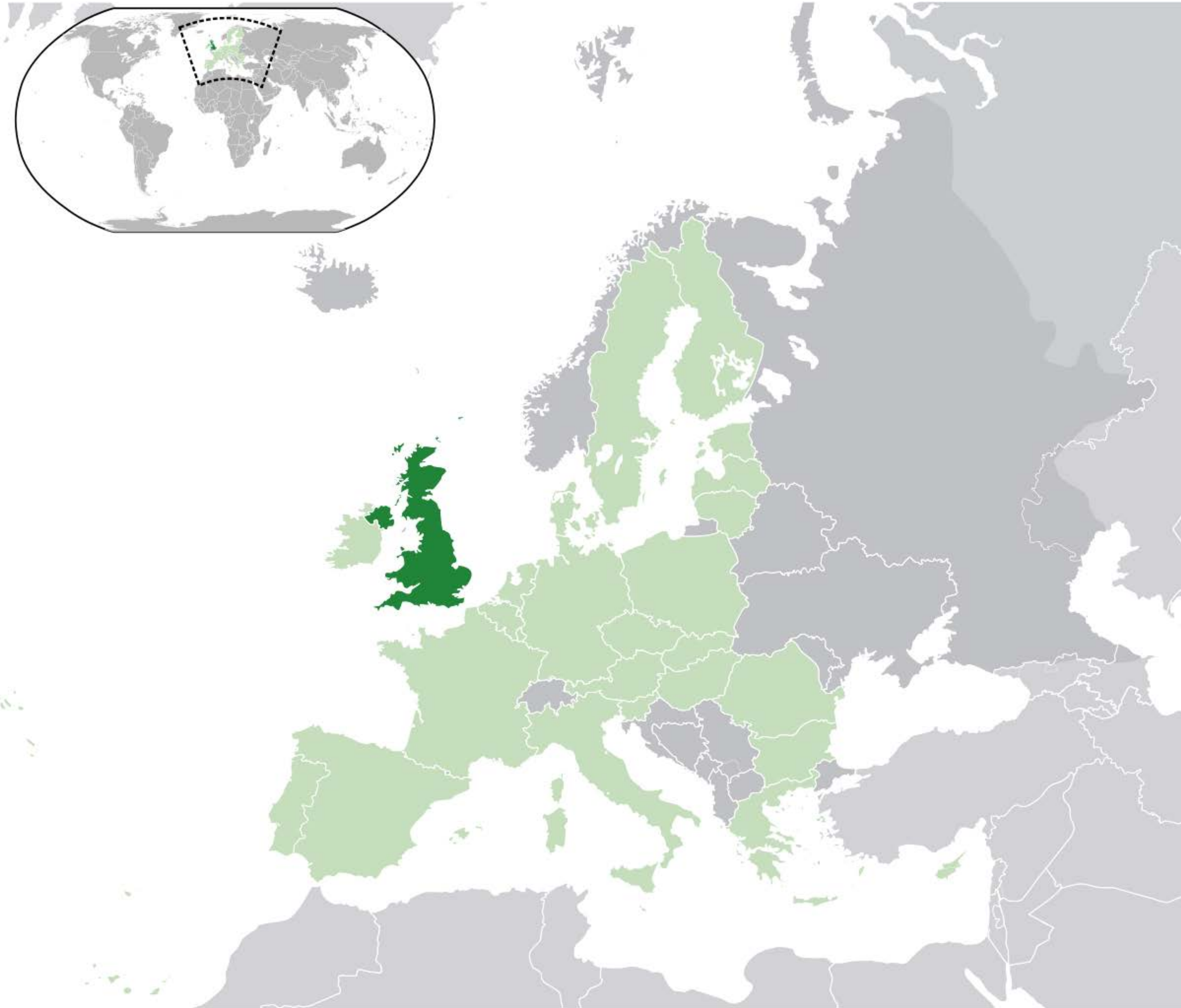

What is the length of coast of Britain?

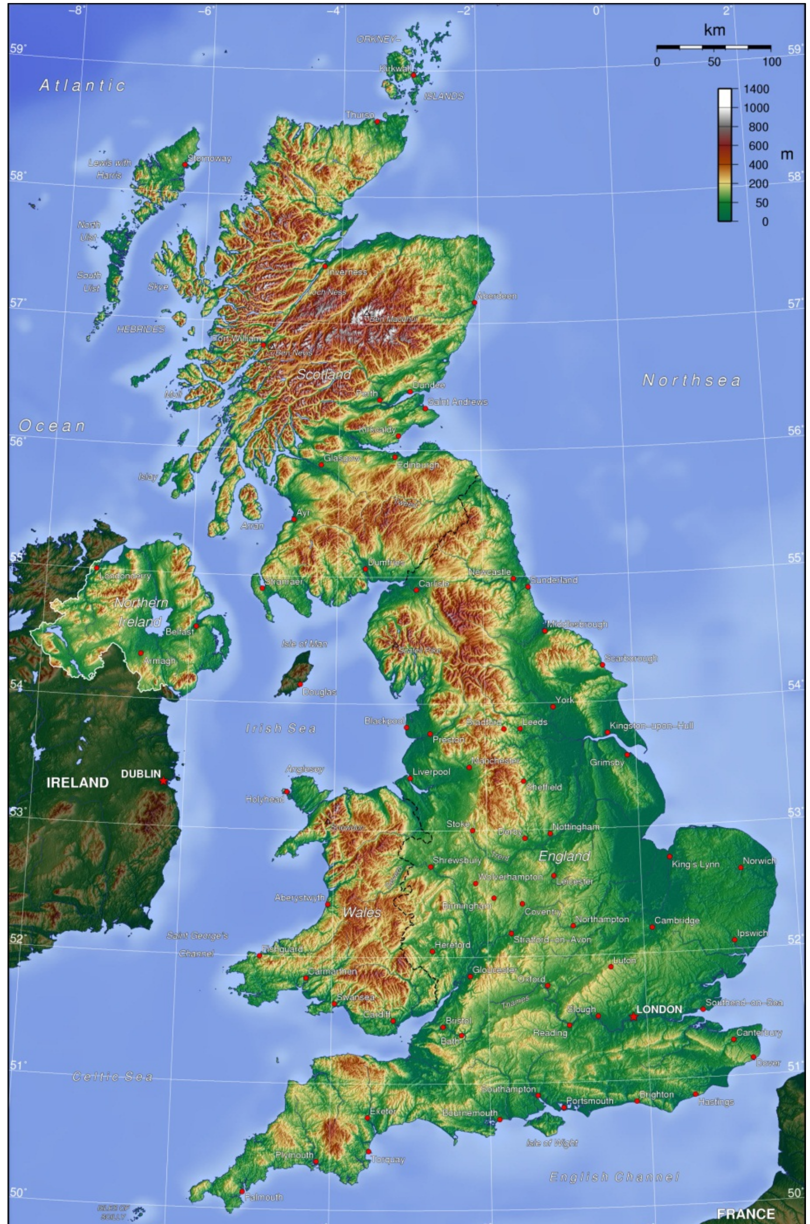

What is the length of coast of Britain?

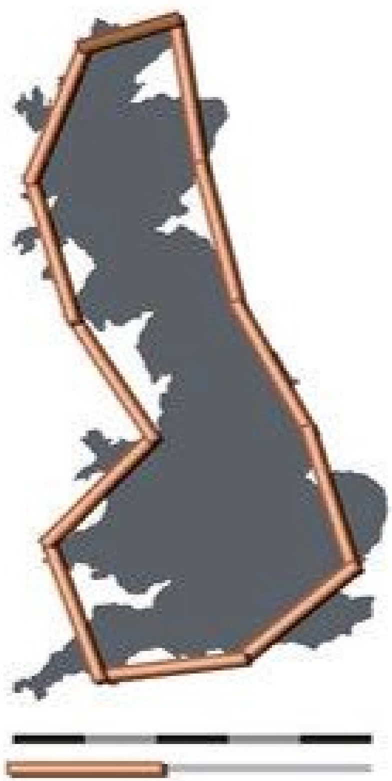

What is the length of coast of Britain?

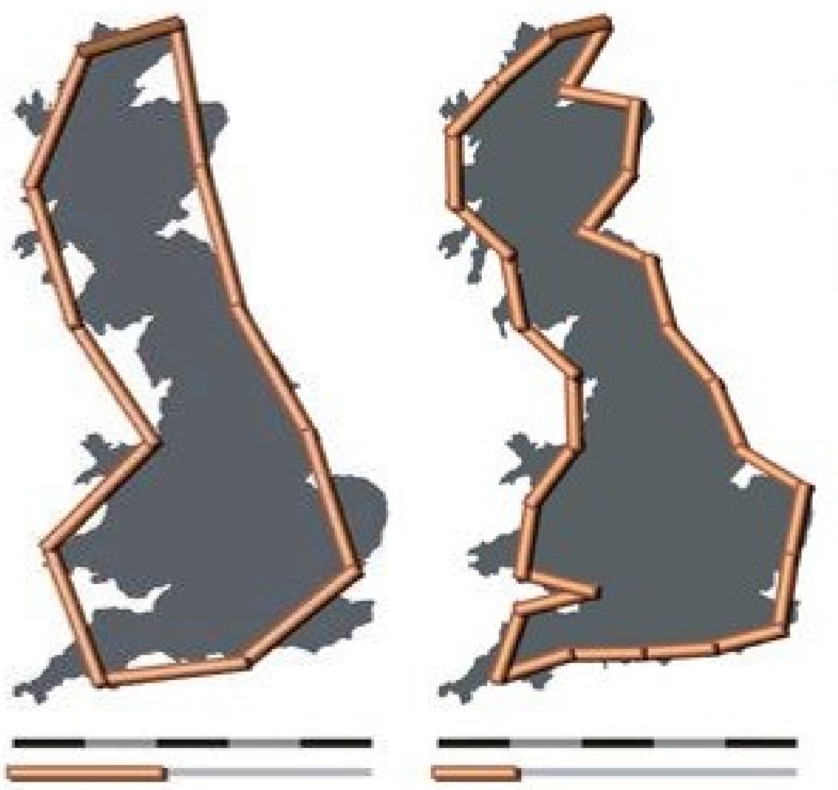

What is the length of coast of Britain?

What is the length of coast of Britain?

measured length $L(G)$ of border is a function of measurement scale G:

$$L(G) = MG^{1-D} \quad \Rightarrow \quad D = \frac{\log N(l)}{\log \frac{1}{l}} \quad \Rightarrow \quad D = \lim_{l \to 0} \frac{\log N(l)}{\log \frac{1}{l}}$$

WIKIPEDIA
The Free Encyclopedia

Main page
Contents
Featured content
Current events
Random article

Interaction
About Wikipedia
Community portal
Recent changes
Contact Wikipedia
Donate to Wikipedia
Help

Toolbox

Print/export

Languages
العربية
Български
Ελληνικά
Español
فارسی
Français
Italiano
Lietuvių

List of countries by length of coastline

From Wikipedia, the free encyclopedia

This is a **list of countries by length of coastline**, in kilometers, based on data for the year 2008 by the CIA World Factbook. A coastline of zero indicates that the country is landlocked.

The coastline paradox states that a coastline does not have a well-defined length. Measurements of the length of a coastline behave like a fractal, being different at different scale intervals (distance between points on the coastline at which measurements are taken). The smaller the scale interval (meaning the more detailed the measurement), the longer the coastline will be.[1] This 'magnifying' effect is greater for convoluted coastlines than for relatively smooth ones. For example, as seen on satellite image websites, the length of Canada's very convoluted coastline at a scale interval of 500 km is only about 20,000 km, less than a tenth of the value given in the table. On the other hand, Australia's coastline at 500 km intervals is about 12,500 km, around half the value in the table.[2]

The **coast/area ratio** measures how many meters of coastline correspond to every square kilometer of land area. The ratio illustrates the ease of accessibility to the country's coast from every point in its interior. Therefore, an island country like Maldives, or a country carved by the sea like Greece, is more likely to have a high ratio, while a landlocked country like Austria will have a ratio of zero.

Note that the scales at which the CIA World Factbook figures were measured are not stated, nor is it known whether the figures are all reported using the same scale. The figures are not necessarily comparable across different countries.

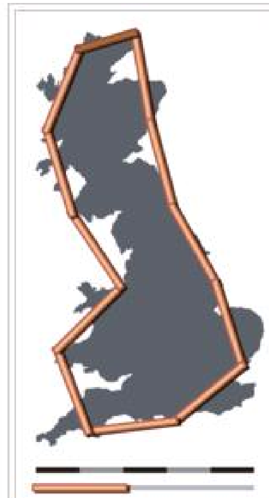

An example of the coastline paradox. The coastline of Britain is measured using Fractal Unit = 200 km, then the length of the coastline = 2400 km (approx.)

Rank	Country	Land area[3] (km²)	Coastline[4] (km)	Coast/Area Ratio (m/km²)
1	Canada	9,984,670	202,080	22.222
2	Indonesia	1,826,440	54,716	29.958
3	Greenland	2,166,086	44,087	20.353
4	Russia	16,995,800	37,653	2.215
5	Philippines	298,170	36,289	121.706

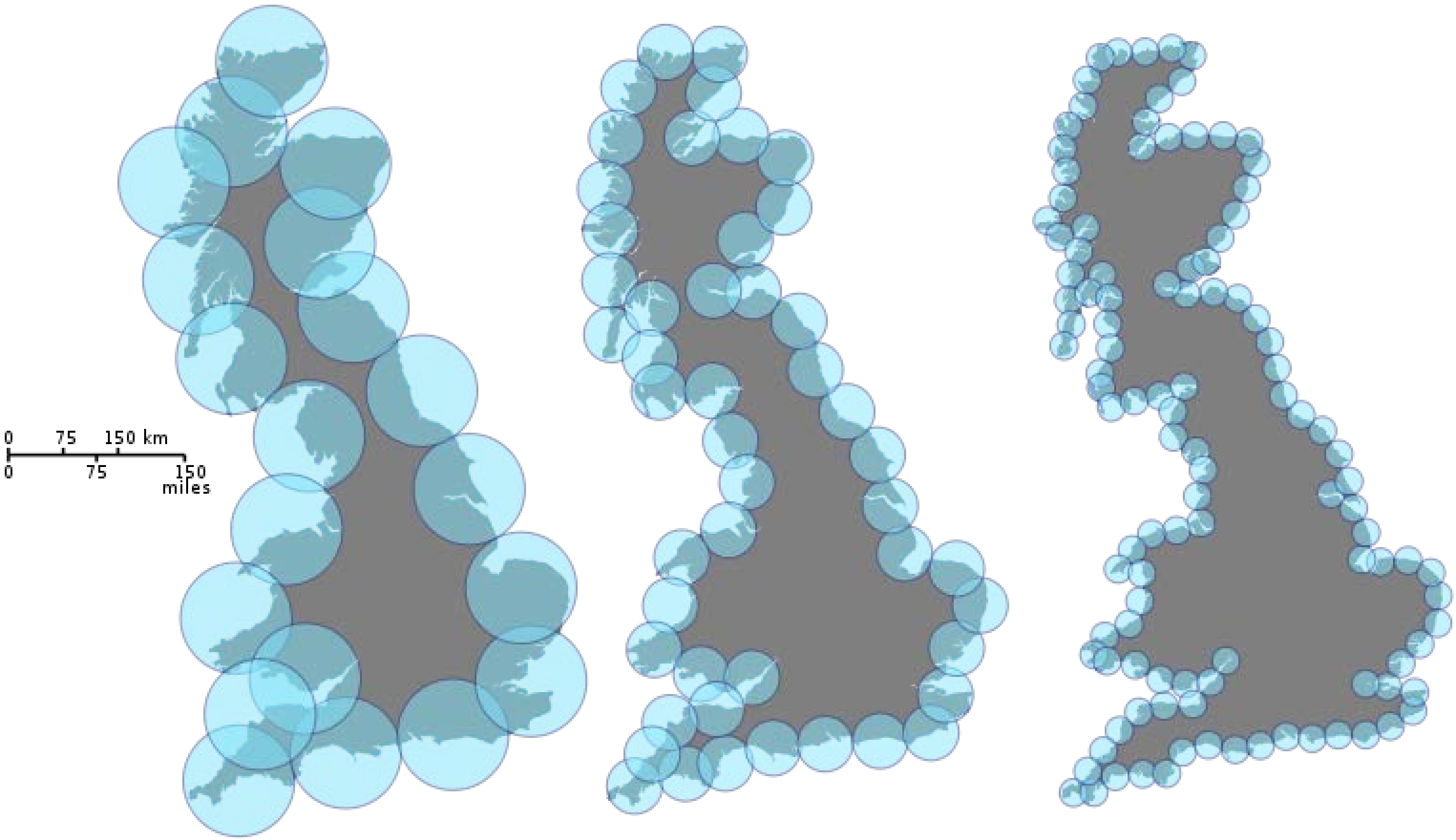
0 75 150 km
0 75 150
miles

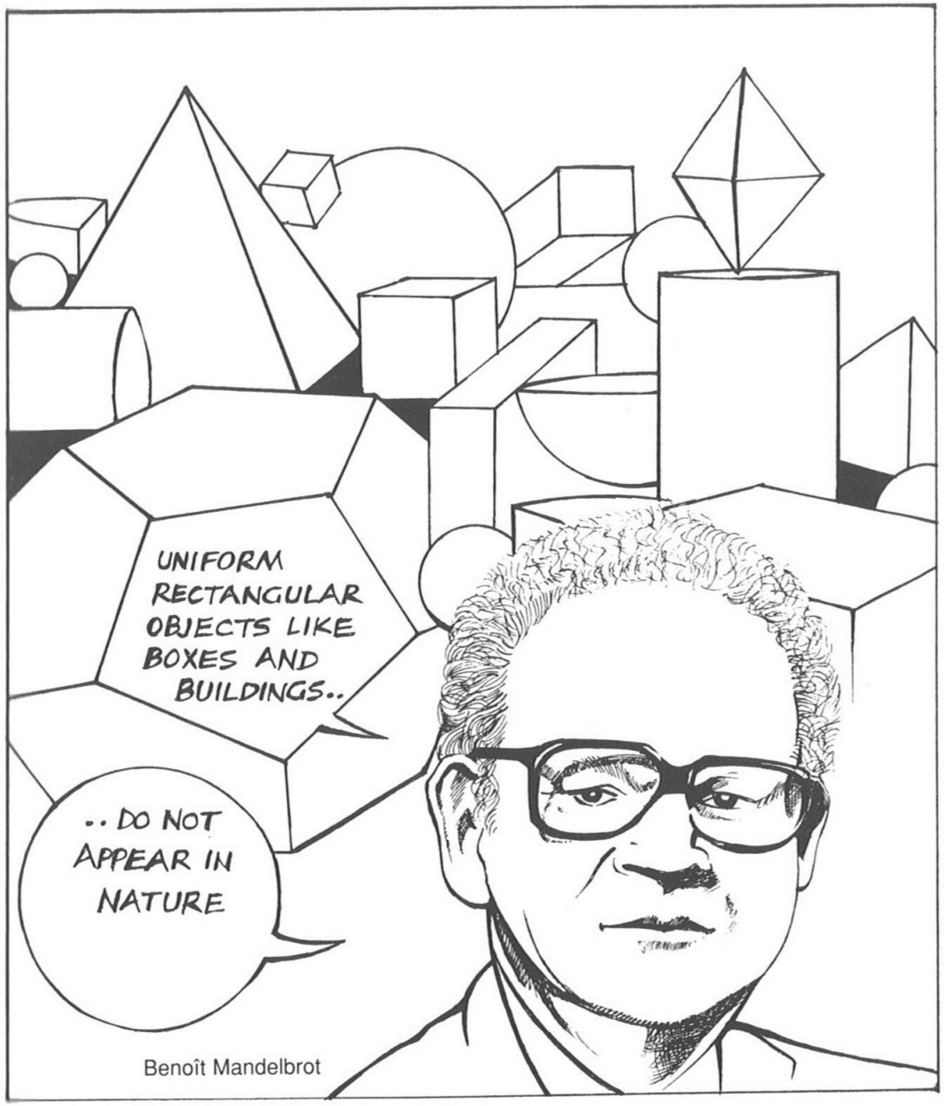

Benoît Mandelbrot

The world that we live in is not naturally smooth-edged. The real world has been fashioned with rough edges. Smooth surfaces are the exception in nature. And yet, we have accepted a geometry that only describes shapes rarely – if ever – found in the real world. The geometry of Euclid describes ideal shapes – the sphere, the circle, the cube, the square. Now these shapes do occur in our lives, but they are mostly man-made and not nature-made.

Here is a plot of how the length of the west coast of Britain depends upon the resolution that we use to measure it. There is no one value that best describes the length of the west coast of Britain. It depends upon the scale (resolution) at which we measure it. As we measure it at a finer scale, we include the segments of the smaller bays and peninsulas, and the coastline is longer. This is one of the surprising way in which fractals change the most basic way that we analyze and understand our data. There is no one number that best describes the length of the west coast of Britain. Instead, what is important is how the length depends upon the resolution that we use to measure it. The more smaller bays and peninsulas, the more the length of the coast increases when it is measured at a finer resolution, and the steeper the slope on this plot. This plot therefore shows that the coast of Britain is rougher than that of Australia, which is rougher than that of South Africa, which is rougher than that of a plain circle.

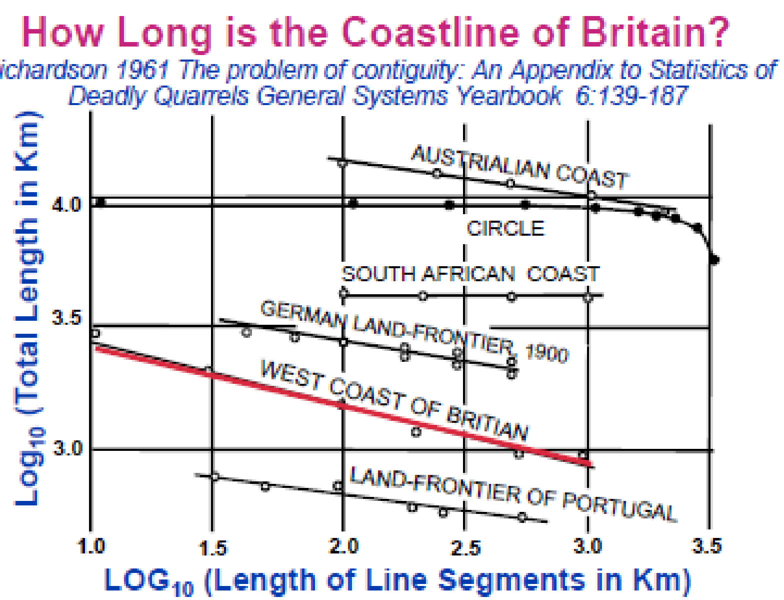

How Long is the Coastline of Britain?

Richardson 1961 The problem of contiguity: An Appendix to Statistics of Deadly Quarrels General Systems Yearbook 6:139-187

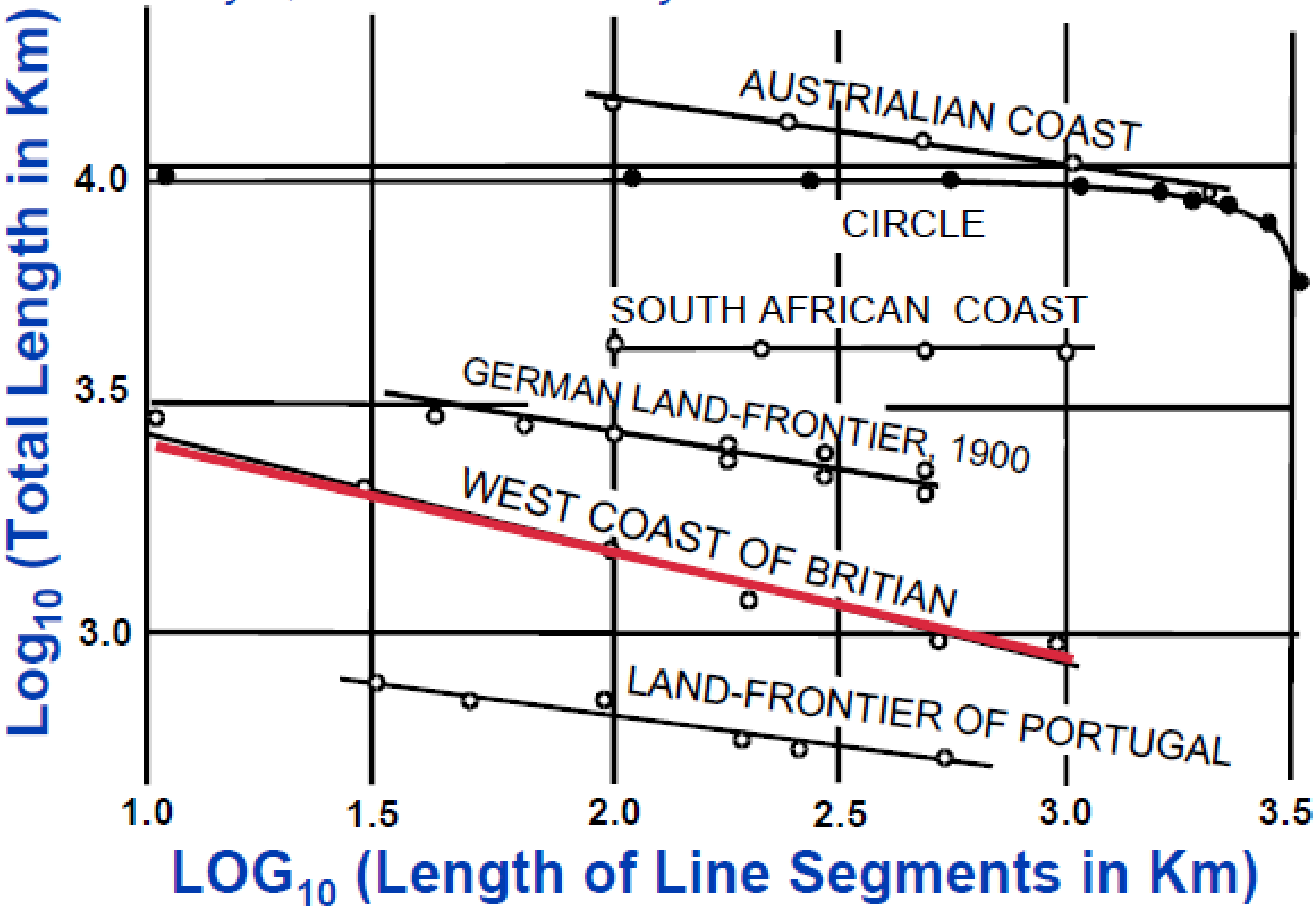

Properties of Objects in Space

Non-Fractal

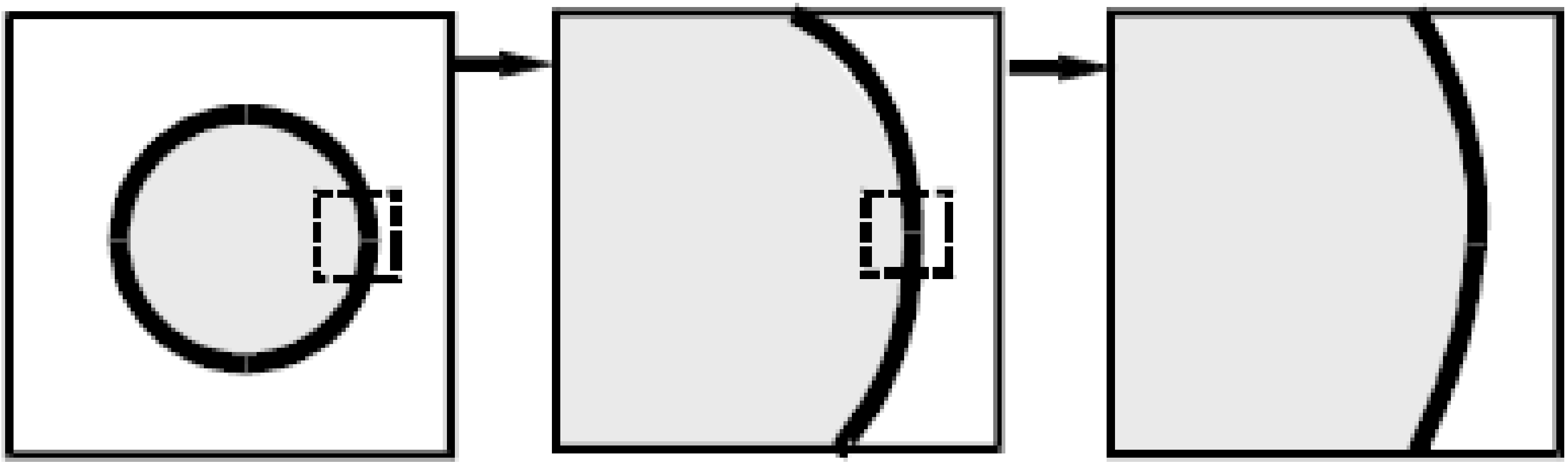

Properties of Objects in Space

Fractal

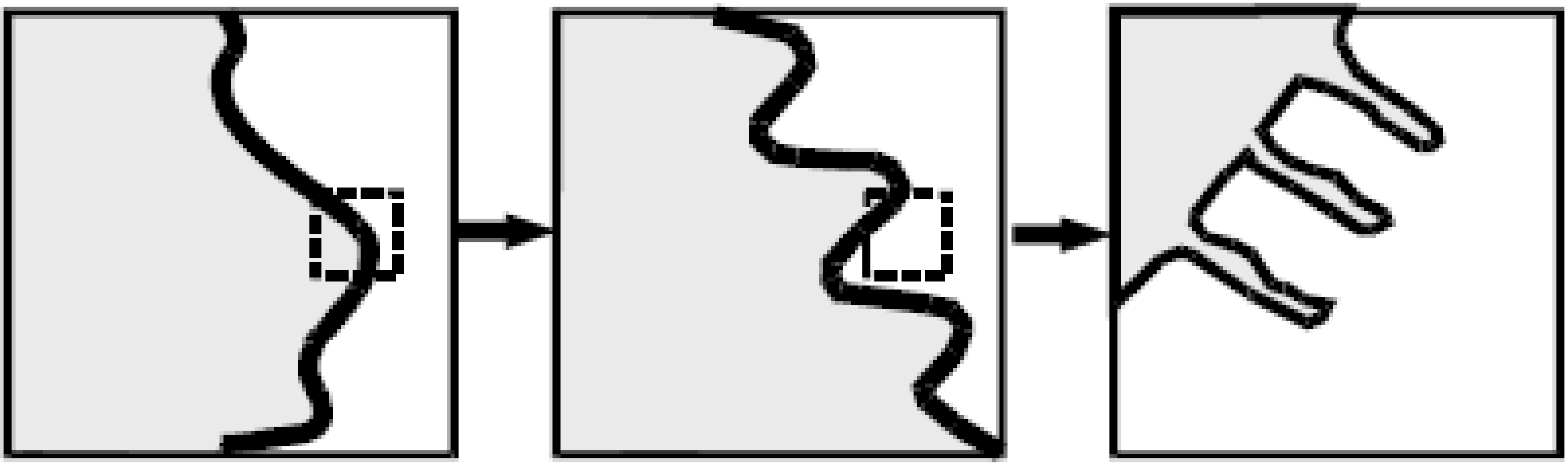

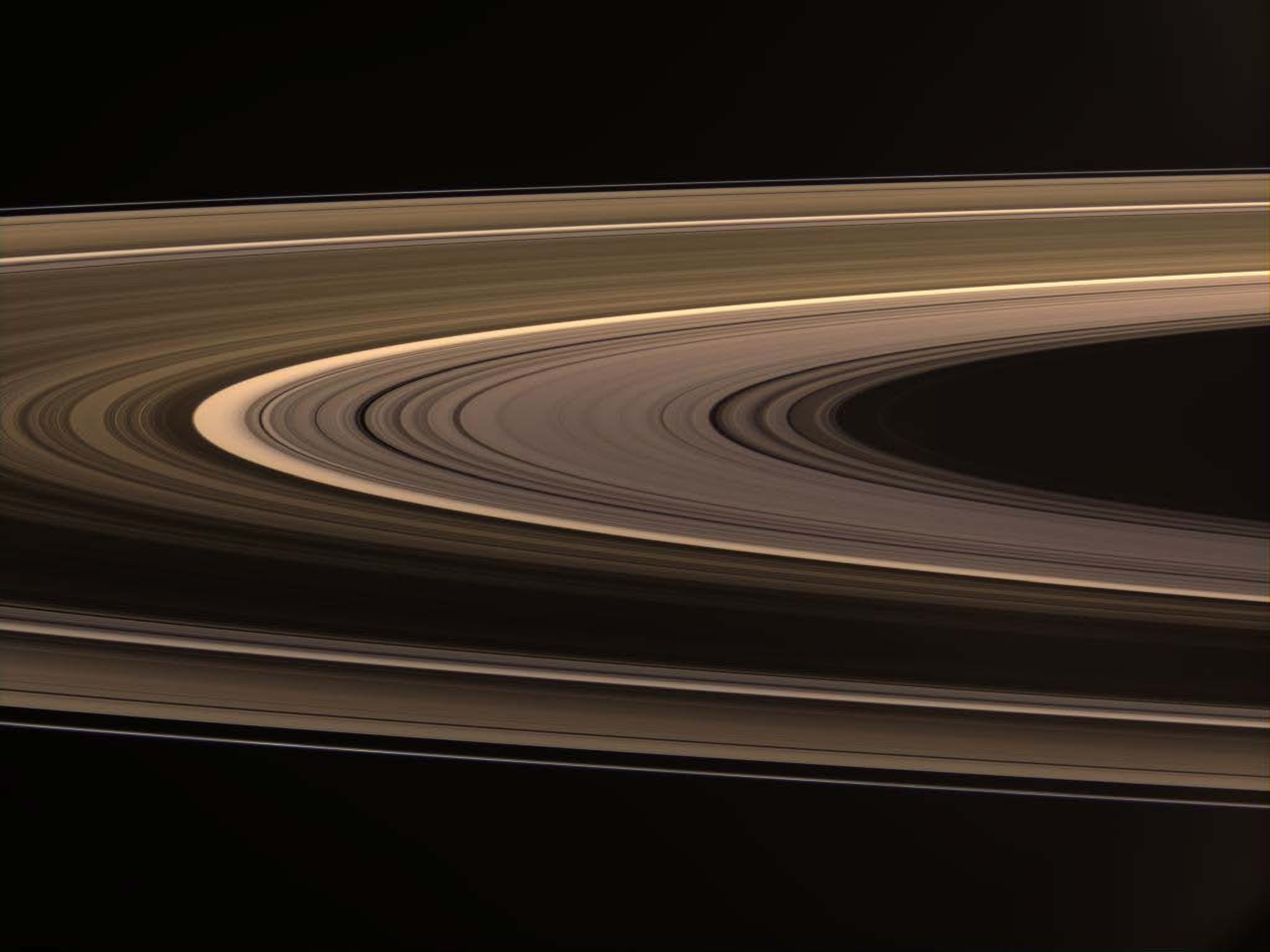

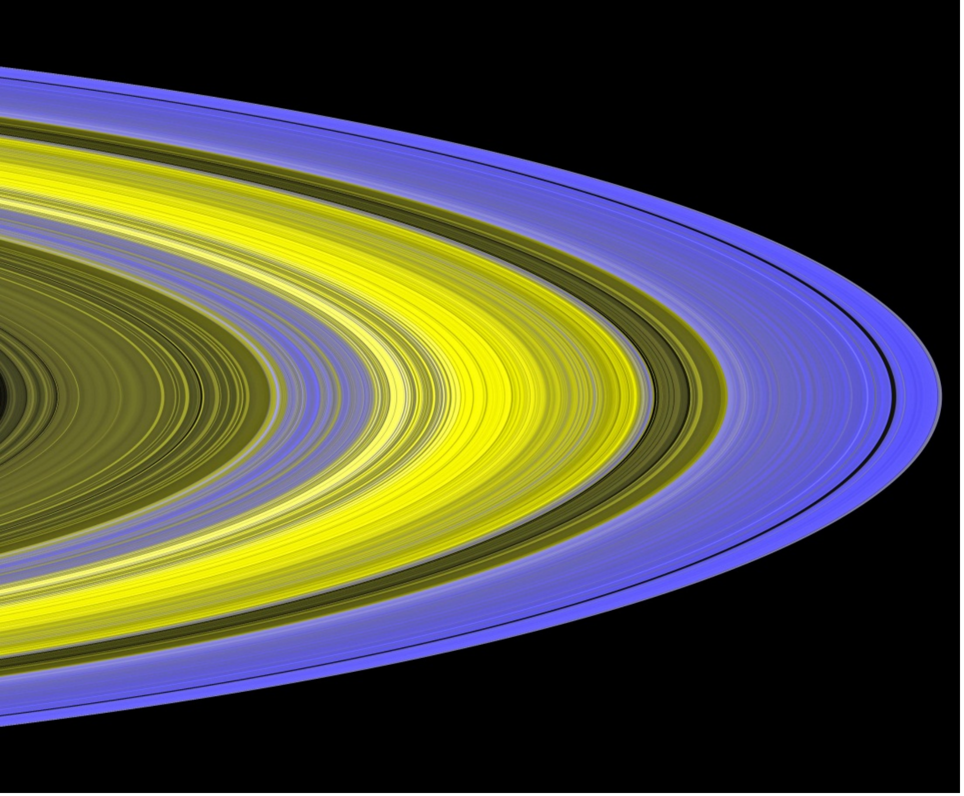 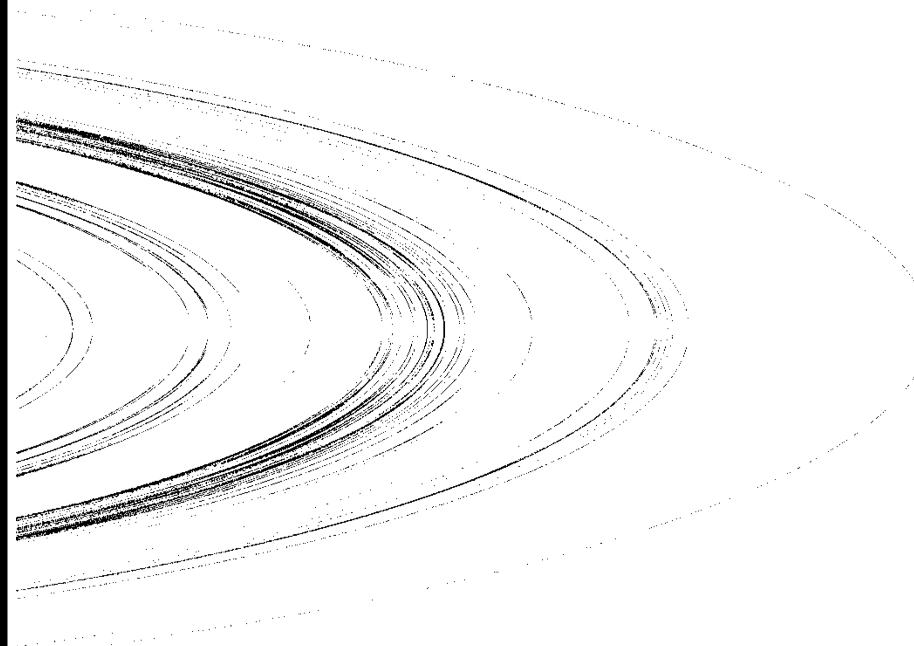

original image from Cassini mission

$\Rightarrow$ image processed to capture ring edges

$D = 1.66$

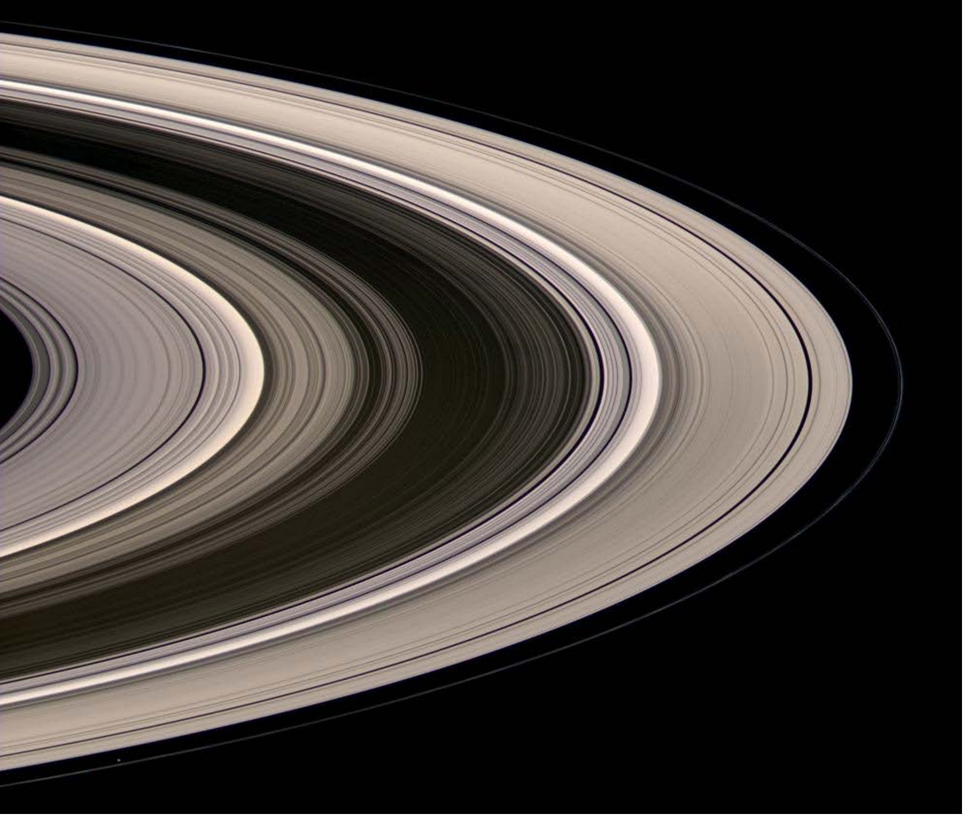 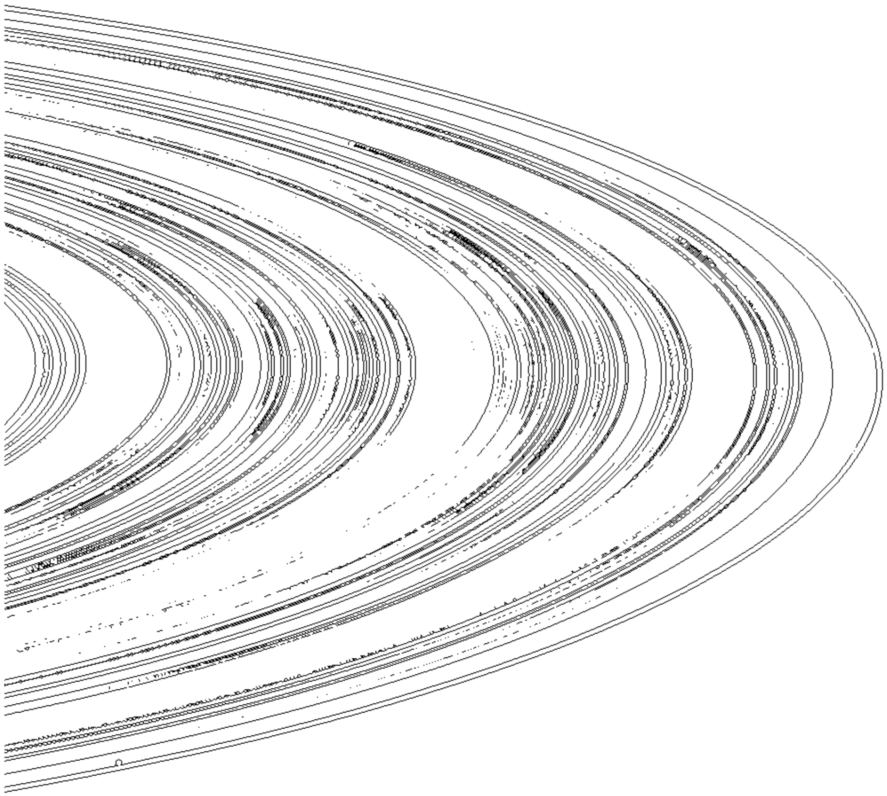

original image from Cassini mission

$\Rightarrow$ image processed to capture ring edges

$D = 1.71$

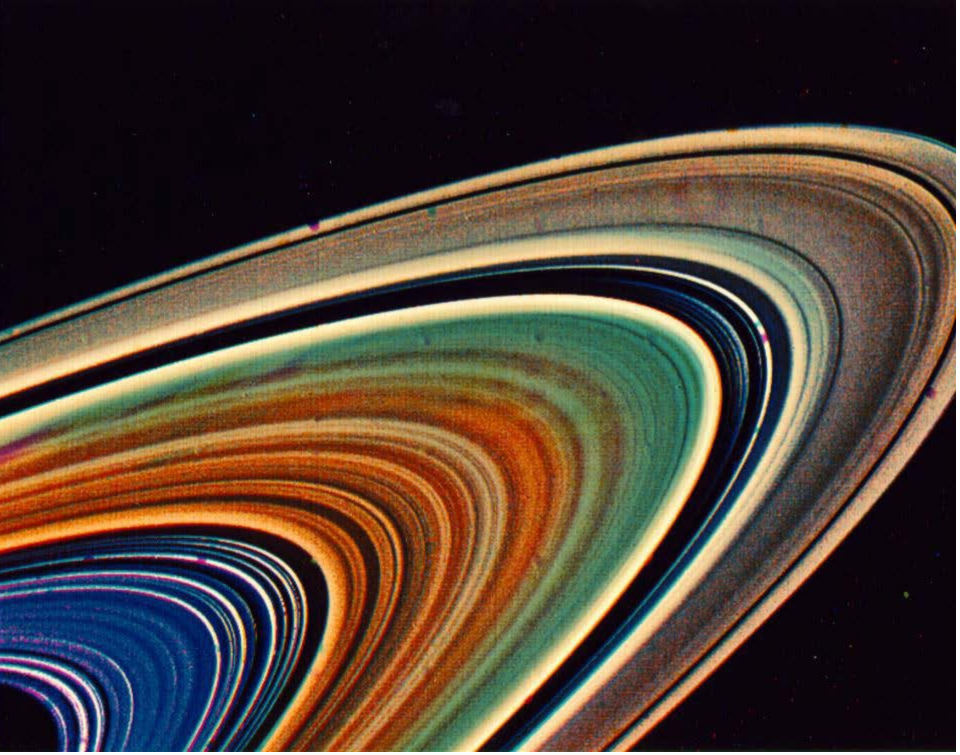

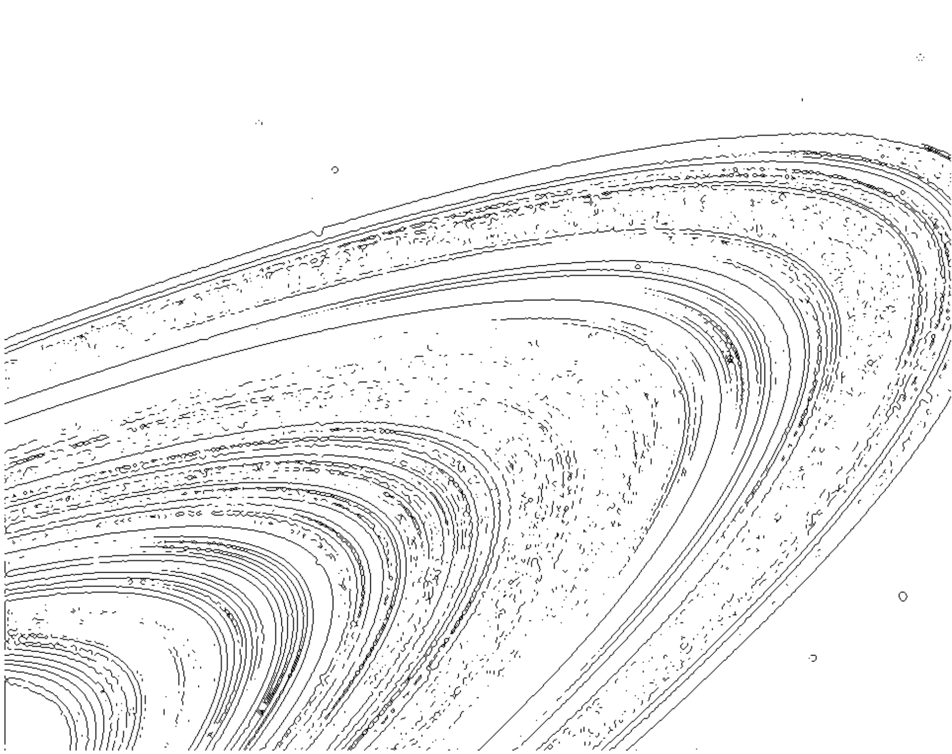

original image from Voyager mission

$\Rightarrow$ image processed to capture ring edges

$D = 1.77$

[*Arxiv*, 1012; *SpringerPlus*, 2015]

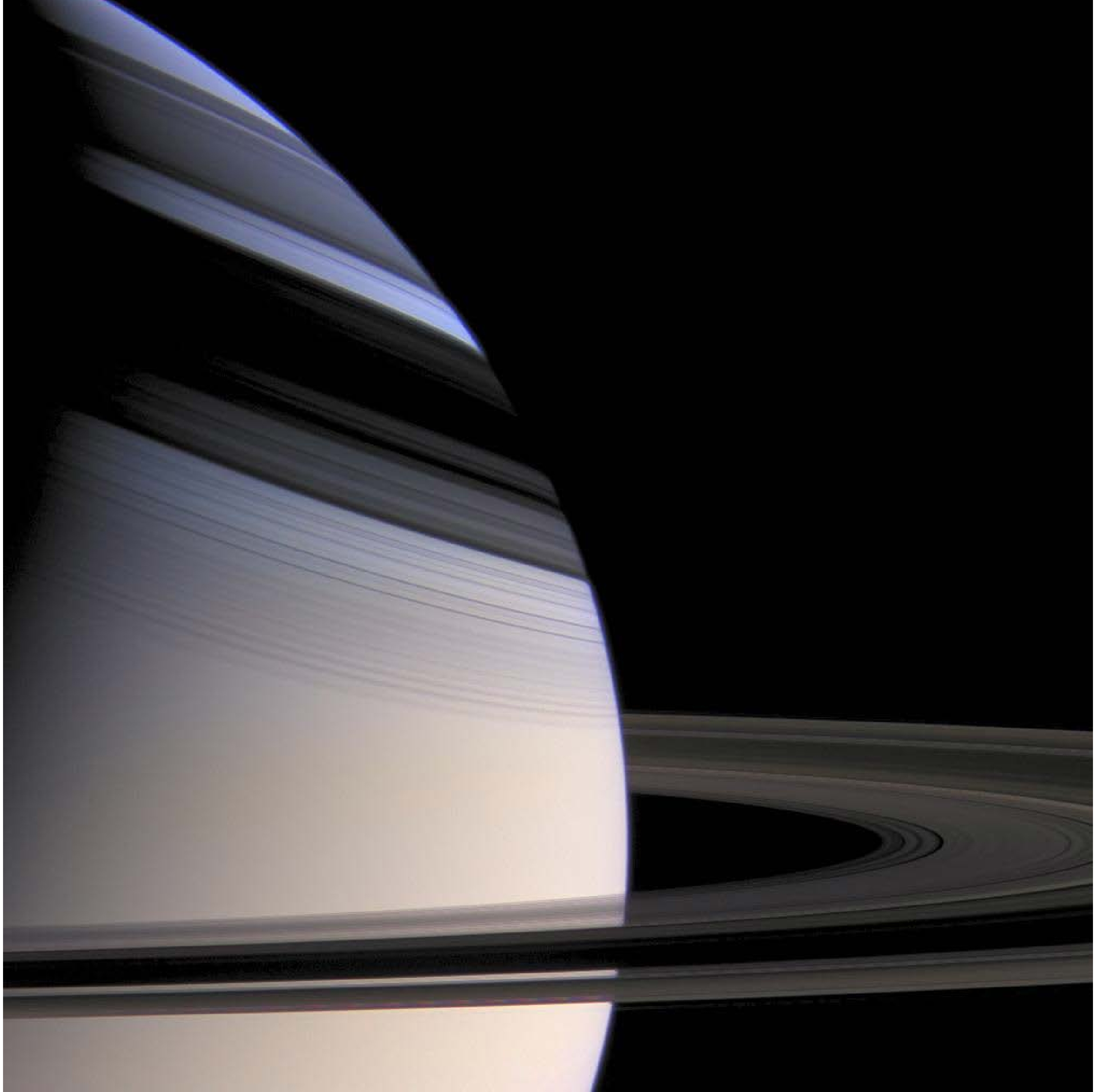


NASA/JPL-CALTECH

Fractal dimension

- Fractal dimension can be non-integer
- Fractal dimension represents the topological space-filling capacity of a geometric pattern
- Fractal dimension characterizes size scaling in detail:

$$N_r \propto r^{-D}$$

N_r : number of covering boxes, r : box size

Fractal dimension: Koch snowflake

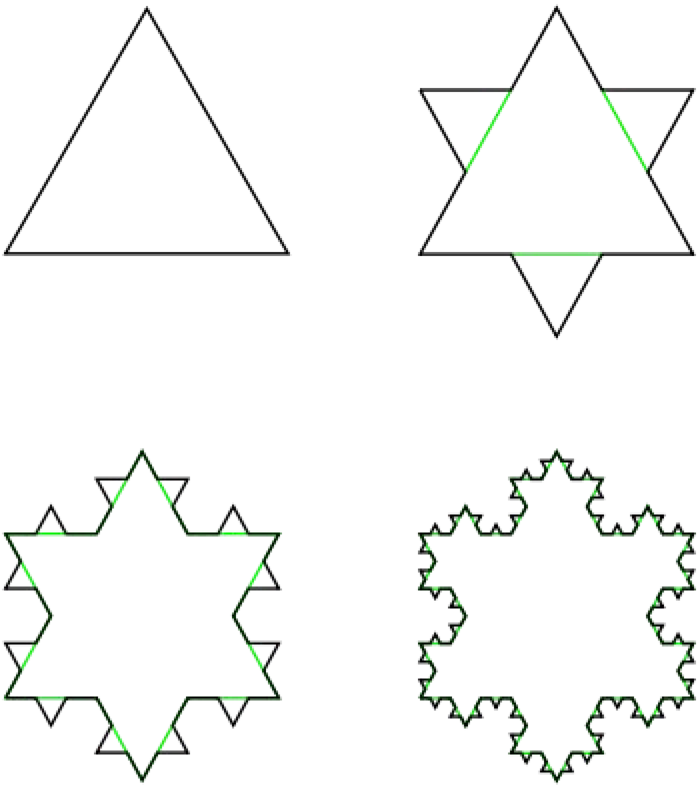

$$r = \frac{1}{3}\ ,\ \ N_r = 4$$

$$D = -\frac{\log(N_r)}{\log(r)} = \frac{\log(4)}{\log(3)} = 1.2618\ldots$$

Mathematical fractal: Koch snowflake

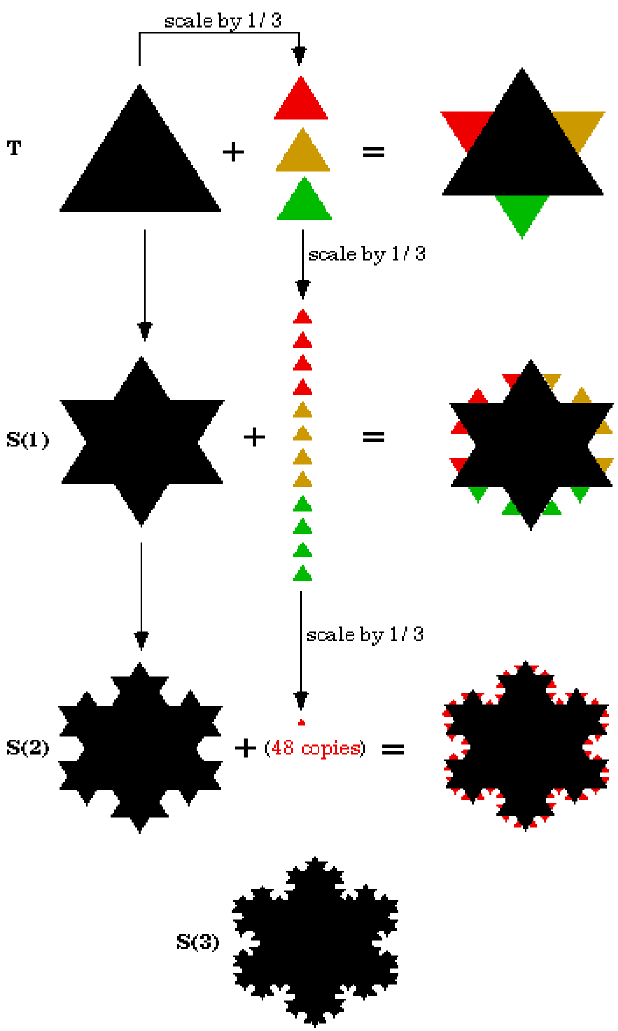

Formation: simple iteration

Feature: infinite perimeter

Fractals in Practice

Variations on the Cantor set occur in everything from frequencies of words and letters in language to noise on telephone lines, while the Koch curve serves as a model for real coastlines. As Mandelbrot wrote in the introduction to his groundbreaking book, *The Fractal Geometry of Nature* (1977) . . .

The number of distinct scales of length of natural patterns is for all practical purposes infinite.

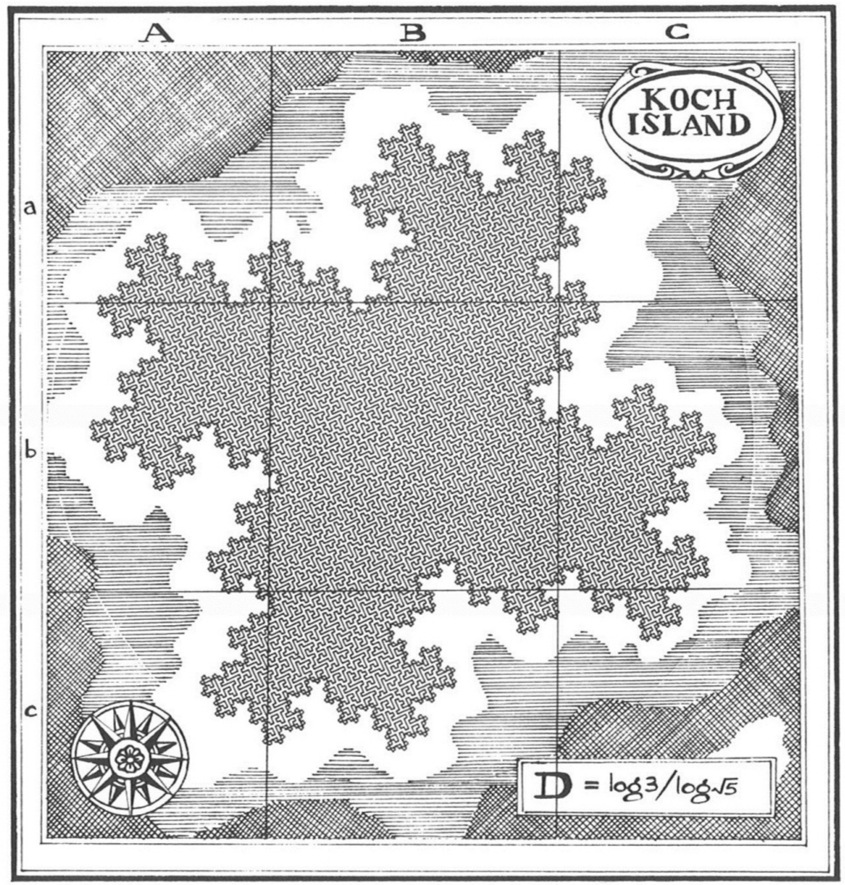

Fractal forgery of an island

Fractal geometry is indeed very much a geometry of the practical, of the real nuts-and-bolts world.

Definition: A **fractal** is "a rough or fragmented geometric shape that can be split into parts, each of which is (at least approximately … statistically) a reduced-size copy of the whole," a property called self-similarity.

<u>Definition</u>: A **fractal** is "a rough or fragmented geometric shape that can be split into parts, each of which is (at least approximately … statistically) a reduced-size copy of the whole," a property called self-similarity.

H.-O. Peitgen (2010): "*if we talk about impact inside mathematics, and applications in the sciences, Benoît B. Mandelbrot is one of the most important figures of the last 50 years*."

…was often criticized for not being rigorous

The world that we live in is not naturally smooth-edged. The real world has been fashioned with rough edges. Smooth surfaces are the exception in nature. And yet, we have accepted a geometry that only describes shapes rarely – if ever – found in the real world. The geometry of Euclid describes ideal shapes – the sphere, the circle, the cube, the square. Now these shapes do occur in our lives, but they are mostly man-made and not nature-made.

5

<u>Typical features of fractals</u>:

- fine structure at arbitrarily small scales
- too irregular to be easily described by traditional Euclidean geometry
- self-similar (at least approximately or stochastically) (but not R^1)
- has a fractal/Hausdorff dimension which is greater than its topological dimension (not space-filling objects in 3d)
- has a simple and recursive definition

Defects in Materials

Dimension (d)	Defect
0	Point defect • Interstitial • Substitutional • Vacancy
1	Line defect • Dislocation
2	Plane defect • Twin planes (twinning)
3	Three dimensional defect

Grain Boundary

- Grain bounda in Al70

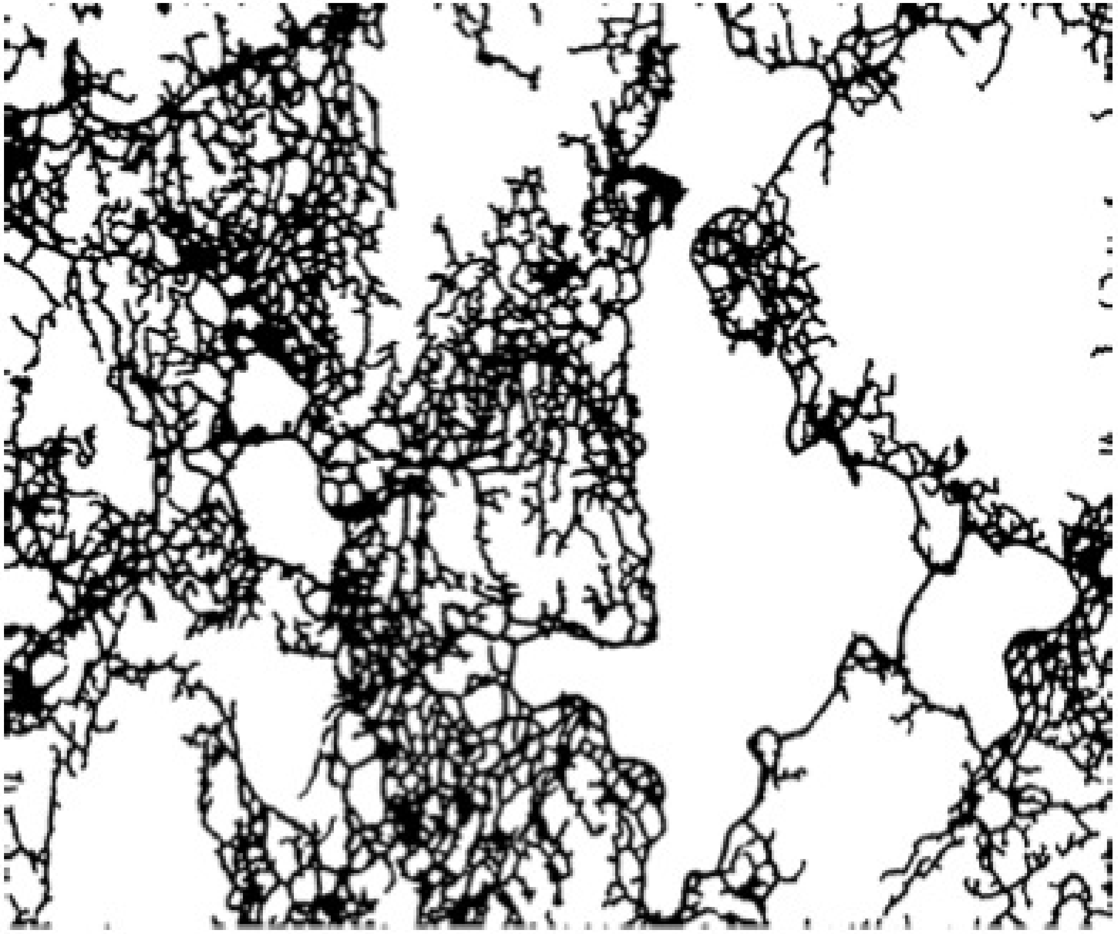

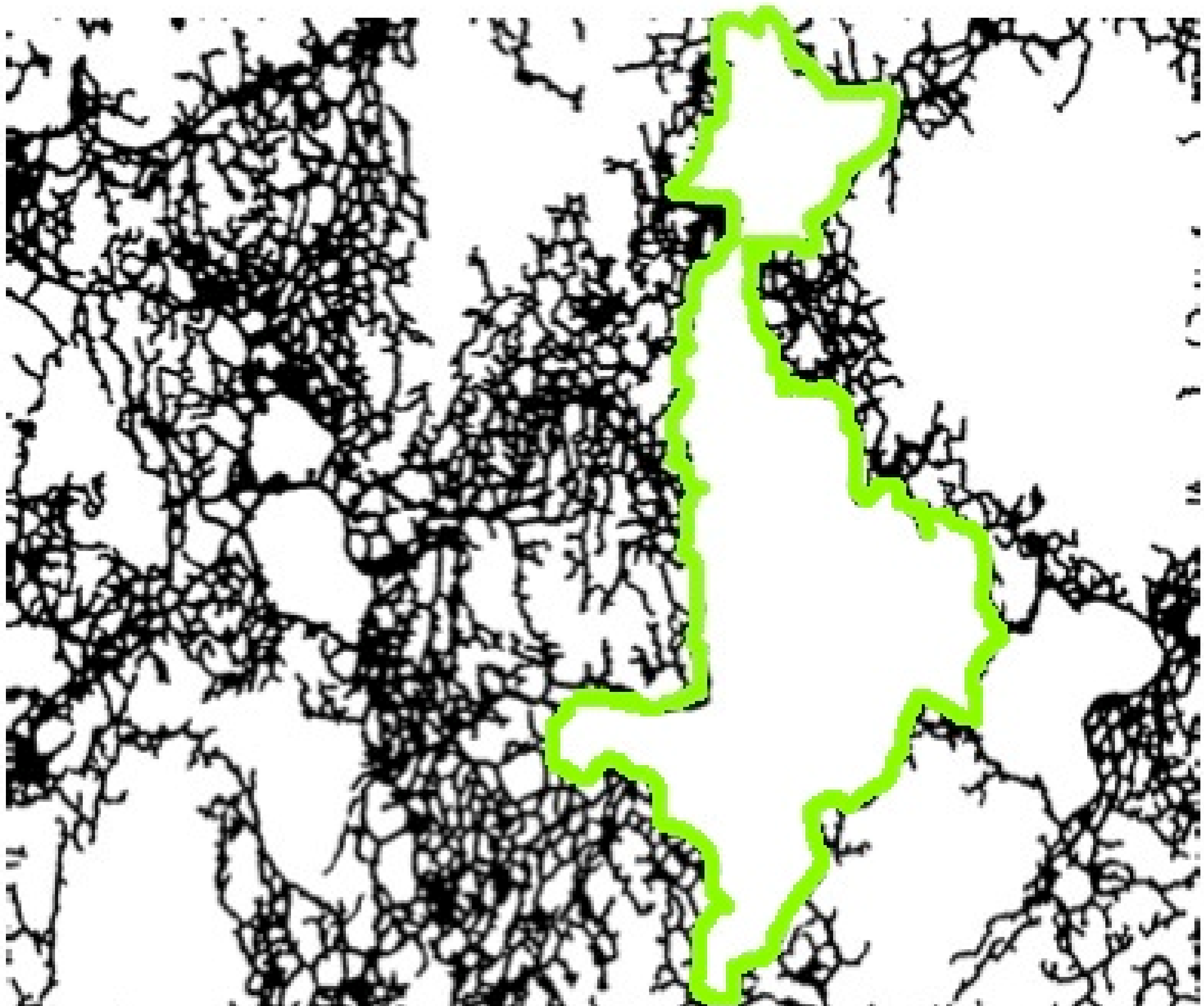

Elements of Random Processes and Fields

Martin Ostoja-Starzewski
Department of Mechanical Science & Engineering
and Institute for Condensed Matter Theory and Beckman Institute
University of Illinois at Urbana-Champaign

[*Math. Mech. Complex Syst. (MEMOCS)*, 2014]
[*Math. Mech. Solids*, 2015]
[*ZAMP*, 2016]
[*J. Elasticity*, 2017]

complete specification of a random field is given in terms of all *n-point probability distributions*:

…*strict-sense stationary* (SSS) if all *n*-order distributions are invariant with respect to arbitrary shifts:

Properties of $\rho(\mathbf{x})$

Describe scalar RF in terms of mean and correlation

$$\langle T(\mathbf{x})\rangle = \mu(\mathbf{x}), \quad \langle T(\mathbf{x}_1)T(\mathbf{x}_2)\rangle = R(\mathbf{x}_1, \mathbf{x}_2) < \infty$$

Work in terms of covariance:

$$R(\mathbf{x}_1, \mathbf{x}_2) = \langle [T(\mathbf{x}_1) - \langle T(\mathbf{x}_1)\rangle][T(\mathbf{x}_2) - \langle T(\mathbf{x}_2)\rangle]\rangle$$

Scalar RF, wide-sense stationary

$$\langle T(\mathbf{x})\rangle = \mu_i, \quad \langle T(\mathbf{x}_1)T(\mathbf{x}_1 + \mathbf{x})\rangle = R(\mathbf{x}) < \infty$$

$$\rho(\mathbf{x}) = \frac{R(\mathbf{x})}{R(\mathbf{0})}$$

Scalar RF wide-sense stationary, isotropic

$$\rho(\mathbf{x}) = \rho(\|\mathbf{x}\|) = \rho(\mathrm{x})$$

Spectral density = Fourier transform of $\rho(x)$:

Basic models:

$$\rho(x) = \exp[-Ax^{\alpha}], \quad A > 0, \quad 0 < \alpha \leq 2$$

$$\rho(x) = [1 + Ax^{\alpha}]^{-1}, \quad A > 0, \quad 0 < \alpha \leq 2$$

$$\rho(x) = \frac{\exp[-Ax^{\alpha}]}{1 + Bx^{\alpha}}, \quad A, B > 0, \quad 0 < \alpha, \beta \leq 2$$

$$\rho(x) = \exp[-\sum_{s=1}^{r} Ax^{\alpha_s}], \quad A_s > 0, \quad 0 < \alpha_s \leq 2, \quad s = 1, \ldots, r$$

$$\rho(x) = [-\prod_{s=1}^{r} (1 + B_s x^{\beta_s}) l_s], \quad B_s > 0, \quad 0 < \beta_s \leq 2, \quad l_s = 1, 2, \ldots$$

$$\rho(x) = \exp[-Ax^{\alpha}](\cosh Bx^{\alpha})^{s}, \quad A + B(2l - s) > 0, \quad 0 < \alpha \leq 2, \quad s = 1, \ldots, r$$

$$\rho(x) = \frac{(\cosh Bx^{\alpha})^{s}}{1 + Ax^{\alpha}}, \quad A + B(2l - s) > 0, \quad 0 < \alpha \leq 2, \quad s = 1, \ldots, r$$

… they do not separate local from long-range effects

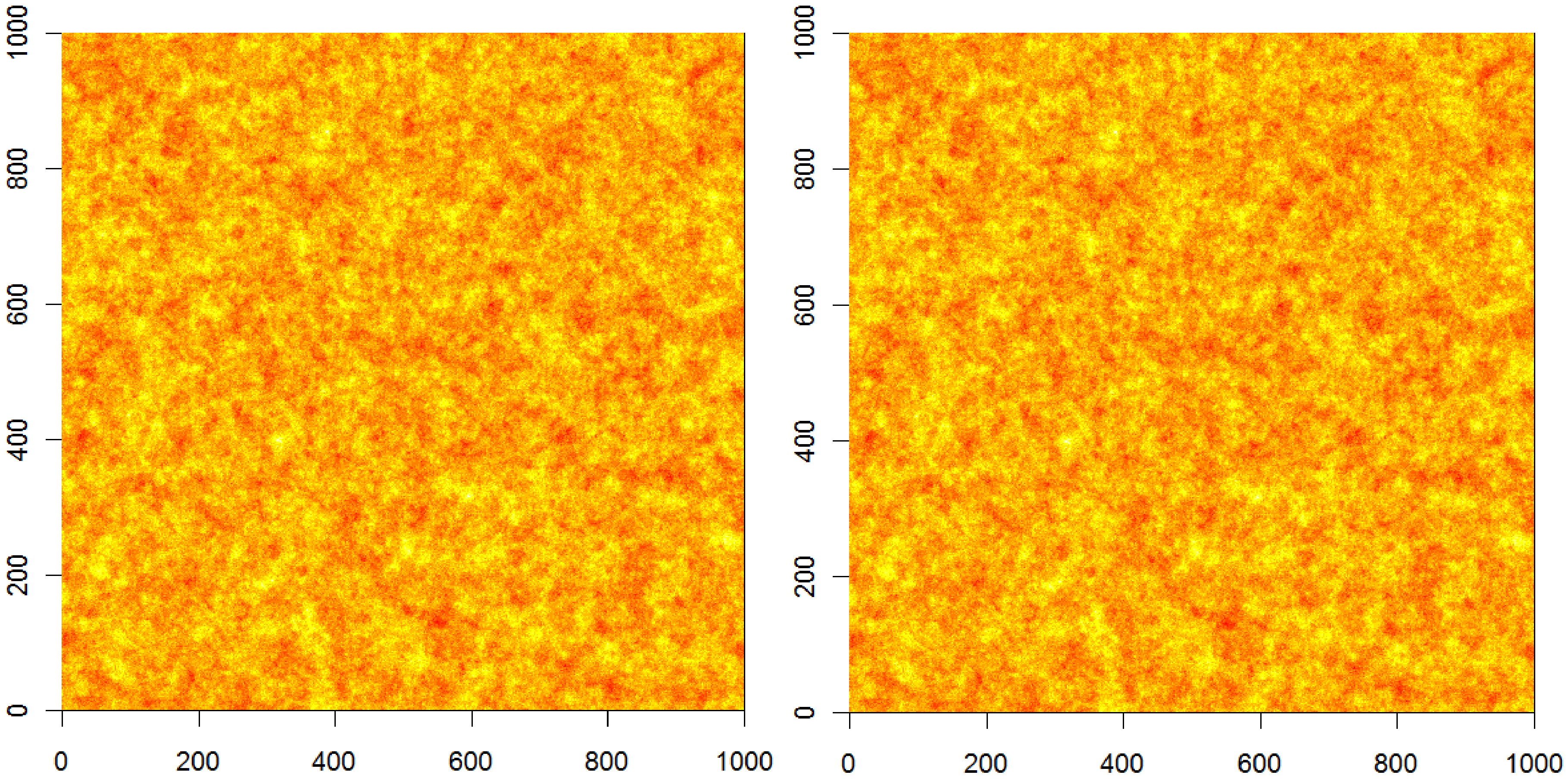

RFs with exponential or Gaussian correlation functions

$$C(x) = \exp[-Ax^{\alpha}], \quad A > 0, \quad 0 < \alpha \le 2$$

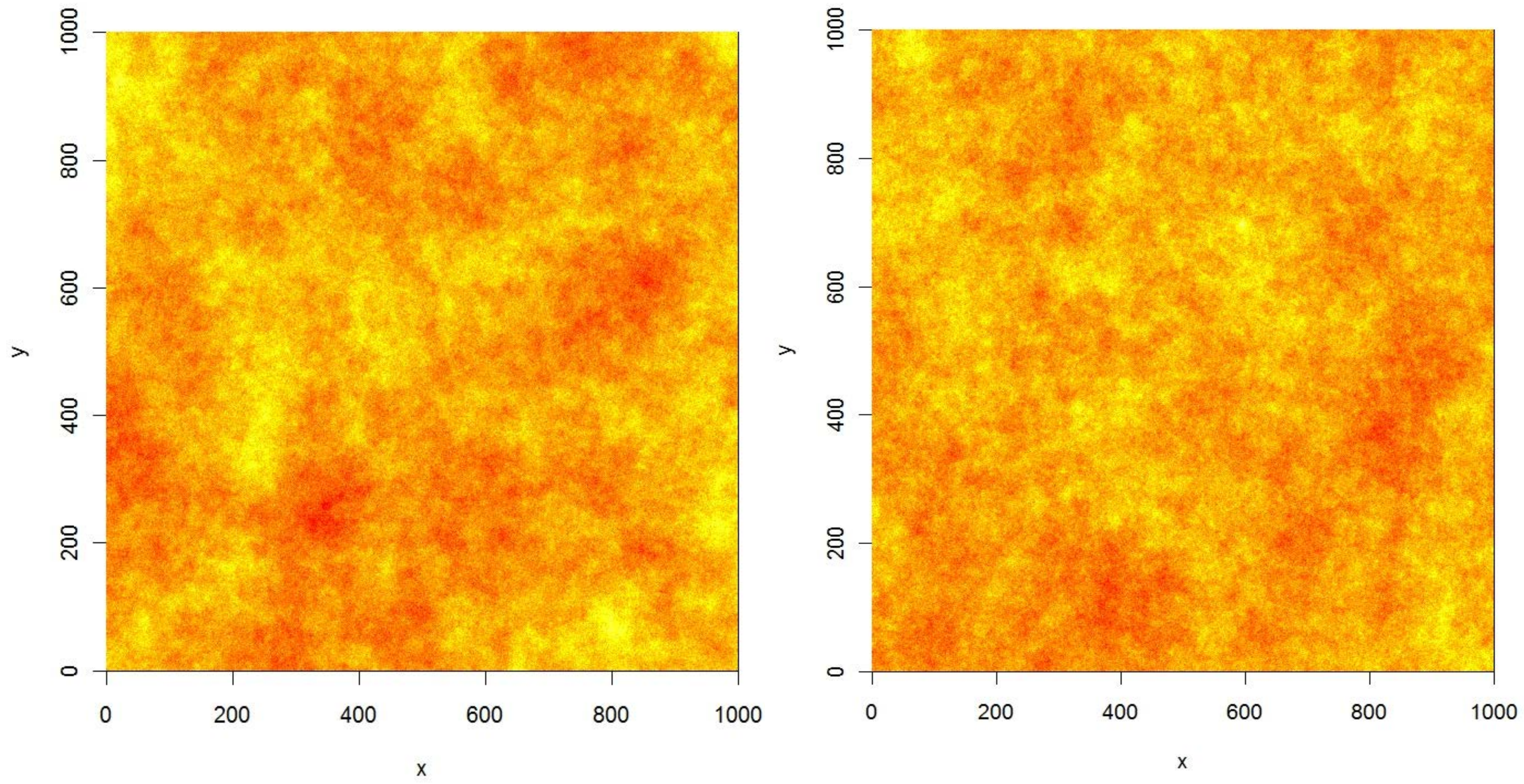

RFs with fractal + Hurst effects

Cauchy

$$C\ (r;\theta,\eta) := \left(1+r^{\theta}\right)^{-\eta/\theta},$$

Dagum

$$C\ (r;\delta,\varepsilon) := 1-\left(1+r^{-\delta}\right)^{-\varepsilon/\delta},$$

$$0<\delta\leq 2$$

Can grasp **fractals** and **Hurst effect**

roughness

heavy-tail behavior of covariance function

A random process Z_x is statistically self-similar if it obeys $Z_x = c^{-H} Z_{cx}$ for some constant c, where H is known as the *Hurst parameter*

- Crudely: when stretched by some factor c in x dimension, Z looks the same if stretched by c^{-H} in the Z dimension

- Most time series Z_t look “flat” if stretched like this

fractals: those enchanting, self-similar things

Hurst effect: long-term memory

$0 < H < 0.5$: time series with negative autocorrelation (e.g. a decrease between values will likely be followed by an increase)

$0.5 < H < 1$: time series with positive autocorrelation (an increase between values followed by another increase)

$H = 0.5$: true random walk, where there is no preference for a decrease or increase following any particular value.

$$Z_L(\omega,\mathbf{x}) := \frac{1}{L^d}\int_{D_L} Z_L(\omega,\mathbf{x}')d\mathbf{x}'$$

Can apply local averaging to constitutive laws in 2d or 3d?

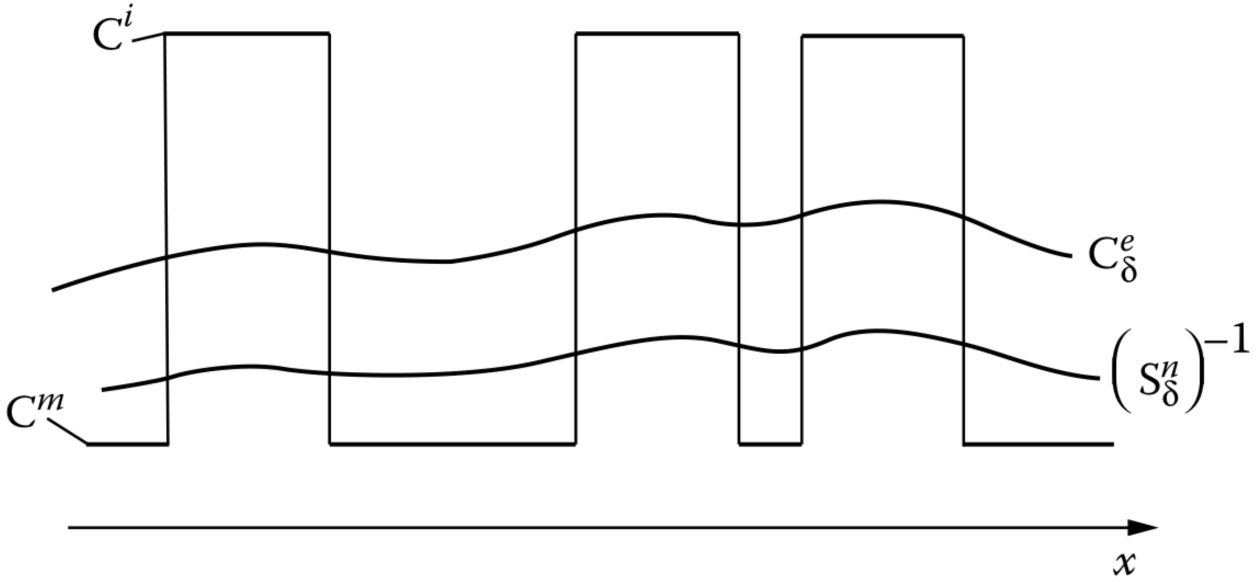

Local averaging is inconsistent with constitutive laws in 2d or 3d!

Because mechanics involves boundary value problems

$$Z_L(\omega, \mathbf{x}) = \frac{1}{L^d} \int_{D_L} Z_L(\omega, \mathbf{x}')\, d\mathbf{x}'$$

Local averaging is inconsistent with constitutive laws in 2D or 3D

- For tensor-type properties of materials,
  need RFs with all kinds of anisotropies

- TRFs are needed as inputs into *stochastic partial differential equations* (SPDEs) and *stochastic finite elements* (SFEs)

$$\nabla \cdot \left(\mathrm{C}(\mathbf{x},\omega)\nabla u \right) = 0, \quad \mathbf{x} \in R^3, \quad \omega \in \Omega$$

$$\nabla \cdot \left(\mathbf{C}(\mathbf{x},\omega) \cdot \nabla u \right) = 0, \quad \mathbf{x} \in R^3, \quad \omega \in \Omega$$

- …same arguments apply to elasticity

$$\mu \nabla^2 \mathbf{u} + (\lambda + \mu)\nabla(\nabla \cdot \mathbf{u}) + \nabla\mu\left(\nabla\mathbf{u} + (\nabla\mathbf{u})^T\right) + \nabla\lambda\nabla \cdot \mathbf{u} = \rho\mathbf{u}$$

(a)
(b)
(c)

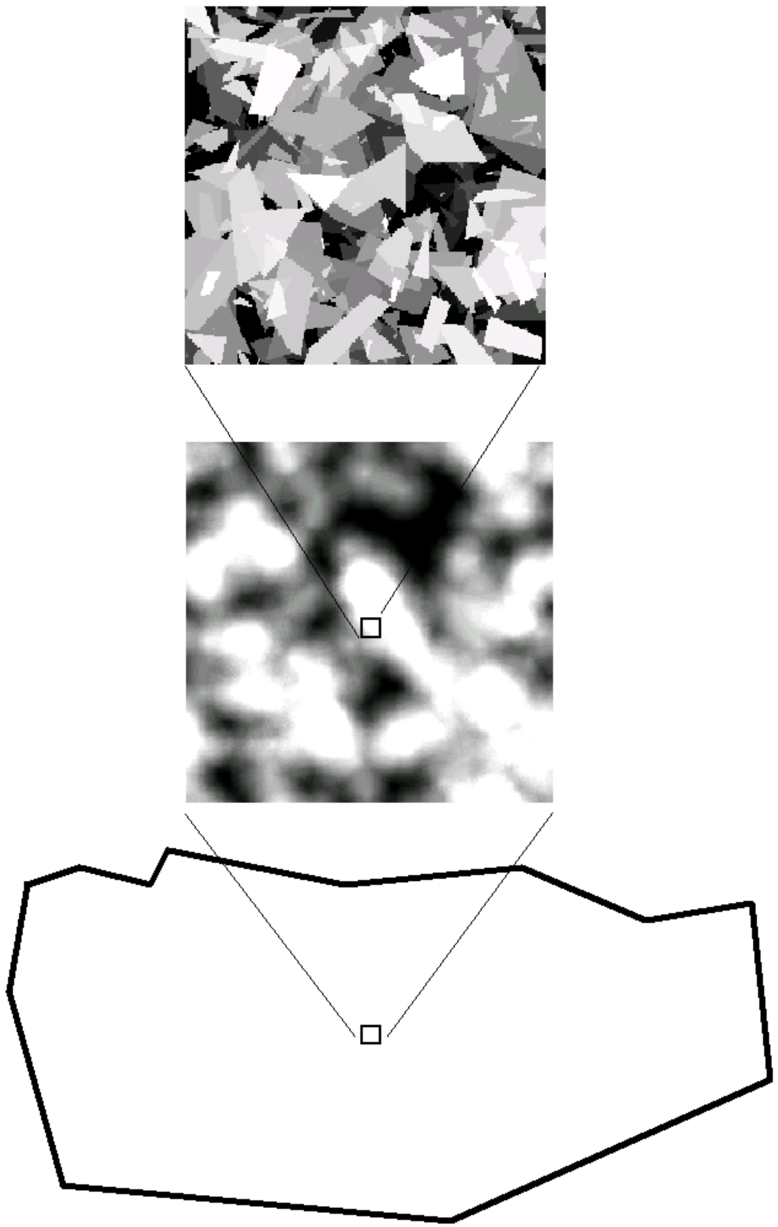

are these equations physically realistic?

Continuum tensor random field (RF) $\mathbf{C}(\omega,\mathbf{x}) = \overline{\mathbf{C}} + \mathbf{C}'(\omega,\mathbf{x})$

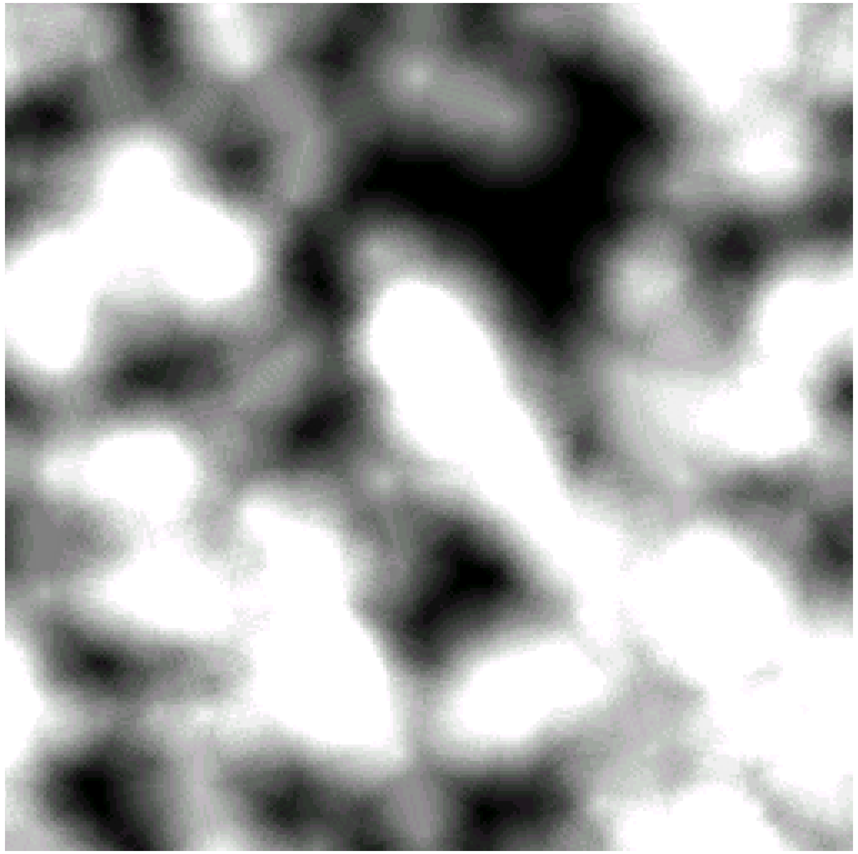

Can it be assumed isotropic (E,v) and smooth? **No**

Can assume a unique tensor RF without reference to spatial resolution? **No**

Can do local averaging of tensor RF for input to stochastic finite elements (SFE)? **No**

Can assume correlation functions of tensor RF w/o reference to micromechanics? **No**

Continuum tensor random field (RF) $\mathbf{C}(\omega, \mathbf{x}) = \overline{\mathbf{C}} + \mathbf{C}'(\omega, \mathbf{x})$

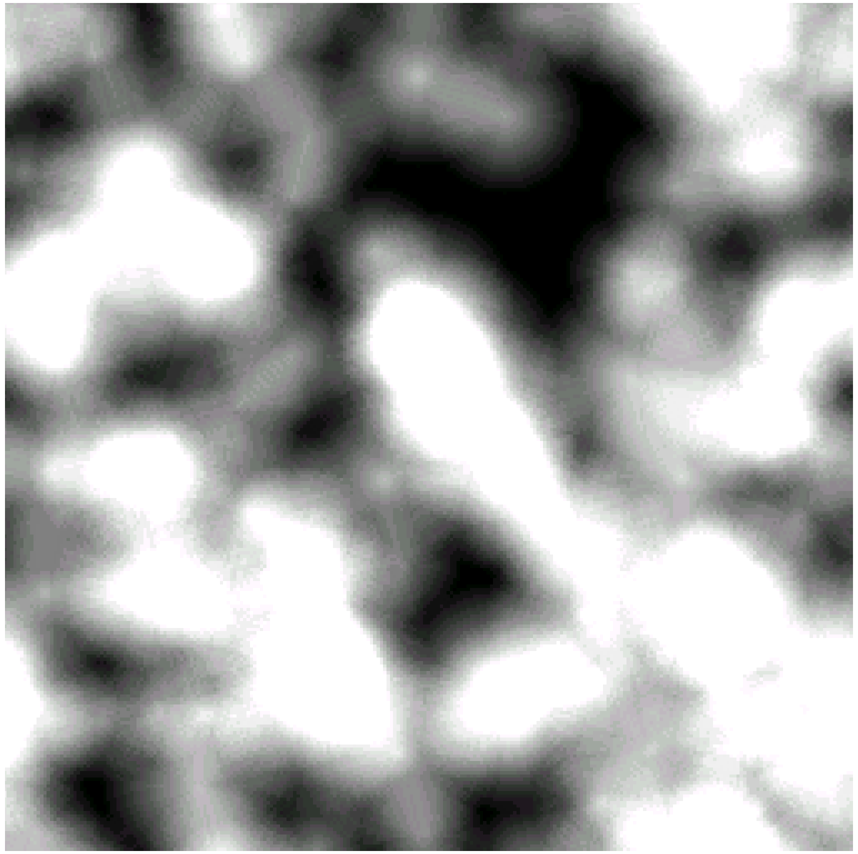

Can it be assumed isotropic (E, v) and smooth? **No**

Can assume a unique tensor RF without reference to spatial resolution? **No**

Can do local averaging of tensor RF for input to stochastic finite elements (SFE)? **No**

Can assume correlation functions of tensor RF w/o reference to micromechanics? **No**

[“Stochastic finite elements: Where is the physics?” *Theor. & Appl. Mech.*, 2011]

Focus on locally anisotropic, and statistically isotropic TRFs

Two kinds of isotropy of tensor random fields (TRFs):

- local $C_{ij} = C\delta_{ij}$
- statistical

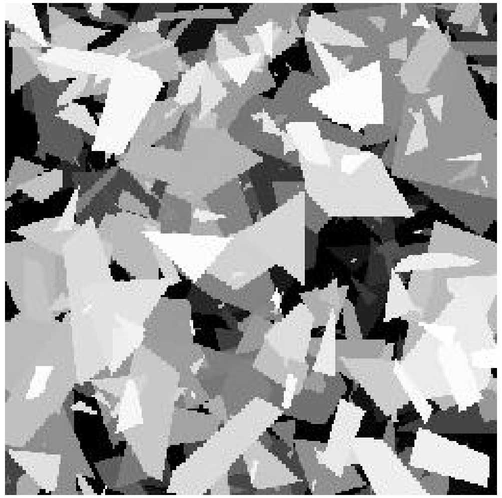

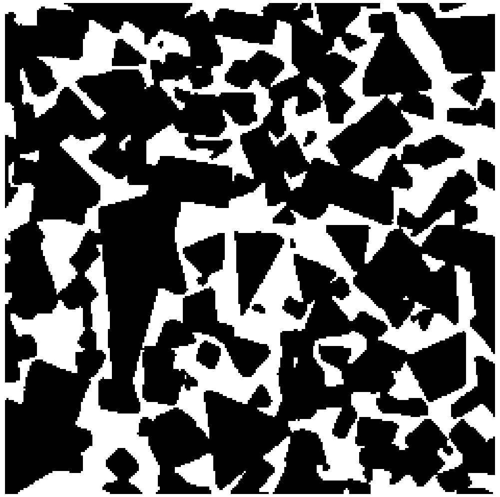

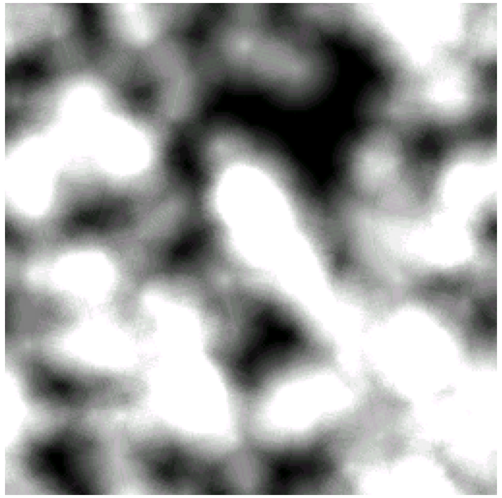

Restrictions on TRFs

- **dependent quantities** (displacement, velocity, deformation, rotation, stress, ...)

  dictated by continuum balance laws and kinematics

[von Kármán 1938; Robertson, 1940; Batchelor 1953; Yaglom, 1957; Lomakin, 1964; Shermergor, 1970; Procaccia, 1999, …]

- **constitutive responses** (conductivity, stiffness, permeability,...)

  positive-definite and dictated by microphysics, micromechanics

[O-S, 1989… ; Soize & Guilleminot, 2004, …, Malyarenko & O-S, 2014]

Representations of statistically isotropic TRFs are needed

- use theory of invariants, group theory, probability theory

Tensor Random Fields (TRF)

$$\mathbf{T}:\Omega \times D \to V$$

- second-order TRF: $\left\langle \| \mathbf{T}(\mathbf{x}) \|^2 \right\rangle < \infty, \quad \mathbf{x} \in R^3.$
- mean-square continuous TRF: $\lim_{\mathbf{x}\to\mathbf{x}_0} \left\langle \| \mathbf{T}(\mathbf{x}) - \mathbf{T}(\mathbf{x}_0) \|^2 \right\rangle = 0, \quad \forall \mathbf{x}_0 \in R^3.$
- wide-sense homogeneous TRF: $R(\mathbf{x},\mathbf{y}) = \left\langle \mathbf{T}(\mathbf{x}) \otimes \mathbf{T}(\mathbf{y}) \right\rangle$

$$R(\mathbf{x},\mathbf{y}) = R(\mathbf{x}-\mathbf{y}), \quad \forall \mathbf{x},\mathbf{y} \in R^3.$$

- 1st-rank (vector) statistically (wide-sense) isotropic TRF:

$$E(k\mathbf{x}) := \langle \mathbf{T}(k\mathbf{x}) \rangle$$

$$R(k\mathbf{x}, k\mathbf{y}) := \left\langle \left[\mathbf{T}(k\mathbf{x}) - \langle \mathbf{T}(k\mathbf{x}) \rangle \right] \otimes \left[\mathbf{T}(k\mathbf{y}) - \langle \mathbf{T}(k\mathbf{y}) \rangle \right] \right\rangle$$

for any rotation

$$E(k\mathbf{x}) = kE(\mathbf{x})$$

$$R(k\mathbf{x}, k\mathbf{y}) = kR(\mathbf{x}, \mathbf{y})k^{-1}$$

- 2nd-rank statistically (wide-sense) isotropic TRF:

$$E(k\mathbf{x}) := \langle \mathbf{T}(k\mathbf{x}) \rangle = \left\langle {}^{2}(k)\mathbf{T}(\mathbf{x}) \right\rangle = {}^{2}(k)\langle \mathbf{T}(k\mathbf{x}) \rangle = {}^{2}(k)E(\mathbf{x})$$

$$R(k\mathbf{x}, k\mathbf{y}) := \left\langle \left[\mathbf{T}(k\mathbf{x}) - \langle \mathbf{T}(k\mathbf{x}) \rangle \right] \otimes \left[\mathbf{T}(k\mathbf{y}) - \langle \mathbf{T}(k\mathbf{y}) \rangle \right] \right\rangle$$

$$= \left[{}^{2}(k) \otimes {}^{2}(k) \right] R(\mathbf{x}, \mathbf{y})$$

symmetric tensor square of k

for any rotation

$$E(k\mathbf{x}) = \langle \mathbf{T}(k\mathbf{x}) \rangle = {}^{2}(k)$$

$$R(k\mathbf{x}, k\mathbf{y}) = \gamma(k)B(\mathbf{x}, \mathbf{y})\gamma^{-1}(k)$$

γ is orthogonal representation of k

Tensor Random Fields (TRF) in 3d

- 0^{th}-rank (scalar): … $R(x) = \dfrac{\exp[-Ax^{\alpha}]}{1+Bx^{\alpha}}, \quad A,B>0, \quad 0<\alpha,\beta\le 2$

$$R(x) = \exp[-\sum_{s=1}^{r} Ax^{\alpha_s}], \quad A_s > 0, \quad 0 < \alpha_s \le 2, \quad s=1,\dots,r$$

- 1^{st}-rank: $R_i^j(\mathbf{x}) = \left\langle T_i(\mathbf{0}) T_j(\mathbf{x}) \right\rangle = \sum_{\alpha=1}^{2} S_\alpha J_i^{j(\alpha)}(\mathbf{x}) = S_1(x)\delta_{ij} + S_2(x) x_i x_j$

$$J_{ij}^{kl(1)} = \delta_{ij}\delta_{kl}, \qquad J_{ij}^{kl(2)} = \delta_{ik}\delta_{jl} + \delta_{il}\delta_{jk}$$

- 2^{nd}-rank: $R_{ij}^{kl}(\mathbf{x}) = \left\langle T_{ij}(\mathbf{0}) T_{kl}(\mathbf{x}) \right\rangle = \sum_{\alpha=1}^{5} S_\alpha(x) J_{ij}^{kl(\alpha)}(\mathbf{x})$

$$J_{ij}^{kl(4)} = x_i x_j \delta_{kl} + x_k x_l \delta_{ij}, \qquad J_{ij}^{kl(5)} = x_i x_j x_k x_l$$

$$J_{ij}^{kl(3)} = x_j x_k \delta_{il} + x_i x_l \delta_{jk} + x_i x_k \delta_{jl} + x_j x_l \delta_{ik}$$

- 3^{rd}-rank: $R_{ijk}^{prs}(\mathbf{x}) = \left\langle T_{ijk}(\mathbf{0}) T_{prs}(\mathbf{x}) \right\rangle = \sum_{\alpha=1}^{21} S_\alpha(x) J_{ijk}^{prs(\alpha)}(\mathbf{x})$ piezoelectricity

- 4^{th}-rank: $R_{ijkl}^{prst}(\mathbf{x}) = \left\langle T_{ijkl}(\mathbf{0}) T_{prst}(\mathbf{x}) \right\rangle = \sum_{\alpha=1}^{29} S_\alpha(x) J_{ijkl}^{prst(\alpha)}(\mathbf{x})$

in all elasticity classes
- tetragonal
- trigonal
- triclinic
- …

Tensor Random Fields (TRF) in 2d (planar)

- 0^{th}-rank (scalar): … $R(x)=\dfrac{\exp[-Ax^{\alpha}]}{1+Bx^{\alpha}},\quad A,B>0,\quad 0<\alpha,\beta\le 2$

$$R(x)=\exp[-\sum_{s=1}^{r}Ax^{\alpha_s}],\quad A_s>0,\quad 0<\alpha_s\le 2,\quad s=1,\ldots,r$$

- 1^{st}-rank: $R_i^{j}(\mathbf{x})=\left\langle T_i(\mathbf{0})T_j(\mathbf{x})\right\rangle=\sum_{\alpha=1}^{2}S_\alpha J_i^{j(\alpha)}(\mathbf{x})=S_1(x)\delta_{ij}+S_2(x)x_i x_j$

$$J_{ij}^{kl(1)}=\delta_{ij}\delta_{kl},\qquad J_{ij}^{kl(2)}=\delta_{ik}\delta_{jl}+\delta_{il}\delta_{jk}$$

- 2^{nd}-rank: $R_{ij}^{kl}(\mathbf{x})=\left\langle T_{ij}(\mathbf{0})T_{kl}(\mathbf{x})\right\rangle=\sum_{\alpha=1,2,4,5}S_\alpha(x)J_{ij}^{kl(\alpha)}(\mathbf{x})$ $J_{ij}^{kl(4)}=x_i x_j\delta_{kl}+x_k x_l\delta_{ij},\quad J_{ij}^{kl(5)}=x_i x_j x_k x_l$

$$\cancel{J_{ij}^{kl(3)}=x_j x_k\delta_{il}+x_i x_l\delta_{jk}+x_i x_k\delta_{jl}+x_j x_l\delta_{ik}}$$

Malyarenko & Ostoja-Starzewski, “Statistically isotropic tensor random fields: Correlation structures,” *Math. Mech. Complex Sys. (MEMOCS)*, 2014.

Malyarenko & Ostoja-Starzewski, “Spectral expansions of homogeneous and isotropic tensor-valued random fields,” *ZAMP*, 2016.

Malyarenko and M. Ostoja-Starzewski, “A random field formulation of Hooke's law in all elasticity classes,” *J. Elast.*, 2017.

3d turbulence of incompressible fluid

Correlation of planar flux TRF: $$R_i^j(\mathbf{x}) := \left\langle u_i(\mathbf{0}) u_j(\mathbf{x}) \right\rangle, \quad i = 1, 2$$

Representation: $$R_i^j(\mathbf{x}) = A(x) x_i x_j + B(x)\delta_{ij}$$

Balance: $$u_{i,i}(\mathbf{x}) = 0$$

$$\Rightarrow \quad R_{i,i}^j(\mathbf{x}) = 0 \qquad \Rightarrow \quad A'x + 4A + B'/x = 0$$

Introduce *longitudinal* and *lateral correlation func*tions:

$$x^2 A(x) + B(x) = \sigma^2 f(x) \qquad B(x) = \sigma^2 g(x) \Rightarrow \quad g = f + xf'$$

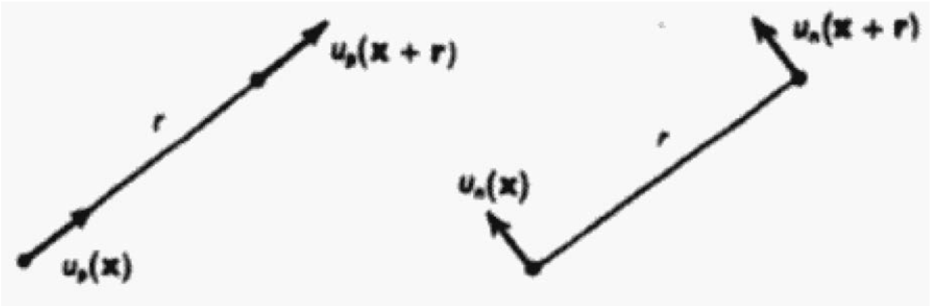

$$g = f + xf'/2$$

(Batchelor, 1953)

2d conductivity heat flow

(or 2d incompressible turbulence)

Correlation of planar flux TRF: $R_i^j(\mathbf{x}) := \left\langle q_i(\mathbf{0}) q_j(\mathbf{x}) \right\rangle, \quad i = 1, 2$

Representation: $R_i^j(\mathbf{x}) = A(x) x_i x_j + B(x)\delta_{ij}$

Balance: $q_{i,i}(\mathbf{x}) = 0$

$$\Rightarrow \quad R_{i,i}^j(\mathbf{x}) = 0 \qquad \Rightarrow \quad A'x + 3A + B'/x = 0$$

Introduce *longitudinal* and *lateral correlation func*tions:

$$x^2 A(x) + B(x) = \sigma^2 f(x) \qquad B(x) = \sigma^2 g(x) \Rightarrow \quad g = f + xf'$$

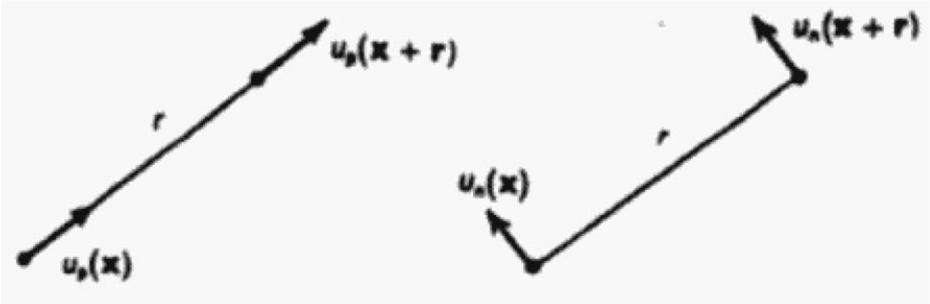

$g = f + xf'$

Anti-plane elasticity $\sigma_i = 2K_{ij}\varepsilon_j$

Correlation of strain TRF: $E_i^j(\mathbf{x}) := \left\langle \varepsilon_i(\mathbf{0})\varepsilon_j(\mathbf{x}) \right\rangle$

Representation: $E_i^j(\mathbf{x}) = D(x)\delta_{ij} + C(x)x_i x_j$

Strain-displacement relation: $\varepsilon_i = u_{,i}$

Correlation of displacement TRF: $U(\mathbf{x}) := \left\langle u(\mathbf{0})\, u(\mathbf{x}) \right\rangle$

$$\Rightarrow \quad E_i^j(\mathbf{x}) = -\frac{1}{4}\frac{\partial^2 U}{\partial x_i \partial x_j}$$

$$\Rightarrow \quad C = D' / x$$

3d random stress field

Correlation of stress TRF: $$R_{ij}^{kl}(\mathbf{x}) := \left\langle \sigma_{ij}(\mathbf{0})\sigma_{kl}(\mathbf{x}) \right\rangle, \quad i, j, k, l = 1, 2$$

Representation: $$R_{ij}^{kl}(\mathbf{x}) = \sum_{\alpha=1}^{5} S_\alpha J_{ij}^{kl(\alpha)}(\mathbf{x})$$

$$J_{ij}^{kl(1)} = \delta_{ij}\delta_{kl}, \qquad J_{ij}^{kl(2)} = \delta_{ik}\delta_{jl} + \delta_{il}\delta_{jk}$$

$$J_{ij}^{kl(3)} = n_i n_j \delta_{kl} + n_k n_l \delta_{ij}, \qquad J_{ij}^{kl(5)} = n_i n_j n_k n_l$$

$$J_{ij}^{kl(4)} = n_j n_k \delta_{il} + n_i n_l \delta_{jk} + n_i n_k \delta_{jl} + n_j n_l \delta_{ik}$$

Balance: $$\Rightarrow \quad R_{ij,i}^{kl}(\mathbf{x}) = 0$$

$$\Rightarrow \qquad 8S_1 = (R+2)(R+4)S_2$$

$$4S_5 = (R+2)S_2 - 2S_3 \qquad R \equiv r\frac{d}{dr}$$

$$8S_4 = 8(R+1)S_3 - R(R+2)S_2$$

$\Rightarrow$ First, must choose S_2, S_3

3d random stress field

Correlation of stress TRF: $$R_{ij}^{kl}(\mathbf{x}) := \left\langle \sigma_{ij}(\mathbf{0})\sigma_{kl}(\mathbf{x}) \right\rangle, \quad i, j, k, l = 1, 2$$

Representation: $$R_{ij}^{kl}(\mathbf{x}) = \sum_{\alpha=1}^{5} S_\alpha J_{ij}^{kl(\alpha)}(\mathbf{x})$$

$$J_{ij}^{kl(1)} = \delta_{ij}\delta_{kl}, \qquad J_{ij}^{kl(2)} = \delta_{ik}\delta_{jl} + \delta_{il}\delta_{jk}$$

$$J_{ij}^{kl(3)} = n_i n_j \delta_{kl} + n_k n_l \delta_{ij}, \qquad J_{ij}^{kl(5)} = n_i n_j n_k n_l$$

$$J_{ij}^{kl(4)} = n_j n_k \delta_{il} + n_i n_l \delta_{jk} + n_i n_k \delta_{jl} + n_j n_l \delta_{ik}$$

Balance: $$\Rightarrow \quad R_{ij,i}^{kl}(\mathbf{x}) = 0$$

$$\Rightarrow \qquad 8S_1 = (R+2)(R+4)S_2$$

$$4S_5 = (R+2)S_2 - 2S_3 \qquad R \equiv r\frac{d}{dr}$$

$$8S_4 = 8(R+1)S_3 - R(R+2)S_2$$

$\Rightarrow$ First, must choose S_2, S_3

Define rotation tensor $\omega := \tfrac{1}{2}\,\mathrm{curl}\; u$

$$\Rightarrow \qquad \Omega_{ij}(\mathbf{r}_1,\mathbf{r}_2) := \langle \omega_i(\mathbf{r}_1)\omega_j(\mathbf{r}_2)\rangle$$

$$\Rightarrow \qquad \Omega = \tfrac{1}{4}\,\mathrm{curl}\; U \qquad\qquad \mathrm{div}\;\Omega = 0$$

If homogeneous and isotropic, $\Omega_{ij} = \Omega_1\delta_{ij} + \Omega_2 r_i r_j$

or $\Omega_{ij} = \Omega_{11}\delta_{ij} + (\Omega_{33} - \Omega_{11}) r_i r_j$

$$\Rightarrow \qquad r\Omega_{33}^{'} + 2(\Omega_{33} - \Omega_{11}) = 0$$

$$\Omega_{11} = \frac{1}{2r}\frac{d}{dr}(r^2\Omega_{33})$$

formally analogous to von Kármán equations

Define curvature tensor $\gamma_{ij} := \omega_{i,j}$

$$\Rightarrow \quad \Gamma_{ijkl}(\mathbf{r}_1, \mathbf{r}_2) := \langle \gamma_{ij}(\mathbf{r}_1)\gamma_{kl}(\mathbf{r}_2) \rangle$$

$$\Rightarrow \quad \Gamma_{ijkl}(\mathbf{r}_1, \mathbf{r}_2) = -\Omega_{ik,jl} \equiv \Theta_{ikjl}$$

$$\Theta_{ikjl} = \Theta_{kijl} = \Theta_{iklj} \neq \Theta_{jlik}$$

$\Rightarrow$ Can estimate RF of grain bending in inhomogeneous medium under homogeneous macro-deformation

micropolar-type

$$\Rightarrow \quad \Theta_{13} = (R-1)\Theta_{12} \qquad \Theta_{31} = R\Theta_{11}/2 = 2\Theta_{12}$$

$$\Theta_{33} = (R-1)(R\Theta_{11} - \Theta_{12}) \qquad 2\Theta_{44} = (R-1)\Theta_{11} - \Theta_{12}$$

$\Rightarrow$ first choose $\Theta_{11},\ \Theta_{12}$

Micropolar continuum

$\Rightarrow$ 5 equations for 13 unknown functions of quasi-static TRFs

kinematics $\Rightarrow$

8 relations for 18 unknown coefficients in 3 correlation functions of displacement, rotation, and torsion-curvature TRFs

OBSERVE

- For tensor random fields (TRFs) we determined explicit correlation functions (and their spectral forms)
- For dependent fields, restrictions are imposed by the governing equations
- For property fields (conductivity, elasticity…) determined correlation functions for all kinds of anisotropies
- such TRFs are needed as inputs into stochastic BVPs [partial differential equations (SPDEs)]
- Random fields of properties are functions of microstructure + mesoscale
- Can go to: micropolar models, coupled field phenomena, inelastic properties,…

(a)
(b)
(c)

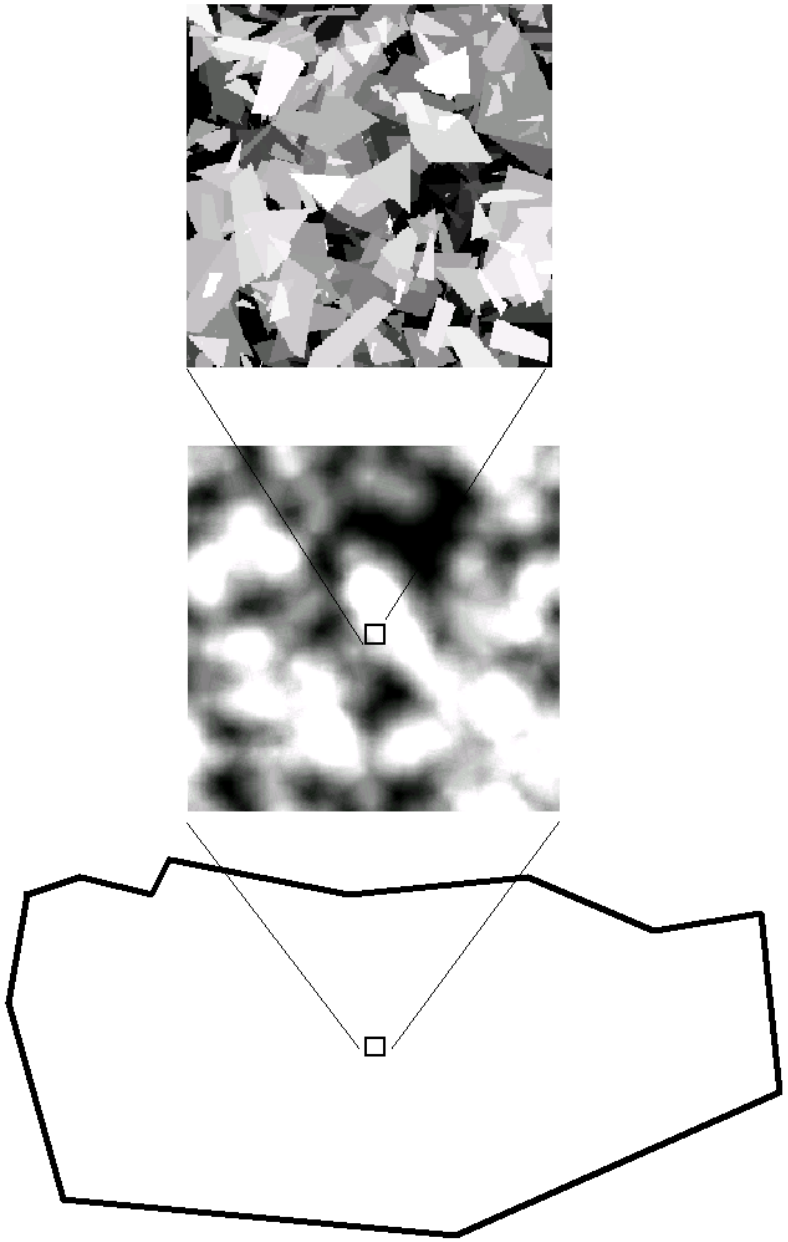

Random fields of constitutive responses from micromechanics

in 2D elasticity C_{ijkl}

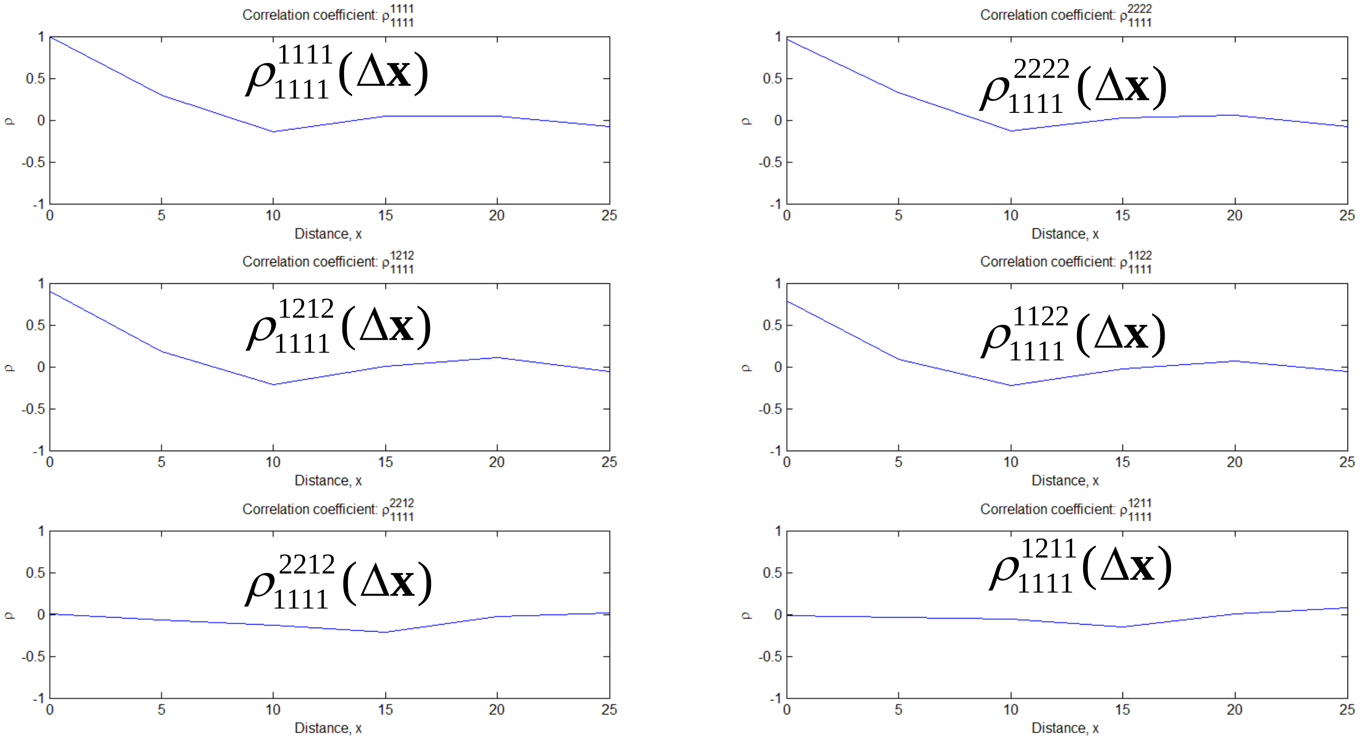

mesoscale = 10

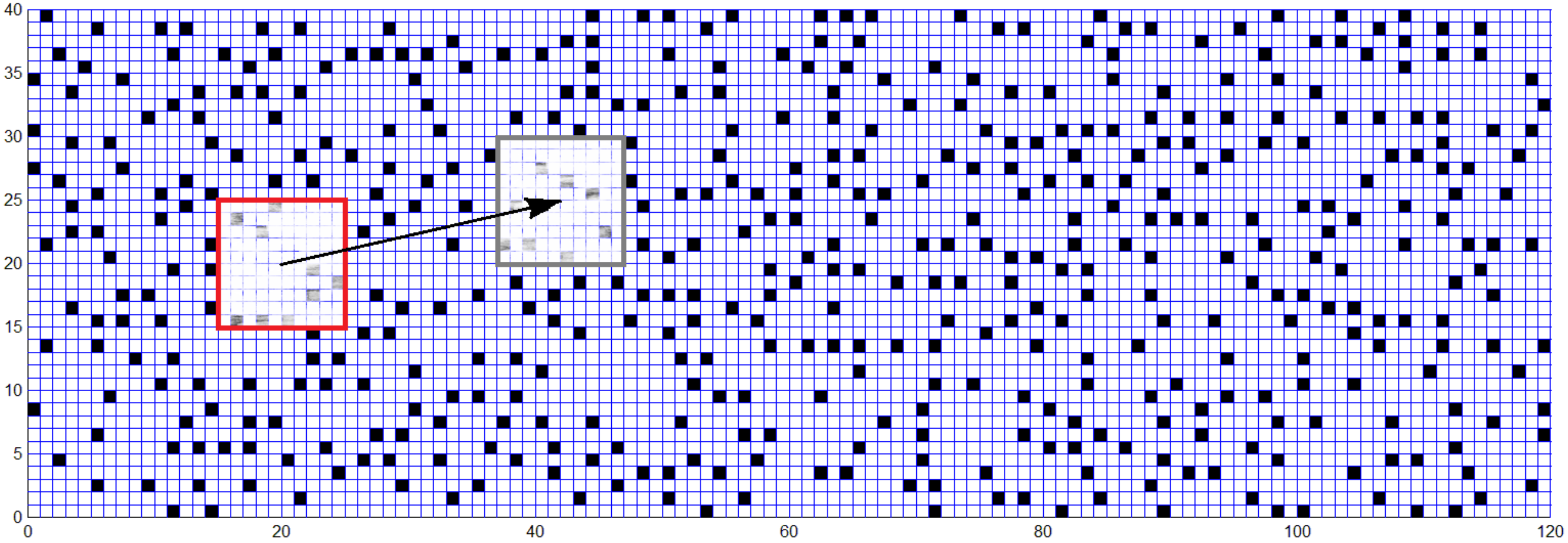

1. auto-correlations of diagonals: ,…

2. cross-correlations of diagonals: ,…

3. auto-correlations of off-diagonals: ,…

4. cross-correlations of off-diagonals: ,…

5. cross-correlations of diagonal with off-diagonal terms: ,…

Tensor RFs of C_{ijkl} in elasticity

$\Rightarrow$ *correlation function:* $R_{ijkl}^{prst}(\mathbf{x}_1,\mathbf{x}_2) = \langle [C_{ijkl}(\mathbf{x}_1) - \langle C_{ijkl}(\mathbf{x}_1)\rangle][C_{prst}(\mathbf{x}_2) - \langle C_{prst}(\mathbf{x}_2)\rangle]\rangle$

… for homogeneous random media: $R_{ijkl}^{prst}(\mathbf{x}_1,\mathbf{x}_2) = R_{ijkl}^{prst}(\mathbf{x})$ $\quad \mathbf{x} = |\mathbf{x}_1 - \mathbf{x}_2|$

$$R_{abcd}^{efgh}(\hat{\mathbf{x}}) = c_{ai}c_{bj}c_{ck}c_{dl}c_{pe}c_{rf}c_{gs}c_{ht}R_{ijkl}^{prst}(\mathbf{x}) = c_{ai}c_{bj}c_{ck}c_{dl}c_{pe}c_{rf}c_{gs}c_{ht}R_{ijkl}^{prst}(c^{-1}\mathbf{x})$$

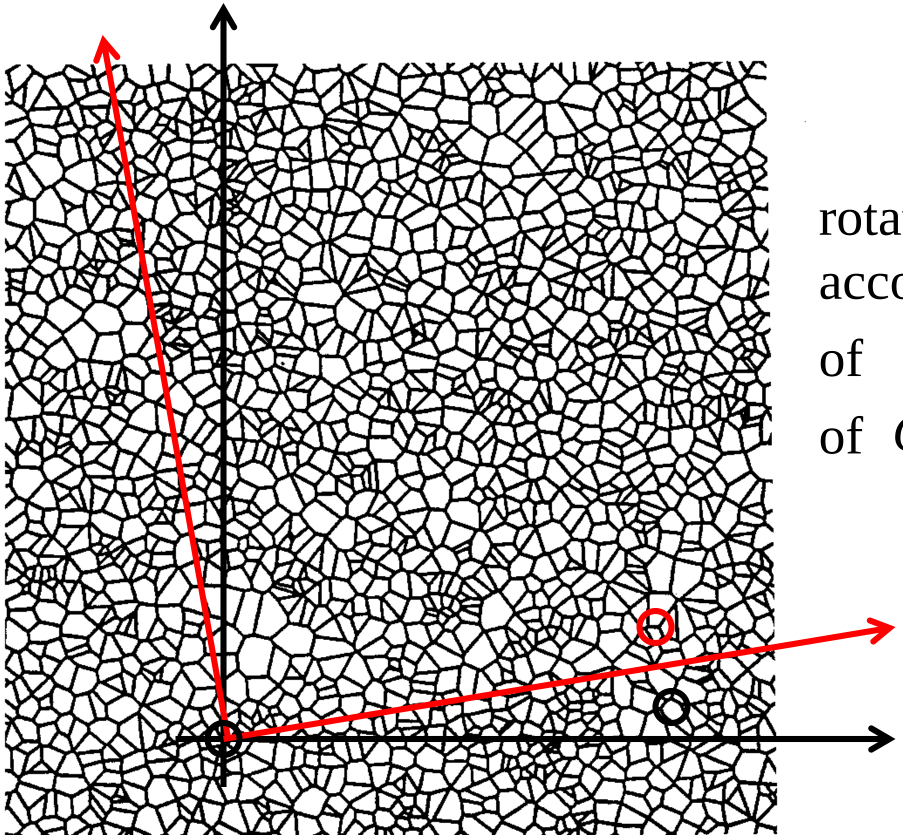

rotation of system $\mathbf{x}$ into $\hat{\mathbf{x}}$ has to be accompanied by a simultaneous rotation [SO(3)] of $C_{ijkl}(\mathbf{x}_1)$ into $\hat{C}_{abcd}(\hat{\mathbf{x}}_1)$ as well as a rotation of $C_{prst}(\mathbf{x}_2)$ into $\hat{C}_{efgh}(\hat{\mathbf{x}}_2)$

Tensor Random Fields (TRF)

- locally isotropic TRF:

1st-rank $\mathbf{T} = \mathbf{0}$

2nd-rank $\mathbf{T} = T\mathbf{1}$ $\qquad C_{ij} = C\mathbf{1}$

4th-rank $\mathbf{T} = \lambda\left(\mathbf{1}\otimes\mathbf{1}\right) + 2\mu\mathbf{1}_4^s \qquad C_{ijkl} = \lambda\left(\mathbf{1}\otimes\mathbf{1}\right) + 2\mu\mathbf{1}_4^s$

$$\mathbf{1}\otimes\mathbf{1} \Leftrightarrow \delta_{ij}\delta_{kl}, \quad \mathbf{1}_4 = \mathbf{1}\overline{\otimes}\mathbf{1} \Leftrightarrow 1_{ijkl} = \delta_{ik}\delta_{jl}, \quad \mathbf{1}\underline{\otimes}\mathbf{1} \Leftrightarrow \delta_{il}\delta_{jk}$$

$$\mathbf{1}_4 = \mathbf{1}_4^s + \mathbf{1}_4^a, \quad \mathbf{1}_4^s = \left(\mathbf{1}\overline{\otimes}\mathbf{1} + \mathbf{1}\underline{\otimes}\mathbf{1}\right)/2, \quad \mathbf{1}_4^a = \left(\mathbf{1}\overline{\otimes}\mathbf{1} - \mathbf{1}\underline{\otimes}\mathbf{1}\right)/2$$

Tensor Random Fields (TRF)

- locally isotropic TRF:

  1^{st}-rank $\quad \mathbf{T}=\mathbf{0}$

  2^{nd}-rank $\quad \mathbf{T}=T\mathbf{1}$

  4^{th}-rank $\quad \mathbf{T}=\lambda\left(\mathbf{1}\otimes\mathbf{1}\right)+2\mu\mathbf{1}_4^s$

$$\mathbf{1}\otimes\mathbf{1}\Leftrightarrow\delta_{ij}\delta_{kl},\quad \mathbf{1}_4=\mathbf{1}\overline{\otimes}\mathbf{1}\Leftrightarrow 1_{ijkl}=\delta_{ik}\delta_{jl},\quad \mathbf{1}\underline{\otimes}\mathbf{1}\Leftrightarrow\delta_{il}\delta_{jk}$$

$$\mathbf{1}_4=\mathbf{1}_4^s+\mathbf{1}_4^a,\quad \mathbf{1}_4^s=\left(\mathbf{1}\overline{\otimes}\mathbf{1}+\mathbf{1}\underline{\otimes}\mathbf{1}\right)/2,\quad \mathbf{1}_4^a=\left(\mathbf{1}\overline{\otimes}\mathbf{1}-\mathbf{1}\underline{\otimes}\mathbf{1}\right)/2$$

- statistically (wide-sense) isotropic TRF:

  0^{th}-rank (scalar)

  1^{st}-rank

  2^{nd}-rank

  4^{th}-rank

- 0^{th}-rank (scalar) statistically (wide-sense) isotropic TRF:

$$E(k\mathbf{x}) := \left\langle T(k\mathbf{x}) \right\rangle$$

$$B(k\mathbf{x}, k\mathbf{y}) := \left\langle \left[T(k\mathbf{x}) - \left\langle T(k\mathbf{x}) \right\rangle \right] \left[T(k\mathbf{y}) - \left\langle T(k\mathbf{y}) \right\rangle \right] \right\rangle$$

for any rotation :

Basic models:

$$\rho(x) = \exp[-Ax^{\alpha}], \quad A > 0, \quad 0 < \alpha \le 2$$

$$\rho(x) = [1 + Ax^{\alpha}]^{-1}, \quad A > 0, \quad 0 < \alpha \le 2$$

$$\rho(x) = \frac{\exp[-Ax^{\alpha}]}{1 + Bx^{\alpha}}, \quad A, B > 0, \quad 0 < \alpha, \beta \le 2$$

$$\rho(x) = \exp[-\sum_{s=1}^{r} Ax^{\alpha_s}], \quad A_s > 0, \quad 0 < \alpha_s \le 2, \quad s = 1, \ldots, r$$

$$\rho(x) = [-\prod_{s=1}^{r} (1 + B_s x^{\beta_s}) l_s], \quad B_s > 0, \quad 0 < \beta_s \le 2, \quad l_s = 1, 2, \ldots$$

$$\rho(x) = \exp[-Ax^{\alpha}](\cosh Bx^{\alpha})^{s}, \quad A + B(2l - s) > 0, \quad 0 < \alpha \le 2, \quad s = 1, \ldots, r$$

$$\rho(x) = \frac{(\cosh Bx^{\alpha})^{s}}{1 + Ax^{\alpha}}, \quad A + B(2l - s) > 0, \quad 0 < \alpha \le 2, \quad s = 1, \ldots, r$$

- 2^{nd}-rank statistically (wide-sense) isotropic TRF:

$$E(k\mathbf{x}) := \left\langle \mathbf{T}(k\mathbf{x}) \right\rangle = \left\langle \;{}^{2}(k)\mathbf{T}(\mathbf{x}) \right\rangle = \;{}^{2}(k)\left\langle \mathbf{T}(k\mathbf{x}) \right\rangle = \;{}^{2}(k)E(\mathbf{x})$$

$$\begin{aligned} B(k\mathbf{x}, k\mathbf{y}) &:= \left\langle \left[\mathbf{T}(k\mathbf{x}) - \left\langle \mathbf{T}(k\mathbf{x}) \right\rangle \right] \otimes \left[\mathbf{T}(k\mathbf{y}) - \left\langle \mathbf{T}(k\mathbf{y}) \right\rangle \right] \right\rangle \\ &= \left[\;{}^{2}(k) \otimes \;{}^{2}(k) \right] B(\mathbf{x}, \mathbf{y}) \end{aligned}$$

for any rotation :

- 4th-rank statistically (wide-sense) isotropic TRF:

for any rotation :

Physical meaning of K_i functions for 2nd rank TRF

$$B_{ij}^{kl}(\mathbf{x}_1,\mathbf{x}_2)=\langle T_{ij}(\mathbf{x}_1)T_{kl}(\mathbf{x}_2)\rangle = K_4\left(x\right)\delta_{ij}\delta_{kl}+K_6\left(x\right)\left[\delta_{ik}\delta_{jl}+\delta_{il}\delta_{jk}\right]$$

$$+\left[K_5\left(x\right)-K_6\left(x\right)\right]\left[n_j n_k\delta_{il}+n_i n_l\delta_{jk}+n_i n_k\delta_{jl}+n_j n_l\delta_{ik}\right]$$

$$+\left[K_3\left(x\right)-K_4\left(x\right)\right]\left[n_i n_j\delta_{kl}+n_k n_l\delta_{ij}\right]$$

$$+\left[K_1\left(x\right)+K_2\left(x\right)-2K_3\left(x\right)-4K_5\left(x\right)\right]n_i n_j n_k n_l,$$

$$\begin{bmatrix} T_{11} & T_{12} & T_{13} \\ & T_{22} & T_{23} \\ & & T_{33} \end{bmatrix}$$

elasticity

Covariance of strain TRF: $$E_{ij}^{kl}(\mathbf{r}) := \left\langle \varepsilon_{ij}^{0}(\mathbf{r}+\mathbf{r}_1)\varepsilon_{kl}^{0}(\mathbf{r}_1) \right\rangle$$

Representation: $$E_{ij}^{kl} = \sum_{\alpha=1}^{5} M_\alpha J_{ij}^{kl(\alpha)}(\mathbf{r})$$

Strain-displacement relation:

Covariance of displacement TRF: $$U_{ij}(\mathbf{r}) = K_1(r) r_i r_j + K_2(r)\delta_{ij}$$

$\Rightarrow$ First, must choose M_1, M_4

damage tensors

Field of damage described by TRF:

Covariance: $$\Phi_{ij}^{kl}(\mathbf{r}) := \left\langle \varphi_{ij}^{0}(\mathbf{r}+\mathbf{r}_1)\varphi_{kl}^{0}(\mathbf{r}_1) \right\rangle$$

Representation: $$\Phi_{ij}^{kl} = \sum_{\alpha=1}^{5} M_{\alpha} J_{ij}^{kl(\alpha)}(\mathbf{r})$$

Damage geometry described by:

Covariance:

Representation:

OBSERVE

- Need to distinguish between local isotropy of continuum fields and statistical isotropy

- For tensor-type properties of materials, need TRFs that are (i) positive-definite and (ii) consistent with micromechanics [as functions of microstructure + mesoscale + Hill-Mandel condition]

- Counterintuitive results

- For dependent tensor fields, covariances are subject to restrictions dictated by field equations

- Once covariance functions are set up, one can simulate realizations of TRFs

- Applications:

- cross-correlations of fields,
- classical or micropolar continua,
- set up stochastic finite element models, …

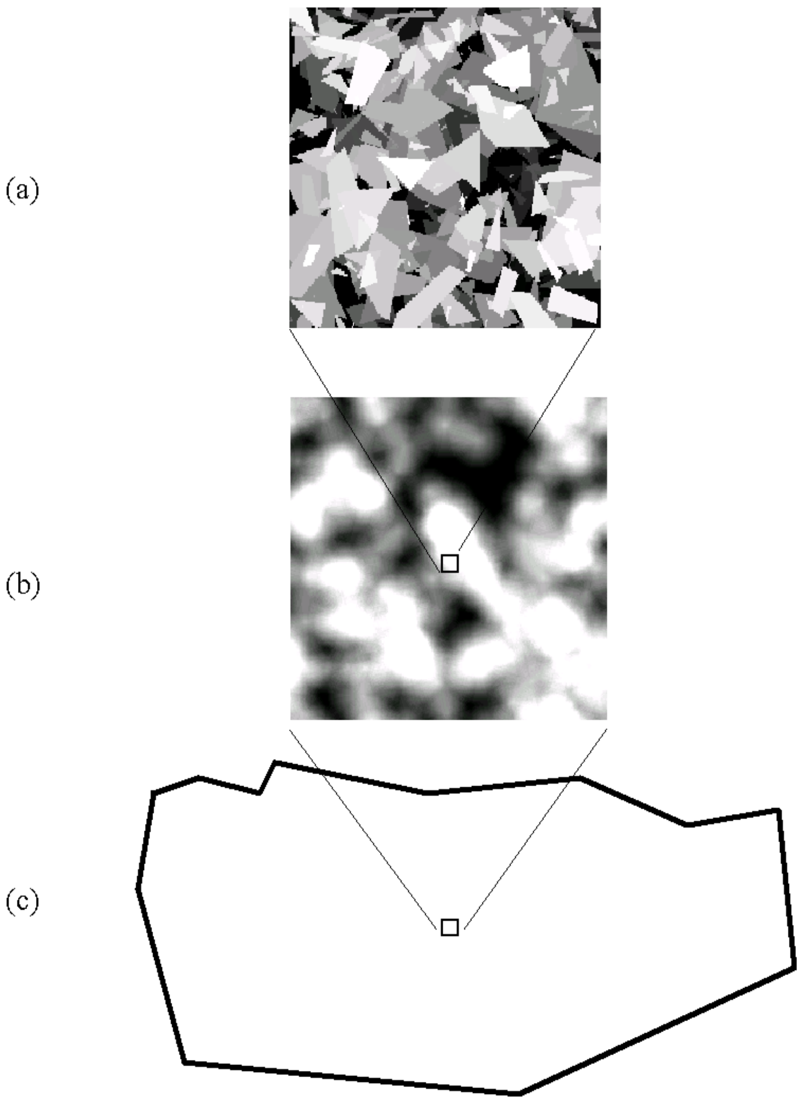

3d conductivity $q_i = -C_{ij} T_{,j}$

Covariance of heat flux TRF: $S_i^j(\mathbf{r}) := \left\langle q_i^0(\mathbf{r}+\mathbf{r}_1) q_j^0(\mathbf{r}_1) \right\rangle, \quad i = 1, 2$

Representation: $S_i^j(\mathbf{r}) = A(r) r_i r_j + B(r)\delta_{ij}$

Equilibrium: $q_{i,i}(\mathbf{r}) = 0$

$$\Rightarrow$$

$$\Rightarrow \quad A'(r) r + 4A(r) + B'/r = 0$$

Introduce *longitudinal* and *lateral correlation functions*:

$$r^2 A(r) + B(r) = \sigma^2 f(r) \qquad B(r) = \sigma^2 g(r)$$

$$\Rightarrow \; g = f + r f'/2$$

3d conductivity

Covariance of temperature gradient TRF: $E_i^j(\mathbf{r}) := \left\langle T,_i^0(\mathbf{r}+\mathbf{r}_1)T,_j^0(\mathbf{r}_1)\right\rangle$

$$T^0,_i(\mathbf{r}) := T,_i(\mathbf{r}) - \left\langle T,_i(\mathbf{r})\right\rangle$$

Representation: $E_i^j(\mathbf{r}) = C(r)r_i r_j + D(r)\delta_{ij}$

$$\Rightarrow \quad C = D'/r$$

Vector RF
wide-sense stationary

$$\langle Z_i(\mathbf{x})\rangle = \mu_i, \quad \langle Z_i(\mathbf{x}_1) Z_j(\mathbf{x}_1 + \mathbf{x})\rangle = R_{ij}(\mathbf{x}) < \infty$$

$$R_{ij}(\mathbf{x}_1, \mathbf{x}_2) = \langle [Z_i(\mathbf{x}_1) - \left\langle Z_i(\mathbf{x}_1)\right\rangle][Z_j(\mathbf{x}_2) - \left\langle Z_j(\mathbf{x}_2)\right\rangle]\rangle$$

$$\rho_{ij}(\mathbf{x}_1, \mathbf{x}_2) = \frac{R_{ij}(\mathbf{x}_1, \mathbf{x}_2)}{\sigma_i(\mathbf{x}_1)\sigma_j(\mathbf{x}_2)}$$

$$\rho_{ij}(\mathbf{x}_1, \mathbf{x}_2) = \rho_{ij}(\left|\mathbf{x}_1 - \mathbf{x}_2\right|)$$

Vector RF: Z_i

$\Rightarrow$ *correlation function*: $R_i^j(\mathbf{x}_1, \mathbf{x}_2) = \langle [Z_i(\mathbf{x}_1) - \langle Z_i(\mathbf{x}_1) \rangle][Z_j(\mathbf{x}_2) - \langle Z_j(\mathbf{x}_2) \rangle] \rangle$

… for homogeneous turbulence: $R_i^j(\mathbf{x}_1, \mathbf{x}_2) = R_i^j(\mathbf{x})$ $\quad \mathbf{x} = |\mathbf{x}_1 - \mathbf{x}_2|$

$$R_a^b(\hat{\mathbf{x}}) = c_{ai} c_{bj} R_i^j(\mathbf{x}) = c_{ai} c_{bj} R_i^j(c^{-1}\mathbf{x})$$

Vector RF: Z_i

$\Rightarrow$ *correlation function*: $R_i^j(\mathbf{x}_1,\mathbf{x}_2) = \langle [Z_i(\mathbf{x}_1) - \langle Z_i(\mathbf{x}_1)\rangle][Z_j(\mathbf{x}_2) - \langle Z_j(\mathbf{x}_2)\rangle]\rangle$

… for homogeneous turbulence: $R_i^j(\mathbf{x}_1,\mathbf{x}_2) = R_i^j(\mathbf{x})$ $\quad \mathbf{x} = |\mathbf{x}_1 - \mathbf{x}_2|$

$$R_a^b(\hat{\mathbf{x}}) = c_{ai}c_{bj}R_i^j(\mathbf{x}) = c_{ai}c_{bj}R_i^j(c^{-1}\mathbf{x})$$

rotation of system $\mathbf{x}$ into $\hat{\mathbf{x}}$ [subject to SO(3)] has to be accompanied by a simultaneous rotation of $Z_i(\mathbf{x}_1)$ into $\hat{Z}_a(\hat{\mathbf{x}}_1)$ as well as a rotation of $Z_j(\mathbf{x}_2)$ into $\hat{Z}_b(\hat{\mathbf{x}}_2)$

2nd rank tensor RF
(e.g. anti-plane elasticity)

$$C_{ij}^{kl}(\mathbf{x}_1,\mathbf{x}_2) = \langle C_{ij}(\mathbf{x}_1) C_{kl}(\mathbf{x}_2)\rangle$$

Stationary RF:

$$\left\langle C_{ij}(\mathbf{x})\right\rangle = const \qquad \forall \mathbf{x}$$

$$R_{ij}^{kl}(\mathbf{x}_1,\mathbf{x}_2) = R_{ij}^{kl}(\mathbf{x}) \qquad \mathbf{x} = \left|\mathbf{x}_1 - \mathbf{x}_2\right|$$

Isotropic RF:

$$\left\langle C_{ij}(\mathbf{x})\right\rangle = C\delta_{ij} \qquad \forall \mathbf{x} \qquad x = \left\|\mathbf{x}\right\|$$

$$\begin{aligned} R_{ij}^{kl}(x) &= K_4(x)\delta_{ij}\delta_{kl} + K_6(x)\left[\delta_{ik}\delta_{jl} + \delta_{il}\delta_{jk}\right] \\ &+ \left[K_5(x) - K_6(x)\right]\left[n_j n_k \delta_{il} + n_i n_l \delta_{jk} + n_i n_k \delta_{jl} + n_j n_l \delta_{ik}\right] \\ &+ \left[K_3(x) - K_4(x)\right]\left[n_i n_j \delta_{kl} + n_k n_l \delta_{ij}\right] \\ &+ \left[K_1(x) + K_2(x) - 2K_3(x) - 4K_5(x)\right] n_i n_j n_k n_l , \end{aligned}$$

(five functions K_i)

$$K_4 + 2K_6 - K_2 = 0$$

Tensor RFs of C_{ijkl} in elasticity

$\Rightarrow$ *correlation function*: $R_{ijkl}^{prst}(\mathbf{x}_1,\mathbf{x}_2) = \langle [C_{ijkl}(\mathbf{x}_1) - \left\langle C_{ijkl}(\mathbf{x}_1)\right\rangle][C_{prst}(\mathbf{x}_2) - \left\langle C_{prst}(\mathbf{x}_2)\right\rangle]\rangle$

… for homogeneous random media: $R_{ijkl}^{prst}(\mathbf{x}_1,\mathbf{x}_2) = R_{ijkl}^{prst}(\mathbf{x})$ $\quad \mathbf{x} = \left|\mathbf{x}_1 - \mathbf{x}_2\right|$

$$R_{abcd}^{efgh}(\hat{\mathbf{x}}) = c_{ai}c_{bj}c_{ck}c_{dl}c_{pe}c_{rf}c_{gs}c_{ht}R_{ijkl}^{prst}(\mathbf{x}) = c_{ai}c_{bj}c_{ck}c_{dl}c_{pe}c_{rf}c_{gs}c_{ht}R_{ijkl}^{prst}(c^{-1}\mathbf{x})$$

Tensor RFs of C_{ijkl} in elasticity

$\Rightarrow$ *correlation function*: $R_{ijkl}^{prst}(\mathbf{x}_1, \mathbf{x}_2) = \langle [C_{ijkl}(\mathbf{x}_1) - \left\langle C_{ijkl}(\mathbf{x}_1) \right\rangle][C_{prst}(\mathbf{x}_2) - \left\langle C_{prst}(\mathbf{x}_2) \right\rangle] \rangle$

… for homogeneous random media: $R_{ijkl}^{prst}(\mathbf{x}_1, \mathbf{x}_2) = R_{ijkl}^{prst}(\mathbf{x})$ $\quad \mathbf{x} = \left| \mathbf{x}_1 - \mathbf{x}_2 \right|$

$$R_{abcd}^{efgh}(\hat{\mathbf{x}}) = c_{ai}c_{bj}c_{ck}c_{dl}c_{pe}c_{rf}c_{gs}c_{ht}R_{ijkl}^{prst}(\mathbf{x}) = c_{ai}c_{bj}c_{ck}c_{dl}c_{pe}c_{rf}c_{gs}c_{ht}R_{ijkl}^{prst}(c^{-1}\mathbf{x})$$

rotation of system $\mathbf{x}$ into $\hat{\mathbf{x}}$ has to be accompanied by a simultaneous rotation [SO(3)] of into $\hat{C}_{abcd}(\hat{\mathbf{x}}_1)$ as well as a rotation of $C_{prst}(\mathbf{x}_2)$ into $\hat{C}_{efgh}(\hat{\mathbf{x}}_2)$

Tensor RFs of C_{ijkl} in elasticity

$\Rightarrow$ *correlation function:* $R^{prst}_{ijkl}(\mathbf{x}_1,\mathbf{x}_2) = \langle [C_{ijkl}(\mathbf{x}_1) - \langle C_{ijkl}(\mathbf{x}_1)\rangle][C_{prst}(\mathbf{x}_2) - \langle C_{prst}(\mathbf{x}_2)\rangle]\rangle$

… for homogeneous random media: $R^{prst}_{ijkl}(\mathbf{x}_1,\mathbf{x}_2) = R^{prst}_{ijkl}(\mathbf{x})$ $\quad \mathbf{x} = |\mathbf{x}_1 - \mathbf{x}_2|$

$$R^{efgh}_{abcd}(\hat{\mathbf{x}}) = c_{ai}c_{bj}c_{ck}c_{dl}c_{pe}c_{rf}c_{gs}c_{ht}R^{prst}_{ijkl}(\mathbf{x}) = c_{ai}c_{bj}c_{ck}c_{dl}c_{pe}c_{rf}c_{gs}c_{ht}R^{prst}_{ijkl}(c^{-1}\mathbf{x})$$

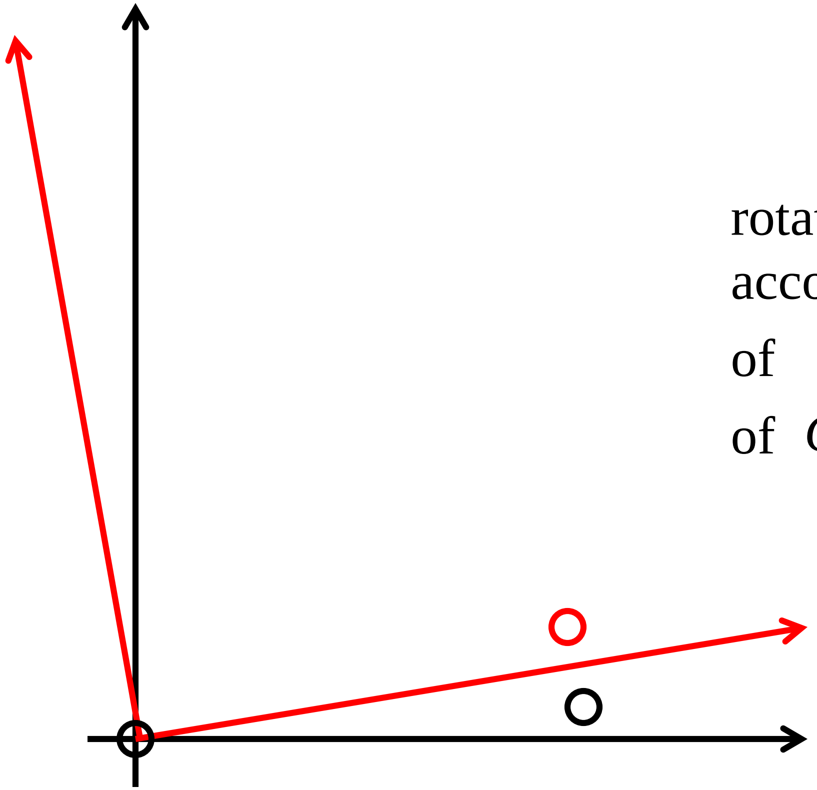

rotation of system $\mathbf{x}$ into $\hat{\mathbf{x}}$ has to be accompanied by a simultaneous rotation [SO(3)] of into $\hat{C}_{abcd}(\hat{\mathbf{x}}_1)$ as well as a rotation of $C_{prst}(\mathbf{x}_2)$ into $\hat{C}_{efgh}(\hat{\mathbf{x}}_2)$

Tensor RFs of C_{ijkl} in elasticity

$\Rightarrow$ *correlation function:* $R^{prst}_{ijkl}(\mathbf{x}_1,\mathbf{x}_2) = \langle [C_{ijkl}(\mathbf{x}_1) - \langle C_{ijkl}(\mathbf{x}_1)\rangle][C_{prst}(\mathbf{x}_2) - \langle C_{prst}(\mathbf{x}_2)\rangle]\rangle$

… for homogeneous random media: $R^{prst}_{ijkl}(\mathbf{x}_1,\mathbf{x}_2) = R^{prst}_{ijkl}(\mathbf{x})$ $\quad \mathbf{x} = |\mathbf{x}_1 - \mathbf{x}_2|$

$$R^{efgh}_{abcd}(\hat{\mathbf{x}}) = c_{ai}c_{bj}c_{ck}c_{dl}c_{pe}c_{rf}c_{gs}c_{ht}R^{prst}_{ijkl}(\mathbf{x}) = c_{ai}c_{bj}c_{ck}c_{dl}c_{pe}c_{rf}c_{gs}c_{ht}R^{prst}_{ijkl}(c^{-1}\mathbf{x})$$

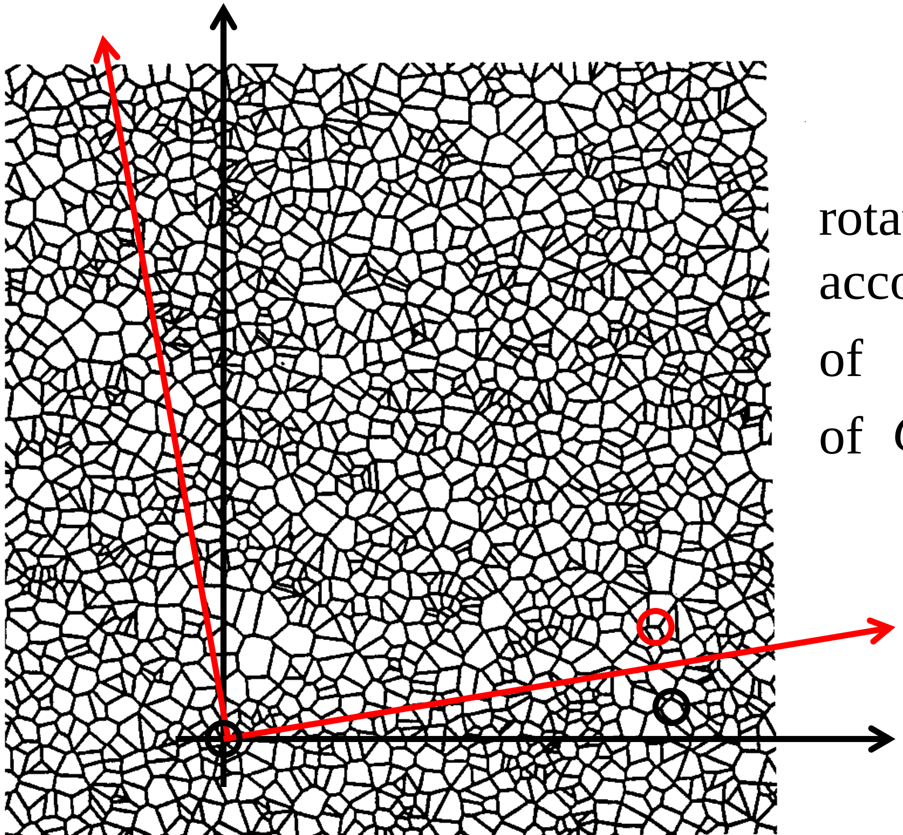

rotation of system $\mathbf{x}$ into $\hat{\mathbf{x}}$ has to be accompanied by a simultaneous rotation [SO(3)] of into $\hat{C}_{abcd}(\hat{\mathbf{x}}_1)$ as well as a rotation of $C_{prst}(\mathbf{x}_2)$ into $\hat{C}_{efgh}(\hat{\mathbf{x}}_2)$

1. With the exception of cross-correlations made with the (1112) and (2212) components, in white-noise checkerboards, correlations generally

- appear to be linear at low contrast α for all volume fractions v_f
- appear to become nonlinear at high α at low v_f, yet to become increasingly linear as v_f increases

2. In general, cross-correlations made with the (1112) and (2212) components are nearly zero for every α and v_f; however, auto- and cross-correlations between the (1112) and (2212) components are highly nonlinear for every α and v_f

3. All correlations approach 0 as $\xi \rightarrow L$ (as windows cease to overlap)

4. In general, the strength of the correlations appears to become weaker with increasing α for all v_f

5. Correlation surfaces and their contours match those of the anti-plane case:

- mismatch in strength along the x and x axes, suggesting an elliptical correlation structure;
- auto- and cross-correlations made with the (1112) and (2212) components appear to have an isotropic correlation structure

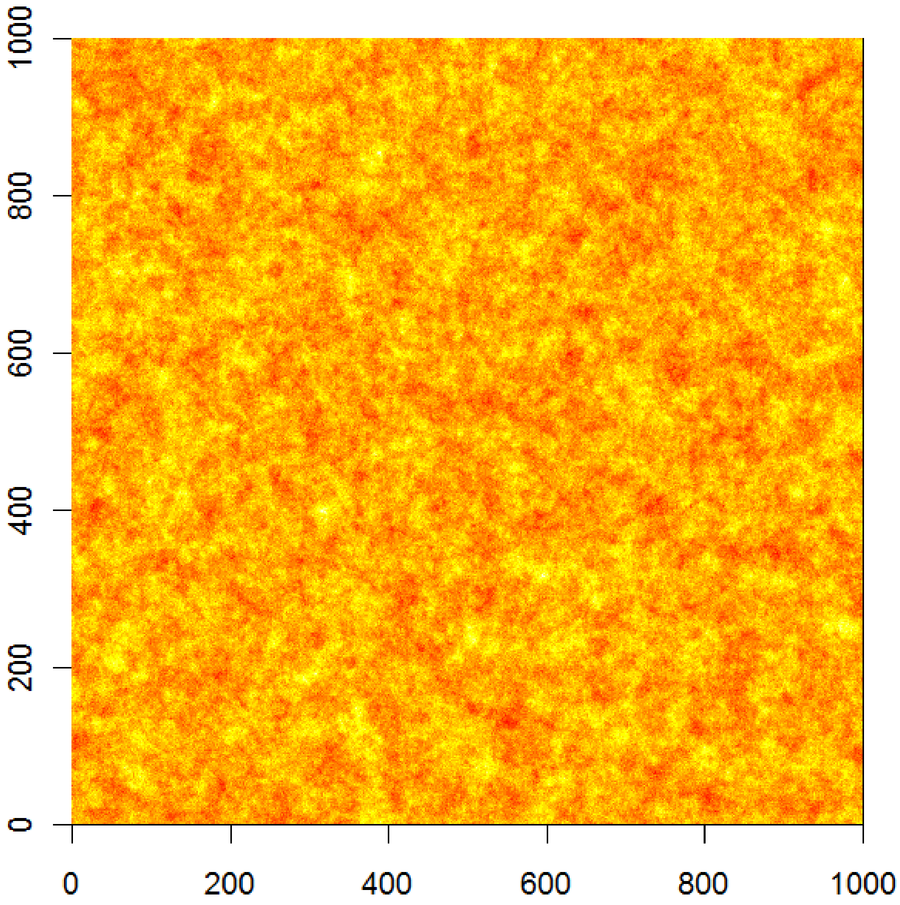

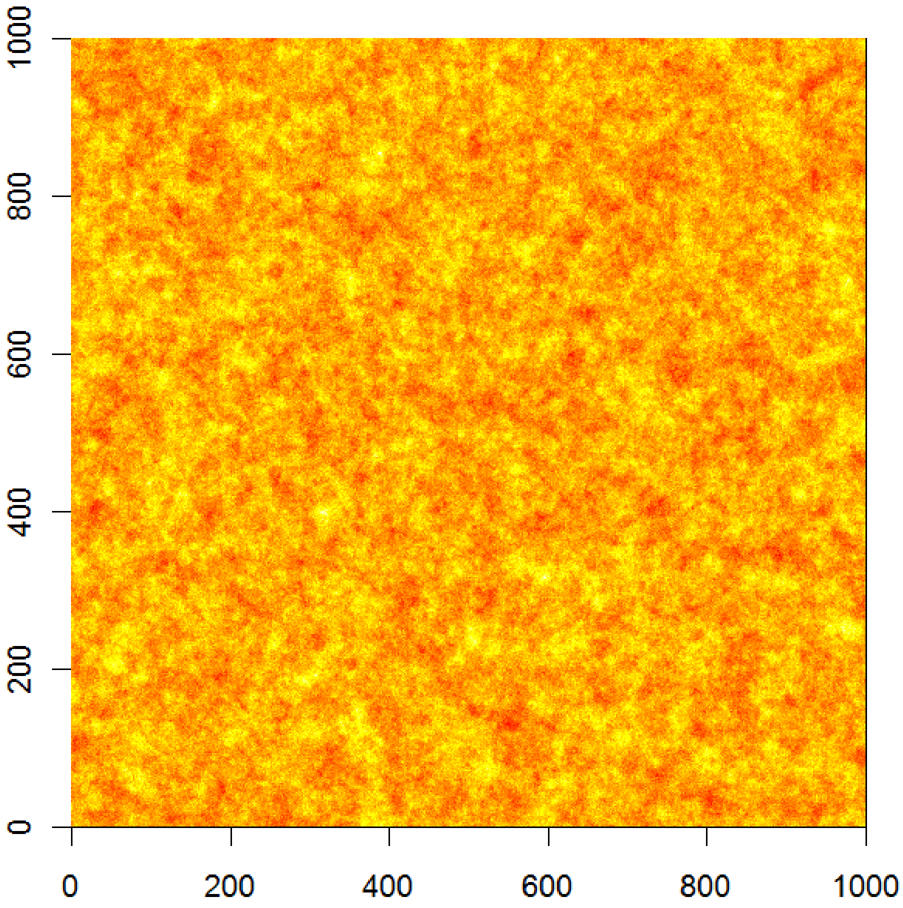

RFs with exponential or Gaussian correlation functions

$$C(x) = \exp[-Ax^{\alpha}], \quad A > 0, \quad 0 < \alpha \le 2$$

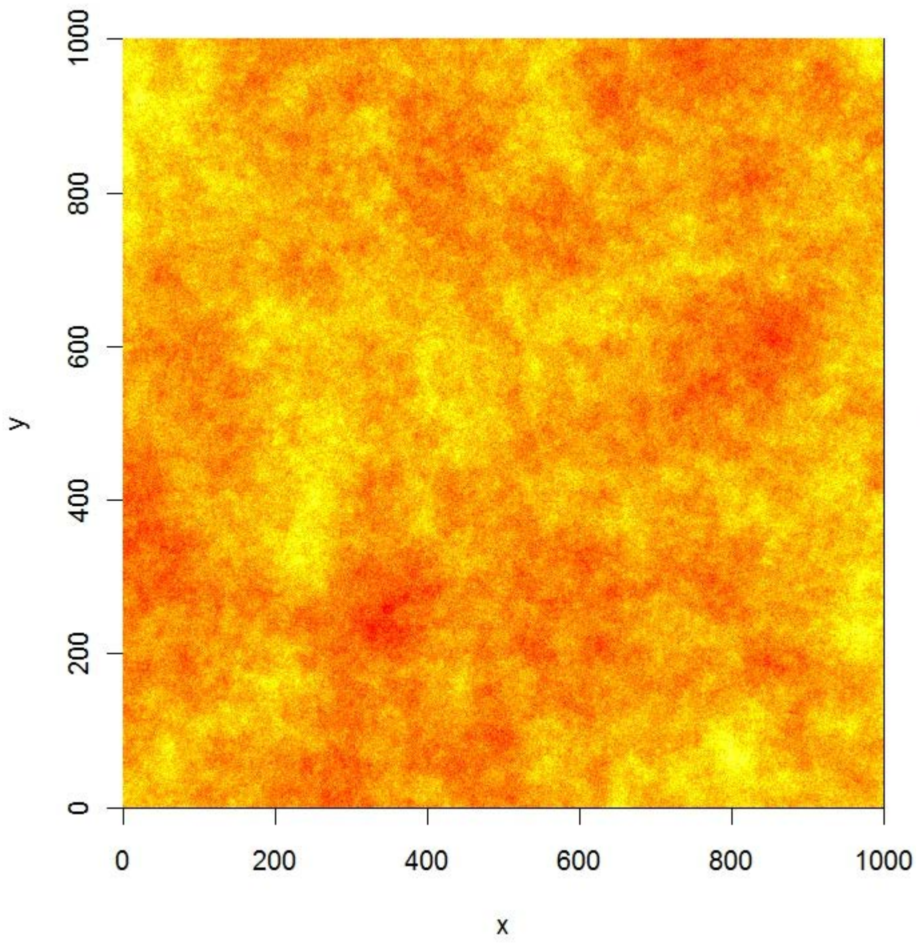

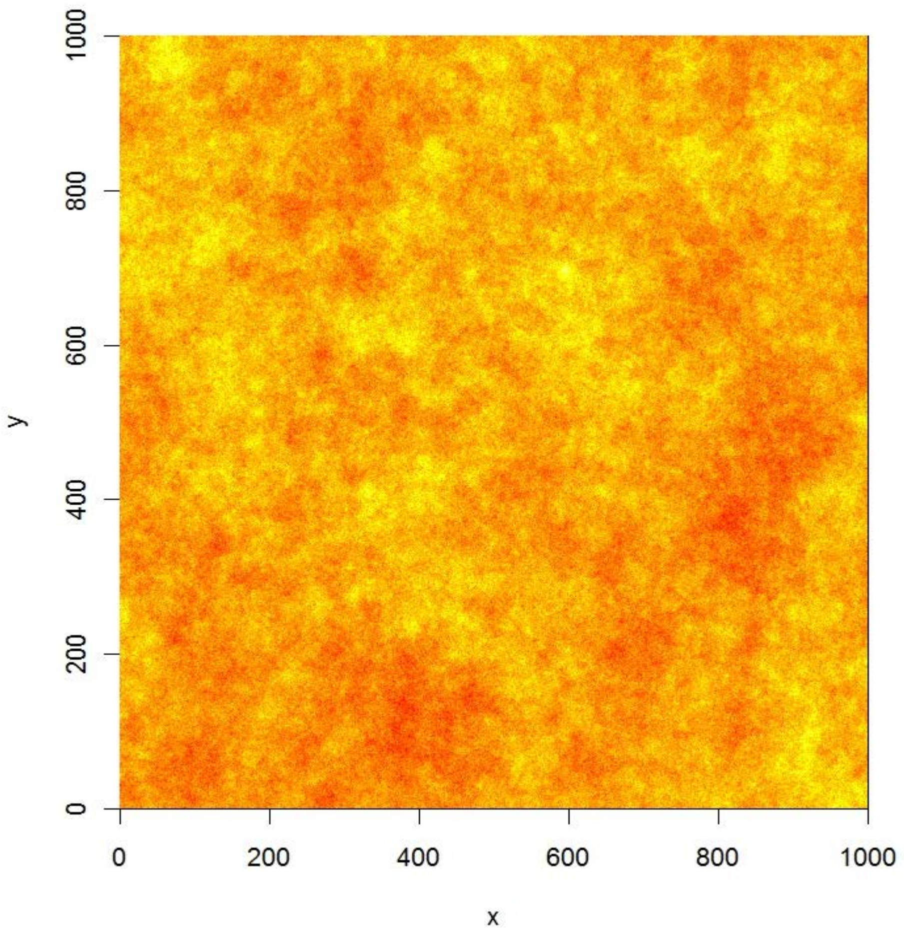

RFs with fractal + Hurst effects

Cauchy Dagum

three scales:

microscale:

mesoscale:

macroscale:

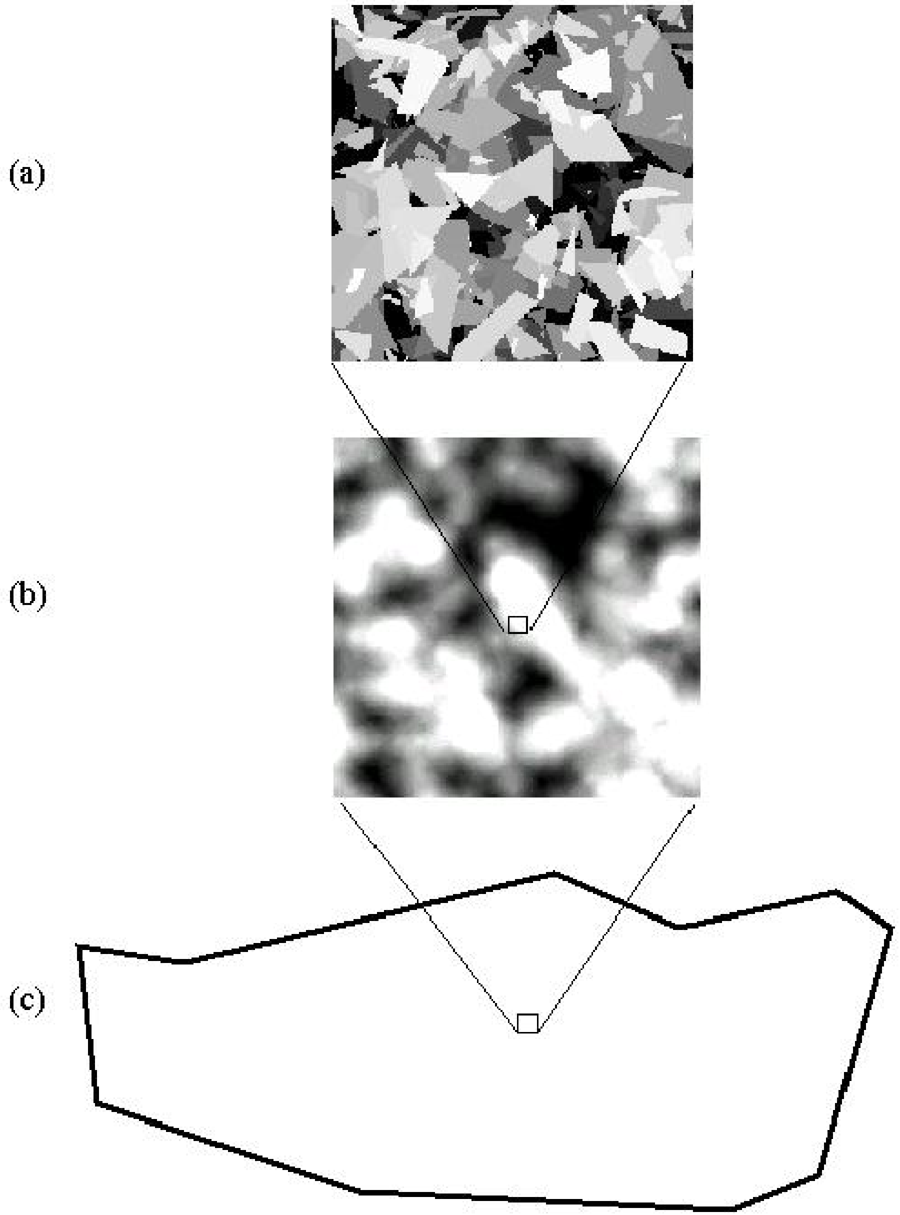

three scales:

microscale: average size of grain d
(microstructure)

mesoscale: L
~~representative volume element (RVE)~~
statistical volume element (SVE)

macroscale: L_{macro}

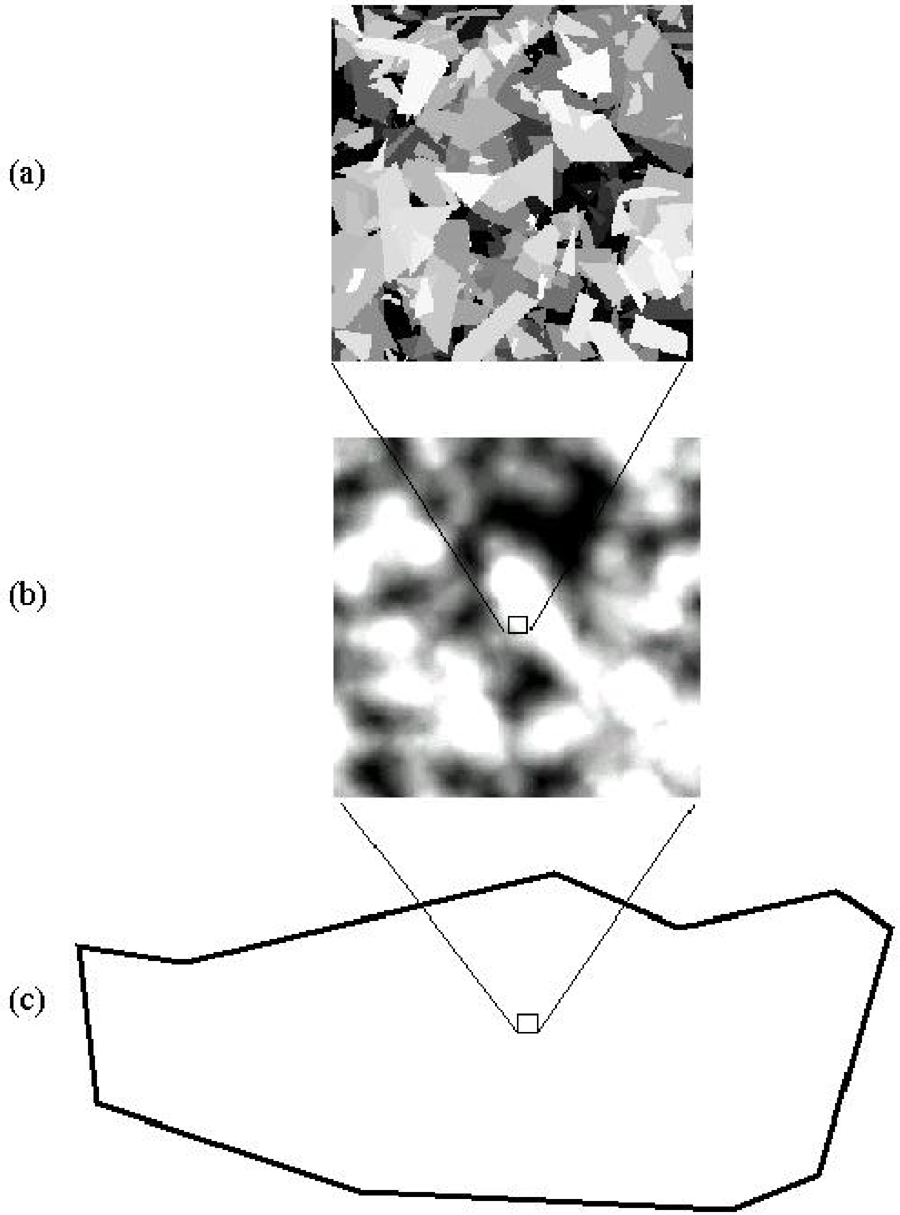

<u>three scales:</u>

microscale: average size of grain d
(microstructure)

mesoscale: L
~~representative volume element (RVE)~~
statistical volume element (SVE)

macroscale: L_{macro}

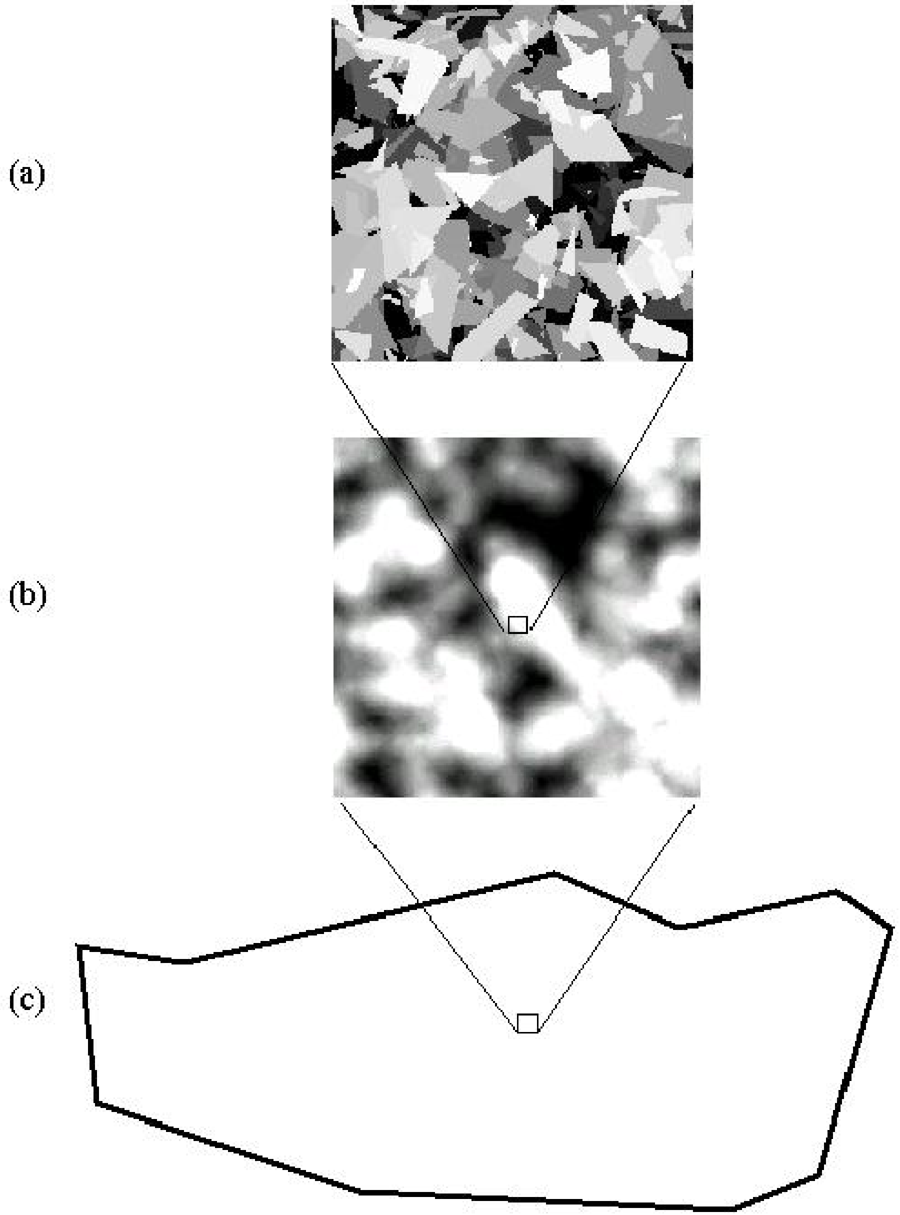

separation of scales $d << L << L_{macro}$
does not generally hold!
even without fractals

Random fields of displacement, strain, stress, rotation, curvature…

Stress RF: $S_{ijkl}(\mathbf{x}_1, \mathbf{x}_2) = \langle \sigma_{ij}(\mathbf{x}_1) \sigma_{kl}(\mathbf{x}_2) \rangle$

Stationary isotropic stress RF: $S_{ijkl}(x) = \sum_{\alpha} S_{\alpha}\left(x\right) J_{ijkl}^{\alpha}$

$$J_{ijkl}^{1} = \delta_{ij}\delta_{kl} \qquad J_{ijkl}^{2} = \delta_{ik}\delta_{jl} + \delta_{il}\delta_{jk}$$

$$J_{ijkl}^{3} = n_i n_j \delta_{kl} + n_k n_l \delta_{ij} \qquad J_{ijkl}^{5} = n_i n_j n_k n_l$$

$$J_{ijkl}^{4} = n_j n_k \delta_{il} + n_i n_l \delta_{jk} + n_i n_k \delta_{jl} + n_j n_l \delta_{ik}$$

$$x_i = n_i / x$$

Stress RF: $$S_{ijkl}(\mathbf{x}_1,\mathbf{x}_2)=\langle\sigma_{ij}(\mathbf{x}_1)\sigma_{kl}(\mathbf{x}_2)\rangle$$

Stationary isotropic stress RF: $$S_{ijkl}(x)=\sum_{\alpha} S_{\alpha}\left(x\right) J_{ijkl}^{\alpha}$$

$$J_{ijkl}^{1}=\delta_{ij}\delta_{kl} \qquad J_{ijkl}^{2}=\delta_{ik}\delta_{jl}+\delta_{il}\delta_{jk}$$

$$J_{ijkl}^{3}=n_i n_j\delta_{kl}+n_k n_l\delta_{ij} \qquad J_{ijkl}^{5}=n_i n_j n_k n_l$$

$$J_{ijkl}^{4}=n_j n_k\delta_{il}+n_i n_l\delta_{jk}+n_i n_k\delta_{jl}+n_j n_l\delta_{ik}$$

$$x_i=n_i / x$$

Strain RF: $$E_{ijkl}(\mathbf{x}_1,\mathbf{x}_2)=\langle[\varepsilon_{ij}(\mathbf{x}_1)-\left\langle\varepsilon_{ij}(\mathbf{x}_1)\right\rangle][\varepsilon_{kl}(\mathbf{x}_2)-\left\langle\varepsilon_{kl}(\mathbf{x}_2)\right\rangle]\rangle$$

Stationary isotropic strain RF: $$\rho_{ij}^{kl}(x)=\sum_{\alpha} E_{\alpha}\left(x\right) J_{ijkl}^{\alpha}$$

Every 2nd rank tensor field T can be decomposed into potential and birotational fields

$$T = T^{(1)} + T^{(2)}, \quad \text{curl } T^{(1)} = 0, \quad \text{div } T^{(2)} = 0$$

such that $T^{(1)} = \text{grad } \phi, \quad T^{(2)} = \text{curl } \Phi, \quad \text{div } \Phi = 0$

vector potential

tensor potential

Every 2nd rank tensor field T can be decomposed into potential and birotational fields

$$T = T^{(1)} + T^{(2)}, \quad \text{curl } T^{(1)} = 0, \quad \text{div } T^{(2)} = 0$$

such that $T^{(1)} = \text{grad } \phi, \quad T^{(2)} = \text{curl } \Phi, \quad \text{div } \Phi = 0$

vector potential   tensor potential

$\Rightarrow$ Given that $\varepsilon_{ij} = u_{(i,j)}$ and $\sigma_{ij,j} = 0$,

ε_{ij} is a potential field

σ_{ij} is birotational in the absence of body forces

Without loss of generality, $n_1 = n_2 = 0$ and $n_3 = n$, in matrix notation

$$S_{ijkl} = S_{12} J^1_{ijkl} + S_{66} J^2_{ijkl} + (S_{13} - S_{12}) J^3_{ijkl}$$
$$+ (S_{44} - S_{66}) J^4_{ijkl} + (S_{11} + S_{33} - 2S_{13} - 4S_{44}) J^5_{ijkl}$$

Since $S_{66} = (S_{11} - S_{12})/2$, only 5 out of 6 components of the stress correlation tensor are algebraically independent

Without loss of generality, $n_1 = n_2 = 0$ and $n_3 = n$, in matrix notation

$$S_{ijkl} = S_{12} J_{ijkl}^{1} + S_{66} J_{ijkl}^{2} + (S_{13} - S_{12}) J_{ijkl}^{3}$$

$$+(S_{44} - S_{66}) J_{ijkl}^{4} + (S_{11} + S_{33} - 2S_{13} - 4S_{44}) J_{ijkl}^{5}$$

Since $S_{66} = (S_{11} - S_{12}) / 2$, only 5 out of 6 components of the stress correlation tensor are algebraically independent

birotational property $\Longrightarrow$ $S_{ijkl,j} = 0$ $\Longrightarrow$ $rS_{13}^{'} + 2(S_{13} + S_{44} - S_{12} - S_{66}) = 0$

$$rS_{33}^{'} + 2(S_{33} - S_{13} - 2S_{44}) = 0$$

$$rS_{44}^{'} + 3S_{44} + S_{13} - S_{12} - 3S_{66} = 0$$

Without loss of generality, $n_1 = n_2 = 0$ and $n_3 = n$, in matrix notation

$$S_{ijkl} = S_{12} J^1_{ijkl} + S_{66} J^2_{ijkl} + (S_{13} - S_{12}) J^3_{ijkl}$$

$$+ (S_{44} - S_{66}) J^4_{ijkl} + (S_{11} + S_{33} - 2S_{13} - 4S_{44}) J^5_{ijkl}$$

Since $S_{66} = (S_{11} - S_{12})/2$, only 5 out of 6 components of the stress correlation tensor are algebraically independent

birotational property $\Longrightarrow$ $S_{ijkl,j} = 0$ $\Longrightarrow$

$$rS'_{13} + 2(S_{13} + S_{44} - S_{12} - S_{66}) = 0$$

$$rS'_{33} + 2(S_{33} - S_{13} - 2S_{44}) = 0$$

$$rS'_{44} + 3S_{44} + S_{13} - S_{12} - 3S_{66} = 0$$

$$\Longrightarrow 8S_{11} = (R+2)(R+4)S_{33} = 0$$

$$4S_{44} = (R+2)S_{33} - 2S_{13} \qquad R \equiv r\frac{d}{dr}$$

$$8S_{12} = 8(R+1)S_{13} - R(R+2)S_{33}$$

$\Longrightarrow$ first choose $S_{13},\ S_{33}$

Strain correlation tensor $E_{ijkl} = -\nabla_{(i}U_{j)(k,l)}$

where $U_{ij}(\mathbf{x}_1, \mathbf{x}_2) = \langle u_i(\mathbf{x}_1) u_j(\mathbf{x}_2) \rangle$

If homogeneous and isotropic, $U_{ij} = U_1\delta_{ij} + U_2 n_i n_j$

Potential property $\Longrightarrow$

$$r^2 E_{12} = -U_2 \qquad r^2 E_{66} = -2(U_2 + rU_1')$$

$$r^2(E_{13} - E_{12}) = 2U_2 + rU_2'$$

$$E_{66} = 2(E_{11} - E_{12})$$

$$r^2(E_{44} - E_{66}) = 6U_2 - 3rU_2' + rU_1' - r^2U_1''$$

$$r^2(E_{11} + E_{33} - 2E_{13} - E_{44}) = -8U_2 + 5rU_2' + r^2U_2''$$

Strain correlation tensor $$E_{ijkl} = -\nabla_{(i}U_{j)(k,l)}$$

where $$U_{ij}(\mathbf{x}_1, \mathbf{x}_2) = \langle u_i(\mathbf{x}_1) u_j(\mathbf{x}_2) \rangle$$

If homogeneous and isotropic, $$U_{ij} = U_1 \delta_{ij} + U_2 n_i n_j$$

Potential property $\Rightarrow$ $$r^2 E_{12} = -U_2 \qquad r^2 E_{66} = -2(U_2 + rU_1^{'})$$

$$r^2 (E_{13} - E_{12}) = 2U_2 + rU_2^{'}$$

$$E_{66} = 2(E_{11} - E_{12})$$

$$r^2 (E_{44} - E_{66}) = 6U_2 - 3rU_2^{'} + rU_1^{'} - r^2 U_1^{''}$$

$$r^2 (E_{11} + E_{33} - 2E_{13} - E_{44}) = -8U_2 + 5rU_2^{'} + r^2 U_2^{''}$$

$$\Rightarrow \quad E_{33} = (R+1)E_{11} + R(R+1)E_{12}$$

$$E_{44} = (R+1)E_{11} - (R-2)E_{12} \qquad R \equiv r\frac{d}{dr}$$

$$E_{13} = (R+1)E_{12}$$

$\Rightarrow$ first choose $E_{11},\ E_{12}$

OBSERVE

- For tensor-type properties of materials, need RFs consistent with mechanics
- Consistent with mechanics iff mechanical definition of properties = energetic definition of properties
- Random fields of properties are functions of microstructure + mesoscale
- Micromechanics analyses lead to counterintuitive results
- Can construct correlation functions from products of basic 1D models
- Can go to: micropolar models, coupled field phenomena, inelastic properties,…

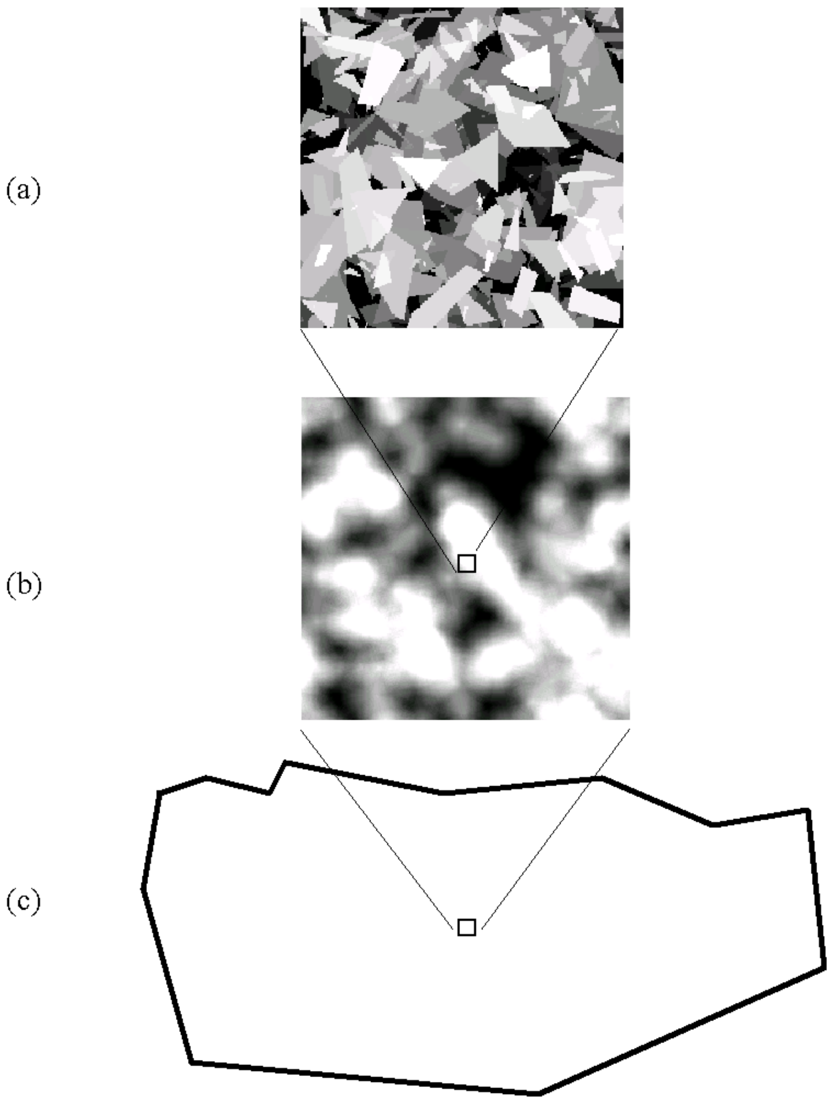

- 1^{th}-rank (scalar) statistically (wide-sense) isotropic TRF: Z_i

$\Rightarrow$ *covariance function*: $B_i^j(\mathbf{x}_1,\mathbf{x}_2) := \langle [T_i(\mathbf{x}_1) - \langle T_i(\mathbf{x}_1)\rangle][T_j(\mathbf{x}_2) - \langle T_j(\mathbf{x}_2)\rangle]\rangle$

… for homogeneous turbulence: $B_i^j(\mathbf{x}_1,\mathbf{x}_2) = B_i^j(\mathbf{x})$ $\quad \mathbf{x} = |\mathbf{x}_1 - \mathbf{x}_2|$

$$B_a^b(\hat{\mathbf{x}}) = c_{ai}c_{bj}B_i^j(\mathbf{x}) = c_{ai}c_{bj}B_i^j(c^{-1}\hat{\mathbf{x}})$$

rotation of system $\mathbf{x}$ into $\hat{\mathbf{x}}$ has to be accompanied by a simultaneous rotation of $T_i(\mathbf{x}_1)$ into $\hat{T}_a(\hat{\mathbf{x}}_1)$ as well as a rotation of $T_j(\mathbf{x}_2)$ into $\hat{T}_b(\hat{\mathbf{x}}_2)$

… the sea surface turbulence is neither spatially homogeneous nor isotropic

- 1^{th}-rank (scalar) statistically (wide-sense) isotropic TRF: Z_i

$\Rightarrow$ *covariance function*: $B_i^j(\mathbf{x}_1,\mathbf{x}_2) := \langle [T_i(\mathbf{x}_1) - \langle T_i(\mathbf{x}_1)\rangle][T_j(\mathbf{x}_2) - \langle T_j(\mathbf{x}_2)\rangle]\rangle$

… for homogeneous turbulence: $B_i^j(\mathbf{x}_1,\mathbf{x}_2) = B_i^j(\mathbf{x})$ $\quad \mathbf{x} = |\mathbf{x}_1 - \mathbf{x}_2|$

$$B_a^b(\hat{\mathbf{x}}) = c_{ai}c_{bj}B_i^j(\mathbf{x}) = c_{ai}c_{bj}B_i^j(c^{-1}\hat{\mathbf{x}})$$

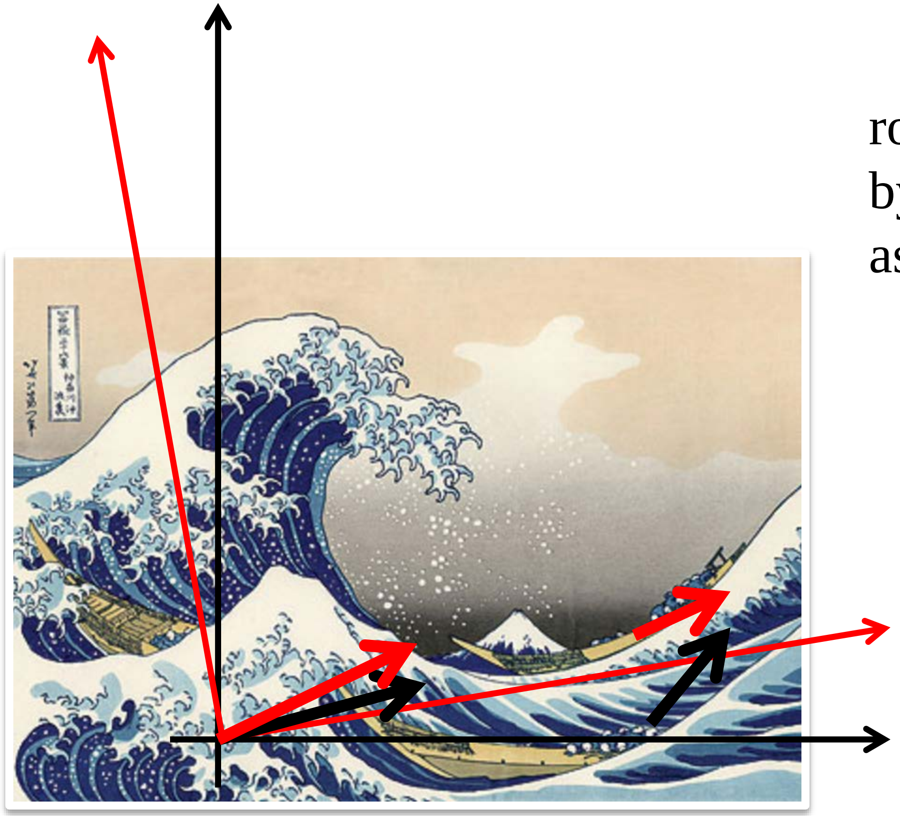

rotation of system $\mathbf{x}$ into $\hat{\mathbf{x}}$ has to be accompanied by a simultaneous rotation of $T_i(\mathbf{x}_1)$ into $\hat{T}_a(\hat{\mathbf{x}}_1)$ as well as a rotation of $T_j(\mathbf{x}_2)$ into $\hat{T}_b(\hat{\mathbf{x}}_2)$

… the sea surface turbulence is neither spatially homogeneous nor isotropic

locally isotropic or anisotropic, and statistically isotropic TRFs

Two kinds of isotropy of tensor random fields (TRFs):

- local $\quad C_{ij} = C\delta_{ij}$
- statistical

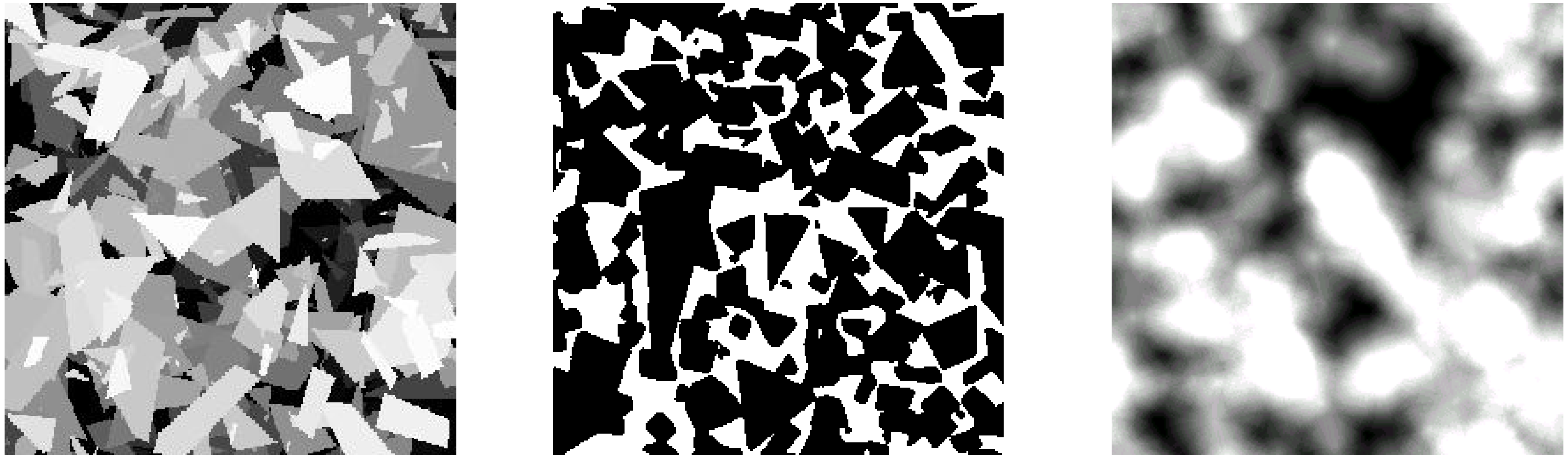

can have locally anisotropic and/or statistically anisotropic TRFs

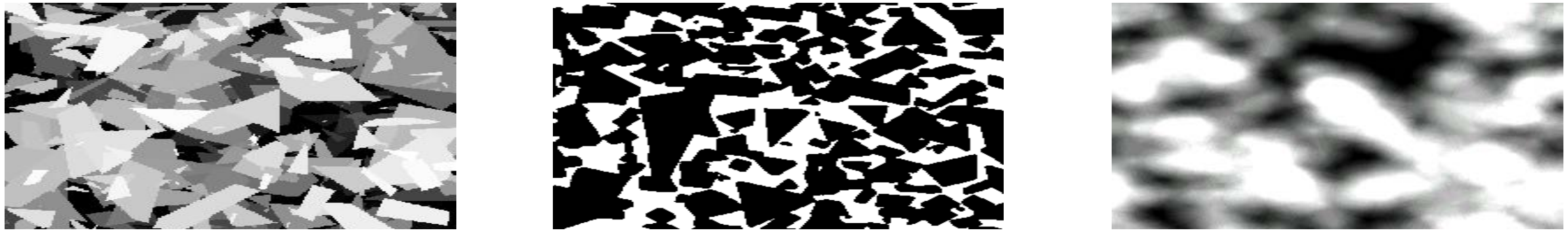

MECHANICS OF RANDOM MATERIALS

Lattice (Spring Network) Models

Martin Ostoja-Starzewski
Mechanical Science & Engineering, UIUC

1. Some One-Dimensional Lattices:

1.1 Simple lattice and elastic string

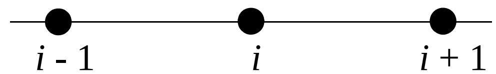

1-D chain of particles of lattice spacing s, connected by axial springs

$$U = \frac{1}{2}\sum_i F_i(u_{i+1} - u_i) = \frac{1}{2}\sum_i K(u_{i+1} - u_i)^2 \qquad T = \frac{1}{2}\sum_i m\dot{u}_i^2 \tag{1.1}$$

$\Rightarrow$

$$K(u_{i+1} - 2u_i + u_{i-1}) = m\ddot{u}_i$$

Taylor expansion up to 2nd derivative: $$u_{i \pm 1} \cong u\big|_{x_i} \pm u_{,x}\big|_{x_i} s + \frac{1}{2!}u_{,xx}\Big|_{x_i} s^2 \tag{1.3}$$

$\Rightarrow$ wave equation

$$EAu_{,xx} = \rho A\ddot{u} \qquad E = \frac{Ks}{A} \qquad \rho = \frac{m}{As} \tag{1.4}$$

Note: this can also be obtained from Hamilton's principle with L in terms of continuum-like quantities, by first introducing (1.3) in $(1.1)_1$ with terms up to 1st derivative

$$U = \frac{AE}{2}\int_0^d (u_{,x})^2 dx \qquad T = \frac{A\rho}{2}\int_0^d (\dot{u})^2 dx \qquad (1.6)$$

1.2 Micropolar lattice and elastic beam

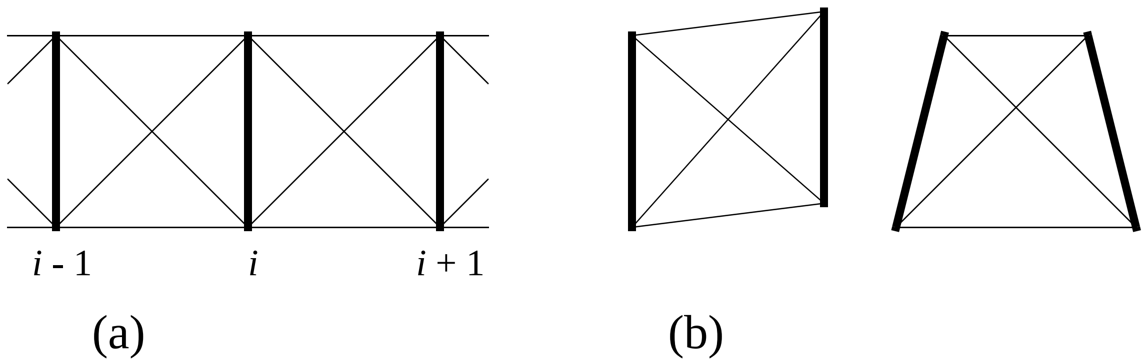

(a) 1-D chain of dumbbell particles (vertical rigid bars) of X-braced girder geometry, pin-connected by axial springs (thin lines); (b) shear and curvature modes of a single bay.

two DOF per particle i: w_i and φ_i.

constitutive laws for a single bay (i to $i+1$)

$$\tilde{F}_i = K_{\perp}(w_{i+1} - w_i - s\varphi_{i+1}) \qquad M_i = -\widehat{K}(\varphi_{i+1} - \varphi_i) \qquad (1.7)$$

... introducing Taylor expansions for w_i and φ_i with terms up to 2nd derivative, and taking the limit $s \to 0$, we find Timoshenko beam equations

$$GA[w_{,x} - \varphi]_{,x} = \rho A\ddot{w} \qquad EI\varphi_{,xx} + GA[w_{,x} - \varphi] = \rho I\ddot{\varphi} \qquad (1.10)$$

$$U = \frac{1}{2}\sum_i K_\perp [w_{i+1} - w_i - s\varphi_{i+1}]^2 + \widehat{K}(\varphi_{i+1} - \varphi_i)^2 \qquad T = \frac{1}{2}\sum_i m\dot{w}_i^2 + J\dot{\varphi}_i^2 \tag{1.8}$$

Note: alternatively, this could be obtained by first introducing Taylor series with terms up to 1st derivative into $(1.8)_1$, to first get

$$U = \frac{1}{2}\int_0^d [GA(w_{,x})^2 + EI(\varphi_{,x})^2]dx \qquad T = \frac{1}{2}\int_0^d [A\rho(\dot{w})^2 + I\rho(\dot{\varphi})^2]dx \tag{1.12}$$

and then, by employing the Hamilton's principle.

Can other, more complex (micro)structures, e.g. made of little beams connected by rigid joints of beam-like geometry, be sufficiently well described by this beam model? No

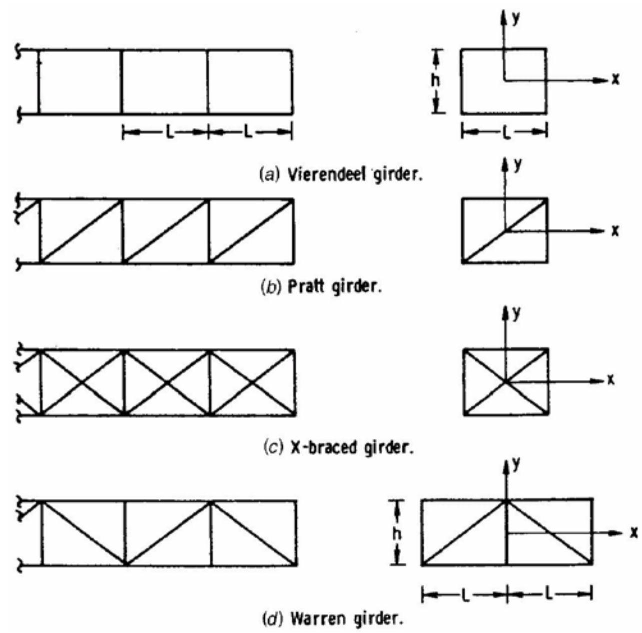

Noor & Nemeth (1980) recommend:

(i) the equivalent micropolar beam model is set up from the postulate $U = K$ stored in the original lattice when both are deformed identically;

(ii) typical repeating element is identified and energies for this element are expressed in terms of nodal displacements, joint rotations, and geometric and material properties of individual members;

(iii) a passage to an effective continuum is carried out via a Taylor expansion, with higher-order terms showing up in the governing continuum equations, depending on the actual microgeometry of the rods making up the structure.

1.3 Axial-twisting coupling and dynamics of a wire rope (helix)

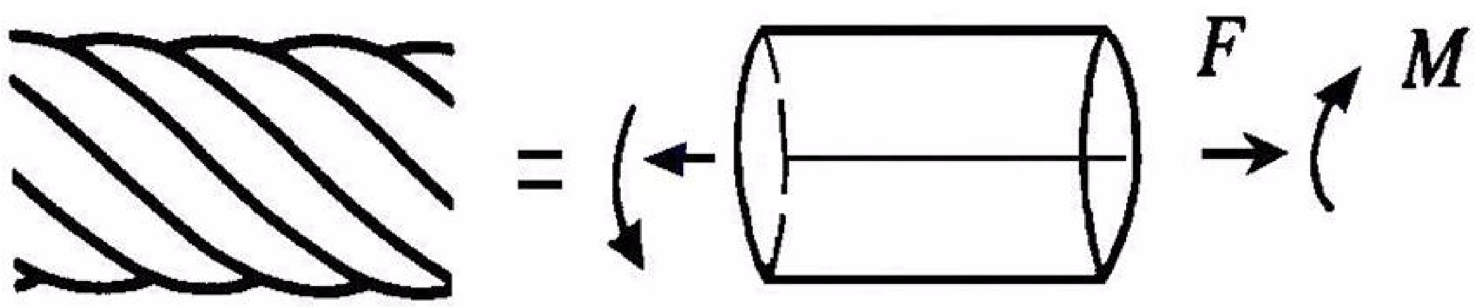

Wire rope of a constant helix angle.

$\Rightarrow$ a coupling between the axial force F and torque M on one hand, and the axial strain ε and rotational strain $\beta = R\tau_s$

$$F = C_{11}\varepsilon + C_{12}\beta \qquad M = C_{21}\varepsilon + C_{22}\beta \qquad (1.12)$$

positive strain energy density $\Rightarrow$

$$C_{12} = C_{21} \qquad C_{11}C_{22} \pm C_{12}C_{21} > 0 \qquad (1.13)$$

$\Rightarrow$ wire rope is a 1-D micropolar medium of a *non-centrosymmetric* type,
also called *hemitropic*, *antisymmetric*, or *chiral composite*

$\Rightarrow$ two coupled wave equations governing the axial-twisting response of a wire

$$C_{11}u_{,xx} + C_{12}\varphi_{,xx} = \rho\ddot{u} \qquad C_{21}u_{,xx} + C_{22}\varphi_{,xx} = J\ddot{\varphi} \tag{1.14}$$

with wave speeds

$$c_{1,2} = \frac{2(C_{11}C_{22} - C_{12}C_{21})}{(C_{11}J + C_{22}\rho) \pm [(C_{11}J - C_{22}\rho)^2 + 4\rho J C_{12}C_{21}]^{1/2}} \tag{1.16}$$

$\Rightarrow c_1 < c_2$

axial vibrations of the wire are described by two types of waves slow and fast

$$\begin{aligned} u(x,t) &= U_1 e^{ik(x-c_1t)} + U_2 e^{ik(x+c_1t)} + U_3 e^{ik(x-c_2t)} + U_4 e^{ik(x+c_2t)} \\ \varphi(x,t) &= \Phi_1 e^{ik(x-c_1t)} + \Phi_2 e^{ik(x+c_1t)} + \Phi_3 e^{ik(x-c_2t)} + \Phi_4 e^{ik(x+c_2t)} \end{aligned} \tag{1.17}$$

Note: the waves that are primarily axial in nature ($U/\Phi > 1$) propagate at speeds c_2,

the waves that are primarily torsional in nature ($U/\Phi < 1$) propagate at speeds c_1.

2. Planar Spring Networks on Periodic Lattices: Classical Continua

2.1 Basic idea of a spring network representation

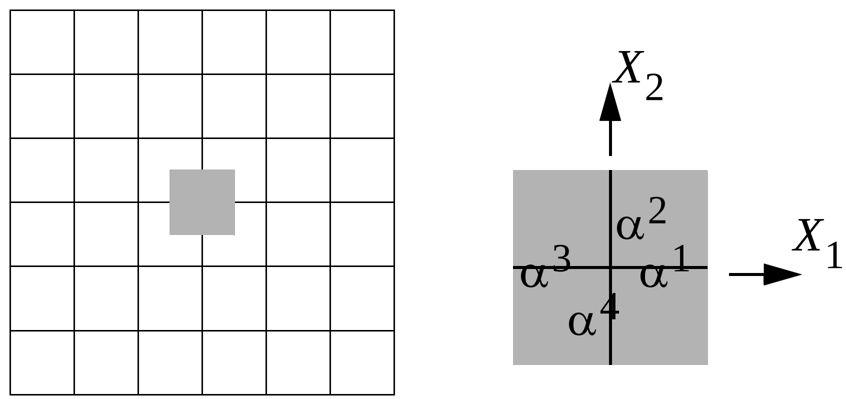

equivalence of strain energies in the unit cell of volume V

$$U_{cell} = U_{continuum} \tag{2.1}$$

where

$$\begin{aligned} U_{cell} &= \sum_b E_b = \frac{1}{2}\sum_b^{N_b} (\boldsymbol{F} \cdot \boldsymbol{u})^{(b)} = \frac{1}{2}\sum_b^{|b|} (k\boldsymbol{u} \cdot \boldsymbol{u})^{(b)} \\ U_{continuum} &= \frac{1}{2}\int_V \sigma \cdot \varepsilon dV = \frac{V}{2}\varepsilon \cdot \boldsymbol{C} \cdot \varepsilon \end{aligned} \tag{2.2}$$

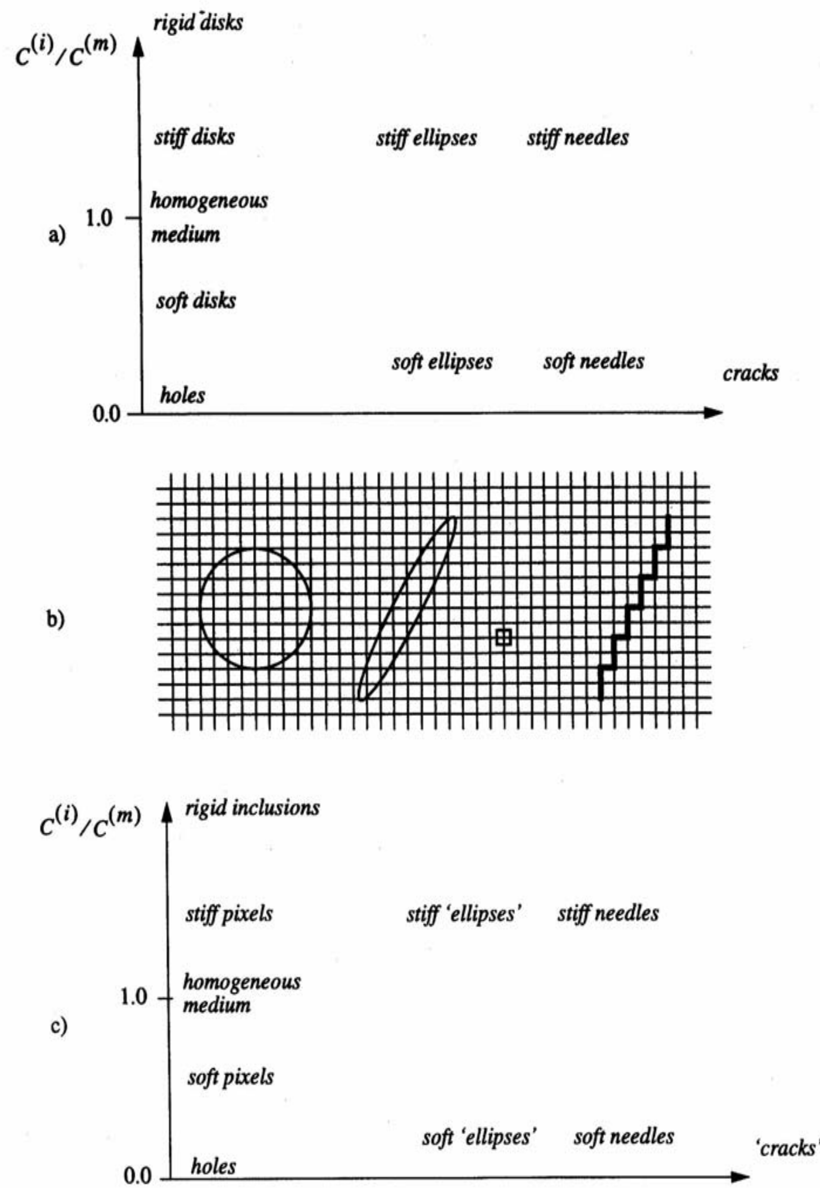

$C^{(i)}/C^{(m)}$
rigid disks
stiff disks
stiff ellipses
stiff needles
homogeneous
medium
1.0
a)
soft disks
soft ellipses
soft needles
cracks
holes
0.0
b)
$C^{(i)}/C^{(m)}$
rigid inclusions
stiff pixels
stiff 'ellipses'
stiff needles
1.0
homogeneous
medium
c)
soft pixels
soft 'ellipses'
soft needles
'cracks'
holes
0.0

2.2 Anti-plane elasticity on square lattice

$$\sigma_i = C_{ij}\varepsilon_j \qquad i, j = 1, 2 \tag{2.4}$$

where $\sigma = (\sigma_1, \sigma_2) \equiv (\sigma^0_{31}, \sigma^0_{32})$ and $\varepsilon = (\varepsilon_1, \varepsilon_2) \equiv (\varepsilon^0_{31}, \varepsilon^0_{32})$

... locally homogeneous medium

$$C_{ij}u_{,ij} = 0 \qquad \Rightarrow \qquad Cu_{,ii} = 0 \tag{2.7}$$

for square lattice:
each node has one DOF (anti-plane displacement u),
nearest neighbor nodes are connected by springs of constant k.

$$U_{cell} = U = \frac{1}{2}k\sum_{b=1}^{4} l_i^{(b)}l_j^{(b)}\varepsilon_i\varepsilon_j \qquad U_{continuum} = \frac{1}{2}\int_V \varepsilon_i C_{ij}\varepsilon_j dV \tag{2.9}$$

$\Rightarrow$

$$C_{11} = C_{22} = \frac{k}{2} \qquad C_{12} = C_{21} = 0 \tag{2.11}$$

2.3 In-plane elasticity: triangular lattice with central interactions

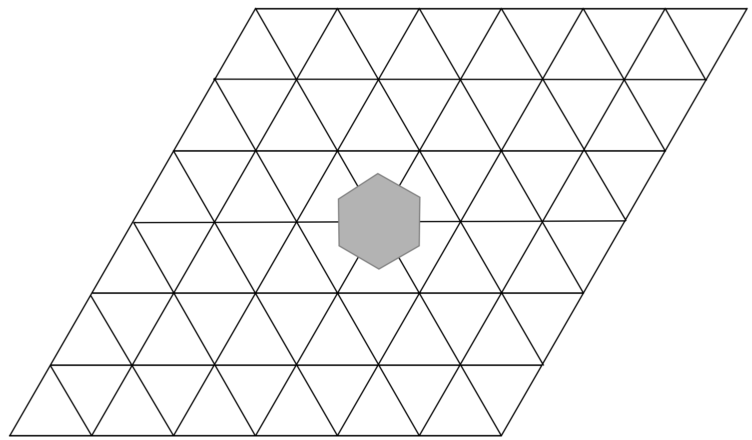

Triangular lattice with a hexagonal unit cell shown.

planar continuum Hooke's law

$$\sigma_{ij} = C_{ijkm}\varepsilon_{km} \qquad i, j, k, m = 1, 2 \tag{2.16}$$

planar Navier's equation for the displacement u_i

$$\mu u_{i,jj} + \kappa u_{j,ji} = 0 \tag{2.18}$$

where μ is defined by $\sigma_{12} = \mu\varepsilon_{12}$ (the same as 3-D)

$$\sigma_{ii} = \kappa\varepsilon_{ii}$$

central force interactions

$$F_i = \Phi_{ij}^{(b)} u_j \qquad where \qquad \Phi_{ij}^{(b)} = \alpha^{(b)} n_i^{(b)} n_j^{(b)} \tag{2.19}$$

$\alpha^{(b)}$ = spring constant of half-lengths of such central (normal) interactions

$$\begin{aligned} \theta^{(1)} &= 0^o & n_1^{(1)} &= 1 & n_2^{(1)} &= 0 \\ \theta^{(2)} &= 60^o & n_1^{(2)} &= \frac{1}{2} & n_2^{(2)} &= \frac{\sqrt{3}}{2} \\ \theta^{(3)} &= 120^o & n_1^{(3)} &= -\frac{1}{2} & n_2^{(3)} &= \frac{\sqrt{3}}{2} \end{aligned} \tag{2.20}$$

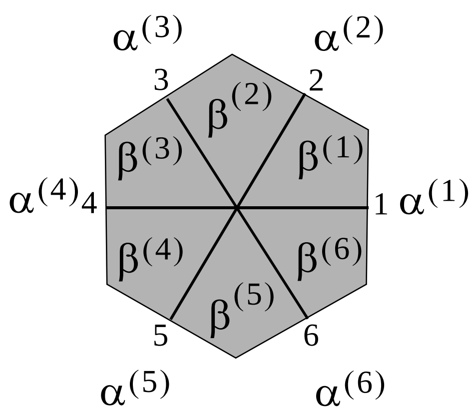

under uniform strain $\varepsilon = (\varepsilon_{11}, \varepsilon_{22}, \varepsilon_{12})$

$$U_{cell} = \frac{l^2}{2} \sum_{b=1}^{6} \alpha^{(b)} n_i^{(b)} n_j^{(b)} n_k^{(b)} n_m^{(b)} \varepsilon_{ij} \varepsilon_{km} \tag{2.21}$$

$\Rightarrow$

$$C_{ijkm} = \frac{l^2}{V} \sum_{b=1}^{6} \alpha^{(b)} n_i^{(b)} n_j^{(b)} n_k^{(b)} n_m^{(b)} \tag{2.22}$$

if $\alpha^{(b)}$ the same,

$$C_{1111} = C_{2222} = \frac{9}{8\sqrt{3}}\alpha \qquad C_{1122} = C_{2211} = \frac{3}{8\sqrt{3}}\alpha \qquad C_{1212} = \frac{3}{8\sqrt{3}}\alpha \tag{2.23}$$

$\Rightarrow$ continuum is isotropic and only one independent elastic modulus

Note: Cauchy symmetry

$$C_{ijkm} = C_{ijmk} = C_{jikm} = C_{kmij} = C_{ikjm} \tag{2.24}$$

$\Rightarrow$

$$C_{ijkm} = \lambda(\delta_{ij}\delta_{km} + \delta_{ik}\delta_{jm} + \delta_{im}\delta_{jk}) \tag{2.25}$$

i.e. classical Lamé constants

$$\lambda = \mu = \frac{3}{4\sqrt{3}}\alpha \tag{2.26}$$

2.4 In-plane elasticity: triangular lattice with central and angular interactions

add angular springs acting between the contiguous bonds incident onto the same node

$\beta^{(b)}$

$\Rightarrow$ six spring constants: $\{\{\alpha^{(1)}, \alpha^{(2)}, \alpha^{(3)}, \beta^{(1)}, \beta^{(2)}, \beta^{(3)}\}$.

$\Rightarrow$ generalization of the *Kirkwood model* (1939) of isotropic material

[the same α and β springs]

$$C_{ijkm} = \frac{\alpha}{2\sqrt{3}} \sum_{b=1}^{6} n_i^{(b)} n_j^{(b)} n_k^{(b)} n_m^{(b)} + \tag{2.30}$$

$$\frac{\beta}{2\sqrt{3}l^2} \sum_{b=1}^{6} \Big\{ 2\delta_{ik} n_j^{(b)} n_m^{(b)} - 2 n_i^{(b)} n_j^{(b)} n_k^{(b)} n_m^{(b)} - \delta_{ik} n_p^{(b)} n_j^{(b+1)} n_p^{(b+1)} n_m^{(b)} +$$

$$n_i^{(b)} n_j^{(b+1)} n_k^{(b+1)} n_m^{(b)} - \delta_{ik} n_p^{(b)} n_j^{(b)} n_p^{(b+1)} n_m^{(b+1)} + n_i^{(b+1)} n_j^{(b)} n_k^{(b)} n_m^{(b+1)} \Big\}$$

$\Rightarrow$

$$C_{1111} = C_{2222} = \frac{1}{2\sqrt{3}}\left(\frac{9}{4}\alpha + \frac{1}{l^2}\beta\right)$$

$$C_{1122} = C_{2211} = \frac{1}{2\sqrt{3}}\left(\frac{3}{4}\alpha - \frac{1}{l^2}\frac{9}{4}\beta\right) \tag{2.31}$$

$$C_{1212} = \frac{1}{2\sqrt{3}}\left(\frac{3}{4}\alpha + \frac{1}{l^2}\frac{9}{4}\beta\right)$$

$\Rightarrow$ two independent: planar bulk and shear moduli

$$\kappa = \frac{1}{2\sqrt{3}}\left(\frac{3}{2}\alpha\right) \qquad \mu = \frac{1}{2\sqrt{3}}\left(\frac{3}{4}\alpha + \frac{1}{l^2}\frac{9}{4}\beta\right) \tag{2.32}$$

$\Rightarrow$ planar Poisson's ratio

$$\nu = \frac{\kappa - \mu}{\kappa + \mu} = \frac{C_{1111} - 2C_{1212}}{C_{1111}} = \left(1 - \frac{3\beta}{\alpha l^2}\right) \Big/ \left(3 + \frac{3\beta}{\alpha l^2}\right) \tag{2.33}$$

$\Rightarrow$

$$\nu = \frac{1}{3} \qquad if \qquad \beta/\alpha \to 0 \qquad \alpha - model$$

$$\nu = -1 \qquad if \qquad \beta/\alpha \to \infty \qquad \beta - model \tag{2.34}$$

2.5 Triple honeycomb lattice Day *et al*. (1992); Snyder *et al*. (1992)

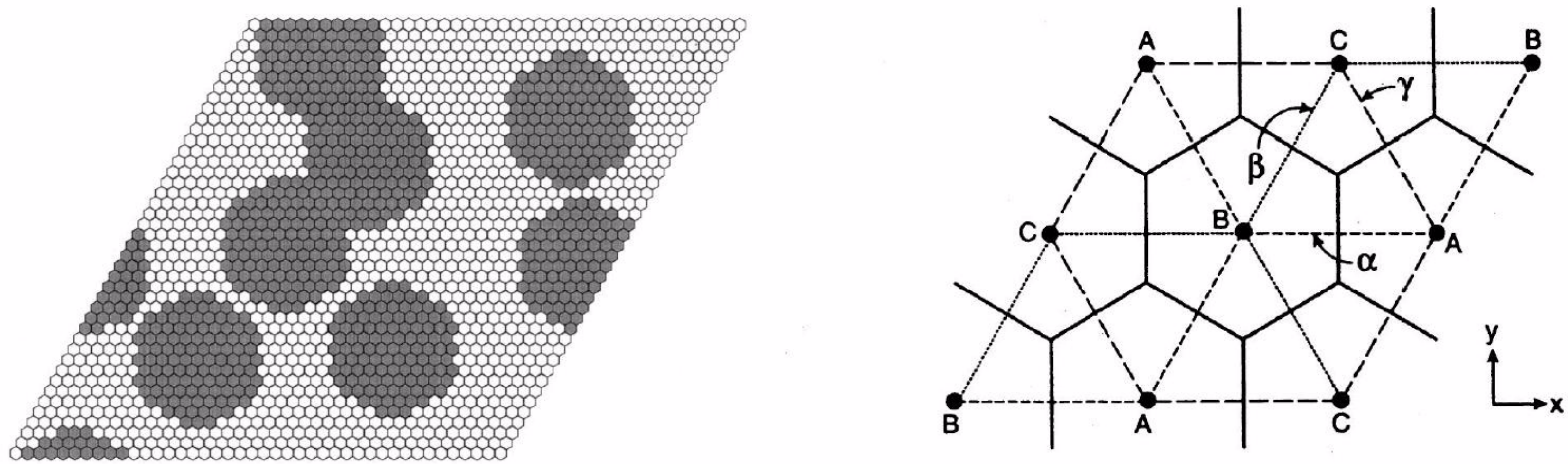

(a) (b)

three honeycomb lattices, with constants α, β, and γ, forming a single triangular lattice

spring assignement $\alpha = [(2\alpha_1)^{-1} + (2\alpha_2)^{-1}]$

$$\kappa = \frac{1}{\sqrt{12}}(\alpha + \beta + \gamma) \qquad \mu = \sqrt{\frac{27}{16}}\left(\frac{1}{\alpha} + \frac{1}{\beta} + \frac{1}{\gamma}\right)^{-1} \tag{2.35}$$

⇒ model permitting planar Poisson's ratio from 1/3 up to 1

3. Applications in Mechanics of Composites

3.1 Representation by a fine mesh

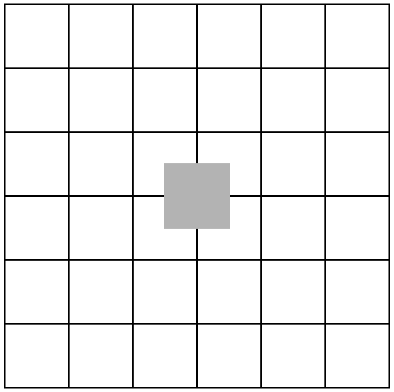

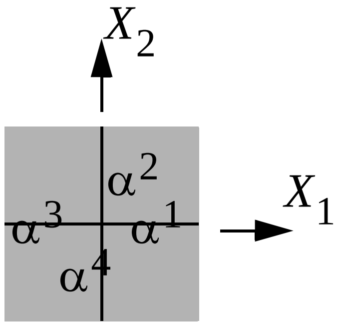

from $\nabla^2 u$ in 2-D $\Rightarrow$

$$[k_r + k_l + k_u + k_d] - u(i+1, j)k_r - u(i-1, j)k_l - u(i, j+1)k_u - u(i, j-1)k_d \quad (3.1)$$

with $[C(i, j)$ is the property at $(i, j)]$

$$\begin{aligned} k_r &= [1/C(i, j) + 1/C(i+1, j)]^{-1} \\ k_l &= [1/C(i, j) + 1/C(i-1, j)]^{-1} \\ k_u &= [1/C(i, j) + 1/C(i, j+1)]^{-1} \\ k_d &= [1/C(i, j) + 1/C(i, j-1)]^{-1} \end{aligned} \quad (3.2)$$

this discretization is equivalent to a finite difference method (via expansions)

$$
\begin{aligned}
u(i \pm 1, j) &= u(i, j) \pm s\frac{\partial}{\partial x_1}(u(i, j))\Big|_{i, j} + \frac{s^2}{2!}\frac{\partial^2}{\partial x_1^2}u(i, j)\Big|_{i, j} \\
u(i, j \pm 1) &= u(i, j) \pm s\frac{\partial}{\partial x_2}(u(i, j))\Big|_{i, j} + \frac{s^2}{2!}\frac{\partial^2}{\partial x_2^2}u(i, j)\Big|_{i, j}
\end{aligned}
\tag{3.3}
$$

in the governing equation $C\left(\frac{\partial^2 u}{\partial x_1^2} + \frac{\partial^2 u}{\partial x_2^2}\right) = 0$

Note: in the case of in-plane elasticity problems, the spring network is not identical to the finite difference method, because the node-node connections of spring network do not have a meaning of springs, whereas the finite difference connections do not.

Parameter plane

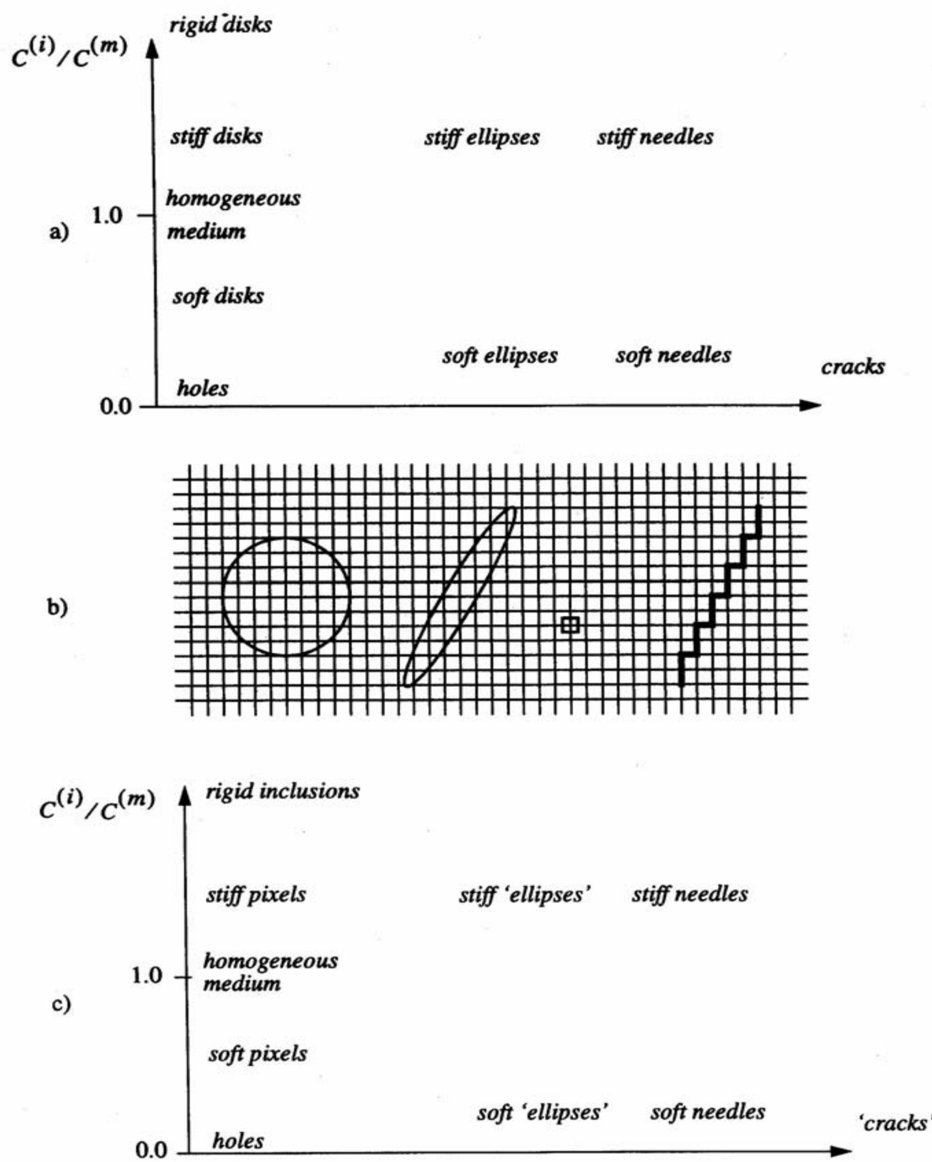

1. for a composite made of two locally isotropic phases: matrix (*m*) and inclusions (*i*)

$$\sigma_i = C_{ij}\varepsilon_j \qquad i, j = 1, 2 \qquad C_{ij} = C^{(m)}\delta_{ij} \qquad or \qquad C^{(i)}\delta_{ij} \tag{3.5}$$

$$\Rightarrow \quad contrast\ C^{(i)}/C^{(m)} \ \ (mismatch)$$

2. aspect ratio of ellipses a/b

3.2 Solutions of linear algebraic problems

elliptic problems in discretized form $\Rightarrow$ linear algebraic systems

$$\boldsymbol{A} \cdot \boldsymbol{x} = \boldsymbol{b} \tag{3.6}$$

$\Rightarrow$ in principle, two methods to set up and solve the governing equations:

(i) exact - via global stiffness matrix accompanied by the connectivity of all the nodes

(ii) iterative - via energy minimization (e.g. *conjugate gradient method*) $\Rightarrow$ energy

$$F(\boldsymbol{x}) = \frac{1}{2}x \cdot \boldsymbol{A} \cdot \boldsymbol{x} - \boldsymbol{b} \cdot \boldsymbol{x} \tag{3.7}$$

with

$$\nabla F(\boldsymbol{x}) = \boldsymbol{A} \cdot \boldsymbol{x} - \boldsymbol{b} \tag{3.8}$$

with respect to all the DOFs
e.g. (*Numerical Receipes*, Press *et al*., 1992)

... other algebraic solvers

Note: the entire task of mesh generation - such as typically required by FE - is absent

Procedure:
(i) the energy and energy gradient subroutines are written only once for the given mesh

(ii) the assignment of all the local spring stiffnesses - according to any chosen lattice model - is done very rapidly in the first stage of the program

(iii) these stiffnesses are stored in the common block (in case of a Fortran program) and are readily accessible to the conjugate gradient subroutines that are activated in the second, and main, stage of the program

(iv) once the energy minimum is reached to within any specified accuracy, this energy is used to compute the overall, effective moduli of a given domain of the lattice based on the postulate of the energy equivalence

Some exact relations that may be used in testing computer programs:

(i) Suppose we have solutions of two elasticity problems on a certain domain B, with boundary ∂B, corresponding to the displacement (d) and traction (t) boundary value problems, respectively. Then we can check whether Betti's reciprocity theorem

$$\int_{\partial B} u_i^{(t)} t_i^{(d)} ds = \int_{\partial B} u_i^{(d)} t_i^{(t)} ds \tag{3.9}$$

is satisfied numerically within some acceptable accuracy.

(ii) Perfect series and parallel systems are well known to result in the arithmetic (Voigt) and harmonic (Reuss) averages

$$C^V = f_1 C_1 + f_2 C_2 \qquad C^R = \left(\frac{f_1}{C_1} + \frac{f_2}{C_2} \right)^{-1} \tag{3.10}$$

where f_1 and f_2 are the volume fractions of phases and 1 and 2, respectively.

(iii) The case of small contrast in properties allows an expansion of, say, effective conductivity to second order in the difference $(C_2 - C_1)$ as follows (Torquato, 1997)

$$C^{eff} = C_1 + f_2(C_2 - C_1) - f_1 f_2 \frac{(C_2 - C_1)^2}{C_1} \frac{1}{d} + O(C_2 - C_1)^3 + \ldots \qquad (3.11)$$

where d is the dimensionality of the space.

(iv) Exact relation in conductivity (Keller, 1964): for a two-phase isotropic system in 2-D,

$$C^{eff}(C_1, C_2) C^{eff}(C_2, C_1) = C_1 C_2 \qquad (3.12)$$

where $C^{eff}(C_1, C_2)$ = effective conductivity of a given system,

$C^{eff}(C_1, C_2)$ = effective conductivity with phases 1 and 2 interchanged.

(v) Note the CLM Theorem (Cherkaev, Lurie, Milton, 1992; Thorpe & Jasiuk, 1992): transformation of an original 2-D material with properties $(\kappa(\boldsymbol{x}), \mu(\boldsymbol{x}))$ into a new material with properties $(\bar{\kappa}(\boldsymbol{x}), \bar{\mu}(\boldsymbol{x}))$

$$\frac{1}{\bar{\kappa}} = \frac{1}{\kappa} + \frac{1}{\Lambda} \qquad \frac{1}{\bar{\mu}} = \frac{1}{\mu} - \frac{1}{\Lambda} \qquad \Lambda = const$$

preserves the stress state

equivalently,

$$A \equiv \frac{1}{\kappa} \qquad S \equiv \frac{1}{\mu} \qquad c = \frac{1}{\Lambda}$$

$\Rightarrow$ effective compliances

$$\frac{1}{\bar{\kappa}^{eff}} = \frac{1}{\kappa^{eff}} + \frac{1}{\Lambda} \qquad \frac{1}{\bar{\mu}^{eff}} = \frac{1}{\mu^{eff}} - \frac{1}{\Lambda} \qquad \Lambda = const$$

... for isotropic or anisotropic materials, compliance is transformed/shifted by $S^I_{ijkl}(\Lambda, -\Lambda)$

$$S^T_{ijkl} = S_{ijkl} + S^I_{ijkl}(\Lambda, -\Lambda)$$

with

$$S^I_{ijkl}(\Lambda, -\Lambda) = \frac{1}{2\Lambda}\left[\frac{1}{2}\delta_{ij}\delta_{kl} - \frac{1}{2}(\delta_{ik}\delta_{jl} + \delta_{il}\delta_{jk} - \delta_{ij}\delta_{kl})\right]$$

$\Rightarrow$ effective compliance tensor of the second material is given by that of the first material plus the same shift as that for the individual phases

$$S^{effT}_{ijkl} = S^{eff}_{ijkl} + S^I_{ijkl}(\Lambda, -\Lambda) \tag{3.16}$$

<u>Parallel computing</u>

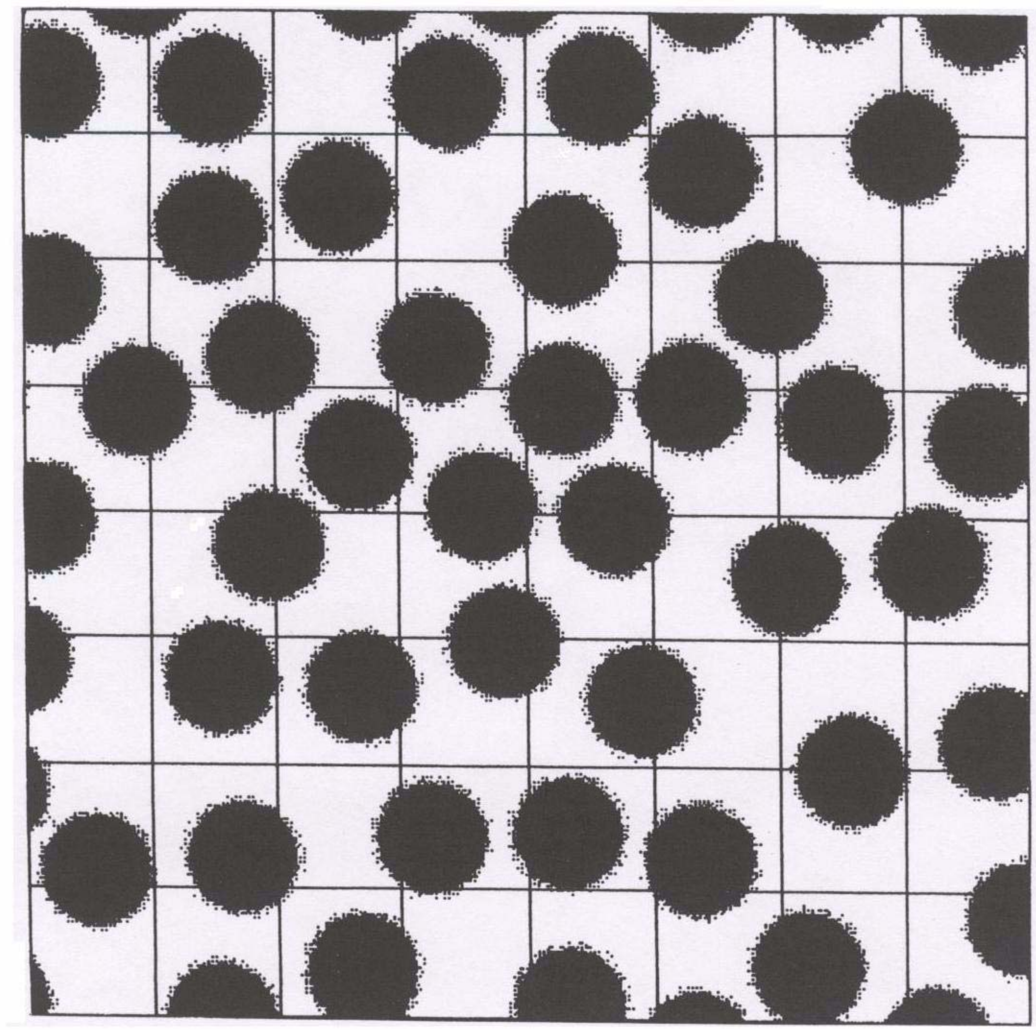

A functionally graded matrix-inclusion composite with 47.2% volume fraction of black phase is partitioned into 8×8 subdomains - 64-processor parallel computer.

3.3 Example simulation of a polycrystal

very thin polycrystalline aluminum specimen (Grah et al., *Acta Mater.* 1996)

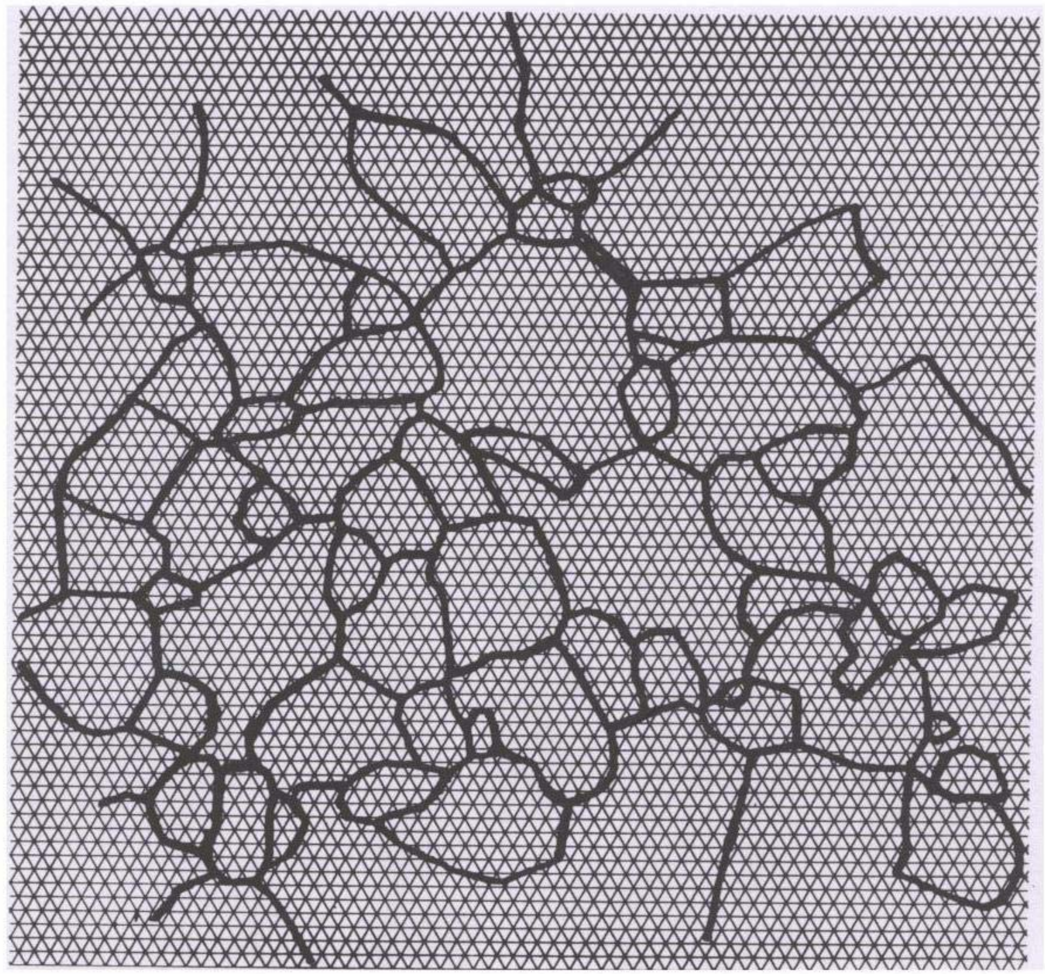

(i) an image of crystal domains is scanned and mapped onto a triangular mesh

the 3-D stiffness tensor C_{ijkm} for each crystal is found according to its transformation matrix a_{ij} $(i, j = 1, 2, 3)$ (via 'Kikuchi surface electron backscattering')

(ii) every bond is assigned its stiffness depending on the domain it falls in, i.e.

- map

$$C_{\alpha\beta}^{Al} = \begin{bmatrix} 10.82 & 6.13 & 6.13 & 0 & 0 & 0 \\ 6.13 & 10.82 & 6.13 & 0 & 0 & 0 \\ 6.13 & 6.13 & 10.82 & 0 & 0 & 0 \\ 0 & 0 & 0 & 2.85 & 0 & 0 \\ 0 & 0 & 0 & 0 & 2.85 & 0 \\ 0 & 0 & 0 & 0 & 0 & 2.85 \end{bmatrix} 10^4 MPa \qquad (4.3.17)$$

- to local stiffnesses via

$$C'_{npqr} = a_{ni}a_{jp}a_{kq}a_{mr}C_{ijkm} \qquad n, p, q, r = 1, 2, 3 \qquad (4.3.18)$$

- and then to $\alpha_1, \alpha_2, \alpha_3, \beta_1, \beta_2, \beta_3$

(iii) computational mechanics of the resulting spring network

- planar dilatation
- intergranular multi-crack propagation

4. Planar Spring Networks on Periodic Lattices: Nonclassical Continua

4.1 Triangular lattice of Bernoulli-Euler beams (Wozniak, 1970)

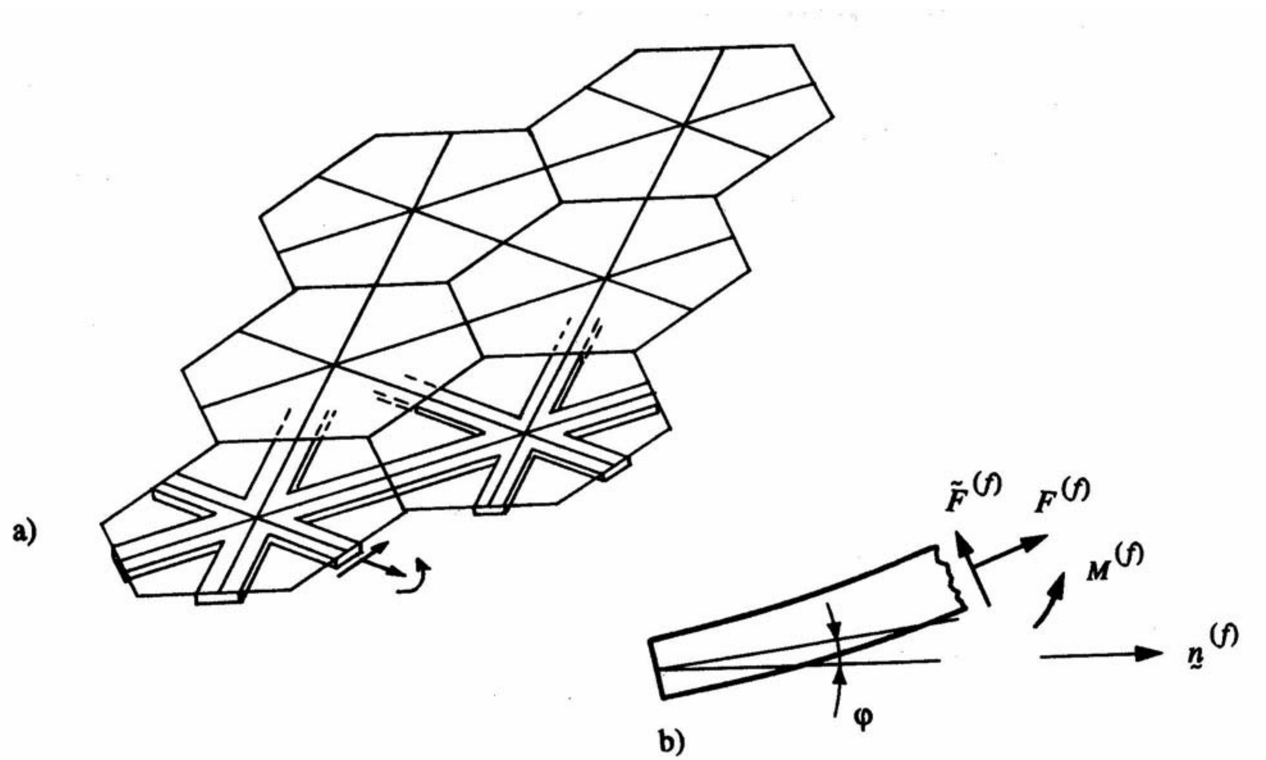

nodes of the network of beams described by

$$u_1(\boldsymbol{x}) \qquad u_2(\boldsymbol{x}) \qquad \varphi(\boldsymbol{x}) \tag{4.1}$$

within each triangular pore, these functions may be assumed to be linear $\Rightarrow$

$$\gamma_{kl} = u_{l,k} + e_{lk}\varphi \qquad \kappa_i = \varphi_{,i} \tag{4.2}$$

elementary beam theory $\Rightarrow$

$$F^{(b)} = E^{(b)}A^{(b)}\gamma^{(b)} \qquad \tilde{F}^{(b)} = \frac{12E^{(b)}I^{(b)}}{s^2}\tilde{\gamma}^{(b)} \qquad M^{(b)} = E^{(b)}I^{(b)}\kappa^{(b)} \tag{4.6}$$

$A^{(b)}$ = beam cross-sectional area

$I^{(b)} = w^3h/12$ = centroidal moment of inertia

$E^{(b)}$ = Young's modulus of beam's material

$s \equiv s^{(b)}$ = mesh spacing

for micropolar continuum

$$U_{continuum} = \frac{V}{2}\gamma_{ij}C_{ijkm}\gamma_{km} + \frac{V}{2}\kappa_i D_{ij}\kappa_j \tag{4.7}$$

$\Rightarrow$

$$C_{ijkm} = \sum_{b=1}^{6} n_i^{(b)}n_k^{(b)}(n_j^{(b)}n_m^{(b)}R^{(b)} + n_j^{(b)}n_m^{(b)}\tilde{R}^{(b)}) \qquad D_{ij} = \sum_{b=1}^{6} n_i^{(b)}n_j^{(b)}S^{(b)} \tag{4.8}$$

$\Rightarrow$

$$R^{(b)} = \frac{2E^{(b)}A^{(b)}}{s^{(b)}\sqrt{3}} \qquad \tilde{R}^{(b)} = \frac{24E^{(b)}I^{(b)}}{(s^{(b)})^3\sqrt{3}} \qquad S^{(b)} = \frac{2E^{(b)}I^{(b)}}{s^{(b)}\sqrt{3}} \tag{4.9}$$

when all the beams the same

$$C_{1111} = C_{2222} = \frac{3}{8}(3R + \tilde{R}) \qquad C_{1212} = \frac{3}{8}(R + 3\tilde{R})$$

$$C_{1122} = C_{2211} = \frac{3}{8}(R - \tilde{R}) \qquad C_{1221} = C_{2112} = \frac{3}{8}(R - \tilde{R}) \tag{4.10}$$

$$D_{11} = D_{22} = \frac{3}{2}S$$

i.e.

$$C_{ijkm} = \delta_{ij}\delta_{km}\Xi + \delta_{ik}\delta_{jm}\Lambda + \delta_{im}\delta_{jk}\Pi \qquad D^{eff}_{ij} = \delta_{ij}\Gamma \tag{4.11}$$

in which

$$\Xi = \Pi = \frac{3}{8}(R - \tilde{R}) \qquad \Lambda = \frac{3}{8}(R + 3\tilde{R}) \qquad \Gamma = \frac{3}{2}S \tag{4.12}$$

... can use four compliances *A*, *S*, *P*, and *M*

$$A = \frac{1}{\Xi + \frac{\Lambda + \Pi}{2}} \qquad S = \frac{2}{\Lambda + \Pi} \qquad P = \frac{2}{\Lambda - \Pi} \qquad M = \frac{2}{3\Gamma} \tag{4.13}$$

$\Rightarrow$

$$\kappa = \frac{3}{4}R \qquad \mu = \frac{3}{8}(R + \tilde{R}) \tag{4.14}$$

$\Rightarrow$

$$E = 3R\frac{1 + \frac{\tilde{R}}{R}}{3 + \frac{\tilde{R}}{R}} \qquad \nu = \frac{1 - \frac{\tilde{R}}{R}}{3 + \frac{\tilde{R}}{R}} \tag{4.15}$$

Note: introduction of beam-type effects has a similar influence on E and ν as the introduction of the angular β-interactions in the Kirkwood model

Note: since $\tilde{R}/R = (w/s)^2$ (w = beam width), given the slenderness assumption of beam elements, this model does not admit Poisson's ratios below ~0.2.

$\Rightarrow$ 2-D compliance tensors

$$S_{ijkm}^{(1)} = \frac{1}{4}[\delta_{ij}\delta_{km}(A-S) + \delta_{ik}\delta_{jm}(S+P) + \delta_{im}\delta_{jk}(S-P)] \qquad S_{ij}^{(2)} = \frac{\delta_{ij}}{\Gamma} \tag{4.16}$$

$\Rightarrow$ micropolar characteristic length

$$l^2 = \frac{S+P}{4M} = \frac{l}{24}\frac{1+3\left(\frac{w}{s}\right)^2}{1+\left(\frac{w}{s}\right)^2} \tag{4.17}$$

$\Rightarrow$ ... compare to computation of l for two-phase composites

4.2 Triangular lattice of Timoshenko beams

solve the b.v.p.

$$EI\theta'' + GA(v' - \theta) = 0 \qquad GA(v'' - \theta') = 0$$

$$v(0) = 0 \qquad \theta(0) = 0 \qquad v'(0) - \theta(0) = 0 \tag{4.20}$$

$$v(s) = \tilde{\gamma}^{(b)} s \qquad \theta(s) = 0 \qquad v'(s) - \theta(s) = 0$$

$\Rightarrow$

$$\tilde{F}^{(b)} = \frac{12E^{(b)}I^{(b)}}{s^3(1+\beta)} s\tilde{\gamma}^{(b)} \tag{4.21}$$

where

$$\beta = \frac{12EI^{(b)}}{GA^{(b)}s^2} = \frac{E}{G}\left(\frac{w}{s}\right)^2 \tag{4.22}$$

Two limiting cases:

$\beta \to 0$, high shear stiffness (less deflection owing to shear) $\Rightarrow$ B-E slender beam;

$\beta > 1$, low shear stiffness (deflection owing to shear dominates over that due to Young's modulus *E*) $\Rightarrow$ general case of the Timoshenko beam.

$\Rightarrow$ effective moduli

$$R^{(b)} = \frac{2E^{(b)}A^{(b)}}{s^{(b)}\sqrt{3}} \qquad \tilde{R}^{(b)} = \frac{24E^{(b)}I^{(b)}}{\left(s^{(b)}\right)^3\sqrt{3}}\frac{1}{1+\beta} \qquad S^{(b)} = \frac{2E^{(b)}I^{(b)}}{s^{(b)}\sqrt{3}} \tag{4.23}$$

with

$$\frac{\tilde{R}}{R} = \left(\frac{w}{s}\right)^2\frac{1}{1+\beta} \tag{4.24}$$

$\Rightarrow$

$$\frac{E^{eff}}{t_a E^{(b)}} = 2\sqrt{3}\frac{w}{s}\frac{1+\left(\frac{w}{s}\right)^2\frac{1}{1+\beta}}{3+\left(\frac{w}{s}\right)^2\frac{1}{1+\beta}}$$

$$\nu^{eff} = \frac{1-\left(\frac{w}{s}\right)^2\frac{1}{1+\beta}}{3+\left(\frac{w}{s}\right)^2\frac{1}{1+\beta}} \tag{4.25}$$

$\Rightarrow$ in terms of the porosity p (pores' volume fraction)

$$\frac{E^{eff}}{t_a E^{(b)}} = 2(1-\sqrt{1-p})\frac{1+\frac{1}{3(1+\beta)}(1-\sqrt{1-p})^2}{3+\frac{1}{3(1+\beta)}(1-\sqrt{1-p})^2}$$

$$\nu^{eff} = \frac{3-(1-\sqrt{1-p})^2\frac{3}{1+\beta}}{9+(1-\sqrt{1-p})^2\frac{3}{1+\beta}} \tag{4.26}$$

4.3 From stubby beams to a perforated plate model

Note: as porosity *p* goes beyond 50%, the beam's aspect ratio w/s increases so high that one can no longer model the connections between the lattice nodes as beams.

Note: as $p \to 1$, "dilute limit" of a locally isotropic material with triangular holes (Jasiuk *et al*., 1994; Jasiuk, 1995)

$$\frac{E^{eff}}{t_a E^{(b)}} = 1 - \alpha(1-p) \qquad \nu^{eff} = \nu^{(b)} - \alpha(\nu^{(b)} - \nu_0)(1-p) \tag{4.27}$$

with $\alpha = 4.2019$ and $\nu_0 = 0.2312$

[analogous coefficients are available for plates with squares, pentagons, ...)

Note: beam effects gain in influence as the pores' volume fraction increases, and lead to an increase of the effective Young's modulus relative to the central-force model.

Note: Timoshenko beams, although more sophisticated than Bernoulli-Euler beams, remain, in principle, one-dimensional objects, of micropolar type in fact. A better approach would have to consider beam segments as little plates, i.e., 2-D objects.

Note: lattice nodes that are taken as rigid objects in this model, could more realistically be modeled by considering their deformability; this will be demonstrated below.

4.4 Square lattice of Bernoulli-Euler beams

(Wozniak, *Surface Lattice Structures* 1970)

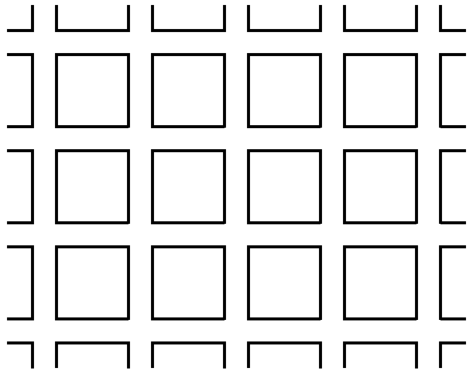

$\Rightarrow$

$$C_{ijkm} = \sum_{b=1}^{4} n_i^{(b)} n_k^{(b)} (n_j^{(b)} n_m^{(b)} R^{(b)} + n_j^{(b)} n_m^{(b)} \tilde{R}^{(b)}) \qquad D_{ij} = \sum_{b=1}^{4} n_i^{(b)} n_j^{(b)} S^{(b)} \tag{4.29}$$

where

$$R^{(b)} = \frac{E^{(b)} A^{(b)}}{s^{(b)}} \qquad \tilde{R}^{(b)} = \frac{12 E^{(b)} I^{(b)}}{(s^{(b)})^3} \qquad S^{(b)} = \frac{E^{(b)} I^{(b)}}{s^{(b)}} \tag{4.30}$$

when all the beams are identical $\Rightarrow$ orthotropic continuum

$$C_{1111} = C_{2222} = R \qquad C_{1212} = C_{2121} = \tilde{R} \qquad D_{11} = D_{22} = S \tag{4.31}$$

$\Rightarrow$ two micropolar characteristic lengths

$$l_1 = \sqrt{\frac{S}{\tilde{R}}} = \frac{s}{2\sqrt{3}} \qquad l_2 = \sqrt{\frac{S}{R}} = r \equiv \sqrt{\frac{I}{A}} \tag{4.32}$$

r = radius of gyration

For lattice nodes taken as deformable nodes,

$$C_{ijkm} = \sum_{b=1}^{4}\left[n_i^{(b)}n_j^{(b)}\sum_{b_\perp=1}^{4} n_k^{(b)}n_m^{(b)}R^{(bb_\perp)} + n_i^{(b)}n_j^{(b)}n_k^{(b)}n_m^{(b)}\tilde{R}^{(b)}\right]$$

$$D_{ij} = \sum_{b=1}^{4} n_i^{(b)}n_j^{(b)}S^{(b)} \qquad (4.33)$$

where

$$R^{(bb_\perp)} = \frac{d}{1-\nu_{(I)}\nu_{(II)}}\begin{bmatrix} \tilde{E}_{(I)} & \nu_{(I)}\tilde{E}_{(I)} \\ \nu_{(II)}\tilde{E}_{(II)} & \tilde{E}_{(II)} \end{bmatrix}$$

$$\tilde{R}^{(b)} = \frac{24E^{(b)}I^{(b)}}{(s^{(b)})^3\sqrt{3}} \qquad S^{(b)} = \frac{2E^{(b)}I^{(b)}}{s^{(b)}\sqrt{3}} \qquad (4.34)$$

Note: a recent extension of such micropolar models to wave propagation and vibration via introduction of internal variables:
(Wozniak, *Arch. Mech.* 1997; Cielecka *et al.*, *Arch. Mech.* 1998)

Note: other recent work: (Pshenichnov, *A Theory of Latticed Plates and Shells* 1993)
(Cioranescu & Saint Jean Paulin, *Homogenization of Reticulated Structures* 1999)

4.5 A honeycomb latitce; three possible periodic unit cells are shown.

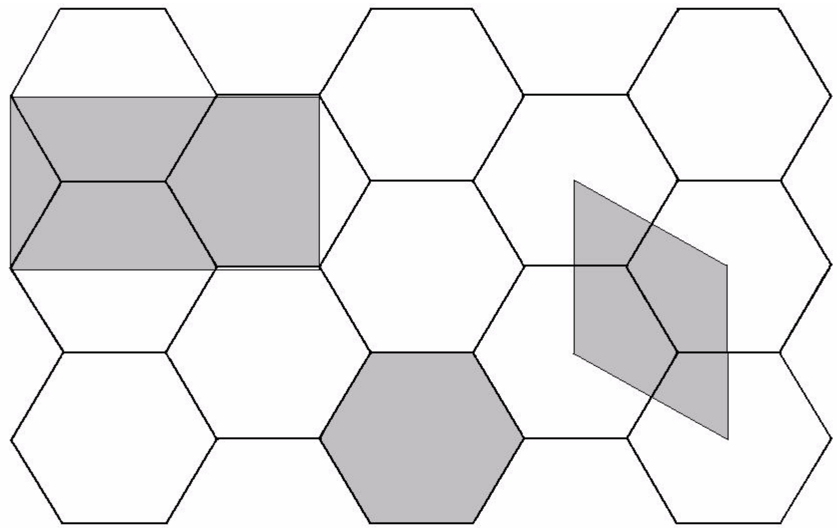

$$C_{ijkm} = \ldots \qquad D_{ij} = \ldots$$

$$l = \ldots$$

4.6 Non-local and gradient elasticity on a lattice with central interactions

(Holnicki-Szulc & Rogula, 1979)

structure I (with short-range interactions) $\alpha^{\boldsymbol{rr}'} = \alpha^{I}$

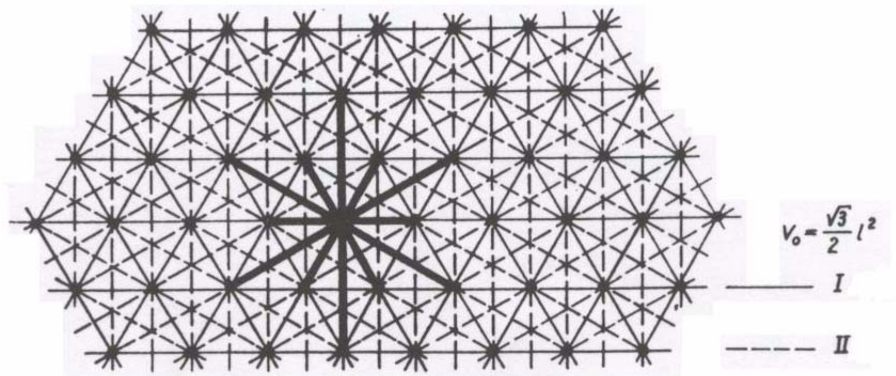

structure II (three regular triangular networks with long-range interactions) $\alpha^{\boldsymbol{rr}'} = \alpha^{II}$

central-force interactions between nodes $\boldsymbol{r}$ and $\boldsymbol{r}'$

$$F_i(\boldsymbol{r}, \boldsymbol{r}') = \Phi_{ij}^{\boldsymbol{rr}'} \Delta u_j(\boldsymbol{r}, \boldsymbol{r}') \tag{4.35}$$

$$\Phi_{ij}^{\boldsymbol{rr}'} = \alpha^{\boldsymbol{rr}'} \Delta r_i \Delta r_j \qquad \Delta u_j(\boldsymbol{r}, \boldsymbol{r}') = u_j(\boldsymbol{r}') - u_j(\boldsymbol{r}) \qquad \Delta r_i = r_i' - r_i \tag{4.36}$$

Q: what continuum model should be set up to approximate this discrete system?
A: three types possible: local, non-local, and strain-gradient.

(a) Local continuum model

... under uniform strain,

$$E = \frac{1}{2}\sum_{\boldsymbol{r},\boldsymbol{r}'} F_i(\boldsymbol{r},\boldsymbol{r}')\Delta u_i(\boldsymbol{r},\boldsymbol{r}') = \frac{1}{2}\sum_{\boldsymbol{r},\boldsymbol{r}'} \Phi_{ij}^{\boldsymbol{r}\boldsymbol{r}'}\Delta u_i(\boldsymbol{r},\boldsymbol{r}')\Delta u_j(\boldsymbol{r},\boldsymbol{r}') \qquad (4.37)$$

equivalent to strain energy of effective continuum

$$E_{continuum} = \frac{1}{2}\int_V \varepsilon_{ij} C_{ijkm} \varepsilon_{km} dV \qquad (4.38)$$

$\Rightarrow$

$$C_{ijkm} = C_{ijkm}^{I} + C_{ijkm}^{II} \qquad (4.4.39)$$

$$C_{ijkm}^{I} = \frac{2}{\sqrt{3}}\alpha^{I} \sum_{b=1,2,3} n_i^{I(b)} n_j^{I(b)} n_k^{I(b)} n_m^{I(b)}$$

$$C_{ijkm}^{II} = \frac{6}{\sqrt{3}}\alpha^{II} \sum_{b=1,2,3} n_i^{II(b)} n_j^{II(b)} n_k^{II(b)} n_m^{II(b)} \qquad (4.4.40)$$

$\Rightarrow$

$$\lambda^{I} = \mu^{I} = \frac{3}{4\sqrt{3}}\alpha^{I} \qquad \lambda^{II} = \mu^{II} = \frac{3}{4\sqrt{3}}\alpha^{II} \qquad (4.4.41)$$

(b) Non-local continuum model

distribute the values of tensors C^{I}_{ijkm} and C^{II}_{ijkm} at point $\boldsymbol{r}$ uniformly over the regions of interactions of structures I and II, and form a new tensor

$$C_{ijkm}(\boldsymbol{r}, \boldsymbol{r}') = C^{I}_{ijkm}(\boldsymbol{r}, \boldsymbol{r}') + C^{II}_{ijkm}(\boldsymbol{r}, \boldsymbol{r}')$$

$$C^{I}_{ijkm}(\boldsymbol{r}, \boldsymbol{r}') = \frac{C^{I}_{ijkm} h^{I}(\boldsymbol{r}, \boldsymbol{r}')}{A^{I}} \qquad C^{II}_{ijkm}(\boldsymbol{r}, \boldsymbol{r}') = \frac{C^{II}_{ijkm} h^{II}(\boldsymbol{r}, \boldsymbol{r}')}{A^{II}} \tag{4.42}$$

$A^{I} = \pi(s^{I})^{2}$, $A^{II} = \pi(s^{II})^{2}$ are the areas,

$h^{I}(\boldsymbol{r}, \boldsymbol{r}')$ and $h^{II}(\boldsymbol{r}, \boldsymbol{r}')$ are the characteristic functions of regions of interaction in the neighborhood of $\boldsymbol{r}$

(c) Strain-gradient continuum model

... a series expansion of the relative displacement field:

$$\Delta u_j(\boldsymbol{r}, \boldsymbol{r}') = \varepsilon_{ij}^{\boldsymbol{r}}(r_j' - r_j) + \frac{1}{2}\gamma_{ijk}^{\boldsymbol{r}}(r_j' - r_j)(r_k' - r_k) \qquad (4.43)$$

where

$$\varepsilon_{ij}^{\boldsymbol{r}} = u_{(i,j)}(\boldsymbol{r}) \qquad \gamma_{ijk}^{\boldsymbol{r}} = \varepsilon_{(i,j,k)}(\boldsymbol{r}) \qquad (4.44)$$

are gradients of 1st and 2nd orders of the displacement field

$\Rightarrow$

$$E = \frac{1}{2}\sum_{\boldsymbol{r},\boldsymbol{r}'} \Phi_{ij}^{\boldsymbol{r}\boldsymbol{r}'}\left[\varepsilon_{ik}^{\boldsymbol{r}}(r_k' - r_k) + \frac{1}{2}\gamma_{ikm}^{\boldsymbol{r}}(r_k' - r_k)(r_m' - r_m)\right] + \left[\varepsilon_{jm}^{\boldsymbol{r}}(r_m' - r_m) + \frac{1}{2}\gamma_{jmn}^{\boldsymbol{r}}(r_m' - r_m)(r_n' - r_m)\right] \qquad (4.45)$$

comparing to

$$E_{continuum} = \frac{1}{2}\int_V (\varepsilon_{ij}C_{ijkl}\varepsilon_{kl} + \gamma_{ijk}C_{ijklmn}\gamma_{lmn})dV \quad (4.46)$$

$\Rightarrow$

$$\begin{aligned} C_{ijkl}(\boldsymbol{r}, \boldsymbol{r}') &= C^I_{ijkl}(\boldsymbol{r}, \boldsymbol{r}') + C^{II}_{ijkl}(\boldsymbol{r}, \boldsymbol{r}') \\ C_{ijklmn}(\boldsymbol{r}, \boldsymbol{r}') &= C^I_{ijklmn}(\boldsymbol{r}, \boldsymbol{r}') + C^{II}_{ijklmn}(\boldsymbol{r}, \boldsymbol{r}') \end{aligned} \quad (4.47)$$

where

$$\begin{aligned} C^I_{ijkl}(\boldsymbol{r}, \boldsymbol{r}') &= \frac{2E^IA^I}{\sqrt{3}s^I}\sum_{b=1,2,3} n_i^{I(b)}n_j^{I(b)}n_k^{I(b)}n_l^{I(b)} \\ C^I_{ijklmn}(\boldsymbol{r}, \boldsymbol{r}') &= \frac{2E^IA^Is^I}{\sqrt{3}}\sum_{b=1,2,3} n_i^{I(b)}n_j^{I(b)}n_k^{I(b)}n_l^{I(b)}n_m^{I(b)}n_n^{I(b)} \end{aligned} \quad (4.48)$$

completely analogous formulas hold for $C^{II}_{ijkl}(\boldsymbol{r}, \boldsymbol{r}')$ and $C^{II}_{ijklmn}(\boldsymbol{r}, \boldsymbol{r}')$

see also (Bardenhagen & Triantafyllidis, 1994) for higher order gradient theories

4.7 Plate-bending response (Wozniak, *Surface Lattice Structures* 1970)

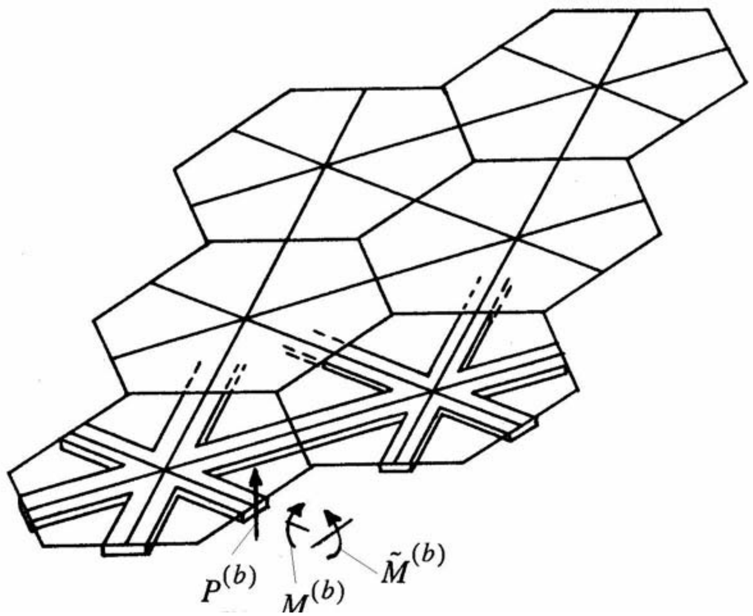

... out-of-plane deformations

$$u(\boldsymbol{x}) \qquad w_1(\boldsymbol{x}) \qquad w_2(\boldsymbol{x}) \tag{4.49}$$

assuming, within each triangular pore, these functions to be linear

$$\kappa_{kl} = v_{l,k} \qquad \gamma_k = u_{,k} + \varepsilon_{kl} v_l \tag{4.50}$$

... for a single beam

$$M^{(b)} = C^{(b)}\kappa^{(b)} \qquad \tilde{M}^{(b)} = E^{(b)}I^{(b)}\tilde{\kappa}^{(b)} \qquad P^{(f)} = \frac{12E^{(b)}I^{(b)}}{s^{(b)}}\tilde{\gamma}^{(b)} \tag{4.51}$$

the strain energy of unit cell

$$U_{continuum} = \frac{V}{2}\bar{\kappa}_{ij}C^{eff}_{ijkl}\bar{\kappa}_{kl} + \frac{V}{2}\bar{\gamma}_i A^{eff}_{ij}\bar{\gamma}_j \tag{4.52}$$

which is consistent with the Hooke's law

$$m_{kl} = C_{ijkl}\kappa_{kl} \qquad p_k = A_{kl}\gamma_l \tag{4.53}$$

m_{kl} = tensor of moment-stresses, p_k = vector of shear tractions.

$$C^{eff}_{ijkl} = \sum_{b=1}^{6} n_i^{(b)}n_k^{(b)}(n_j^{(b)}n_l^{(b)}S^{(b)} + n_j^{(b)}n_l^{(b)}\tilde{S}^{(b)}) \qquad A^{eff}_{ij} = \sum_{b=1}^{6} n_i^{(b)}n_j^{(b)}R^{(b)} \tag{4.54}$$

$$S^{(b)} = \frac{C^{(b)}}{s^{(b)}} \qquad \tilde{S}^{(b)} = \frac{E^{(b)}I^{(b)}}{s^{(b)}} \qquad \widehat{R}^{(b)} = \frac{12E^{(b)}I^{(b)}}{\tilde{s}^{(b)}(s^{(b)})^2} \tag{4.55}$$

... if lattice made of identical beams,

$$C_{ijkl} = \delta_{ij}\delta_{kl}\Delta + \delta_{ik}\delta_{jl}Y + \delta_{il}\delta_{jk}\Omega \qquad A_{ij} = \delta_{ij}B \tag{4.56}$$

in which

$$\Delta = \Omega = \frac{3}{8}(S - \tilde{S}) \qquad Y = \frac{3}{8}(S + 3\tilde{S}) \qquad B = \frac{3}{2}\widehat{R}$$

$$S = \frac{2C}{s\sqrt{3}} \qquad \tilde{S} = \frac{2EI}{s\sqrt{3}} \qquad \widehat{R} = \frac{24EI}{s^3\sqrt{3}} \tag{4.57}$$

5. Rigidity of Networks

5.1 Structural topology and rigidity percolation

Q: Given the topology of a central force (or truss) system $G(V, E)$, e.g.

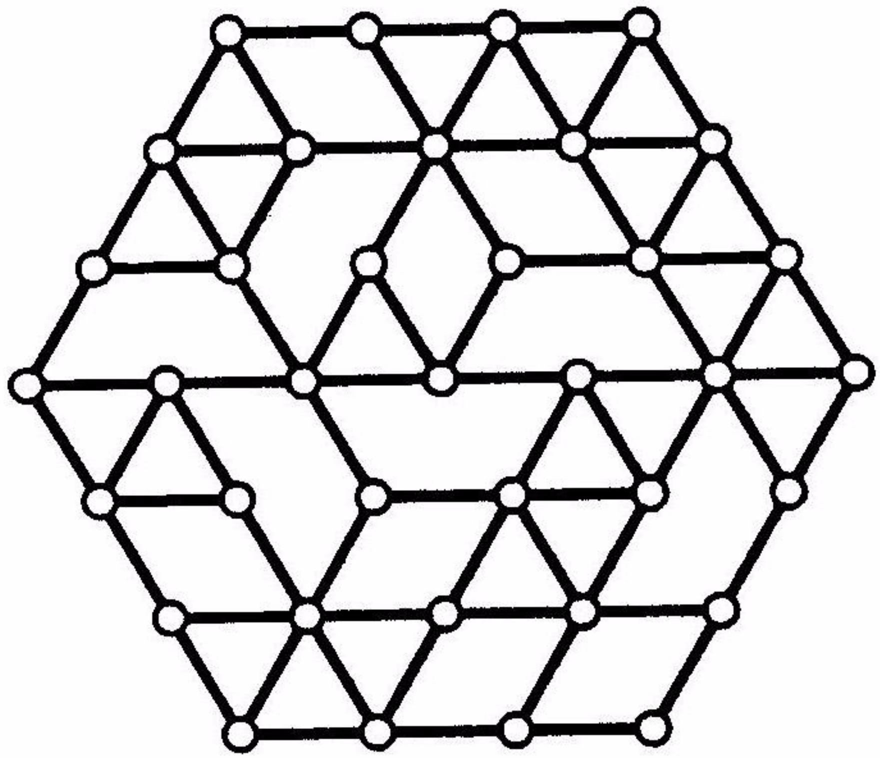

$|E| = 71$ $|V| = 37$

is it a sufficiently constrained system or not?
i.e., is it an intrinsically rigid body?

Two approaches to structural rigidity: static or kinematic.

Static approach:

A system of forces assigned to the nodes of a network is said to be an *equilibrium load* iff the sum of the assigned vectors is the zero vector, and the total moment of those vectors about any one point is zero.

A network resolves an equilibrium load iff there is an assignment of tensions and compressions to all the bars of E, such that the sum at each node is equal and opposite to its assigned load. A structure is said to be *statically rigid* iff it resolves all equlibrium loads.

Kinematic approach:

infinitesimal motion = assignment of velocities to all the nodes of V, such that the difference of velocities assigned to the ends of any bar is perpendicular to the bar itself;

i.e. the motion does not result in any extension or compression of the bar.

$\Rightarrow$ every connected plane structure has at least three DOF (two translations and one rotation), called a *rigid motion.*

Def: A structure is said to be *infinitesimally rigid* if and only if all its infinitesimal motions are rigid motions.

Thm. (Crapo & Whiteley, 1989): A structure is statically rigid iff it is infinitesimally rigid.

Def: A structure is said to be *isostatic* iff it is minimally rigid, i.e., when it is infinitesimally rigid but the removal of any bar introduces some infinitesimal motion.

Note: in an isostatic strcuture all the bars are necessary to maintain the overall rigidity. In statics this is called a *statically determinate structure*, as opposed to the indeterminate one which has more than a minmally sufficient number of bars for the global rigidity.

A well known result (necessary condition) for rigidity in 2-D:

$$|E| = 2|V| - 3 \tag{5.1}$$

... for sufficiency: Thm (e.g., Laman, 1970; Asimov & Roth, 1978):

$G(V, E)$ is isostatic iff it has $2|V| - 3$ bars, and for every m, $2 \le m \le |V|$, no subset of m nodes has more than $2m - 3$ bars connecting it.

$\Rightarrow$ can check whether the edges of the graph are not distributed spatially in a uniform manner. If they are crowded locally, than the odds are that the structure is not isostatic.

Note: the isostatic concept falls in the category of generic rigidity, where only the topological information on a graph's connectivity comes into picture.

! one may also deal with unexpected infinitesimal motions:
e.g. two edges incident onto the same vertex lie on a straight line (Guyon *et al*, 1990):

in condensed matter physics $\Rightarrow$ very large systems $\Rightarrow$ need to ask:
what critical fraction, p_r, of edges of E *is* needed to render the structure isostatic?

$\Rightarrow$ would have $|E'| = p_r|E|$ new edges of thus modified, or depleted, set E'

Note: $|E'| = 2|V| - 3 \quad \Rightarrow \quad p_r = 2/3$

a simple estimate of the so-called *rigidity percolation*
e.g., (Shechao Feng *et al*., 1985), (Thorpe *et al*., 1986), (Boal, 1993)

Note: the rigidity percolation typically occurs above the connectivity percolation: $p_r > p_c$

Poisson line field e.g. (Miles, 1964, Santaló, 1976)

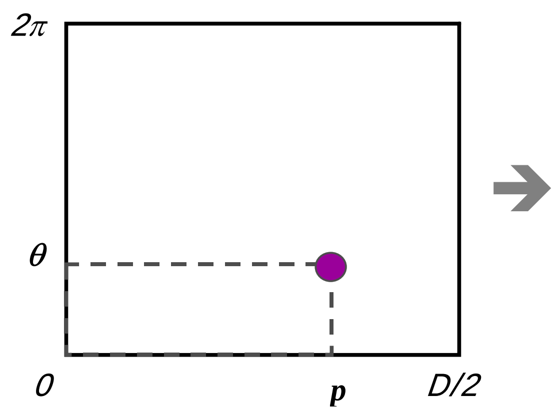

Random generation of p and θ

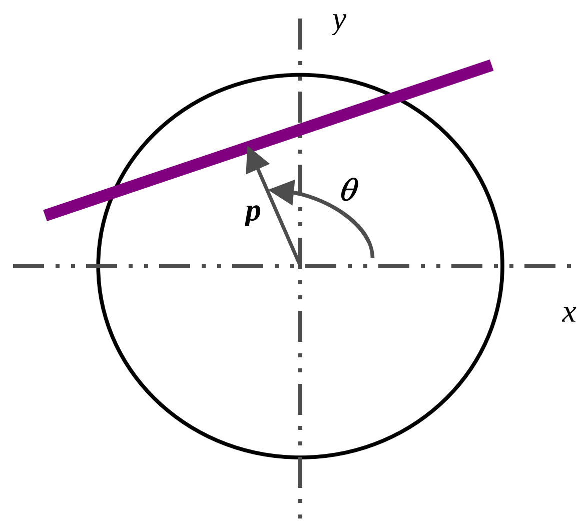

Poisson line field

1. Poisson point field in (p, θ)-plane

2. Hesse normal form:

$$x\cos\theta + y\sin\theta = p$$

to get a field of lines, homogeneous in (x, y)-plane

Note: other methods do not result in homogeneous line fields!

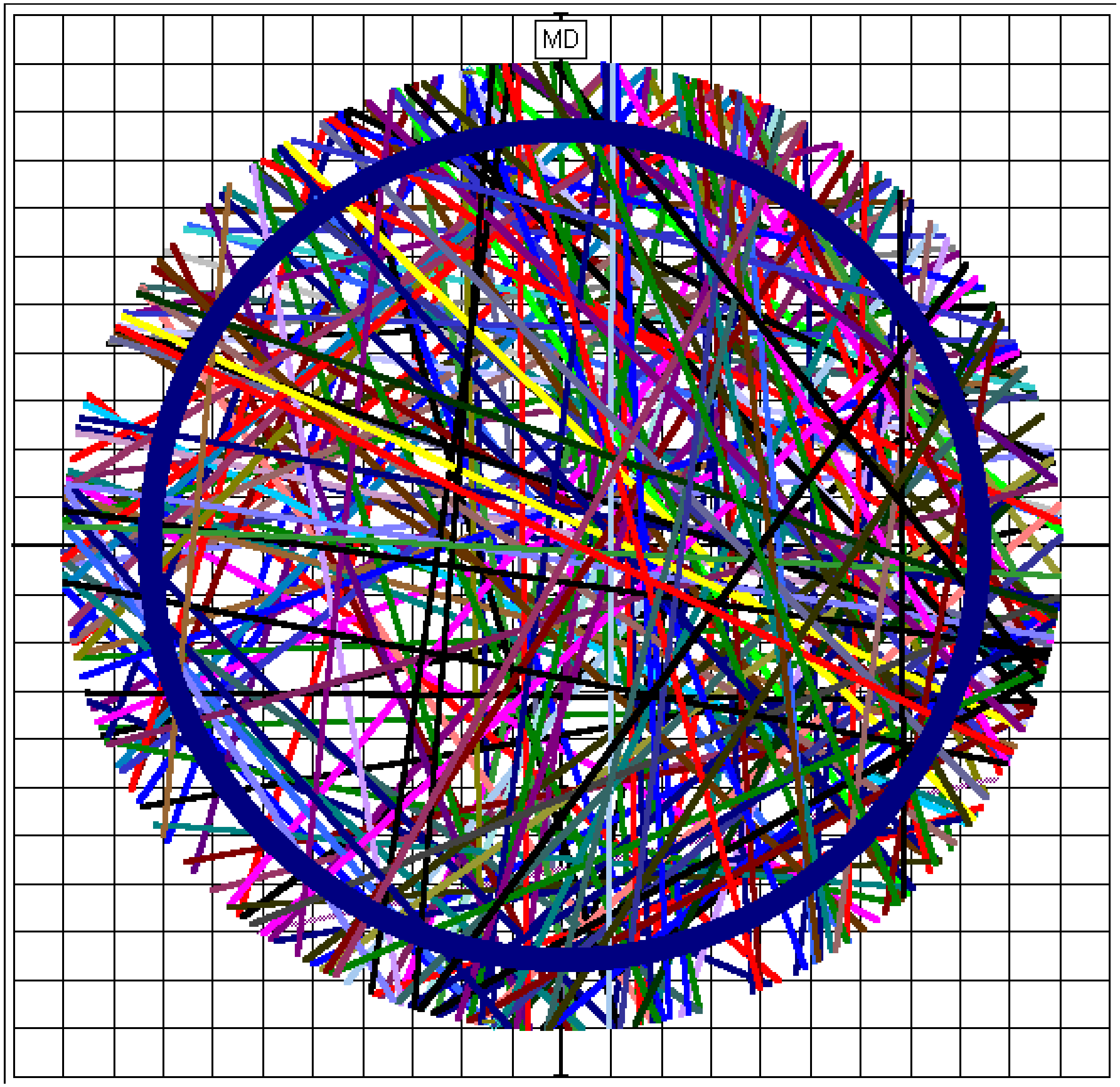
MD

5.2 Rigidity of a <u>truss</u> of Poisson line field geometry

$\Rightarrow$ basic model of cellulose fiber networks and some other composites (Cox, 1952)

Note: typical vertices have connectivity 4, i.e., V_4

... can calculate the total number of edges in the bold drawn graph $G(V, E)$

$$|E| = |V_2| + \frac{3}{2}|V_3| + 2|V_4| \tag{5.2}$$

but, since $V = V_2 \cup V_3 \cup V_4$,

$$|V| = |V_2| + |V_3| + |V_4| \tag{5.3}$$

so that $|E| < 2|V| - 3$ - the system is not isostatic, i.e., a mechanism

$\Rightarrow$ the Poisson line field of axial force fiber segments (so-called Cox model) - is not a valid model of paper, or any other solid material

In real 2-D networks fibers have finite length $\Rightarrow$ fibers' ends are loose

$\Rightarrow$ $|V_2|$ and $|V_3|$ increase!

Note: Going to 3-D requires an even more stringent condition as more constraints are needed when dealing with the additional degrees of freedom (e.g., Asimov & Roth, 1978).

5.3 Rigidity of a fiber-beam network

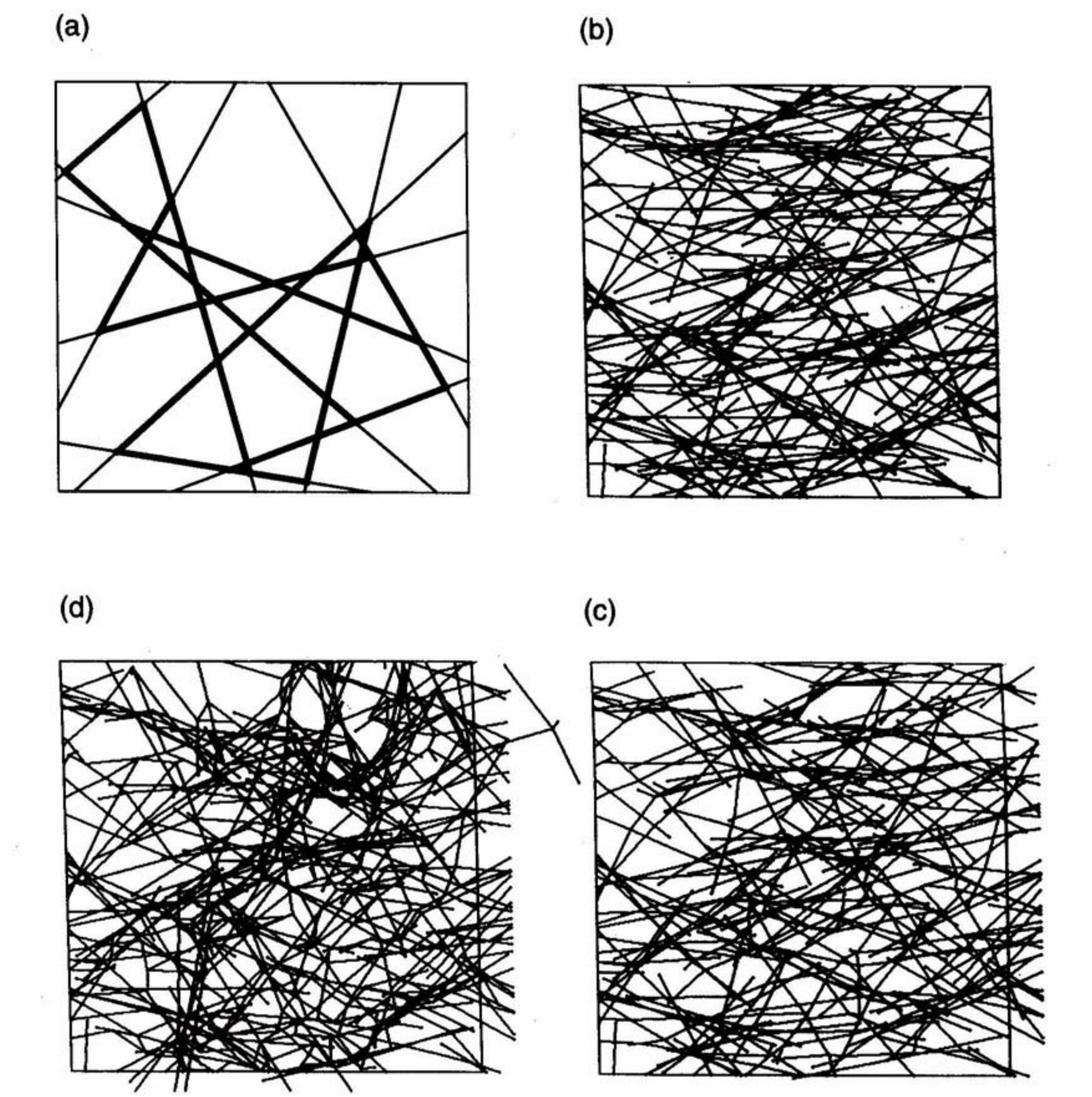

... highly porous materials (Chung *et al*., 1996)
cement-coated wood strands composites (Stahl & Cramer, 1998)
fiber networks (Ostoja-Starzewski *et al*., 1999, 2000)

Construction:

(i) Boolean model: floc centers: fiber clusters/flocs
fibers are laid in 3-D on top of one another with possible non-zero out-of-plane angle
(ii) Fibers are homogenous, but each fiber may have different dimensions and mechanical properties, all sampled from any prescribed statistical distribution
(iii) Each fiber is a series of linear elastic 3-D extensible Timoshenko beam elements. stiffness matrix, written here in an abbreviated form set up in a corotational coordinate system (Cook *et al*., 1989)

$$g = 12\frac{EI_y}{GA} \qquad h = 12\frac{EI_z}{GA} \qquad a = \frac{EI_y}{l(12g + l^2)} \qquad b = \frac{EI_z}{l(12h + l^2)} \tag{5.5}$$

F, T = axial force and twisting moment,

$M_y^a, M_z^a, M_y^b, M_z^b$ = bending moments around the y and z axes at the a and b ends

$$
\begin{bmatrix} F \\ T \\ M_y^a \\ M_z^a \\ M_y^b \\ M_z^b \end{bmatrix} = \begin{bmatrix} \frac{EA}{l} & 0 & 0 & 0 & 0 & 0 \\ 0 & \frac{GJ}{l} & 0 & 0 & 0 & 0 \\ 0 & 0 & 4a(l^2+3g) & 0 & 2a(l^2-6g) & 0 \\ 0 & 0 & 0 & 4b(l^2+3h) & 0 & 2b(l^2-6h) \\ 0 & 0 & 2a(l^2-6g) & 0 & 4a(l^2+3g) & 0 \\ 0 & 0 & 0 & 2b(l^2-6h) & 0 & 4a(l^2+3g) \end{bmatrix} \begin{bmatrix} \Delta L \\ \Delta\theta_x \\ \theta_y^a \\ \theta_z^a \\ \theta_y^b \\ \theta_z^b \end{bmatrix} \tag{5.4}
$$

ΔL, $\Delta\theta_x$, θ_y^a, θ_z^a, θ_y^b, θ_z^b = axial elongation, angle of twist, four angles of rotation

l, A, J, I_x, and I_y = length, cross-sectional area,

J, I_x, and I_y = cross-sectional polar moment of inertia, moments of inertia

E and G are the Young's modulus and shear modulus of a fiber-beam

(iv) All the intersection points are identified so as to set up a connectivity matrix.

(v) Equilibrium is found under kinematic boundary conditions $u_i = \bar{\varepsilon}_{ij} x_j$.

Note:

(i) The sharp kinks we see in both figures are only the artifact of simple computer graphics---the micromechanical model assumes fibers deform into differentiable curves. Magnification creates the appearance of large displacements - actually, an infinitesimal displacement assumption is used in the computational mechanics program.

(ii) The kinks are far more pronounced when fibers have low flexural stiffness. Portions of the network where connected fibers do not form triangular pores can generate significant forces in response to deformation when fibers have high flexural stiffness, but they cannot do so when fibers rely almost entirely on axial stiffness. These portions of the network are not stable in the sense of loss of generic rigidity discussed earlier.

(iii) We do not study this rigid-floppy transition by turning, in an *ad hoc* fashion, all the connections into pivots. Rather, with the model taking into account all the displacements and rotations of nodes, we can study it as a continuous function of fiber slenderness; see also (Kuznetsov, 1991). This aspect is impossible to investigate with models based on central-force potentials for single fiber segments (e.g., Kellomaki *et al*., 1996).

5.5 Rigidity percolation in a triangular truss

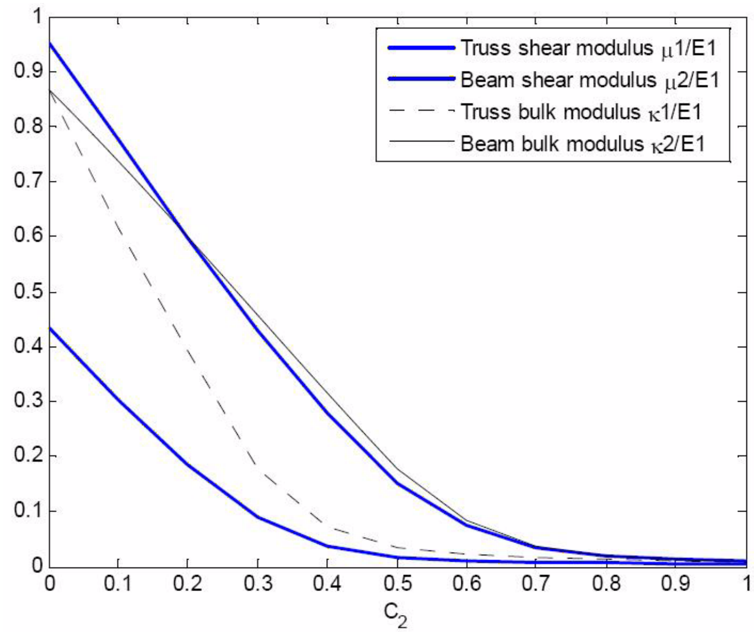

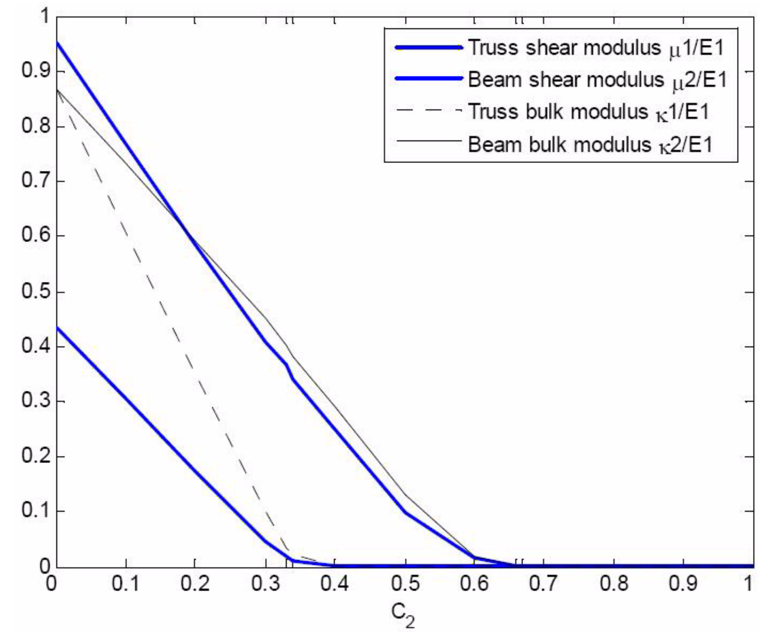

5.5 Rigidity percolation in a Poisson-Delaunay truss

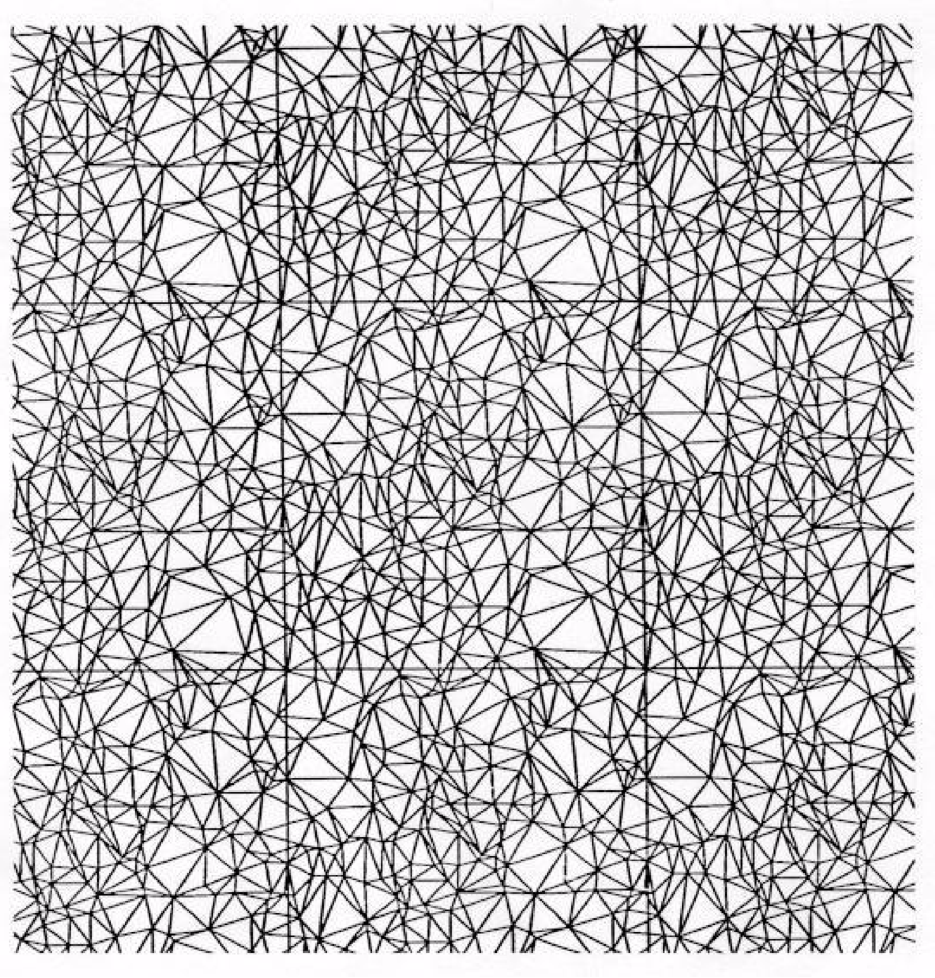

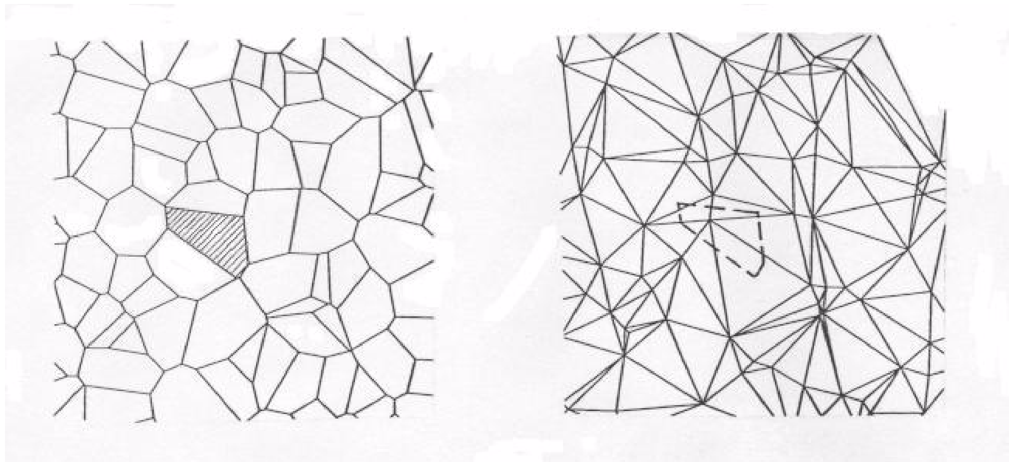

spider-inclusion analogy: an inclusion as a cell in a Voronoi tessellation, and a corresponding spider in the dual Delaunay network.

6. Spring Network Models: Disordered Topologies

6.1 Load transfer mechanisms in heterogeneous media

granular medium via *discrete elements (DE)* - (Cundall & Strack, 1978)

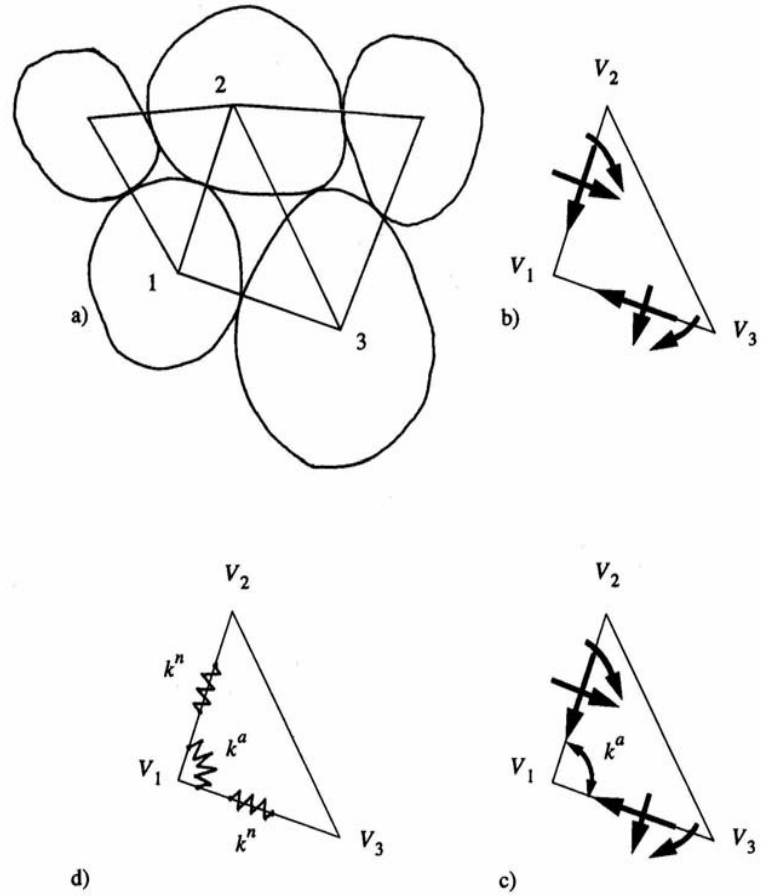

Fig. 6.1(a) A cluster of five grains showing the lines of interactions; (b) a discrete element model showing the normal force, the shear force, and the moment exerted by grains 2 and 3 each onto the grain 1; (c) a most general model showing the same grain-grain interactions as before but augmented by an internal, angular spring constant k^a; (d) a simplified model adopted in this paper, showing only normal (k^n) and angular (k^a) effects.

Types of DE models:

- Central interactions:

$$U = U^{central} \tag{6.1}$$

- Central and angular interactions:

$$U = U^{central} + U^{angular} \tag{6.2}$$

a generalization of Section 2.4

- Central, shear and bending interactions:

$$U = U^{central} + U^{shear} + U^{moment} \tag{6.3}$$

a generalization of Sections 4.1 and 4.2

$\Rightarrow$ a locally inhomogeneous micropolar continuum

- Central, shear, bending, and angular interactions: the total energy is

$$U = U^{central} + U^{shear} + U^{moment} + U^{angular} \tag{6.4}$$

Note: there exist successful DE models which account for normal and shear forces only (Bathurst & Rothenburg, 1988, 89)... although lacking rotational invariance of energy.

Note: correspondence between a system of convex grains and its graph model:

Table 1:

assembly of grains	graph	index	number of elements
grain	vertex	v	$\lvert V \rvert$
contacting point	edge	e	$\lvert E \rvert$
void (in 2-D)	loop	l	$\lvert L \rvert$

$\Rightarrow$ assignment of mechanical quantities:

Table 2:

quantity	notation	number of elements	notation	quantity
body force	$\boldsymbol{B}^{v}$	$\lvert V \rvert$	$\boldsymbol{u}^{v}$	grain displacement
body couple	$\boldsymbol{N}^{v}$	$\lvert V \rvert$	$\boldsymbol{w}^{e}$	grain rotation
contact force	$\boldsymbol{F}^{e}$	$\lvert E \rvert$	$\Delta\boldsymbol{u}^{e}$	relative displacement
contact couple	$\boldsymbol{M}^{e}$	$\lvert E \rvert$	$\Delta\boldsymbol{w}^{e}$	relative rotation

connectivity of $G(V, E)$ is described by the incidence matrix D^{ve} (Satake, 1976, 1978)

$\Rightarrow$ total of $3|V|$ equilibrium equations, each w.r.t. a grain of radius r^v and volume V^v

$$D^{ve}\begin{bmatrix} \boldsymbol{F}^e \\ \boldsymbol{M}^e \end{bmatrix} + V^v \begin{bmatrix} \boldsymbol{B}^v \\ \boldsymbol{N}^v \end{bmatrix} = 0 \qquad (6.5)$$

$$\tilde{D}^{ve} = \begin{bmatrix} D^{ve} & 0 \\ r^v D^{ve} \boldsymbol{n}^e \times & D^{ve} \end{bmatrix} \qquad (6.6)$$

$\boldsymbol{n}^e$ = unit vector of edge e in nonoriented graph

kinematics of all the edges

$$\begin{bmatrix} \Delta \boldsymbol{u}^e \\ \Delta \boldsymbol{w}^e \end{bmatrix} = -\tilde{D}^{ev} \begin{bmatrix} \boldsymbol{u}^v \\ \boldsymbol{w}^v \end{bmatrix} \qquad (6.7)$$

subject to $3|L|$ compatibility constraints written for all loops

$$\tilde{D}^{ev} = \begin{bmatrix} D^{ev} & -\boldsymbol{n}^{e} \times r^{v} D^{ev} \\ 0 & D^{ev} \end{bmatrix} \tag{6.8}$$

This is augmented by $3|E|$ constitutive equations relating contact force $\boldsymbol{F}^e$ and moment $\boldsymbol{M}^e$ with relative displacement $\Delta\boldsymbol{u}^e$ and rotation $\Delta\boldsymbol{w}^e$.

Note: Given 3 global equilibrium conditions, we have a total of

$$3(|V| - 1 + |E| + |L|) = 6|E| \tag{6.9}$$

equations.

$\Rightarrow$ given Euler relation $|V| - |E| + |L| = 1$, this budget of equations agrees with $6|E|$ unknowns - i.e., $\boldsymbol{F}^e$, $\boldsymbol{M}^e$, $\Delta\boldsymbol{u}^e$ and $\Delta\boldsymbol{w}^e$ - defined on edges of E.

Note: formal analogy of (6.5) and (6.7) to equilibrium and strain-displacement equations of Cosserat continua

$$Div\begin{bmatrix}\sigma \\ \mu\end{bmatrix} + \begin{bmatrix}\boldsymbol{b} \\ \boldsymbol{m}\end{bmatrix} = \boldsymbol{0} \qquad \begin{bmatrix}\gamma \\ \kappa\end{bmatrix} = Grad\begin{bmatrix}\boldsymbol{u} \\ \boldsymbol{w}\end{bmatrix} \tag{6.10}$$

6.3 Periodic graphs with topological disorder (e.g., Ziman, 1979)

two basic possibilities of randomness:

substitutional disorder

topological disorder (departure from the periodic topology)
e.g., incompatibility of crystal-like domains in a granular material

geometric disorder (e.g., uneven lengths of various bonds)

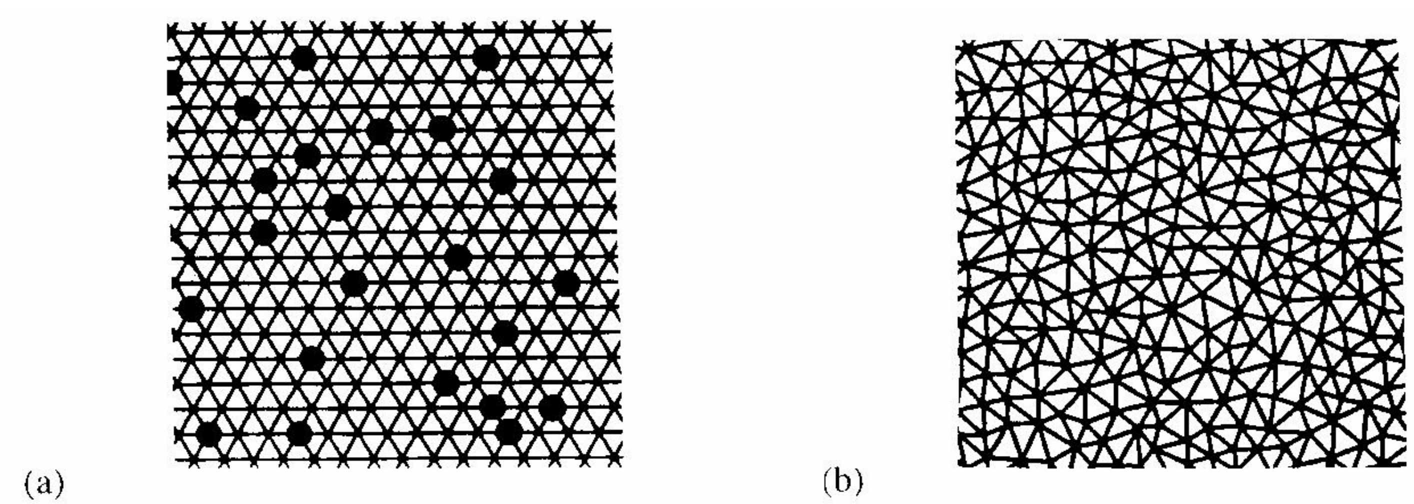

(a) (b)

Fig. 6.2 Substitutional (a) versus topological disorder (b) of a hard-core Delaunay network.

for *effective* (macroscopic) moduli $\boldsymbol{C}_L^{eff}$,

use *periodic boundary conditions* on $L \times L$ square B

$$u_i(\underset{\sim}{x} + \underset{\sim}{L}) = u_i(\underset{\sim}{x}) + \bar{\varepsilon}_{ij}x_j \qquad t_i(\underset{\sim}{x}) = -t_i(\underset{\sim}{x} + \underset{\sim}{L}) \qquad \forall \underset{\sim}{x} \in \partial B \tag{6.11}$$

$\Rightarrow$

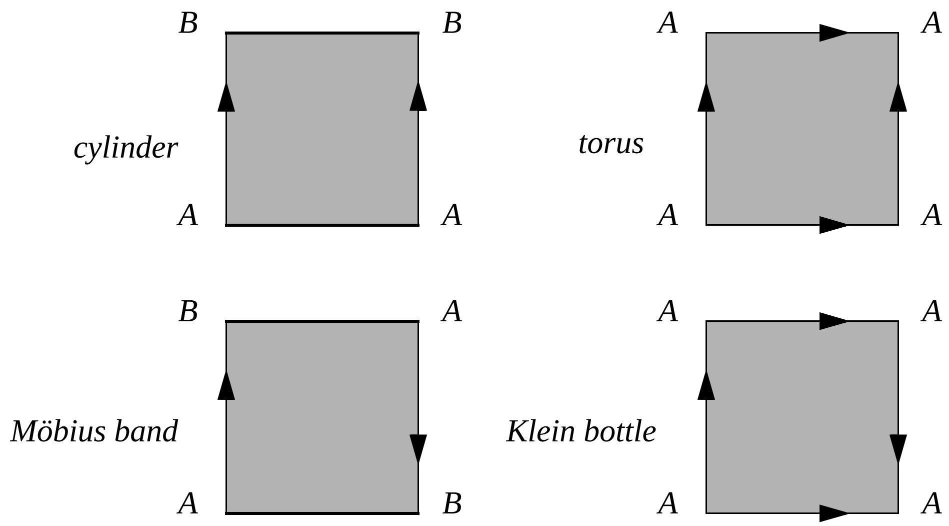

Poisson point field has space-homogeneous and isotropic statistics

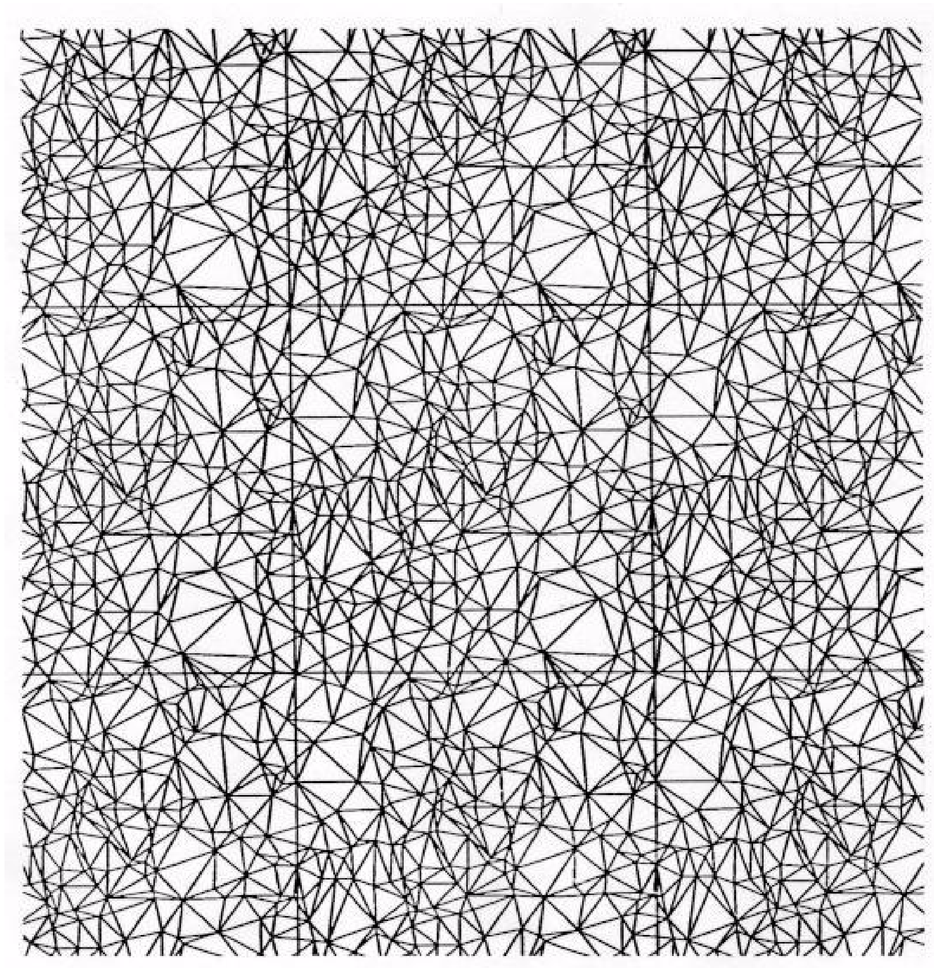

$\boldsymbol{C}_L^{eff}$ ($\equiv C_{ijkl}^{eff}$) is isotropic

... calculate effective moduli κ and μ:

biaxial extension $\bar{\varepsilon}_{11} = \bar{\varepsilon}_{22}$

shear deformation $\bar{\varepsilon}_{11} = -\bar{\varepsilon}_{22}$

from equivalent continuum of area $V = L^2$

$$U = \frac{V}{2}\left[\kappa\bar{\varepsilon}_{ii}\bar{\varepsilon}_{jj} + 2\mu\left(\bar{\varepsilon}_{ij}\bar{\varepsilon}_{ij} - \frac{1}{2}\bar{\varepsilon}_{ii}\bar{\varepsilon}_{jj}\right)\right] \tag{6.12}$$

in a Monte Carlo sense ... via ensemble averages: $\langle\kappa\rangle$, $\langle\mu\rangle$

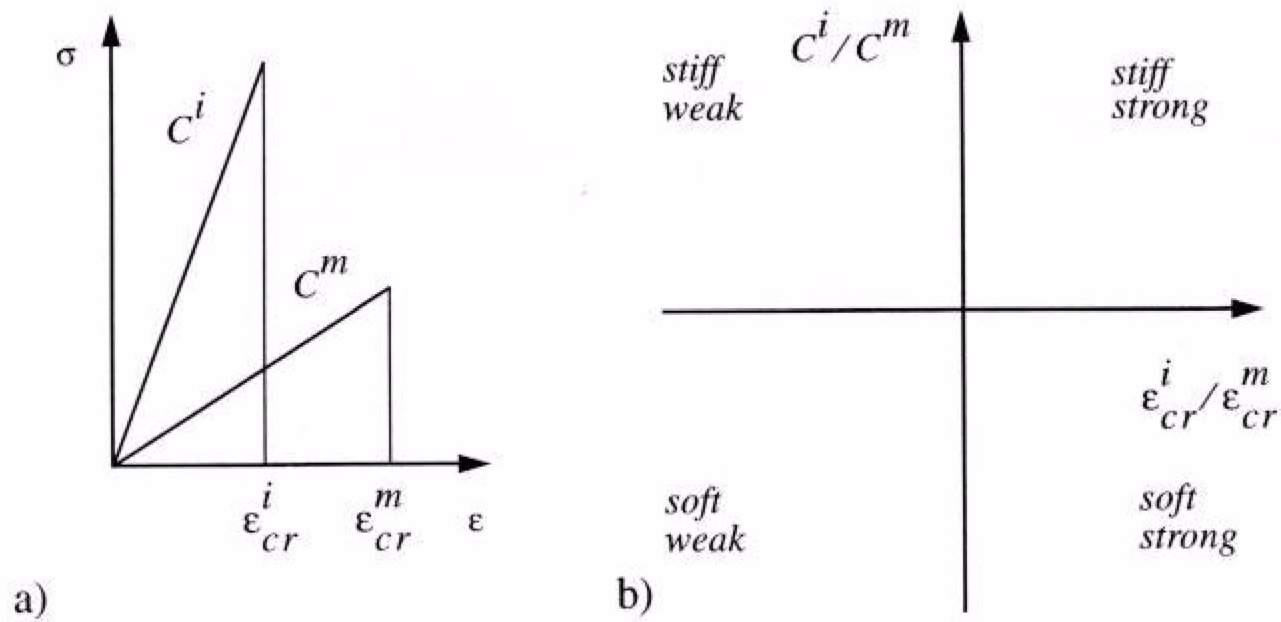

σ
C^i
C^m
ε^i_{cr}
ε^m_{cr}
ε
a)
C^i/C^m
stiff
weak
stiff
strong
$\varepsilon^i_{cr}/\varepsilon^m_{cr}$
soft
weak
soft
strong
b)

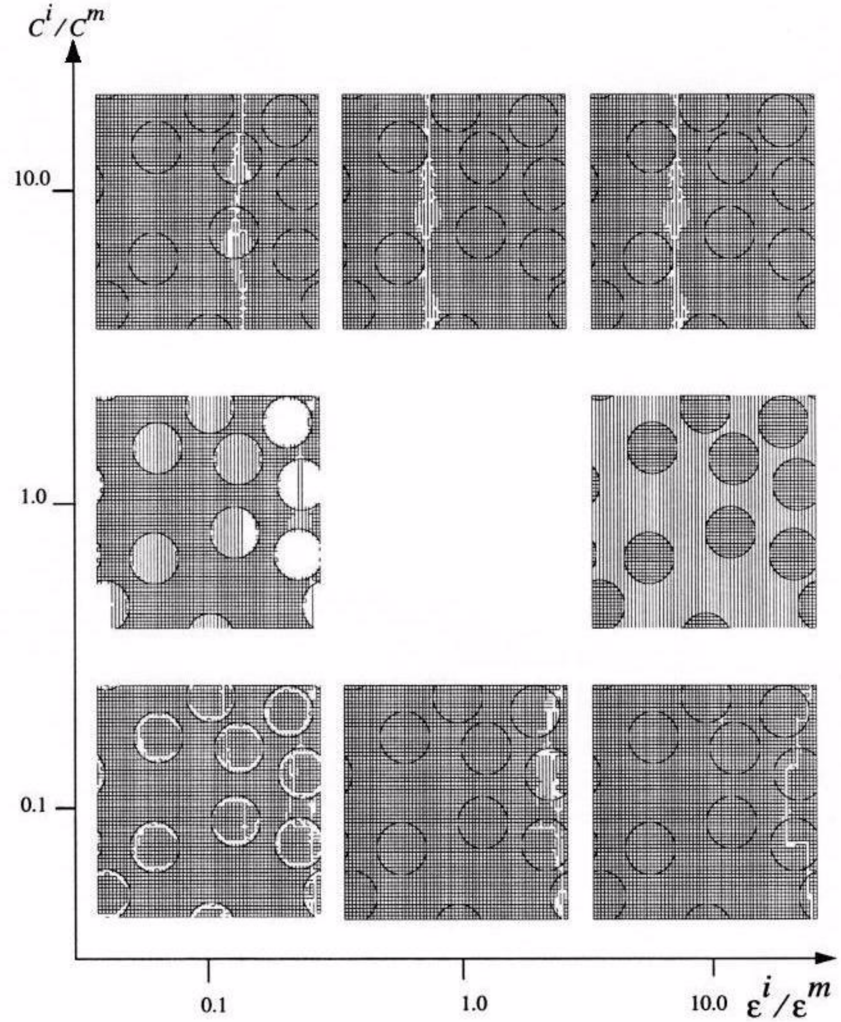
C^i/C^m
10.0
1.0
0.1
0.1
1.0
10.0
$\varepsilon^i/\varepsilon^m$

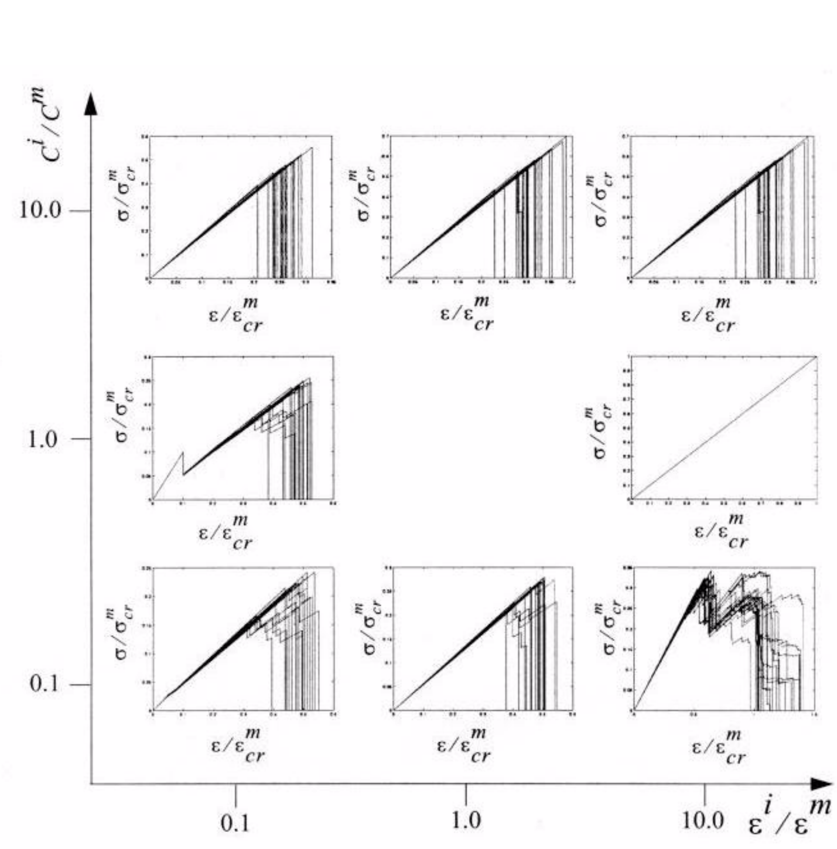

c^i/c^m
10.0
1.0
0.1
$\varepsilon^i/\varepsilon^m$
0.1
1.0
10.0
σ/σ^m_{cr}
$\varepsilon/\varepsilon^m_{cr}$

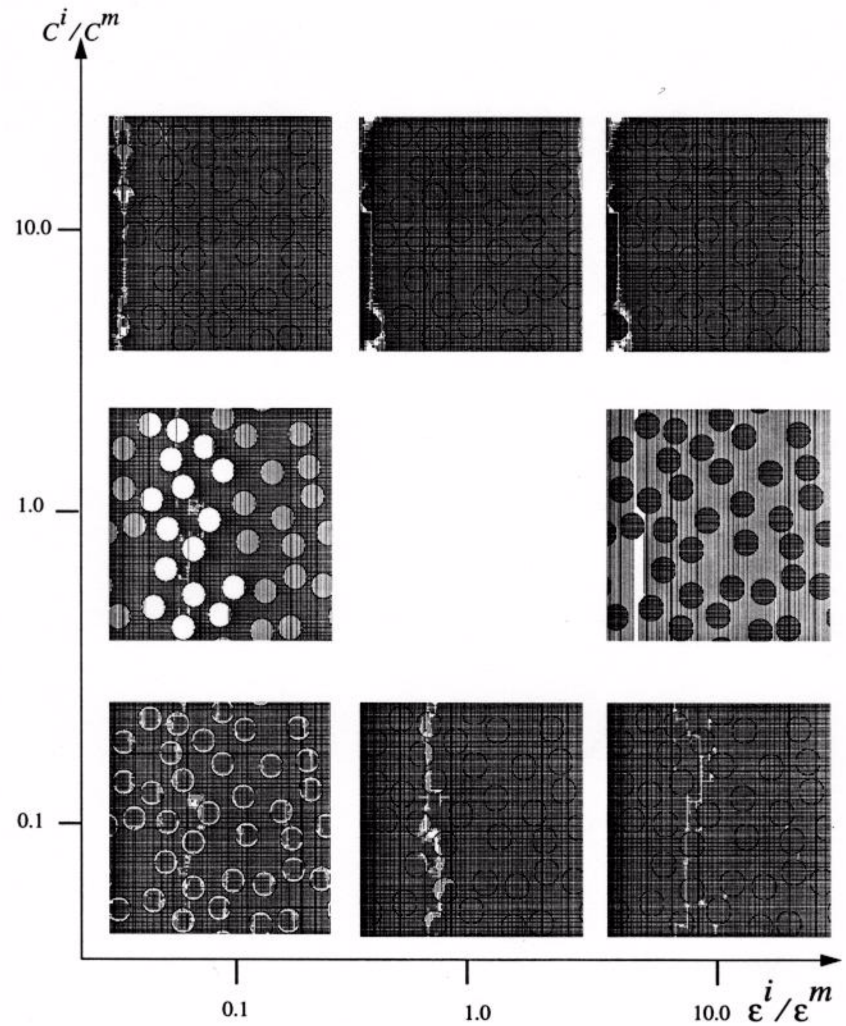

c^i/c^m
10.0
1.0
0.1
0.1
1.0
10.0
$\varepsilon^i/\varepsilon^m$

Simulations of Evolving Damage

quasi-static

dynamic

8. Spring networks: classifications, pros and cons

Resolution of a planar mosaic by the square lattice indicates that there are several possible ways of classifying spring network models - they include:

(a) static versus dynamic;

(b) lattice topology directly given by the material microstructure, or assigned by another rule;

(c) springs modeling central-force interactions only, or also non-central and other;

(d) elastic versus inelastic;

(e) physical system dimensionality (D = 1, 2, or 3).

Ad (a): Static version of lattice modeling neglects the inertia forces, as opposed to the dynamic version, which belongs to molecular dynamics; the latter one covers also non-lattice systems such as fluids. There is a trade-off here: including dynamics forces one to integrate forward in time by time steps small enough so as to satisfy some stability condition appropriate for am explicit scheme adopted (e.g. leap-frog). As a result, having a very fine lattice, one is likely to work on very short time scales that are suitable for high-speed transient rather than quasi-static phenomena which would necessitate a huge number of forward time steps. In molecular dynamics one can also use an implicit scheme allowing for larger time steps, but at a costly expense of having to solve an algebraic system for many interacting bodies.

Ad (b): Spring networks are most natural when the lattice topology is directly given by the material - some examples are:

- cellulose fiber network with each fiber treated as a 3-D rod element (e.g., Ostoja-Starzewski *et al.*, 1999);
- granular media with each grain modeled by a vertex interacting via central and shear forces, plus moments, with contiguous grains (e.g., Alzebdeh and Ostoja-Starzewski, 1999). Such an assignment is not possible in the case of polycrystals and other continuum-like systems, Fig. 26. Evidently, modeling a crystal by a single vertex would be primitive (though sometimes employed with success), and a number of vertices is needed to get a finer resolution. The latter option seems to be better accomplished by finite elements, but the great advantage of a regular, periodic network is no need for costly remeshing (preprocessing) and, therefore, the possibility to easily automate the procedure so as to run in a Monte Carlo fashion (!).

Ad (c): By going to a triangular lattice arrangement, the central-force lattice outlined above can be used to model in-plane elasticity. To cover the entire range of continuum stiffnesses one may have to introduce non-central potentials. By allowing for the inter-vertex moments, one goes to micropolar continua; e.g. (Ostoja-Starzewski *et al.*, 1996). Furthermore, by allowing for interactions between further neighbors, one may model non-local continua (Askar, 1985). A lot of work on micropolar, and higher-order, models of plate- and shell-like systems was reported in (Wozniak, 1970) and Noor (1988). For more recent work on models of lattice structures we refer to (Pshenichnov, 1993), and for mathematical aspects of their homogenization to (Cioranescu and Saint Jean Paulin, 1999). Finally, we mention here recent work on honeycomb lattices (Chen *et al.*, 1998), which treats the issue of effective elastic moduli as well continuum-type fracture of porous materials with such microgeometry.

Ad (d): Spring networks work best for linear elastic materials (e.g., Alzebdeh *et al.*, 1998), but some extensions even to plasticity have recently been carried out; see (Monette and Anderson, 1999) and references therein.

Statistical Continuum and Bounding Methods for Effective Transport and Elastic Properties

Martin Ostoja-Starzewski

Department of Mechanical Science & Engineering

University of Illinois at Urbana-Champaign

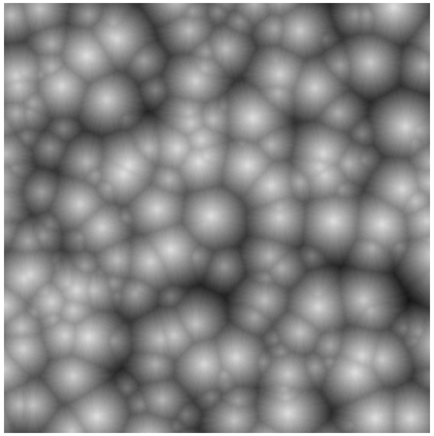

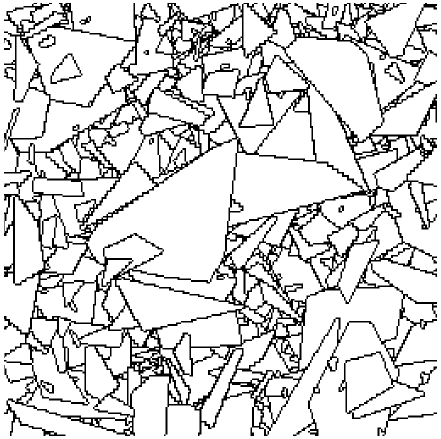

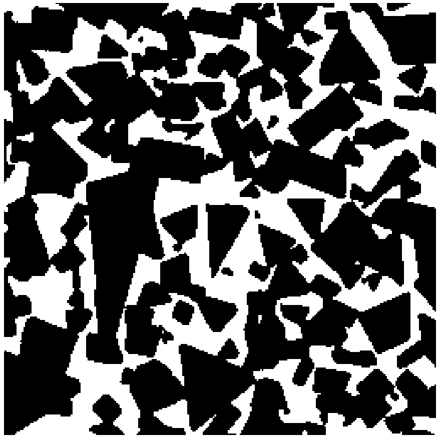

1 Random Processes and Fields

1.1 Elements of 1D random fields

1.1.1 Scalar random fields

(scalar) random variable (r.v.)

$$Z : \Omega \longrightarrow \mathbb{R}, \;\; Z(\omega) = z. \tag{1.1}$$

Note: The term random variable is a misnomer as it is a function in the first place.

probability distribution of Z

$$F_Z(z) = P\{Z \leq z\} \tag{1.2}$$

if differentiable, $\Longrightarrow$ probability density of Z

$$f_Z(z) = \frac{dF_Z(z)}{dz}. \tag{1.3}$$

Example 1: Measurements of random paper stiffness modulus $Z = E$ of 1" $\times$ 1" specimens, separated by 1.5", at n ($= 500$) points along a paper web, $\Longrightarrow E_i$, $i \in I = \{1, 2, ..., n\}$.

$\{Z(\omega, i); \omega \in \Omega, i \in I\} =$ (scalar) random field parametrized by i.

May parametrize Z by a continuous x.

$\Longrightarrow I$ is replaced by $X \subset R$, and Z is a 1D random field (or random/stochastic process in 1D). It assigns to $\forall\omega$ a realization (or trajectory) over X:

$$Z : \Omega \times X \to \mathbb{R}, \;\; Z(\omega, x) = z. \tag{1.4}$$

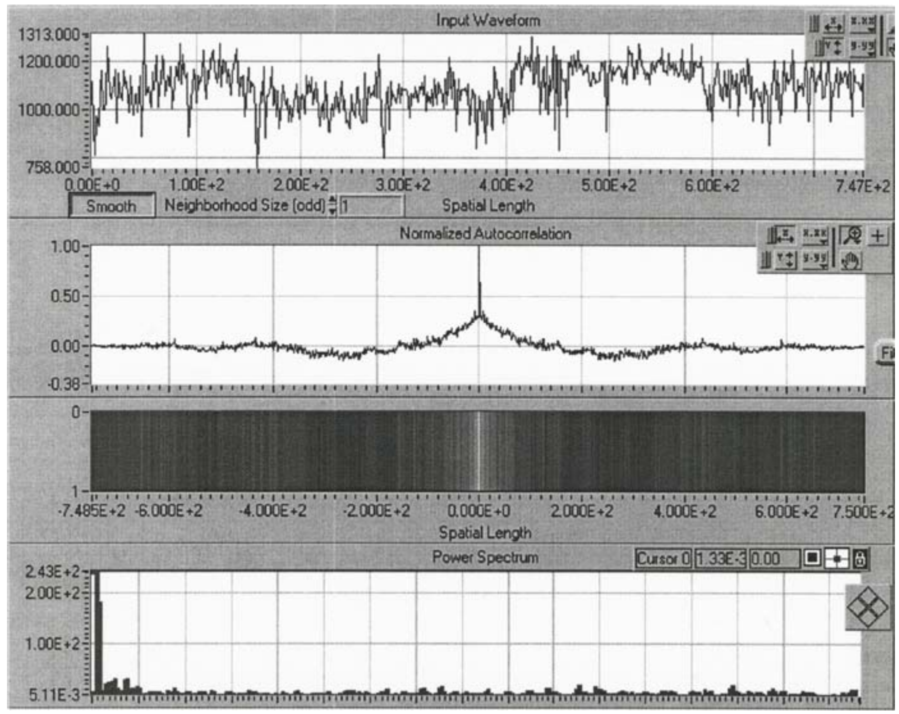

Figure 1.1: A sample realization of random process E (Young's modulus), its autocorrelation, and spectrum.

Note: Four interpretations of Z:

(1) a set, or ensemble, of all functions $Z(\omega, x)$: ω and x are variable;

(2) a single deterministic function (a realization) $Z(\omega)$: ω is fixed but x is variable;

(3) a random variable $Z(x)$: ω is variable but x is fixed;

(4) a deterministic number z: ω and x are fixed.

Note: Conventional literature on random/stochastic processes typically introduces a parametrization by the time (t) rather than space (x) coordinate.

$\forall x$ introduce a first-order (or one-point) probability distribution of the process Z

$$F_Z(z;x) \equiv F_1(z;x) = P\{Z(x) \leq e\}, \tag{1.5}$$

if $F_Z(z;x)$ is differentiable w.r.t. z, have first-order probability density of Z

$$f_Z(z;x) \equiv f_1(z;x) = \frac{dF_1(z;x)}{dz}. \tag{1.6}$$

... second-order (or two-point) probability distribution

$$F_2(z_1, z_2; x_1, x_2) = P\{Z(x_1) \leq z_1, Z(x_2) \leq z_2\}, \tag{1.7}$$

with

$$f_2(z_1, z_2; x_1, x_2) = \frac{\partial^2 F_2(z_1, z_2; x_1, x_2)}{\partial z_1 \partial z_2}. \tag{1.8}$$

... n-th-order (or n-point) probability distribution of Z

$$F_n(z_1, ..., z_n; x_1, ..., x_n) = P\{Z(x_1) \leq z_1, ..., Z(x_n) \leq z_n\}. \tag{1.9}$$

i.e., a function of $2n$ variables; n-th-order probability density

$$f_n(z_1, ..., z_n; x_1, ..., x_n) = \frac{\partial^n F_n(z_1, ..., z_n; x_1, ..., x_n)}{\partial z_1 ... \partial z_n}. \tag{1.10}$$

Q: given a family of functions F_n, can we find a stochastic process such that F_n's are its n-th order probability distributions?

A: *Kolmogorov conditions*: if F_n's is a family of distributions dependent on n, such that for any n, any $x_i \in X$, and any permutation $i_1, ..., i_n$ of numbers $1, ..., n$, the following must hold:

(i) symmetry (i.e., invariance w.r.t. permutation)

$$F_n(z_{i_1}, ..., z_{i_n}; x_{i_1}, ..., x_{i_n}) = F_n(z_1, ..., z_n; x_1, ..., x_n); \tag{1.11}$$

(ii) consistency $\forall m < n$

$$F_n(z_1, ..., z_m, \infty, ..., \infty; x_1, ..., x_n) = F_n(z_1, ..., z_m; x_1, ..., x_m). \tag{1.12}$$

Example 2: Consider the case $n = 2$, and

$$f\left(z_1, z_2; x_1, x_2\right) = \frac{1}{2\pi\sigma_1\sigma_2\sqrt{1-r^2}} \exp\left[\frac{-1}{2\left(1-\rho^2\right)}\left(\frac{z_1^2}{\sigma_1^2} - 2\rho\frac{z_1}{\sigma_1}\frac{z_2}{\sigma_2} + \frac{z_2^2}{\sigma_2^2}\right)\right], \tag{1.13}$$

where $\sigma_1 = x_1$, $\sigma_2 = x_2 - x_1$, $0 < x_1 < x_2$, $z_i \in \mathbb{R}^1$, $i = 1, 2$. Then the marginal densities are

$$\int_{\mathbb{R}^1} f\left(z_1, z_2; x_1, x_2\right) dz_2 = \frac{1}{x_1\sqrt{2\pi}} \exp\left[-\frac{z_1^2}{\sigma_1^2}\right]$$

$$\int_{\mathbb{R}^1} f\left(z_1, z_2; x_1, x_2\right) dz_1 = \frac{1}{\left(x_2 - x_1\right)\sqrt{2\pi}} \exp\left[-\frac{z_2^2}{2\left(x_2 - x_1\right)^2}\right] \tag{1.14}$$

$$= \varphi\left(x_1, x_2, z_2\right).$$

$\Longrightarrow \varphi\left(x_1, x_2, z_2\right)$ depends on x_1 and x_2, $\Longrightarrow f\left(z_1, z_2; x_1, x_2\right)$ does not satisfy the Kolmogorov conditions, $\Longrightarrow$ it cannot represent a second-order density function $f_2(z_1, z_2; x_1, x_2)$ of a stochastic process $Z(x)$.

Mean (or average $\mu(x)$) of the process Z is

$$\langle Z(x)\rangle = \int_{\mathbb{R}} z dF_1(z; x) = \int_{\mathbb{R}} z f_1(z; x) dz, \tag{1.15}$$

$\langle\ \rangle \equiv$ ensemble averaging

... autocorrelation

$$R(x_1, x_2) \equiv R_Z(x_1, x_2) = \langle Z(x_1)Z(x_2)\rangle = \int_{\mathbb{R}} z_1 z_2 f_2(z_1, z_2; x_1, x_2) dz_1 dz_2, \tag{1.16}$$

autocovariance (covariance of $Z(x_1)$ and $Z(x_2)$)

$$C(x_1, x_2) \equiv C_Z(x_1, x_2) = \langle [Z(x_1) - \mu(x_1)][Z(x_2) - \mu(x_2)]\rangle. \tag{1.17}$$

$\Longrightarrow C_Z(x_1, x_2) = R_Z(x_1, x_2) - \mu(x_1)\mu(x_2)$.

... setting $x_1 = x_2 = x$, $\Longrightarrow$ variance of $Z(x)$

$$\sigma^2_{Z(x)} = C_Z(x, x) = R_Z(x) - \mu^2(x) = \langle Z(x)^2\rangle - \langle Z(x)\rangle^2. \tag{1.18}$$

Note: The covariance is symmetric $C(x_1, x_2) = C(x_2, x_1)$; when the process is complex-valued, it is Hermitian. Furthermore, by the Cauchy-Schwartz inequality, the squared modulus of $C(x_1, x_2)$ never exceeds the product of the variances $\sigma^2(x_1)$ and $\sigma^2(x_2)$

$$C^2(x_1, x_2) \leq \sigma^2(x_1)\sigma^2(x_2) = C(x_1, x_1)C(x_2, x_2). \tag{1.19}$$

Example 3: A point is at (O, P) at time $t_0 = 0$ in the (t, x)-plane, and then moves with a velocity Q on the straight line. (P, Q) is a random vector $\mathbf{Z}$. At time t the point is at $(t, X(\omega, t))$ where $X(\omega, t) = P(\omega) + tQ(\omega)$. Realizations of the $X(\omega, t)$ process are rays $x(t) = p + qt$ for $t \geq 0$; p and q are fixed. The mean and the autocorrelation are found to be (Problem 2)

$$\langle X(t) \rangle = \langle P \rangle + t \langle Q \rangle \quad R_X(t_1, t_2) = \left\langle P^2 \right\rangle + \langle PQ \rangle (t_1 + t_2) + \left\langle Q^2 \right\rangle t_1 t_2 \ . \tag{1.20}$$

Example 4: With P and Q as above, we form a differential equation for $t > 0$

$$P \frac{dX}{dt} + QX = 0 \tag{1.21}$$

with the initial condition $X(t) = 2H(t)$, $H(t)$ being the Heaviside function. Obviously, the solution is $X(t) = 2 \exp(-qt/p) H(t)$ and this stochastic process consists of a family of exponentials.

Example 5: Consider a random process $Z(x) = Y \sin \pi x$, where $F_Y(y)$ is given and x is a deterministic parameter $x \in [1/4, 1/2]$. Then, the first-order distribution function is

$$F_Z(z) = P\{Y \sin \pi x \leq z\} = P\left\{Y \leq \frac{z}{\sin \pi x}\right\} = F_Y\left(\frac{z}{\sin \pi x}\right). \quad (1.22)$$

Example 6: Consider

$$Y(\omega, x) = \begin{cases} \sin x & \text{if} \quad \omega = tails \\ 2x & \text{if} \quad \omega = heads \end{cases}. \quad (1.23)$$

$\Longrightarrow$ process Y_x consists of two very regular curves.

We are rather interested in processes where randomness is "richer" and "extends into infinity".

... a classical example

$$Y(\omega, x) = A(\omega) \cos kx + B(\omega) \sin kx, \tag{1.24}$$

where $k > 0$, and A, B are ind. r.v.'s with standard Gaussian densities $N(0, \sigma)$, or

$$Y(\omega, x) = C(\omega)[\cos kx + \Phi(\omega)], \tag{1.25}$$

with

$$\langle Y(x) \rangle = 0 \quad R_X(x_1, x_2) = \sigma^2 \cos k(x_2 - x_1) \ . \tag{1.26}$$

... more general model

$$Y(x, \omega) = \sum_{i=1}^{n} [A_i(\omega) \cos k_i x + B_i(\omega) \sin k_i x], \tag{1.27}$$

where $k_i > 0$, and A_i, B_i, for $i = 1, ..., n$, are independent random variables with $N(0,1)$.

... richer model, (Rice noise)

$$Y(\omega, x) = \sum_{i=1}^{n} A_i(\omega) \cos\left[\upsilon_i(\omega)x + \Phi_i(\omega)\right], \qquad (1.28)$$

where A_i's, B_i's, υ_i's and Φ_i's are r.v.'s with known statistics

... random Fourier series

$$Y(\omega, x) = \sum_{m=1}^{\infty} V_m(\omega) e^{imgx}, \tag{1.29}$$

$V_1, V_2, \ldots$ are mutually uncorrelated, zero-mean r.v.'s

$$\langle V_m \rangle = 0 \quad \langle V_m V_n \rangle = \begin{cases} W_m^2 & \text{if} \quad m = n \\ 0 & \text{if} \quad m \neq n \end{cases} \tag{1.30}$$

For $Y(\omega, x)$ to represent $\widetilde{Y}(\omega, x)$ adequately (in mean-square sense) $\forall x \in [-X, X]$

$$4 \sin^2 \frac{gX}{4} \ll 1. \tag{1.31}$$

Random processes whose values e_1, ..., e_n, at respective positions x_1, ..., x_n, are independent r.v.'s (recall Bernoulli and binomial processes)

$$f_n(e_1, ..., e_n; x_1, ..., x_n) = \prod_{i=1}^{n} f_1(e_i; x_i). \tag{1.32}$$

A process is strict-sense stationary (SSS) if all n-order distributions F_n are invariant w.r.t. arbitrary shifts x', and for any x_i's

$$F_n(z_1, ..., z_n; x_1, ..., x_n) = F_n(z_1, ..., z_n; x_1+x', ..., x_n+x'). \tag{1.33}$$

A process is wide-sense stationary (WSS) if its mean is constant and its finite-valued autocorrelation depends only on $x = x_2 - x_1$

$$\langle Z(x)\rangle = \mu, \;\; \langle Z(x_1)Z(x_1+x)\rangle = R_Z(x) < \infty. \tag{1.34}$$

Note: WSS is much less restrictive than SSS.

Note: If r.p. is specified via 1st and 2nd moments, then WSS $\Longrightarrow$ SSS; e.g. Gaussian

Note: r.p.'s can be classified as stationary versus evolutionary.

normalized autocovariance (*correlation coefficient*)

$$\rho(x_1, x_2) \equiv \rho_Z(x_1, x_2) = \frac{C_Z(x_1, x_2)}{\sigma_{Z_1}\sigma_{Z_2}}. \tag{1.35}$$

Example: Gaussian curve

$$\rho(x) = \mathrm{exp}[-x^2/2l^2]; \tag{1.36}$$

Example: exponential curve

$$\rho(x) = \mathrm{exp}[-x/l]. \tag{1.37}$$

Defines *spectral density* $s(\gamma)$ of $\rho(x)$ as its Fourier transform

$$s(\gamma) = \frac{1}{2\pi}\int_{-\infty}^{\infty} \rho(x)e^{-i\gamma x}dx, \;\; \rho(x) = \int_{-\infty}^{\infty} s(\gamma)e^{i\gamma x}d\gamma \tag{1.38}$$

Note: For a real-valued r.p.:

$$\rho(x) = \int_{-\infty}^{\infty} s(\gamma) \cos(\gamma x) d\gamma \tag{1.39}$$

By Bochner's Theorem: every non-negative definite function has a non-negative Fourier transform, i.e. $s(\gamma) \geq 0$. A simple application

$$\rho(x) = \begin{cases} \rho_0, & |x| < x_c \\ 0, & else \end{cases} . \tag{1.40}$$

But, since

$$s(\gamma) = \frac{1}{2\pi} \int_{-\infty}^{\infty} \rho(x) e^{-i\gamma x} dx = \frac{\rho_0}{2\pi} \int_{-x_c}^{x_c} \cos(\gamma x) dx = \frac{\rho_0}{\pi\gamma} \sin(\gamma x_c) \tag{1.41}$$

model (1.41) is inadmissible.

For a WSS r.p. — in analogy to random processes parametrized by time — one can define a *correlation length* (or *correlation radius*)

$$l_c = \frac{1}{\sigma^2} \int_0^{\infty} R(x) dx = \int_0^{\infty} \rho(x) dx. \tag{1.42}$$

For Gaussian autocovariance: $l_c = l(\pi/2)^{-1/2}$; for exponential $l_c = l$.

Note: the integral may diverge, e.g. $\rho(x) = [1 + x^2/l^2]^{-a}$, $a < 1/2$.

Note: In practice, autocovariances and spectra are often estimated from single realizations of r.p.'s; this is based on the *ergodic assumption*.

Local averaging: given any $Z(\omega)$, consider a new r.p. with realization $Z_L(\omega)$

$$Z_L(\omega, x) = \frac{1}{2L}\int_{x-L}^{x+L} Z_L(\omega, x')dx'. \tag{1.43}$$

Note: autocorrelations are changed with L.

1.1.2 Vector random fields

Example: Return to paper properties, and also report strength σ_{max}

$\Longrightarrow$*vector random variable*

$$\begin{bmatrix} E \\ \sigma_{\mathsf{max}} \end{bmatrix} : \Omega \rightarrow \mathbb{R}, \;\; E(\omega) = e, \;\; \sigma_{\mathsf{max}}(\omega) = s, \tag{1.44}$$

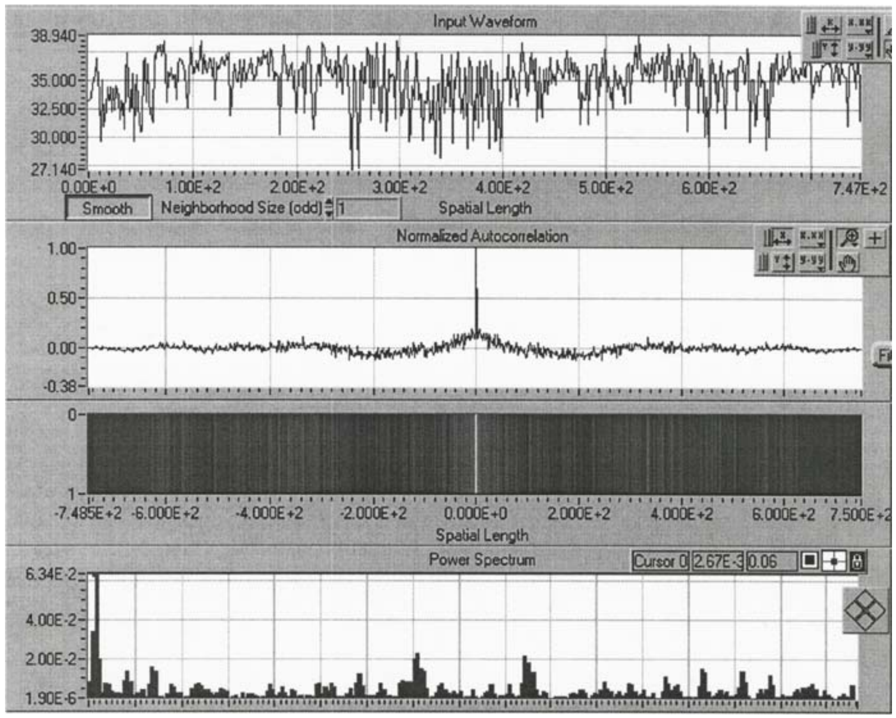

Figure 1.2: A sample realization of random process σ_{max}, its autocorrelation, and spectrum.

$\Longrightarrow$*vector random process*

$$\begin{bmatrix} E \\ \sigma_{\mathsf{max}} \end{bmatrix} : \Omega \times X \to \mathbb{R}^2, \;\; E(\omega, x) = e, \;\; \sigma_{\mathsf{max}}(\omega, x) = s. \tag{1.45}$$

In general, $\mathbf{Z} : \Omega \times X \to \mathbb{R}^n$, $\mathbf{Z}(\omega, x) = \mathbf{z}$.

Complete specification via n-point probability distributions

$$F_n(z_1, ..., z_n; x_1, ..., x_n) = P\{Z(x_1) \leq z_1, ..., Z(x_n) \leq z_n\}, \tag{1.46}$$

which again are subject to Kolmogorov conditions. But, such a description is very difficult to achieve in practice. $\Longrightarrow$ focus on WSS fields.

... *joint covariance*

$$C_{ij}(x_1, x_2) = \langle [Z_i(x_1) - \langle Z_i(x_1) \rangle][Z_j(x_2) - \left\langle Z_j(x_2) \right\rangle] \rangle \tag{1.47}$$

$\Longrightarrow$*correlation coefficient*

$$\rho_{ij}(x_1, x_2) = \frac{C_{ij}(x_1, x_2)}{\sigma_i \sigma_j}, \tag{1.48}$$

for $i = j$, *autocovariance*; else *crosscovariance*

Setting $x_1 = x_2 = x$, get *covariance matrix*

$$\rho_{ij}(x) = \frac{C_{ij}(x)}{\sigma_i \sigma_j}. \tag{1.49}$$

Example of paper: E, σ_{max}, strain-to-failure $\varepsilon_{\mathsf{max}}$, tensile energy absorption TEA

$\Longrightarrow \mathbf{Z}^T = [E, \sigma_{\mathsf{max}}, \varepsilon_{\mathsf{max}}, TEA]$.

1.2 Mechanics problems on 1D random fields

In continuum mechanics often consider a superposition

$$Z(\omega, x) = \langle Z \rangle + Z'(\omega, x) \quad \langle Z' \rangle = 0 \quad \forall \omega, x \tag{1.50}$$

and assume

$$\left\langle \frac{\partial}{\partial x} Z \right\rangle = \frac{\partial}{\partial x} \langle Z \rangle \quad \left\langle \frac{\partial}{\partial t} Z \right\rangle = \frac{\partial}{\partial t} \langle Z \rangle \, . \tag{1.51}$$

... generalize to vector random processes and random fields.

Note: In general, $(2.2)_2$ is not true, e.g. in thermodynamics.

1.2.1 Propagation of surface waves along random boundaries

... random surface profile ζ_x of half-space $\{-\infty \leq x, y \leq \infty; z \geq \zeta(x, y)\}$

$$\left|\frac{l_c}{\lambda}\right| \ll 1 \quad \left|\frac{d\zeta}{dx}\right| \ll 1. \tag{1.52}$$

and for $\mathbf{n} = (n_x, n_y, n_z) \perp$ surface

$$n_x = -\frac{d\zeta}{dx}/S \ll 1 \quad n_z = 1/S \simeq 1, \quad S = \left[1 - (\partial\zeta/\partial x)^2\right]^{1/2}. \tag{1.53}$$

Take ζ_x as a zero-mean WSS r.p. modeled by random Fourier series.

Recall: unperturbed, harmonic ($e^{-i\gamma t}$) Rayleigh wave, propagating in x:

$$\phi = e^{ipx-az} \quad \psi = e^{ipx-bz}, \tag{1.54}$$

where

$$a^2 = p^2 - k_L^2 \quad k_L^2 = \frac{\rho\omega^2}{\lambda + 2\mu}$$
$$b^2 = p^2 - k_T^2 \qquad k_T^2 = \frac{\rho\omega^2}{\mu} \tag{1.55}$$

Approximate zero-traction b.c.'s by those at mean surface $z = 0$:

$$\sigma_{zx}^1 - \sigma'_{zx} = \sigma_{zx} = 0 \quad \sigma_{zz}^1 - \sigma'_{zz} = \sigma_{zz} = 0, \tag{1.56}$$

where each field, say, $\sigma_{zx} = \sigma_{zx}^1$ (scattered) $+ \sigma'_{zx}$ (perturbed). Note

$$\sigma_{ij}(x, \zeta) = \sigma_{ij}(x, 0) + \left.\frac{\partial \sigma_{ij}}{\partial z}\right|_{z=0}, \tag{1.57}$$

and rejecting higher order terms

$$\sigma'_{zx} = \left.\frac{\partial \sigma_{zx}^0}{\partial z}\right|_{z=0} \zeta - \sigma_{xx}^0 \frac{d\zeta}{dx} \quad \sigma'_{zz} = -\left.\frac{\partial \sigma_{zz}^0}{\partial z}\right|_{z=0} \zeta, \tag{1.58}$$

where σ^0_{zx}, σ^0_{zz} are unperturbed wave (2.3).

Introduce a system of plane waves $\{\phi_n, \psi_n; n = 1, 2, ...\}$

$$\phi_n = e^{ip_n x - \eta_n z} \quad \psi_n = e^{ip_n x - \nu_n z}, \tag{1.59}$$

with $p_n = p + ng$ for $\forall n$, so that $\eta_n = \sqrt{k_L - p_n^2}$, $\nu_n = \sqrt{k_T - p_n^2}$. Hence

$$\sigma^1_{zx} = \sum_{n=1}^{\infty} \sigma^{1(n)}_{zx} = \sum_{n=1}^{\infty} \mu \left[-2A_n p_n \eta_n + B_n \left(\nu_n^2 - \eta_n^2 \right) \right] e^{ip_n x}, \quad \sigma^1_{zz} = ... \tag{1.60}$$

1.2.2 Fracture of brittle micro-beams

Randomness of micro-beams Linear elastic fracture mechanics involves stiffness E and surface energy γ.

$\Longrightarrow$ pair $[E, \gamma]$. Given a randomly micro-heterogeneous material structure, admit a vector r.p. $[E, \gamma]_x$.

Note: randomness of E arises when the Representative Volume Element (RVE) cannot be safely assumed, i.e. when micro-beam is so thin that its lateral dimension L (defining its E) is comparable to crystal size d.

$\Longrightarrow$ consider scaling from a Statistical Volume Element (SVE) to RVE,.

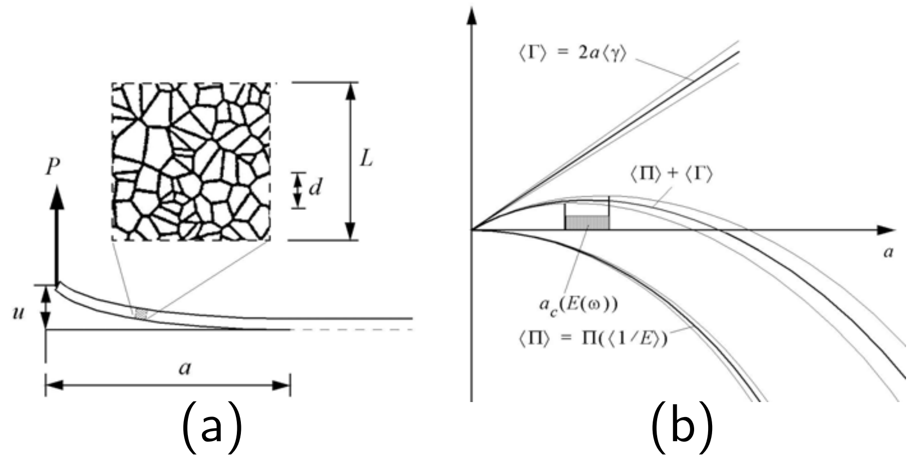

Figure 1.3: (a) Fracturing of a micro-beam of thickness L off a substrate, where a Statistical Volume Element imposed by the random microstructure characterized by a scale d is shown. (b) Potential energy $\Pi(\langle 1/E \rangle)$ (thick line) and its scatter shown by a parabolic wedge (thin lines), summed with the surface energy $\langle \Gamma \rangle = 2a \langle \gamma \rangle$ (thick line) and its scatter shown by a straight wedge (thin lines), results in $\Pi(\langle 1/E \rangle) + \langle \Gamma \rangle$ (thick line) and having scatter shown by a wider parabolic wedge (thin lines). Dashed region indicates the range of a random critical crack length $a_c(E(\omega))$.

Strain energy release rate in random beam (Griffith, 1921)

$$G = \frac{\partial W}{\partial A} - \frac{\partial U}{\partial A} = 2\gamma \tag{1.61}$$

where $A =$ crack surface area formed, $W =$work performed by applied loads, $U =$elastic strain energy, $\gamma =$energy to form a unit of new surface.

Dead-loading: force is not random, but kinematic variable is, $\Longrightarrow$

$$U(a) = \int_0^a \frac{M^2}{2IE} dx, \quad a = A/B \tag{1.62}$$

By Clapeyron's theorem, U is a random integral

$$U(a, E(\omega)) = \int_0^a \frac{M^2 dx}{2IE(\omega, x)}, \tag{1.63}$$

$\Longrightarrow$

$$\langle U(a, E) \rangle = \left\langle \int_0^a \frac{M^2 dx}{2I\left[\langle E \rangle + E'(\omega, x)\right]} \right\rangle . \tag{1.64}$$

In conventional formulation of deterministic fracture mechanics, random microscale heterogeneities $E'(x,\omega)$ are disregarded, and (2.14) is evaluated from $\langle E\rangle$

$$U(a,\langle E\rangle)=\int_0^a \frac{M^2dx}{2I\,\langle E\rangle}. \tag{1.65}$$

This corresponds to replacing $\left\langle \mathcal{L}^{-1}\right\rangle^{-1}$ by $\langle \mathcal{L}\rangle$

What about $\langle U(a,E)\rangle$ versus $U(a,\langle E\rangle)$, and $\langle G(E)\rangle$ versus $G(\langle E\rangle)$?

Note: r.p. E is positive-valued almost surely $\Longrightarrow$ Jensen's inequality

$$\frac{1}{\langle E\rangle}\leq\left\langle\frac{1}{E}\right\rangle. \tag{1.66}$$

$\Longrightarrow$

$$U(a, \langle E \rangle\,) = \int_0^a \frac{M^2 dx}{2I\,\langle E \rangle} \leq \int_0^a \frac{M^2}{2I} \left\langle \frac{1}{E} \right\rangle dx = \left\langle \int_0^a \frac{M^2 dx}{2IE(\omega, x)} \right\rangle = \langle U(a, E) \rangle \tag{1.67}$$

... hypothetical material specified by $\langle E \rangle$, versus properly ensemble averaged random material

$$G(a, \langle E \rangle) = \frac{\partial U(a, \langle E \rangle)}{B\partial a} \quad \langle G(a, E) \rangle = \frac{\partial \langle U(a, E) \rangle}{B\partial a}, \tag{1.68}$$

noting

$$U(a, \langle E \rangle) \mid_{a=0} = 0, \qquad \langle U(a, E) \rangle \mid_{a=0} = 0, \tag{1.69}$$

$\Longrightarrow$

$$G(a, \langle E \rangle) \leq \langle G(a, E) \rangle\,. \tag{1.70}$$

Note: can generalize to Timoshenko beams

Note: as mesoscale L/d grows, $E' \to 0$. $\Longrightarrow \left\langle E^{-1} \right\rangle^{-1} \to \langle E \rangle$, recover deterministic fracture mechanics.

Fixed-grip: displacement is non-random, but load is $\Longrightarrow$

$$G = -\frac{\partial U^e(a)}{B \partial a} = -\frac{u}{2B} \frac{\partial P}{\partial a}, \tag{1.71}$$

and G can be computed by direct ensemble averaging of E.

Mixed-loading conditions:

$$G_u \leq G_{mixed} \leq G_P. \tag{1.72}$$

Stochastic crack stability ... in any particular micro-beam ($B(\omega); \omega \in \Omega$),

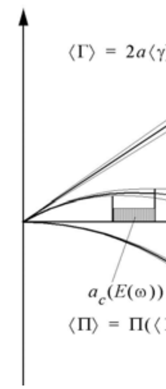

under general loading:

$$\frac{\partial^2 \left(\Pi\left(\omega\right) + \Gamma\left(\omega\right)\right)}{\partial a^2} \begin{array}{ll} < 0: & \text{unstable equilibrium} \\ = 0: & \text{neutral equilibrium} \\ > 0: & \text{stable equilibrium} \end{array}$$

potential energy $\Pi\left(\langle 1/E \rangle\right)$ and its scatter, summed with surface energy $\langle \Gamma \rangle = 2a \langle \gamma \rangle$ and its scatter, results in $\Pi\left(\langle 1/E \rangle\right) + \langle \Gamma \rangle$ having scatter shown by a parabolic wedge

$\Rightarrow$ random critical crack length $a_c\left(E\left(\omega\right)\right)$ has wide scatter!

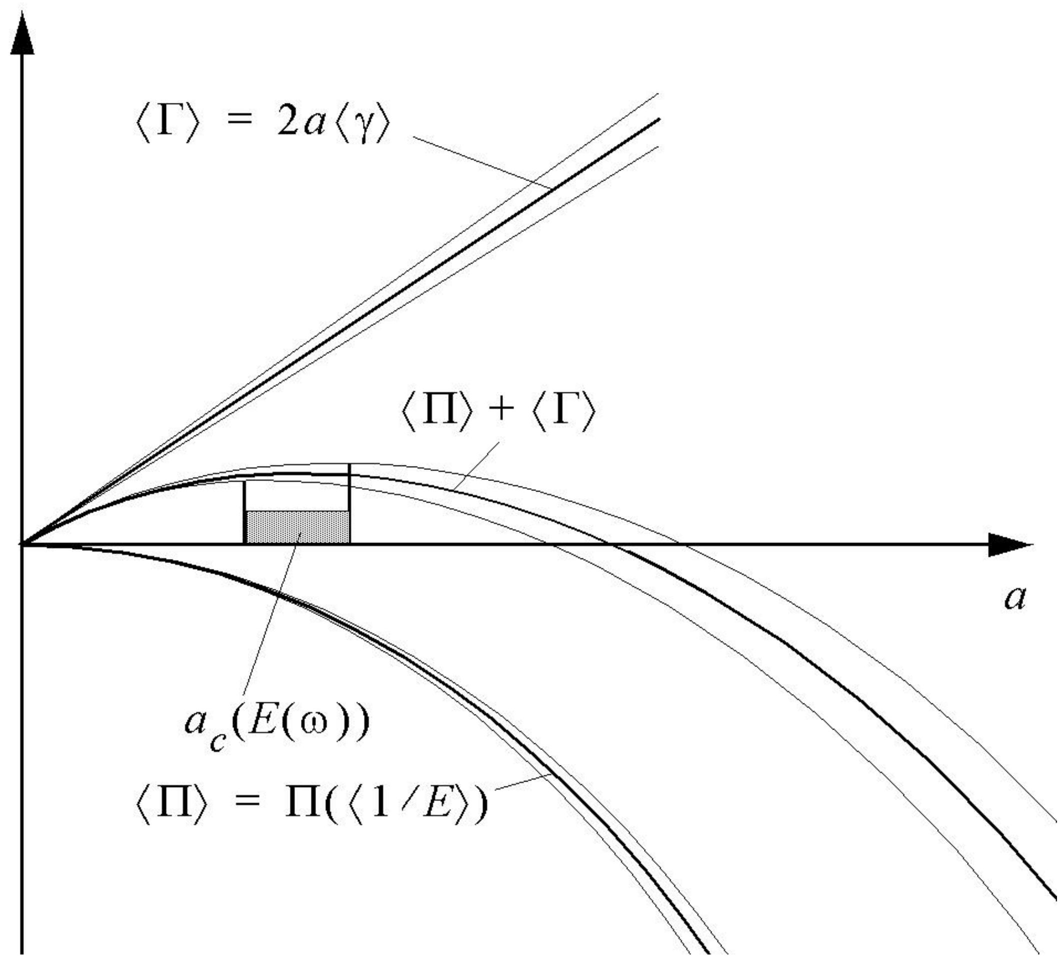

$\langle\Gamma\rangle = 2a\langle\gamma\rangle$
$\langle\Pi\rangle + \langle\Gamma\rangle$
a
$a_c(E(\omega))$
$\langle\Pi\rangle = \Pi(\langle 1/E\rangle)$

Note:

1. Potential energy $\Pi(\omega)$ is sensitive to fluctuations in E, which die out as $L/d \to \infty$ (L beam thickness, d grain size)

2. Surface energy $\Gamma(\omega)$ is sensitive to fluctuations in γ, but randomness in γ is independent of L/d

$\Rightarrow$ cracking of micro-beams is more sensitive to randomness of elastic moduli than cracking of large plates

3. Can show that under dead-load conditions:

and small random fluctuations in E and γ lead to relatively much stronger (!) fluctuations in a_c

$\Longrightarrow$ Even weak random perturbation in properties may be very significant!

Recall

$$\mathcal{L}(\omega)\phi = f \qquad \text{versus} \qquad \left\langle \mathcal{L}^{-1} \right\rangle^{-1} \langle \phi \rangle = f. \tag{1.73}$$

Note: $\langle \phi \rangle \neq \phi$ obtained by straightforward averaging: $\langle \mathcal{L} \rangle \, \phi^{\text{det}} = f$, as done in deterministic continuum mechanics.

... other aspects of mechanics of random micro-beams (Altus, 2001; Altus & Givli, 2003; Beran, 1998; Givli & Altus, 2003).

1.3 Elements of 2D and 3D random fields

1.3.1 Random scalar and vector fields

… return to paper: 2D random field of $[E, \sigma_{\mathsf{max}}, \varepsilon_{\mathsf{max}}, TEA]$

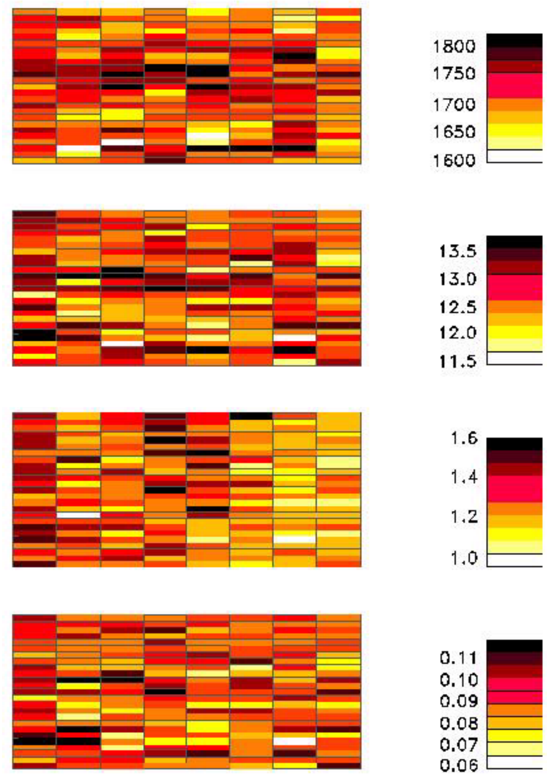

1800
1750
1700
1650
1600
13.5
13.0
12.5
12.0
11.5
1.6
1.4
1.2
1.0
0.11
0.10
0.09
0.08
0.07
0.06

random scalar field in D dimensions

$$Z : \Omega \times X \to \mathbb{R}, \;\; Z(\omega, \mathbf{x}) = z, \tag{1.74}$$

random vector field in D dimensions

$$\mathbf{Z} : \Omega \times X \to \mathbb{R}^n, \;\; \mathbf{Z}(\omega, \mathbf{x}) = \mathbf{z}. \tag{1.75}$$

Note: complete specification via *n-point probability distributions*

$$F_n(\mathbf{z}_1, ..., \mathbf{z}_n; \mathbf{x}_1, ..., \mathbf{x}_n) = P\{\mathbf{Z}(\mathbf{x}_1) \leq \mathbf{z}_1, ..., \mathbf{Z}(\mathbf{x}_n) \leq \mathbf{z}_n\}. \tag{1.76}$$

... correlation function $\rho(\mathbf{x}_1, \mathbf{x}_2)$ has properties:

(a) $\rho(\mathbf{x}_1, \mathbf{x}_2) \geq 0$,

(b) $\rho(\mathbf{x}_1, \mathbf{x}_2) = \overline{\rho(\mathbf{x}_1, \mathbf{x}_2)}$,

(c) $|\rho(\mathbf{x}_1, \mathbf{x}_2)|^2 \leq \rho(\mathbf{x}_1, \mathbf{x}_1)\rho(\mathbf{x}_2, \mathbf{x}_2)$.

Focus on WSS random fields

$$\langle Z(\mathbf{x})\rangle = \mu, \quad \langle Z(\mathbf{x}_1)Z(\mathbf{x}_1 + \mathbf{x})\rangle = R_Z(\mathbf{x}) < \infty. \tag{1.77}$$

... correlation (and covariance) functions

$$C_{ij}(\mathbf{x}_1, \mathbf{x}_2) = \langle [Z_i(\mathbf{x}_1) - \langle Z_i(\mathbf{x}_1)\rangle][Z_j(\mathbf{x}_2) - \left\langle Z_j(\mathbf{x}_2)\right\rangle]\rangle \tag{1.78}$$

correlation coefficient

$$\rho_{ij}(\mathbf{x}_1, \mathbf{x}_2) = \frac{C_{ij}(\mathbf{x}_1, \mathbf{x}_2)}{\sigma_i(\mathbf{x}_1)\sigma_j(\mathbf{x}_2)}, \tag{1.79}$$

$\Longrightarrow$for WSS field

$$\rho_{ij}(\mathbf{x}) = \frac{C_{ij}(\mathbf{x})}{\sigma_i(\mathbf{x})\sigma_j(\mathbf{x})}. \tag{1.80}$$

one-point special case

$$\rho_{ij}(\mathbf{0}) = \frac{C_{ij}(\mathbf{0})}{\sigma_i(\mathbf{0})\sigma_j(\mathbf{0})}. \tag{1.81}$$

Isotropic random fields

$$\rho(\mathbf{x}) = \rho(x), \ \ x \equiv |\mathbf{x}| = \sqrt{x_i x_i}. \tag{1.82}$$

Note: An analogue of isotropy property for random fields in 1D is: $\rho(x) = \rho(-x)$, $x = x_1 - x_2$.

Note: As before, can define a correlation length (radius).

Two classes of isotropic random fields:

$$\rho(x) = \exp[-Ax^{\alpha}], \;\; A > 0, \;\; 0 < \alpha \leq 2; \tag{1.83}$$

$$\rho(x) = [1 + Ax^{\alpha}]^{-1}, \;\; A > 0, \;\; 0 < \alpha \leq 2. \tag{1.84}$$

Note: For an isotropic field on $\mathbb{R}^D$, $\rho\,(x) \geq -1/D$.

Note: A valid isotropic $\rho(x)$ in $\mathbb{R}^{D_2}$ is always a valid isotropic $\rho\,(x)$ in $\mathbb{R}^{D_1}$, where $D_2 > D_1$. But, the converse is not true as this 'tent' example shows

$$\rho(x) = \begin{cases} \sigma^2(1 - |x|\,/a), & 0 \leq |x| < a \\ 0, & |x| > a \end{cases} \qquad \text{valid in } \mathbb{R}^1\text{, but not in } \mathbb{R}^2. \tag{1.85}$$

$\Longrightarrow$May construct new, more complex correlation functions. Note:

(i) a convex combination of p.d.f.'s is a p.d.f.

(ii) a convex combination of correlation fn's is a correlation fn

(iii) a finite product of correlation fn's is a correlation fn

$$\rho(x) = \frac{\exp[-Ax^{\alpha}]}{1 + Bx^{\alpha}}, \quad A, B > 0, \quad 0 < \alpha, \beta \leq 2; \tag{1.86}$$

$$\rho(x) = \exp[-\sum_{s=1}^{r} Ax^{\alpha_s}], \quad A_s > 0, \quad 0 < \alpha_s \leq 2, \quad s = 1, ..., r; \tag{1.87}$$

$$\rho(x) = [-\prod_{s=1}^{r} (1 + B_s x^{\beta_s}) l_s], \quad B_s > 0, \quad 0 < \beta_s \leq 2, \quad l_s = 1, 2, ...; \tag{1.88}$$

$$\rho(x) = \exp[-Ax^{\alpha}](\cosh Bx^{\alpha})^{s}, \quad A{+}B(2l{-}s) > 0, \quad 0 < \alpha \leq 2, \quad s = 1, ..., r; \tag{1.89}$$

$$\rho(x) = \frac{(\cosh Bx^{\alpha})^s}{1 + Ax^{\alpha}}, \quad A + B(2l - s) > 0, \quad 0 < \alpha \leq 2, \quad s = 1, ..., r. \quad (1.90)$$

Example: paper properties - $\rho_{ij}(x)$ is estimated from stationarity and ergodicity

$$\rho_{ij}(\mathbf{0}) \equiv \begin{bmatrix} \rho_{E,E} & & & \\ \rho_{E,\sigma_{\mathsf{max}}} & \rho_{\sigma_{\mathsf{max}},\sigma_{\mathsf{max}}} & sym & \\ \rho_{E,\varepsilon_{\mathsf{max}}} & \rho_{\sigma_{\mathsf{max}},\varepsilon_{\mathsf{max}}} & \rho_{\varepsilon_{\mathsf{max}},\varepsilon_{\mathsf{max}}} & \\ \rho_{E,TEA} & \rho_{\sigma_{\mathsf{max}},TEA} & \rho_{\varepsilon_{\mathsf{max}},TEA} & \rho_{TEA,TEA} \end{bmatrix} = \begin{bmatrix} 1 & & & \\ 0.43 & 1 & sym & \\ 0.10 & 0.56 & 1 & \\ 0.14 & 0.90 & 0.69 & 1 \end{bmatrix}. \quad (1.91)$$

(i) cross-correlations between E and inelastic parameters $\sigma_{\mathsf{max}}, \varepsilon_{\mathsf{max}}, TEA$ are weak, although we note that $\rho_{E,\sigma_{\mathsf{max}}}$ is greater than $\rho_{E,\varepsilon_{\mathsf{max}}}$ or $\rho_{E,TEA}$;

(ii) cross-correlations between $\sigma_{\mathsf{max}}, \varepsilon_{\mathsf{max}}$, and TEA are v. similar.

Anisotropy of correlation function

... introduce a transformation

$$T(\mathbf{x}) = [T_1(\mathbf{x}), ..., T_1(\mathbf{x})], \;\; \mathbf{x} = (x_1, ..., x_D) \tag{1.92}$$

of $\mathbb{R}^D$ into $\mathbb{R}^D$. If J of T is $\neq 0$, there exists T^{-1}. Let $|\mathbf{x}|$ denote a norm in $\mathbb{R}^D$ and $||\mathbf{y}||$ a norm in $\mathbb{R}^D$ after T. If a WSS field Z has a property that $|\mathbf{x}| = ||\mathbf{y}||$ implies

$$\rho(\mathbf{x}) = \rho(\mathbf{y}), \tag{1.93}$$

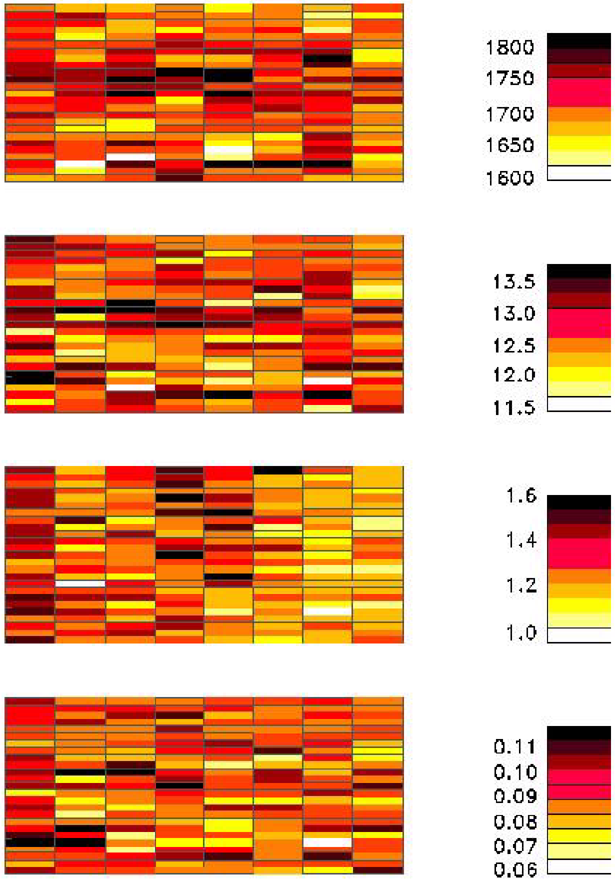

Figure 1.4: A map (from the top) of stiffness, strength, strain-to-failure, and tensile energy absorption for a 25×8 array of 7" $\times$ 1" specimens, after (DiMillo and Ostoja-Starzewski, 1998); paper web provided by Champion Corp.

then Z is called a *WSS quasi-isotropic random field.*

... *ellipsoidal structure* with b_{ij} a positive-definite quadratic form

$$||\mathbf{y}||^2 = \sum_{i,j=1}^{n} b_{ij} y_i y_j, \tag{1.94}$$

Consider $\rho(||\mathbf{y}||)$. Then the Jacobian of T is the determinant of matrix b_{ij}. For example, the Gaussian autocovariance of a random process on $\mathbb{R}^1$ can now be generalized as

$$\rho(\mathbf{y}) = \exp[-\sum_{i,j=1}^{n} b_{ij} y_i y_j]. \tag{1.95}$$

Another model of a quasi-isotropic field on $\mathbb{R}^D$ is

$$T(\mathbf{x}) = [a_1 x_1, ..., a_D x_D], \text{ all } a_i > 0. \tag{1.96}$$

Note: Distinguish the anisotropy in terms of correlation function from the (local) anisotropy of realizations.

Note: Models of correlation function for isotropic random fields (3.9) carry over to quasi-isotropic fields provided we replace x by $\left\|T^{-1}(\mathbf{y})\right\|$. $\Longrightarrow$

$$\rho(x) = \exp[-A \left\|T^{-1}(\mathbf{y})\right\|^{\alpha}], \;\; A > 0, \;\; 0 < \alpha \leq 2. \tag{1.97}$$

Fully separable correlation function

$$\rho(\mathbf{x}) = \rho(x_1)\rho(x_2)...\rho(x_D), \tag{1.98}$$

partially separable structure, as in

$$\rho(\mathbf{x}) = \rho(x_1, x_2)...\rho(x_D). \tag{1.99}$$

... common model in fluid mechanics: $\rho(\mathbf{x}, t) = \rho(\mathbf{x})\rho(t)$.

Local averaging:

$$Z_L(\omega, \mathbf{x}) = \frac{1}{L^2} \int_{D_L} Z_L(\omega, \mathbf{x}') d\mathbf{x}', \tag{1.100}$$

Note: If applied to a stiffness $\mathbf{C}$ (resp., compliance $\mathbf{S}$) tensor field, it yields a Voigt-type (Reuss-type) estimate/bound of the stiffness (compliance) for the domain D_L.

... local averaging is a simple operation, but it may yield very misleading estimates of actual material properties.

... D_L plays the role of a mesoscale, but mechanics is unaccounted for !

... which L to choose? ... what is the L-dependence!

1.3.2 Random tensor fields

Consider $\mathbf{z} = \mathbf{Z}(\omega, \mathbf{x})$ to be a first-rank tensor:

$$\mathbf{z}' = Q \cdot \mathbf{z}, \tag{1.101}$$

where Q is a matrix giving $\mathbf{x}' = Q \cdot \mathbf{x}$ upon rotation.

For an nth-rank tensor we have

$$\mathbf{z}' = Q ... Q \cdot \mathbf{z}, \tag{1.102}$$

where Q appears n times.

$\Longrightarrow$ define a random tensor field of first-rank to be *wide-sense stationary* (WSS) and isotropic whenever the mean $\langle \mathbf{Z}(\mathbf{x}) \rangle$ and the correlation $\rho_i^k(\mathbf{x})$ do not change when subjected to arbitrary shifts and when transforming by rotation in (3.31) according to

$$\langle \mathbf{Z}' \rangle = Q \cdot \langle \mathbf{Z} \rangle \,, \quad \rho_i^j(\mathbf{x}') = Q \cdot \rho_i^j(\mathbf{x}), \tag{1.103}$$

with $\mathbf{x}$ transformed into $\mathbf{x}'$ also according to (3.30).

Note: This may be extended to *strict-sense stationarity* (SSS) by requiring (3.30) to hold for all n-order distributions F_n, not just for two moments.

In (3.33) we employ the correlation coefficient

$$\rho_i^j(\mathbf{x}_1, \mathbf{x}_2) = \frac{\langle [\Theta_i(\mathbf{x}_1) - \langle \Theta_i(\mathbf{x}_1) \rangle][\Theta_j(\mathbf{x}_2) - \left\langle \Theta_j(\mathbf{x}_2) \right\rangle] \rangle}{\sigma_i(\mathbf{x}_1)\sigma_j(\mathbf{x}_2)}, \tag{1.104}$$

... same thing as (3.6), but notation ρ_i^j is superior to ρ_{ij} for tensors.

The WSS property means that, for any pair $(\mathbf{x}_1, \mathbf{x}_2)$,

$$\rho_i^j(\mathbf{x}_1, \mathbf{x}_2) = \rho_i^j(\mathbf{x}), \qquad \mathbf{x} = |\mathbf{x}_1 - \mathbf{x}_2| \,. \tag{1.105}$$

Isotropy $\Longrightarrow$

$$\rho_i^j(\mathbf{x}) = \rho_i^j(x), \;\; x \equiv |\mathbf{x}| = \sqrt{x_i x_i}. \tag{1.106}$$

Robertson (*Proc. Camb. Phil. Soc.*, 1940): ρ_i^j in 3D admits this representation:

$$\rho_i^j\,(\mathbf{x}) = K_1\,(x)\,x_i x_k + K_2\,(x)\,\delta_{ik} \tag{1.107}$$

where K_i's are real-valued functions of $x = |\mathbf{x}|$ s.t.

$$K_1 = \rho_{11}^1 = \rho_{22}^1 \quad K_1 + K_2 = \rho_{33}^1 \tag{1.108}$$

and $n_i = x_i/x$. Here ρ_{ij}^1 = correlation $\rho_i^j\,(\mathbf{x})$ between $C_i\,(\mathbf{x}_1)$ and $C_j\,(\mathbf{x}_2)$ in a coordinate system centered at $\mathbf{x}_1$ and directed to $\mathbf{x}_2$.

Second-rank random tensor fields

In general, $\mathbf{Z}$ is a *random tensor field* in D dimensions if

$$\mathbf{Z} : \Omega \times X \to \mathbb{R}^n, \ \ \mathbf{Z}(\omega, \mathbf{x}) = \mathbf{z}, \, \forall \mathbf{x} \in X \tag{1.109}$$

Note: for $D = 2$, $n = 4$, while, for $D = 3$, $n = 9$, etc. The concept of a random tensor field may be applied to any tensor field in continuum mechanics.

The normalized correlation function of, say, a second-rank tensor field is

$$\rho_{ij}^{kl}(\mathbf{x}_1, \mathbf{x}_2) = \frac{\langle [Z_{ij}(\mathbf{x}_1) - \left\langle Z_{ij}(\mathbf{x}_1) \right\rangle][Z_{kl}(\mathbf{x}_2) - \langle Z_{kl}(\mathbf{x}_2) \rangle] \rangle}{\sigma_{ij}(\mathbf{x}_1) \sigma_{kl}(\mathbf{x}_2)}, \tag{1.110}$$

where $\sigma_{ij}(\mathbf{x}_1)$ and $\sigma_{kl}(\mathbf{x}_2)$ are the standard deviations of the pair $[z_{ij}(\mathbf{x}_1),$ $z_{kl}(\mathbf{x}_2)]$ at respective points. It follows from the tensor property of $\mathbf{z}$, that ρ_{ij}^{kl} is a fourth-rank tensor.

Special case: $\mathbf{Z}$ = anti-plane stiffness tensor $\mathbf{C}$ ($\equiv C_{ij}$) of a hyperelastic material (or a conductivity tensor). Then, $\forall \mathbf{x} \in X$ of every $\mathbf{C}(\omega)$ of the random field

$$C_{ij} = C_{ji} \tag{1.111}$$

implying these symmetries

$$\rho_{ij}^{kl} = \rho_{ji}^{kl} = \rho_{ij}^{lk}. \tag{1.112}$$

Robertson (1940): ρ_{ij}^{kl} in 3D admits this representation

$$\begin{gathered}
\rho_{ij}^{kl}(x) = K_4(x)\,\delta_{ij}\delta_{kl} + K_6(x)\left[\delta_{ik}\delta_{jl} + \delta_{il}\delta_{jk}\right] \\
+\left[K_5(x) - K_6(x)\right]\left[n_j n_k \delta_{il} + n_i n_l \delta_{jk} + n_i n_k \delta_{jl} + n_j n_l \delta_{ik}\right] \\
+\left[K_3(x) - K_4(x)\right]\left[n_i n_j \delta_{kl} + n_k n_l \delta_{ij}\right] \\
+\left[K_1(x) + K_2(x) - 2K_3(x) - 4K_5(x)\right] n_i n_j n_k n_l,
\end{gathered} \tag{1.113}$$

where K_i's are s.t.

$$\begin{array}{lll} K_1 = \rho^1_{1111} & K_2 = \rho^1_{2222} & K_3 = \rho^1_{1122} \\ K_4 = \rho^1_{2233} & K_5 = \rho^1_{1212} & K_6 = \rho^1_{2323} \end{array}, \tag{1.114}$$

and satisfy

$$K_4 + 2K_6 - K_2 = 0, \tag{1.115}$$

and $n_i = x_i/x$. Here ρ^1_{ijkl} = correlation between $C_{ij}(\mathbf{x}_1)$ and $C_{kl}(\mathbf{x}_2)$ in a coordinate system centered at $\mathbf{x}_1$ and directed to $\mathbf{x}_2$.

Note: while a second-rank tensor in 3D generally has 9 independent components, the assumption of isotropy of its realizations reduces the number of parameters of its correlation function to 6.

Fourth-rank tensor fields

$\mathbf{Z}$ is a *random tensor field* in D dimensions if

$$\mathbf{Z} : \Omega \times X \to \mathbb{R}^n, \;\; \mathbf{Z}(\omega, \mathbf{x}) = \mathbf{z}, \forall \mathbf{x} \in X \tag{1.116}$$

Note: for $D = 2$, $n = 16$, while, for $D = 3$, $n = 81$. For example, in classical (non-micropolar) hyperelasticity, where $\mathbf{Z}$ = stiffness tensor, $n = 21$. As an example, if we were able to measure not just the uniaxial stiffness (E) but the entire stiffness tensor ($\mathbf{C} = C_{ijkl}$) at each and every point $\mathbf{x}$ of a realization of random medium, we would deal with a random field of stiffness tensor.

Focus on $\mathbf{Z}$ being WSS. $\Longrightarrow$

$$\rho_{ijkl}^{prst}(\mathbf{x}_1, \mathbf{x}_2) = \frac{\langle [Z_{ijkl}(\mathbf{x}_1) - \left\langle Z_{ijkl}(\mathbf{x}_1) \right\rangle][Z_{prst}(\mathbf{x}_2) - \left\langle Z_{prst}(\mathbf{x}_2) \right\rangle] \rangle}{\sigma_{ijkl}(\mathbf{x}_1)\sigma_{prst}(\mathbf{x}_2)}, \tag{1.117}$$

where $\sigma_{ijkl}(\mathbf{x}_1)$ and $\sigma_{prst}(\mathbf{x}_2)$ are the standard deviations of $[Z_{ijkl}(\mathbf{x}_1),$ $Z_{prst}(\mathbf{x}_2)]$. Tensor property of $\mathbf{Z} \Longrightarrow \rho_{ijkl}^{prst}$ is an eighth-rank tensor.

$\mathbf{Z}$ is WSS $\Longrightarrow$

$$\rho_{ijkl}^{prst}(\mathbf{x}_1, \mathbf{x}_2) = \rho_{ijkl}^{prst}(\mathbf{x}), \tag{1.118}$$

where $\mathbf{x} = \mathbf{x}_2 - \mathbf{x}_1$.

If the correlation function is isotropic,

$$\rho_{ijkl}^{prst}(\mathbf{x}) = \rho_{ijkl}^{prst}(x). \tag{1.119}$$

Example: $\mathbf{Z}$ = random stiffness tensor $\mathbf{C}$ in a linear hyperelastic material. Then, at $\forall \mathbf{x} \in X$ of every $\mathbf{C}(\omega)$

$$C_{ijkl} = C_{jikl} = C_{ijlk} = C_{klij} \tag{1.120}$$

so that

$$\rho_{ijkl}^{prst} = \rho_{jikl}^{prst} = \rho_{ijlk}^{prst} = \rho_{klij}^{prst} = \rho_{ijkl}^{rpst} = \rho_{ijkl}^{prts} = \rho_{ijkl}^{stpr} \tag{1.121}$$

Lomakin (1965, 1970): $\rho_{ijkl}^{prst}(x)$ in 3D admits this representation

$$\begin{gathered}\rho_{ijkl}^{prst}(x) = F_{12} + K_{13}(x)\,\delta_{ij}\delta_{kl}\delta_{pr}\delta_{st} \\ +K_{14}(x)\left[\delta_{ij}\delta_{kl}\delta_{ps}\delta_{rt} + \delta_{ij}\delta_{kl}\delta_{pt}\delta_{rs} + \delta_{ik}\delta_{jl}\delta_{pr}\delta_{st} + \delta_{il}\delta_{jk}\delta_{pr}\delta_{st}\right] \\ +K_{15}(x)\left[\delta_{ij}\delta_{jl}\delta_{ps}\delta_{rt} + \delta_{ik}\delta_{jl}\delta_{pt}\delta_{rs} + \delta_{il}\delta_{jk}\delta_{ps}\delta_{rt} + \delta_{il}\delta_{jk}\delta_{pt}\delta_{rs}\right]\end{gathered} \tag{1.122}$$

Concepts of separable structure, local averaging, ... apply, in appropriately generalized forms, to random fourth-rank tensor fields.

1.4 Mechanics problems on 2D and 3D random fields

4.1 Mean field equations of random materials

Recall from Preface: $\mathbf{u}$ is governed by $\mathcal{L}\mathbf{u} = \mathbf{f}$. Use decompositions

$$\mathbf{u} = \langle \mathbf{u} \rangle + \mathbf{u}' \quad \mathcal{L} = \langle \mathcal{L} \rangle + \mathcal{L}', \tag{1.123}$$

First averaging the original equation, and then subtract the result from it, to obtain an equation for $\mathbf{u}'$

$$\langle \mathcal{L} \rangle \mathbf{u}' + (I - P) \mathcal{L}' \mathbf{u}' = -\mathcal{L}' \langle \mathbf{u} \rangle . \tag{1.124}$$

Here P is a so-called *projection*, basically an averaging operation.

Solving for $\mathbf{u}'$,

$$\left(\langle\mathcal{L}\rangle - \mathcal{M}\right)\langle\mathbf{u}\rangle = \mathbf{f}, \tag{1.125}$$

where

$$\mathcal{M} = \left\langle \mathcal{L}'\left[\langle\mathcal{L}\rangle + (I-P)\,\mathcal{L}'\right]^{-1}\mathcal{L}'\right\rangle = -\mathcal{L}'\,\langle\mathbf{u}\rangle \tag{1.126}$$

stands for the so-called *mass operator*; $^{-1}$ indicates an inversion.

Fishman & McCoy (1981); consider heat conduction problem in a medium described by a random field $\left\{K_{ij}\left(\omega,\mathbf{x}\right);\omega\in\Omega\right\}$, under a source term $f\left(\mathbf{x}\right)$ and boundary temperature field $T^0\left(\mathbf{x}\right)$, both slowly varying on macroscale.

Thus, $\forall B(\omega) \in \mathcal{B}$

$$\begin{aligned} q_{i,i} &= f(\mathbf{x}) & \mathbf{x} &\in \mathcal{B} \\ q_i &= K_{ij}(\omega, \mathbf{x})\, T_{,j} & \mathbf{x} &\in \mathcal{B} \\ T(\mathbf{x}) &= T^0(\mathbf{x}) & \mathbf{x} &\in \partial\mathcal{B}, \end{aligned} \tag{1.127}$$

Note: $K_{ij}(\omega, \mathbf{x}) = \left\langle K_{ij} \right\rangle + K'_{ij}(\omega, \mathbf{x})$, so that, upon averaging,

$$\begin{aligned} \langle q_i \rangle_{,i} &= f(\mathbf{x}) & \mathbf{x} &\in \mathcal{B} \\ \langle q_i \rangle &= \left\langle K_{ij} \right\rangle \left\langle T_{,j} \right\rangle + \left\langle K'_{ij}(\omega, \mathbf{x})\, T'_{,j} \right\rangle & \mathbf{x} &\in \mathcal{B} \\ \langle T(\mathbf{x}) \rangle &= T^0(\mathbf{x}) & \mathbf{x} &\in \partial\mathcal{B}. \end{aligned} \tag{1.128}$$

From the equations governing the fluctuations

$$\begin{aligned} \left\langle q'_i \right\rangle_{,i} &= 0 & \mathbf{x} &\in \mathcal{B} \\ q'_i &= \left\langle K_{ij} \right\rangle T'_{,j} + (I - P)\, K'_{ij}(\omega, \mathbf{x})\, T'_{,j} + K'_{ij}(\omega, \mathbf{x}) \left\langle T'_{,j} \right\rangle & \mathbf{x} &\in \mathcal{B} \\ T'(\mathbf{x}) &= 0 & \mathbf{x} &\in \partial\mathcal{B}, \end{aligned} \tag{1.129}$$

derive an analog

$$\left\langle K_{ij}\right\rangle T'_{,ji}+(I-P)\left[K'_{ij}\left(\omega,\mathbf{x}\right)T'_{,j}\right]_{,i}=-K'_{ij}\left(\omega,\mathbf{x}\right)\left\langle T'_{,j}\right\rangle . \qquad (1.130)$$

$\Longrightarrow$ constitutive equation for average fields is

$$\left\langle q_i\left(\mathbf{x}\right)\right\rangle = K^{*}_{ij}\left\langle T_{,j}\right\rangle+\int_{\mathcal{B}}\left[K_{ij}\left(\mathbf{x},\mathbf{x}'\right)\left\langle T_{,j}\left(\mathbf{x}'\right)\right\rangle\right]_{,i}d\mathbf{x}'. \qquad (1.131)$$

Note: Effective constitutive response has a non-local character; this result carries over to random elastic and inelastic materials.

4.2 Mean field equations of turbulent media

Recall

$$v_{i,i} = 0 \quad \rho \dot{v}_i = \sigma_{ij,j} \quad \rho \dot{u} = \sigma_{ij} d_{ij} - q_{i,i} \ , \tag{1.132}$$

Assuming (2.2) to hold for all the fields, find

$$\langle v \rangle_{i,i} = 0 \quad \rho \langle \dot{v}_i \rangle = \sigma^*_{ij,j} \quad \rho \dot{u}^* = \sigma^*_{ij} \left\langle d_{ij} \right\rangle - q^*_{i,i} \ , \tag{1.133}$$

with Reynolds stress $(= R_{ij})$

$$\sigma^*_{ij} = \sigma_{ij} - \rho \left\langle v'_i v'_j \right\rangle , \tag{1.134}$$

$$u^* = \langle u \rangle + \frac{1}{2} \left\langle v'_i v'_i \right\rangle \tag{1.135}$$

$$q^*_i = q_i - \left\langle \sigma'_{ij} v'_i \right\rangle + \rho \left\langle \left(u' + \frac{1}{2} v'_j v'_j \right) v'_i \right\rangle \tag{1.136}$$

i.e. effective heat flux = original heat flux + rate of work of fluctuating stresses on dV's surface +stochastic energy convection through that surface.

Note: Average field $\langle v_i \rangle$ satisfies the same continuity equation as v_i. Divergence of Reynolds stress may be interpreted as the force density on the fluid due to turbulent fluctuations. Reynolds stress also appears when analyzing the Euler or N-S equations.

Note: While, formally, $\langle v_i \rangle$ = ensemble average, in practice, it is sometimes also thought of as a spatial average over some length scale, or a temporal average. Accordingly, $\mathbf{v}'$ is then interpreted not as a statistical one, but a spatial or temporal one. One then works with *separation of scales*: time scale of variation of $\langle \mathbf{v} \rangle$ is much larger than that of $\mathbf{v}'$. The equivalence between such averages in statistical turbulence is an open problem, but is justified in the more established field of equilibrium statistical mechanics by the ergodic theorem.

1.5 Ergodicity

1.5.1 Basic considerations

Can one determine probabilistic characteristics (moments, distributions, ...) of a random process or field in terms of a set of values $\{z(x_1), .., z(x_n)\}$ observed over just one realization $Z(\omega, x)$, $x \in \mathbb{R}$?

If yes, have a possibility of treating $Z(\omega)$ at hand as 'typical' (in a certain sense...) of the whole random field Z, recall measurements of paper properties.

$\Longrightarrow$ *ergodic property* (or *ergodicity*), but in mathematics these terms have a narrower meaning (be careful).

$\Longrightarrow$ *ergodicity in the mean* (or, r.p. is *mean-ergodic*) means that any realization $Z(\omega), \omega \in \Omega$ is sufficient to get the ensemble average $\langle Z(x) \rangle$ at any x from its spatial average $\overline{Z(\omega)}$ for any $\omega \in \Omega$ taken over a sufficiently large interval:

$$\overline{Z(\omega)} \equiv \lim_{L \to \infty} \frac{1}{2L} \int_{-L}^{L} Z(\omega, x) dx = \int_{\Omega} Z(\omega, x) dP(\omega) \equiv \langle Z(x) \rangle \,. \quad (1.137)$$

Computation of (5.1)

LHS of (5.1) may be evaluated only with some accuracy, due to finite scale discretization of measurements and impossibility of carrying out the limit $L \to \infty$. In practice:

$$\overline{Z(\omega)} \equiv \frac{1}{N} \sum_{n=1}^{N} Z(\omega, x_n) \quad (1.138)$$

and

$$\langle Z(x)\rangle \equiv \frac{1}{M}\sum_{m=1}^{M} Z(\omega_m, x). \tag{1.139}$$

Conditions for (5.1) to hold

Assuming the limit in (5.1) exists, its value $\overline{Z(\omega)}$, depends on ω. Under what conditions does it equal the constant μ?

$\Longrightarrow$ ergodic theorems; the process is mean-ergodic iff its autocovariance is such that

$$\lim_{L\to\infty} \frac{1}{4L^2} \int_{-L}^{L} \int_{-L}^{L} C(x_1, x_2) dx_1 dx_2 = 0 \tag{1.140}$$

Prove this by noting that σ_L^2 of r.v. $S_L(\omega) = (2L)^{-1} \int_{-L}^{L} Z(\omega, x) dx$ is

$$\sigma_L^2 = \left\langle |S_L - \mu_L|^2 \right\rangle = \frac{1}{4L^2} \int_{-L}^{L} \int_{-L}^{L} C(x_1, x_2) dx_1 dx_2 \tag{1.141}$$

where $\mu_L = \langle S_L(\omega) \rangle$.

Note: A process may be ergodic without being stationary.

If Z is WSS $\Longrightarrow$ r.p. is mean-ergodic if its $C(x) = R(x) - \mu^2$ is s.t.

$$\lim_{L\to\infty} \frac{1}{2L} \int_{-2L}^{2L} C(x) \left(1 - \frac{|x|}{2L}\right) dx = 0 \tag{1.142}$$

One gets sufficiency here if $\int_{-\infty}^{\infty} C(x)dx < \infty$.

There also are other kinds of ergodicity: e.g. correlation-ergodic, distribution-ergodic, e.g.

$$\begin{gathered}\overline{R_Z(\omega, x)} \equiv \lim_{L\to\infty} \frac{1}{2L} \int_{-L}^{L} Z(\omega, x_1 + x) Z(\omega, x_1) dx_1 = \\ \int_{\Omega} Z(\omega, x_1 + x) Z(\omega, x_1) dP(\omega) \equiv \langle Z(\omega, x_1 + x) Z(\omega, x_1) \rangle \,,\end{gathered} \tag{1.143}$$

which, in fact, was the basis for computation of autocorrelations in Figs. 1.1 and 1.2.

Under what conditions does the limit $\overline{Z(\omega)}$ in (5.1) exist? This is known as '*ergodic problem*' in mathematics, having roots in statistical mechanics, where one is interested in estimating system properties from a single trajectory over a relatively very long period of time. Since a trajectory occurs in a phase space, this leads us to the concept of an *ergodic flow* in the phase space, i.e. a flow for which the integral with respect to a time parameter t converges to a random variable $\widehat{Z(\omega)}$

$$\lim_{L\to\infty} \frac{1}{L} \int Z(\omega, t) dx = \widehat{Z(\omega)}. \tag{1.144}$$

More generally, for r.p. $Z(t)$ can define a flow in phase (or state) space of Z as a transformation mapping this space onto itself, whereby any event A is transformed into some other one, A_τ, via operator $T(\tau)$:

$$A \to A_\tau = T(\tau)A. \tag{1.145}$$

$\Longrightarrow$ a set function $g(A)$ transforms as

$$g(A) \to g(A_\tau) = g[T(\tau)A]. \tag{1.146}$$

In classical statistical mechanics one focuses on Hamiltonian flows (total system energy $= const$), which are *measure-preserving* in the sense that

$$P(A) = P(A_\tau). \tag{1.147}$$

In (5.8) A and A_τ stand for an initial set and a set after the transformation (5.6). The counterpart of measure in physics is the *density* $\rho\,(q_n, p_n, t)$ in phase space (q_i, p_n; $n = 1, ..., N$); this needed to pass from statistical mechanics to continuum thermodynamics.

Note: a Hamiltonian system is measure-preserving because of *Liouville's theorem* (expressed in terms of convective derivative being zero)

$$\frac{d\rho}{dt} = \frac{\partial \rho}{\partial t} + \frac{\partial \rho}{\partial q_n}\dot{q}_n + \frac{\partial \rho}{\partial p_n}\dot{p}_n = 0, \tag{1.148}$$

Recall here Hamilton's equations

$$\dot{q}_n = \frac{\partial H}{\partial p_n} \quad \dot{p}_n = -\frac{\partial H}{\partial q_n}. \tag{1.149}$$

Consider three basic types of measure-preserving flows in phase space. Let the set A modeling the state of system evolve while keeping another set B fixed.

Case (a): moves in a periodic fashion through phase space, visiting just a fraction of it without ever entering other regions (e.g. harmonic oscillator)

$$H(q,p) = \frac{p^2}{2m} + \frac{1}{2}kq^2 \tag{1.150}$$

Case (b): A is only slowly altered during its motion, while it sweeps the entire space if observed for a sufficiently long (infinite) time $\Longrightarrow$ ergodic flow. G.D. Birkhoff (1931): every invariant set has measure 0 or 1, i.e. no trajectory can be confined to a finite portion of phase space because it has to wander (*ergodos* in Greek) through all of it. Another way to express this: trajectory is not sensitive to initial conditions.

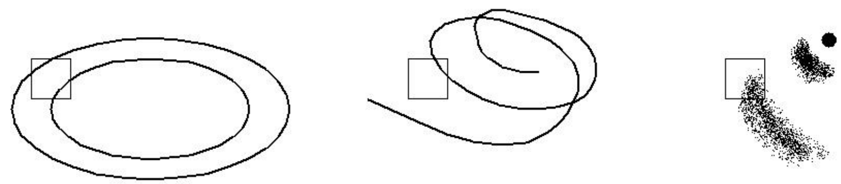

(a) (b) (c)

Figure 1.5: Three types of flow in phase space: (a) periodic, non-ergodic; (b) ergodic, non-mixing; (c) ergodic, mixing; after Balescu (1975). In each case, a square-shaped set B is shown.

Case (c): A not only sweeps the entire space, but its shape is being altered during its motion so as to fill the entire space through a multitude of growing branches, subbranches, and so on $\Longrightarrow$ *(strong) mixing flow*:

... A diffuses from small blob, and tends to a 'uniformly mixed situation': volume fraction of A in B equals the initial volume fraction of A in Ω:

$$\lim_{\tau \to \infty} P(A_\tau \cap B) = P(A)P(B) \tag{1.151}$$

Note: mixing $\Longrightarrow$ ergodicity, but $\exists$ ergodic flows that are not mixing.

... *weak mixing* defined via

$$\lim_{\tau \to \infty} \frac{1}{\tau} \int_0^\tau [P(A_\tau \cap B) - P(A)P(B)]\, d\tau = 0 \tag{1.152}$$

...an even weaker mixing

$$\lim_{\tau\to\infty} \frac{1}{\tau} \int_0^{\tau} [P(A_\tau \cap B)]\, d\tau = P(A)P(B). \tag{1.153}$$

Note: all these are various extensions of the independence property $[P(A \cap B) = P(A)P(B)]$ when the time evolution is involved.

Take a random field E, defined on $\mathbb{R}^D$, $D = 1, ..., 3$. By analogy to (5.9), consider a family of shift transformations

$$g(E) \to g(E_\xi) = g[T_\xi^{(j)} E] \tag{1.154}$$

where

$$T_\xi^{(j)} g(x_1, ..., x_j, ..., x_D) = g(x_1, ..., x_j + \xi, ..., x_D) \tag{1.155}$$

Here $g(x) = \omega \in \Omega$, each of which takes a set $S \subset \Omega$ into a set $S_\xi^{(j)}$ composed of functions of S shifted by ξ at their jth parameter x_j. If r.f. is SSS, then these transformations are measure preserving

$$P(S) = P(S_\xi^{(j)}) \tag{1.156}$$

Set S is called invariant if, $\forall j$ and ξ, sets S and $S_\xi^{(j)}$ differ at most by a set of P-measure zero. $\Longrightarrow$ every invariant set has either $P = 0$ or 1.

1.6 Maximum entropy method

6.1 Cracks in plates with holes

Al-Ostaz & Jasiuk (1997) investigated fracture response in tension of elastic-brittle (epoxy) and ductile (aluminum) plates. Macroscopically identical specimens were tested under the same conditions, and each displayed a different crack pattern. Nominally identical plates (8.25 x 33.02 x 0.38cm), epoxy (PSM-5). Each plate: same non-periodic distribution of 31 circular holes (diameter=1") from a hard-core r.f.; subjected to tensile loading in y at 0.03cm/s initially, and then decreased to ~0.0017cm/s.

Non-uniqueness of experimental results!

Note from combinatorics: that there exists a large number of geometrically acceptable (plausible) crack paths cutting the specimen across having very

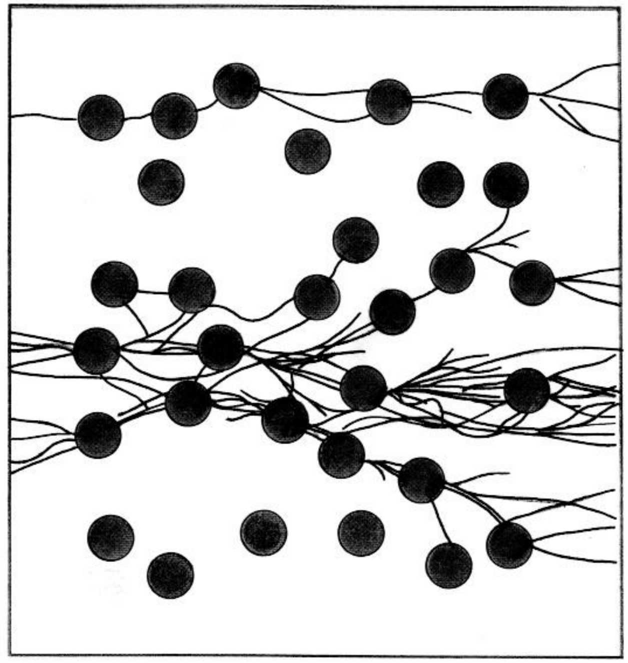

Figure 1.6: Schematic plot of final crack patterns superposed from seven epoxy specimens (in various colors) under the same uniaxial vertical tensile loading conditions, obtained experimentally; after (Al-Ostaz & Jasiuk, 1997).

similar energy values. $\Longrightarrow$ minute material and geometric imperfections decide which crack path will actually take place in a particular specimen.

Material imperfections arise from the intrinsic nature of materials which are all heterogeneous at a microscopic level.

Geometric imperfections include roughness of holes' surfaces and microscopic surface damage from drilling.

6.2 Disorder and information entropy

Compute crack paths using FE or spring networks...

But, which crack path should actually be used as a guidance in fine tuning the computational mechanics model?

Note: FE in mechanics of random media ($\forall$body $B(\omega) \in \mathcal{B}$) based on

$$\min \left[U\left(\omega\right) - W\right] \tag{1.157}$$

... to investigate effects of microscale randomness, need to carry out a finite (necessarily limited!) number of studies on a subset $\Omega_{MC} \subset \Omega$.

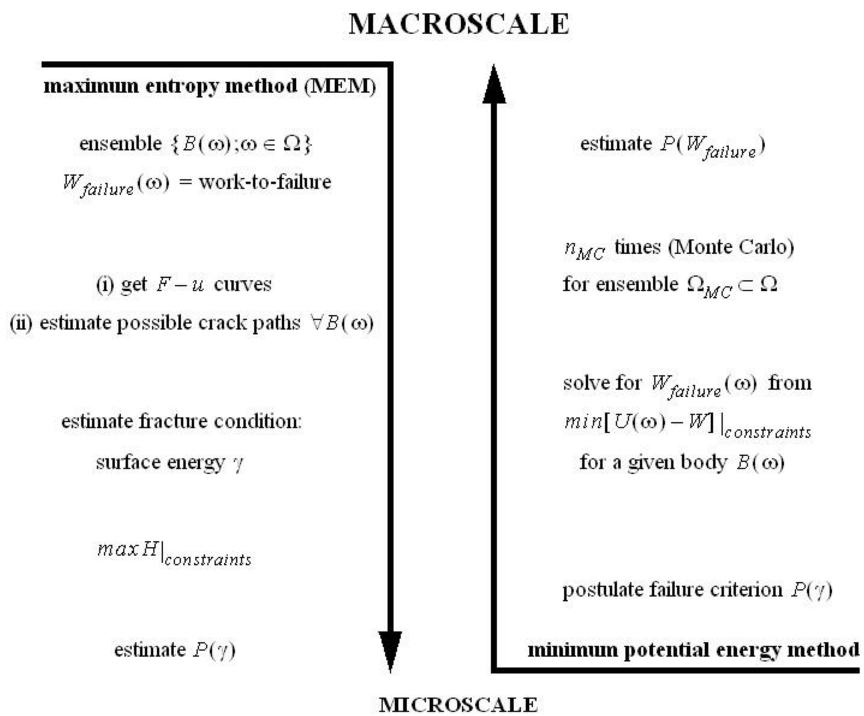

Figure 1.7: Two variational principle philosophies in mechanics of random media, and their roles in establishing a connection between microscale and macroscale responses. Left column illustrates a maximum entropy approach where the microscale probabilities are determined from the macroscale statements and observations, which represent constraints. The right column illustrates a (usually) much more familiar variational method of deterministic mechanics extended to a representative subset of heterogeneous specimens of a random medium.

Another possibility: *maximum entropy method* (MEM): for ensemble Ω (on which r.v. $X = \{X(\omega); \omega \in \Omega\}$ is defined), maximize the possible disorder expressed via *information entropy*

$$h(X) = \langle -\ln p(x) \rangle = -\int_{-\infty}^{\infty} p(x) \ln p(x)\, dx, \tag{1.158}$$

subject to condition that $\mu = \langle g_i(x) \rangle$ of n known functions $g_i(x)$ of X are given.

For discrete-type r.v. (with values $i = 1, ..., I$),

$$h(X) = \langle -\ln p(x) \rangle = -\sum_{i=1}^{I} p_i(x) \ln p_i(x), \tag{1.159}$$

one may show that the probability density of X is given by

$$p(x) = A \exp\left[-\lambda_1 g_1(x) - ... - \lambda_I g_I(x)\right] \tag{1.160}$$

Note: The entropy definition (6.2) represents the measure of uncertainty, or lack of information, for a continuous valued random variable.

Note: The conditions involved in finding the solution $p(x)$ represent our limited knowledge of possible *constraints*. If all the constraints were known, we would get exactly same solution as by conducting a deterministic mechanics study ω-by-ω according to the right column $\Longrightarrow$ no philosophical conflict between both methods. Usually, however, the knowledge of all the constraints is not there, or their introduction into the analysis is prohibitively complex. MEM is complementary to conventional variational principles.

Cracks in plates with holes via MEM

The MEM outlined in the left column of Fig. 6.2 is ideally suited to study the microscale material randomness, as expressed by the surface energy density fluctuations. We proceed in the following steps:

(i) Fracture occurs at the expense of dissipated energy $E(\omega)$, and the fracture path has a length $L(\omega)$. The two quantities can be computed from Fig. 6.1.

(ii) Calculate surface energy per unit length $\gamma(\omega) = E(\omega)/L(\omega)$. Let us note here that γ (and hence its probability density $p(\gamma)$) is now assessed on the mesoscale l, which is the mean hole spacing, rather than on, say, a molecular scale.

(iii) Given the results for N specimens, we get $\{\gamma(\omega_n); \omega_1, ..., \omega_N\}$, each of probability

$$P\{\omega_1\} = ... = P\{\omega_N\} = \frac{1}{N} \tag{1.161}$$

(iv) Compute moments $\langle\gamma\rangle, \left\langle\gamma^2\right\rangle, \left\langle\gamma^3\right\rangle, ...$ to get, according to (6.4),

$$p(\gamma) = A \exp\left[-\lambda_1 \langle\gamma\rangle - \lambda_2 \left\langle\gamma^2\right\rangle - \lambda_3 \left\langle\gamma^3\right\rangle - ...\right] \tag{1.162}$$

subject to

$$\begin{gathered} A \int_0^\infty \exp\left[-\lambda_1\gamma - \lambda_2\gamma^2 - \lambda_3\gamma^3 - ...\right] d\gamma = 1 \\ A \int_0^\infty \gamma \exp\left[-\lambda_1\gamma - \lambda_2\gamma^2 - \lambda_3\gamma^3 - ...\right] d\gamma = \langle\gamma\rangle \\ A \int_0^\infty \gamma^2 \exp\left[-\lambda_1\gamma - \lambda_2\gamma^2 - \lambda_3\gamma^3 - ...\right] d\gamma = \left\langle\gamma^2\right\rangle \\ ... \end{gathered} \tag{1.163}$$

(v) This basic model can be improved to account for:

- orientation of cracks with respect to the macroscopic loading direction;

- local crack (hole-hole) interactions;

- further crack (hole-hole) interactions; etc.

(vi) With $p(\gamma)$ one can predict the probability of occurrence of any other crack path.

Note: The MEM provides a closure method for many nonlinear problems of stochastic mechanics – e.g., fragmentation under dynamic impact, turbulence, nonlinear random vibration, effective response of random materials, contact forces in granular media...

2 Mesoscale random fields

From discrete to continuum random fields

... random medium is a set of deterministic media: $\mathcal{B} = \{B(\omega); \omega \in \Omega\}$.

e.g. anti-plane elasticity of a matrix-inclusion composite ($B(\omega) = B_m \cup B_i$) with locally isotropic phases of properties $C^{(m)}$ (matrix) and $C^{(i)}$ (inclusion). The most complete description of this two-phase microstructure is given in terms of an indicator (or characteristic) function

$$\chi_m(\omega, \mathbf{x}) = \begin{cases} 1 & if \quad \mathbf{x} \in B_m \\ 0 & if \quad \mathbf{x} \in B_i \end{cases} \qquad \text{or} \qquad \chi_m : \Omega \times \mathbb{R}^2 \to \{0, 1\}. \tag{2.1}$$

$\Longrightarrow$ local property at any point

$$C(\omega, \mathbf{x}) = \chi_m(\omega, \mathbf{x}) C^{(m)} + [1 - \chi_m(\omega, \mathbf{x})] \, C^{(i)}. \tag{2.2}$$

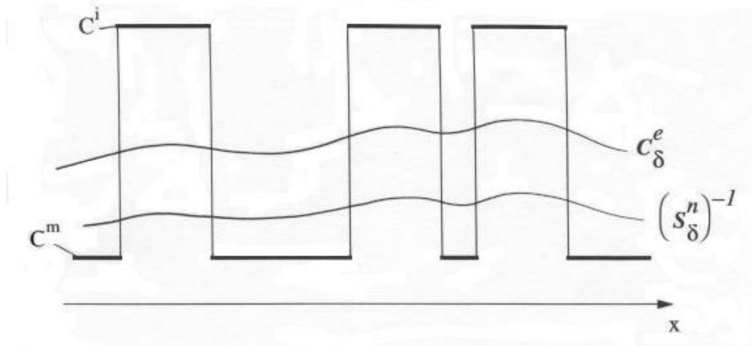

Figure 2.1: The setup of random fields: from a piecewise-constant realization of a composite to two approximating continua at a finite mesoscale.

$\Longrightarrow$ r.f. with discrete-valued realizations for $\mathbf{x}$: $\{\chi_m(\omega, \mathbf{x}); \omega \in \boldsymbol{\Omega}, \mathbf{x} \in \mathbb{R}^2\}$.
$\Longrightarrow$ discrete-valued r.f. with a continuous parameter

$$\mathbf{C} : \boldsymbol{\Omega} \times \mathbb{R}^2 \to \{\mathbf{I}C^{(i)}, \mathbf{I}C^{(m)}\} \quad \text{or} \quad \{\mathbf{C}(\omega, \mathbf{x}); \omega \in \boldsymbol{\Omega}, \mathbf{x} \in \mathbb{R}^2\}, \quad (2.3)$$

δ-dependent hierarchy of bounds $\Longrightarrow \forall \mathbf{x}$ in the material and $\forall \delta$, two bounding estimates of $\mathbf{C}^{eff}$ may be introduced: $\mathbf{C}_\delta^e$ and $\mathbf{C}_\delta^n \equiv (\mathbf{S}_\delta^n)^{-1}$. $\Longrightarrow$ two *mesoscale r.f.'s* (continuous-valued with continuous parameter)

$$\mathbf{C}_\delta^e : \Omega \times \mathbb{R}^2 \to \mathbb{R}^3 \qquad \mathbf{S}_\delta^n : \Omega \times \mathbb{R}^2 \to \mathbb{R}^3. \tag{2.4}$$

$\Longrightarrow$ approximate description of the composite material via two sets: $\{\mathbf{C}_\delta^e(\omega, \mathbf{x}); \omega \in \Omega, \mathbf{x} \in \mathbb{R}^2\}$ and $\{\mathbf{S}_\delta^n(\omega, \mathbf{x}); \omega \in \Omega, \mathbf{x} \in \mathbb{R}^2\}$ $\Longrightarrow$ two alternate inputs to field equation for global response on a smoothing mesoscale δ

$$[C_{ij}(\omega, \mathbf{x}) T_{,j}]_i = 0. \tag{2.5}$$

... in fact three approximating random fields

$$\mathcal{B}^d = \{B(\omega); \omega \in \Omega\},\ \mathcal{B}^t = \{B(\omega); \omega \in \Omega\},\ \mathcal{B}^{dt} = \{B(\omega); \omega \in \Omega\}, \tag{2.6}$$

$\Longrightarrow$ no unique way of setting up a continuum r.f.!

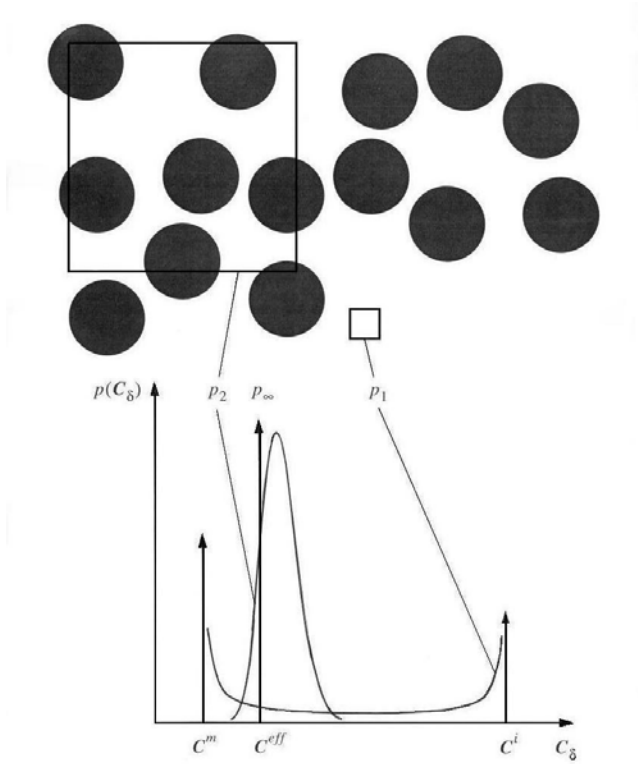

Figure 2.2: Sampling of the mesoscale property (trace of apparent tensor C_δ) of a disk-matrix composite via windows of different sizes. The beta distribution gives a practical approximation for the entire range of window sizes, showing four cases: the pointwise limit of eq. (1.7); the scale δ_1 and fit p_1; the scale δ_2 and fit p_2; and the scale δ_∞ and the causal distribution p_∞.

Scale dependence via beta distribution

Assume the statistics of χ_m to be homogeneous, isotropic. $\Longrightarrow$

$$p[C(\mathbf{x})] = f^{(m)}\delta\left[C(\mathbf{x}) - C^{(m)}\right] + f^{(i)}\delta\left[C(\mathbf{x}) - C^{(i)}\right]. \tag{2.7}$$

Note: of all classical p.d.f.'s, beta is the most convenient one to describe this scale effect:

$$p\left[C, a, b, C^{(m)}, C^{(i)}\right] = \frac{C^{a-1}(1-C)^{b-1}}{[C^{(i)} - C^{(m)}]B(a,b)} \quad \text{for} \quad C^{(m)} < C < C^{(i)}\ , \tag{2.8}$$

where

$$B[a,b] = \frac{\Gamma(a+b)}{\Gamma(a)\Gamma(b)} \quad \text{for} \quad C^{(m)} < C < C^{(i)}, \tag{2.9}$$

with Γ being the gamma function.

3 Second-order properties of mesoscale r.f.'s

Start from equilibrium eqn

$$\sigma_{j,j} = f, \tag{3.1}$$

and take both fields as superpositions:

$$\sigma_j(\mathbf{x}) = \left\langle \sigma_j \right\rangle + \sigma'_j(\mathbf{x}) \quad f(\mathbf{x}) = \langle f \rangle + f'(\mathbf{x}), \tag{3.2}$$

Multiplying $\sigma_{j,j}$ at $\mathbf{x}_1$ by $\sigma_{j,j}$ at $\mathbf{x}_2$, and ensemble averaging,

$$\frac{\partial^2 C_i^j(\mathbf{x}_1, \mathbf{x}_2)}{\partial x_{1i} \partial x_{2j}} = \frac{\partial^2 \langle \sigma'_i(\mathbf{x}_1)\, \sigma'_j(\mathbf{x}_2) \rangle}{\partial x_{1i} \partial x_{2j}} = \langle f'(\mathbf{x}_1)\, f'(\mathbf{x}_2) \rangle = F(\mathbf{x}_1, \mathbf{x}_2), \tag{3.3}$$

where C_i^j = correlation f'n of $\boldsymbol{\sigma}'$, $F(\mathbf{x}_1, \mathbf{x}_2)$ = correlation f'n of f'.

In the case of

$$\sigma_{ij,j} = f_i, \tag{3.4}$$

obtain

$$\frac{\partial^2 C_{ij}^{kl}(\mathbf{x}_1, \mathbf{x}_2)}{\partial x_{1j} \partial x_{2l}} = F_i^k(\mathbf{x}_1, \mathbf{x}_2), \tag{3.5}$$

Can generalize to micropolar bodies..., etc.

3.1 Universal properties of mesoscale bounds

Consider four types of microstructures (*Phys. Rev.*, 2000):

- matrix-needle composites with stiff needles

- multi-phase Poisson-Voronoi mosaics, Fig. 8.1(a),

- matrix-disk composites with circular or elliptical disks,

- superpositions of the latter with matrix-disk composites, Fig. 8.2(b).

For $\mathbf{C}_\delta^e$ and $\mathbf{S}_\delta^n$ (for any $B(\omega)$) can compute 2nd invariants

$$R_\delta^e(\omega) = \sqrt{(C_{11} - C_{22})^2/4 + C_{12}^2}, \quad R_\delta^n(\omega) = \sqrt{(S_{11} - S_{22})^2/4 + S_{12}^2}. \tag{3.6}$$

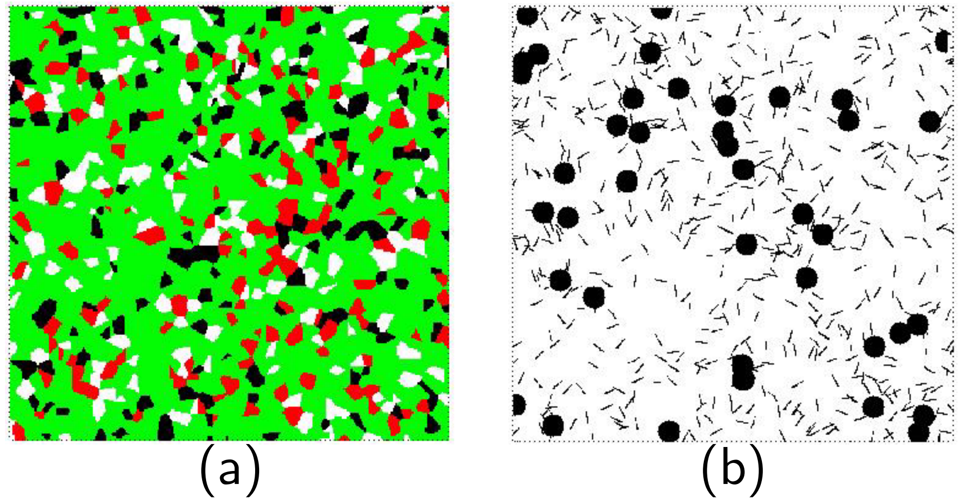

Figure 3.1: Two planar random microstructures: (a) four-phase Poisson-Voronoi mosaics; (b) superposition of a matrix-disk composite with a matrix-needle composite.

$\Longrightarrow$ two random invariants: $\{R_\delta^e(\omega); \omega \in \Omega\}$ or $\{R_\delta^n(\omega); \omega \in \Omega\}$. $\Longrightarrow$ coefficient of variation of each of these invariants

$$CV_\delta^e = \frac{\sigma(R_\delta^e)}{\mu(R_\delta^e)}, \quad CV_\delta^n = \frac{\sigma(R_\delta^n)}{\mu(R_\delta^n)}. \tag{3.7}$$

Find: for any $\delta > 1$, these equal ~0.55 ± 0.1 irrespective of:

(a) window size δ;

(b) b.c.'s applied (Dirichlet or Neumann);

(c) contrasts $\alpha^{(p)}$ ($p = 2, ..., 4$), and inclusion's shape;

(d) volume fraction $f^{(p)}$ of any phase $p = 1, ..., 4$, providing its conductivity is not 0 or ∞.

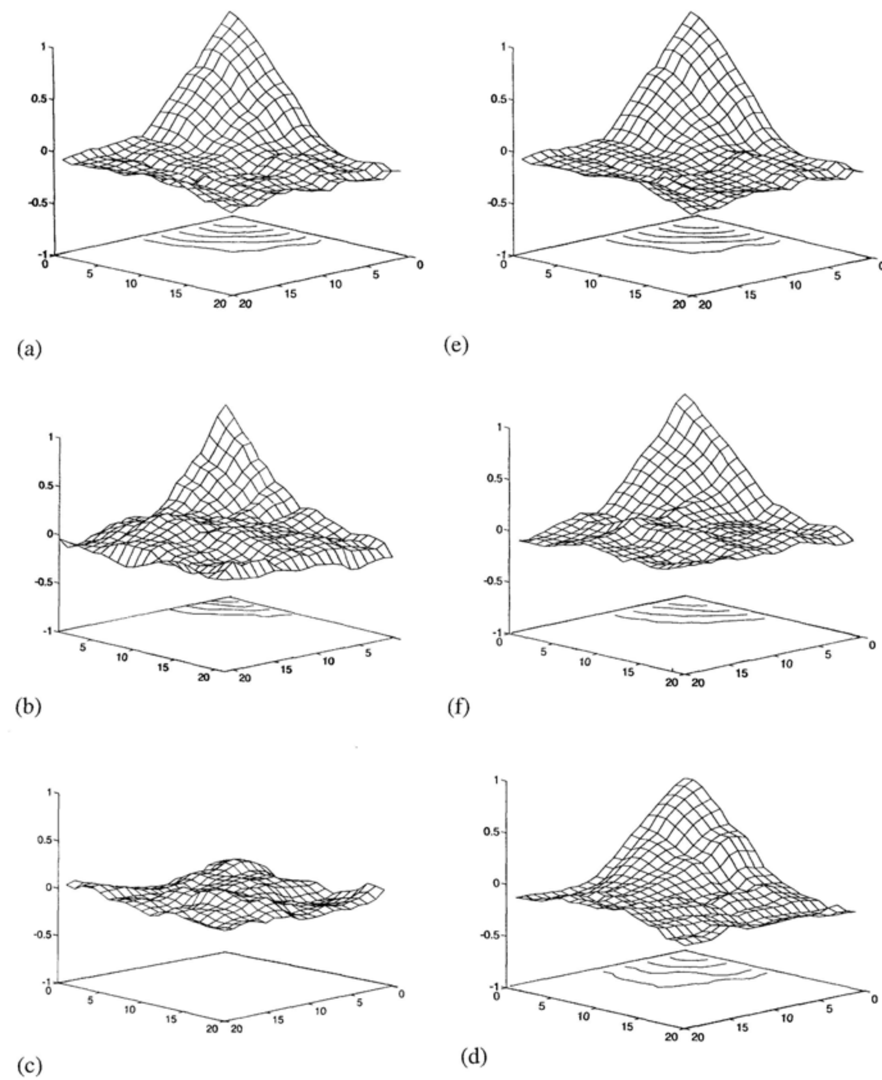

Figure 3.2: Graphs of the correlation coefficient $\rho_{ijkl}(\mathbf{r}) = \rho_{G_{ij}G_{kl}}(\mathbf{r})$ of the

$\Longrightarrow$ a universal nature of CV_δ^e and CV_δ^n for planar random media generated from Poisson point patterns.

Correlation structure of mesoscale r.f.'s of stiffness

For composite having SSS statistics of properties, mesoscale r.f. $\mathbf{C}$ is SSS:

$$\rho_{C_{ij}C_{kl}}(\mathbf{x}_1, \mathbf{x}_2) = \rho_{C_{ij}C_{kl}}(\mathbf{r}) \qquad \mathbf{r} = \mathbf{x}_1 - \mathbf{x}_2. \tag{3.8}$$

Q: For a composite having also an isotropic statistics of its properties, is $\mathbf{C}$ field isotropic in terms of its correlation function?

$$\rho_{C_{ij}C_{kl}}(\mathbf{r}) \stackrel{?}{=} \rho_{C_{ij}C_{kl}}(|\mathbf{r}|), \tag{3.9}$$

Note from computations of anti-plane mesoscale stiffnesses of two systems: binomial fields on square lattices and disk-matrix composites:

(i) autocovariance $\rho_{C_{11}C_{11}}$ is not isotropic as there is a stronger correlation in x_1 than in x_2;

(ii) autocovariance $\rho_{C_{12}C_{12}}$ is isotropic;

(iii) crosscovariance $\rho_{C_{11}C_{12}}$ is practically zero;

(iv) crosscovariance $\rho_{C_{11}C_{22}}$ attains, at the origin, a maximum value of ˜0.75 rather than 1.0 as might intuitively be expected;

(v) practically identical plots of $\rho_{C_{ij}C_{kl}}$ are obtained under the assumption of uniform strain [(e), (f)].

4 Does there exist a locally isotropic, smooth elastic material?

The correlation theory of random fields implies $\rho_{1212}(x) = 0$, which is possible only for $C_{12} = 0$ everywhere, i.e. for mesoscale $\delta = 0$, discrete medium description - non-smooth!

$\Longrightarrow$ cannot assume smooth $\mathbf{C}(\mathbf{x}, \delta) = C(\mathbf{x}, \delta)\,\mathbf{I}$

$\Longrightarrow$ In the model

$$\boldsymbol{\varepsilon} = \mathbf{S}(\omega, \mathbf{x}) \colon \boldsymbol{\sigma} \quad \boldsymbol{\sigma} = \mathbf{C}(\omega, \mathbf{x}) \colon \boldsymbol{\varepsilon} \quad \mathbf{S}(\omega, \mathbf{x}) = \mathbf{C}^{-1}(\omega, \mathbf{x}), \tag{4.1}$$

$\boldsymbol{\sigma}$ and $\boldsymbol{\varepsilon}$ are fields on a hypothetical, unspecified RVE / SVE of a random medium.

$\Longrightarrow$ 4th rank, isotropic tensor random field is also unjustified

$$\varepsilon = \frac{1}{E(\omega, \mathbf{x})}[(1+\nu(\omega, \mathbf{x}))\sigma_{ij} - \nu(\omega, \mathbf{x})\delta_{ij}\sigma_{kk}] \ \ \omega \in \mathbf{\Omega} \ \ \mathbf{x} \in B \subset \mathbb{R}^D \quad (4.2)$$

5 Stochastic finite elements for elastic media

Consider a (scalar) problem of torsion of a bar made of a two-phase microstructure (e.g. duplex steel)

$$\begin{array}{l} [C_{ij}(\omega, \mathbf{x})\phi_{,j}]_{,i} + f = 0, \;\; \mathbf{x} \in B(\omega) \\ \phi = 0, \;\; \mathbf{x} \in \partial B(\omega). \end{array} \tag{5.1}$$

ϕ = stress function, $\mathbf{C}(\omega, \mathbf{x})$ ($\equiv C_{ij}(\omega, \mathbf{x})$) corresponds to one particular realization $B(\omega)$ (of volume V) of $\mathcal{B}$

Note: lower and upper bounds on global response of $B(\omega)$ are obtained, respectively, from two dual energy principles: the minimum potential energy principle

$$\inf_{\phi \in H_0^1(V)} \frac{1}{2} \int_V \boldsymbol{\eta}^T \mathbf{C}_\delta(\omega) \boldsymbol{\eta} dV - \frac{1}{2} \int_V f \phi dV, \tag{5.2}$$

and, the minimum complementary energy principle

$$\inf_{\phi \in H_0^1(V)} \frac{1}{2} \int_V \boldsymbol{\xi}^T \mathbf{S}_\delta(\omega) \boldsymbol{\xi} dV \;\; \forall \boldsymbol{\xi} \in H = \{ \boldsymbol{\xi} \in (L(V))^2 | \nabla \cdot \boldsymbol{\xi} + f = 0 \}. \quad (5.3)$$

Here $\mathbf{C}_\delta(\omega)$ and $\mathbf{S}_\delta(\omega)$ are stiffness and compliance tensor fields on mesoscale δ (set by the size L of the finite element relative to the grain size d), while $\boldsymbol{\eta}$ and $\boldsymbol{\xi}$ stand for $\nabla\phi$ and $\mathbf{C}_\delta(\omega)\boldsymbol{\eta}$, respectively.

$\Longrightarrow$ two algebraic problems

$$[\mathbf{K}(\omega)] \{\Phi\} = \{f\} \;\; \omega \in \Omega, \quad (5.4)$$

where $[\mathbf{K}(\omega)]$ = global stiffness matrix, and

$$[\mathbf{L}(\omega)] \{\varphi\} = \{\Lambda\} \;\; \omega \in \Omega, \quad (5.5)$$

where $[\mathbf{L}(\omega)]$ = global flexibility matrix. Here Φ and φ are the respective vector solutions; see the first reference above for all the details.

... these two energy principles ensure a monotonic convergence of the lower and upper bounds of the energy norm from below and above, respectively,

$$\|\phi\|_E = \frac{1}{2}\int_V \eta^T C(\omega)\eta dV \quad \omega \in \mathbf{\Omega}. \tag{5.6}$$

provided (i) we have a homogeneous material and (ii) the mesh resolution $\delta \longrightarrow 0$

This is the classical limit of infinitesimal finite elements solving a deterministic continuum problem without identifying any microstructure.

In a heterogeneous material, the tendency of global FE methods to converge with δ decreasing is hindered by the fact that the mesoscale (i.e. apparent) responses $\mathbf{C}_\delta(\omega)$ and $\mathbf{S}_\delta(\omega)$ tend to diverge as δ decreases.

i.e. no separation of scales!

Example: torsion of a duplex-steel bar (bi-percolating)

Note: competition of two opposing trends:

(i) global responses tend to converge as δ decreases;

(ii) mesoscale responses, serving as input to (i), computed resp. from essential and natural boundary conditions, are well defined via micromechanics but tend to diverge as δ decreases.

(iii) ... SVE = ‘mesoscale finite element’

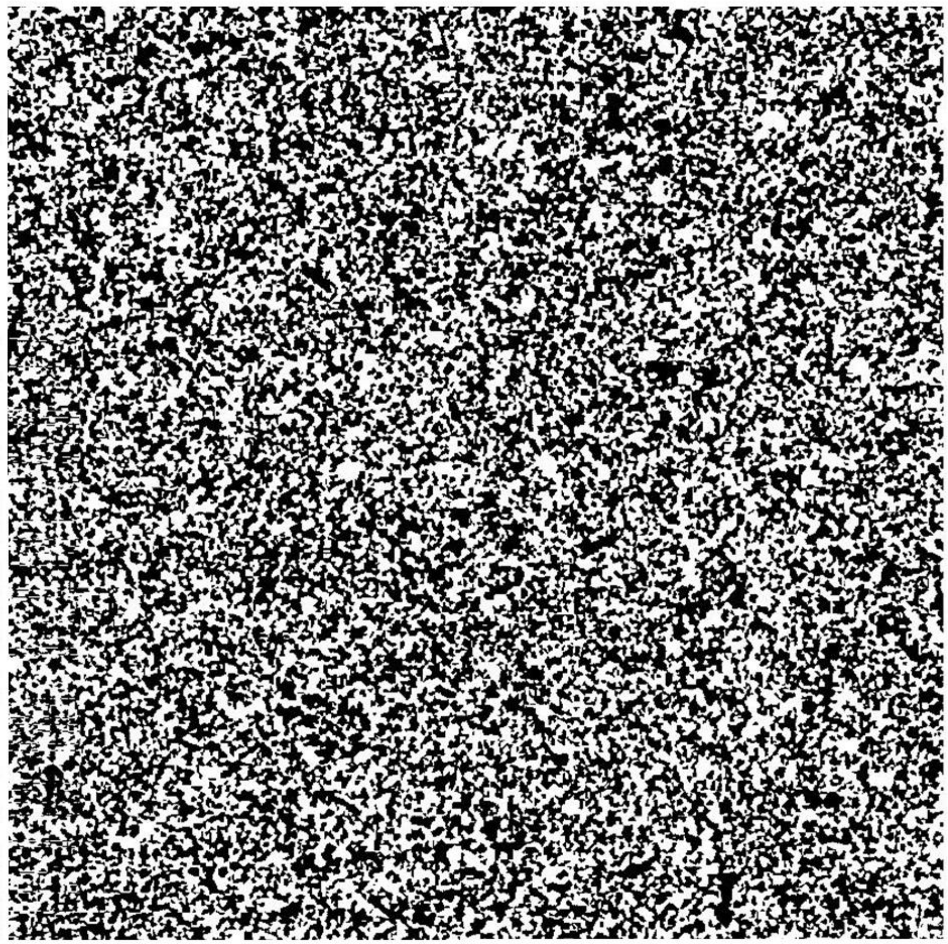

Figure 5.1: A two-phase material with a Voronoi mosaic microgeometry of a total 104,858 black and white cells, at volume fraction 50% each.

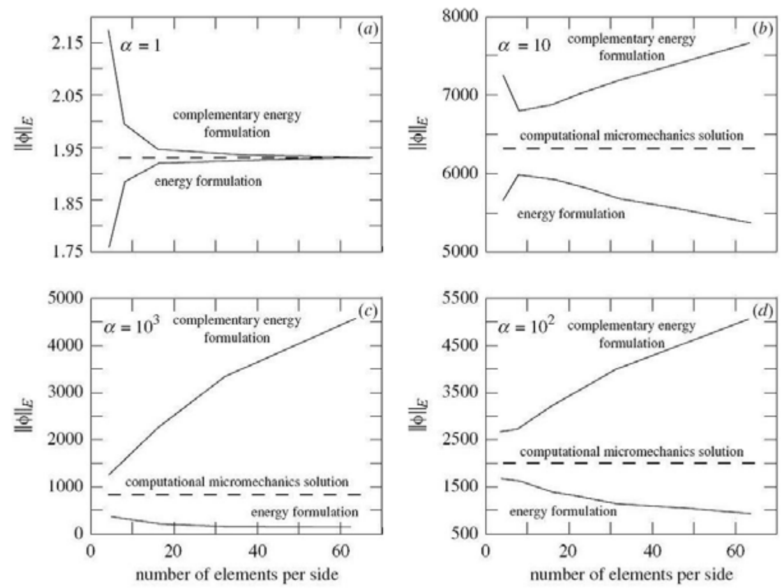

Figure 5.2: Behavior of the energy norm (3.6) with respect to a sequence of self-accommodating finite element meshes, in terms of the increasing finite element resolution, for: (a) a homogeneous material domain contrast $= 1$, and (b) for contrast $\alpha = 10$, (c) same domain for $\alpha = 100$, and (d) same domain for $\alpha = 1000$. Computational micromechanics solutions taking account entire microstructure of are also shown.

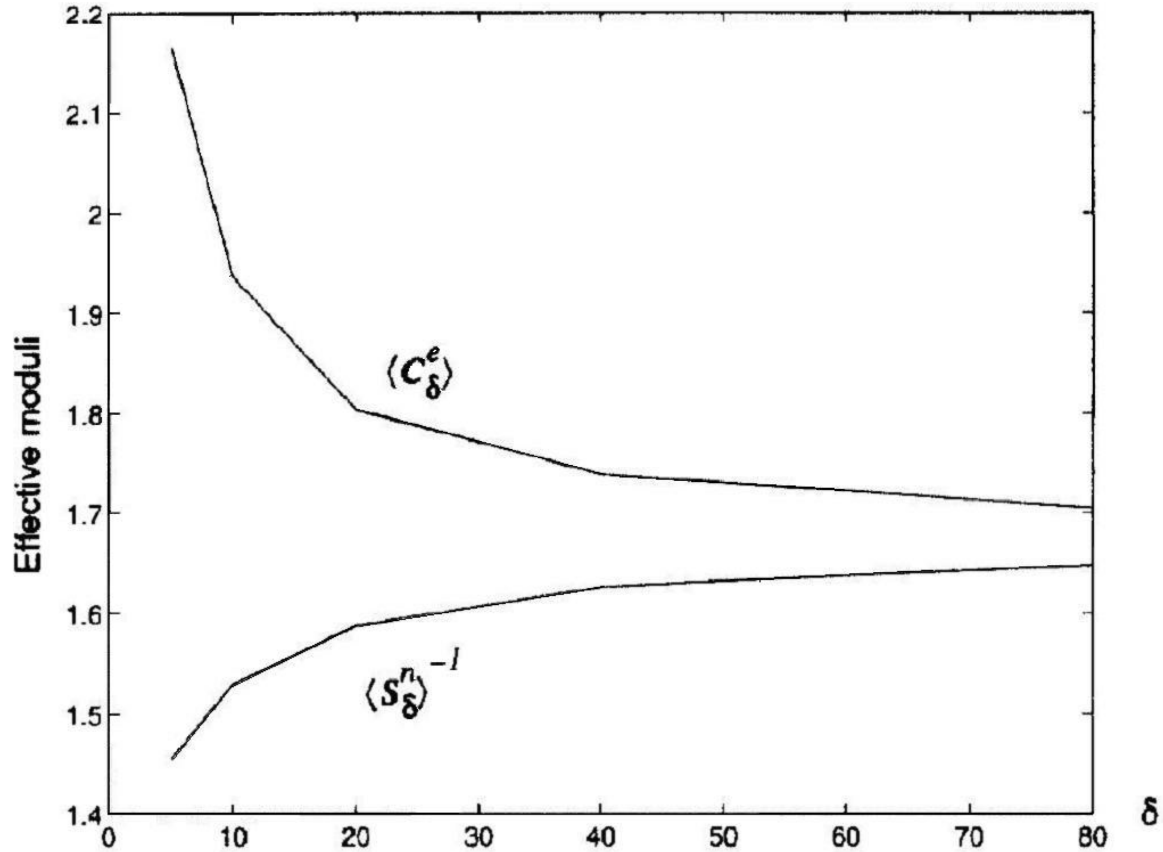

Figure 5.3: Hierarchies of bounds $\left\langle \mathbf{C}_\delta^e(\omega) \right\rangle$ and $\left\langle \mathbf{S}_\delta^n(\omega) \right\rangle^{-1}$ for the two-phase microstructure of Fig. 6 at volume fraction and contrast $\alpha = 10$; five data sets are shown.

Mesoscale Bounds for Random Media - Elastic

Martin Ostoja-Starzewski
Department of Mechanical Science & Engineering
Institute for Condensed Matter Theory,
and Beckman Institute
University of Illinois at Urbana-Champaign

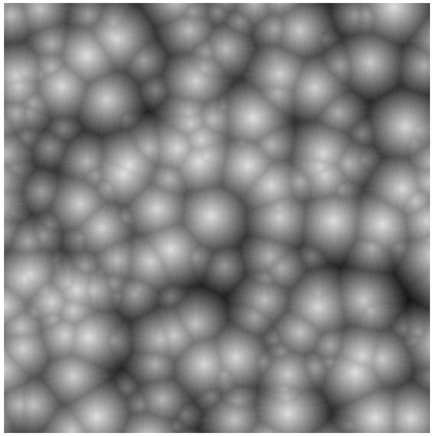

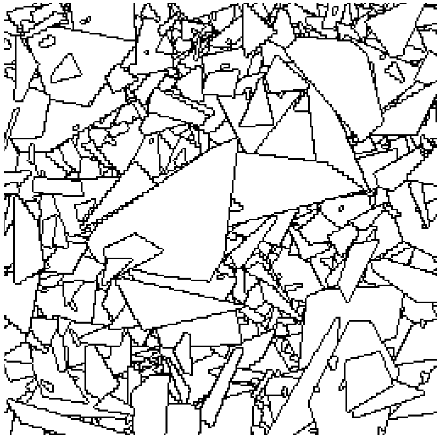

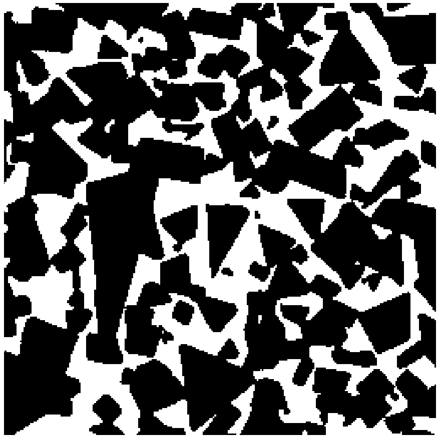

three scales:

microscale: average size of grain d
(microstructure)

mesoscale: L
if not RVE, then
inhomogeneous continuum

macroscale: L_{macro}

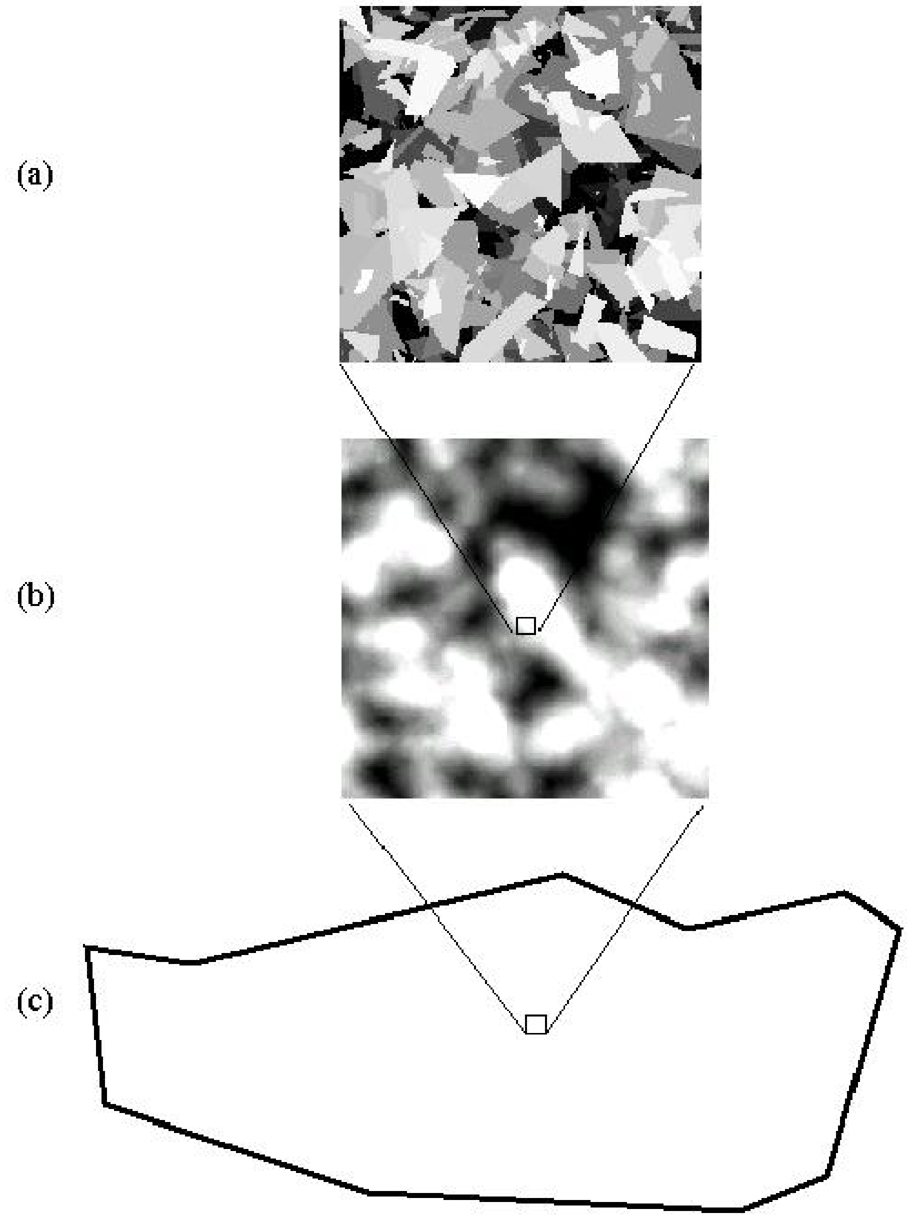

three scales:

microscale: average size of grain d
(microstructure)

mesoscale: L
if not RVE, then
inhomogeneous continuum

macroscale: L_{macro}

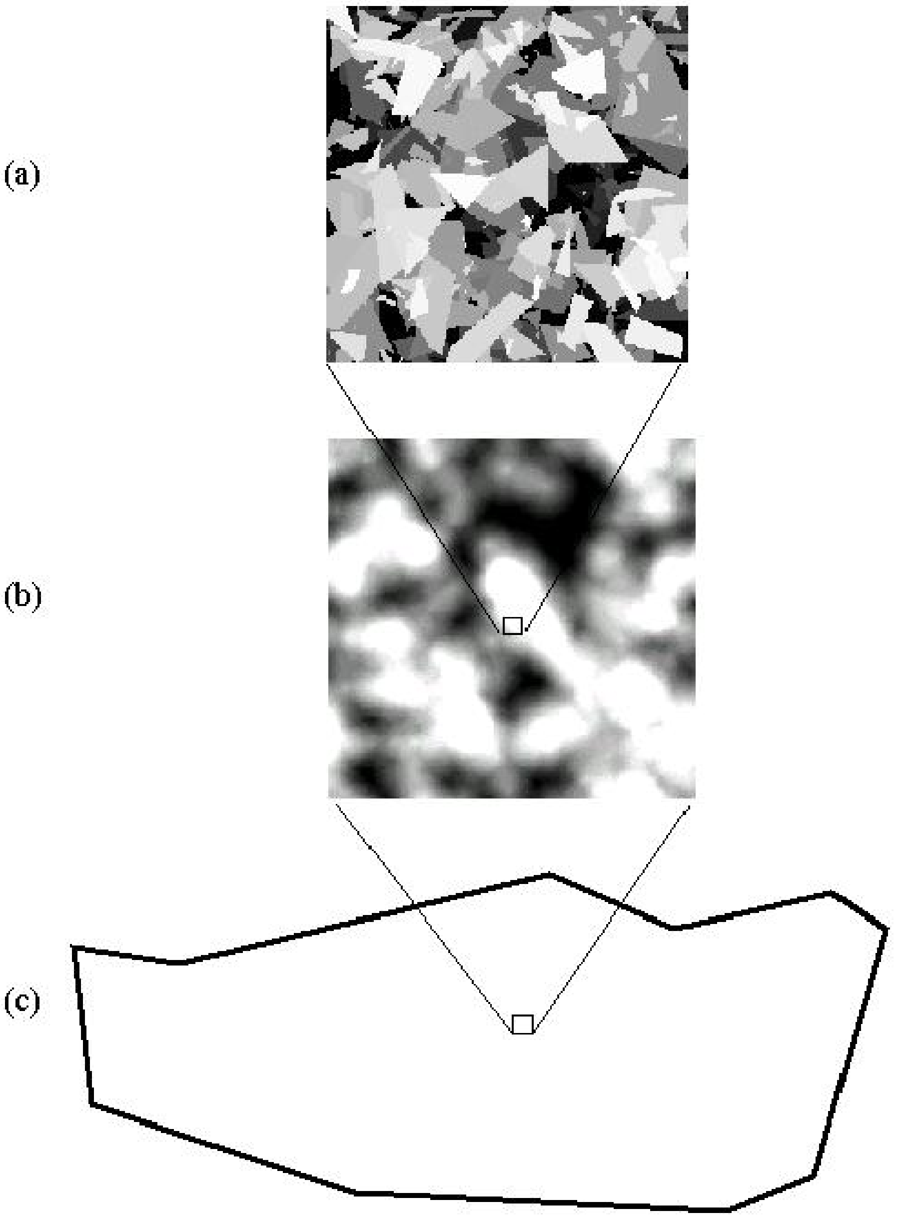

separation of scales $d << L << L_{macro}$
does not always hold!

three scales:

microscale: average size of grain d
(microstructure, non-fractal)

mesoscale: L
if not RVE, then
inhomogeneous continuum

macroscale: L_{macro}

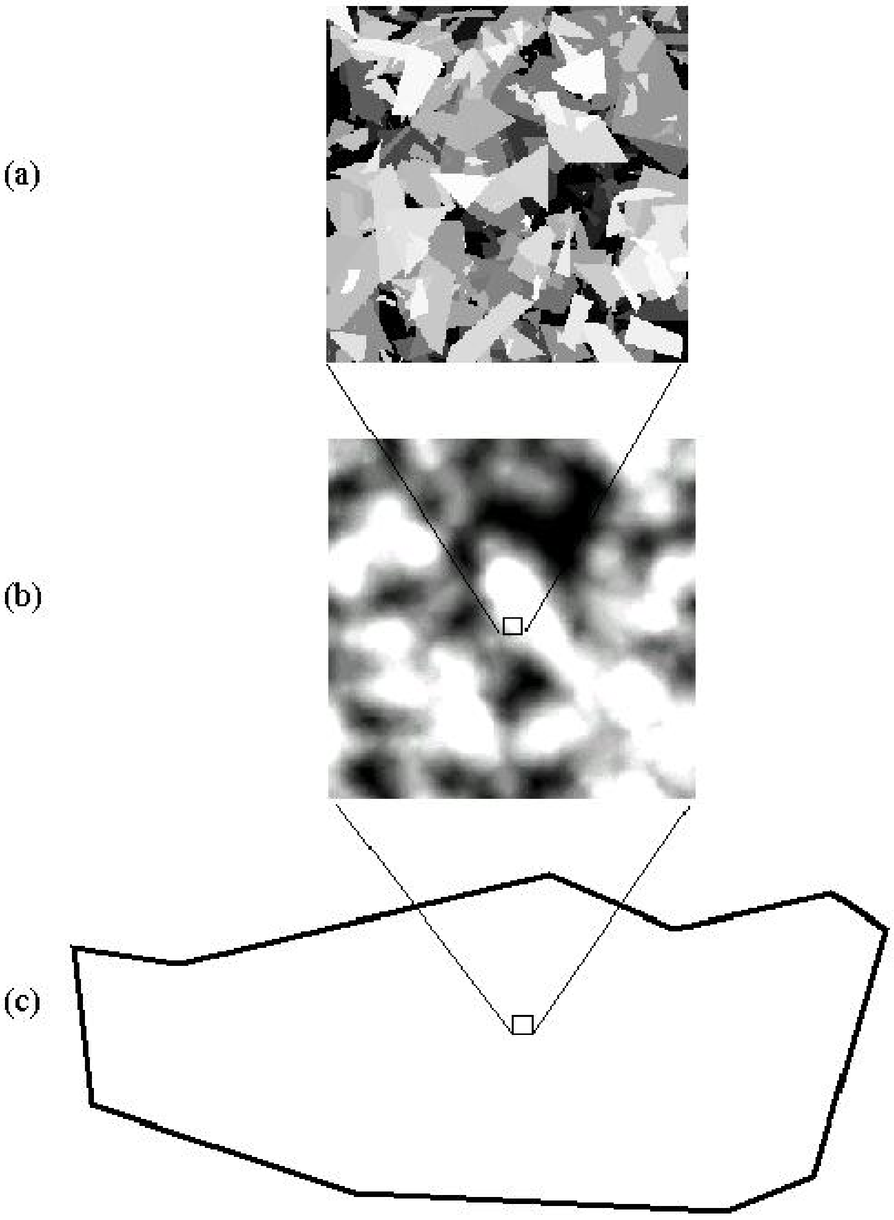

separation of scales $d << L << L_{macro}$
does not always hold!

Three ways for randomness to enter a problem in solid mechanics

$$Lu = f$$

L = field (differential) operator

- via forcing: $Lu = f(\omega) \qquad \omega \in \Omega$
- via boundary conditions: $u(\omega)$ on ∂B
- via field operator: $L(\omega)u = f$

Outline

1. Finite-size-scaling and convergence of Statistical Volume Element (SVE) to Representative Volume Element (RVE)

2. Problems/challenges w/o separation of scales
   - stochastic boundary value probems
   - random fields, stochastic finite elements
   - wavefronts in random media
   - fracture mechanics of micro-beams
   - shape optimization in presence of microscale material randomness
   - …

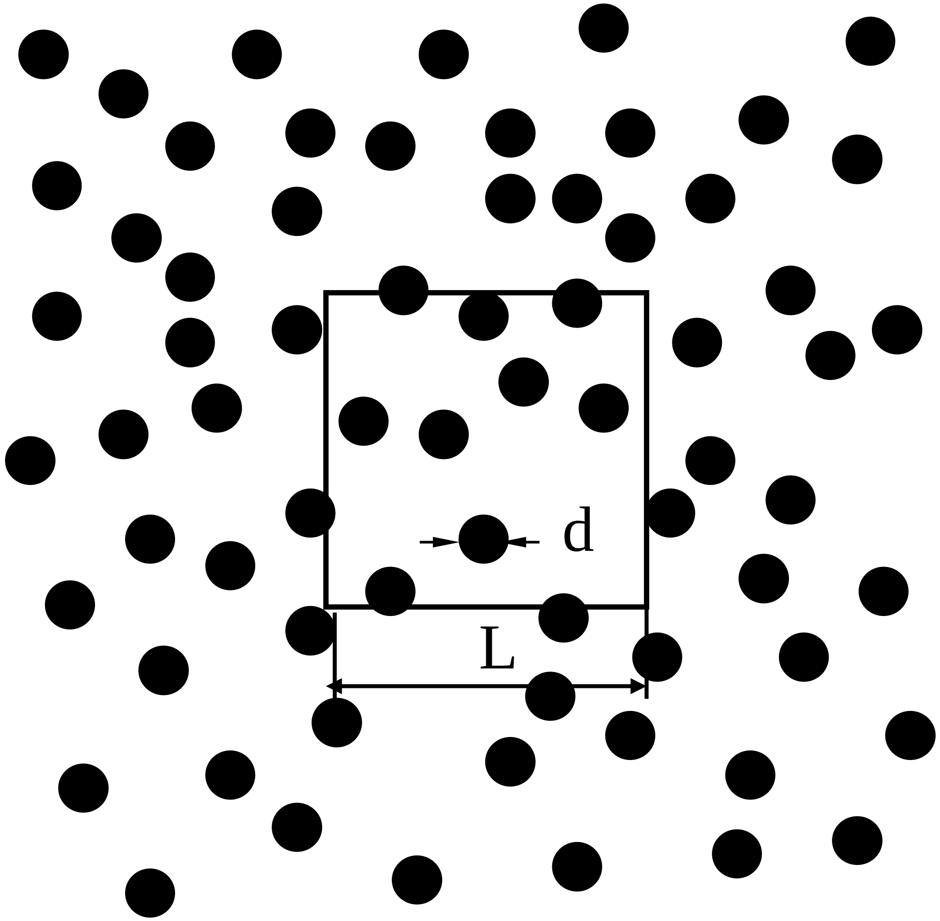

mesoscale: $\delta = L / d$

How large must the mesoscale domain be to qualify as RVE?

Definition of RVE [Hill, 1963]

- RVE is structurally entirely typical of the whole mixture on average

- contains a sufficient number of inclusions for the apparent overall moduli to be effectively independent of the surface values of traction and displacement, as long as these values are 'macroscopically uniform'

Definition of RVE [Hill, 1963]

- RVE is structurally entirely typical of the whole mixture on average
  $\Longrightarrow$ **need spatially homogeneous and ergodic statistics**

- contains a sufficient number of inclusions for the apparent overall moduli to be effectively independent of the surface values of traction and displacement, as long as these values are 'macroscopically uniform'
  $\Longrightarrow$ **need a *mesoscale* for both bvp's**

Hill (-Mandel) condition: Equivalence of energetic and mechanical definitions of Hooke's law:

$$\overline{\sigma : \varepsilon} = \overline{\sigma} : \overline{\varepsilon} \qquad \Leftrightarrow \qquad \int_{\partial B_\delta} (t - \overline{\sigma} \cdot n) \cdot (u - \overline{\varepsilon} \cdot x)\, dS = 0$$

Uniform boundary conditions: $\qquad \forall x \in \partial B_\delta$

- displacement (Dirichlet) b.c. $\qquad u = \overline{\varepsilon} \cdot x$

- traction (Neumann) b.c. $\qquad t = \overline{\sigma} \cdot n$

- displacement-traction b.c. (mixed-orthogonal) $\qquad (t - \overline{\sigma} \cdot n) \cdot (u - \overline{\varepsilon} \cdot x) = 0$

$$\frac{C^{(i)}}{C^{(m)}} = 1$$

$$\frac{C^{(i)}}{C^{(m)}} = 0.2$$

$$\frac{C^{(i)}}{C^{(m)}} = 0.05$$

$$\frac{C^{(i)}}{C^{(m)}} = 0.02$$

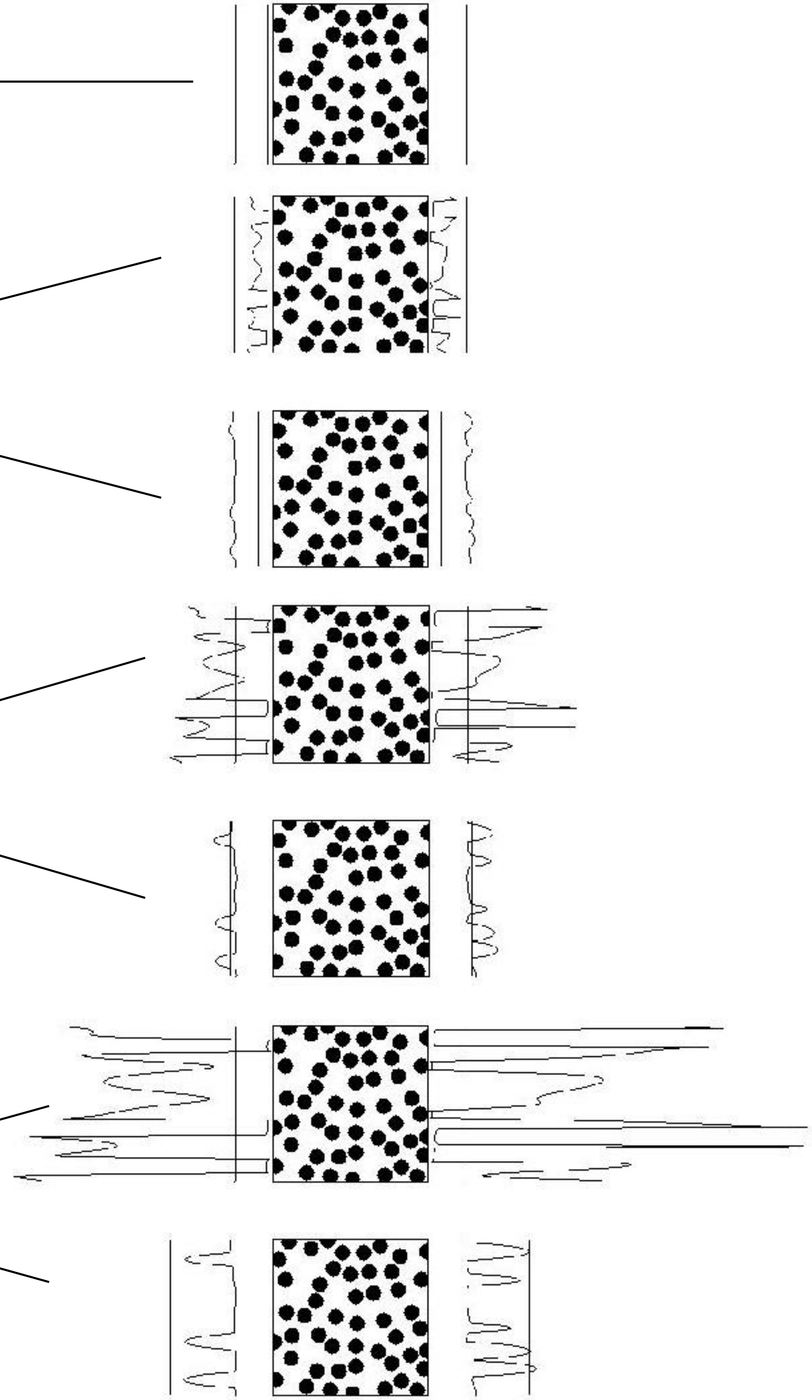

stiff inclusions in soft matrix

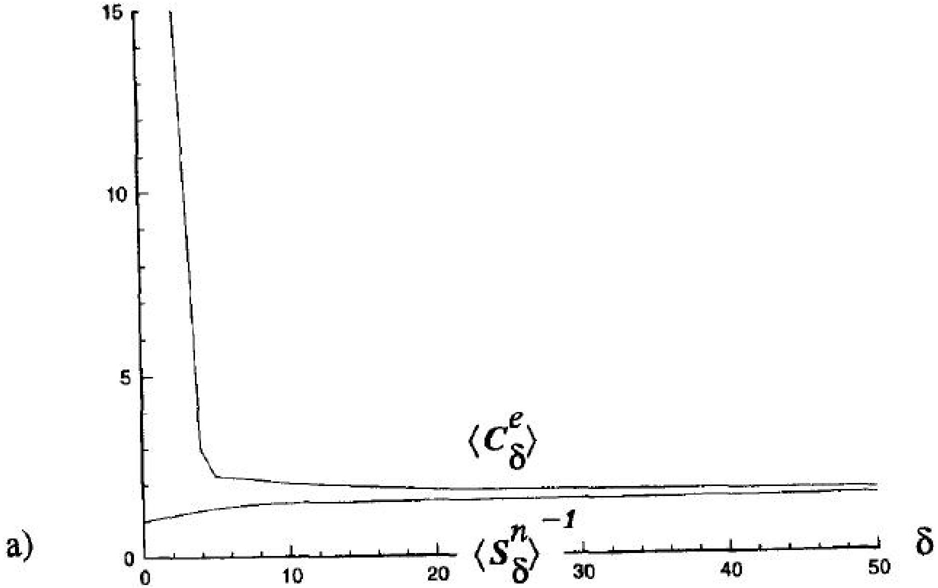

$$\frac{C^{(i)}}{C^{(m)}} = 10^2$$

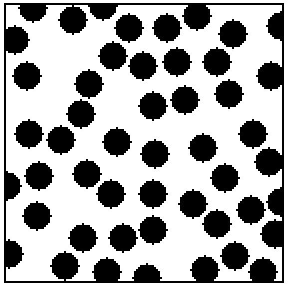

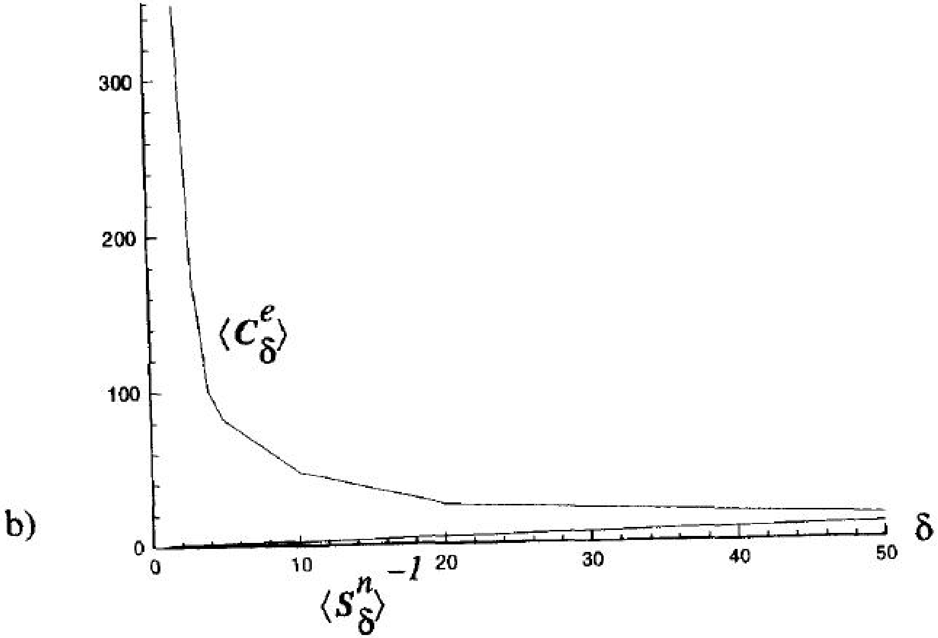

$$\frac{C^{(i)}}{C^{(m)}} = 10^4$$

soft inclusions in stiff matrix

a)

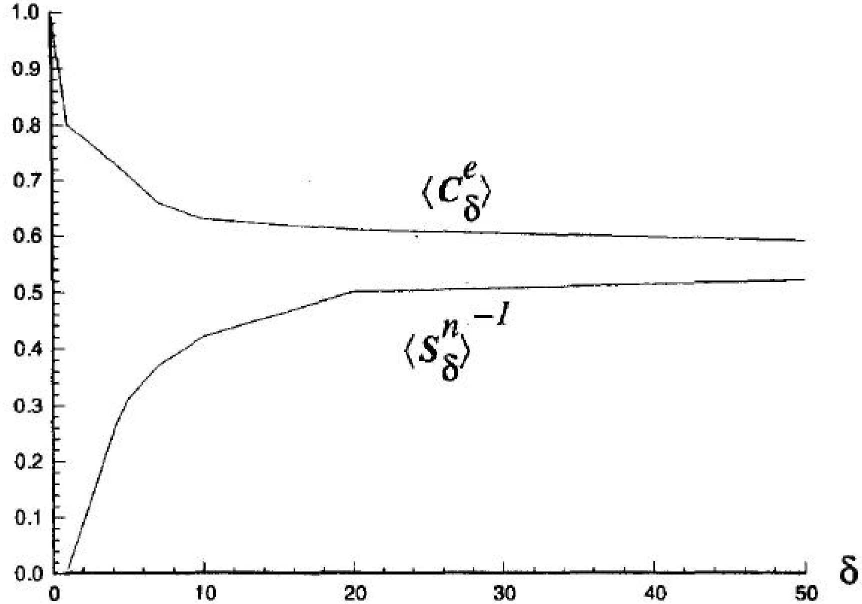

$$\frac{C^{(i)}}{C^{(m)}} = 10^{-2}$$

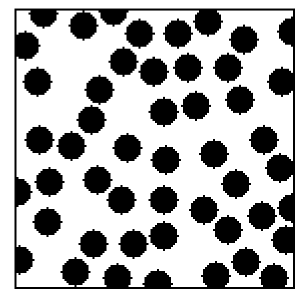

b)

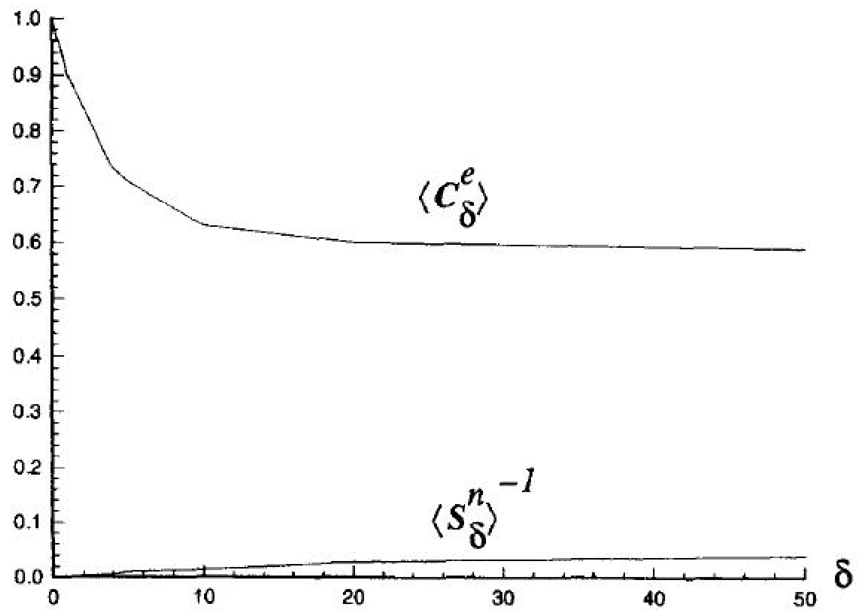

$$\frac{C^{(i)}}{C^{(m)}} = 10^{-4}$$

Linear elastic random composites

$$w(\varepsilon^0,\delta)=\frac{1}{2}\varepsilon^0:C_\delta^d:\varepsilon^0 \qquad w^*(\sigma^0,\delta)=\frac{1}{2}\sigma^0:S_\delta^t:\sigma^0$$

$$C^R\equiv(S^R)^{-1}\equiv\langle S_1^t\rangle^{-1}\leq\langle S_{\delta'}^t\rangle^{-1}\leq\langle S_\delta^t\rangle^{-1}\leq C^{eff}$$

$$\forall\,\delta'<\delta \qquad \leq\langle C_\delta^d\rangle\leq\langle C_{\delta'}^d\rangle\leq\langle C_1^d\rangle\equiv C^V$$

Unrestricted b.c.:

$$u_i = \varepsilon_{ij}^0 x_j , \qquad x \in \partial B_\delta$$

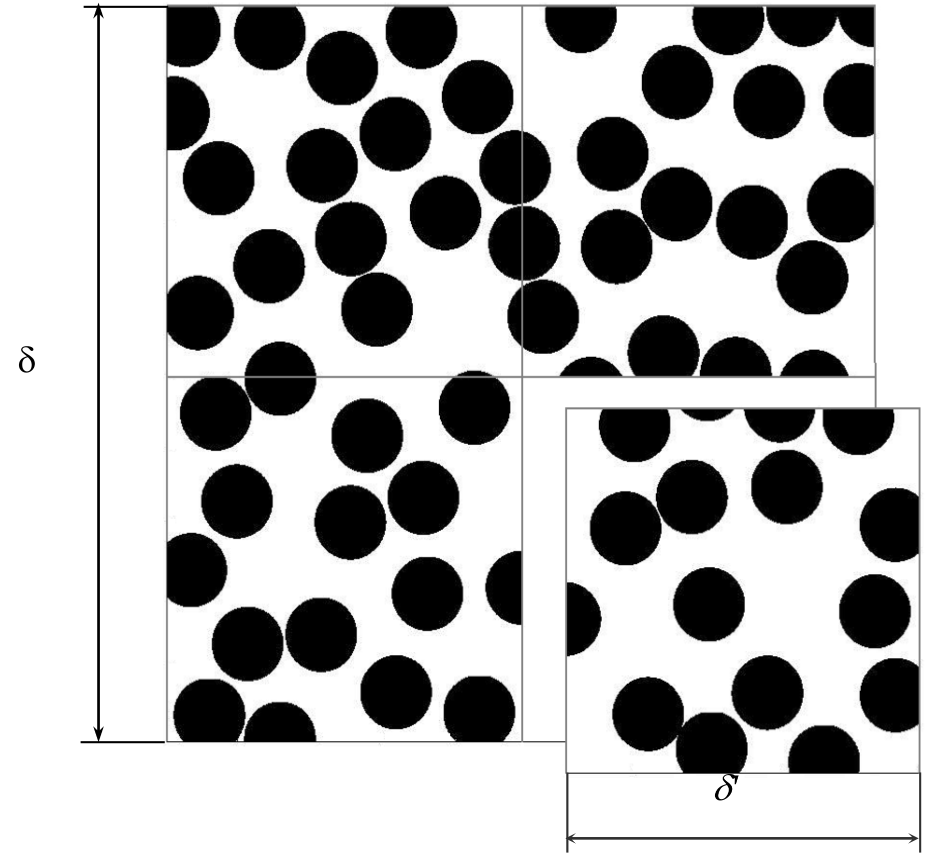

Restricted b.c.:

$$u_i^r = \varepsilon_{ij}^0 x_j , \qquad x \in \partial B_{\delta'} , \qquad s = 1,2,\ldots,n^2$$

randomly placed elliptical inclusions

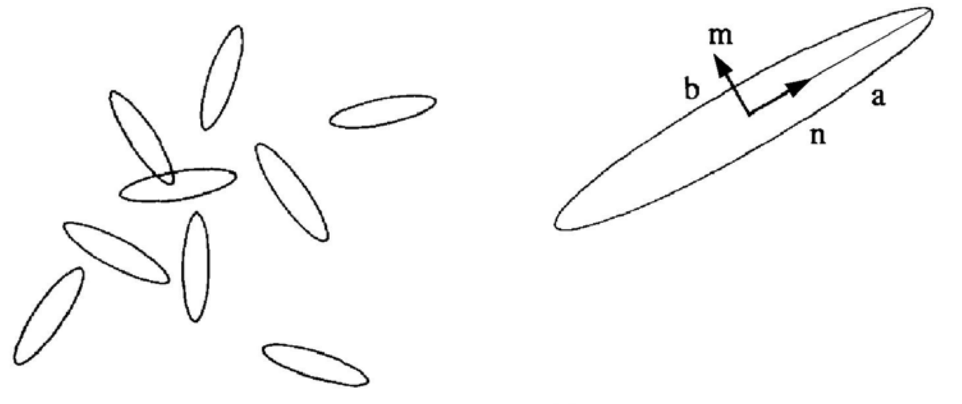

a) b)

randomly placed elliptical inclusions

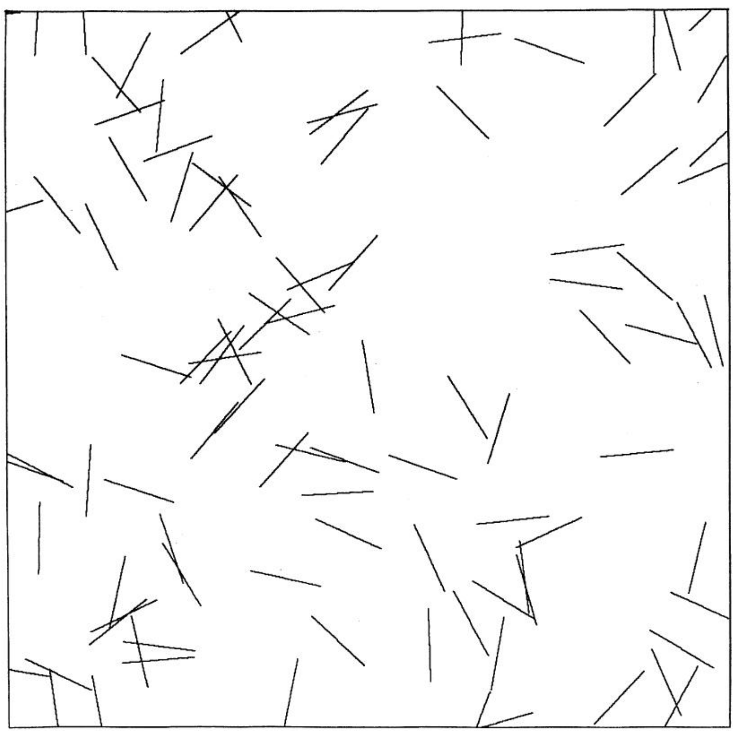

Fig. 2. A field of long (1×100) needles in a 1000×1000 square, generated from a Poisson point process of density $\lambda = 10^{-4}$, i.e. there are 100 needles.

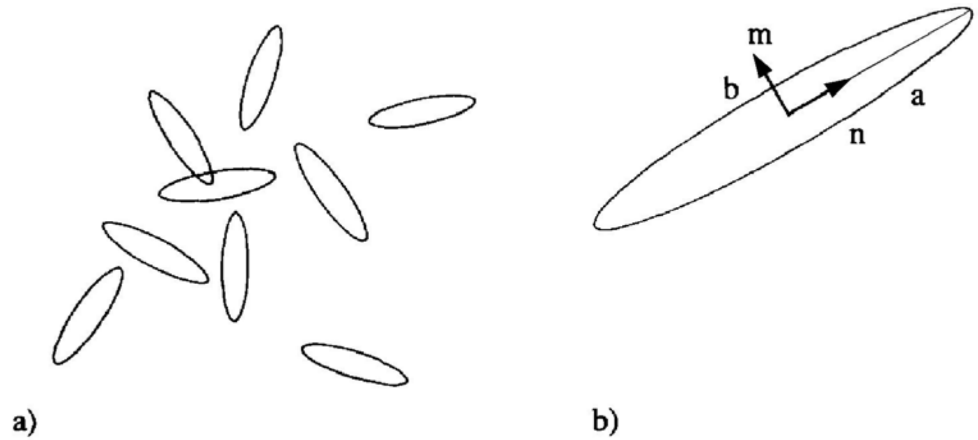

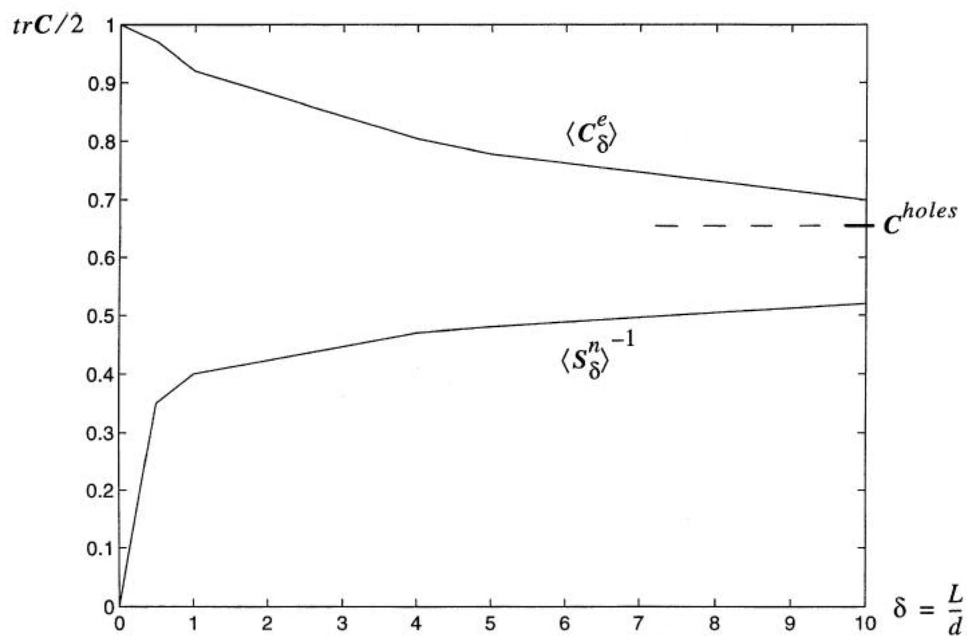

randomly placed needles or cracks

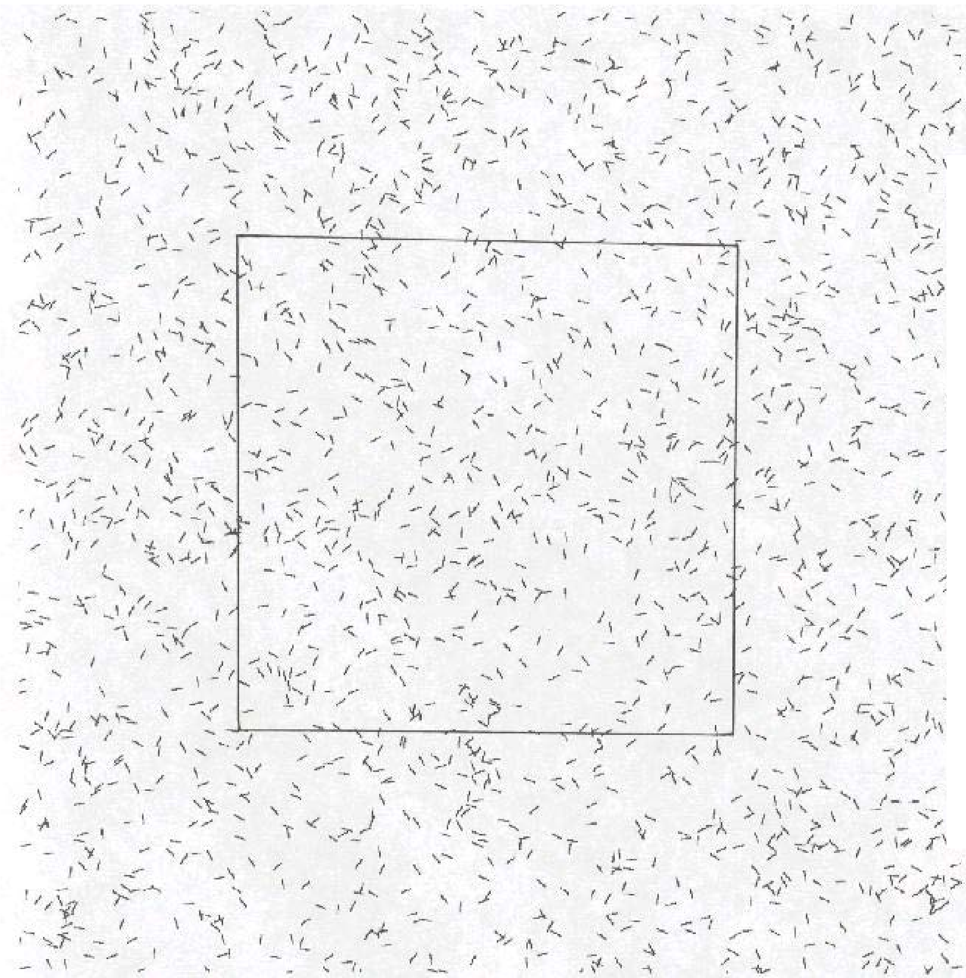

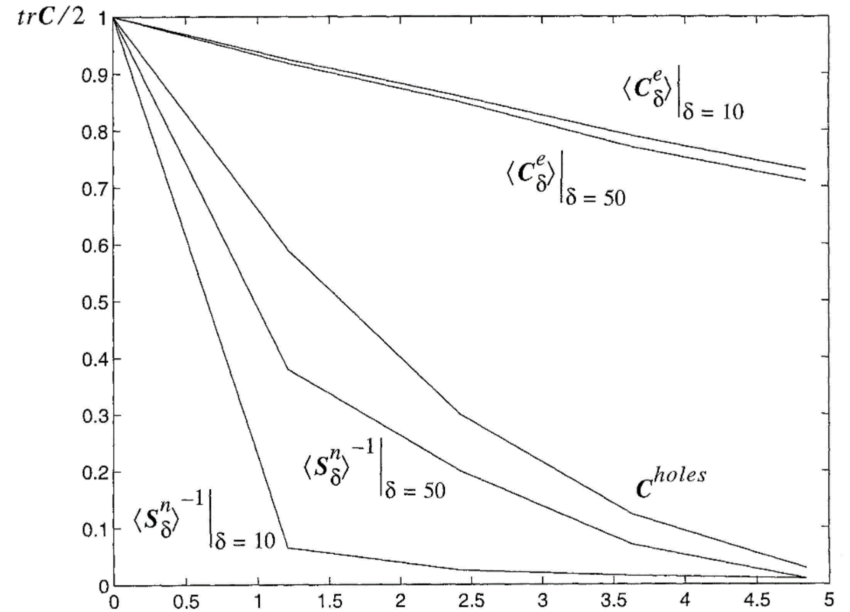

[*Mech. Mater.*, 1999]

In two-phase media, <u>beta</u> p.d.f approximates scale change for entire range of mesoscales: from SVE to RVE

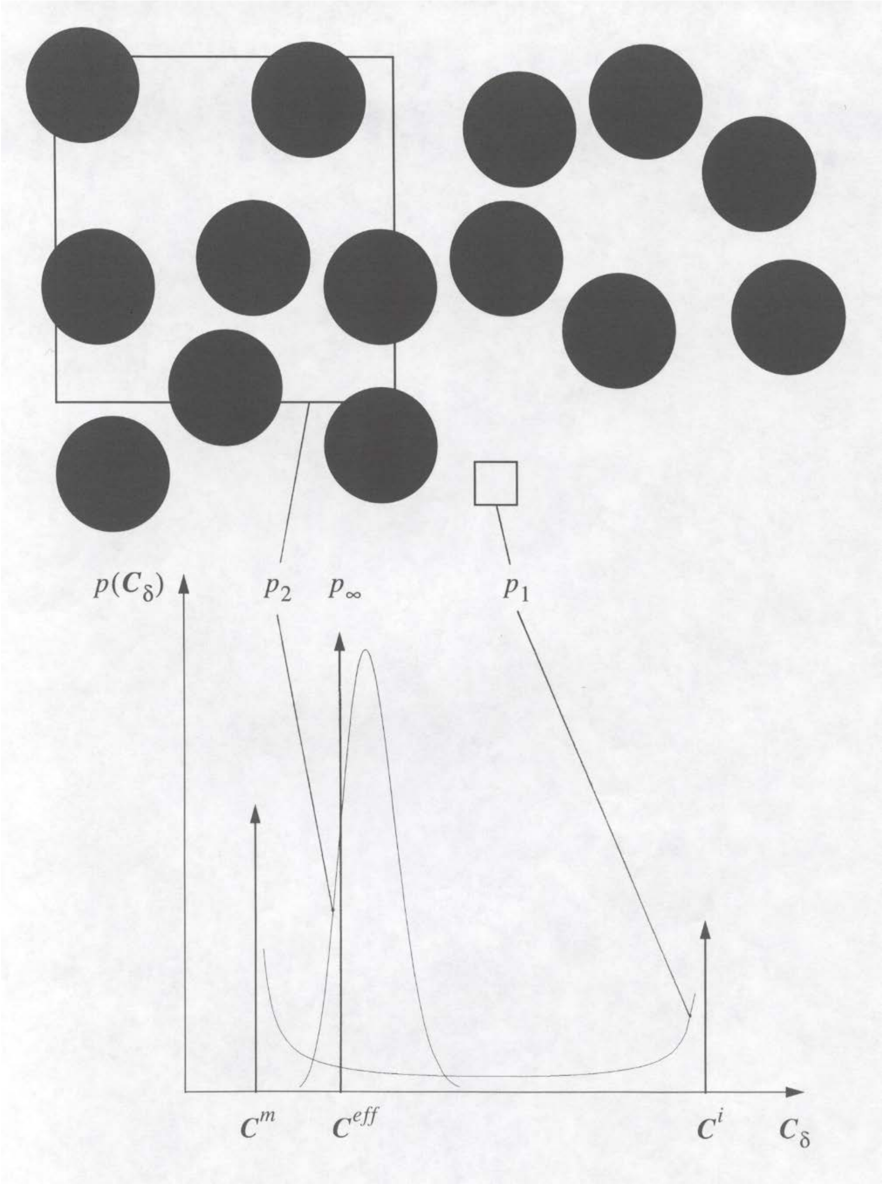

[*IJSS*, 1998]

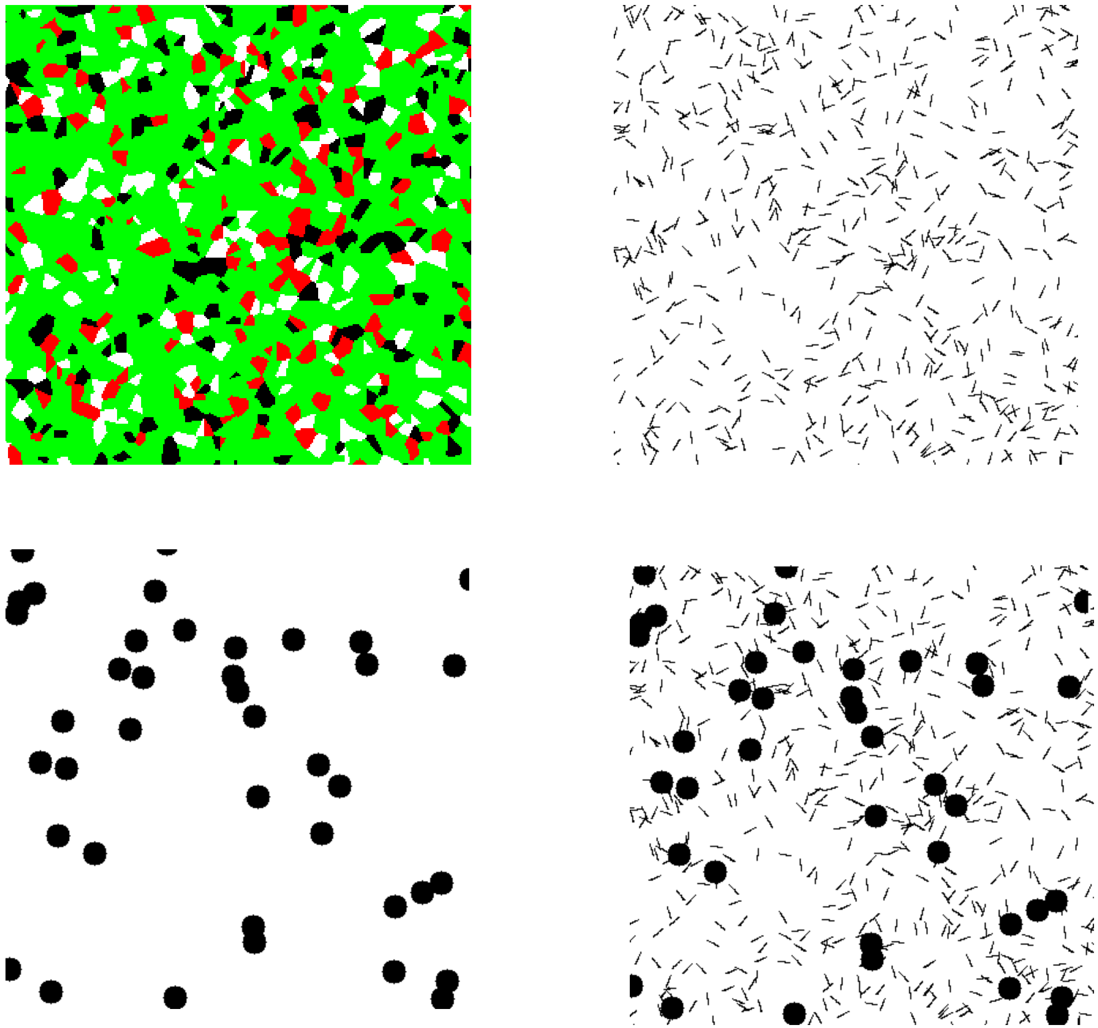

In-plane conductivity

- For each of mesoscale 2^{nd} rank tensors, consider 2^{nd} invariants

- Take coefficients of variation of these invariants
- These equal ~0.55, irrespective of:

  (a) mesoscale

  (b) the b.c.'s (uniform Dirichlet or Neumann)

  (c) the contrasts, and the inclusion's shape

  (d) the volume fraction of any phase

…universal property on mesoscale

[*Phys. Rev. B*, 2000]

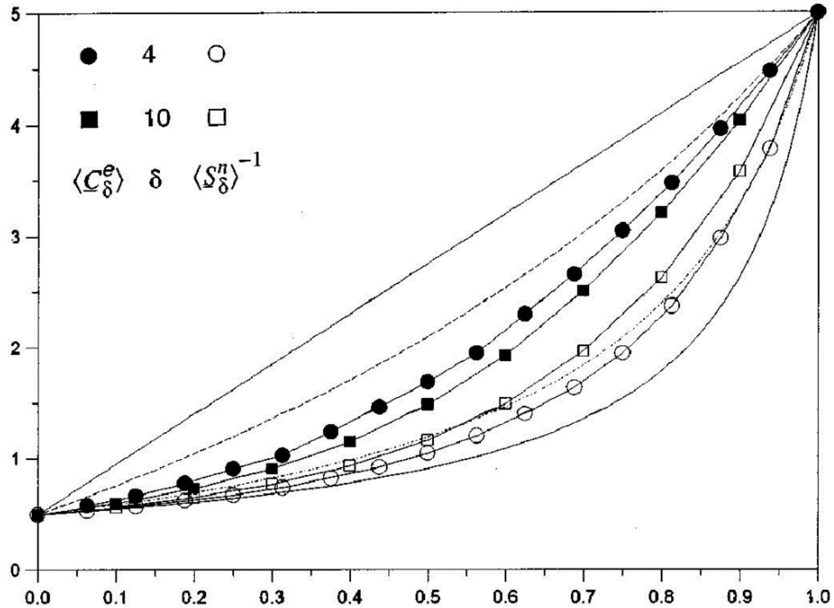

Mesoscale bounds on $tr\boldsymbol{C}^{eff}$ for a random two-phase square lattice
at contrasts 10, 100, 1000
at $\delta = 4$ and 10
Hashin-Shtrikman bounds (-------)

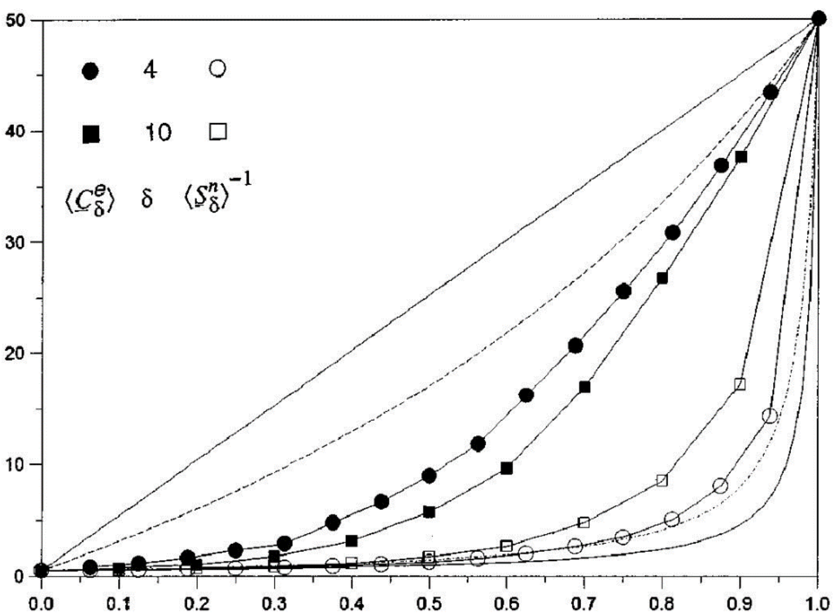

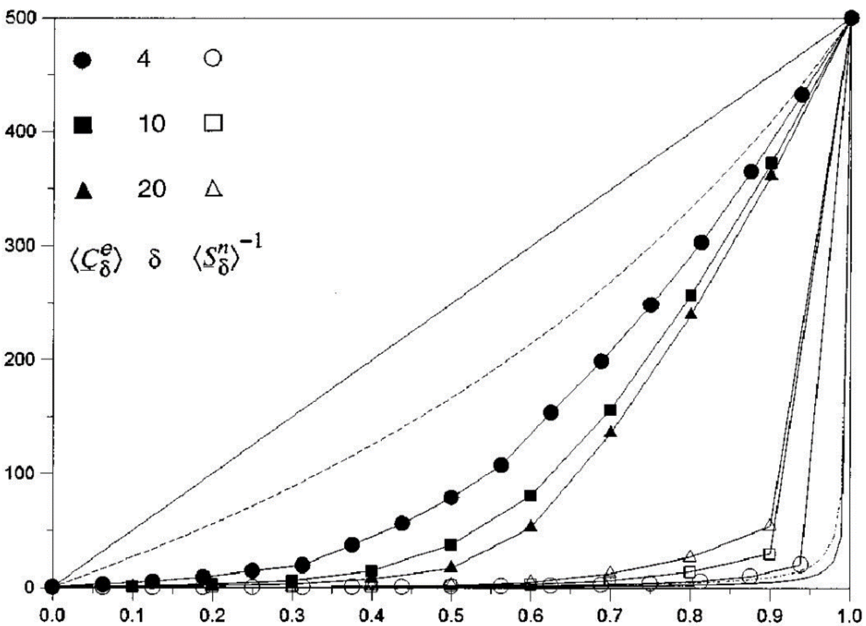

α

Finite-size scaling in random chessboards

$$C_\delta{}^e = \exp[-\delta^{-m_e}] \qquad S_\delta{}^n = \exp[\delta^{-m_n}]$$

$$m_e = 3.8\alpha^{0.14} \qquad m_n = 2.4\alpha^{0.59}$$

α = contrast

up to δ =1000

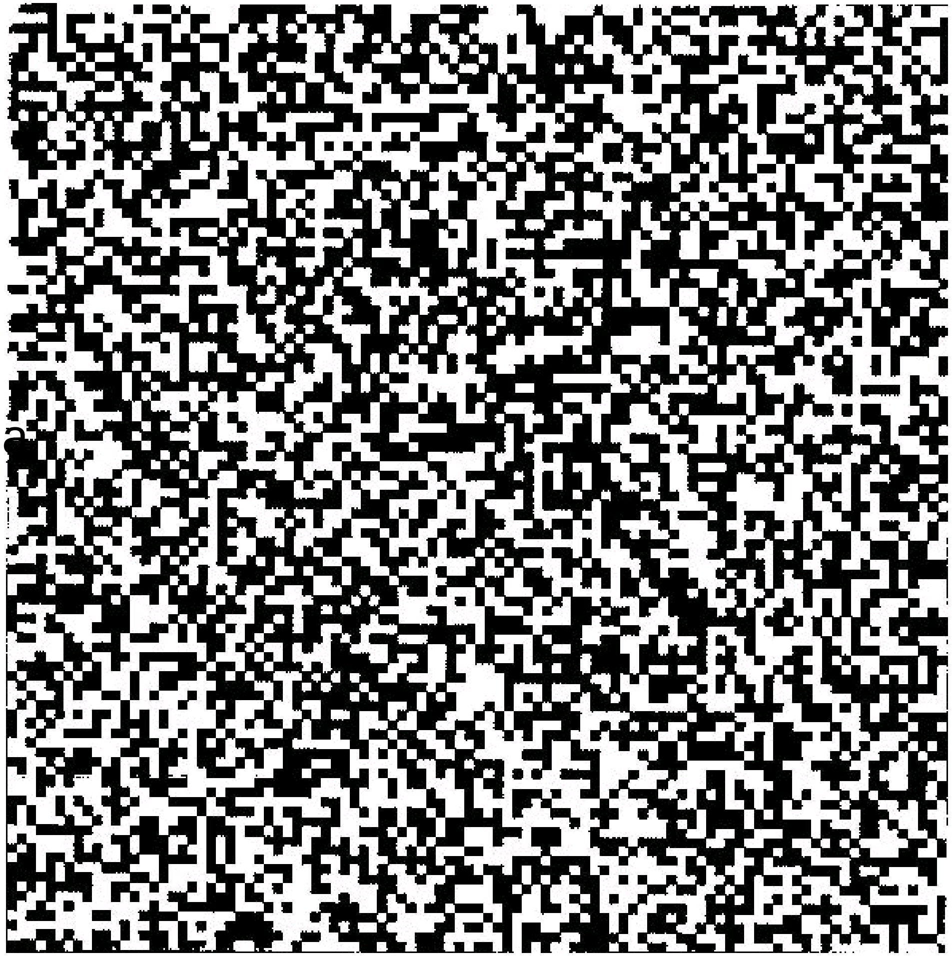

[*Phys. Rev. B*, 1996]

microscale

mesoscale

macroscale

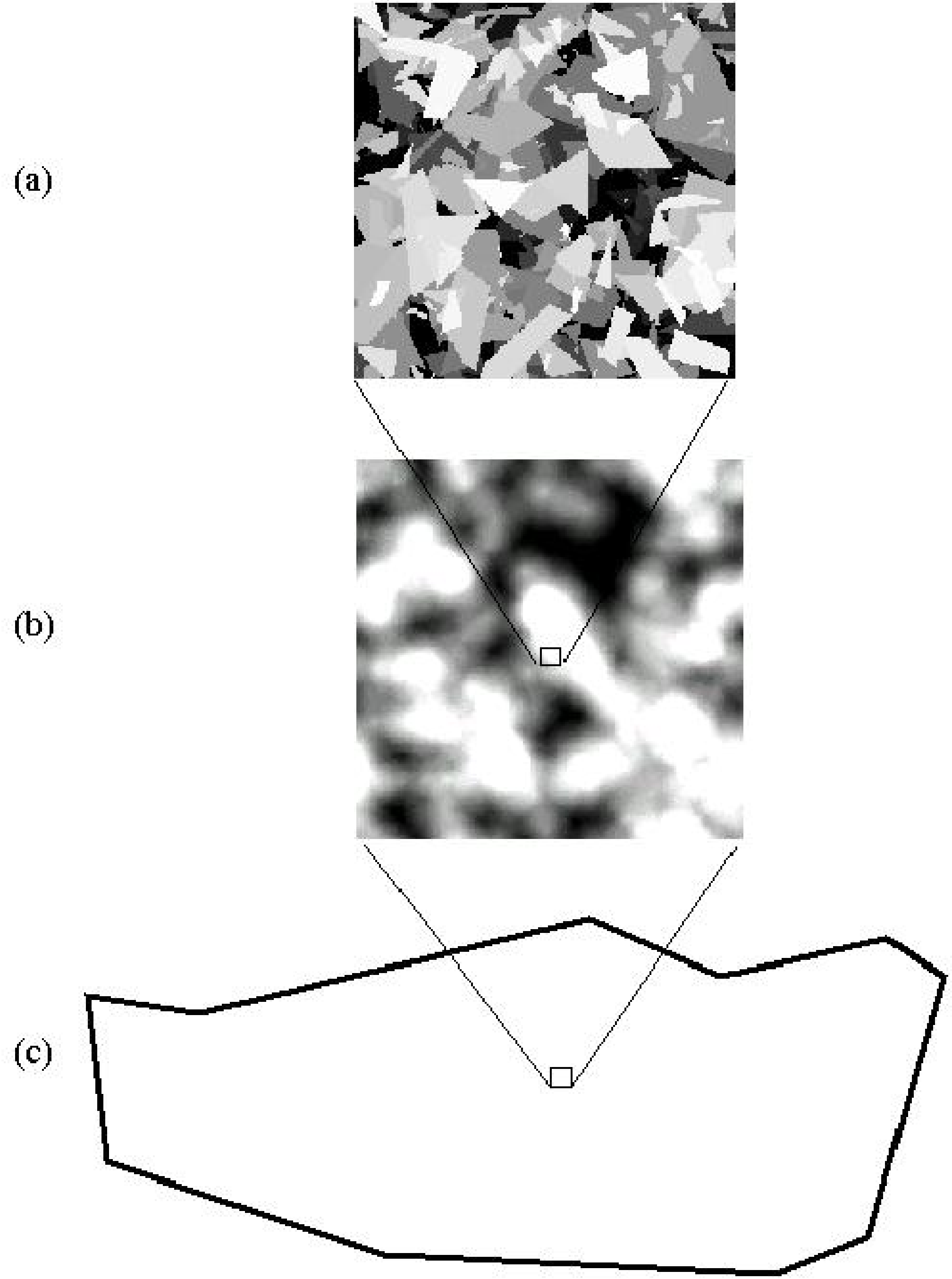

Continuum random tensor field

$$\mathbf{C}(\omega, \mathbf{x}) = \overline{\mathbf{C}} + \mathbf{C}'(\omega, \mathbf{x})$$

can it be assumed isotropic?

… can assume *E* and *v* to be smooth functions?

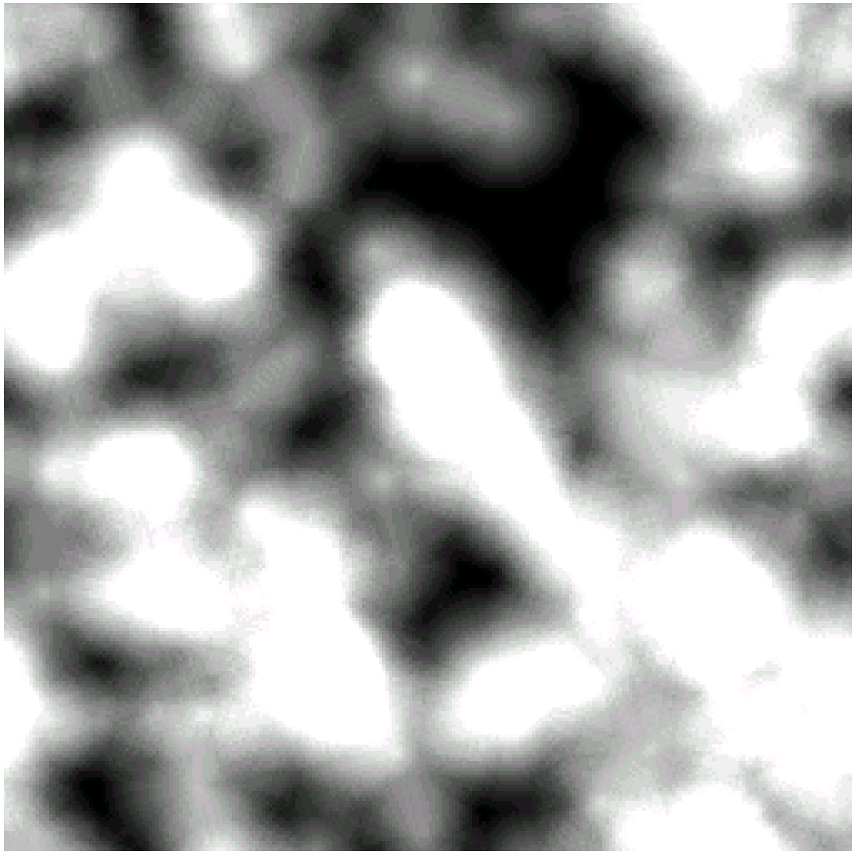

Continuum random tensor field

$$\mathbf{C}(\omega, \mathbf{x}) = \overline{\mathbf{C}} + \mathbf{C}'(\omega, \mathbf{x})$$

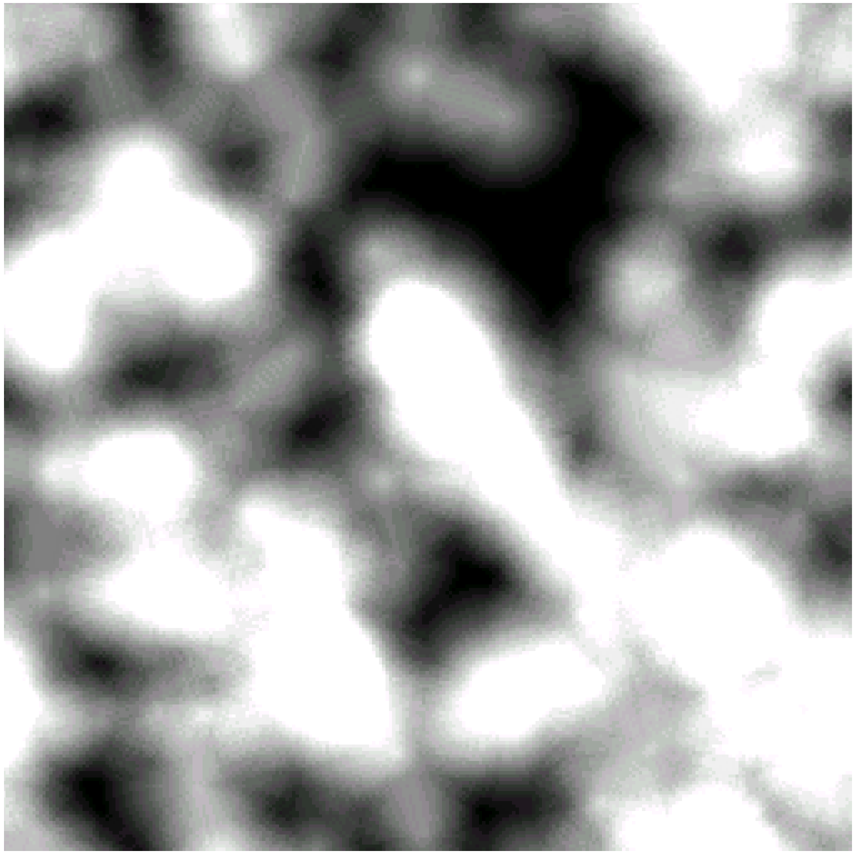

can it be assumed isotropic?

… can assume *E* and *v* to be smooth functions?

No!

Continuum random tensor field

$$\mathbf{C}(\omega,\mathbf{x}) = \overline{\mathbf{C}} + \mathbf{C}'(\omega,\mathbf{x})$$

can it be assumed isotropic?

… can assume *E* and *v* to be smooth functions?

No!

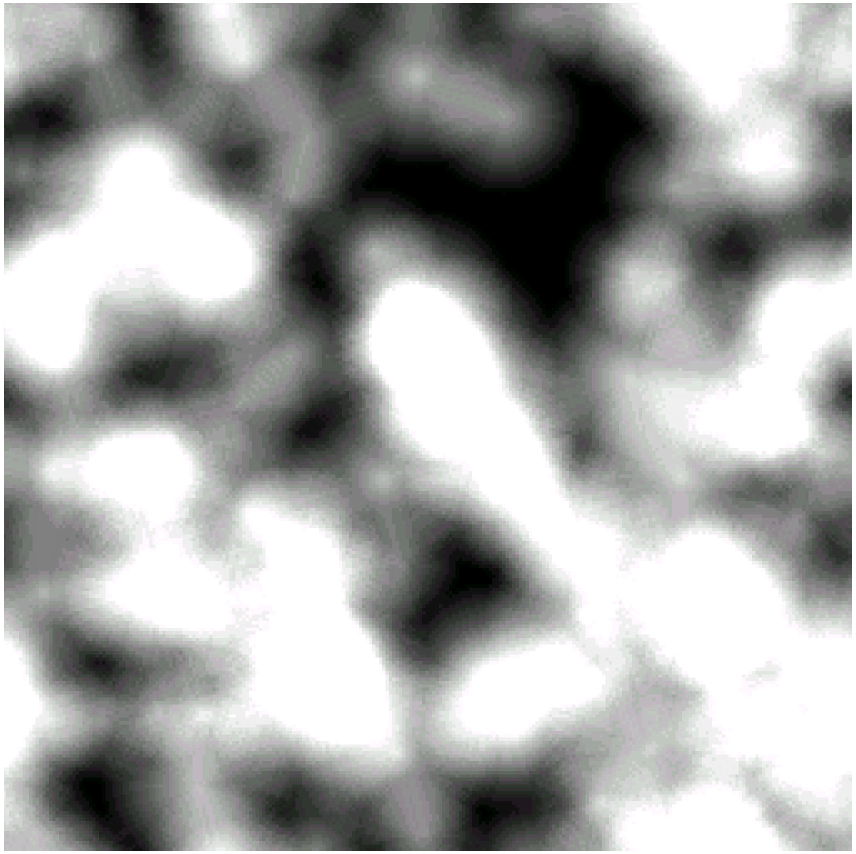

Applications:

random field models

stochastic finite elements

waves in random media

FGM …

Observe

- spatial inhomogeneity (gradient) prevents local isotropy of approximating smooth continuum

- assuming any smooth realization of random tensor field to be locally isotropic is in contradiction with the admissible correlation structure of random tensor fields, stationary and isotropic in wide sense

  [proof via representation theory of tensor fields, holds in mean-square]

- must admit anisotropy of **C’** tensor

<u>Hill condition</u>: Equivalence of energetic and mechanical definitions of Darcy's law:

$$\overline{p_{,i}U_i} = \overline{p_{,i}}\,\overline{U_i} \Leftrightarrow \int_{\partial B} (p - \overline{p_{,j}}x_j)(U_i n_i - \overline{U_i}\, n_i) dS = 0$$

$$\left.\begin{array}{ll} \text{(i)} & p = \overline{\nabla p} \cdot \vec{x} \quad \text{or} \quad p = \overline{p_{,i}} x_i \\ \text{(ii)} & \vec{U} \cdot \vec{n} = \vec{U}_0 \cdot \vec{n} \quad \text{or} \quad U_i n_i = U_{0i} n_i \\ \text{(iii)} & (p - \overline{p_{,i}} x_i)(U_i n_i - U_{0i} n) = 0 \\ \text{or} & (p - \overline{\nabla p} \cdot \vec{x}) \cdot (\vec{U} \cdot \vec{n} = \vec{U}_0 \cdot \vec{n}) = 0 \end{array}\right\} \text{on} \quad \partial B$$

$$\left\langle \tilde{\tilde{K}}_{\delta}{}^{e} \right\rangle \geq \left\langle \tilde{\tilde{K}}_{2\delta}{}^{e} \right\rangle \geq \cdots \geq \tilde{\tilde{K}}^{eff} = (\tilde{\tilde{R}}^{eff})^{-1} \geq \cdots \geq \left\langle \tilde{\tilde{R}}_{2\delta}{}^{n} \right\rangle^{-1} \geq \left\langle \tilde{\tilde{R}}_{\delta}{}^{n} \right\rangle^{-1}$$

Thermal expansion of random composites

$$\varepsilon_{ij} = S_{ijkl}(\omega, x)\sigma_{kl} + \alpha_{ij}(\omega, x)\theta$$

$$\Gamma_{ij} = -C_{ijkl}\alpha_{kl}$$

$$\sigma_{ij} = C_{ijkl}(\omega, x)\varepsilon_{kl} + \Gamma_{ij}(\omega, x)\theta$$

$$U = \frac{1}{V}\int_V AdV - \int_V F_i u_i dV - \int_{St} t_i u_i dS$$

$$A = \frac{1}{2}C_{ijkl}\varepsilon_{ij}\varepsilon_{kl} - \Gamma_{ij}\varepsilon_{ij}\theta - \frac{1}{2}c_v\frac{\theta^2}{T}$$

$$U^* = -\frac{1}{V}(\int_V Gdv + \int_{Su} t_i u_i ds)$$

$$G = -\frac{1}{2}S_{ijkl}\sigma_{ij}\sigma_{kl} - \alpha_{ij}\sigma_{ij}\theta - \frac{1}{2}c_p\frac{\theta^2}{T}$$

$$\delta = \frac{L}{d} = 2$$

$$\delta = \frac{L}{d} = 16$$

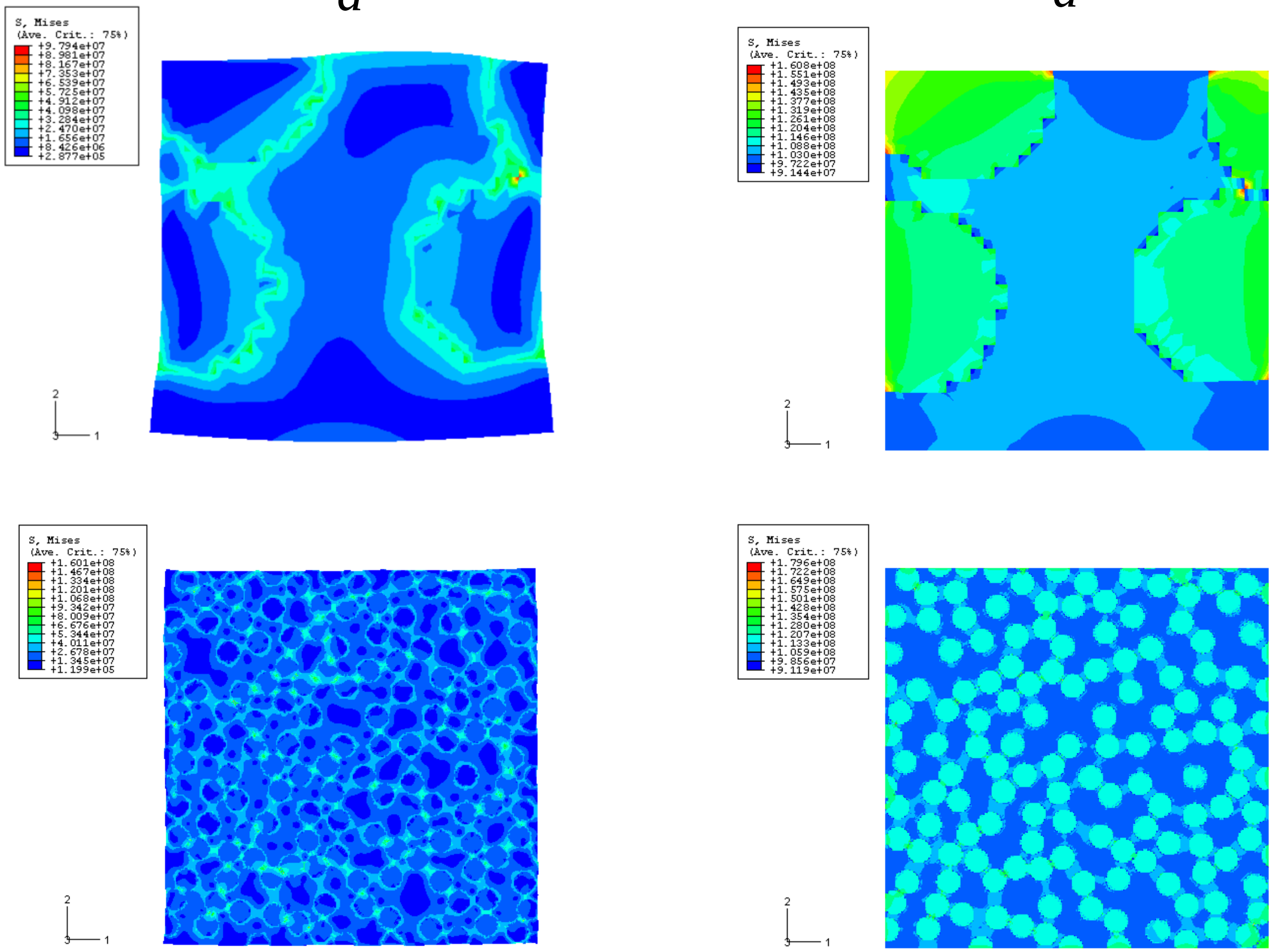

Neumann b.c.

Dirichlet b.c.

$$\Gamma_{ij}^{eff} \geq \cdots \geq \left\langle \Gamma_{ij} \right\rangle_{4\delta}^{d} \geq \left\langle \Gamma_{ij} \right\rangle_{2\delta}^{d} \geq \left\langle \Gamma_{ij} \right\rangle_{\delta}^{d} \geq \left\langle \Gamma_{ij} \right\rangle_{1}^{d}$$

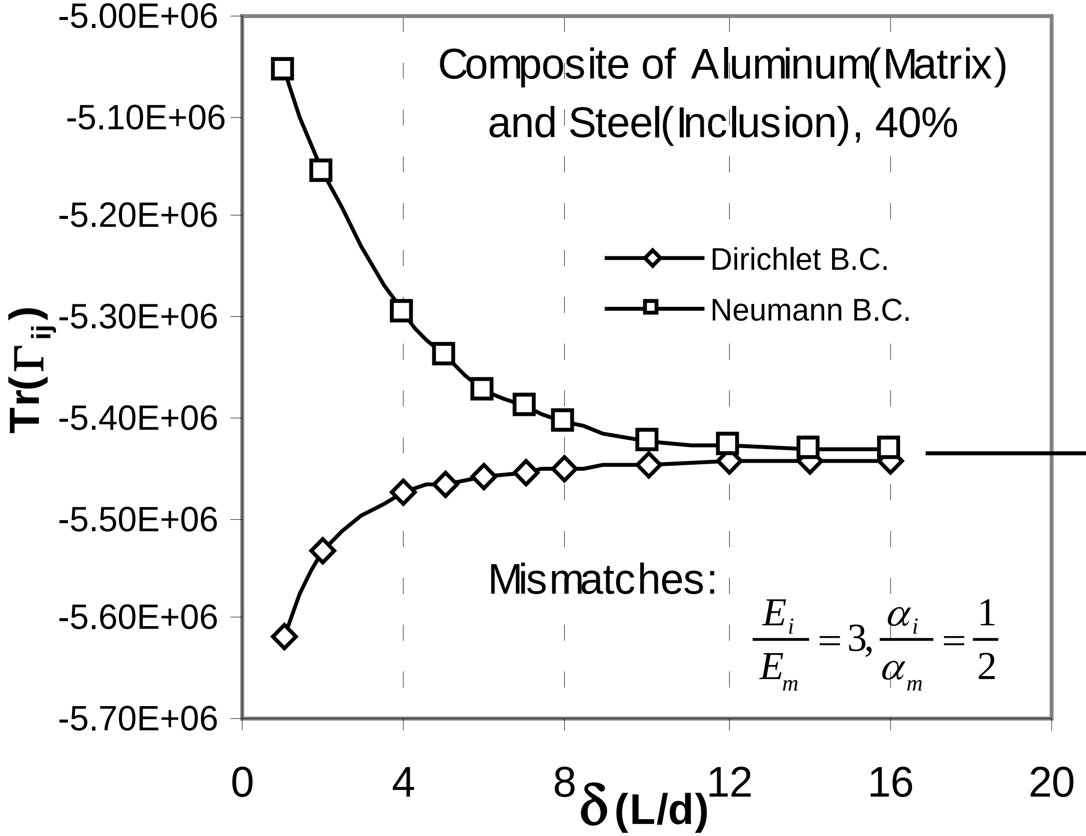

$$\Gamma_{ij}^{eff} = -C_{ijkl}^{eff} \alpha_{kl}^{eff}$$

$$\alpha_{ij}^{eff} \leq \cdots \leq \left\langle \alpha_{ij} \right\rangle_{4\delta}^{n} \leq \left\langle \alpha_{ij} \right\rangle_{2\delta}^{n} \leq \left\langle \alpha_{ij} \right\rangle_{\delta}^{n} \leq \left\langle \alpha_{ij} \right\rangle_{1}^{n}$$

[*Networks & Heterogeneous Media*, 2006]

quartets of Legendre transformations

classical →

$$X(x_i, \alpha_i)$$
$$y_i = \frac{\partial X}{\partial x_i}, \ \beta_i = \frac{\partial X}{\partial \alpha_i}$$

$$X(x_i, \alpha) + Y(y_i, \alpha_i) = x_i y_i$$

$$X(x_i, \alpha) + V(x_i, \beta_i) = \alpha_i \beta_i$$

$$Y(y_i, \alpha_i)$$
$$x_i = \frac{\partial Y}{\partial y_i}, \ \beta_i = -\frac{\partial Y}{\partial \alpha_i}$$

$$V(x_i, \beta_i)$$
$$y_i = -\frac{\partial V}{\partial x_i}, \ \alpha_i = \frac{\partial V}{\partial \beta_i}$$

$$Y(y_i, \alpha_i)) + W(y_i, \beta_i) = -\alpha_i \beta_i$$

$$V(x_i, \beta_i) + W(y_i, \beta_i) = -x_i y_i$$

$$W(y_i, \beta_i)$$
$$x_i = -\frac{\partial W}{\partial y_i}, \ \alpha_i = -\frac{\partial W}{\partial \beta_i}$$

stochastic ↓

$$\langle X(x_i, \alpha_i) \rangle$$
$$\langle y_i \rangle = \frac{\partial \langle X \rangle}{\partial x_i}, \ \langle \beta_i \rangle = \frac{\partial \langle X \rangle}{\partial \alpha_i}$$

$$\langle X(x_i, \alpha_i) \rangle + Y(\langle y_i \rangle, \alpha_i) = x_i \langle y_i \rangle$$

$$\langle X(x_i, \alpha_i) \rangle + V(x_i, \langle \beta_i \rangle) = \alpha_i \langle \beta_i \rangle$$

$$Y(\langle y_i \rangle, \alpha_i)$$
$$x_i = \frac{\partial Y}{\partial \langle y_i \rangle}, \ \langle \beta_i \rangle = -\frac{\partial Y}{\partial \alpha_i}$$

$$V(x_i, \langle \beta_i \rangle)$$
$$\langle y_i \rangle = -\frac{\partial V}{\partial x_i}, \ \alpha_i = \frac{\partial V}{\partial \langle \beta_i \rangle}$$

$$Y(\langle y_i \rangle, \alpha_i)) + W(\langle y_i \rangle, \langle \beta_i \rangle) = -\alpha_i \langle \beta_i \rangle$$

$$V(x_i, \langle \beta_i \rangle) + W(\langle y_i \rangle, \langle \beta_i \rangle) = -x_i \langle y_i \rangle$$

$$W(\langle y_i \rangle, \langle \beta_i \rangle)$$
$$x_i = -\frac{\partial W}{\partial \langle y_i \rangle}, \ \alpha_i = -\frac{\partial W}{\partial \langle \beta_i \rangle}$$

[*J. Non-Equilib. Thermodyn.*, 2002]

Thermomechanics of random media

(generalizing formulation of H. Ziegler)

Thermodynamics with internal variables

orthogonality in space of forces

orthogonality in space of velocities

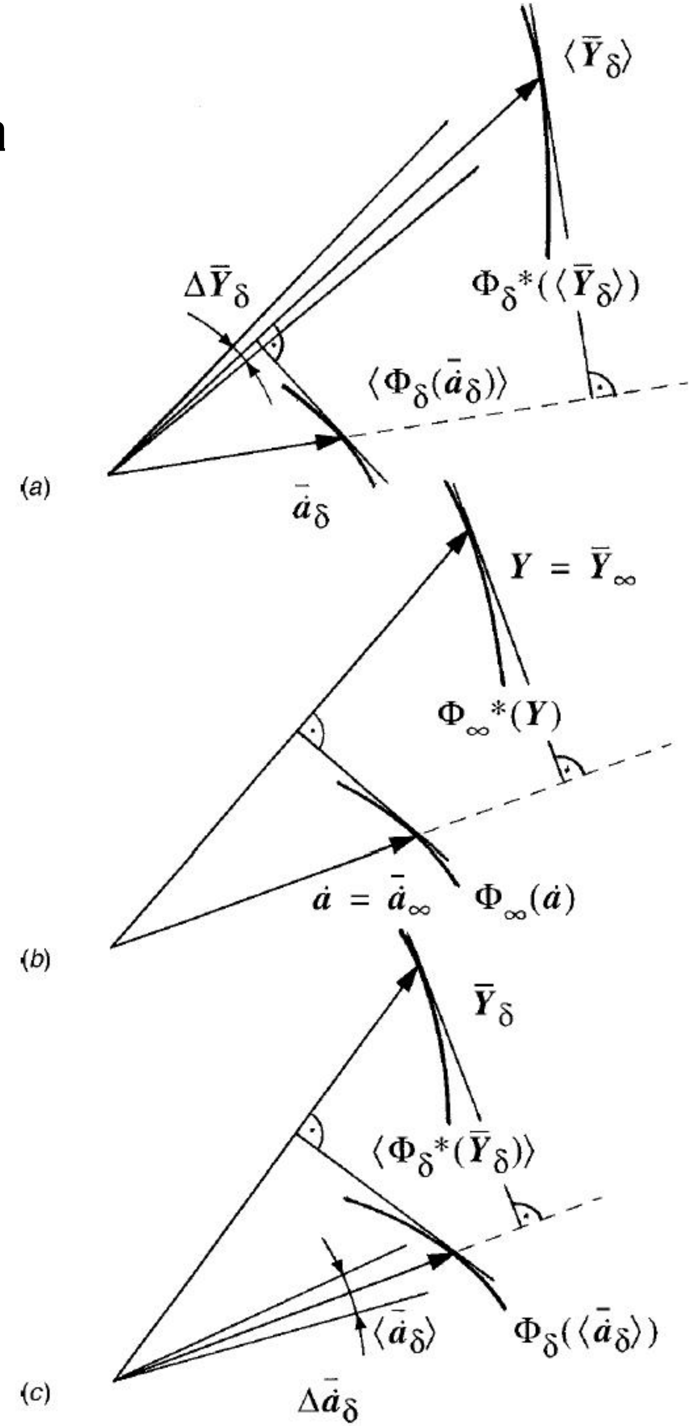

Mesoscale bounds in finite elasticity of random composites

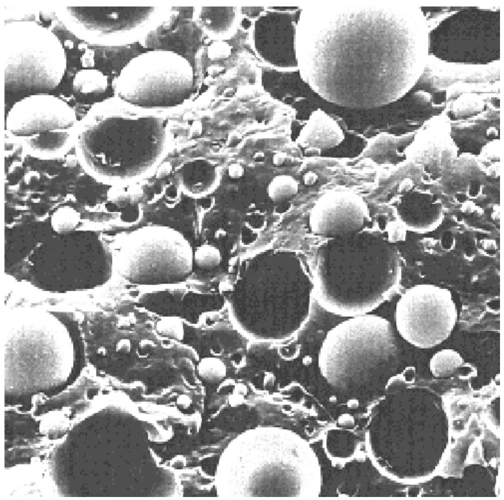

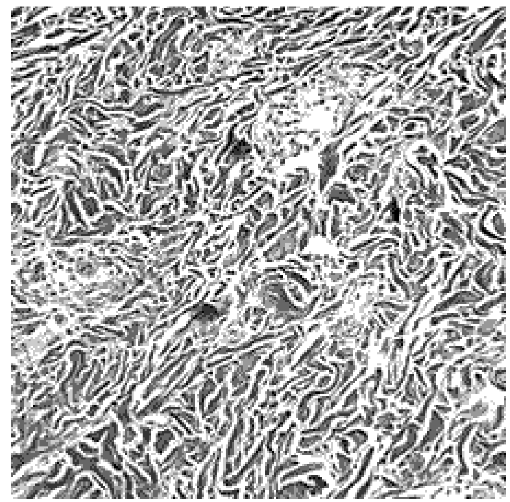

ternary phase rubber composite

leg muscle tissue

P.R. Hornsby & K. Premphet, *J. Appl. Polym.Sci.* 70, 587 (1998)

L.E. Eldsberg *et al*., *J. Rehab. Res. Develop.* 37, (2000)

Finite elasticity of random media

Hill condition: $\overline{\mathbf{P}:\mathbf{F}} = \overline{\mathbf{P}}:\overline{\mathbf{F}} \quad \Rightarrow \quad \frac{1}{V_0}\int_{\partial V_0} (\mathbf{t} - \overline{\mathbf{P}}\cdot\mathbf{N})\cdot(\mathbf{u} - [\overline{\mathbf{F}} - \mathbf{1}]\cdot\mathbf{X})dS = 0$

Kinematic uniform b.c. $\mathbf{u} = [\mathbf{F}^0 - \mathbf{1}]\cdot\mathbf{X}\,, \quad \forall\mathbf{X}\in\partial V_0$

Static uniform b.c. $\mathbf{t} = \mathbf{P}^0\cdot\mathbf{N}, \quad \forall\mathbf{X}\in\partial V_0$

Mixed uniform b.c. $(\mathbf{t} - \mathbf{P}^0\cdot\mathbf{N})\cdot(\mathbf{u} - [\mathbf{F}^0 - \mathbf{1}]\cdot\mathbf{X}) = 0, \quad \forall\mathbf{X}\in\partial V_0$

Minimum potential energy: $P\{U_i\} = \int_{V_0} \psi(U_{i,k})dV - \int_{S_T} t_i^0 U_i dS$

P assumes local minimum for actual solution u_{ij} provided

Under kinematic b.c: $P\{U_i\} = \int_{V_0} \psi(U_{i,k})dV$

$$\int_{V_0} \frac{\partial^2 \psi}{\partial u_{i,k} \partial u_{p,q}} d_{i,k} d_{p,q} dV > 0$$

Complementary type functional:

$$Q\{U_{ik}\} = \int_{V_0} \left\{ \frac{\partial \psi(U_{ik})}{\partial U_{ik}} U_{ik} - \psi(U_{ik}) \right\} dV - \int_{S_D} \frac{\partial \psi(U_{ik})}{\partial U_{ik}} n_k u_i^0 dS$$

where $\frac{\partial}{\partial x_k}\left(\frac{\partial \psi(U_{ik})}{\partial U_{ik}} \right) = 0$ in V_0, $\frac{\partial \psi(U_{ik})}{\partial U_{ik}} n_k = t_i^0$ on S_T

Q assumes a local minimum for the actual solution u_{ij} provided

$$\int_{V_0} \frac{\partial^2 \psi}{\partial u_{i,k} \partial u_{p,q}} d_{ik} d_{pq} dV > 0$$

[S.J. Lee & R.T. Shield, “Variational principles in finite elastostatics”, *ZAMP*, 1980]

Scale-dependent hierarchies in finite elasticity:

Lower bound: $\left\langle \Psi(\mathbf{F}^0,\Delta)\right\rangle \le \left\langle \Psi(\mathbf{F}^0,\delta)\right\rangle \le \left\langle \Psi(\mathbf{F}^0,\delta')\right\rangle \le \left\langle \Psi(\mathbf{F}^0,1)\right\rangle$

Upper bound: $\left\langle Q(\mathbf{P}^0,\Delta)\right\rangle \le \left\langle Q(\mathbf{P}^0,\delta)\right\rangle \le \left\langle Q(\mathbf{P}^0,\delta')\right\rangle \le \left\langle Q(\mathbf{P}^0,1)\right\rangle$

for $1<\delta'<\delta<\Delta$

$$\Psi(\omega)=\int_{V_0}\psi(\omega,\mathbf{X})dV \qquad Q(\mathbf{P}^0)=\mathbf{P}^0:\overline{\mathbf{F}}-\Psi(\omega,\mathbf{P}^0)$$

[*Proc. Roy. Soc. Lond. A*; *J. Elast.*, 2006]

Numerical simulations

$$\Psi = \sum_{i=1}^{N} \frac{2\mu_i}{\alpha_i^2}(\overline{\lambda_1}^{\alpha_i} + \overline{\lambda_2}^{\alpha_i} + \overline{\lambda_3}^{\alpha_i} - 3) + \sum_{i=1}^{N} \frac{1}{D_i}(J^{el} - 1)^{2i}$$

	Matrix	Inclusion
Energy function	Ogden model	Neo-Hookean model
	$\mu_1 = 4.095 \cdot 10^5\,Nm,\quad \alpha_1 = 1.3,$ $\mu_2 = 0.03 \cdot 10^5\,Nm,\quad \alpha_2 = 5.0,$ $\mu_3 = 0.01 \cdot 10^5\,Nm,\quad \alpha_3 = -2.0.$	$\mu_1 = 4.095 \cdot 10^6\,Nm,\quad \alpha_1 = 2,$ $\mu_2 = 0,\quad \alpha_2 = 0,$ $\mu_3 = 0,\quad \alpha_3 = 0.$

$$\alpha = \frac{\mu_0^{(i)}}{\mu_0^{(m)}} = 10, \quad \frac{K_0^{(i)}}{K_0^{(m)}} = 1, \quad \frac{V^{(i)}}{V^{(m)}} = 0.35$$

	δ=1	δ=2	δ=4	δ=8	δ=16
Number of samples	512	384	160	40	10

Stress-strain curves

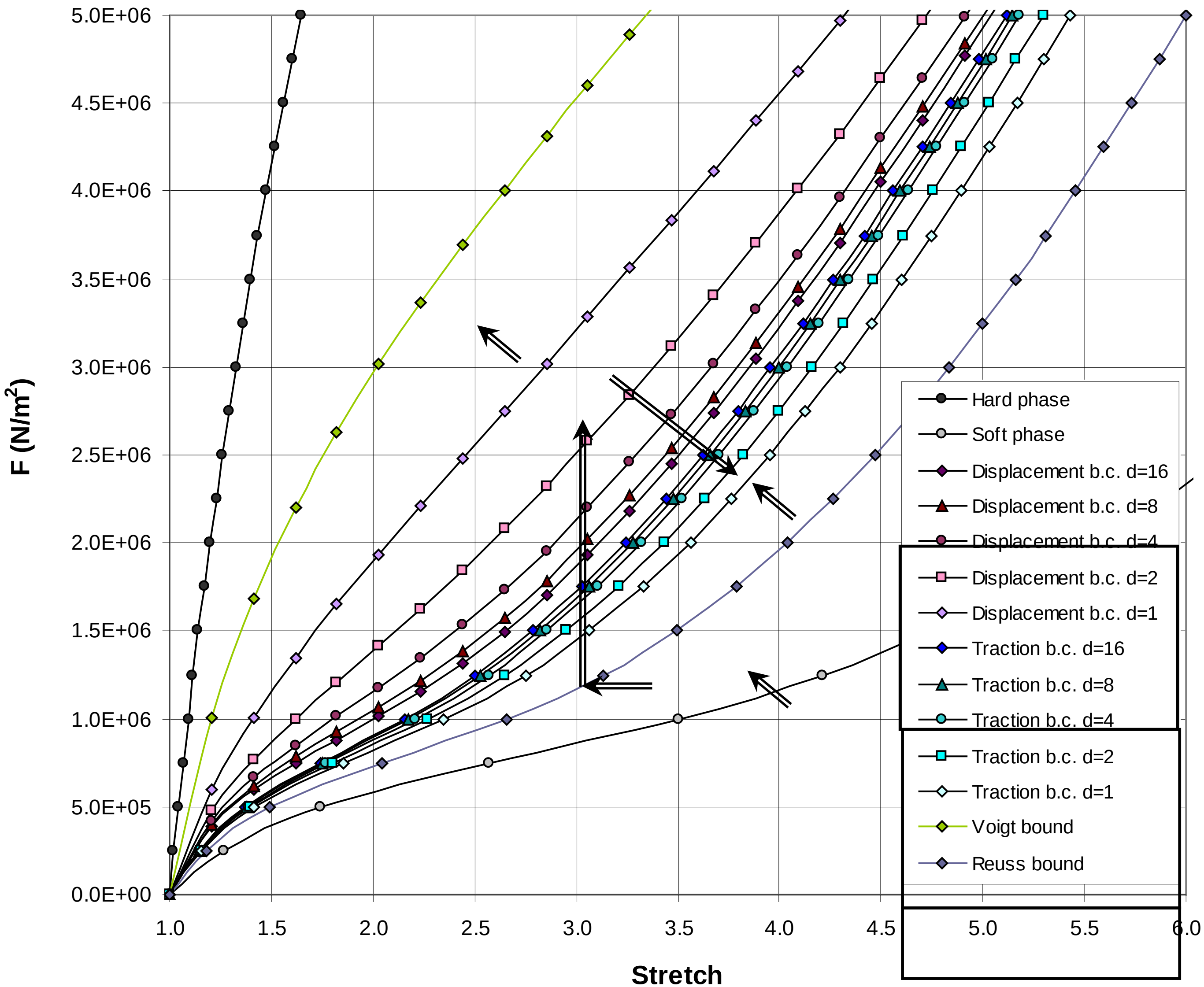

Elementary bounds

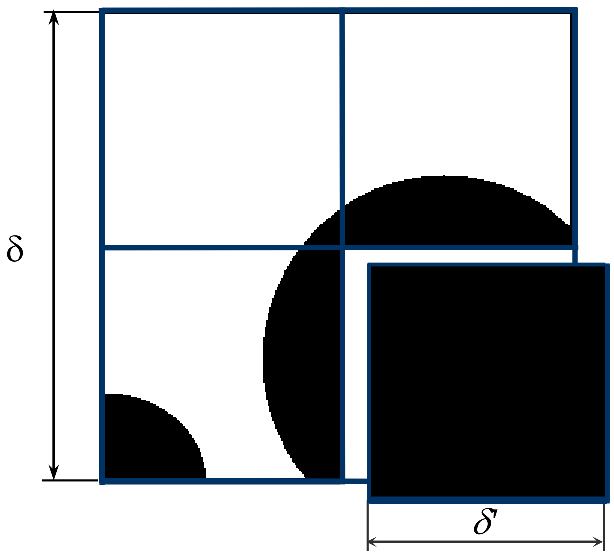

Voigt upper bound:

$$\Psi_V(\overline{\mathbf{F}}) \geq \Psi_\delta^d$$

$$\Psi_V = c_1\Psi_1 + c_2\Psi_2$$

$$\mu_V = 0.35\mu_{Neo-hookean} + 0.65\mu_{Ogden}$$

Reuss lower bound:

$$\Psi_R^*(\overline{\mathbf{P}}) \geq \Psi_\delta^{*t}$$

$$\mu_R = ?$$

Energy Bounds

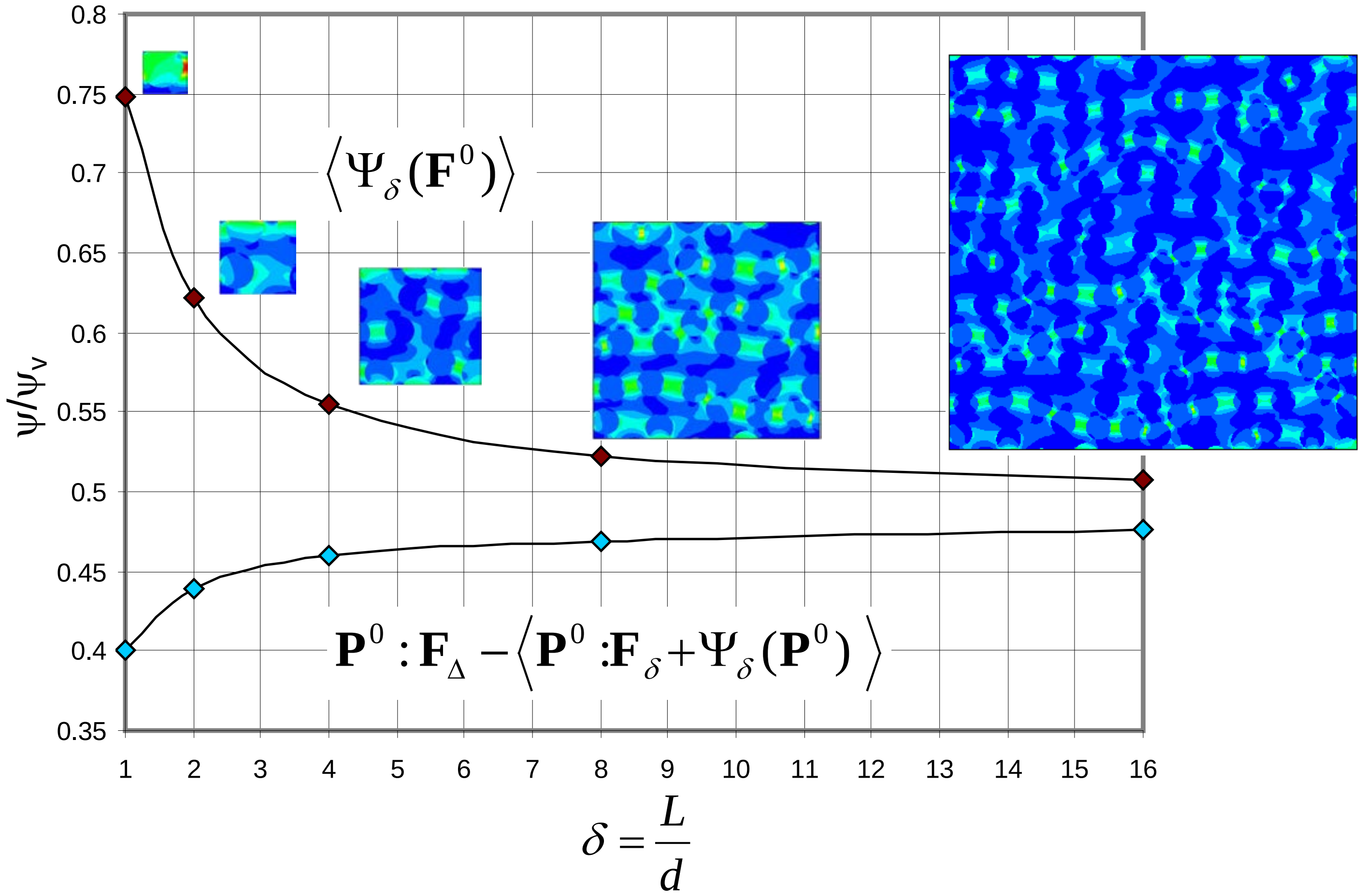

Mixed Boundary Conditions

$$\Psi_{\delta}^{d} \geq \Psi_{\delta}^{m}$$

$$\Psi_{\delta}^{*t} \geq \Psi_{\delta}^{*m}$$

1st type

$$\begin{bmatrix} F_{11}^{0} & F_{12}^{0} = 0 \\ P_{21}^{0} = 0 & P_{22}^{0} = 0 \end{bmatrix}$$

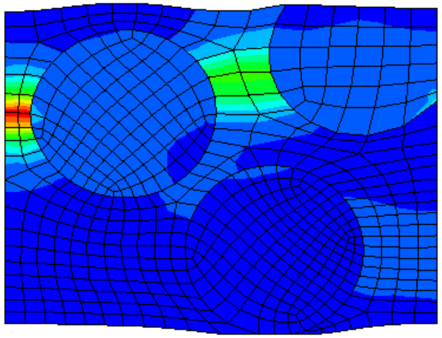

2nd type

$$\begin{bmatrix} F_{11}^{0} & P_{12}^{0} = 0 \\ P_{21}^{0} = 0 & F_{22}^{0} \end{bmatrix}$$

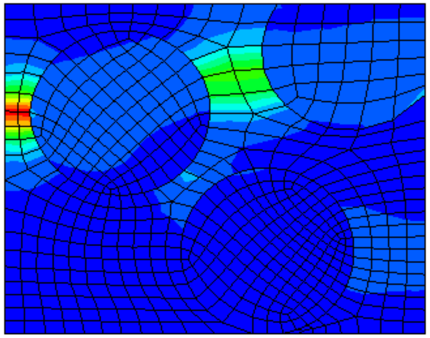

Mesh dependence (40% inclusions)

material properties:

$E_i / E_m = 5$

Poisson ratio is the same

$\alpha_i / \alpha_m = 10$

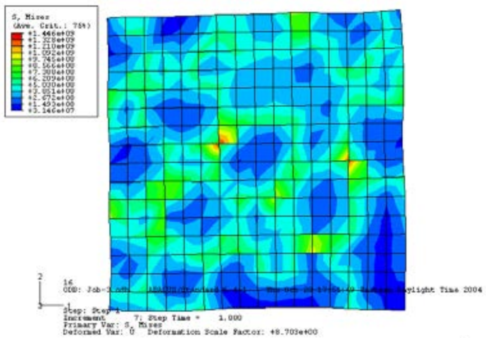

$$\frac{d_{inclusion}}{dx} = 8$$

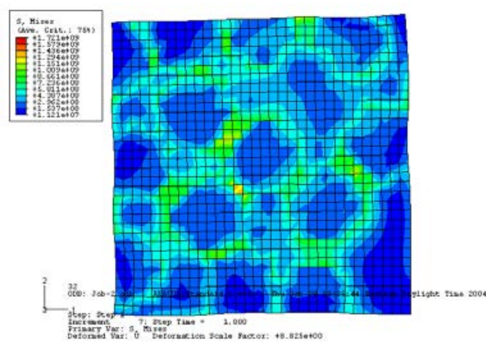

$$\frac{d_{inclusion}}{dx} = 16$$

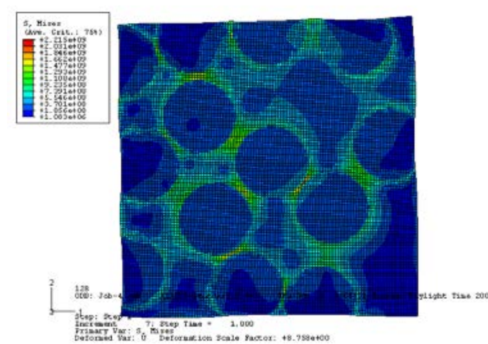

$$\frac{d_{inclusion}}{dx} = 32$$

Tr(α)

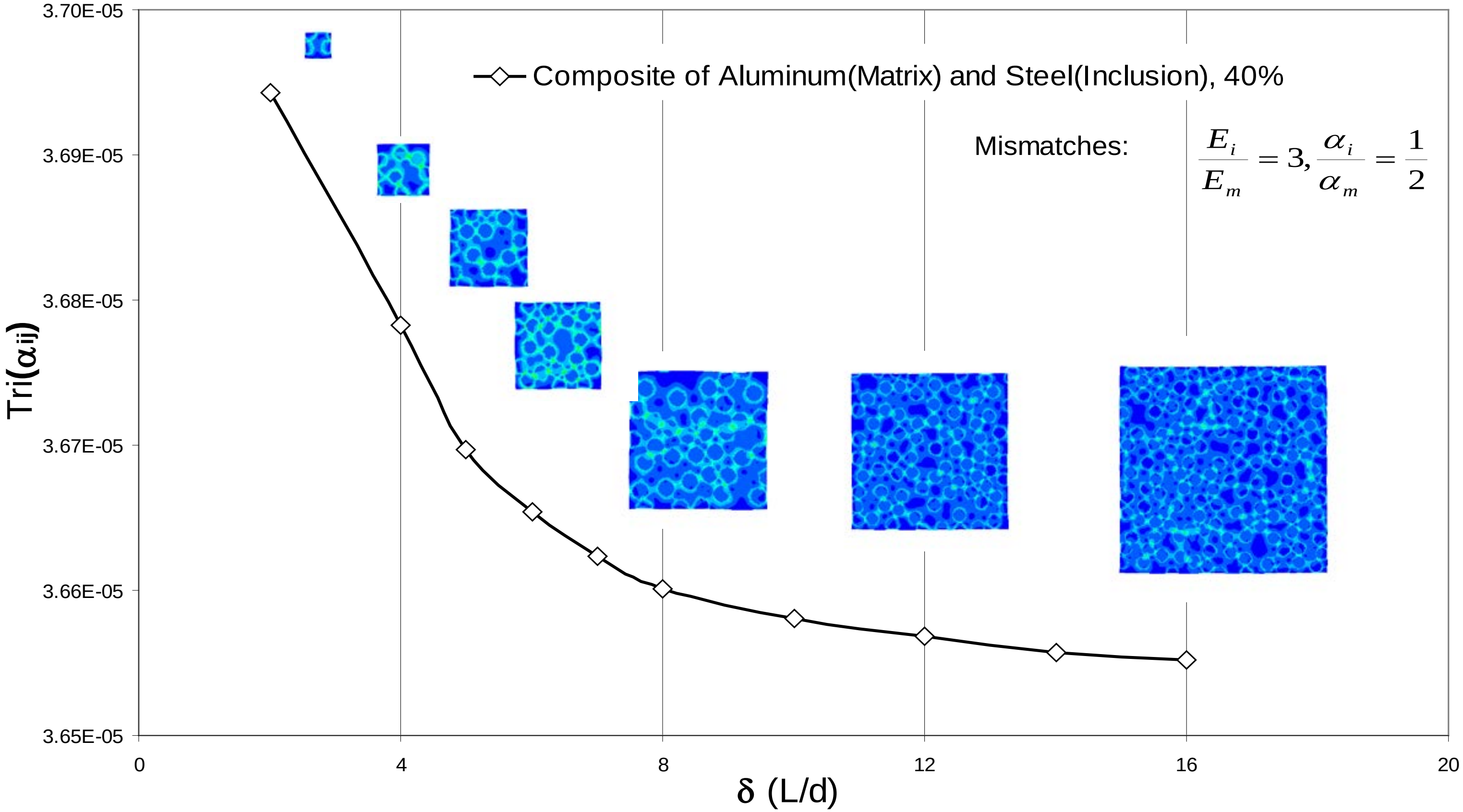

Composite of Aluminum(Matrix) and Steel(Inclusion), 40%
Mismatches: $\frac{E_i}{E_m} = 3, \frac{\alpha_i}{\alpha_m} = \frac{1}{2}$
Tri(αij)
3.70E-05
3.69E-05
3.68E-05
3.67E-05
3.66E-05
3.65E-05
0
4
8
12
16
20
δ (L/d)

$Tr(\Gamma)$

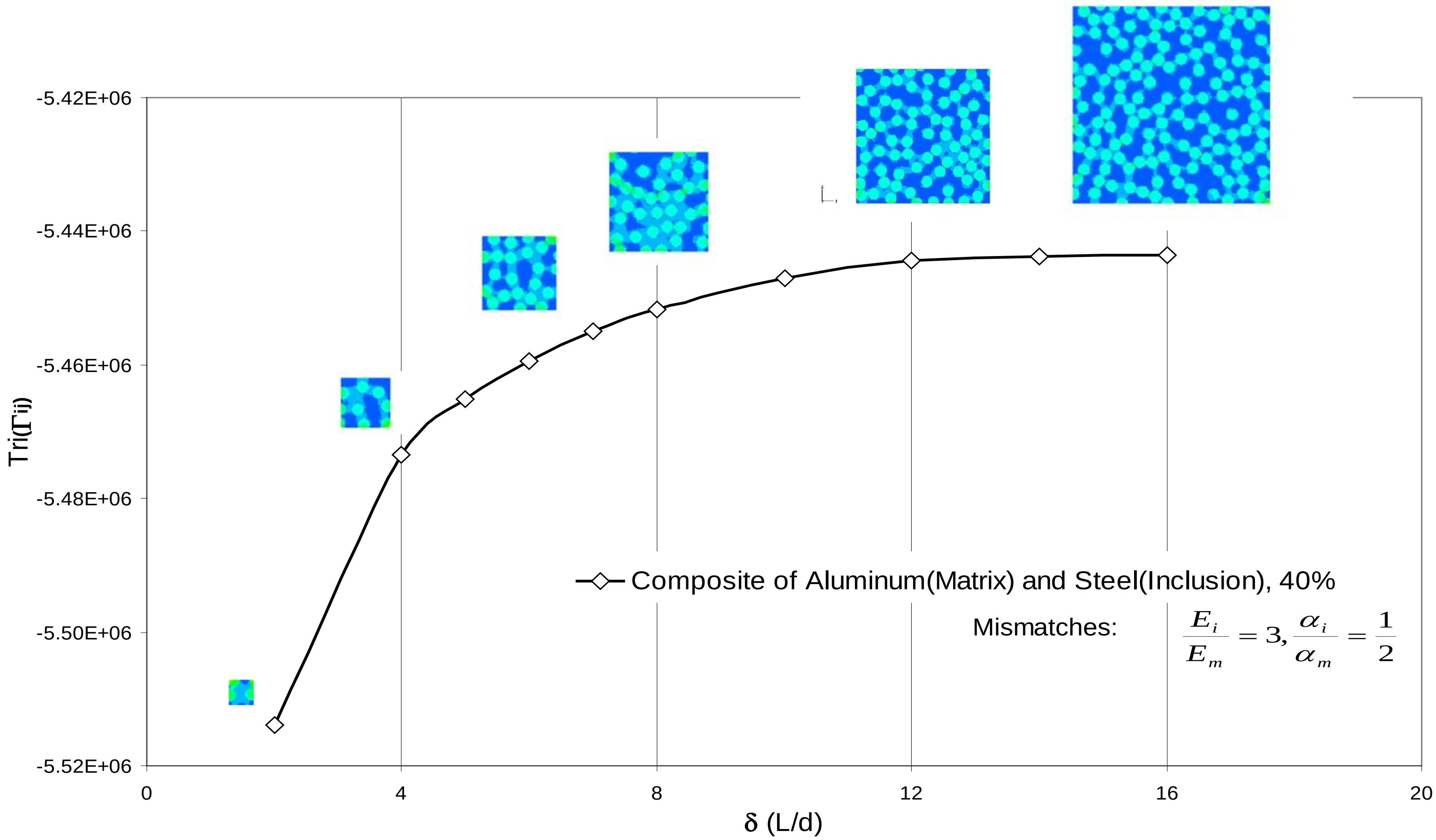

-5.42E+06
-5.44E+06
-5.46E+06
-5.48E+06
-5.50E+06
-5.52E+06
Tri(Γij)
0
4
8
12
16
20
δ (L/d)
Composite of Aluminum(Matrix) and Steel(Inclusion), 40%
Mismatches: $\frac{E_i}{E_m} = 3, \frac{\alpha_i}{\alpha_m} = \frac{1}{2}$

Energy Bounds – Uniaxial Tension

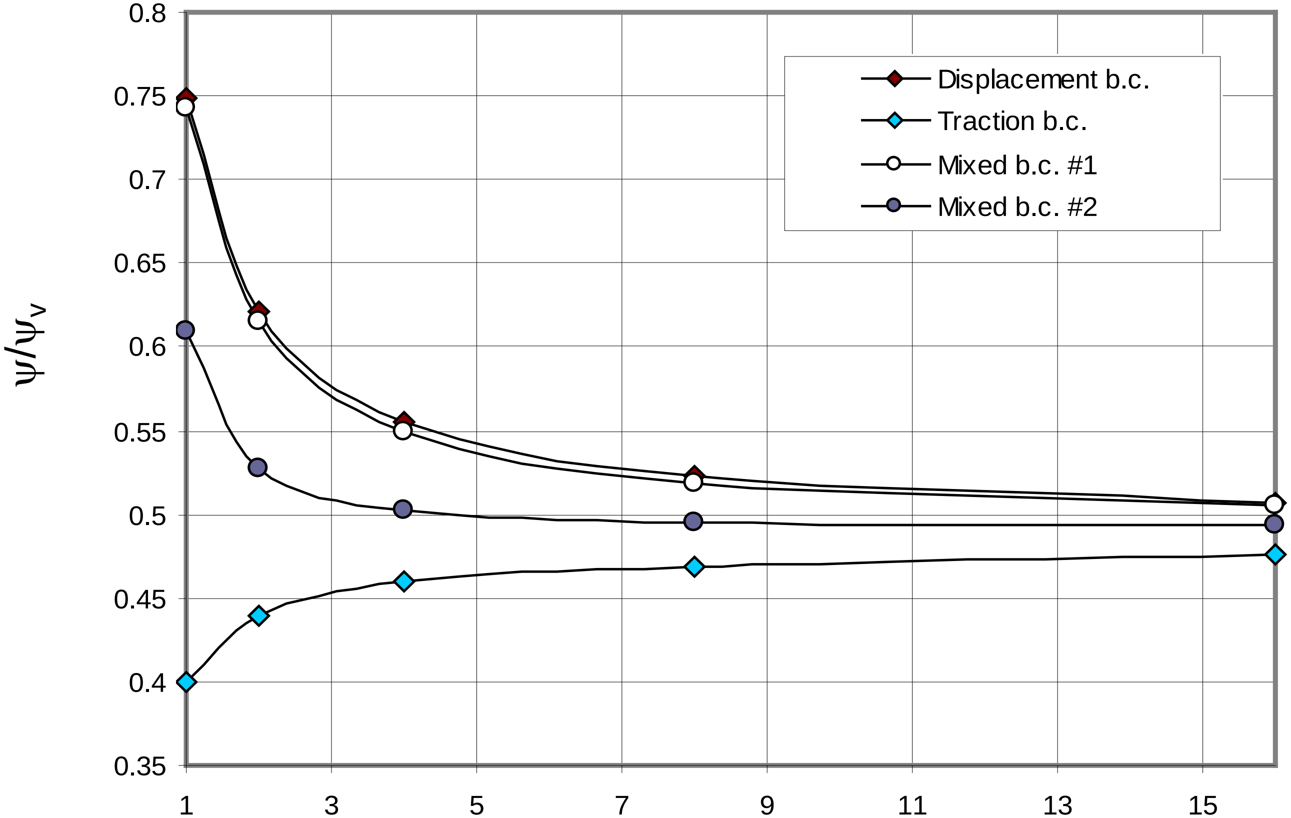

$$\delta = \frac{L}{d}$$

Comparison of scaling trends

$$D = \frac{R_\delta^e - R_\delta^n}{\left(R_\delta^e + R_\delta^n\right)/2}$$

Table 1 Mismatch and discrepancy (D) values on mesoscale $\delta = 16$

	Mismatch	D [%]
Linear elasticity	$\frac{\mu^{(i)}}{\mu^{(m)}} = 10, \frac{\kappa^{(i)}}{\kappa^{(m)}} = 1$	2.28
Linear thermoelasticity	$\frac{\mu^{(i)}}{\mu^{(m)}} = 10, \frac{\kappa^{(i)}}{\kappa^{(m)}} = 10, \frac{\alpha^{(i)}}{\alpha^{(m)}} = \frac{1}{10}$	5.51
Plasticity	$\frac{h^{(i)}}{h^{(m)}} = 10, \frac{E^{(i)}}{E^{(m)}} = 1$	2.29
Nonlinear elasticity	$\frac{\mu_0^{(i)}}{\mu_0^{(m)}} = 10, \frac{\kappa_0^{(i)}}{\kappa_0^{(m)}} = 1$	5.86
Flow in porous media	$\frac{tr(\mathbf{K}^{(i)})}{tr(\mathbf{K}^{(m)})} = \infty$	27

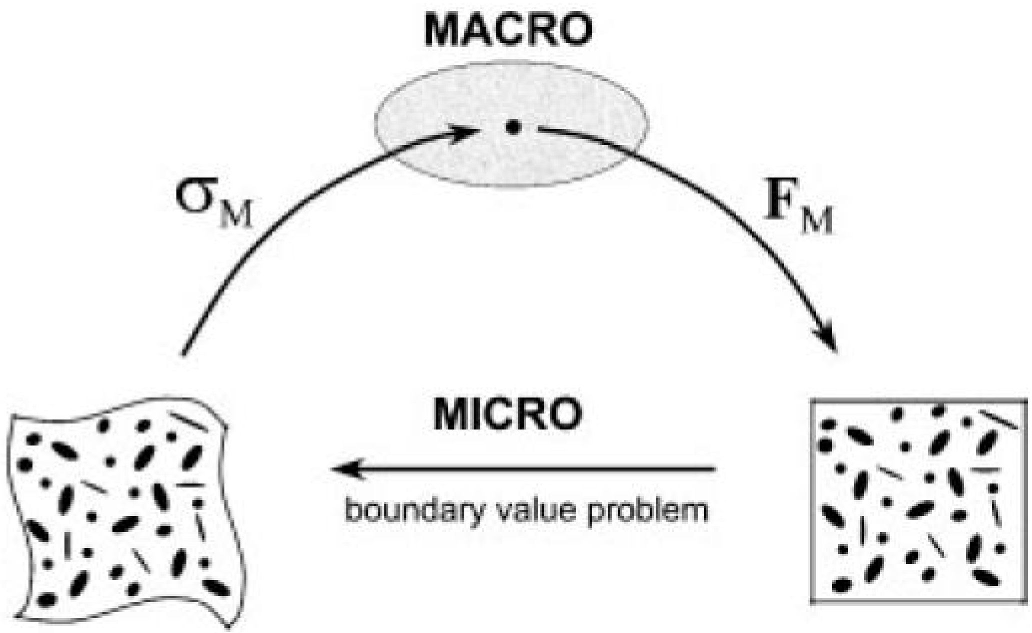

first-order
homogenization scheme

second-order
homogenization scheme

[Forest & Sab, Jasiuk & O-S, Kuznetsova & Geers, Onck …]

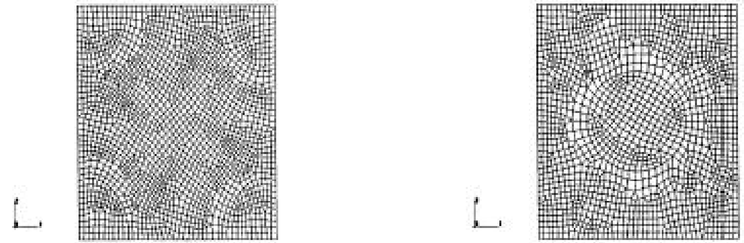

$u_1(\mathbf{x}) = 0, \quad u_2(\mathbf{x}) = \gamma_{22} x_2$

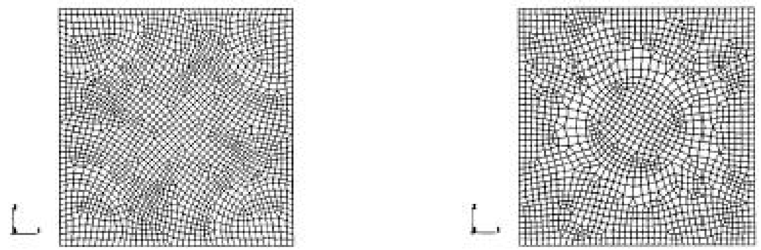

$u_1(\mathbf{x}) = \gamma_{11} x_1, \quad u_2(\mathbf{x}) = \gamma_{22} x_2$

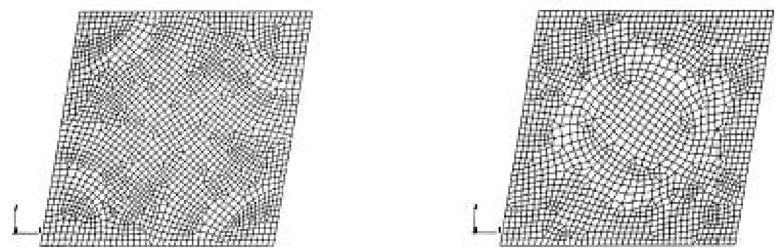

$u_1(\mathbf{x}) = \gamma_{12} x_2, \quad u_2(\mathbf{x}) = 0$

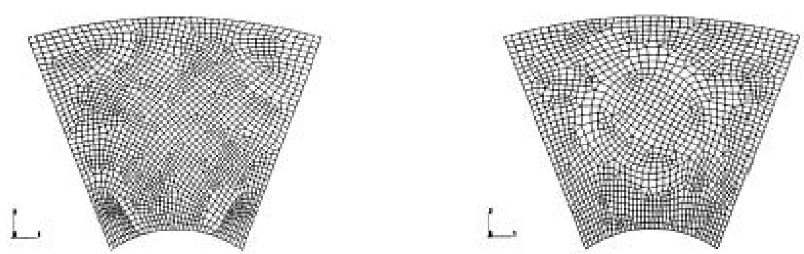

$u_1(\mathbf{x}) = -x_1 x_2 \kappa_{13}, \quad u_2(\mathbf{x}) = \dfrac{{x_1}^2}{2} \kappa_{13}$

- **Convergence to RVE depends on:**
  - Elastic versus inelastic microstructure

    faster slower
  - mismatch in properties
  - 2-D or 3-D
  - microscale geometries (disks *versus* ellipses, spatial clustering…)

- **Convergence to RVE in linear elastic microstructures:**
  - mesoscale moduli of stiff matrix w. soft inclusions converge (much) more slowly to RVE than those of soft matrix w. stiff inclusions
  - convergence to RVE is slowest in anti-plane, faster in in-plane, and fastest in 3-D elasticity

- **In problems w/o separation of scales need to work with random fields and solve stochastic b.v.p. (e.g. via stochastic FE), …**

Microstructural Randomness and Scaling in Mechanics of Materials, Taylor & Francis/CRC Modern Mech. Math. Series, 2007.

Coupled scale and b.c. effects in random media:

linear elasticity:
random: Huet (1990, …), O-S (1989, …), Sab (1992), Terada & Kikuchi (2002),
Forest & Jeulin (2003) …
periodic: Hollister & Kikuchi (1992), Pecullan, Gibiansky & Torquato (1999)
Jiang, Jasiuk & O-S (2002, …) …

nonlinear elasticity: Hazanov (1999), …

viscoelasticity: Huet (1998)

elasto-plasticity: Jiang, O-S & Jasiuk (2001)

rigid-perfect plasticity, elasto-plasticity

thermoelasticity: O-S

elasticity + damage

THANK YOU!

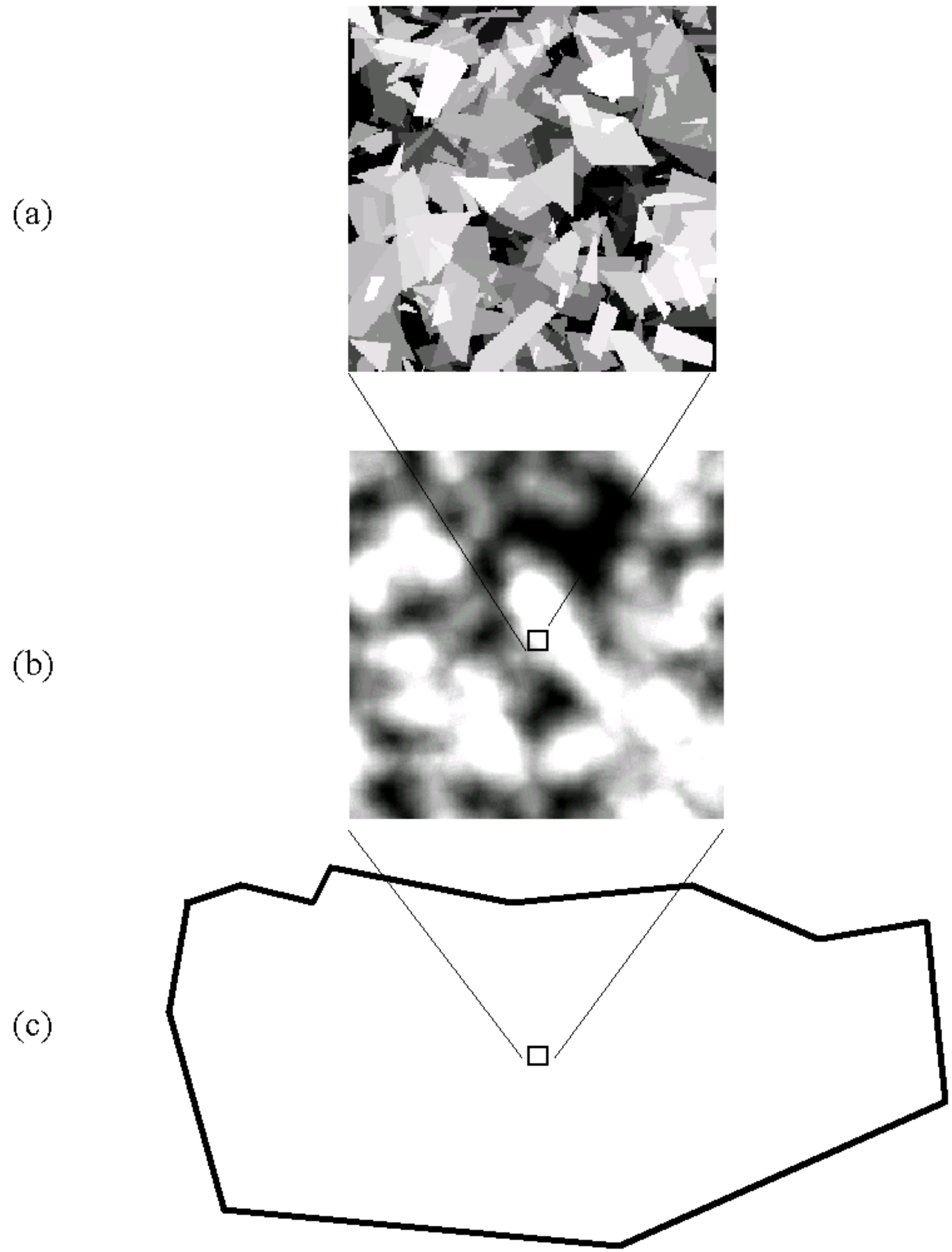

paradigm of inhomogeneous continua: FGM

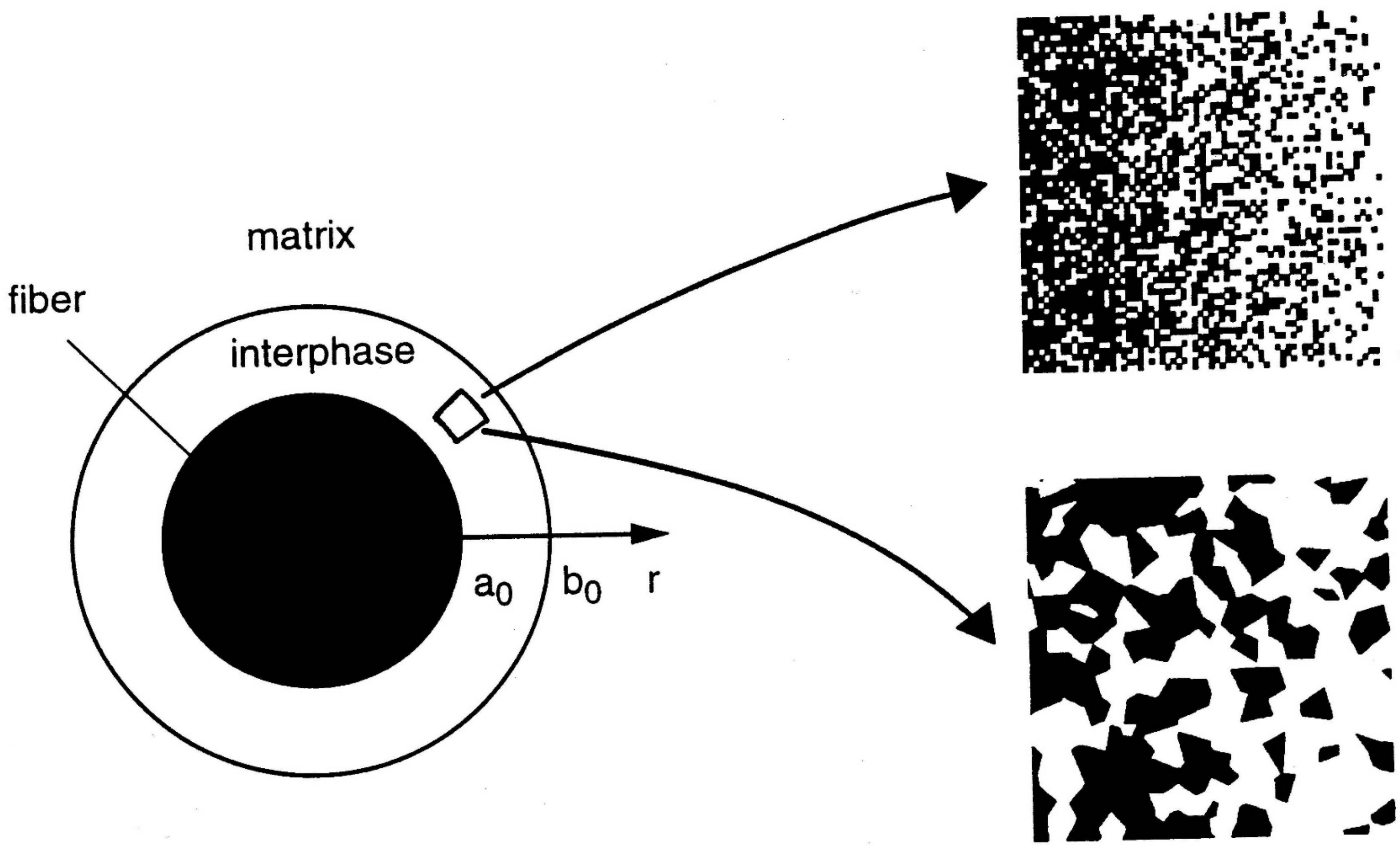

mesoscale property is anisotropic

bounded by Dirichlet and Neumann b.c.'s

[*Acta Mater.*, 1996]

Mesoscale random fields:
as a bridge from micro (nano) to macro scales
as a basis of stochastic finite elements (SFE)

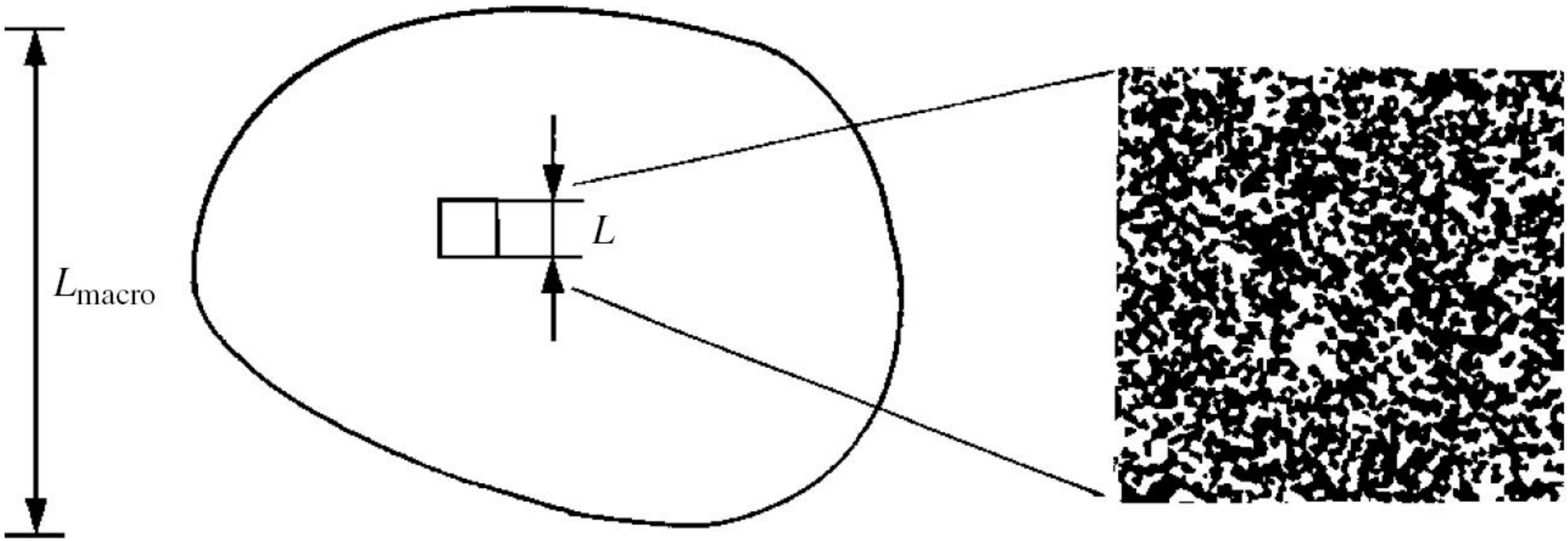

Figure 1. A macroscopic body with a mesoscale window (or finite element) of size L, in which a microstructure of grain size d is shown.

[*CMAME*, 1999; *Proc. Roy Soc. Lond. A*, 1999]

Torsion of a bar
of square cross section with bi-percolating microstructure

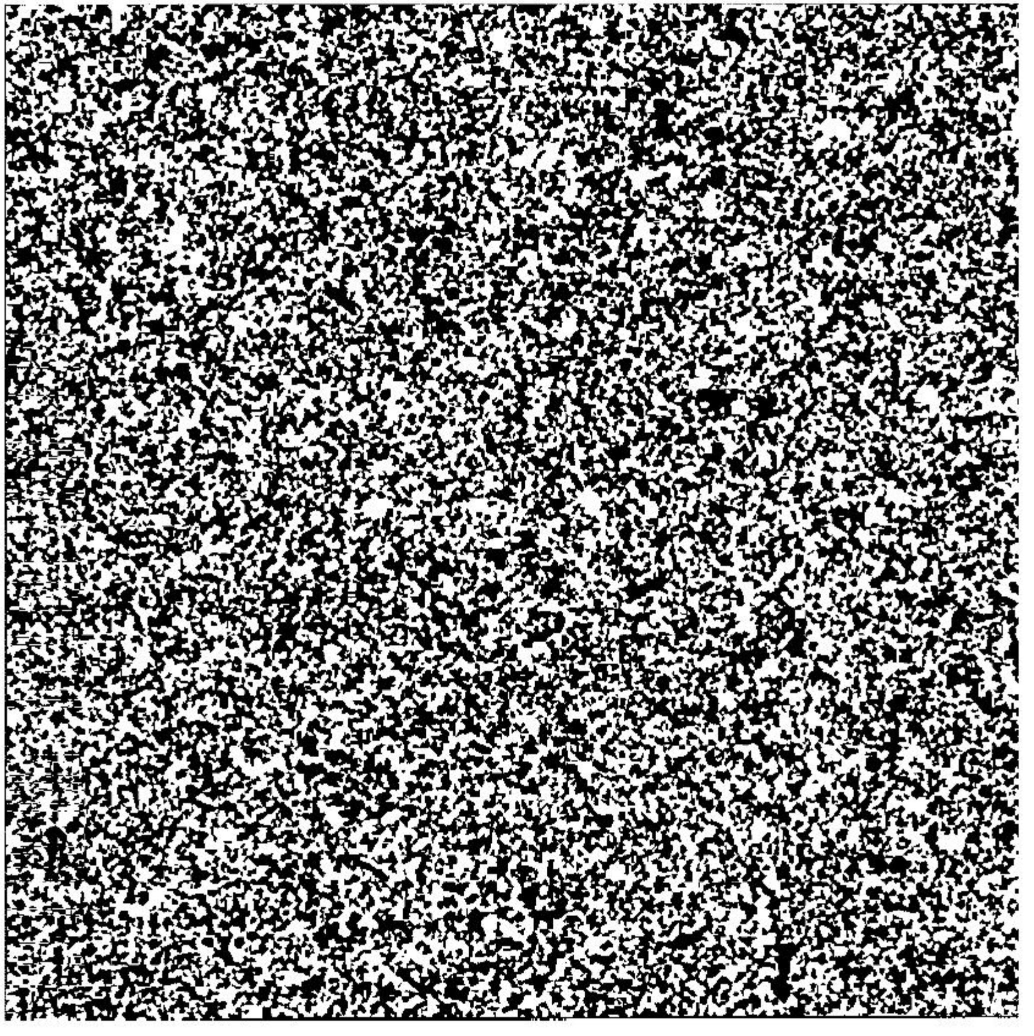

Figure 2. A two-phase material with a Voronoi mosaic microgeometry of a total 104 858 black and white cells, at volume fraction 50% each.

Mesoscale bounds:

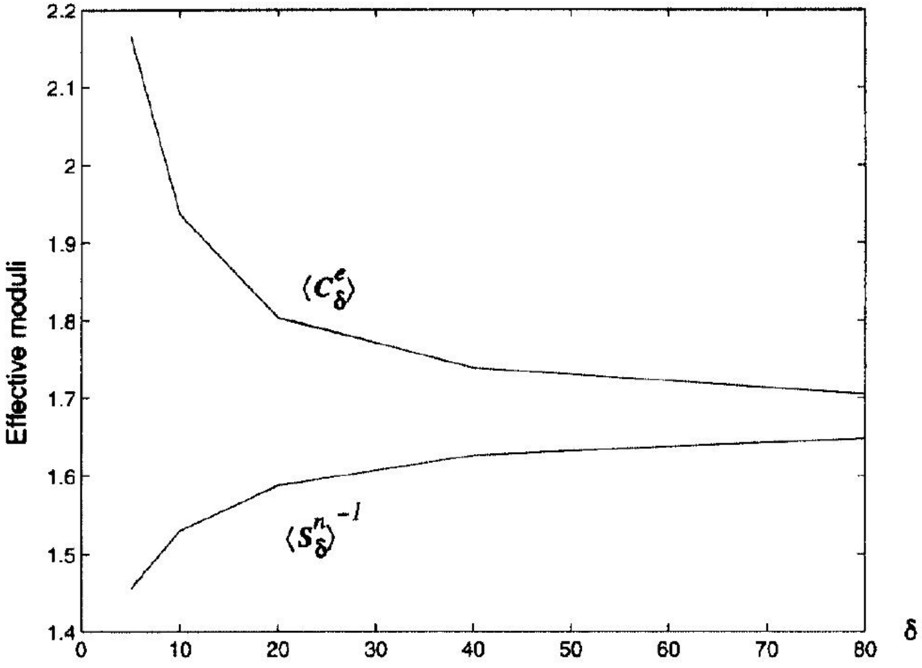

Mesoscale bounds:

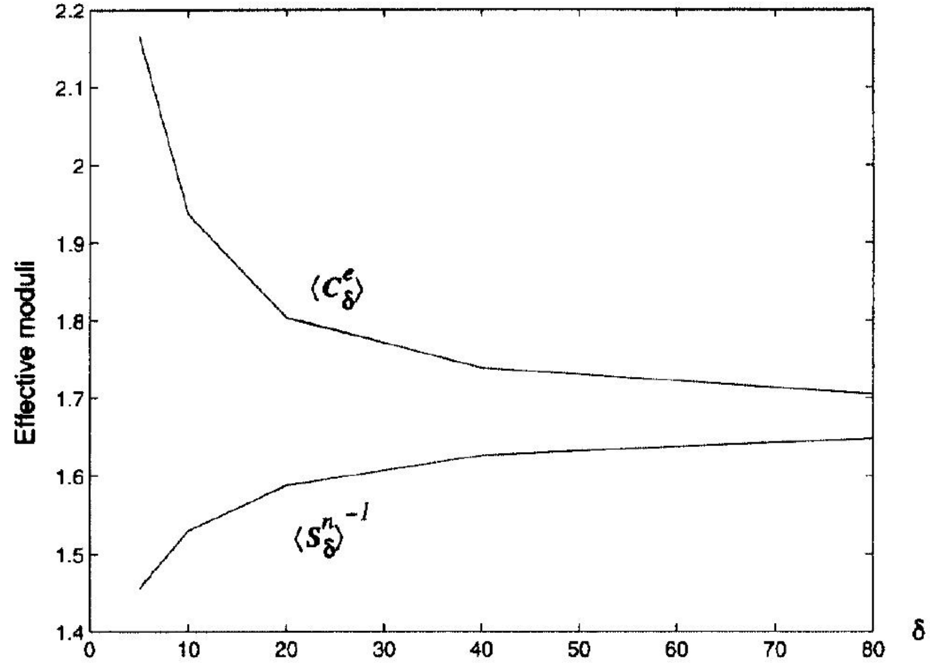

Convergence of torsion solutions
for a homogeneous bar:

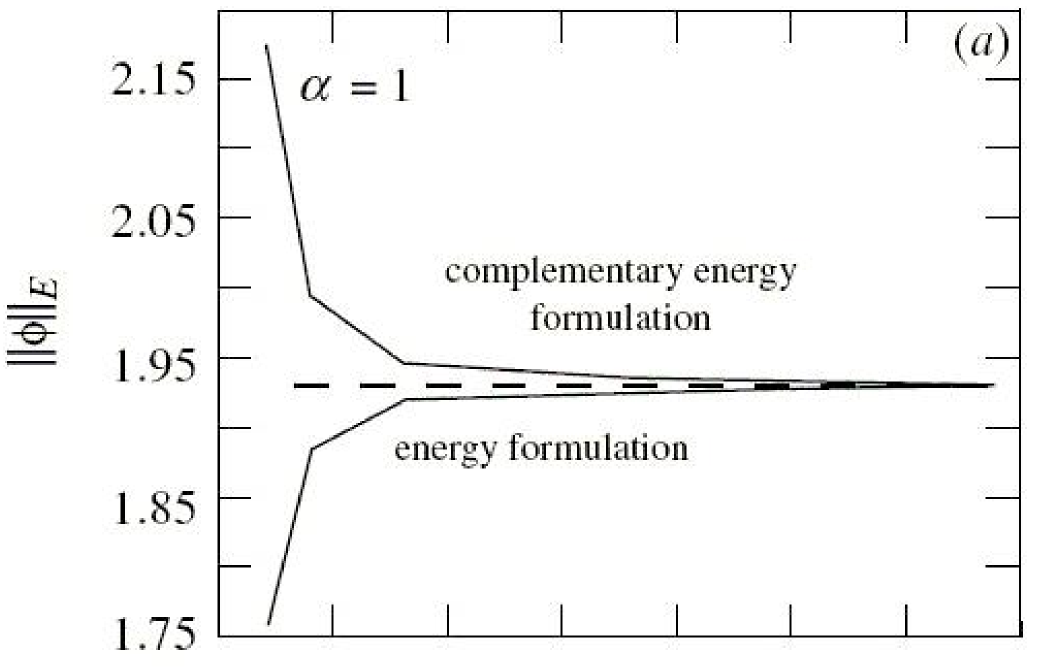

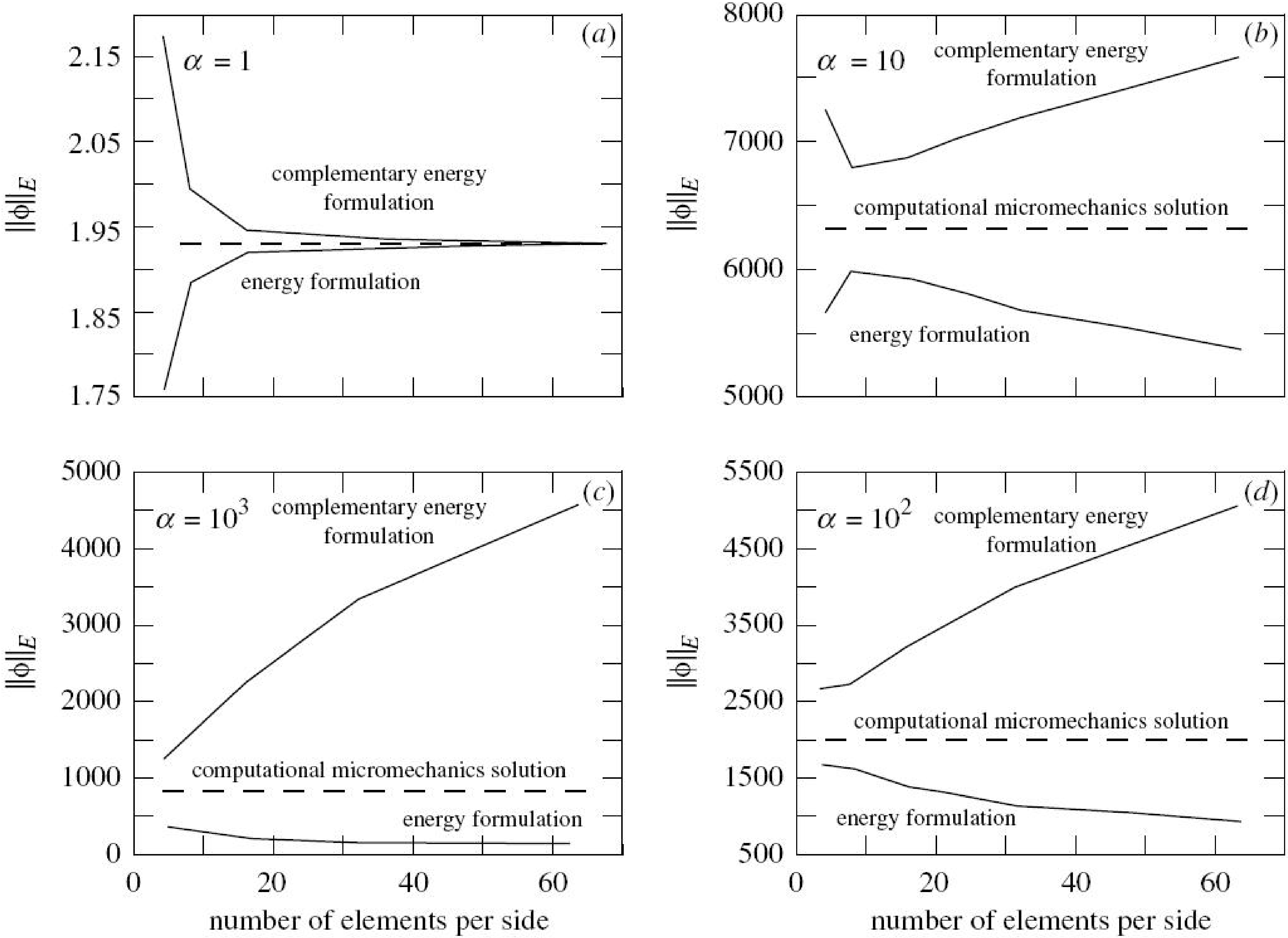

(a)
$\alpha = 1$
complementary energy formulation
energy formulation
2.15
2.05
1.95
1.85
1.75
$\|\phi\|_E$
(b)
$\alpha = 10$
complementary energy formulation
computational micromechanics solution
energy formulation
8000
7000
6000
5000
$\|\phi\|_E$
(c)
$\alpha = 10^3$
complementary energy formulation
computational micromechanics solution
energy formulation
5000
4000
3000
2000
1000
0
$\|\phi\|_E$
0
20
40
60
number of elements per side
(d)
$\alpha = 10^2$
complementary energy formulation
computational micromechanics solution
energy formulation
5500
4500
3500
2500
1500
500
$\|\phi\|_E$
0
20
40
60
number of elements per side

Shape optimization

Optimal truss (Michell, 1904)**:**
a minimum-weight design of a planar truss that transmits a given load to a rigid foundation with axial stresses in all the bars: $-\sigma_0 \leq \sigma \leq \sigma_0$

Solution found by solving a hyperbolic problem

n = # of nodes

$Eff = V/\, V(n)$ ***efficiency***

V = volume of *Michell truss-like continuum*

$V(n)$ = volume of 'finite' truss

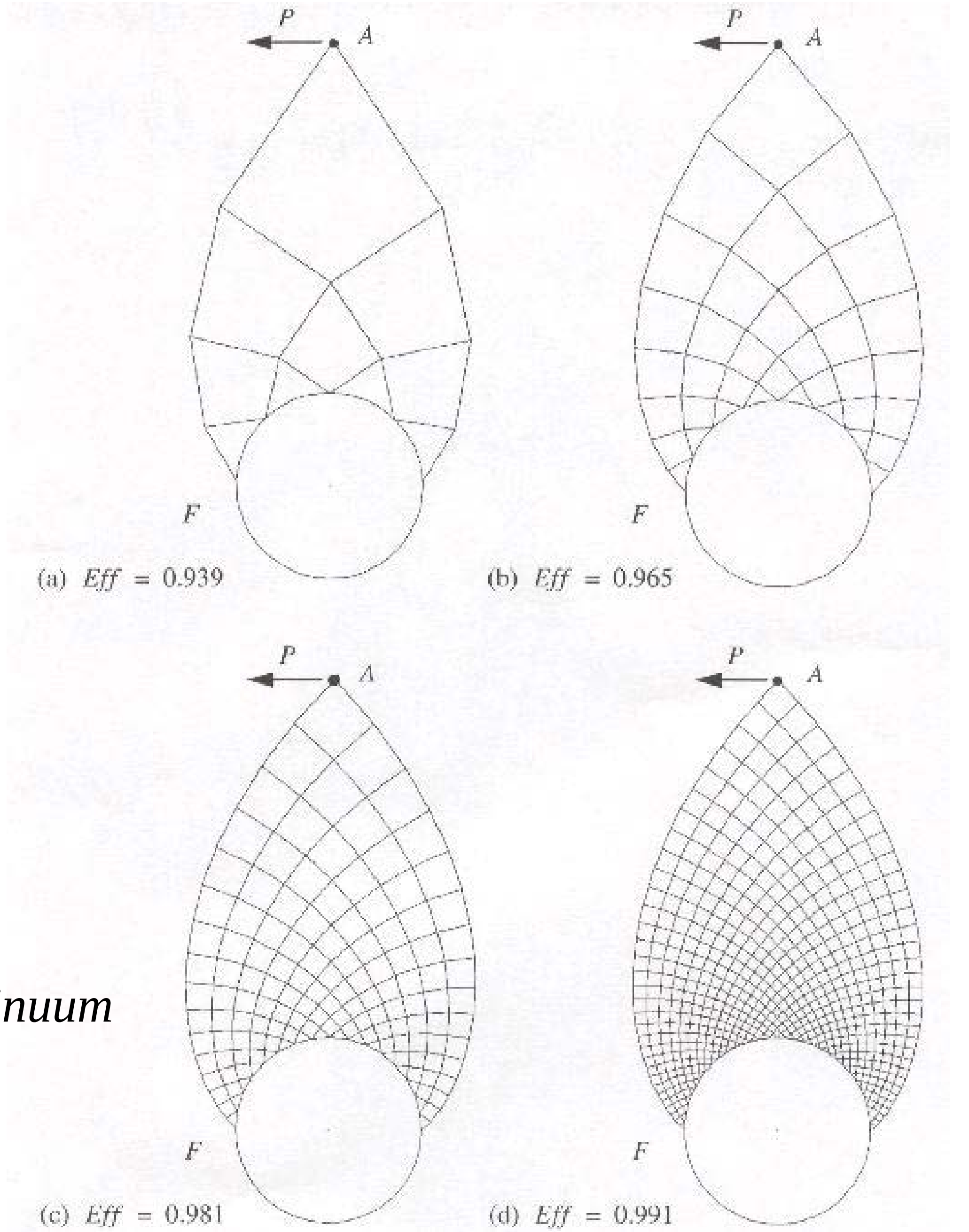

Manufacturing of a truss from a polycrystal

…as the mesh is refined,

random noise in σ_0 grows

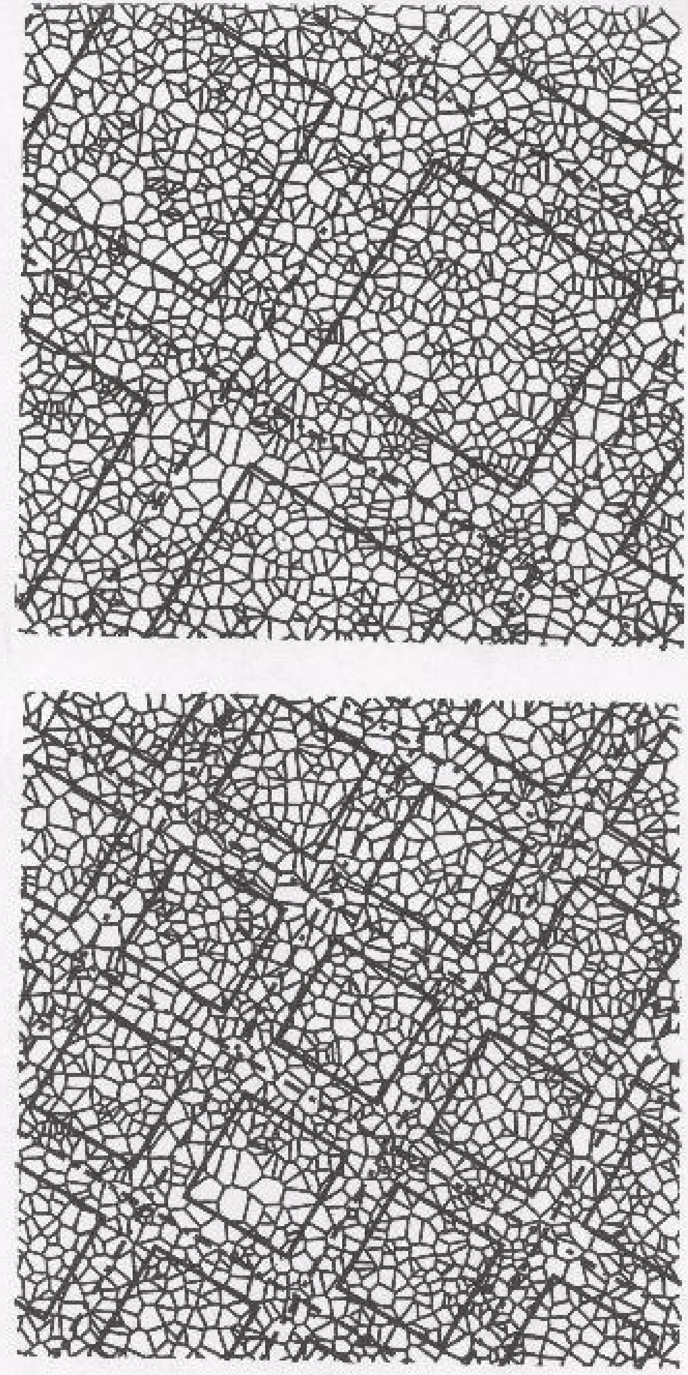
(a)

(b)

Truss made of 'real' material:
a minimum-weight design in
the presence of random strengths σ_0

n = # of nodes

$Eff = V/\,V(n)$

V = volume of Michell truss-like continuum

$V(n)$ = volume of 'finite' truss

As randomness in σ_0 grows,
characteristics get more scattered

… beyond (d), characteristics intersect!

Material spatial randomness
prevents the attainment of $Eff = 1$

[*Proc. Roy. Soc. Lond. A*, 2003]

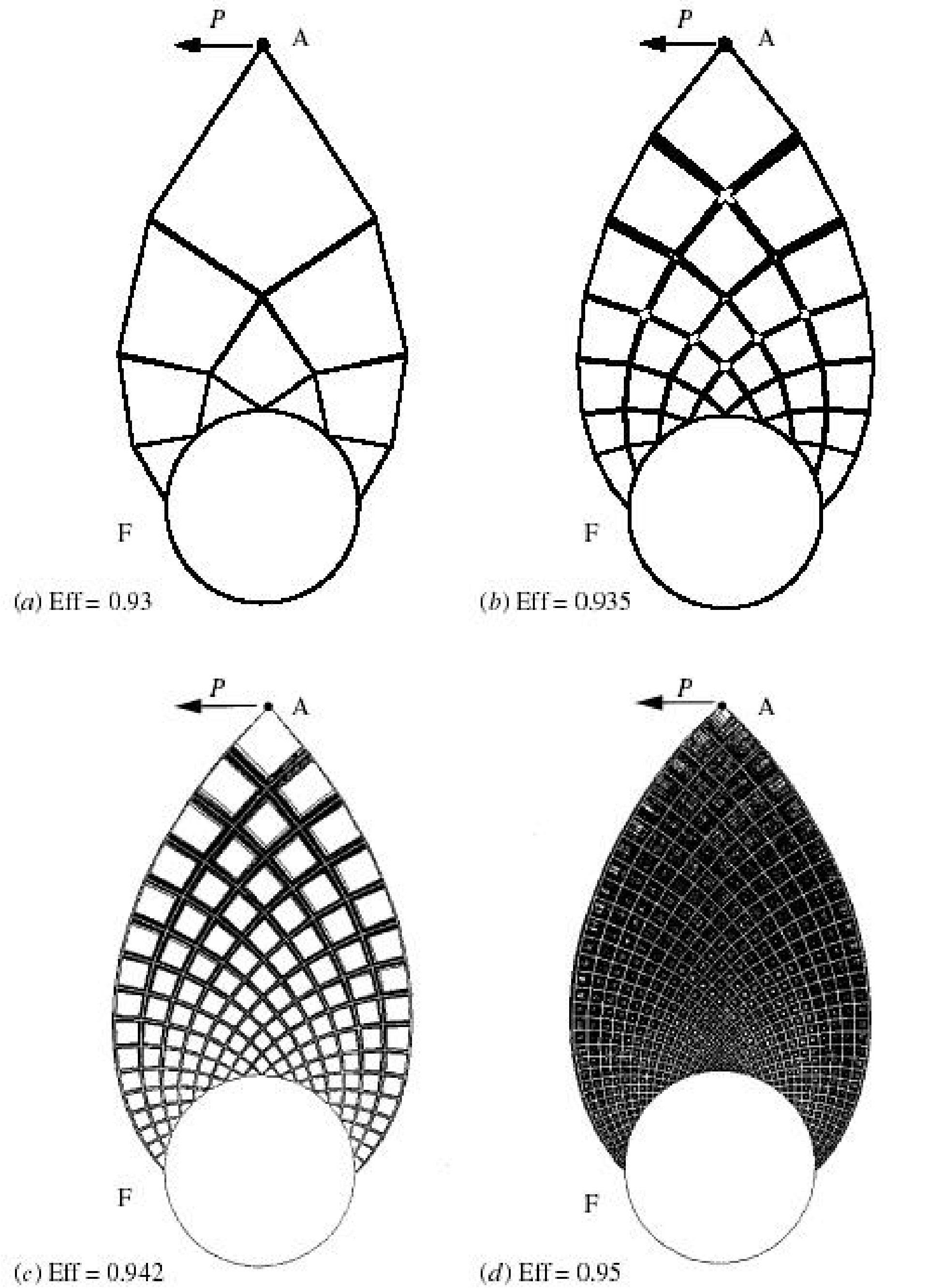

(a) Eff = 0.93 (b) Eff = 0.935 (c) Eff = 0.942 (d) Eff = 0.95

Shape optimization of an elastic structure with minimum compliance, having a prescribed weight

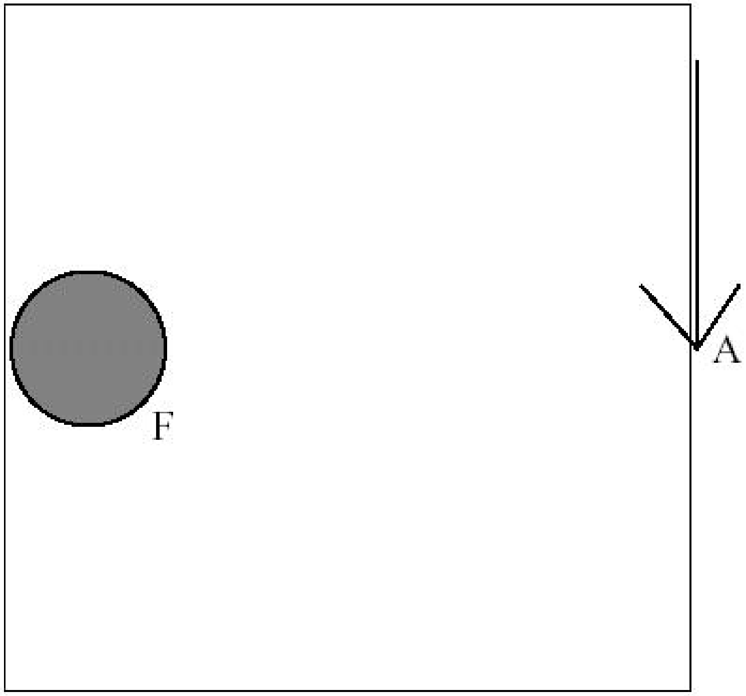

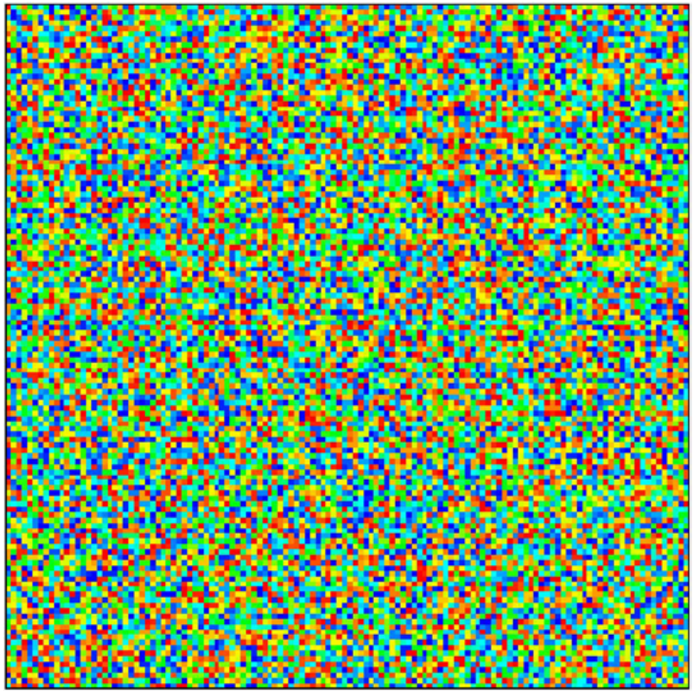

Rigid foundation F

Force applied at A

Material = square mosaic with random stiffnesses:

$$E(\omega) = E + E'(\omega)$$

homogeneous medium case

E = const

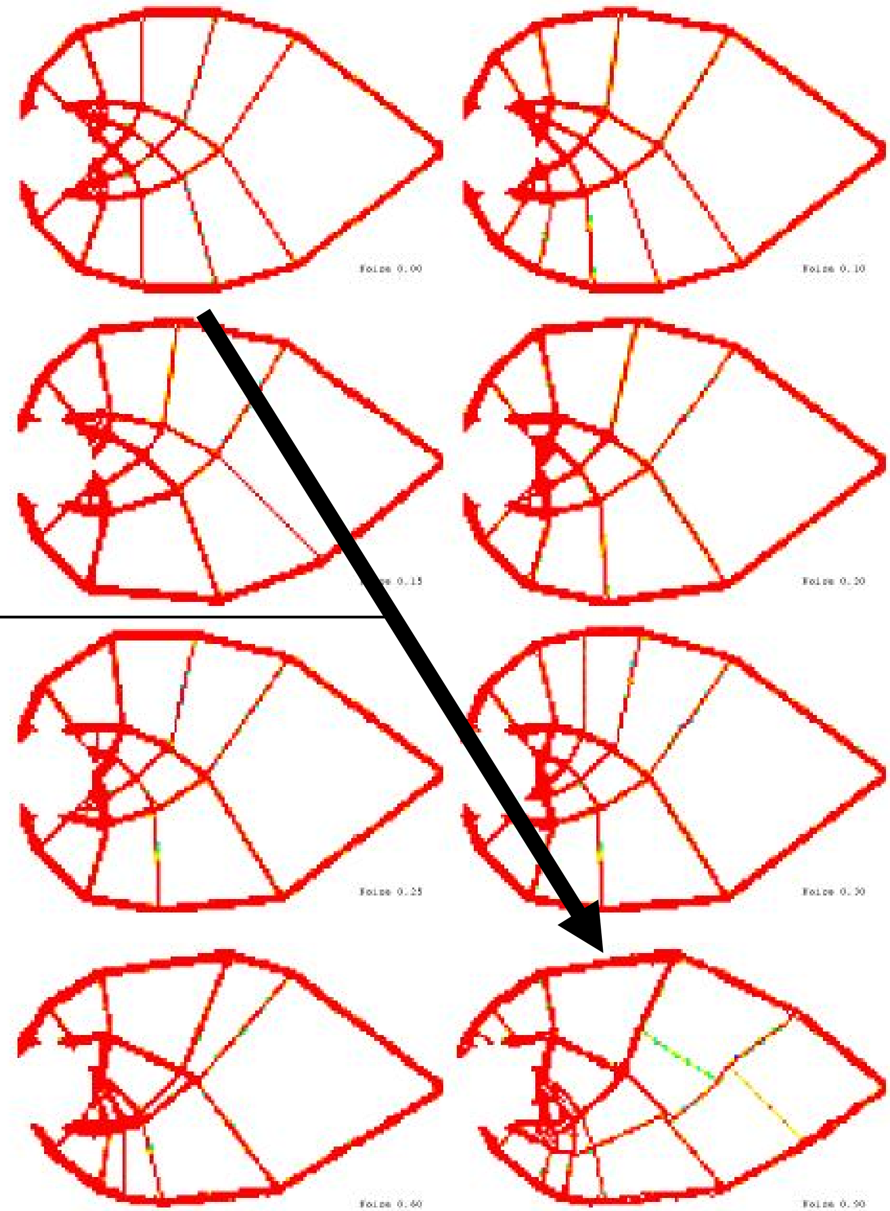

increasing randomness in stiffness

generally, compliance increases

but, for some realizations,

the algorithm may find a lower compliance than in homogeneous medium case

[*Struct. Multidiscipl. Optim.* 2003]

Conclusions

Studies of finite-size-scaling in random media allow assessment of RVE size for:

- linear elasticity and conductivity (thermal, electrical, magnetic,…)
- physically nonlinear elasticity
- viscoelasticity
- elasto-plasticity
- rigid-perfect plasticity
- finite elasticity
- thermoelasticity
- permeability
- …

These issues are critical where separation of scales is missing

- in micro- and nano-structured materials
- biological systems
- geophysical problems
- …

Many complex microstructures may be modeled via mathematical morphology

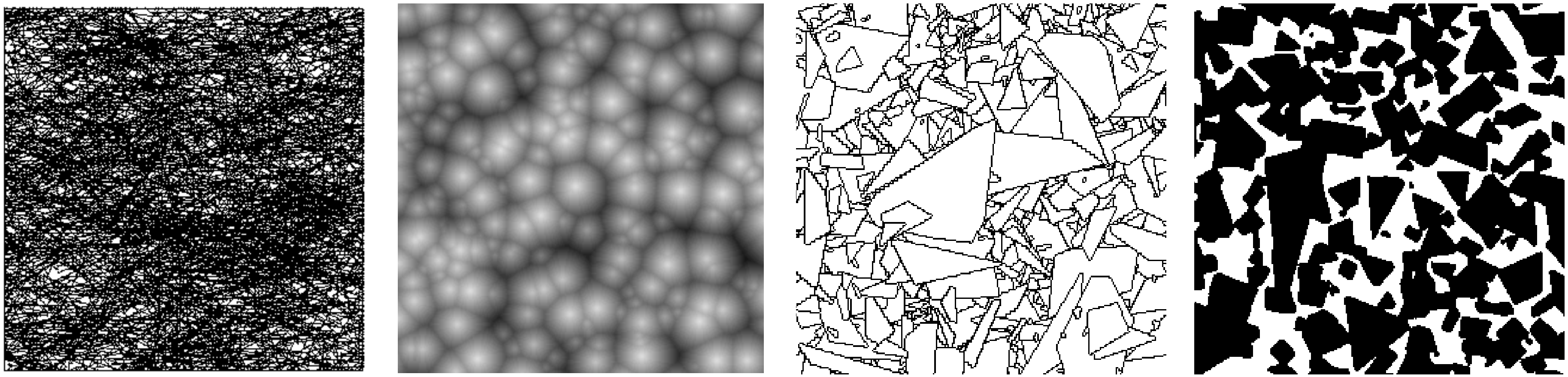

(a) (b) (c) (d)

(a) germ-grain fiber model (… fiber structures)

(b) hard-core Boolean random function (… cellular/biological tissues)

(c) dead leaves random tessellation of Poisson polygons

(… randomly micro-layered systems)

(d) Boolean model of Poisson polygons

(… tungsten-carbide [black] and cobalt [white])

THANK YOU!

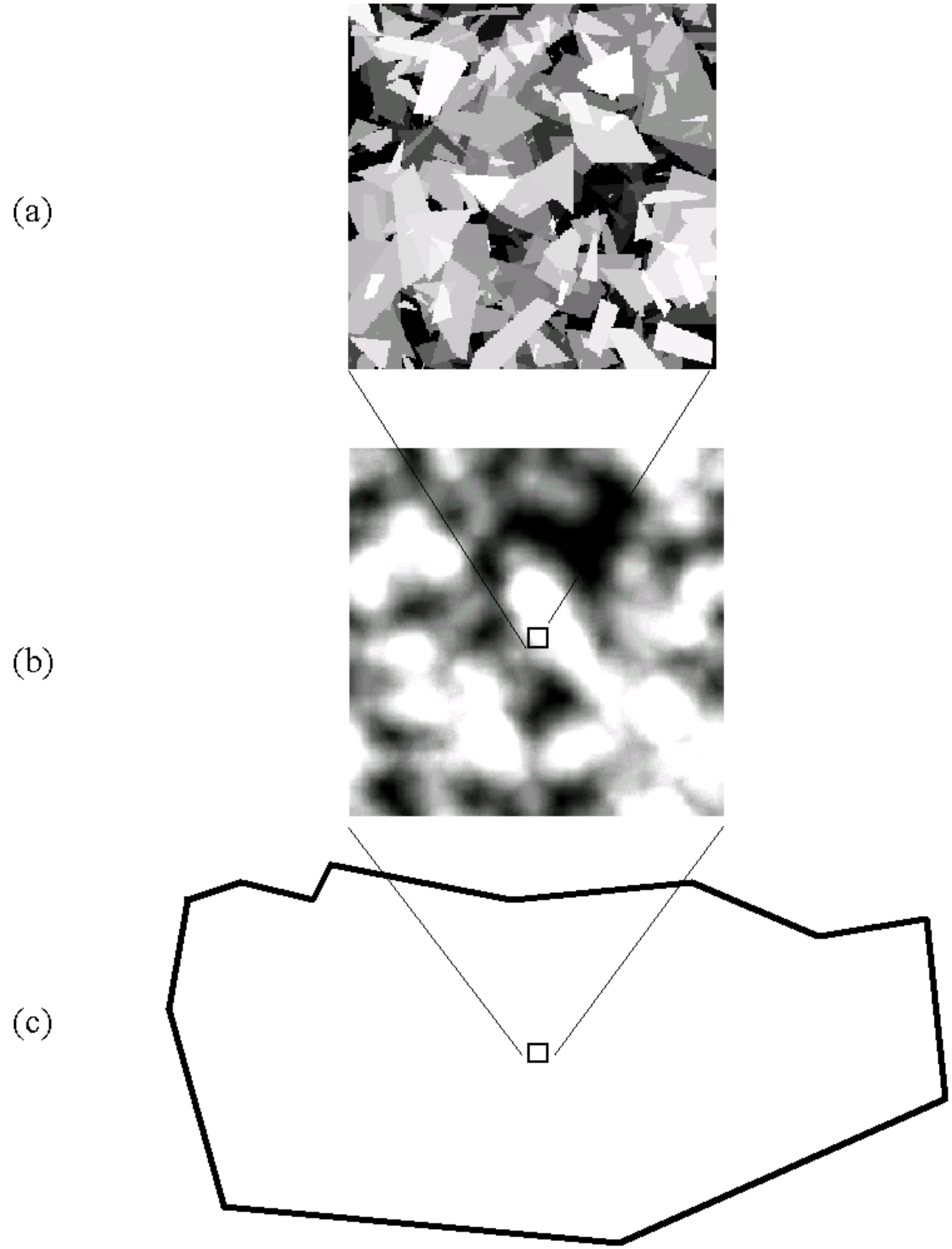

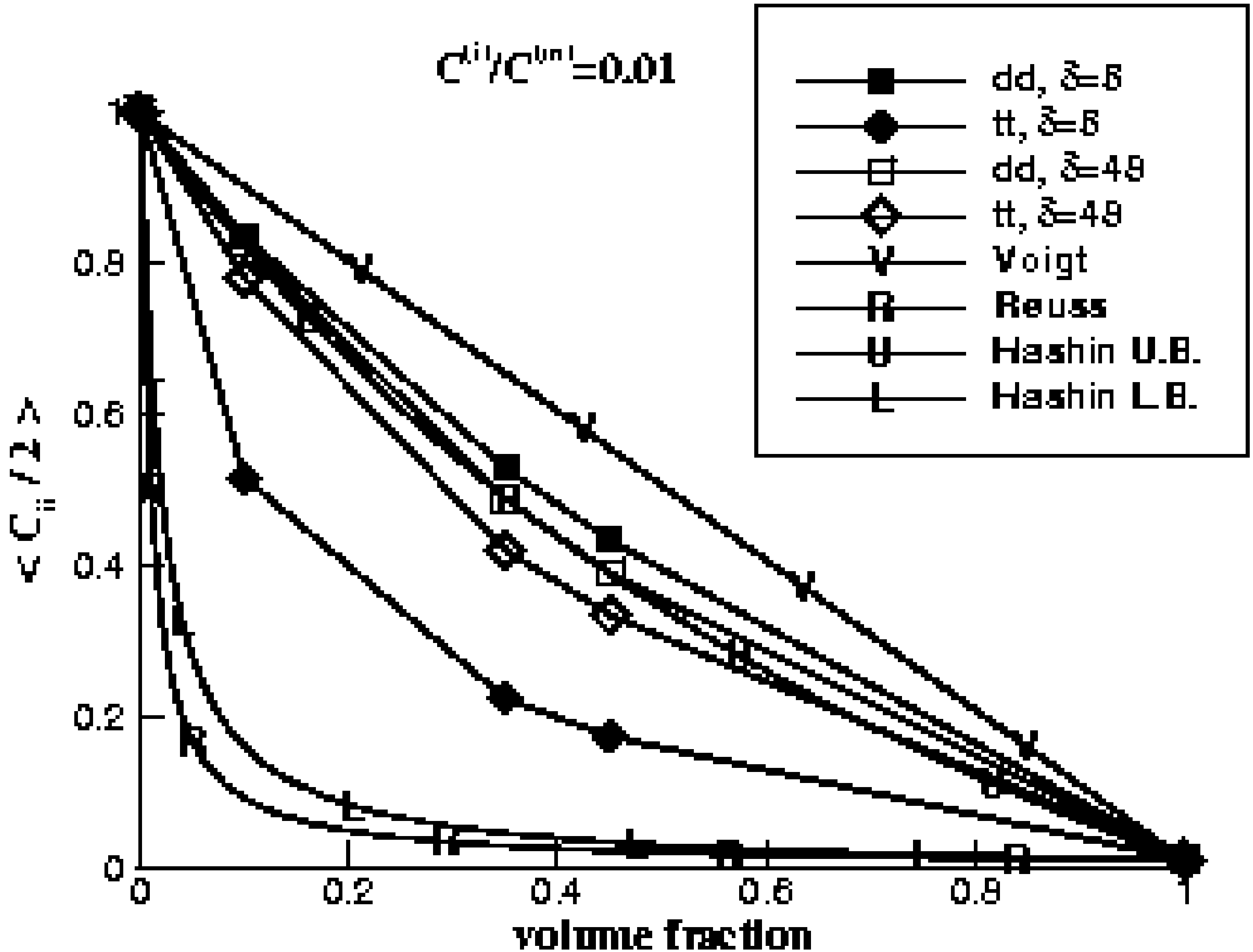

C(i)/C(m)=0.01
dd, δ=6
tt, δ=6
dd, δ=49
tt, δ=49
Voigt
Reuss
Hashin U.B.
Hashin L.B.
< C_ii / 2 >
0
0.2
0.4
0.6
0.8
1
volume fraction

Mesoscale Bounds for Random Media - Inelastic

Martin Ostoja-Starzewski
Department of Mechanical Science & Engineering
also Institute for Condensed Matter Theory, and Beckman Institute
University of Illinois at Urbana-Champaign

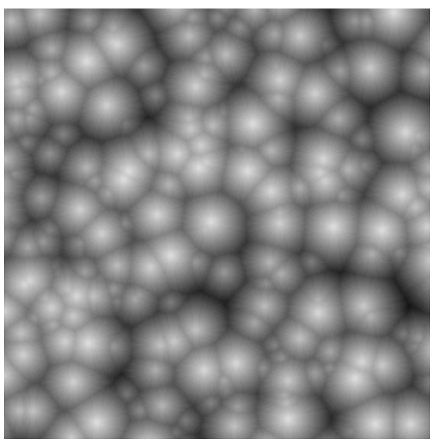

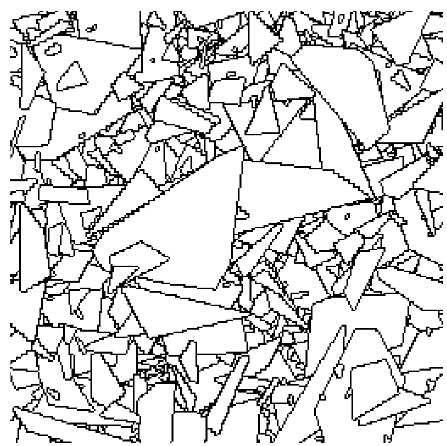

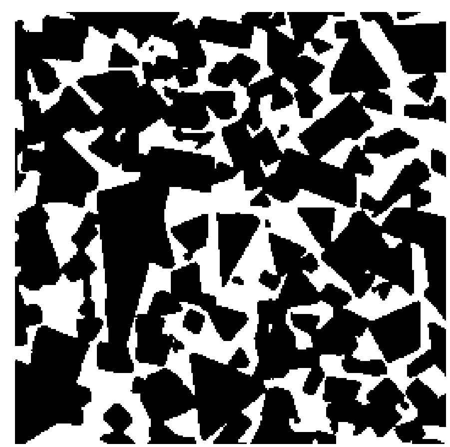

Elasto-plastic random composite

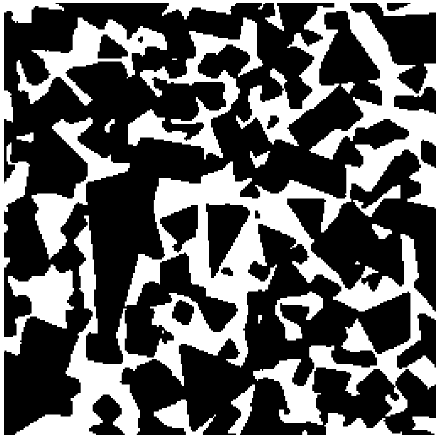 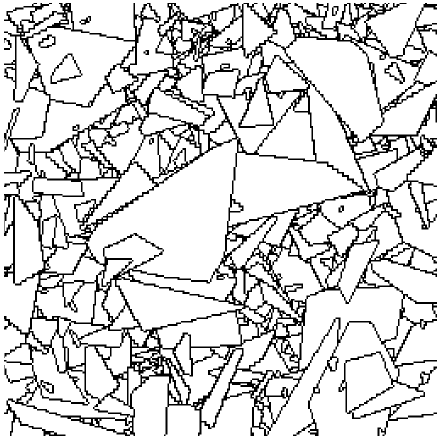 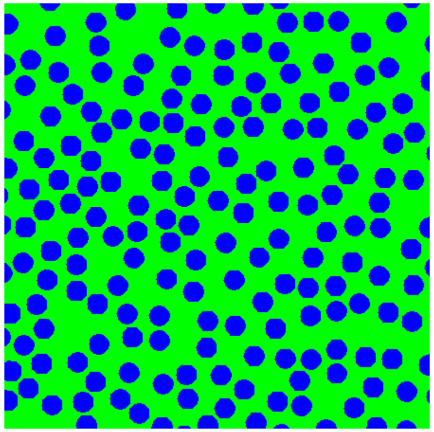

Mesoscale (apparent) **elasto-plastic response**,
under proportional monotonic loading,
can be treated within the framework of deformation theory

… formally equivalent to **physically nonlinear**,
small-deformation elasticity theory.

Minimum potential energy principle

$$\Pi(\tilde{\varepsilon}) = \int w(\tilde{\varepsilon}_{ij})dV - \int_{\partial B_\delta^t} t_i u_i dS$$

because $$\partial B_\delta = \partial B_\delta^d, \quad \partial B_\delta^t = \phi$$

we have $$W(\omega;\varepsilon^0) \leq W^r(\omega;\varepsilon^0)$$

$$W(\omega;\varepsilon^0) = \int w dV, \qquad W^r(\omega;\varepsilon^0) = \int w^r dV$$

$$W(\varepsilon^0,\Delta) \le W(\varepsilon^0,\delta) \le W(\varepsilon^0,\delta') \le W(\varepsilon^0,1) \equiv W^V$$

$$w(\varepsilon^0,\Delta) \le w(\varepsilon^0,\delta) \le w(\varepsilon^0,\delta') \le w(\varepsilon^0,1) \equiv w^V$$

$$\delta' < \delta < \Delta$$

Minimum complementary energy principle

$$\Pi^*(\tilde{\sigma}) = \int w^*(\tilde{\sigma})dV - \int_{\partial B_\delta^d} t_i u_i dS$$

because $\partial B_\delta = \partial B_\delta^t \qquad \partial B_\delta^d = \phi$

we have

$$W^*(\omega;\sigma^0) \leq W^{*r}(\omega;\sigma^0)$$

$$W^*(\omega;\sigma^0) = \int w^* dV, \qquad W^{*r}(\omega;\sigma^0) = \int w^{*r} dV$$

$$W^{*}(\sigma^{0},\Delta)\leq W^{*}(\sigma^{0},\delta)\leq W^{*}(\sigma^{0},\delta')\leq W^{*}(\sigma^{0},1)\equiv W^{*R}$$

$$w(\varepsilon^{0},\Delta)\leq w(\varepsilon^{0},\delta)\leq w(\varepsilon^{0},\delta')\leq w(\varepsilon^{0},1)\equiv w^{V}$$

$$w^{eff}=w(\varepsilon^{0},\Delta)\leq\langle w(\varepsilon^{0},\delta)\rangle\leq\langle w(\varepsilon^{0},\delta')\rangle\leq\langle w(\varepsilon^{0},1)\rangle\equiv w^{V}$$

$$w^{*eff}=w^{*}(\sigma^{0},\Delta)\leq\langle w^{*}(\sigma^{0},\delta)\rangle\leq\langle w^{*}(\sigma^{0},\delta')\rangle\leq\langle w^{*}(\sigma^{0},1)\rangle\equiv w^{*R}$$

$$\delta'<\delta<\Delta$$

Thermal expansion of random composites

$$\varepsilon_{ij} = S_{ijkl}(\omega, x)\sigma_{kl} + \alpha_{ij}(\omega, x)\theta$$

$$\Gamma_{ij} = -C_{ijkl}\alpha_{kl}$$

$$\sigma_{ij} = C_{ijkl}(\omega, x)\varepsilon_{kl} + \Gamma_{ij}(\omega, x)\theta$$

$$U = \frac{1}{V}\int_V A dV - \int_V F_i u_i dV - \int_{St} t_i u_i dS$$

$$A = \frac{1}{2}C_{ijkl}\varepsilon_{ij}\varepsilon_{kl} - \Gamma_{ij}\varepsilon_{ij}\theta - \frac{1}{2}c_v\frac{\theta^2}{T}$$

$$U^* = -\frac{1}{V}\left(\int_V G dv + \int_{Su} t_i u_i ds\right)$$

$$G = -\frac{1}{2}S_{ijkl}\sigma_{ij}\sigma_{kl} - \alpha_{ij}\sigma_{ij}\theta - \frac{1}{2}c_p\frac{\theta^2}{T}$$

Elementary bounds

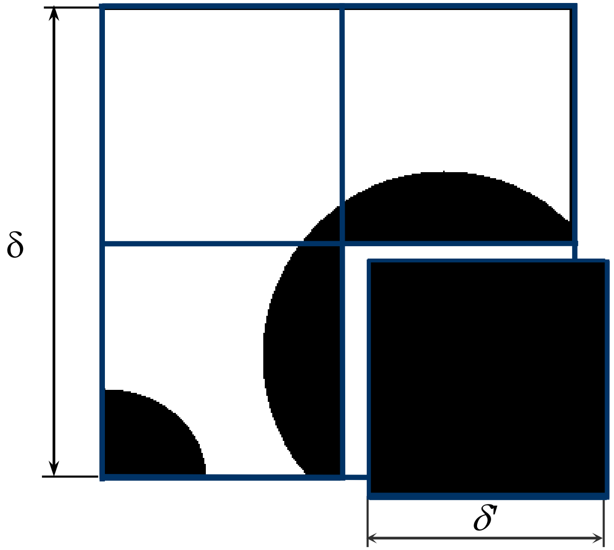

Voigt upper bound:

$$\Psi_V(\overline{\mathbf{F}}) \geq \Psi_\delta^d$$

$$\Psi_V = c_1\Psi_1 + c_2\Psi_2$$

$$\mu_V = 0.35\mu_{Neo-hookean} + 0.65\mu_{Ogden}$$

Reuss lower bound:

$$\Psi_R^*(\overline{\mathbf{P}}) \geq \Psi_\delta^{*t}$$

$$\mu_R = ?$$

$$\delta = \frac{L}{d} = 2$$

$$\delta = \frac{L}{d} = 16$$

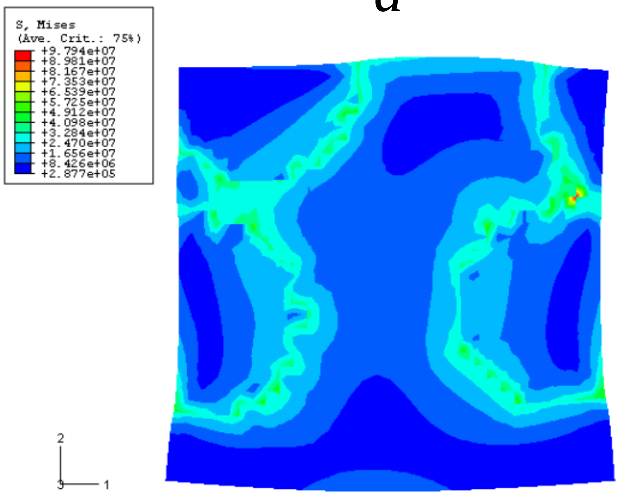

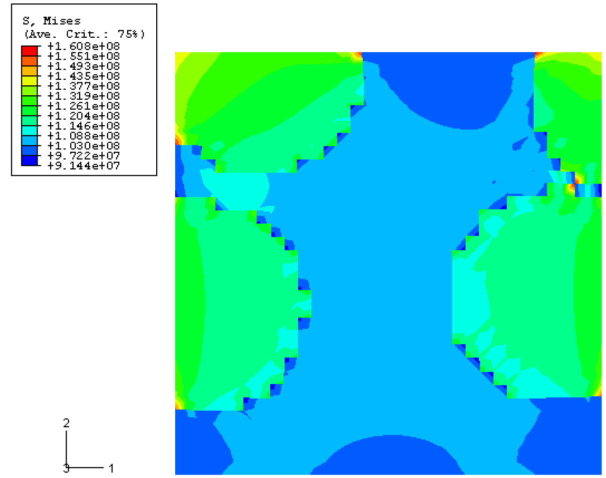

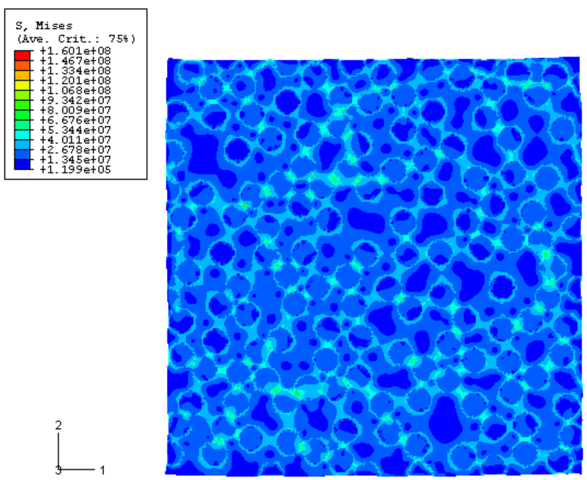

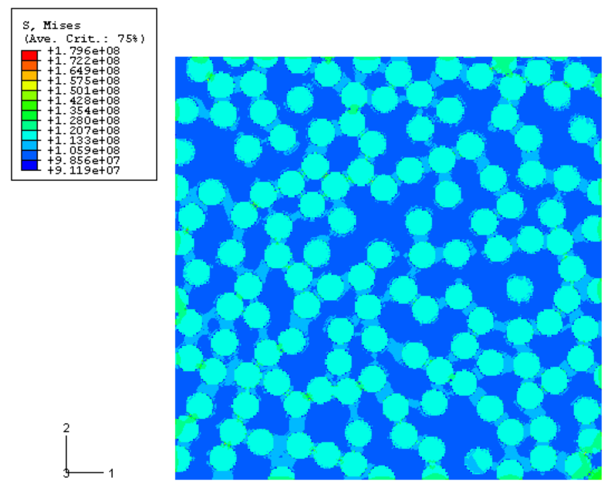

Neumann b.c.

Dirichlet b.c.

Energy Bounds

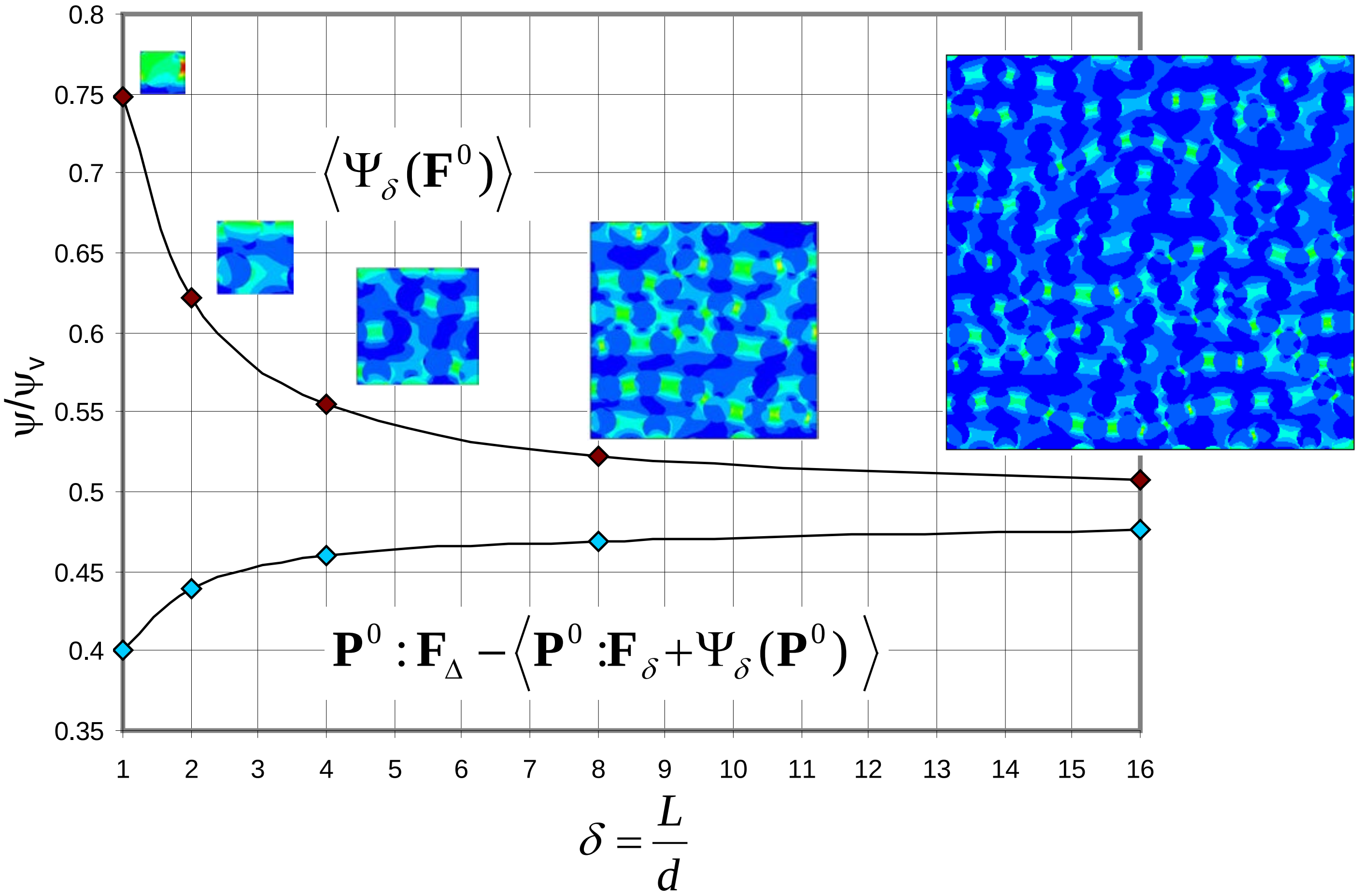

$$\Gamma_{ij}^{eff} \geq \cdots \geq \left\langle \Gamma_{ij} \right\rangle_{4\delta}^{d} \geq \left\langle \Gamma_{ij} \right\rangle_{2\delta}^{d} \geq \left\langle \Gamma_{ij} \right\rangle_{\delta}^{d} \geq \left\langle \Gamma_{ij} \right\rangle_{1}^{d}$$

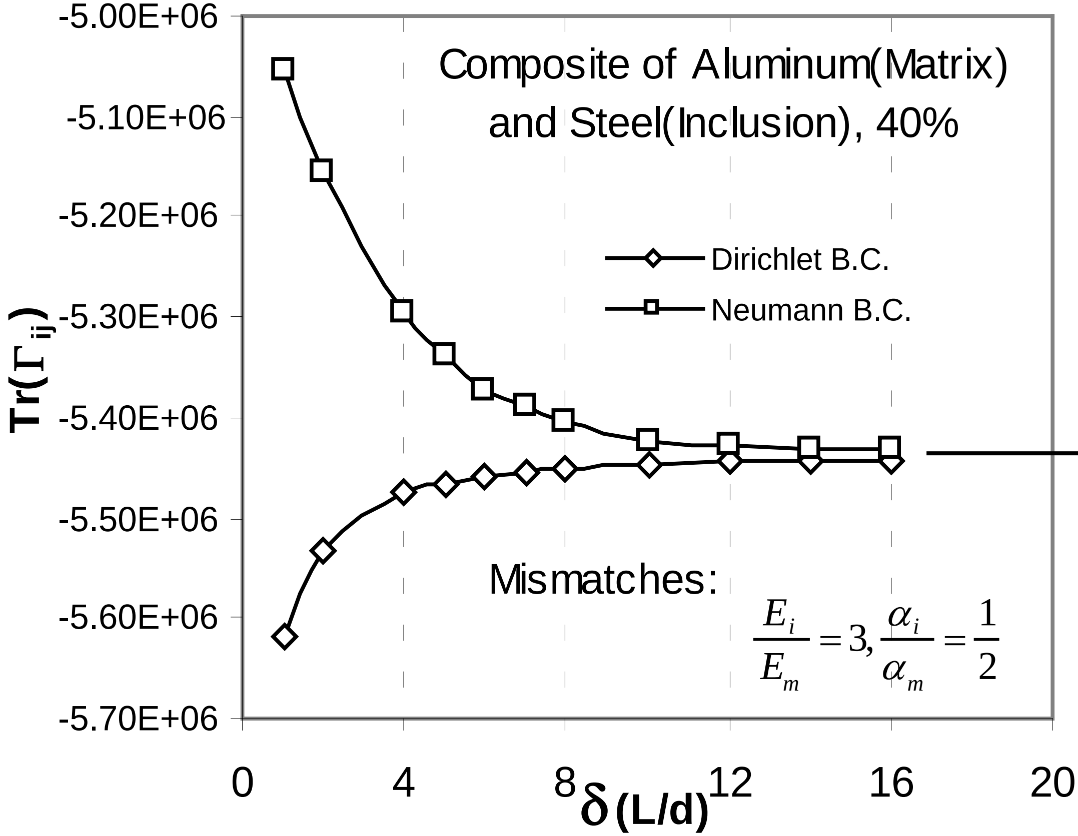

$$\Gamma_{ij}^{eff} = -C_{ijkl}^{eff} \alpha_{kl}^{eff}$$

$$\alpha_{ij}^{eff} \leq \cdots \leq \left\langle \alpha_{ij} \right\rangle_{4\delta}^{n} \leq \left\langle \alpha_{ij} \right\rangle_{2\delta}^{n} \leq \left\langle \alpha_{ij} \right\rangle_{\delta}^{n} \leq \left\langle \alpha_{ij} \right\rangle_{1}^{n}$$

[*Networks & Heterogeneous Media*, 2006]

Mixed Boundary Conditions

$$\Psi_{\delta}^{d} \geq \Psi_{\delta}^{m}$$

$$\Psi_{\delta}^{*t} \geq \Psi_{\delta}^{*m}$$

1st type

$$\begin{bmatrix} F_{11}^{0} & F_{12}^{0} = 0 \\ P_{21}^{0} = 0 & P_{22}^{0} = 0 \end{bmatrix}$$

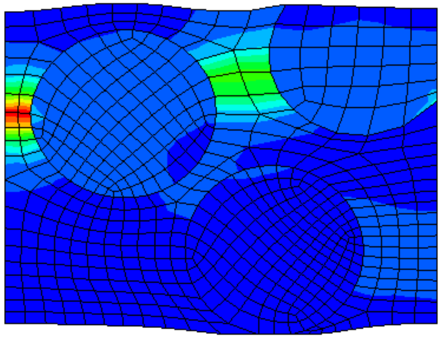

2nd type

$$\begin{bmatrix} F_{11}^{0} & P_{12}^{0} = 0 \\ P_{21}^{0} = 0 & F_{22}^{0} \end{bmatrix}$$

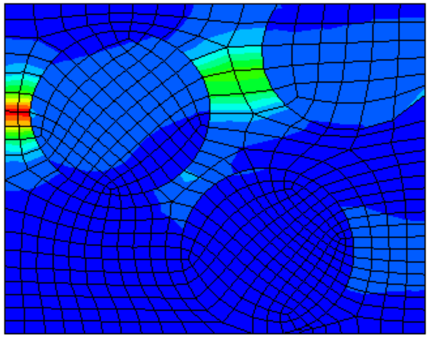

Energy Bounds – Uniaxial Tension

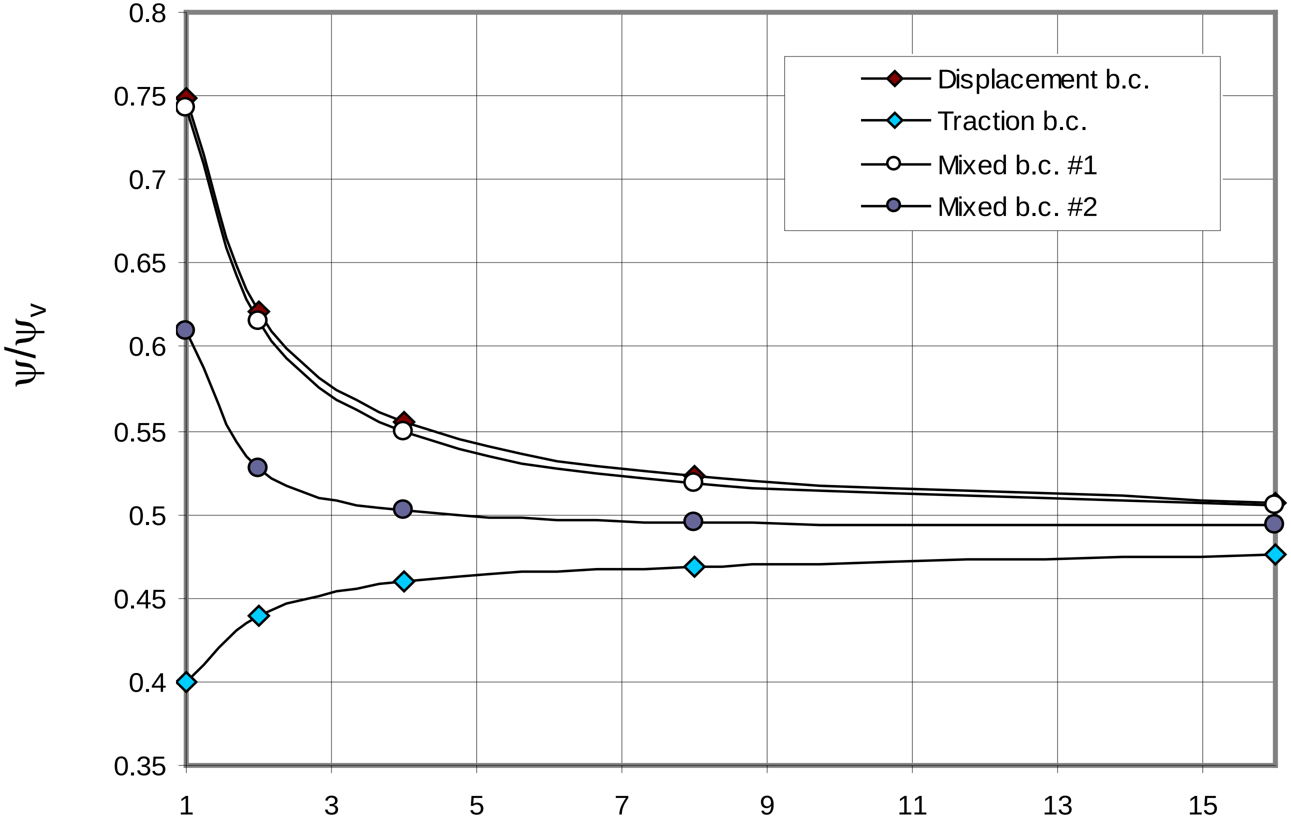

$$\delta = \frac{L}{d}$$

[Scaling function, anisotropy and the size of RVE in elastic random polycrystals, *J. Mech. Phys. Solids* 2008]

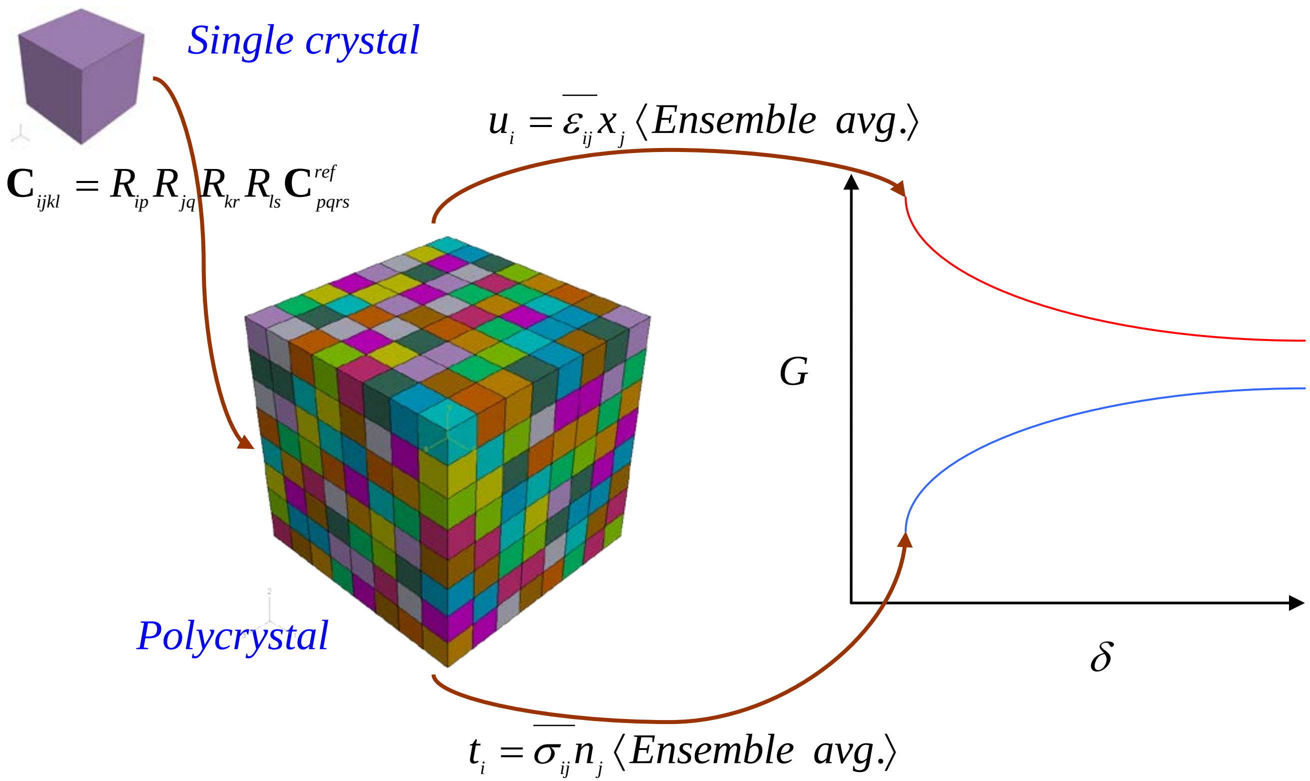

[Scaling function, anisotropy and the size of RVE in elastic random polycrystals, *J. Mech. Phys. Solids* 2008]

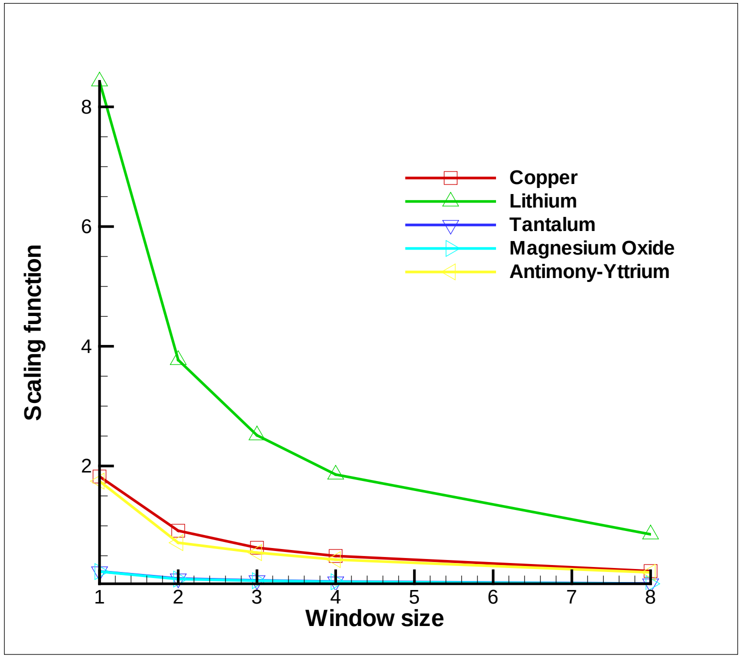

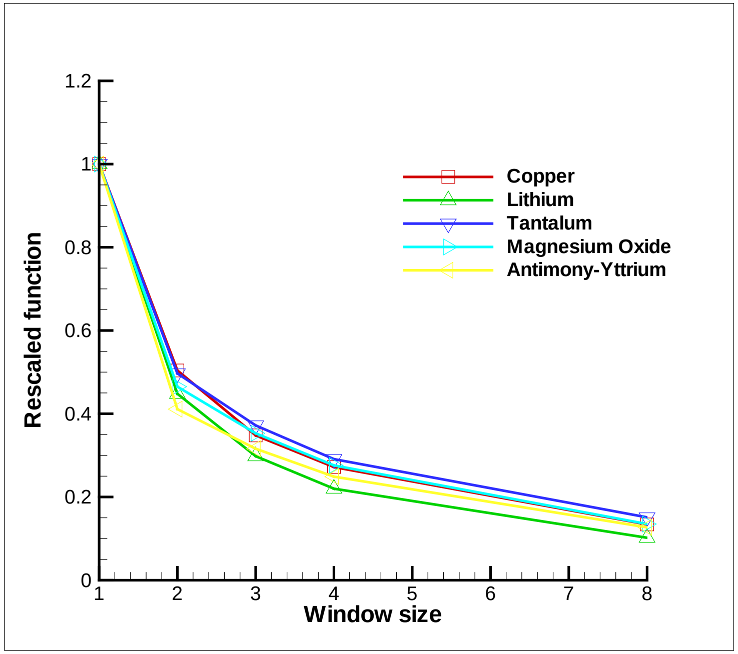

[Scaling function, anisotropy and the size of RVE in elastic random polycrystals, *J. Mech. Phys. Solids* 2008]

$$\left\langle \mathbf{C}_\delta^d \right\rangle = 2\left\langle G_\delta^d \right\rangle \mathbf{K} + 3\left\langle K_\delta^d \right\rangle \mathbf{J}$$

$$\left\langle \mathbf{S}_\delta^t \right\rangle = \frac{1}{2\left\langle G_\delta^t \right\rangle}\mathbf{K} + \frac{1}{3\left\langle K_\delta^t \right\rangle}\mathbf{J} \qquad \Rightarrow \qquad \left\langle \mathbf{C}_\delta^d \right\rangle : \left\langle \mathbf{S}_\delta^t \right\rangle = 5\frac{\left\langle G_\delta^d \right\rangle}{\left\langle G_\delta^t \right\rangle} + \frac{\left\langle K_\delta^d \right\rangle}{\left\langle K_\delta^t \right\rangle}$$

$$\Rightarrow \quad \lim_{\delta\to\infty} \left\langle \mathbf{C}_\delta^d \right\rangle : \left\langle \mathbf{S}_\delta^t \right\rangle = 6 \qquad \left\langle \mathbf{C}_\delta^d \right\rangle : \left\langle \mathbf{S}_\delta^t \right\rangle = \lim_{\delta\to\infty} \left\langle \mathbf{C}_\delta^d \right\rangle : \left\langle \mathbf{S}_\delta^t \right\rangle + f\left(C_{11}, C_{12}, A, \delta\right)$$

$$\Rightarrow \quad f\left(C_{11}, C_{12}, A, \delta\right) = 5\frac{\left\langle G_\delta^d \right\rangle}{\left\langle G_\delta^t \right\rangle} + \frac{\left\langle K_\delta^d \right\rangle}{\left\langle K_\delta^t \right\rangle} - 6$$

$$f\left(A, \delta\right) = \frac{6}{5}\left(\sqrt{A} - \frac{1}{\sqrt{A}}\right)^2 \exp\left[-0.767\left(\delta - 1\right)^{0.504}\right], \quad \delta = N_G^{\frac{1}{3}}$$

Can one grasp the entire anisotropy of a crystal via one number?

Zener index:
$$A := \frac{2C_{44}}{C_{11} - C_{12}}$$

Chung & Buessem index:
$$A^c := \frac{G^V - G^R}{G^V + G^R} = \frac{3(A-1)^2}{3(A-1)^2 + 25A}$$

Ledbetter & Migliori index:
$$A^* := \frac{v_2^2}{v_1^2}$$

$$\Rightarrow \quad A^U := \mathbf{C}^V : \mathbf{S}^R - 6 = 5\frac{G^V}{G^R} + \frac{K^V}{K^R} - 6 \geq 0$$

[Universal elastic anisotropy index, *Phys. Rev. Lett.* **101**, 2008]

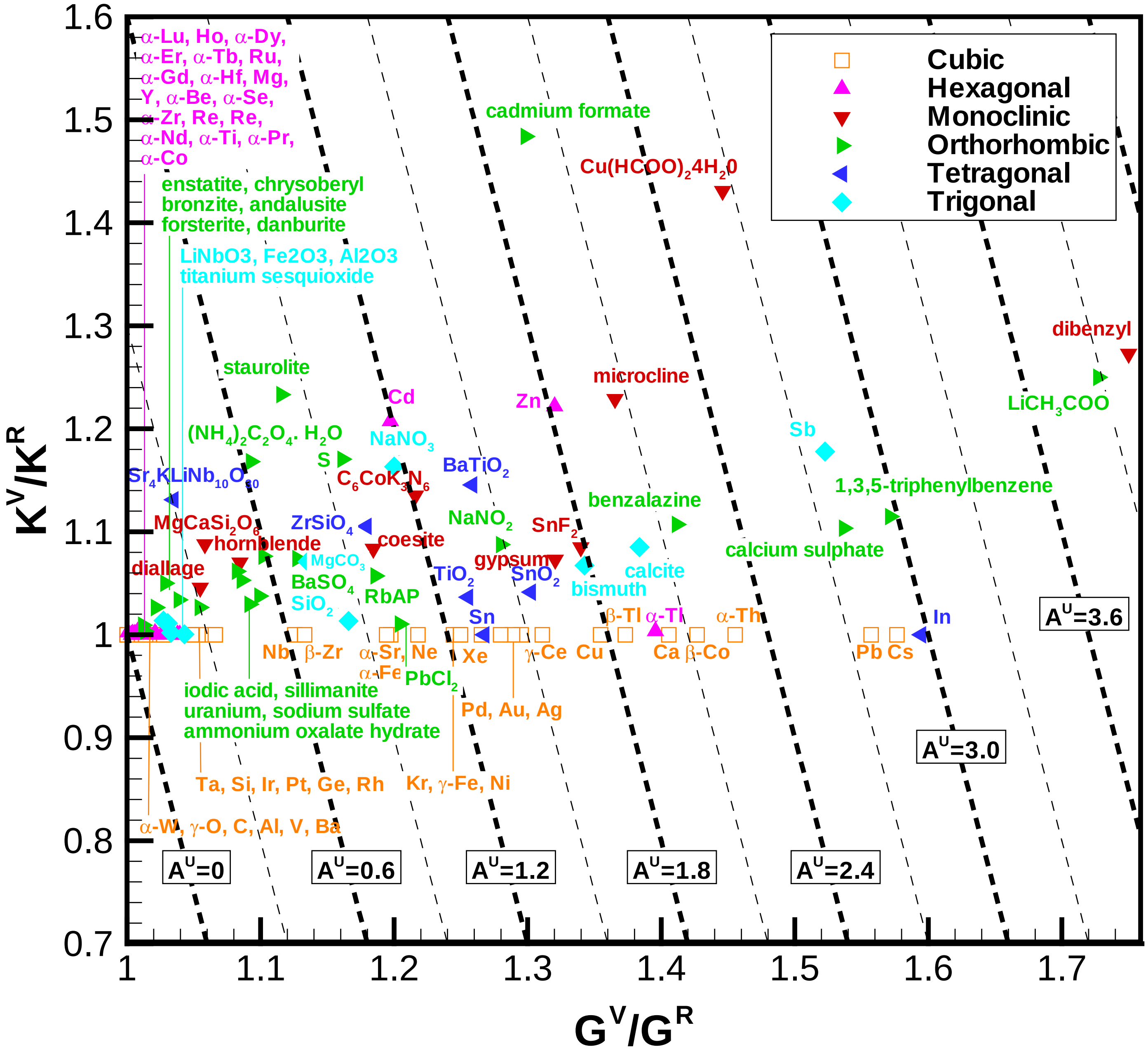

[Universal elastic anisotropy index, *Phys. Rev. Lett.* **101**, 2008]

Mesoscale bounds in finite elasticity of random composites

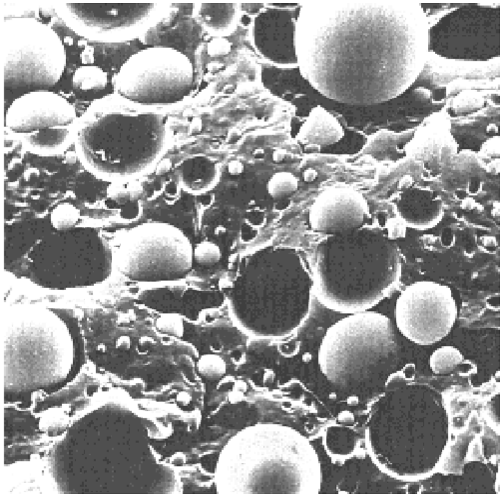

ternary phase rubber composite

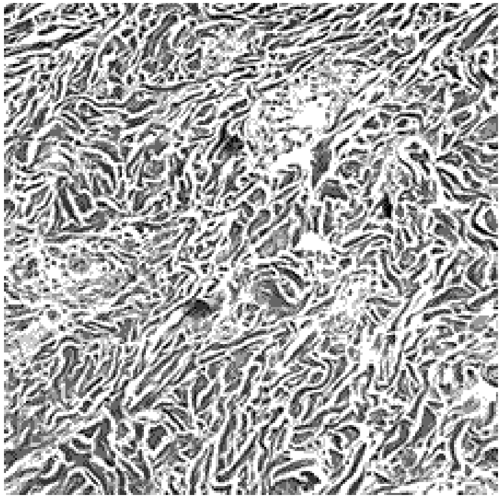

leg muscle tissue

P.R. Hornsby & K. Premphet, *J. Appl. Polym.Sci.* 70, 587 (1998)

L.E. Eldsberg *et al*., *J. Rehab. Res. Develop.* 37, (2000)

Finite elasticity of random media

Hill condition: $\overline{\mathbf{P}:\mathbf{F}} = \overline{\mathbf{P}}:\overline{\mathbf{F}} \quad \Rightarrow \quad \frac{1}{V_0}\int_{\partial V_0} (\mathbf{t}-\overline{\mathbf{P}}\cdot\mathbf{N})\cdot(\mathbf{u}-\left[\overline{\mathbf{F}}-\mathbf{1}\right]\cdot\mathbf{X})dS = 0$

Kinematic uniform b.c. $\mathbf{u} = [\mathbf{F}^0 - \mathbf{1}]\cdot\mathbf{X}\,, \quad \forall\mathbf{X}\in\partial V_0$

Static uniform b.c. $\mathbf{t} = \mathbf{P}^0\cdot\mathbf{N}, \quad \forall\mathbf{X}\in\partial V_0$

Mixed uniform b.c. $(\mathbf{t}-\mathbf{P}^0\cdot\mathbf{N})\cdot(\mathbf{u}-[\mathbf{F}^0-\mathbf{1}]\cdot\mathbf{X}) = 0, \quad \forall\mathbf{X}\in\partial V_0$

Finite elasticity of random media

Hill condition: $\overline{\mathbf{P}:\mathbf{F}} = \overline{\mathbf{P}}:\overline{\mathbf{F}} \qquad \Rightarrow \qquad \frac{1}{V_0}\int_{\partial V_0}(\mathbf{t}-\overline{\mathbf{P}}\cdot\mathbf{N})\cdot(\mathbf{u}-\left[\overline{\mathbf{F}}-\mathbf{1}\right]\cdot\mathbf{X})dS = 0$

Kinematic uniform b.c. $\mathbf{u} = [\mathbf{F}^0 - \mathbf{1}]\cdot\mathbf{X}\,, \quad \forall\mathbf{X}\in\partial V_0$

Static uniform b.c. $\mathbf{t} = \mathbf{P}^0\cdot\mathbf{N}, \quad \forall\mathbf{X}\in\partial V_0$

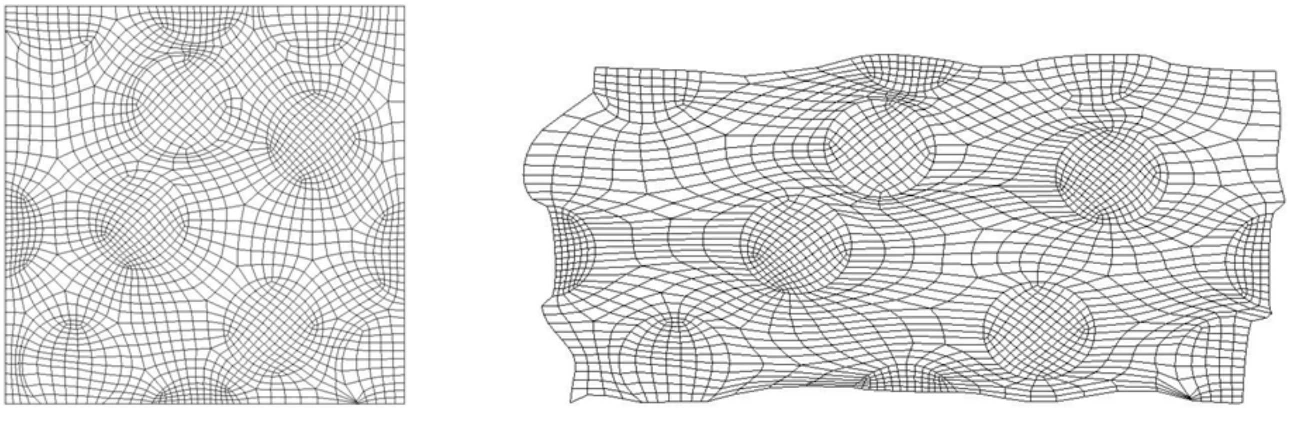

(a) (b)

Minimum Potential Energy Theorem

$$P\{U_i\} = \int_{V_0} \psi(U_{i,k})\, dV - \cancel{\int_{S_T} t_i^0 x_i dS}$$

P assumes a local ***minimum*** for the actual solution u_{ij} provided

$$\int_{V_0} \frac{\partial^2 \psi}{\partial u_{i,k} \partial u_{p,q}} d_{i,k} d_{p,q} dV > 0$$

Under ***kinematic*** uniform boundary conditions

$$P\{U_i\} = \int_{V_0} \psi(U_{i,k}) dV$$

Partitioning of a Body

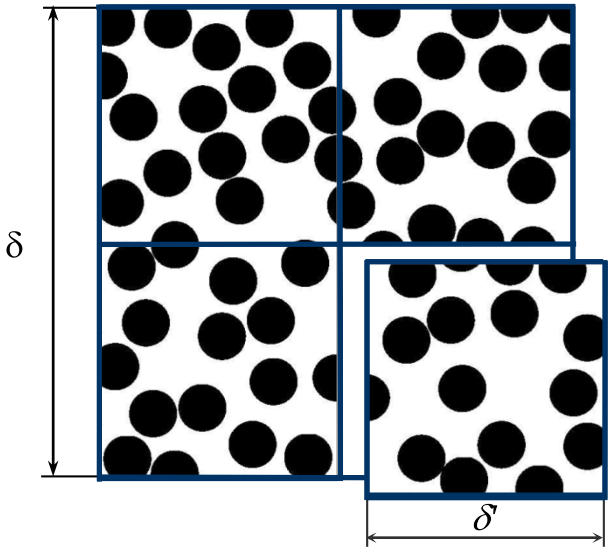

Introducing ***unrestricted*** and ***restricted*** boundary conditions, we obtain the following inequality:

$$P\{u_i\} \leq P\{U_i\}^r$$

For ***KUBC***

$$\Psi(\omega, \mathbf{F}^0) \leq \Psi^r(\omega, \mathbf{F}^0)$$

Scale-dependent Hierarchies

Upper bound:

$$\left\langle \Psi(\mathbf{F}^0, \Delta) \right\rangle \le \left\langle \Psi(\mathbf{F}^0, \delta) \right\rangle \le \left\langle \Psi(\mathbf{F}^0, \delta') \right\rangle \le \left\langle \Psi(\mathbf{F}^0, 1) \right\rangle$$

for $1 < \delta' < \delta < \Delta \quad , \quad \delta = \dfrac{L}{d}$

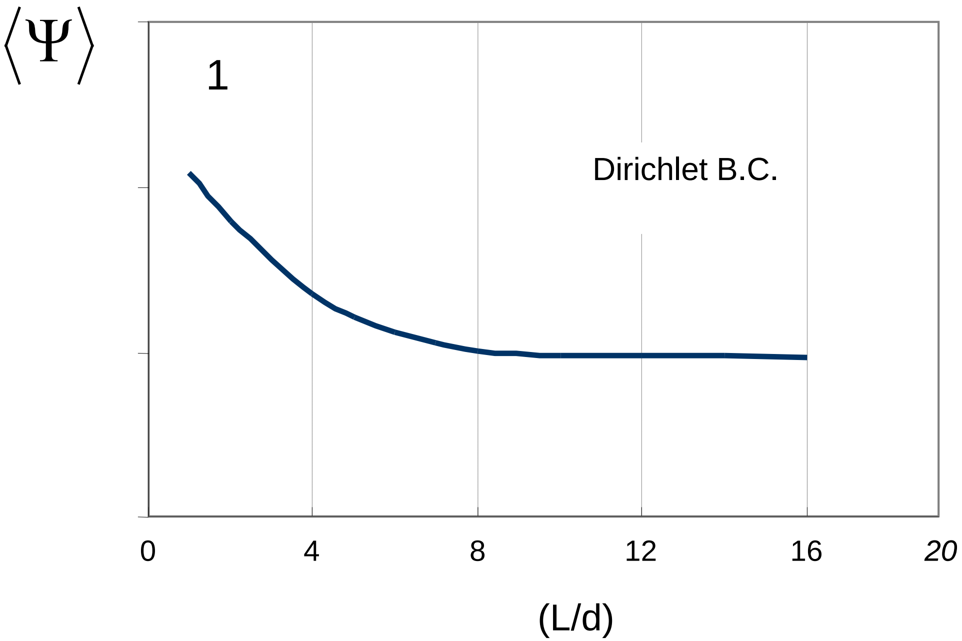

Complementary Type Functional

$$Q\{U_{ik}\} = \int_{V_0} \left\{ \frac{\partial \psi(U_{ik})}{\partial U_{ik}} U_{ik} - \psi(U_{ik}) \right\} dV - \int_{S_D} \frac{\partial \psi(U_{ik})}{\partial U_{ik}} n_k x_i^{0*} dS$$

where $\frac{\partial}{\partial x_k}\left(\frac{\partial \psi(U_{ik})}{\partial U_{ik}} \right) = 0$ in V_0, $\frac{\partial \psi(U_{ik})}{\partial U_{ik}} n_k = t_i^0$ *on* S_T

Q assumes a local ***minimum*** for the actual solution $U_{ij}=u_{i,j}$ provided

$$\int_{V_0} \frac{\partial^2 \psi}{\partial u_{i,k} \partial u_{p,q}} d_{ik} d_{pq} dV > 0$$

*S.J. Lee and R.T. Shield, "Variational principles in finite elastostatics", *ZAMP*, 31, 437-453 (1980).

Partitioning of a Body

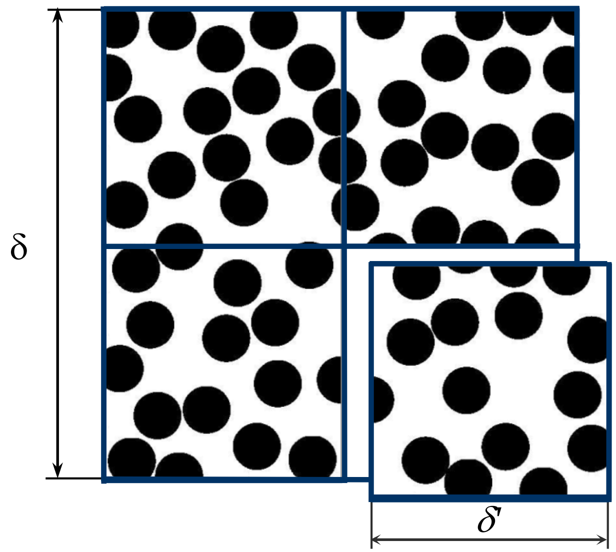

Introducing ***unrestricted*** and ***restricted*** boundary conditions, we obtain the following inequality:

$$Q\left\{u_{i,k}\right\} \le Q\left\{U_{ik}\right\}^{r}$$

For ***SUBC***

$$Q(\omega, \mathbf{P}^{0}) \le Q^{r}(\omega, \mathbf{P}^{0})$$

Scale-dependent Hierarchies

Lower bound:

$$\langle Q(\mathbf{P}^0, \Delta)\rangle \le \langle Q(\mathbf{P}^0, \delta)\rangle \le \langle Q(\mathbf{P}^0, \delta')\rangle \le \langle Q(\mathbf{P}^0, 1)\rangle$$

for $1 < \delta' < \delta < \Delta \quad , \quad \delta = \frac{L}{d}$

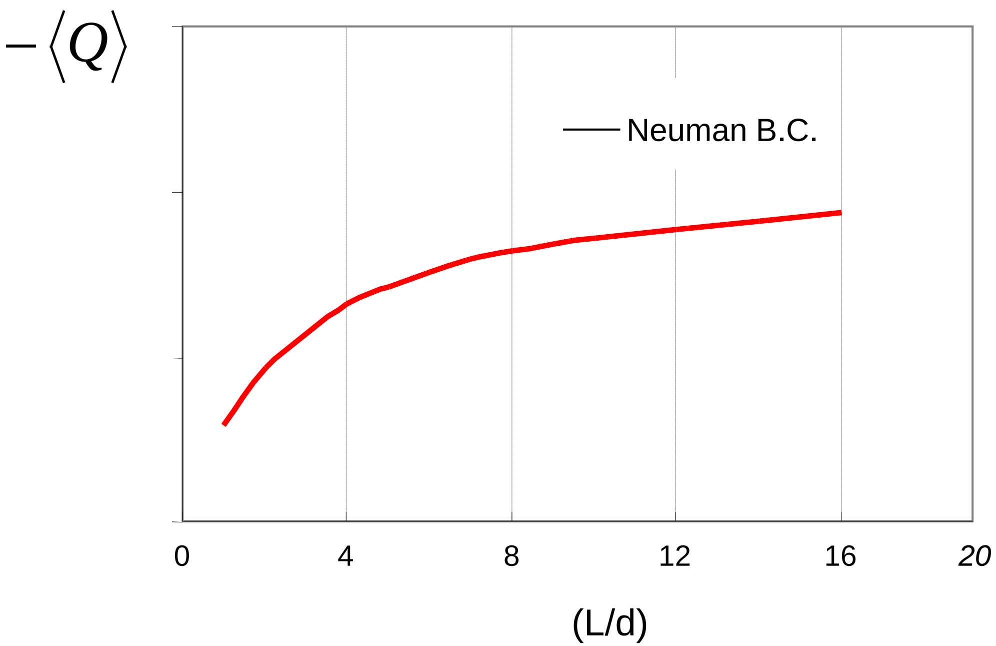

Scale-dependent Hierarchies

Upper bound:

$$\left\langle \Psi(\mathbf{F}^0, \Delta) \right\rangle \le \left\langle \Psi(\mathbf{F}^0, \delta) \right\rangle \le \left\langle \Psi(\mathbf{F}^0, \delta') \right\rangle \le \left\langle \Psi(\mathbf{F}^0, 1) \right\rangle$$

for $\quad 1 < \delta' < \delta < \Delta \qquad \delta = \dfrac{L}{d}$

Lower bound:

$$\left\langle Q(\mathbf{P}^0, \Delta) \right\rangle \le \left\langle Q(\mathbf{P}^0, \delta) \right\rangle \le \left\langle Q(\mathbf{P}^0, \delta') \right\rangle \le \left\langle Q(\mathbf{P}^0, 1) \right\rangle$$

where $\quad \Psi(\omega) = \int_{V_0} \psi(\omega, \mathbf{X})\, dV$

$$Q(\mathbf{P}^0) = \mathbf{P}^0 : \overline{\mathbf{F}} - \Psi(\omega, \mathbf{P}^0)$$

Computational Results: Material Models

$$\Psi = \sum_{i=1}^{N} \frac{2\mu_i}{\alpha_i^2}\left(\overline{\lambda_1}^{\alpha_i} + \overline{\lambda_2}^{\alpha_i} + \overline{\lambda_3}^{\alpha_i} - 3\right) + \sum_{i=1}^{N} \frac{1}{D_i}(J-1)^{2i}$$

$$\overline{\lambda_i} = J^{-\frac{1}{3}}\lambda_i$$

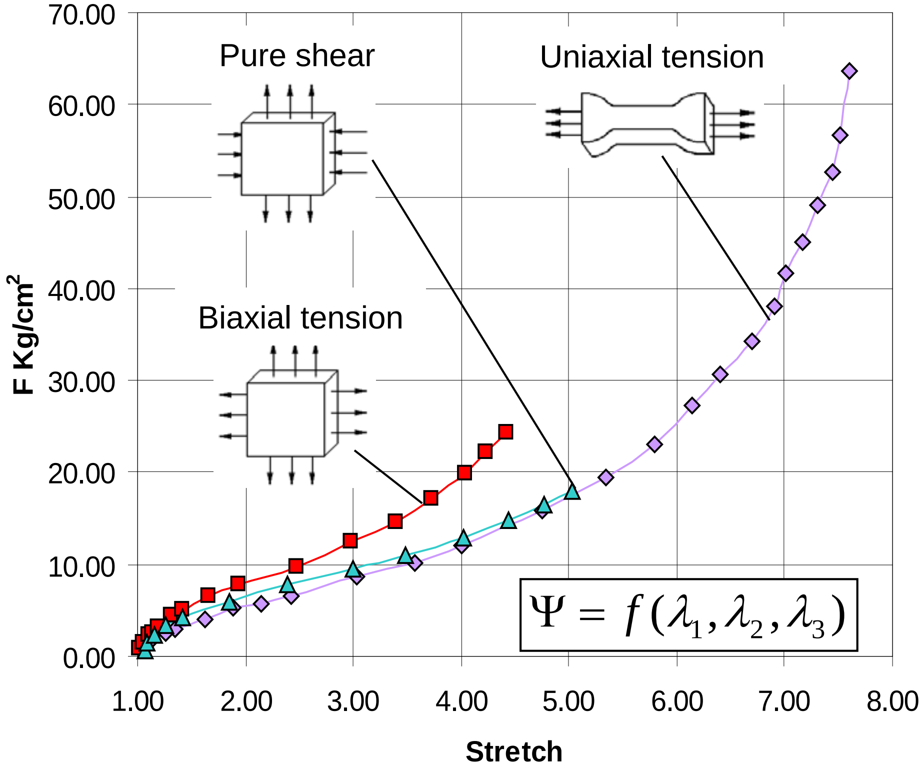

[*Treloar*, 1975]

Composite Models

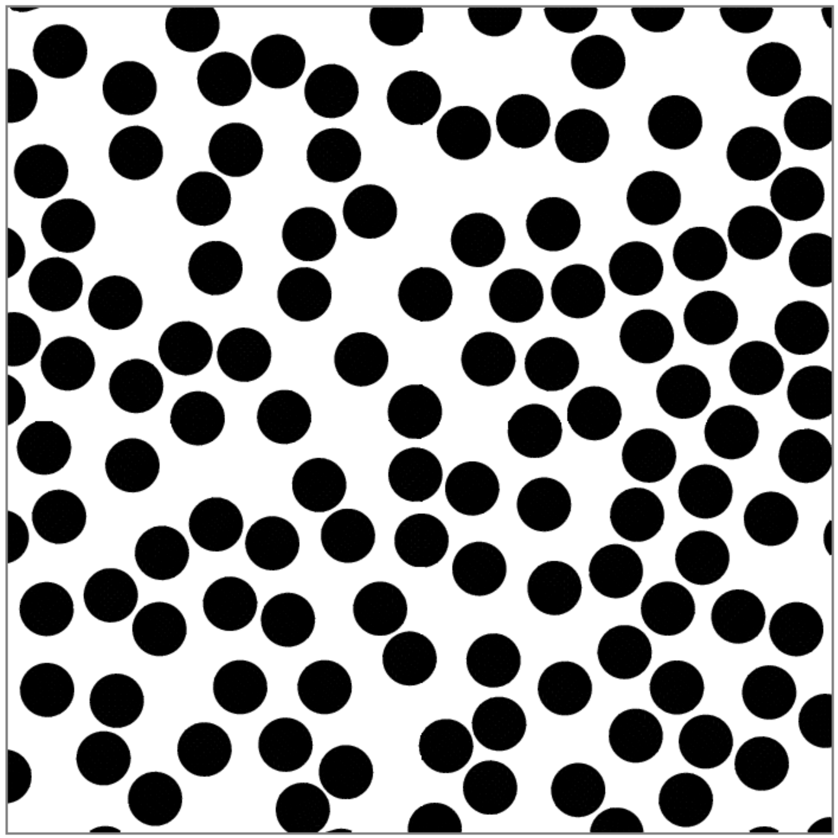

$$\frac{K_0^{(i)}}{K_0^{(m)}} = 1, \qquad \frac{V^{(i)}}{V^{(m)}} = 0.35$$

Boundary Conditions

Deformation modes	Uniaxial tension	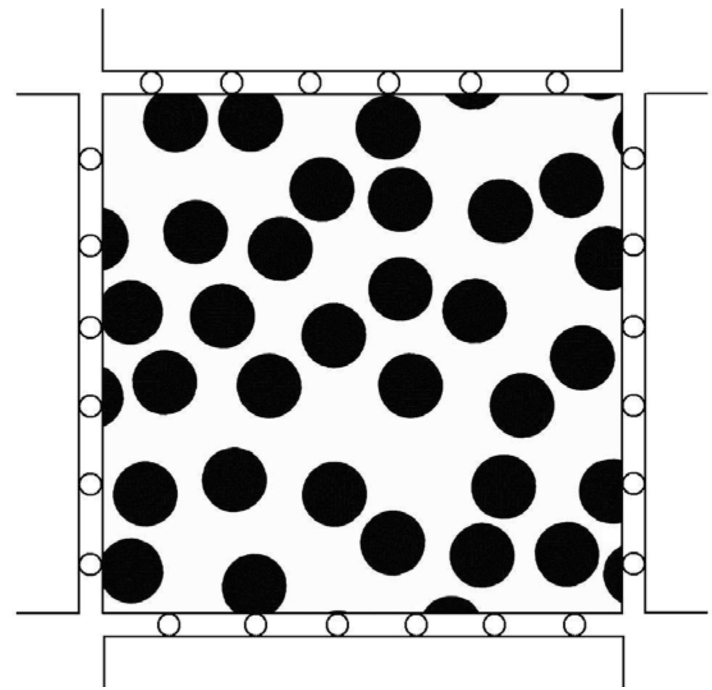	
Uniform static b.c. (USBC)	$P_{11}^0 = P$ $P_{22}^0 = P_{12}^0 = P_{21}^0 = 0$		
Uniform kinematic b.c. (UKBC)	$F_{11}^0 = \langle \overline{\lambda_1} \rangle^{\mathbf{P}}$, $F_{22}^0 = \langle \overline{\lambda_2} \rangle^{\mathbf{P}}$ $F_{12}^0 = F_{21}^0 = 0$		
Orthogonal mixed b.c. (MIXED)	$F_{11}^0 = \langle \overline{\lambda_1} \rangle^{\mathbf{P}}$, $F_{22}^0 = \langle \overline{\lambda_2} \rangle^{\mathbf{P}}$ $P_{12}^0 = P_{21}^0 = 0$		
	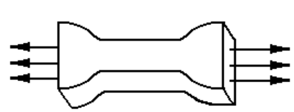	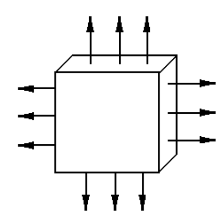	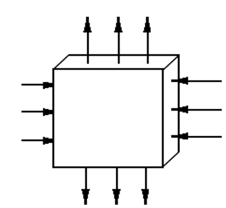

Scale-dependent hierarchies in finite elasticity:

Lower bound: $$\left\langle \Psi(\mathbf{F}^0, \Delta) \right\rangle \le \left\langle \Psi(\mathbf{F}^0, \delta) \right\rangle \le \left\langle \Psi(\mathbf{F}^0, \delta') \right\rangle \le \left\langle \Psi(\mathbf{F}^0, 1) \right\rangle$$

Upper bound: $$\left\langle Q(\mathbf{P}^0, \Delta) \right\rangle \le \left\langle Q(\mathbf{P}^0, \delta) \right\rangle \le \left\langle Q(\mathbf{P}^0, \delta') \right\rangle \le \left\langle Q(\mathbf{P}^0, 1) \right\rangle$$

for $$1 < \delta' < \delta < \Delta$$

$$\Psi(\omega) = \int_{V_0} \psi(\omega, \mathbf{X}) dV \qquad Q(\mathbf{P}^0) = \mathbf{P}^0 : \overline{\mathbf{F}} - \Psi(\omega, \mathbf{P}^0)$$

[*Proc. Roy. Soc. Lond. A*; *J. Elast.*, 2006]

Numerical simulations

$$\Psi = \sum_{i=1}^{N} \frac{2\mu_i}{\alpha_i^2}(\overline{\lambda_1}^{\alpha_i} + \overline{\lambda_2}^{\alpha_i} + \overline{\lambda_3}^{\alpha_i} - 3) + \sum_{i=1}^{N} \frac{1}{D_i}(J^{el} - 1)^{2i}$$

	Matrix	Inclusion
Energy function	Ogden model	Neo-Hookean model
	$\mu_1 = 4.095\cdot 10^5\, Nm,\quad \alpha_1 = 1.3,$ $\mu_2 = 0.03\cdot 10^5\, Nm,\quad \alpha_2 = 5.0,$ $\mu_3 = 0.01\cdot 10^5\, Nm,\quad \alpha_3 = -2.0.$	$\mu_1 = 4.095\cdot 10^6\, Nm,\quad \alpha_1 = 2,$ $\mu_2 = 0,\quad \alpha_2 = 0,$ $\mu_3 = 0,\quad \alpha_3 = 0.$

$$\alpha = \frac{\mu_0^{(i)}}{\mu_0^{(m)}} = 10, \quad \frac{K_0^{(i)}}{K_0^{(m)}} = 1, \quad \frac{V^{(i)}}{V^{(m)}} = 0.35$$

	δ=1	δ=2	δ=4	δ=8	δ=16
Number of samples	512	384	160	40	10

Stress-strain curves

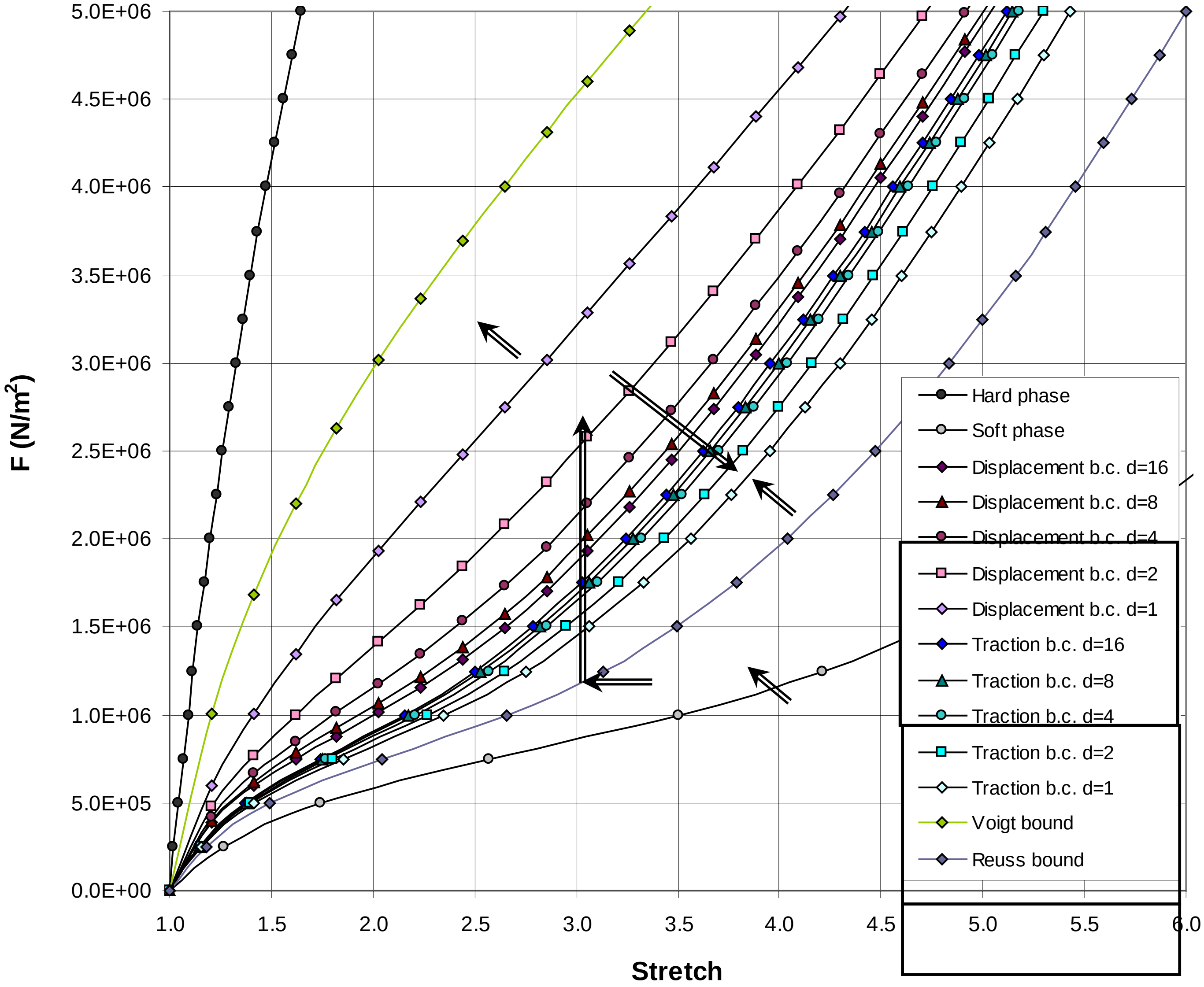

Energy Bounds

$$\left\langle \Psi^{*}(\mathbf{P}^{0}) \right\rangle_{\delta} \Longrightarrow \lambda_i^{0} = \left\langle \overline{\lambda_i} \right\rangle^{\mathbf{P}}_{\delta=\delta_{\max}} \Longrightarrow \left\langle \Psi(\mathbf{F}^{0}) \right\rangle_{\delta}$$

$$\Longrightarrow \left\langle \Psi(\mathbf{P}^{0}) \right\rangle_{\delta} = \mathbf{P}_{\delta=\delta_{\max}} : \mathbf{F}_{\delta=\delta_{\max}} - \left\langle \Psi^{*}(\mathbf{P}^{0}) \right\rangle_{\delta}$$

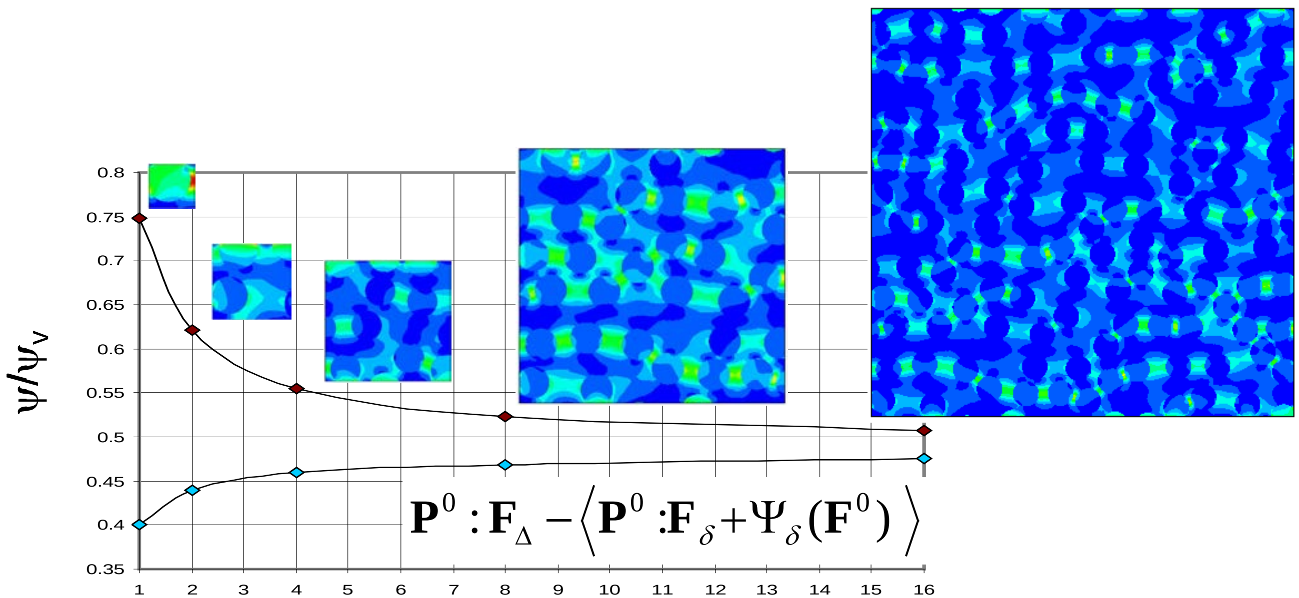

$$\delta = \frac{L}{d}$$

Energy Bounds
Dependence on Deformation Mode

Uniaxial Tension | Biaxial Tension | Pure Shear

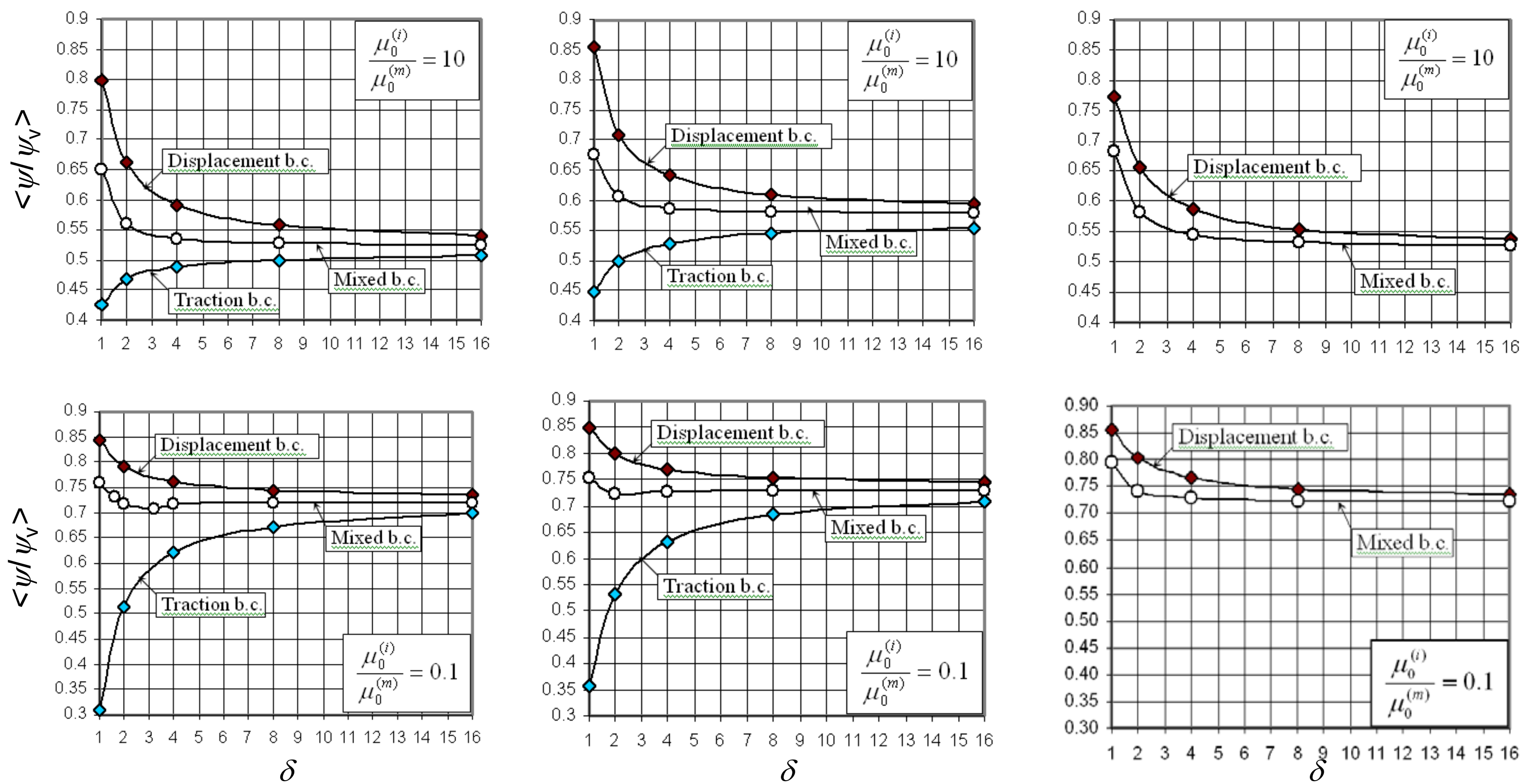

Energy Bounds
Dependence on Deformation

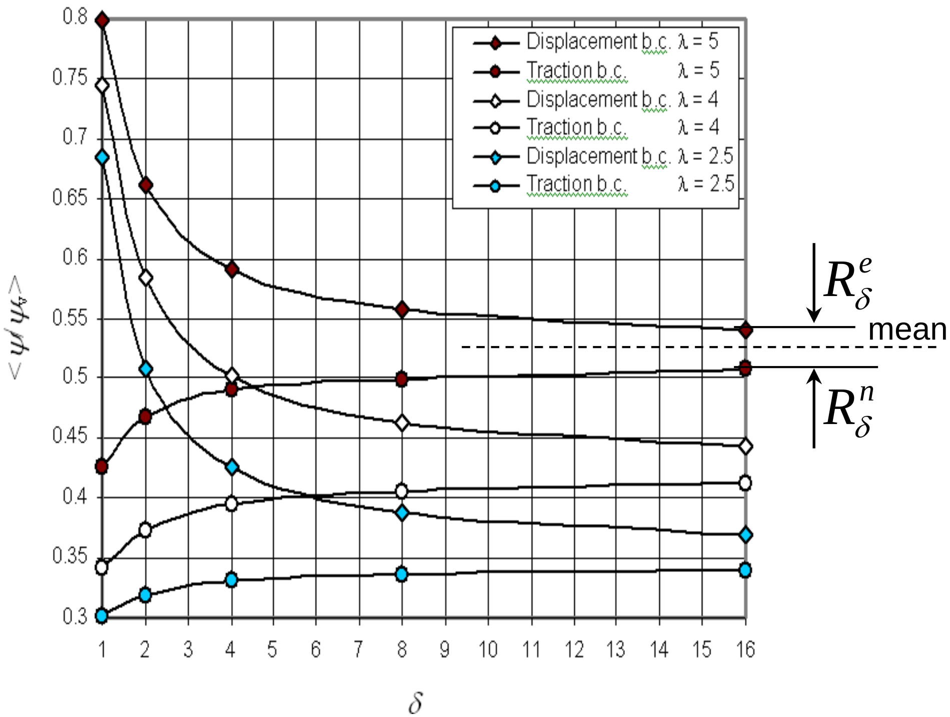

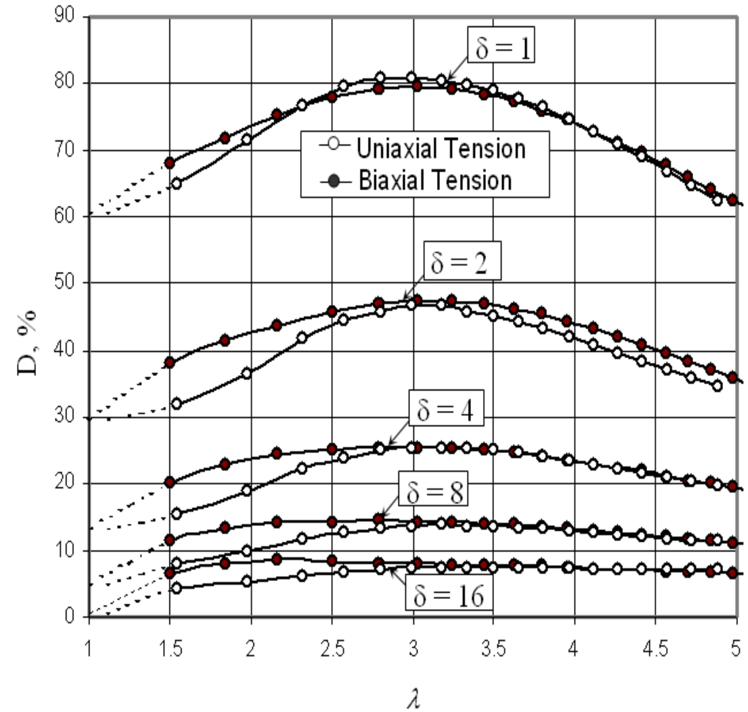

$$D = \frac{R_\delta^e - R_\delta^n}{\left(R_\delta^e + R_\delta^n\right)/2} \cdot 100\%$$

Scale-dependent Hierarchies in Finite Thermoelasticity

Upper bound:

$$\left\langle \Psi(\mathbf{F}^0, \theta_0) \right\rangle_\Delta \le \left\langle \Psi(\mathbf{F}^0, \theta_0) \right\rangle_\delta \le \left\langle \Psi(\mathbf{F}^0, \theta_0) \right\rangle_{\delta'} \le \left\langle \Psi(\mathbf{F}^0, \theta_0) \right\rangle_1$$

for $1 < \delta' < \delta < \Delta \qquad \delta = \dfrac{L}{d}$

Lower bound:

$$\left\langle G(\mathbf{P}^0, \theta_0) \right\rangle_\Delta \ge \left\langle G(\mathbf{P}^0, \theta_0) \right\rangle_\delta \ge \left\langle G(\mathbf{P}^0, \theta_0) \right\rangle_{\delta'} \ge \left\langle G(\mathbf{P}^0, \theta_0) \right\rangle_1$$

where $G(\omega, \mathbf{P}^0, \theta_0) = \dfrac{1}{V_0} \displaystyle\int_{V_0} g(\omega, \mathbf{X}, \mathbf{P}, \theta_0)\, dV$

Thermodynamic Potential of the Mesoscale

Linear Thermoelasticity:

$$\Psi = \frac{1}{2} C_{ijkl}(\omega)\varepsilon_{ij}^{0}\varepsilon_{kl}^{0} + \Gamma_{ij}(\omega)\varepsilon_{ij}^{0}\Delta T - \frac{1}{2} c_v(\omega)\frac{\Delta T^2}{T_0}$$

Nonlinear Thermoelasticity:

$$\Psi(\omega,\mathbf{F}^0,\theta_0) = \frac{1}{V_0}\int_{V_0}\left[\psi_\Delta(\omega,\mathbf{F}^0,\theta_0) + \psi'(\omega,\mathbf{X},\mathbf{F},\theta_0)\right]dV$$

local fluctuation

$$\psi_\Delta(\omega,\mathbf{F}^0,\theta_0) = \frac{1}{2}\left[\mu_\Delta(T)(\tilde{\lambda}_1^{0\,2} + \tilde{\lambda}_2^{0\,2} + \tilde{\lambda}_3^{0\,2} - 3) + \kappa_\Delta(T)\left(\frac{J^0}{(1+\alpha_\Delta \Delta T)^3} - 1\right)^2\right] + \tilde{T}(T)$$

Composite Models

Mismatch	μ_0, MPa	κ_0, MPa	$\alpha \cdot 10^4$, $^oC^{-1}$	c_υ, J/gK
Rubber-Polystyrene	$\frac{\mu_0^{(i)}}{\mu_0^{(m)}} = 0.5 \cdot 10^{-3}$	$\frac{\kappa_0^{(i)}}{\kappa_0^{(m)}} = 0.5$	$\frac{\alpha^{(i)}}{\alpha^{(m)}} = 5$	$\frac{c_p^{(i)}}{c_p^{(m)}} = 1.5$
Sodium-chloride-rubber	$\frac{\mu_0^{(i)}}{\mu_0^{(m)}} = 3.2 \cdot 10^{3}$	$\frac{\kappa_0^{(i)}}{\kappa_0^{(m)}} = 12.8$	$\frac{\alpha^{(i)}}{\alpha^{(m)}} = 0.17$	$\frac{c_p^{(i)}}{c_p^{(m)}} = 0.5$

$$\psi = \frac{1}{2}\left[\mu(T)(\tilde{\lambda}_1^2 + \tilde{\lambda}_2^2 + \tilde{\lambda}_3^2 - 3) + \kappa(T)(J_M - 1)^2\right] + \tilde{T}(T)$$

$$\tilde{\lambda}_a = J^{-\frac{1}{3}} \lambda_a$$

Energy Bounds

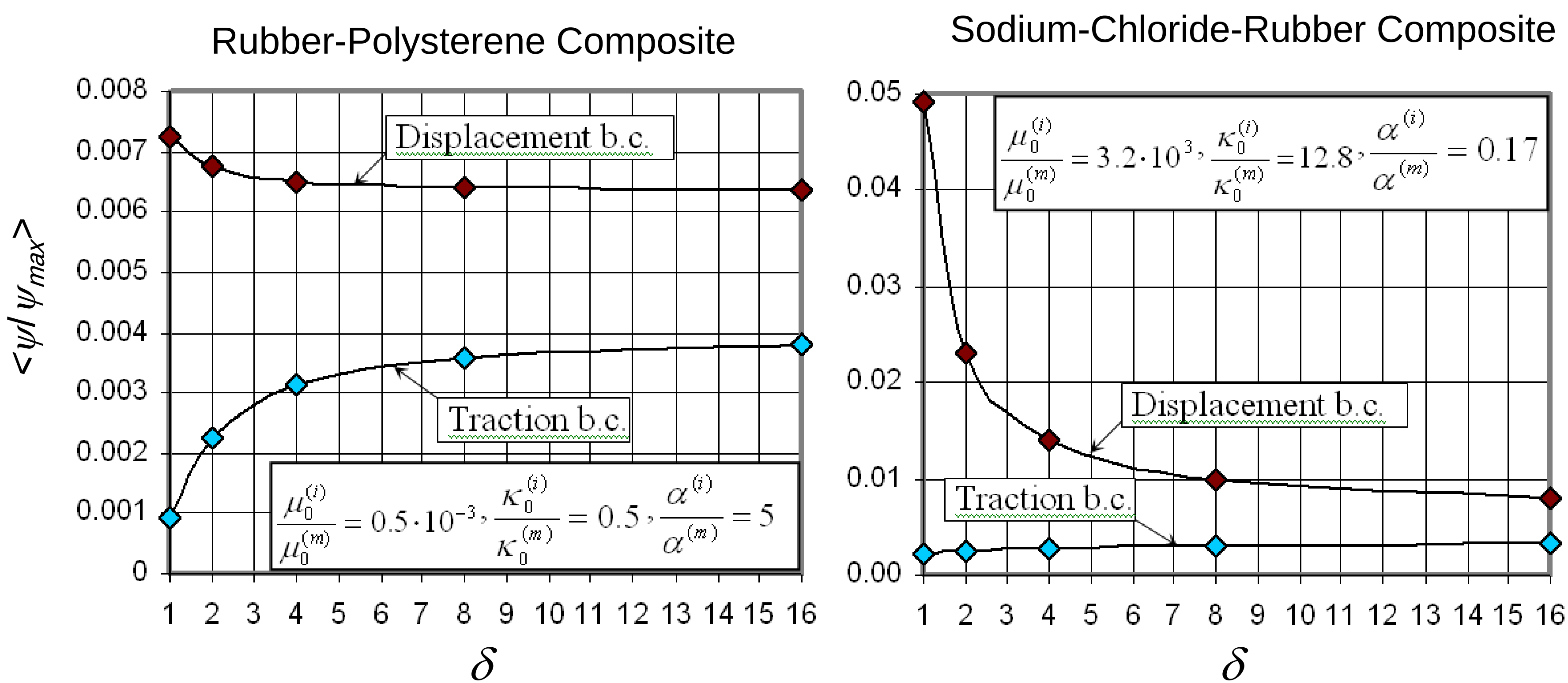

Bounds on Thermal Stress and Strain Coefficients

Rubber-Polysterene

Sodium-chlorid-Rubber

Hypothetical

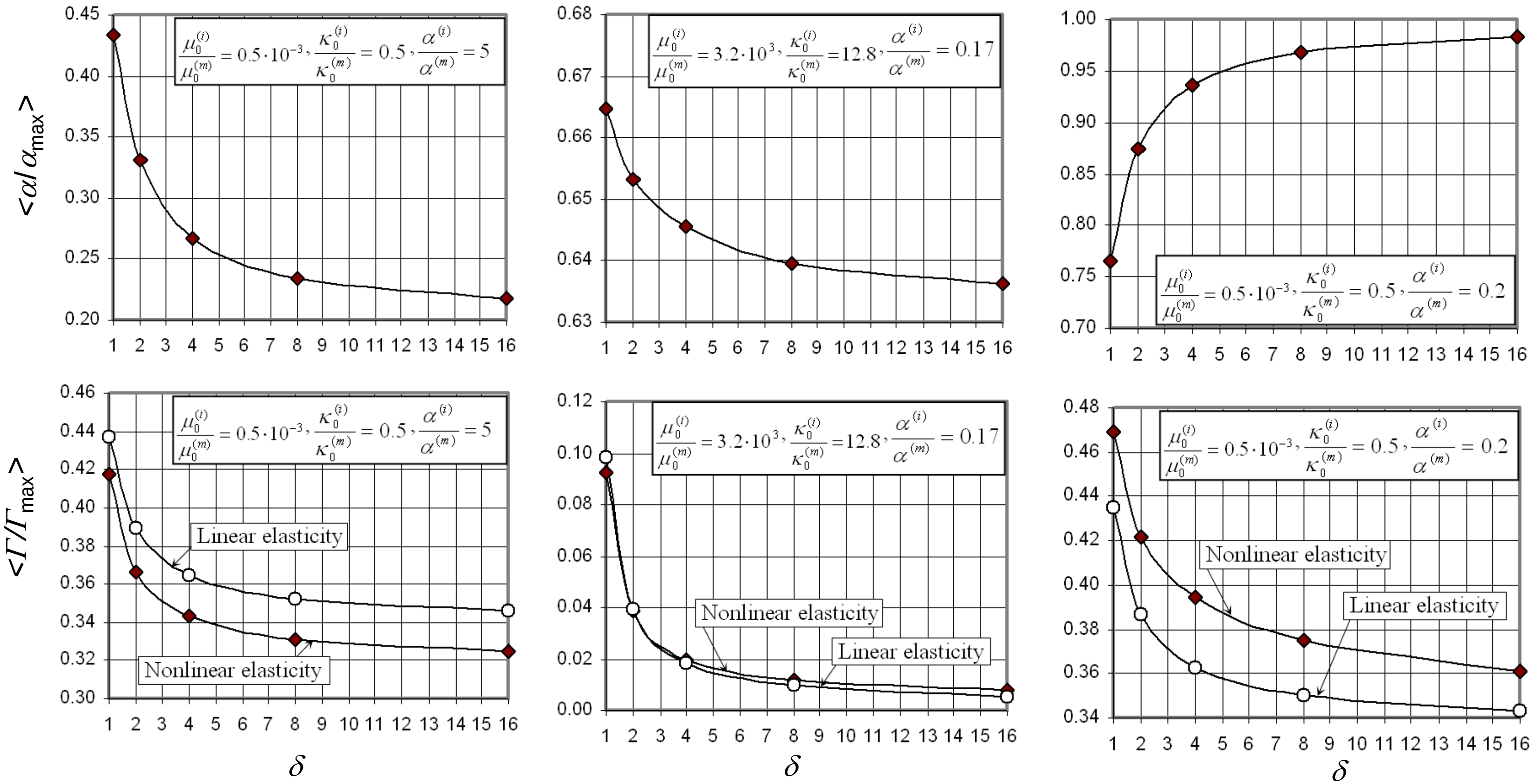

Functionally graded materials

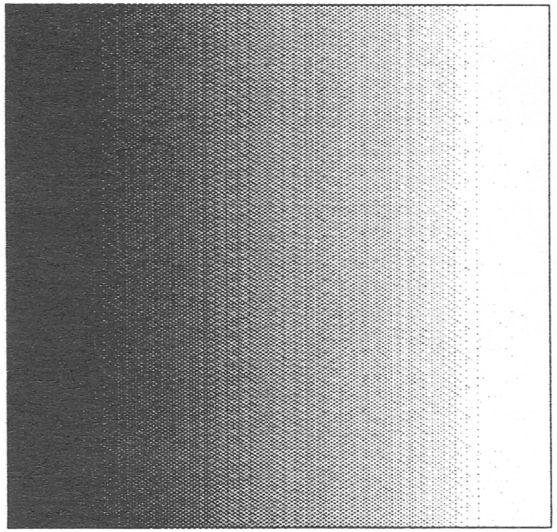

Random medium

$$\mathrm{B} = \{B(\omega); \omega \in \Omega\}$$

A. Saharan, M. Ostoja-Starzewski and S. Koric, “Fractal geometric characterization of functionally graded materials,” *ASCE J. Nanomech. Micromech.*, 2013.

Functionally graded materials

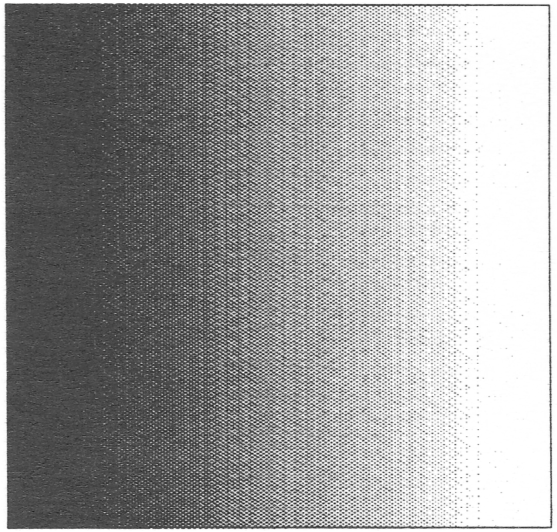

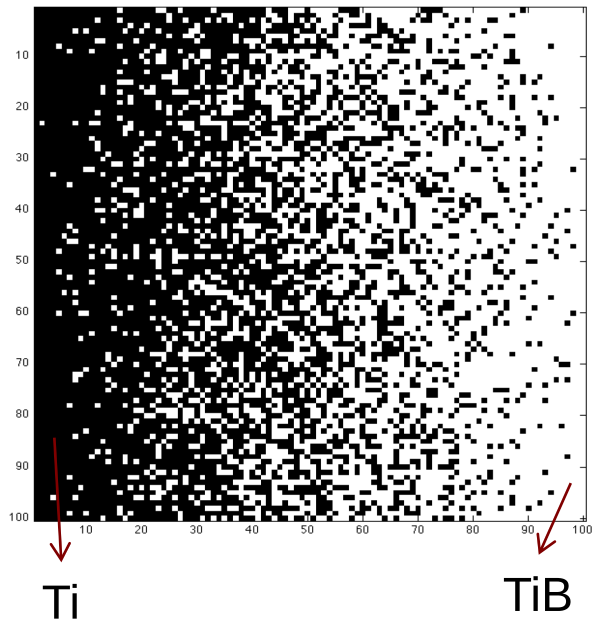

Random medium

$$\mathrm{B} = \{B(\omega); \omega \in \Omega\}$$

A. Saharan, M. Ostoja-Starzewski and S. Koric, "Fractal geometric characterization of functionally graded materials," *ASCE J. Nanomech. Micromech.*, 2013.

Functionally graded materials

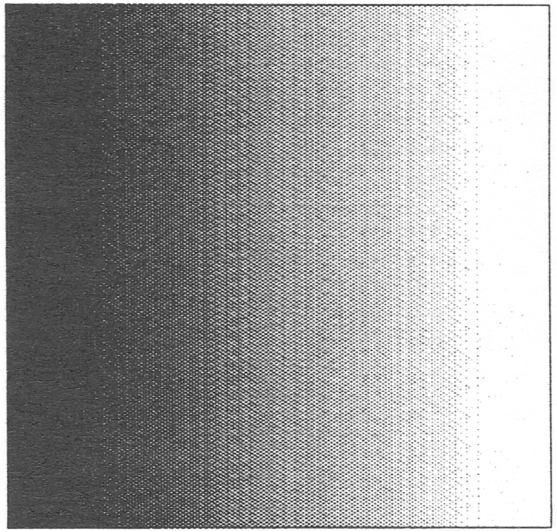

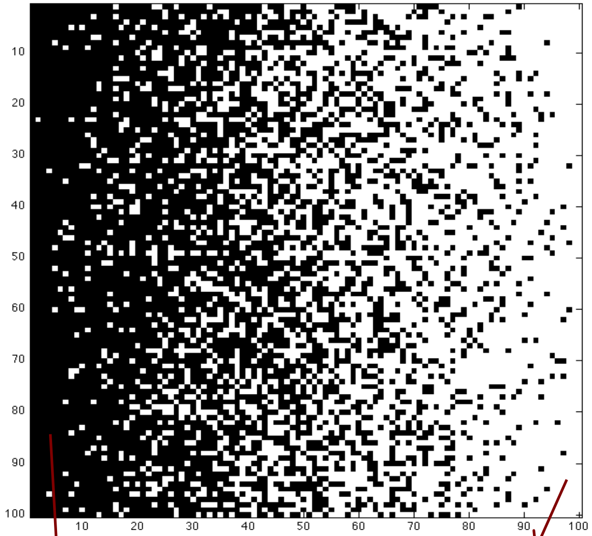

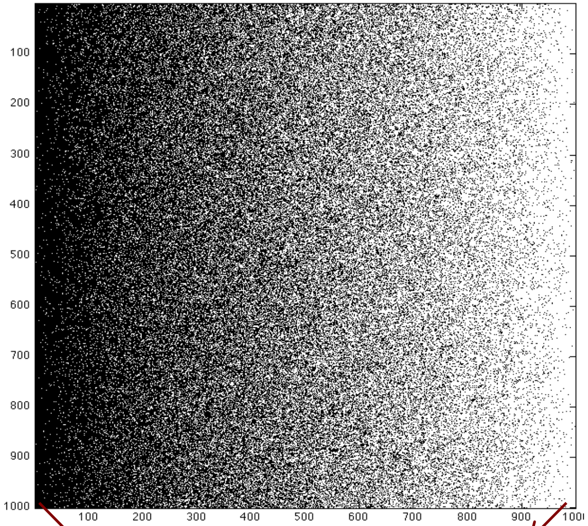

Ti TiB Ti TiB

Random medium

$$\mathrm{B} = \{B(\omega); \omega \in \Omega\}$$

A. Saharan, M. Ostoja-Starzewski and S. Koric, "Fractal geometric characterization of functionally graded materials," *ASCE J. Nanomech. Micromech.*, 2013.

Edge Plots

Fineness: 100

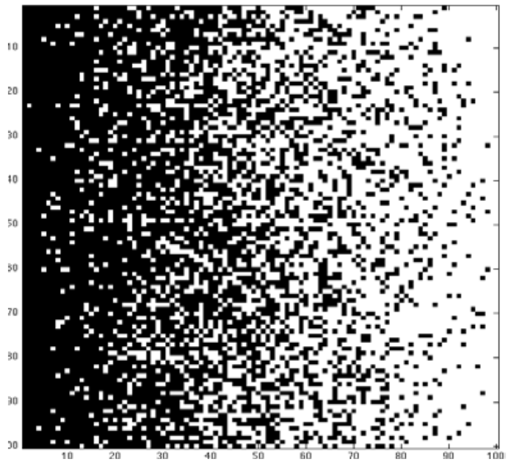

Edge Plots

Fineness: 100

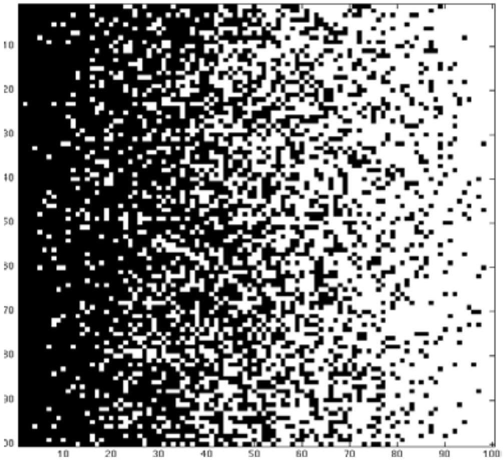

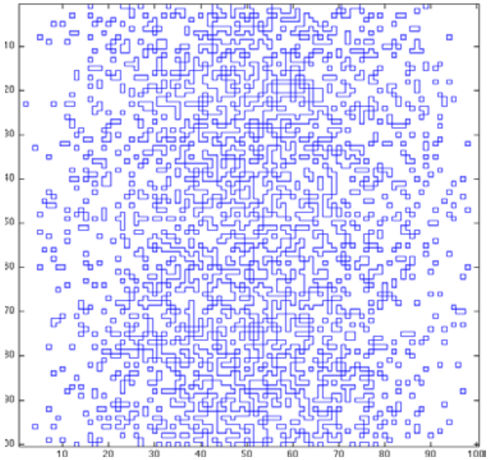

Edge Plots

Fineness: 100

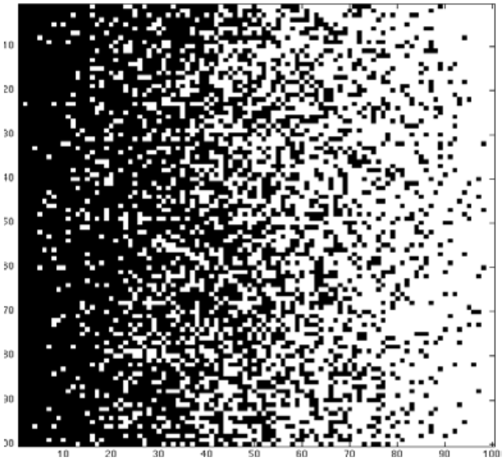

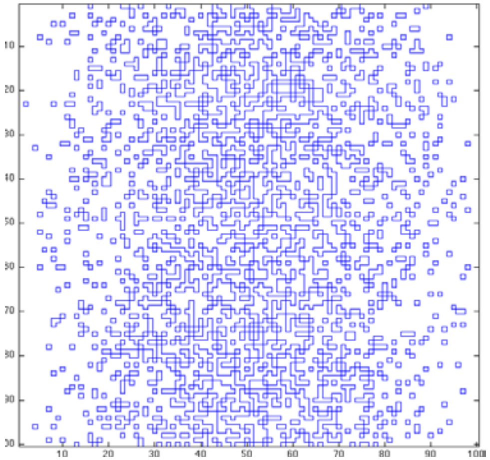

Fineness: 1000

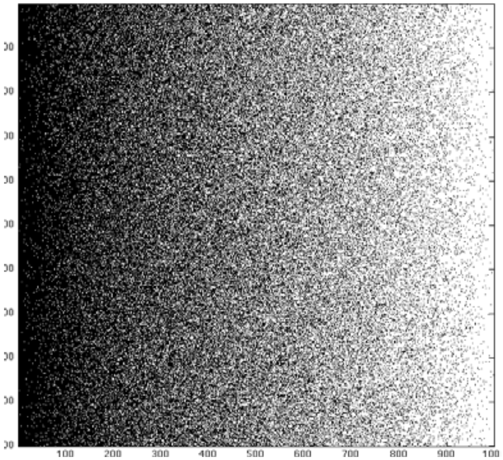

Edge Plots

Fineness: 100

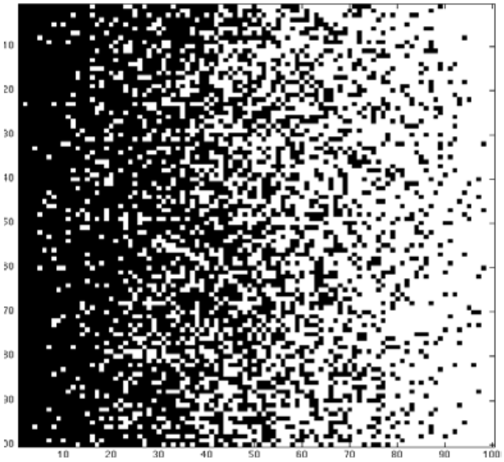

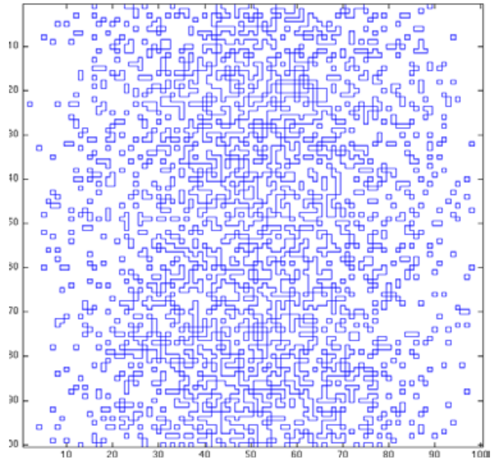

D ~ 1.7–1.8

Fineness: 1000

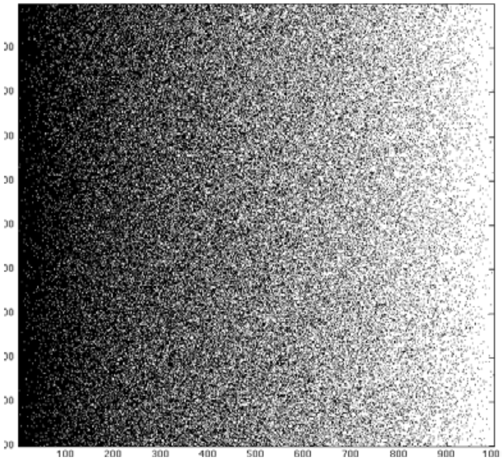

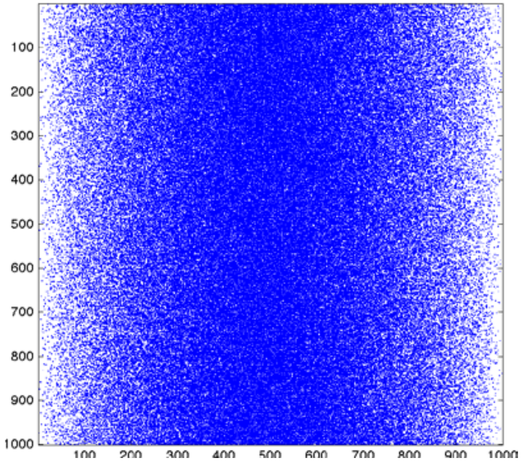

Mechanical formulation

Property	Value	Units
Young's modulus	104	GPa
Poisson's ratio	0.3	
Yield strength	482.633	MPa
Density	4512	Kg/mm^3

Material properties of commercially pure Titanium (A70) at room temperature

Property	Value	Units
Young's modulus	370	GPa
Poisson's ratio	0.14	
density	4630	Kg/mm^3

Material properties of Titanium Monoboride (TiB) at room temperature

Welsch, Boyer, Collings E.W. (1994), Larson (2008)

- FGM: Ti-TiB
- Hill-Mandel condition:

$$\overline{\sigma : \varepsilon} = \overline{\sigma} : \overline{\varepsilon} \quad \Leftrightarrow \int_{\partial B_\delta} (t - \overline{\sigma} \cdot n) \cdot (u - \overline{\varepsilon} \cdot x) \, dS = 0$$

$\forall x \in \partial B_\delta$

- Uniform boundary conditions:
- Displacement B.C. : $u = \overline{\varepsilon} \cdot x$
- Traction B.C. : $t = \overline{\sigma} \cdot n$

2d FGM microstructures

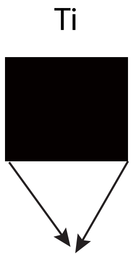

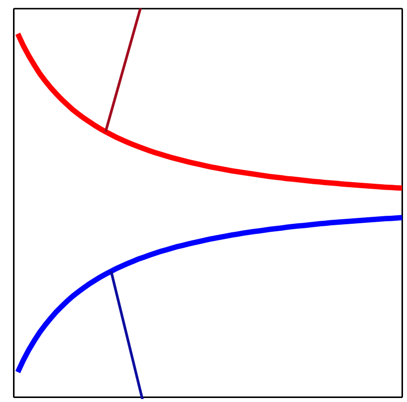

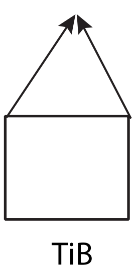

Homogenization procedure for 2d graded microstructures

Stress-strain plots and fractal dimension (*D*)

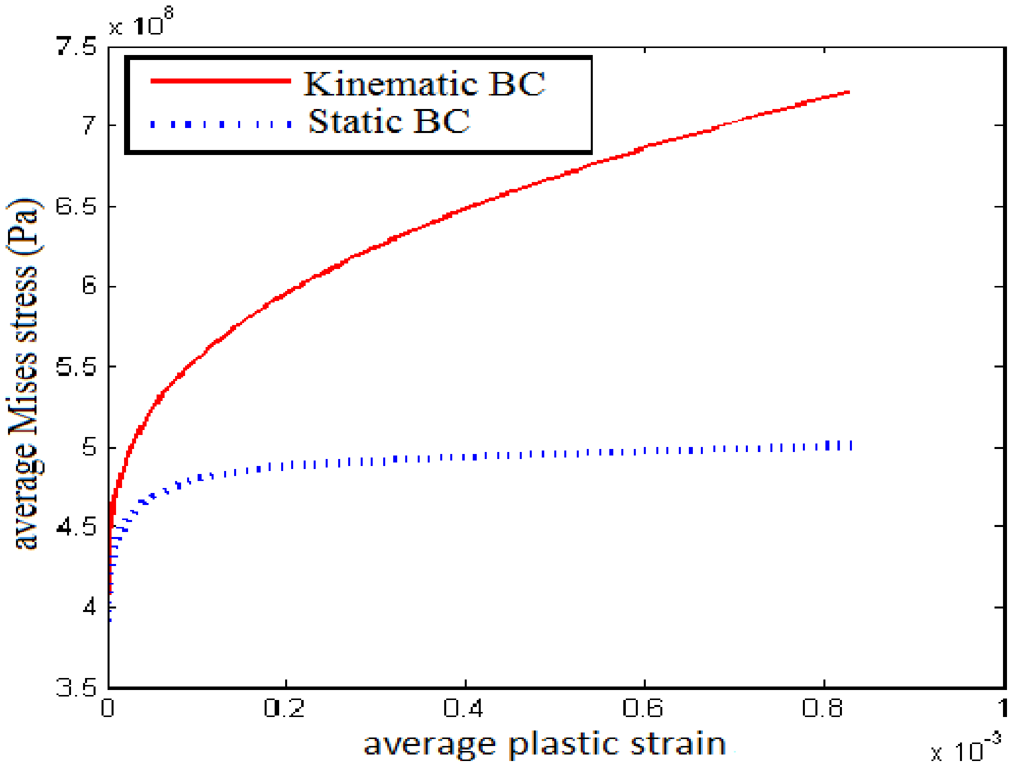

Fineness: 100

Stress-strain plots and fractal dimension (*D*)

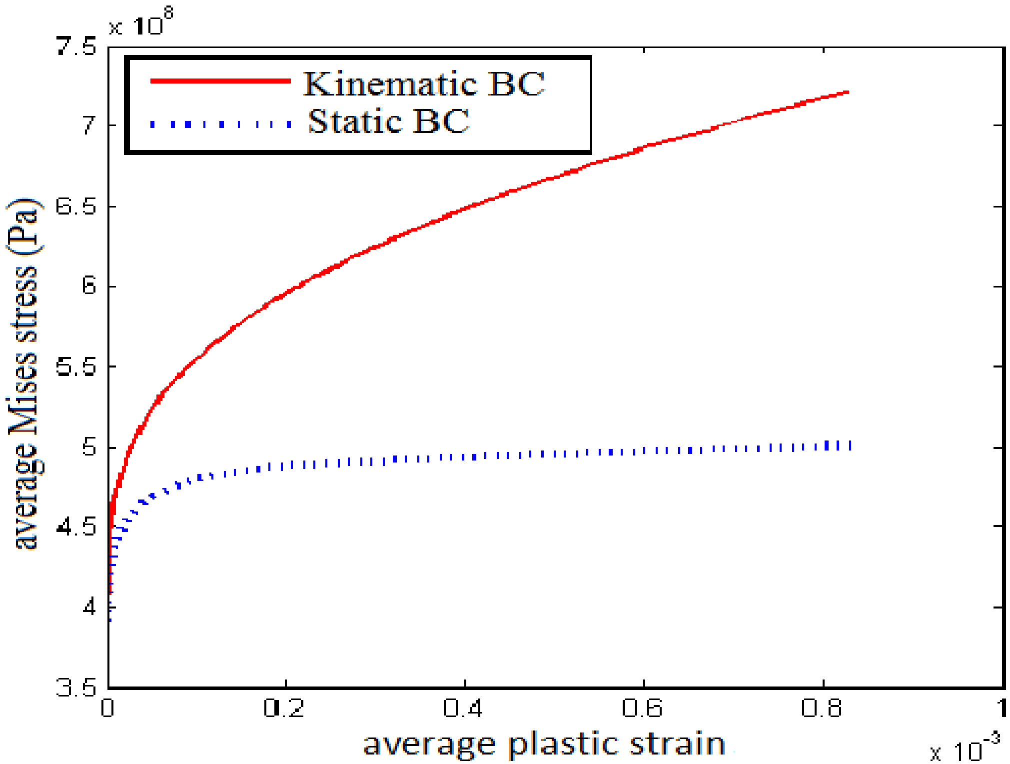

Fineness: 100

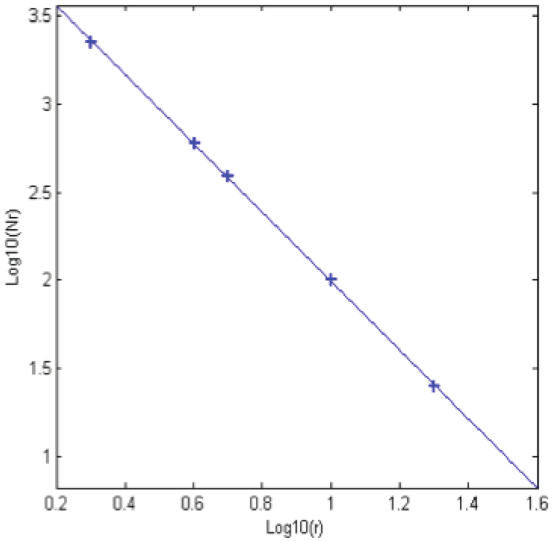

***D* = 1.955 (UKBC)**

***D* = 1.784 (USBC)**

3d Functionally graded materials (FGM)

- Homogenization of functionally graded materials (FGM) in 3d carried out using Hill’s condition:

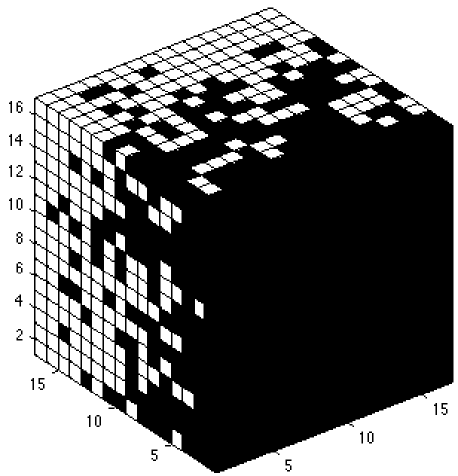

$\delta = 16$

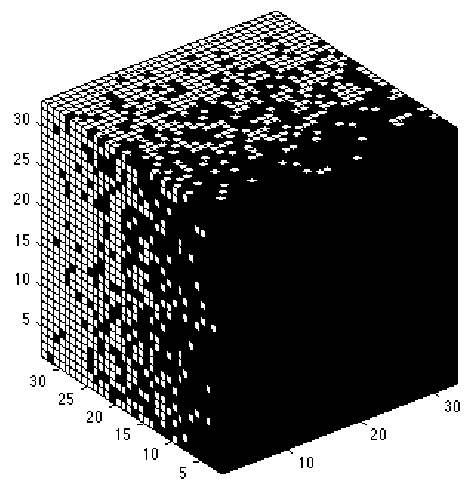

$\delta = 32$

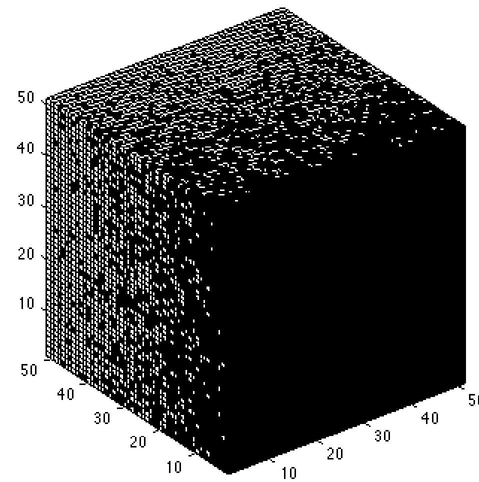

$\delta = 50$

3d FGM microstructures

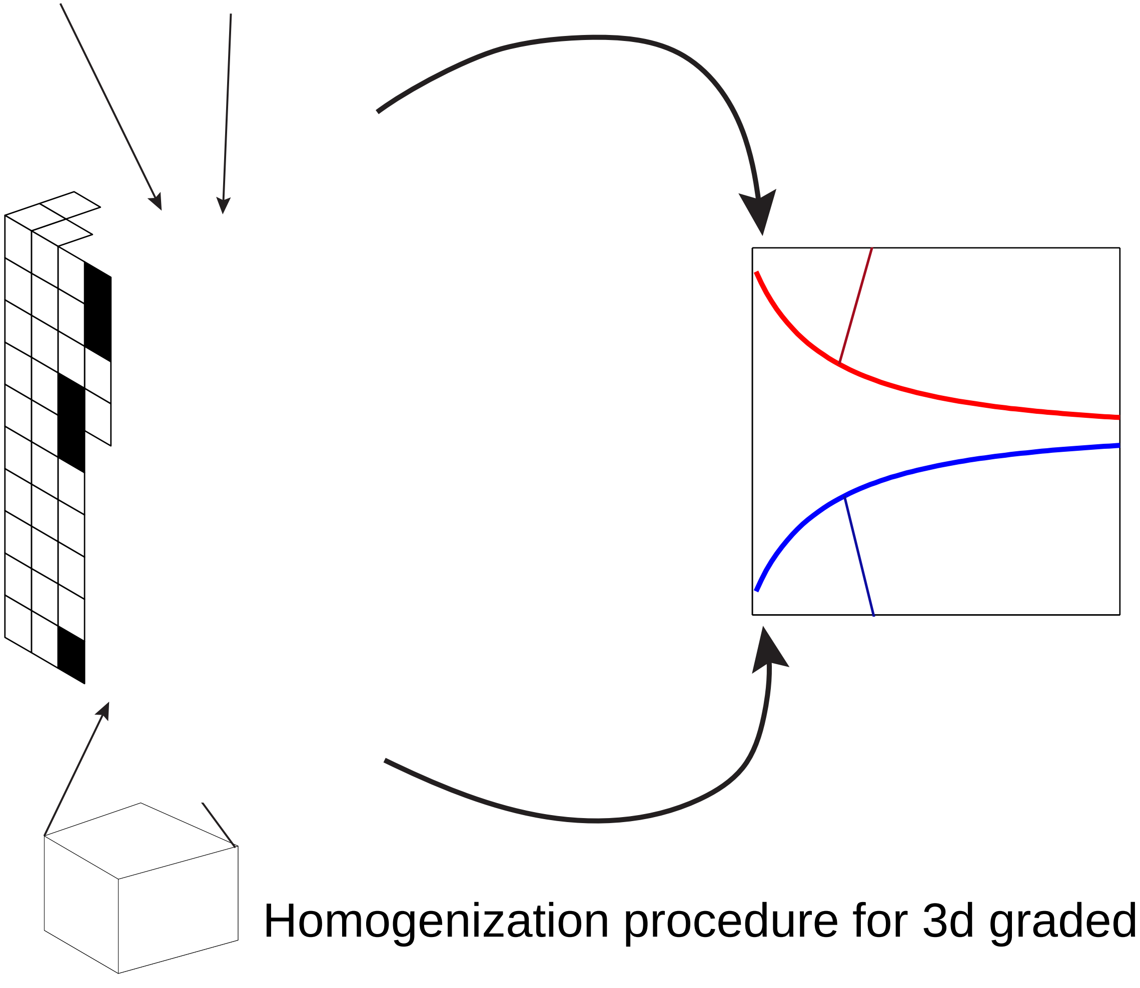

Homogenization procedure for 3d graded microstructures

Convergence of bounds (Ti-TiB)

Property	Value	Units
Young's modulus	104	GPa
Poisson's ratio	0.3	

Material properties of commercially pure Titanium (A70) at room temperature

Property	Value	Units
Young's modulus	370	GPa
Poisson's ratio	0.14	

Material properties of Titanium Monoboride (TiB) at room temperature

Welsch, Boyer, Collings E.W. (1994), Larson (2008)

Convergence of bounds (Ti-TiB)

Property	Value	Units
Young's modulus	104	GPa
Poisson's ratio	0.3	

Material properties of commercially pure Titanium (A70) at room temperature

Property	Value	Units
Young's modulus	370	GPa
Poisson's ratio	0.14	

Material properties of Titanium Monoboride (TiB) at room temperature

Welsch, Boyer, Collings E.W. (1994), Larson (2008)

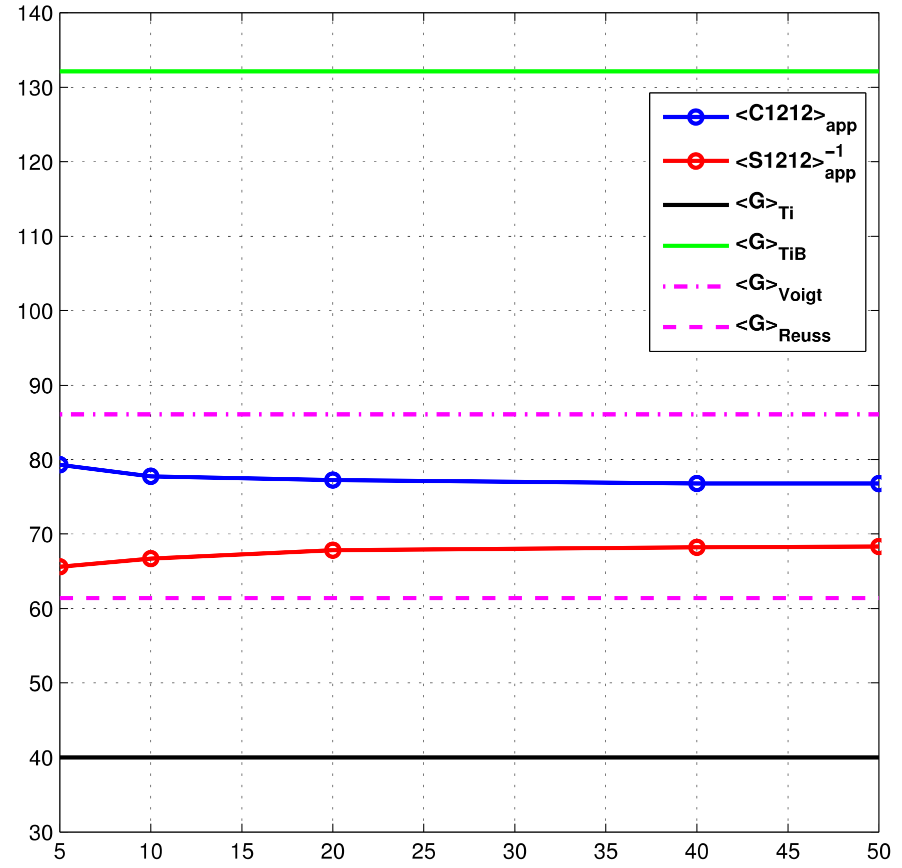

Convergence of bounds (Ti-TiB)

Property	Value	Units
Young's modulus	104	GPa
Poisson's ratio	0.3	

Material properties of commercially pure Titanium (A70) at room temperature

Property	Value	Units
Young's modulus	370	GPa
Poisson's ratio	0.14	

Material properties of Titanium Monoboride (TiB) at room temperature

Welsch, Boyer, Collings E.W. (1994), Larson (2008)

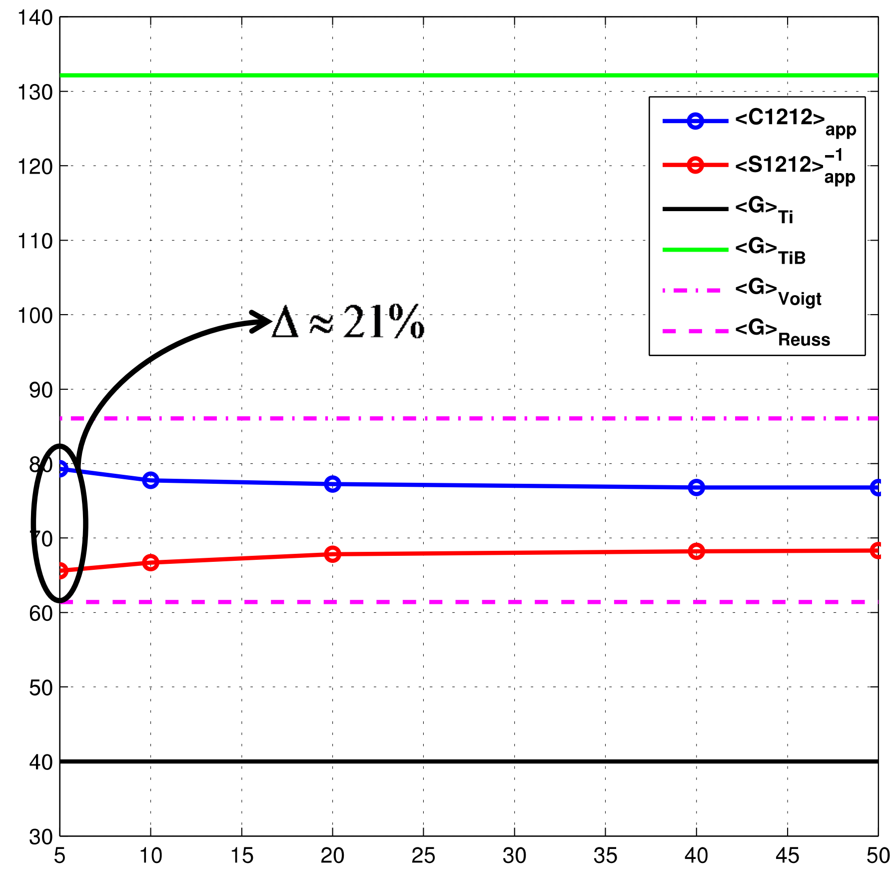

Convergence of bounds (Ti-TiB)

Property	Value	Units
Young's modulus	104	GPa
Poisson's ratio	0.3	

Material properties of commercially pure Titanium (A70) at room temperature

Property	Value	Units
Young's modulus	370	GPa
Poisson's ratio	0.14	

Material properties of Titanium Monoboride (TiB) at room temperature

Welsch, Boyer, Collings E.W. (1994), Larson (2008)

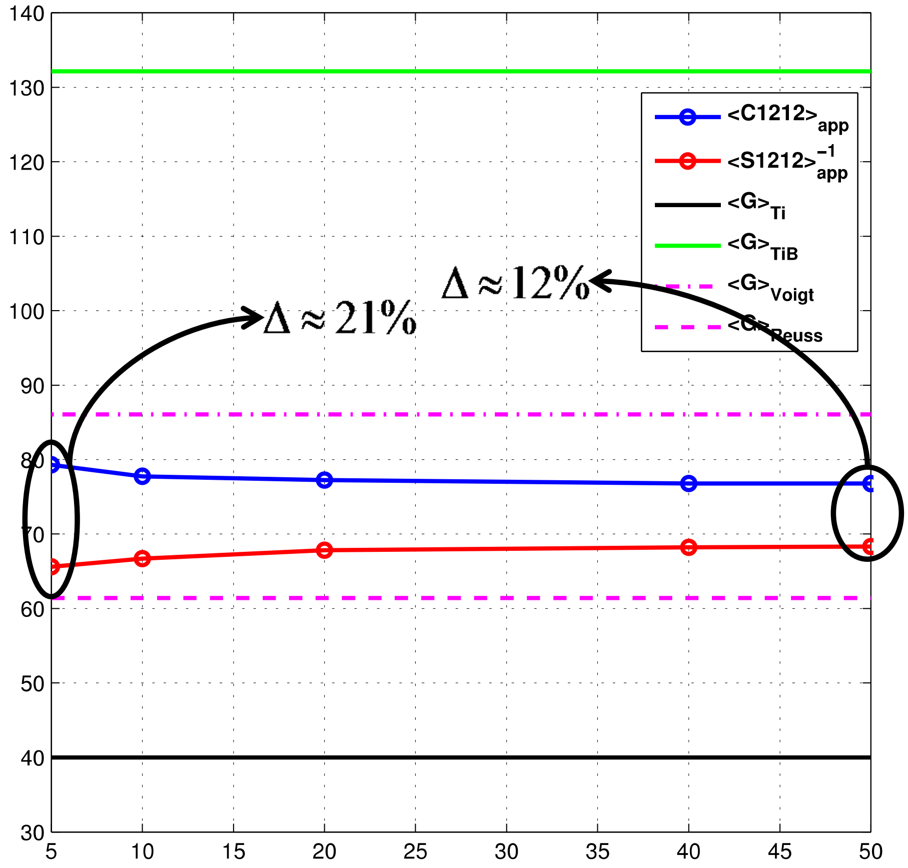

Convergence of bounds (Cu-Ni)

Property	Value	Units
Young's modulus	122.7	GPa
Poisson's ratio	0.32	

Material properties of Copper

Property	Value	Units
Young's modulus	199.8	GPa
Poisson's ratio	0.32	

Material properties of Nickel

Wilfredo Montealegre Rubio *et al.*, 2012

Convergence of bounds (Cu-Ni)

Property	Value	Units
Young's modulus	122.7	GPa
Poisson's ratio	0.32	

Material properties of Copper

Property	Value	Units
Young's modulus	199.8	GPa
Poisson's ratio	0.32	

Material properties of Nickel

Wilfredo Montealegre Rubio *et al.*, 2012

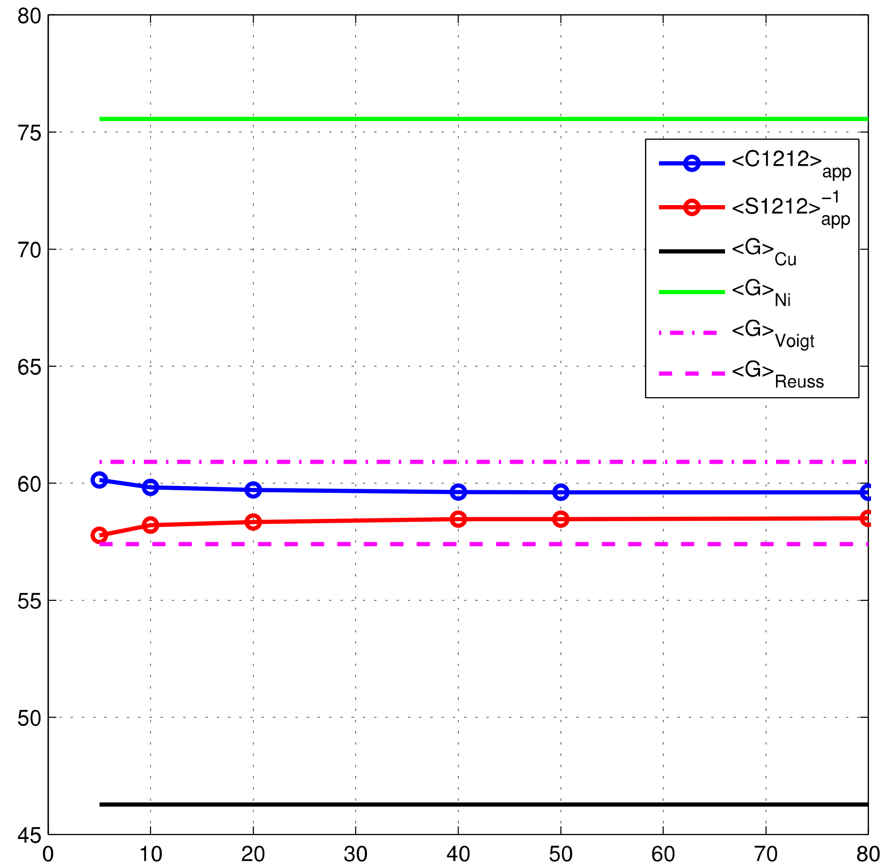

Convergence of bounds (Cu-Ni)

Property	Value	Units
Young's modulus	122.7	GPa
Poisson's ratio	0.32	

Material properties of Copper

Property	Value	Units
Young's modulus	199.8	GPa
Poisson's ratio	0.32	

Material properties of Nickel

Wilfredo Montealegre Rubio *et al.*, 2012

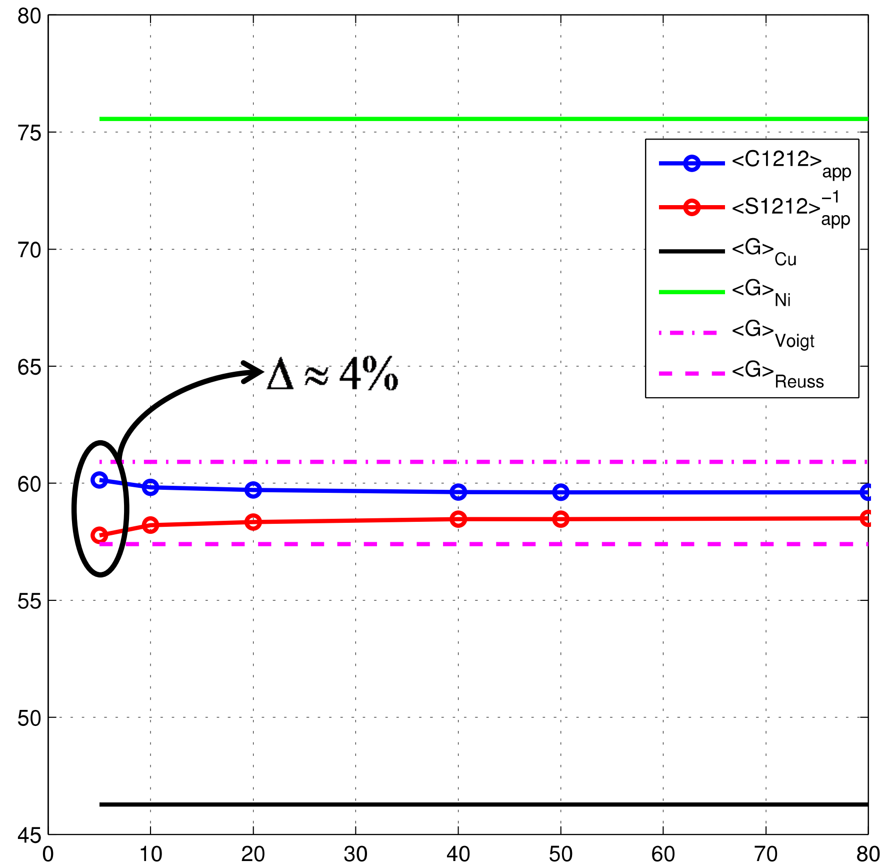

Convergence of bounds (Cu-Ni)

Property	Value	Units
Young's modulus	122.7	GPa
Poisson's ratio	0.32	

Material properties of Copper

Property	Value	Units
Young's modulus	199.8	GPa
Poisson's ratio	0.32	

Material properties of Nickel

Wilfredo Montealegre Rubio *et al.*, 2012

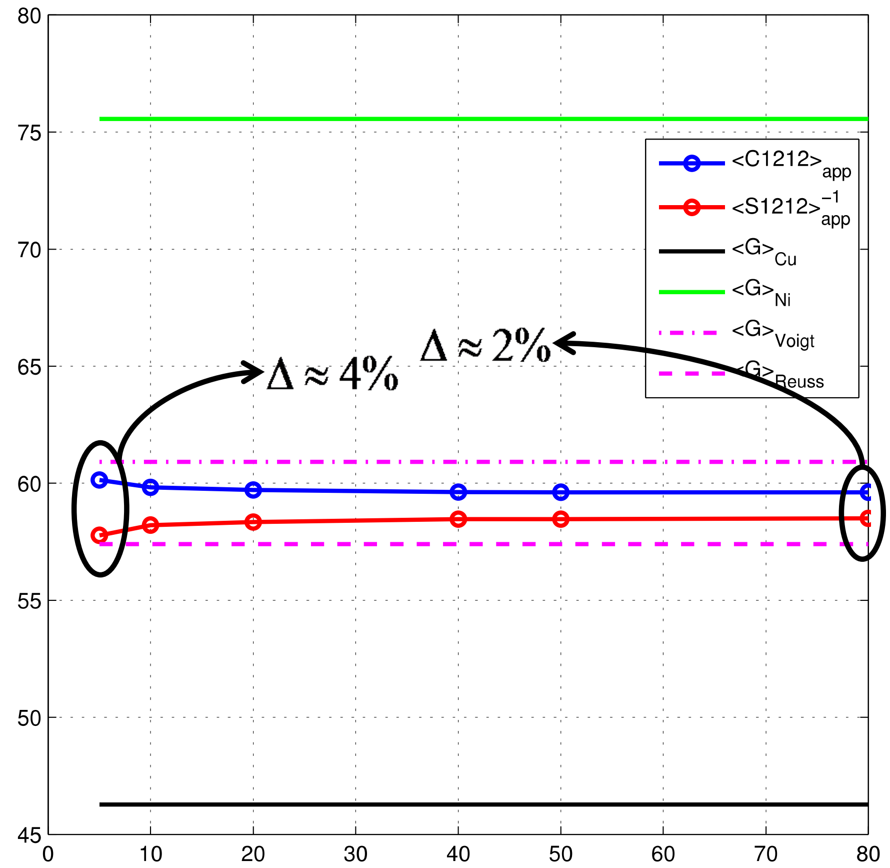

Results – scaling function

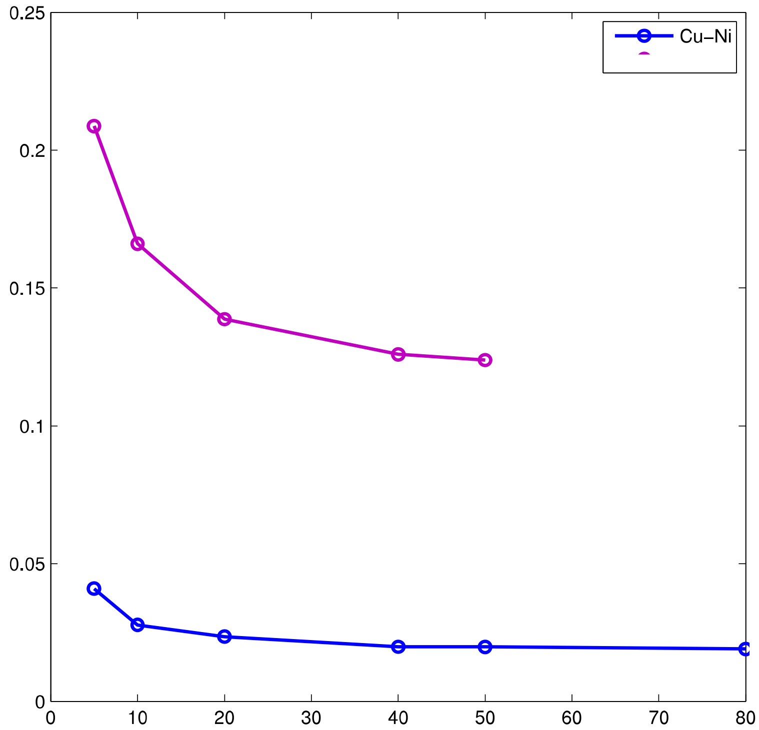

$$f(\alpha,\mu_1,\mu_2,\delta)=\frac{\langle \mu_\delta^d \rangle}{\langle \mu_\delta^t \rangle}-1 \qquad g(\alpha,\mu_1,\mu_2,\delta)=\left(\frac{\langle \mu_\delta^d \rangle}{\langle \mu_\delta^t \rangle}-1\right)\left(\frac{\mu^V}{\mu^R}-1\right)^{-1}$$

Results – scaling function

- On the basis of the mean values of the normalized scaling function, the data was fitted using a *'stretch exponential function.*

$$g(\delta)=0.687\exp[-0.331(\delta-1)^{0.732}]+0.313$$

- More material models need to be simulated to get a reliable fit of the normalized scaling function (*g*).
- Using *g(δ)*, we can predict convergence the convergence of bounds for any material combinations of FGM type.

Comparison of scaling trends

$$D = \frac{R_\delta^e - R_\delta^n}{\left(R_\delta^e + R_\delta^n\right)/2}$$

Table 1 Mismatch and discrepancy (D) values on mesoscale $\delta = 16$

	Mismatch	D [%]
Linear elasticity	$\frac{\mu^{(i)}}{\mu^{(m)}} = 10, \frac{\kappa^{(i)}}{\kappa^{(m)}} = 1$	2.28
Linear thermoelasticity	$\frac{\mu^{(i)}}{\mu^{(m)}} = 10, \frac{\kappa^{(i)}}{\kappa^{(m)}} = 10, \frac{\alpha^{(i)}}{\alpha^{(m)}} = \frac{1}{10}$	5.51
Plasticity	$\frac{h^{(i)}}{h^{(m)}} = 10, \frac{E^{(i)}}{E^{(m)}} = 1$	2.29
Nonlinear elasticity	$\frac{\mu_0^{(i)}}{\mu_0^{(m)}} = 10, \frac{\kappa_0^{(i)}}{\kappa_0^{(m)}} = 1$	5.86
Flow in porous media	$\frac{tr(\mathbf{K}^{(i)})}{tr(\mathbf{K}^{(m)})} = \infty$	27

Thermomechanics of random media

(generalizing the formulation of H. Ziegler)

Thermodynamics with internal variables

orthogonality in space of forces

orthogonality in space of velocities

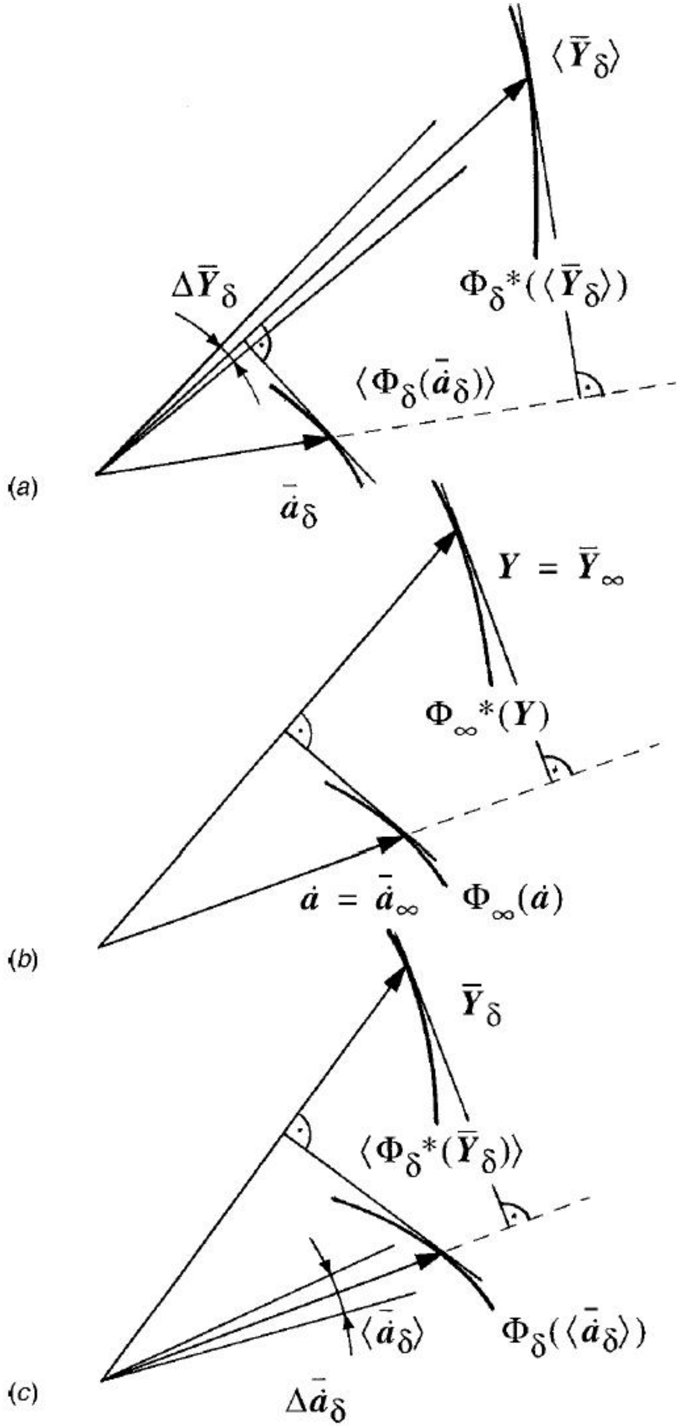

quartets of
Legendre transformations

classical →

$$X(x_i, \alpha_i)$$
$$y_i = \frac{\partial X}{\partial x_i},\ \beta_i = \frac{\partial X}{\partial \alpha_i}$$

$$X(x_i, \alpha) + Y(y_i, \alpha_i) = x_i y_i$$

$$X(x_i, \alpha) + V(x_i, \beta_i) = \alpha_i \beta_i$$

$$Y(y_i, \alpha_i)$$
$$x_i = \frac{\partial Y}{\partial y_i},\ \beta_i = -\frac{\partial Y}{\partial \alpha_i}$$

$$V(x_i, \beta_i)$$
$$y_i = -\frac{\partial V}{\partial x_i},\ \alpha_i = \frac{\partial V}{\partial \beta_i}$$

$$Y(y_i, \alpha_i)) + W(y_i, \beta_i) = -\alpha_i \beta_i$$

$$V(x_i, \beta_i) + W(y_i, \beta_i) = -x_i y_i$$

$$W(y_i, \beta_i)$$
$$x_i = -\frac{\partial W}{\partial y_i},\ \alpha_i = -\frac{\partial W}{\partial \beta_i}$$

quartets of Legendre transformations

classical →

$$X(x_i, \alpha_i)$$
$$y_i = \frac{\partial X}{\partial x_i}, \ \beta_i = \frac{\partial X}{\partial \alpha_i}$$

$$X(x_i, \alpha) + Y(y_i, \alpha_i) = x_i y_i$$

$$X(x_i, \alpha) + V(x_i, \beta_i) = \alpha_i \beta_i$$

$$Y(y_i, \alpha_i)$$
$$x_i = \frac{\partial Y}{\partial y_i}, \ \beta_i = -\frac{\partial Y}{\partial \alpha_i}$$

$$V(x_i, \beta_i)$$
$$y_i = -\frac{\partial V}{\partial x_i}, \ \alpha_i = \frac{\partial V}{\partial \beta_i}$$

$$Y(y_i, \alpha_i)) + W(y_i, \beta_i) = -\alpha_i \beta_i$$

$$V(x_i, \beta_i) + W(y_i, \beta_i) = -x_i y_i$$

$$W(y_i, \beta_i)$$
$$x_i = -\frac{\partial W}{\partial y_i}, \ \alpha_i = -\frac{\partial W}{\partial \beta_i}$$

stochastic ↓

$$\langle X(x_i, \alpha_i)\rangle$$
$$\langle y_i\rangle = \frac{\partial \langle X\rangle}{\partial x_i}, \ \langle \beta_i\rangle = \frac{\partial \langle X\rangle}{\partial \alpha_i}$$

$$\langle X(x_i, \alpha_i)\rangle + Y(\langle y_i\rangle, \alpha_i) = x_i \langle y_i\rangle$$

$$\langle X(x_i, \alpha_i)\rangle + V(x_i, \langle \beta_i\rangle) = \alpha_i \langle \beta_i\rangle$$

$$Y(\langle y_i\rangle, \alpha_i)$$
$$x_i = \frac{\partial Y}{\partial \langle y_i\rangle}, \ \langle \beta_i\rangle = -\frac{\partial Y}{\partial \alpha_i}$$

$$V(x_i, \langle \beta_i\rangle)$$
$$\langle y_i\rangle = -\frac{\partial V}{\partial x_i}, \ \alpha_i = \frac{\partial V}{\partial \langle \beta_i\rangle}$$

$$Y(\langle y_i\rangle, \alpha_i)) + W(\langle x_i\rangle, \langle \beta_i\rangle) = -\alpha_i \langle \beta_i\rangle$$

$$V(x_i, \langle \beta_i\rangle) + W(\langle y_i\rangle, \langle \beta_i\rangle) = -x_i \langle y_i\rangle$$

$$W(\langle y_i\rangle, \langle \beta_i\rangle)$$
$$x_i = -\frac{\partial W}{\partial \langle y_i\rangle}, \ \alpha_i = -\frac{\partial W}{\partial \langle \beta_i\rangle}$$

[*J. Non-Equilib. Thermodyn.*, 2002]

Hill-Mandel condition

quasi-static responses

- (non)linear (thermo)elastic
- rigid-plastic
- elasto-plastic
- viscoelastic
- permeable
- poroelastic
- thermoelastic
- …

Hill-Mandel condition

<u>quasi-static responses</u>

•(non)linear (thermo)elastic
•rigid-plastic
•elasto-plastic
•viscoelastic
•permeable
•poroelastic
•thermoelastic
•…

<u>dynamic responses</u>

Hill-Mandel condition

<u>quasi-static responses</u>

•(non)linear (thermo)elastic
•rigid-plastic
•elasto-plastic
•viscoelastic
•permeable
•poroelastic
•thermoelastic
•…

<u>dynamic responses</u>

<u>non-Cauchy materials</u>

- Cosserat
- dynamic responses

Hill-Mandel condition

<u>quasi-static responses</u>

•(non)linear (thermo)elastic
•rigid-plastic
•elasto-plastic
•viscoelastic
•permeable
•poroelastic
•thermoelastic
•…

<u>formulation of tensor random fields</u>

- one-point statistics
- scaling laws
- correlation structure
- …

<u>dynamic responses</u>

<u>non-Cauchy materials</u>

- Cosserat
- dynamic responses

Determine mesoscale properties from Hill-Mandel condition: for dynamics of Cauchy materials

$$\overline{\sigma_{ji}\ \dot{\varepsilon}_{ji}} = \overline{\sigma_{ji}}\ \overline{\dot{\varepsilon}_{ji}} \quad \Leftrightarrow \quad \frac{1}{V}\int_S \left(t_i - \overline{\sigma_{ki}}\ n_k\right)\left(\dot{u}_i - \overline{\dot{\varepsilon}_{ij}}\ x_j\right)\ dS - \overline{\dot{k}} + (\overline{k})^{\cdot} = 0$$

$\Rightarrow$ Uniform boundary conditions: $\quad \forall x \in \partial B_\delta$

- displacement (Dirichlet) b.c. $\quad \dot{u}_i - \overline{\dot{\varepsilon}_{ij}}\ x_j$

- traction (Neumann) b.c. $\quad t_i = \overline{\sigma_{ki}}\ n_k$

- displacement-traction b.c. (mixed-orthogonal) $\quad \left(t_i - \overline{\sigma_{ki}}\ n_k\right)\left(\dot{u}_i - \overline{\dot{\varepsilon}_{ij}}\ x_j\right) = 0$

Determine mesoscale properties from Hill-Mandel condition: for dynamics of Cosserat materials

$$\overline{\tau_{ji}\ \dot{\gamma}_{ji}} - \overline{\tau_{ji}}\ \overline{\dot{\gamma}_{ji}} + \overline{\mu_{ji}\ \dot{\kappa}_{ji}} - \overline{\mu_{ji}}\ \overline{\dot{\kappa}_{ji}} =$$

$$\tfrac{1}{V}\int_S \left(t_i - \overline{\tau_{ki}}\ n_k\right)\left(\dot{u}_i - \overline{\dot{u}_{i,j}}\ x_j\right)\ dS + \tfrac{1}{V}\int_S \left(m_i - \overline{\mu_{ki}}\ n_k\right)\left(\dot{\phi}_i - \overline{\dot{\phi}_{i,j}}\ x_j\right)\ dS +$$

$$-\overline{\dot{k}_c} + (\overline{k_c})^{\cdot} - \overline{\dot{k}_m} + (\overline{k_m})^{\cdot}$$

$\Longrightarrow$ Uniform boundary conditions:

$$t_i(\mathbf{x}) = \overline{\tau_{ki}}\ n_k \quad \text{and} \quad m_i(\mathbf{x}) = m_i^0 + \overline{\mu_{ji}}\ n_j \qquad \forall \mathbf{x} \in \partial B$$

$$t_i(\mathbf{x}) = \overline{\tau_{ki}}\ n_k \quad \text{and} \quad \dot{\phi}_i(\mathbf{x}) = \frac{1}{2} e_{lji}\ \overline{\dot{\alpha}_{ji}} + \overline{\dot{\kappa}_{ji}}\ \left(x_j - X_j\right) \qquad \forall \mathbf{x} \in \partial B$$

$$m_i(\mathbf{x}) = m_i^0 + \overline{\mu_{ji}}\ n_j \quad \text{and} \quad \dot{u}_i(\mathbf{x}) = \overline{\dot{\varepsilon}_{ji}}\ x_j \qquad \forall \mathbf{x} \in \partial B$$

$$\dot{u}_i(\mathbf{x}) = \overline{\dot{\varepsilon}_{ji}}\ x_j \quad \text{and} \quad \dot{\phi}_i(\mathbf{x}) = \frac{1}{2} e_{lji}\ \overline{\dot{\alpha}_{ji}} + \overline{\dot{\kappa}_{ji}}\ \left(x_j - X_j\right) \qquad \forall \mathbf{x} \in \partial B$$

$$\dot{\gamma}_{ji} = \dot{u}_{i,j} - e_{kji}\dot{\phi}_k \qquad \dot{\kappa}_{ji} = \dot{\phi}_{i,j}$$

Define:

classical and micropolar kinetic energies

$$k_c = \tfrac{1}{2}\rho\upsilon_i\upsilon_i \qquad \upsilon_i \equiv \dot{u}_i$$

$$k_m = \tfrac{1}{2}I_{ij}w_iw_j \qquad w_i \equiv \dot{\phi}_i$$

their volume averages

$$\overline{k_c} = \tfrac{1}{V}\int_V k_c dV$$

$$\overline{k_m} = \tfrac{1}{V}\int_V k_m dV$$

time rates of these averages

$$(\overline{k_c})^{\cdot} \equiv \tfrac{d}{dt}\left(\tfrac{1}{V}\int_V k_c dV\right) = \tfrac{d}{dt}\left(\tfrac{1}{V}\int_V \tfrac{1}{2}\rho\boldsymbol{\upsilon}\cdot\boldsymbol{\upsilon}dV\right)$$

$$(\overline{k_m})^{\cdot} \equiv \tfrac{1}{V}\int_V k_m dV = \tfrac{d}{dt}\left(\tfrac{1}{V}\int_V \tfrac{1}{2}\mathbf{I} \,:\, \mathbf{w}\cdot\mathbf{w}dV\right)$$

volume averages of rates of volume averaged kinetic energies

$$\overline{\dot{k}_c} \equiv \tfrac{1}{V}\int_V \dot{k}_c dV = \tfrac{1}{V}\int_V\left(\tfrac{1}{2}\rho\upsilon_i^2\right)^{\cdot} dV = \tfrac{1}{V}\int_V \rho\upsilon_i\dot{\upsilon}_i dV \equiv \tfrac{1}{V}\int_V \rho\dot{u}_i\ddot{u}_i dV$$

$$\overline{\dot{k}_m} \equiv \tfrac{1}{V}\int_V \dot{k}_m dV = \tfrac{1}{V}\int_V\left(\tfrac{1}{2}\rho\phi_i^2\right)^{\cdot} dV = \tfrac{1}{V}\int_V \rho w_i\dot{w}_i dV \equiv \tfrac{1}{V}\int_V \rho\dot{\phi}_i\ddot{\phi}_i dV$$

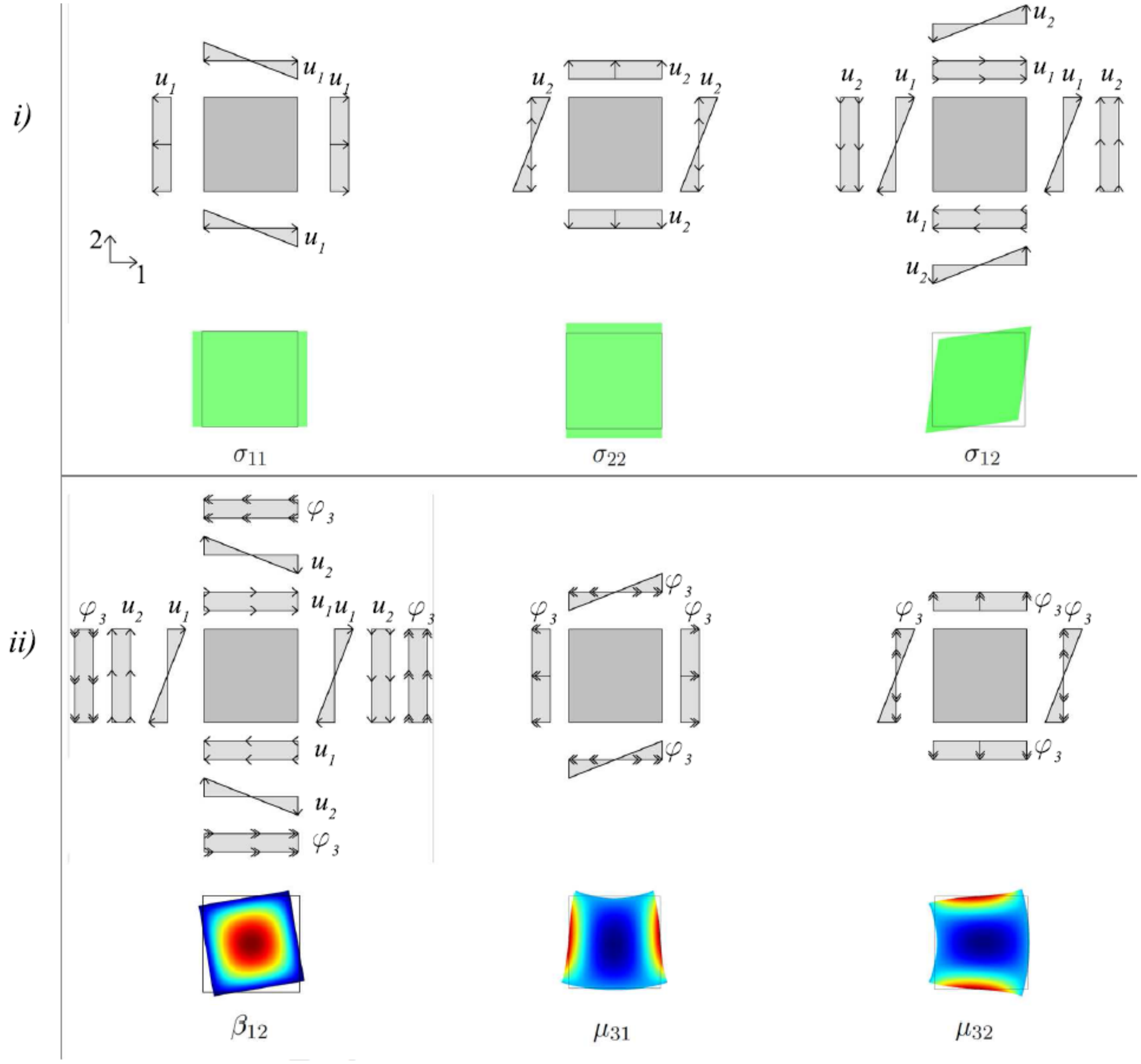

[P. Trovalusci, “Particulate random composites homogenized as micropolar materials,” *Meccanica* **49**, 2014]
[P. Trovalusci, “Scale-dependent homogenization of random composites as micropolar continua,” *Europ. J. Mech./A: Solids* **49**, 2014]

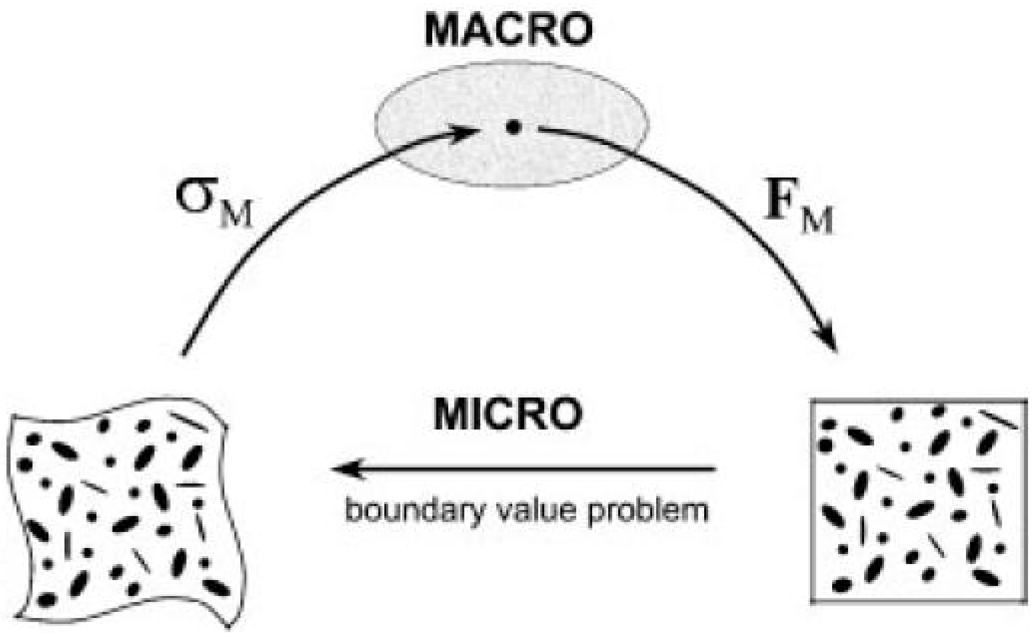

first-order
homogenization scheme

↓

second-order
homogenization scheme

[Forest & Sab, Kuznetsova & Geers, Onck, Trovalusci, …]

- **Convergence to RVE depends on:**
  - Elastic versus inelastic microstructure
    faster slower
  - mismatch in properties
  - 2d or 3d
  - microscale geometries (disks *versus* ellipses, spatial clustering…)

- **Convergence to RVE in linear elastic microstructures:**
  - mesoscale moduli of stiff matrix w. soft inclusions converge (much) more slowly to RVE than those of soft matrix w. stiff inclusions
  - convergence to RVE is slowest in anti-plane, faster in in-plane, and fastest in 3-D elasticity

- **In problems w/o separation of scales need to work with random fields and solve stochastic b.v.p. (e.g. via stochastic FE), …**

Microstructural Randomness and Scaling in Mechanics of Materials, Taylor & Francis/CRC Modern Mech. Math. Series, 2007.

Coupled scale and b.c. effects in random media:

linear elasticity:
random: Huet (1990, …), O-S (1989, …), Sab (1992), Terada & Kikuchi (2002), Forest & Jeulin (2003) …
periodic: Hollister & Kikuchi (1992), Pecullan, Gibiansky & Torquato (1999) Jiang, Jasiuk & O-S (2002, …) …

nonlinear elasticity: Hazanov (1999), …

viscoelasticity: Huet (1998)

elasto-plasticity: Jiang, O-S & Jasiuk (2001)

rigid-perfect plasticity, elasto-plasticity

thermoelasticity: O-S

elasticity + damage

Viscoelastic random materials

- Constitutive law

$$\sigma_{ij}(t) = \int_{0^-}^{t} r_{ijkl}(t-\tau)\dot{\varepsilon_{kl}}(\tau)d\tau\,;\ \varepsilon_{ij}(t) = \int_{0^-}^{t} f_{ijkl}(t-\tau)\dot{\sigma_{kl}}(\tau)d\tau$$

where $r_{ijkl}(t)$ and $f_{ijkl}(t)$ are the ***relaxation modulus*** and ***creep compliance***

- Special case: steady harmonic oscillation
  - Let $\varepsilon_{ij}(t) = \varepsilon_{ij}{}^{A} e^{i\omega t}$ and $\sigma_{ij}(t) = \sigma_{ij}{}^{A} e^{i\omega t}$

$$\sigma_{ij}{}^{A}(i\omega) = r^{*}{}_{ijkl}(i\omega)\varepsilon_{ij}{}^{A}(i\omega);\ \ \varepsilon_{ij}{}^{A}(i\omega) = f^{*}{}_{ijkl}(i\omega)\sigma_{ij}{}^{A}(i\omega)$$

where $r^{*}{}_{ijkl}(i\omega)$ and $f^{*}{}_{ijkl}(i\omega)$ are ***complex modulus*** and ***complex compliance***

- Modified Hill-Mandel condition

$$\overline{\boldsymbol{\sigma}:\dot{\boldsymbol{\varepsilon}}} = \overline{\boldsymbol{\sigma}}:\overline{\dot{\boldsymbol{\varepsilon}}}$$

[Huet, 1995]

- Time-dependent:
  - Kinematic Uniform Boundary Condition (KUBC)

$$u_i(x,t) = \varepsilon_{ij}{}^0\,(t)x_j \quad \forall x \in \partial V \qquad \boxed{\overline{\varepsilon_{ij}(x,t)} = \varepsilon_{ij}{}^0\,(t)}$$

  - Static Uniform Boundary Condition (SUBC)

$$t_i(x,t) = \sigma_{ij}{}^0(t)n_j \quad \forall x \in \partial V \qquad \boxed{\overline{\sigma_{ij}(x,t)} = \sigma_{ij}{}^0\,(}$$

mesoscale properties

- Time-domain properties:

$$\textit{Let } u_i(x,t) = \varepsilon_{ij}{}^0\, x_j(x)H(t) \;\; \textit{on} \;\; \partial V$$
$$\overline{\boldsymbol{\sigma}_{ij}(\boldsymbol{t})} = \overline{r_{ijkl}(x,t) \circ \varepsilon_{kl}(x,t)} = r^d_{ijkl,\delta}(t)\varepsilon_{kl}{}^0$$

$$\textit{Let } \boldsymbol{t}_i(x,t) = \boldsymbol{\sigma}_{ij}{}^0\, \boldsymbol{n}_j(x)H(t) \;\; \textit{on} \;\; \partial V$$
$$\overline{\boldsymbol{\varepsilon}_{ij}(\boldsymbol{t})} = \overline{f_{ijkl}(x,t) \circ \sigma_{kl}(x,t)} = f^t_{ijkl,\delta}(t)\sigma_{kl}{}^0$$

$$\langle r^d_{ijkl,\delta}(t)\rangle$$
$$\langle f^t_{ijkl,\delta}(t)\rangle$$

- Frequency-domain properties:

$$\textit{Let } u_i(x,t) = \varepsilon_{ij}{}^0\, x_j(x)\boldsymbol{e}^{\boldsymbol{i\omega t}} \;\; \textit{on} \;\; \partial V$$
$$\overline{\boldsymbol{\sigma}_{ij}\ (\boldsymbol{i\omega})}^A = \overline{r^*{}_{ijkl}(x,i\omega)\varepsilon_{kl}(x,i\omega)} = r^*{}^d_{ijkl,\delta}(i\omega)\varepsilon_{kl}{}^0$$

$$\textit{Let } t_i(x,t) = \sigma_{ij}{}^0\, n_j(x)e^{i\omega t} \;\; \textit{on} \;\; \partial V$$
$$\overline{\boldsymbol{\varepsilon}_{ij}\ (\boldsymbol{i\omega})}^A = \overline{f^*{}_{ijkl}(x,i\omega)\sigma_{kl}(x,i\omega)} = f^*{}^t_{ijkl,\delta}(i\omega)\sigma_{kl}{}^0$$

$$\langle r^*{}^d_{ijkl,\delta}(i\omega)\rangle$$
$$\langle f^*{}^t_{ijkl,\delta}(i\omega)\rangle$$

scale dependent homogenization

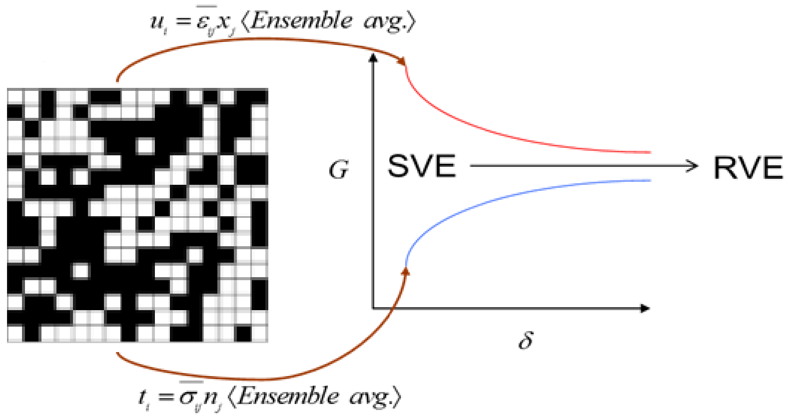

- Viscoelastic minimum theorems [Huet, 1995, 1999]
  - time domain properties

$$f^{eff}(t) \leq \ldots \leq \langle f_{\delta'}(t)\rangle \leq \langle f_{\delta}(t)\rangle \leq \ldots \leq \langle f_1(t)\rangle$$

$$r^{eff}(t) \leq \ldots \leq \langle r_{\delta'}(t)\rangle \leq \langle r_{\delta}(t)\rangle \leq \ldots \leq \langle r_1(t)\rangle \qquad \forall \delta' > \delta\,, t > 0$$

  - frequency domain properties

$$Re\left(r^*{}_{eff}\right) \leq \ldots \leq Re(\langle r^*{}_{\delta'}\rangle) \leq Re(\langle r^*{}_{\delta}\rangle) \leq \ldots \leq Re(\langle r^*{}_1\rangle)$$

$$Im\left(r^*{}_{eff}\right) \leq \ldots \leq Im(\langle r^*{}_{\delta'}\rangle) \leq Im(\langle r^*{}_{\delta}\rangle) \leq \ldots \leq Im(\langle r^*{}_1\rangle) \qquad \forall \delta' = 2\delta\,, t > 0$$

$$Re\left(f^*{}_{eff}\right) \leq \ldots \leq Re(\langle f^*{}_{\delta'}\rangle) \leq Re(\langle f^*{}_{\delta}\rangle) \leq \ldots \leq Re(\langle f^*{}_1\rangle)$$

$$-Im\left(f^*{}_{eff}\right) \leq \ldots \leq -Im(\langle f^*{}_{\delta'}\rangle) \leq -Im(\langle f^*{}_{\delta}\rangle) \leq \ldots \leq -Im(\langle f^*{}_1\rangle)$$

computational procedure

- Material representation (Prony series)
  - isotropic linear viscoelastic phases

$$r_R(t) = 1 - \sum_{i=1}^{N} \bar{r}_i (1 - e^{-\frac{t}{\tau_i}})$$

	Type	E	v	g_1	k_1	τ_1
Mat 1	Elastic	60	0.3			
Mat 2	Viscoelastic	30	0.3	0.9	0.25	0.25

- Finite element analysis
  - perfect bonding between interfaces
  - quasi-static loading
  - small strain, plane stress

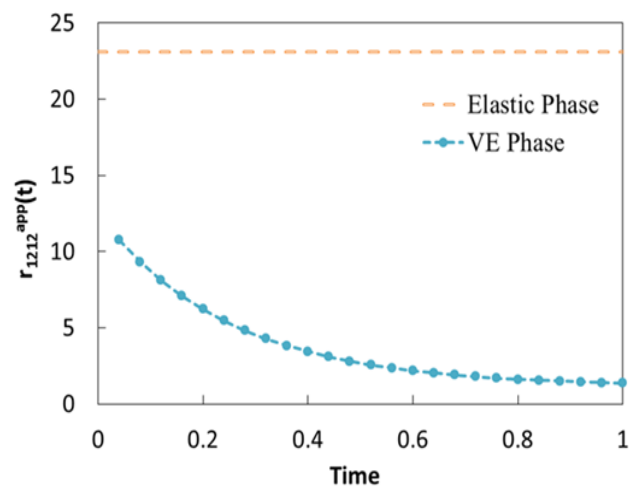

$$g_R(t) = 1 - \sum_{i=1}^{N} \bar{g}_i \, (1 - e^{-\frac{t}{\tau_i}}) \text{ and } G(t) = G \, * \, g_R(t)$$
$$k_R(t) = 1 - \sum_{i=1}^{N} \bar{k}_i \, (1 - e^{-\frac{t}{\tau_i}}) \text{ and } \mathrm{K}(t) = K \, * \, k_R(t)$$

- Simulation in the time domain :
  - Relaxation shear modulus $\mu_\delta(t)$
  - BCs: prescribed tensor $\varepsilon_{ij}^0 = \varepsilon_{12}^0 \begin{bmatrix} 0 & 1 \\ 1 & 0 \end{bmatrix}$; $\sigma_{ij}^0 = \sigma_{12}^0 \begin{bmatrix} 0 & 1 \\ 1 & 0 \end{bmatrix}$
    - KUBC: $u_i(x,t) = \varepsilon_{ij}{}^0\, x_j(x) T(t) \quad \forall x \in \partial V$
    - SUBC: $t_i(x,t) = \sigma_{ij}{}^0\, n_j(x) T(t) \quad \forall x \in \partial V$

Scenario 1 : Let $T(t) = \boldsymbol{H(t)}$

$$\mu_\delta^d(t) = \frac{\overline{\sigma_{12}(t)}}{\varepsilon_{12}^0}; \quad J_\delta^t(t) = \frac{\overline{\varepsilon_{12}(t)}}{\sigma_{12}^0}$$

$\Rightarrow$

$\langle \mu_\delta^d(t) \rangle$

$\langle J_\delta^t(t) \rangle$

Hierarchies of mesoscale bounds

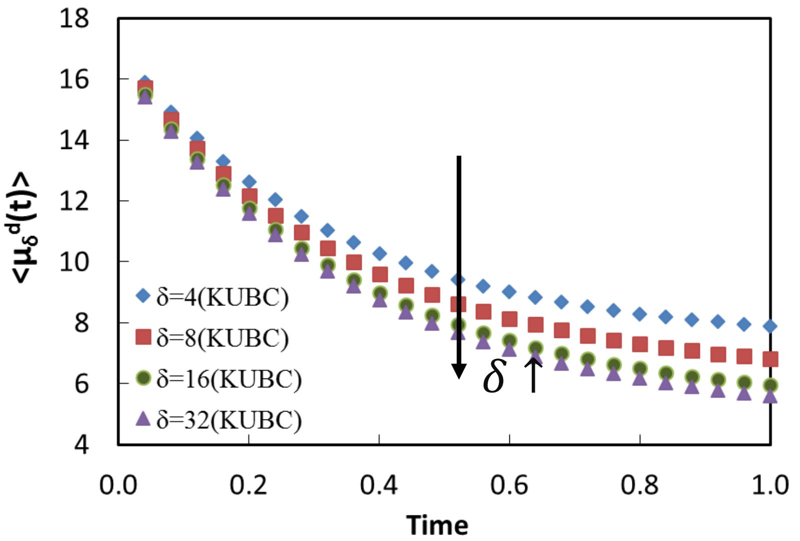

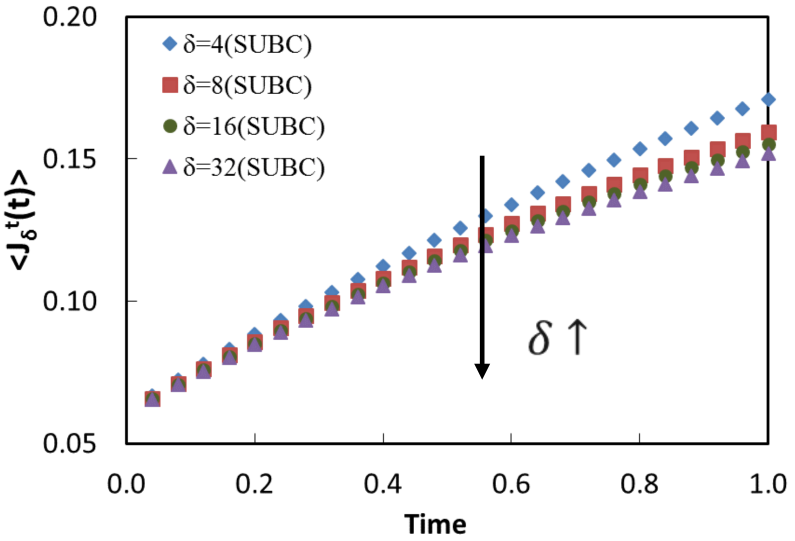

$$f^{eff}(t) \leq \ldots \leq \langle f_{\delta'}(t)\rangle \leq \langle f_{\delta}(t)\rangle \leq \ldots \leq \langle f_1(t)\rangle$$

$$r^{eff}(t) \leq \ldots \leq \langle r_{\delta'}(t)\rangle \leq \langle r_{\delta}(t)\rangle \leq \ldots \leq \langle r_1(t)\rangle$$

$$\forall \delta' = 2\delta\, , t > 0$$

$$\boxed{\langle f_1(t)\rangle^{-1} \leq .. \leq \langle f_{\delta}(t)\rangle^{-1} \leq \langle f_{\delta'}(t)\rangle^{-1} \leq .. \leq f^{eff}(t)^{-1} = r^{eff}(t) \leq .. \leq \langle r_{\delta'}(t)\rangle \leq \langle r_{\delta}(t)\rangle \leq .. \leq \langle r_1(t)\rangle}$$

[Hazanov, 1996; Huet, 1999]

Scaling from SVE to RVE

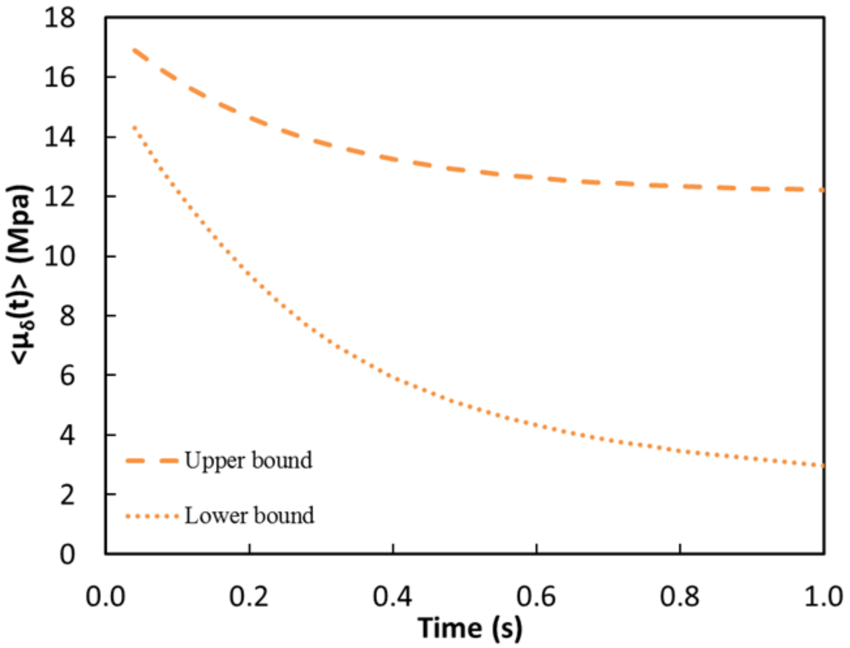

Scaling from SVE to RVE

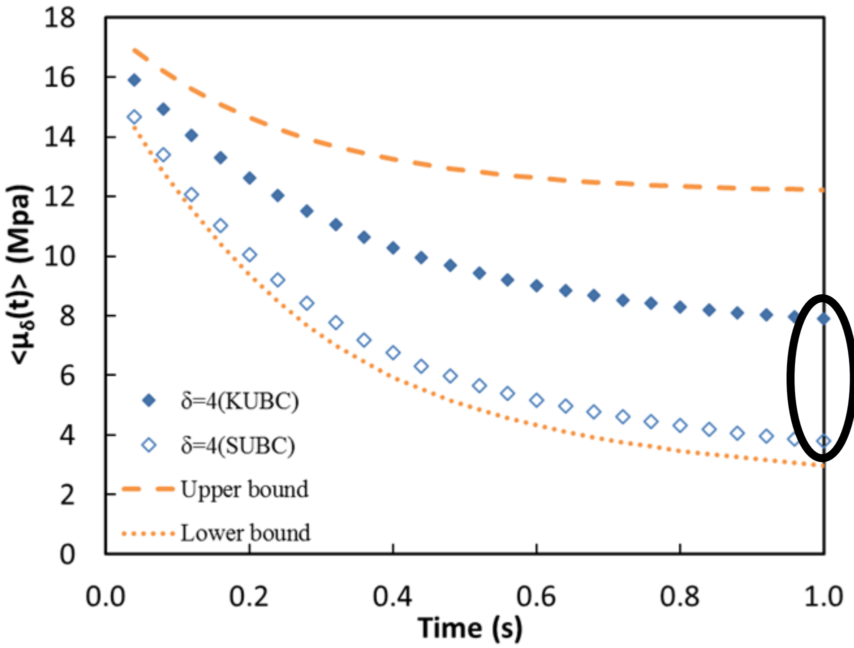

$\langle C_{\delta=4}(t=1.0\,\mathrm{s})\rangle = 7.889MPa$

$\langle S_{\delta=4}(t=1.0\,\mathrm{s})\rangle^{-1} = 3.810MPa$

$\Delta = 4.079MPa$

Scaling from SVE to RVE

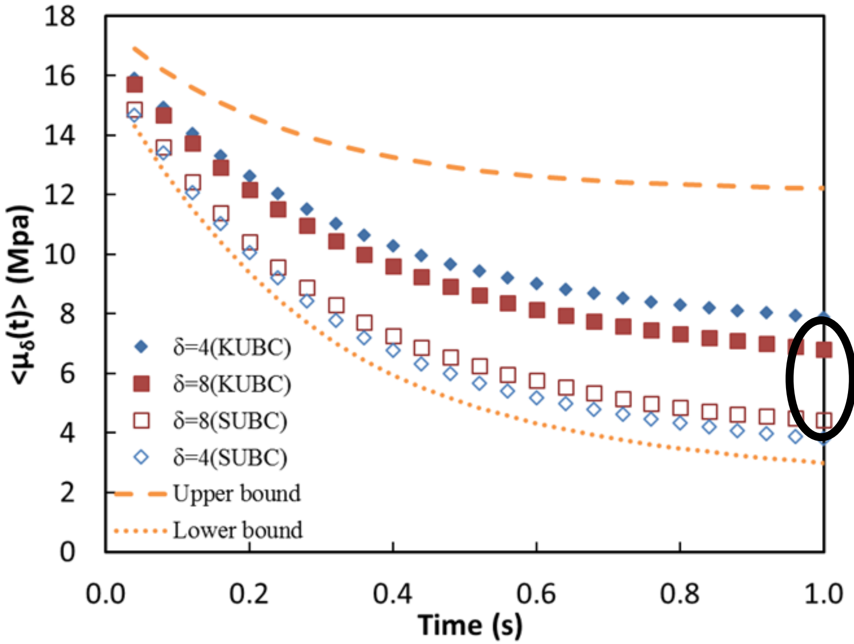

$$\left\langle C_{\delta=8}(t=1.0\,\mathrm{s})\right\rangle = 6.815MPa$$
$$\left\langle S_{\delta=8}(t=1.0\,\mathrm{s})\right\rangle^{-1} = 4.382MPa$$
$$\Delta = 2.433MPa$$

Scaling from SVE to RVE

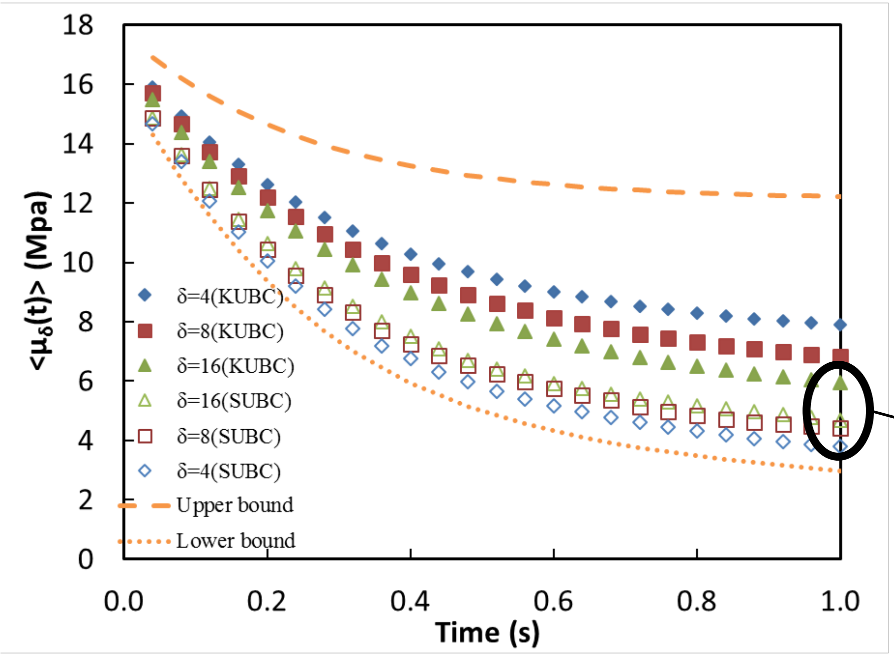

$$\left\langle C_{\delta=16}(t=1.0\,\mathrm{s})\right\rangle = 5.951MPa$$

$$\left\langle S_{\delta=16}(t=1.0\,\mathrm{s})\right\rangle^{-1} = 4.667MPa$$

$$\Delta = 1.284MPa$$

Scaling from SVE to RVE

- Interconversion between $\langle \mu_\delta(t) \rangle$ and $\langle J_\delta\,(t) \rangle$
  - analytical: $\int_0^t \mu_\delta(t-s) J_\delta(s) ds = t$, i.e. $\langle \mu_\delta(t) \rangle \neq \langle J_\delta\,(t) \rangle^{-1}$
  - engineering approach: $\mu(t) J(t) \approx \frac{\sin n\pi}{n\pi}$

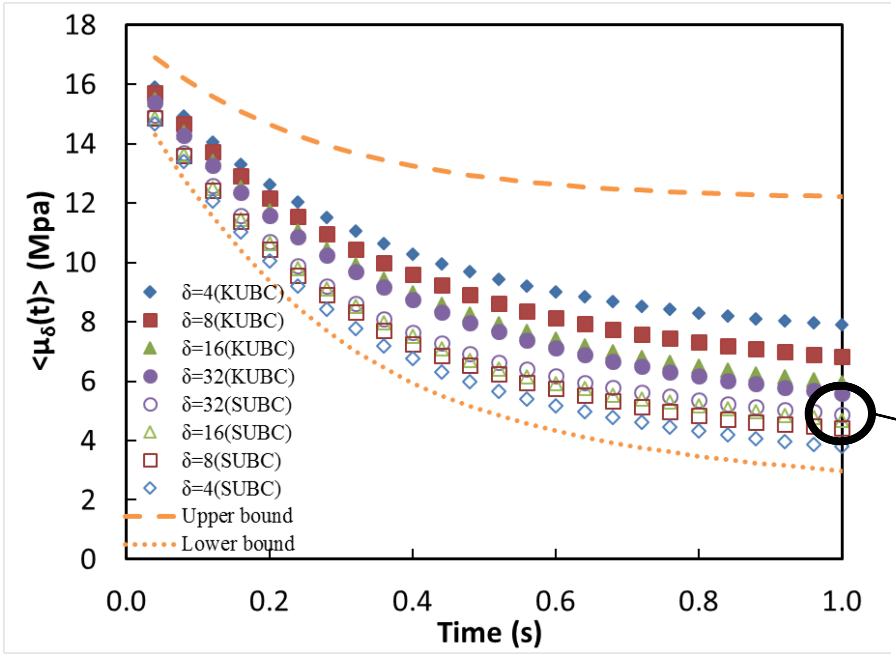

$\left\langle C_{\delta=32}(t=1.0\,\mathrm{s}) \right\rangle = 5.594 MPa$

$\left\langle S_{\delta=32}(t=1.0\,\mathrm{s}) \right\rangle^{-1} = 4.889 MPa$

$\Delta = 0.705 MPa$

[*Mech. Res. Comm*, 2015]

Scaling from SVE to RVE

- Observation
  - A good estimation for the effective properties can be approached by deriving mesoscale bounds
  - At $\delta = 32$, the maximum statistical scatter is $\Delta = 0.705MPa$

- Compare with elasticity

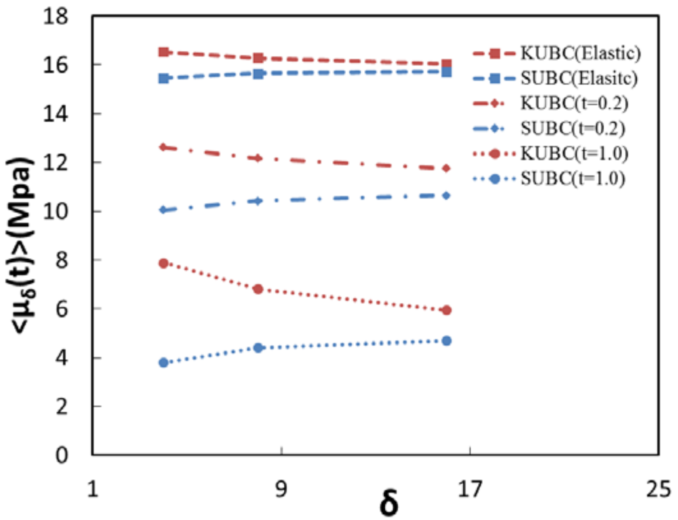

- discrepancy in viscoelastic mesoscale bounds is time dependent
- convergence rate is slower than in the analogous problem with elasticity
- viscoelasticity requires larger mesoscale to homogenize SVE to RVE

- Analysis in the **frequency domain**
  - Complex shear modulus $\mu_\delta{}^*(i\omega)$ and complex bulk modulus $k_\delta{}^*(i\omega)$
  - Constitutive relation becomes quasi-static at each given frequency
  - It is much easier for interconversion between modulus and compliance

Scenario 2 : Let T(t) = $e^{i\omega t}$

$$\mu^{*d}_{\delta} = \frac{\overline{\sigma_{12}}^A}{\varepsilon^0_{12}}; \quad J^{*t}_{\delta} = \frac{\overline{\varepsilon_{12}}^A}{\sigma^0_{12}} = (\mu^{*t}_{\delta})^{-1}$$

$$k^{*d}_{2D,\delta} = \frac{\overline{\sigma_{11} + \sigma_{22}}^A}{3(\varepsilon^0_{11} + \varepsilon^0_{22})}; \quad L^{*t}_{2D,\delta} = \frac{3(\overline{\varepsilon_{11} + \varepsilon_{22}}^A)}{\sigma^0_{11} + \sigma^0_{22}} = (k^{*t}_{2D,\delta})^{-1}$$

$\Rightarrow$

$$\langle \mu^{*d}_{\delta}(i\omega) \rangle$$

$$\langle \mu^{*t}_{\delta}(i\omega) \rangle$$

$$\langle k^{*d}_{2D,\delta}(i\omega) \rangle$$

$$\langle k^{*t}_{2D,\delta}(i\omega) \rangle$$

[*Proc. Roy. Soc. A*, 2016]

Frequency – dependent mesoscale bounds

- complex shear modulus

absolute value

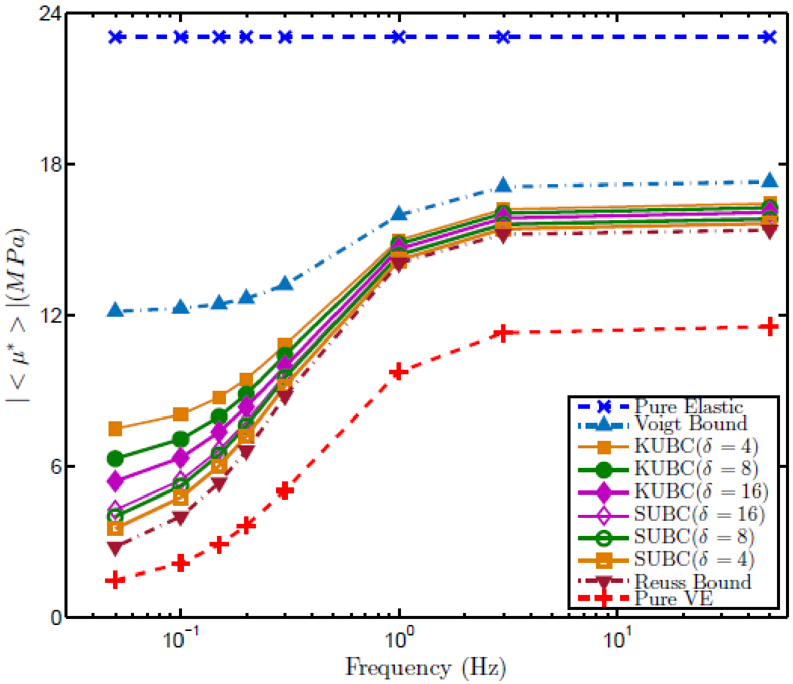

phase angle

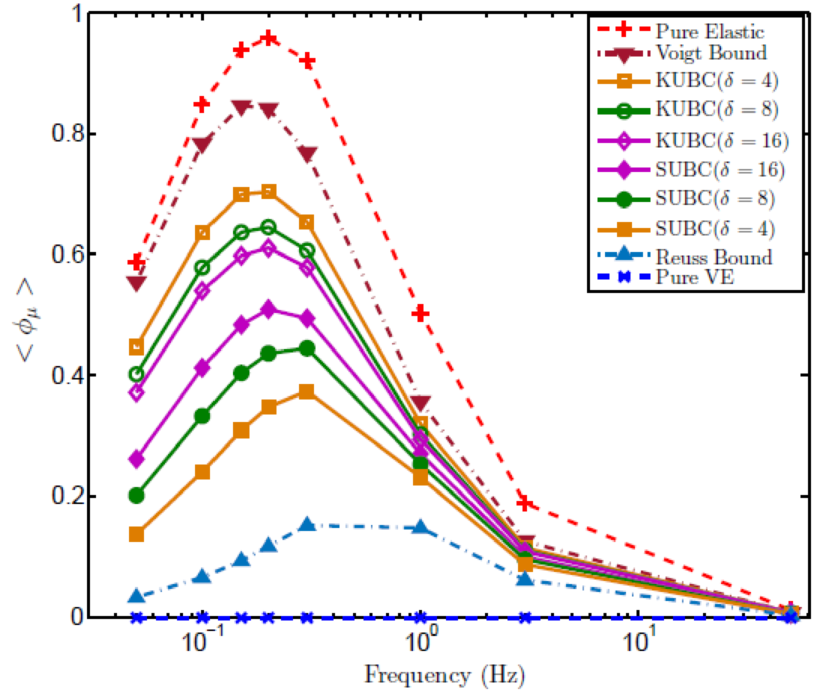

Frequency – dependent mesoscale bounds

- complex bulk modulus

absolute value

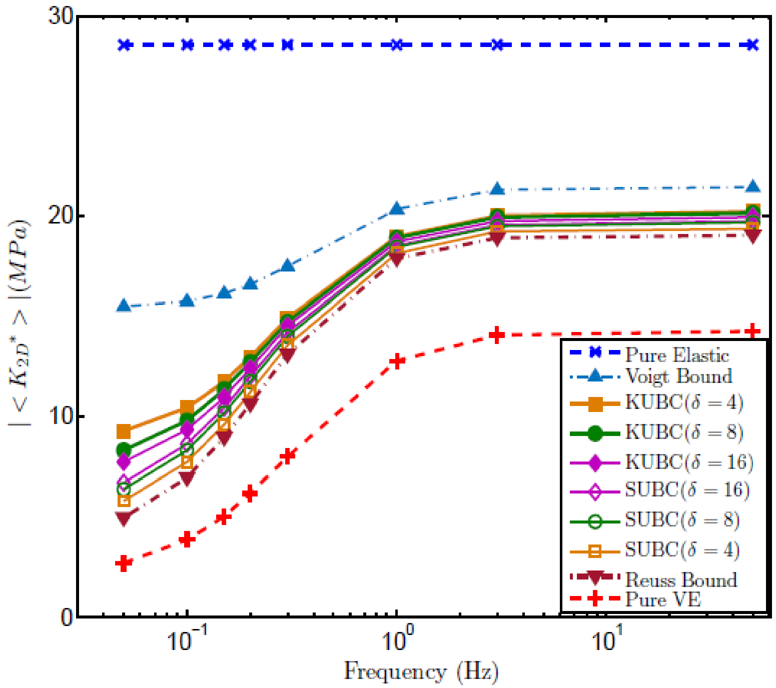

phase angle

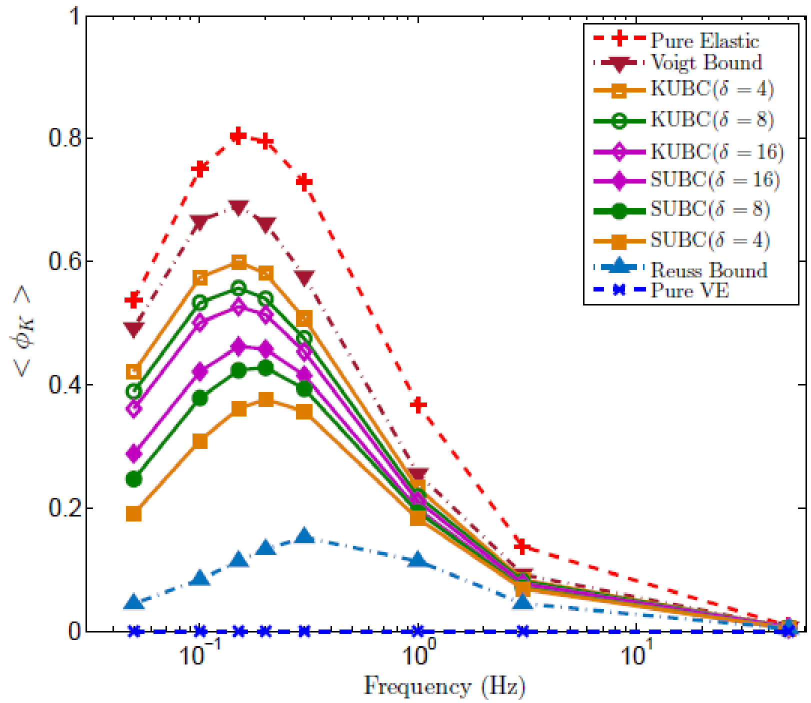

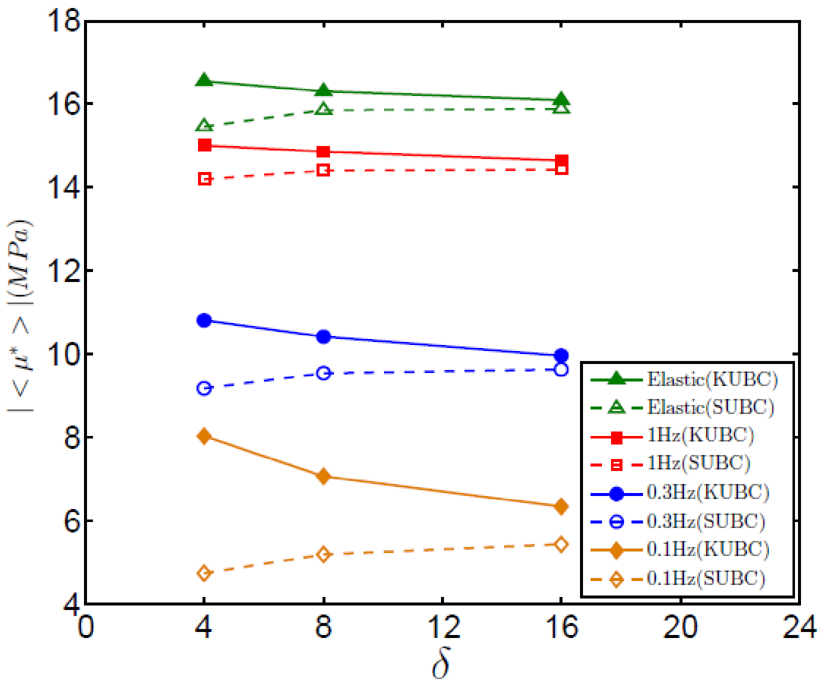

- VE mesoscale bounds are developed in a similar fashion as those in elasticity at each single frequency

- Convergence of mesoscale bounds depends on loading frequency

- Load frequency determines the physical properties of VE phase, or more fundamentally, the mismatch between component phases

- recall **scaling function** in
  - conductivity
  - linear and nonlinear elasticity
  - permeability

- **scaling function** for plane stress viscoelasticity

$$f^*(\delta, k_1^*, k_2^*, \mu_1^*, \mu_2^*, i\omega) = 2\frac{< {\mu^*}^d_{2D,\delta}(i\omega) >}{< {\mu^*}^t_{2D,\delta}(i\omega) >} + \frac{< {k^*}^d_{2D,\delta}(i\omega) >}{< k^t_{2D,\delta}(i\omega) >} - 3$$

  - f^* is complex
  - f^* is monotonically decreasing with mesoscale δ
  - $|f^*(\delta = \infty)| = 0$ which implies $\lim_{\delta\to\infty} Re(f^*) = \lim_{\delta\to\infty} Im\,(f^*) = 0$

- At $\delta = 1$, the controlled moduli equal the Voigt and Reuss bounds

$$f^*(\delta = 1\,) = 2\frac{{\mu^*}^{V}_{2D,\delta}(i\omega)}{{\mu^*}^{R}_{2D,\delta}(i\omega)} + \frac{{k^*}^{V}_{2D,\delta}(i\omega)}{k^{R}_{2D,\delta}(i\omega)} - 3$$

- Introduce a normalized scaling function $g^*(\delta)$

$$g^*(\delta\,) = \frac{f^*}{|f^*|_{\delta=1}}$$

  - $g^*(\delta)$ satisfies $0 \leq |g^*(\delta)| \leq 1$, $|g^*(1)| = 1$ and $|g^*(\infty)| = 0$

- Simulations on planar random checkerboard for:
  - wide range of loading frequencies (from 0.05 Hz to 50Hz)
  - many different materials combinations (VE-Elastic, Elastic-Elastic, VE-VE)

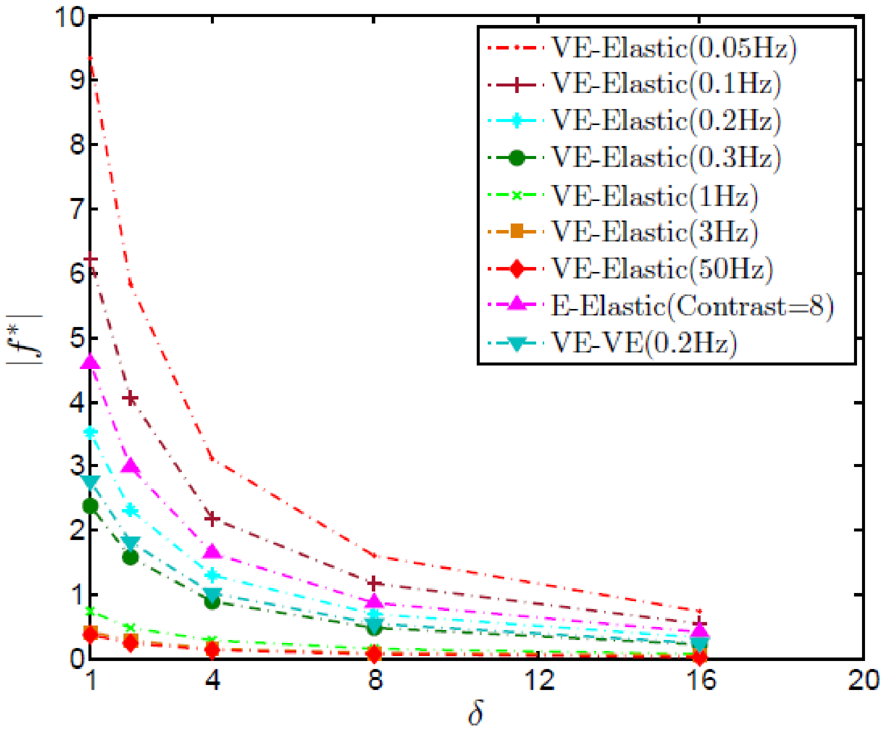

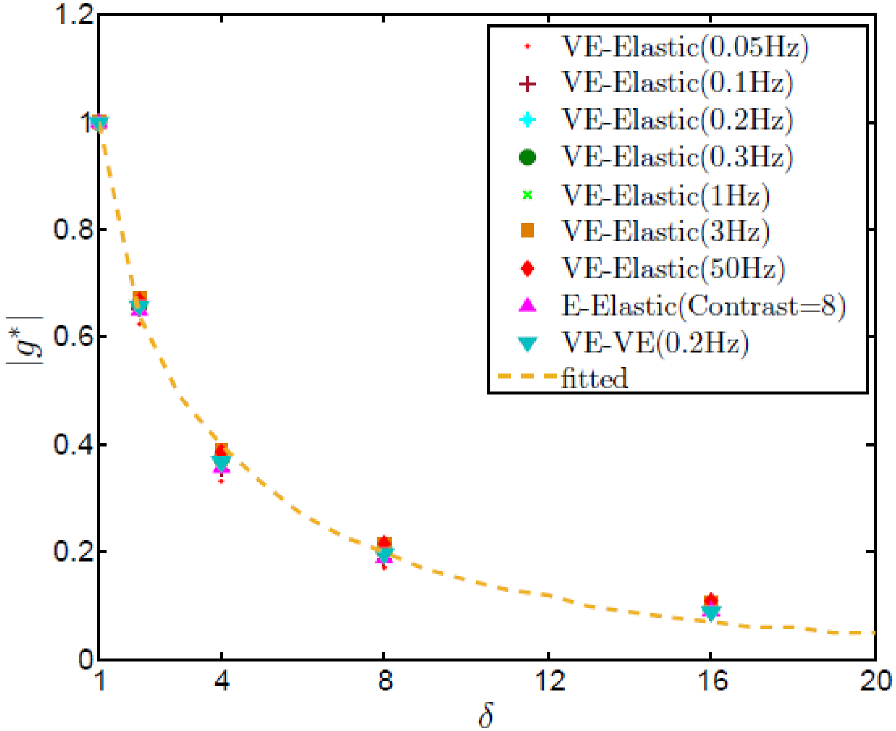

$$|g^*(\delta)| = \exp(-0.45 * (\delta - 1)^{0.66})$$

Conclude…

- Mesoscale bounds provide monotonically convergent bounds on RVE response of viscoelastic composites

- Viscoelastic composite generally requires larger domain to homogenize to within the same error than the elastic composite, to capture the long time and full frequency range behavior

- Normalized complex scaling function tracks the characteristic of microstructure and predicts the mesoscale behavior for any combinations of micro-constituents' properties

- Analogous scalings have been established in elastic and inelastic random microstructures [*Adv. Appl. Mech.*, 2016]

Random Field Models and Stochastic FE

Martin Ostoja-Starzewski
Department of Mechanical Science & Engineering
also Institute for Condensed Matter Theory, and Beckman Institute
University of Illinois at Urbana-Champaign

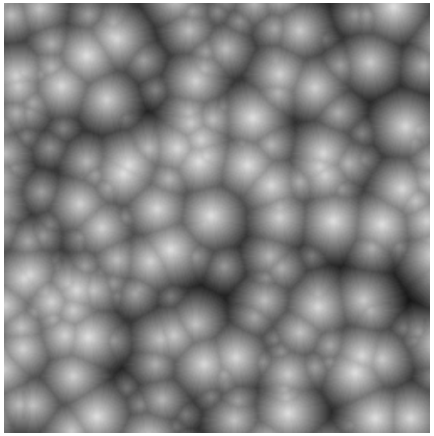

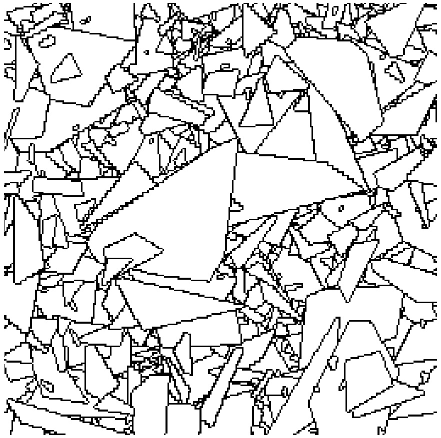

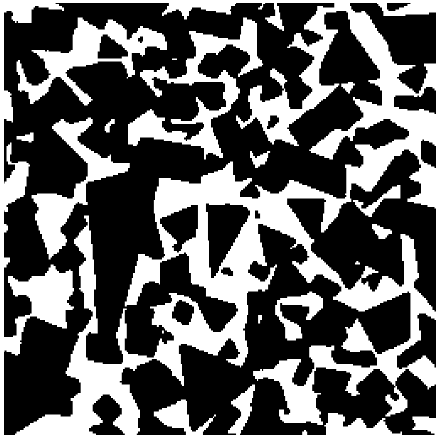

three scales:

microscale: average size of grain d
(microstructure)

mesoscale: L
if not RVE, then
inhomogeneous continuum

macroscale: L_{macro}

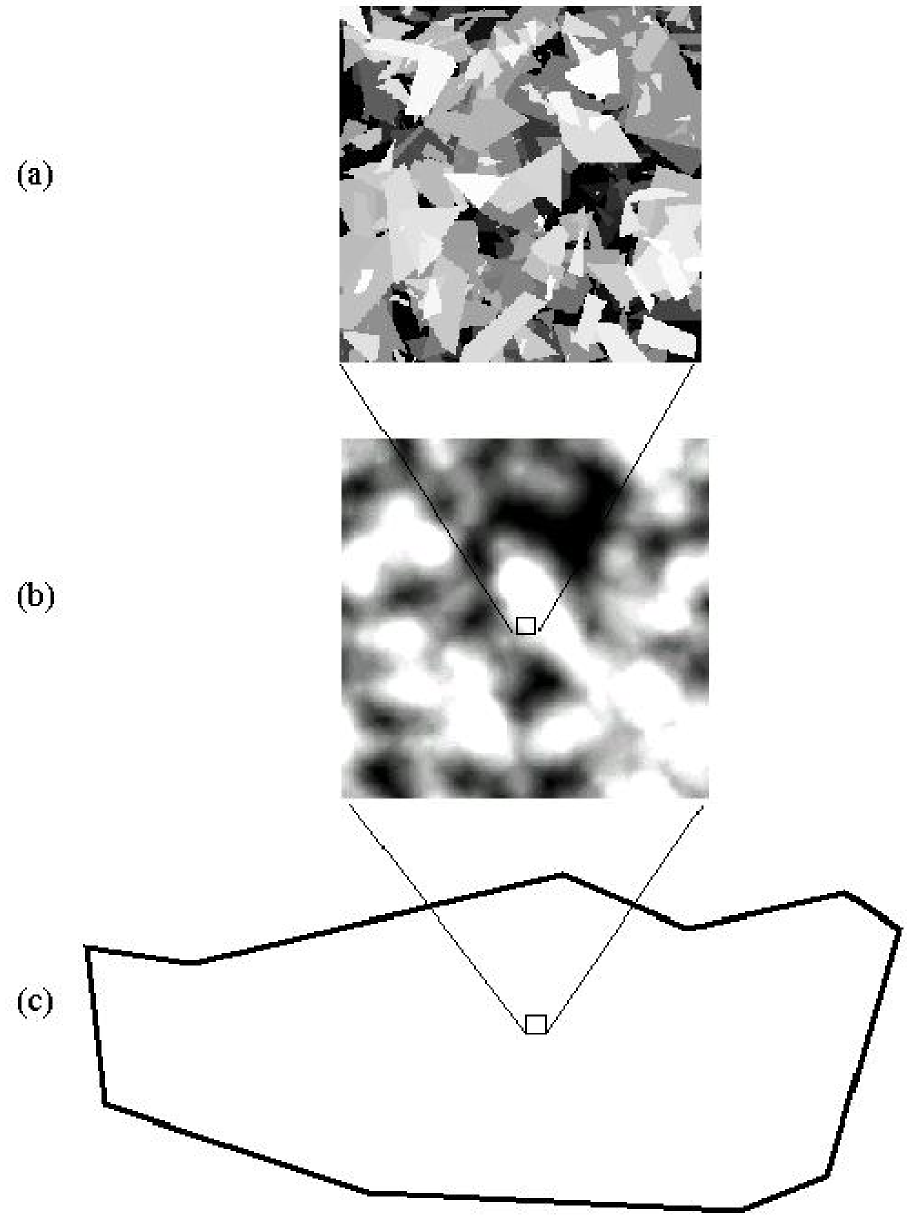

three scales:

microscale: average size of grain d
(microstructure)

mesoscale: L
if not RVE, then
inhomogeneous continuum

macroscale: L_{macro}

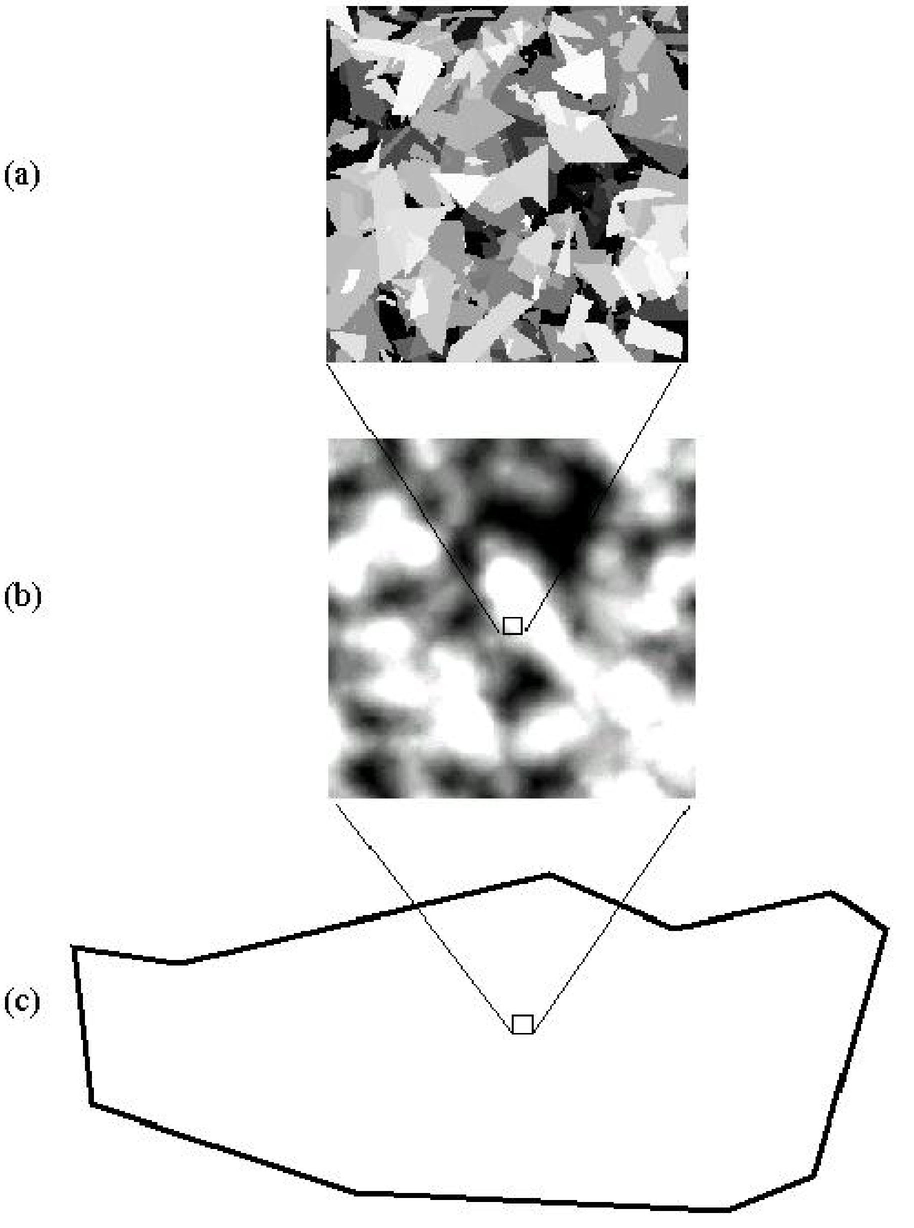

separation of scales $d << L << L_{macro}$
does not always hold!

three scales:

microscale: average size of grain d
(microstructure, non-fractal)

mesoscale: L
if not RVE, then
inhomogeneous continuum

macroscale: L_{macro}

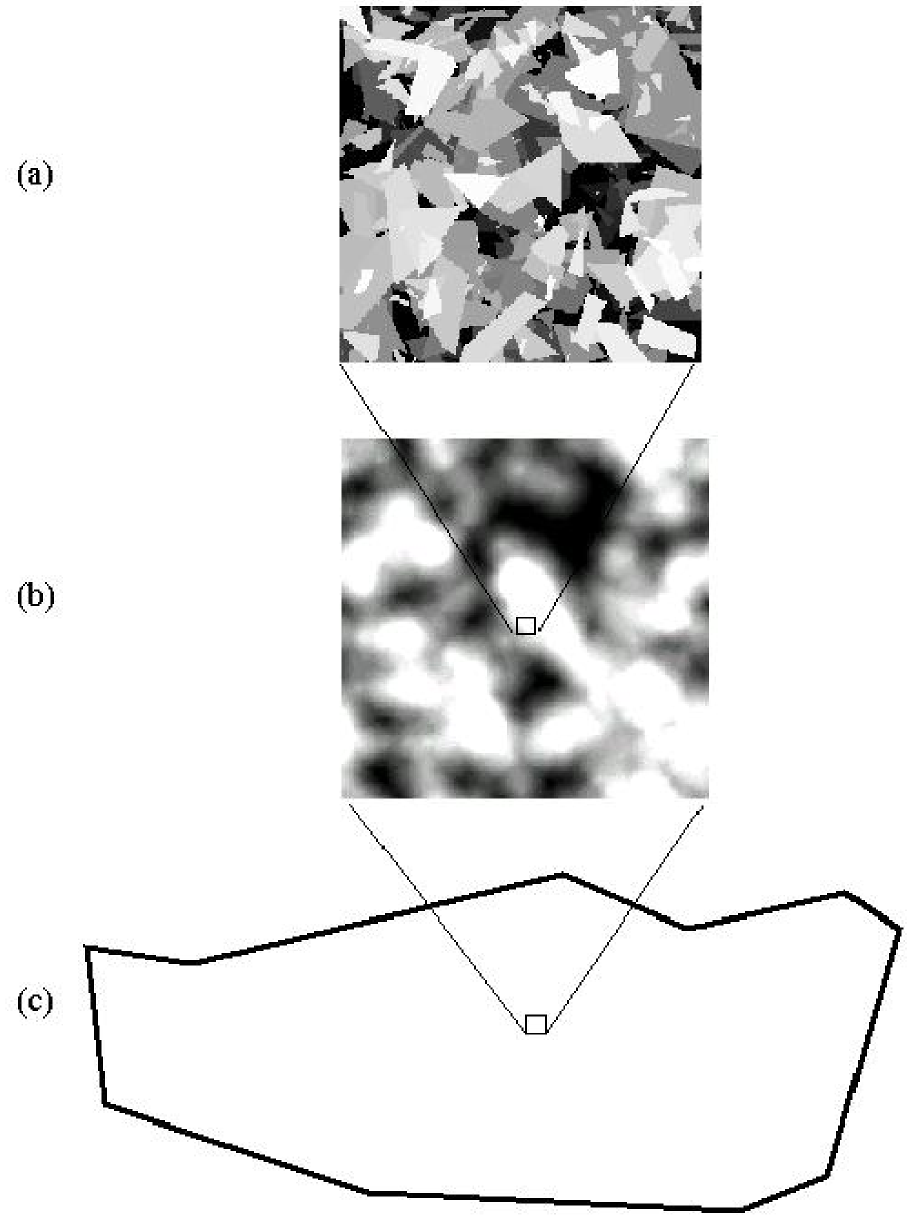

separation of scales $d << L << L_{macro}$
does not always hold!

Three ways for randomness to enter a problem in solid mechanics

$$Lu = f$$

L = field (differential) operator

- via forcing: $Lu = f(\omega) \qquad \omega \in \Omega$
- via boundary conditions: $u(\omega)$ on ∂B
- via field operator: $L(\omega)u = f$

Navier equation of linear elasticity (homogeneous, isotropic)

$$\mu u_{i,jj} + (\mu + \lambda) u_{j,ij} + f_i = 0$$

Beltrami-Michell equations of compatibility

$$\sigma_{ij,kk} + \frac{1}{1+\nu} \sigma_{kk,ij} + f_{i,j} + f_{j,i} + \frac{\nu}{1-\nu} \delta_{ij} f_{k,k} = 0$$

Navier-Stokes equation

$$\frac{\partial}{\partial t} v_i + v_{i,j} v_j = f_i - \frac{1}{\rho} p_{,i} + \frac{\mu}{\rho} v_{i,jj}$$

Wave equation in media with RF of mass density

Hyperbolic equation in media with vector RF (ρ,E)

…popular model in stochastic PDE literature

Not very physical

Assume $E=const$ $\Longrightarrow$ *stochastic Helmholtz equation*

Wave equation in media with RF of mass density

Hyperbolic equation in media with vector RF (ρ,E)

…very popular model in stochastic PDE literature

Not very physical!

Assume $E=const$ $\Longrightarrow$ *stochastic Helmholtz equation*

α

Recall finite-size scaling (in random chessboards)

$$C_\delta{}^{e} = \exp[-\delta^{-m_e}] \qquad S_\delta{}^{n} = \exp[\delta^{-m_n}]$$

$$m_e = 3.8\alpha^{0.14} \qquad m_n = 2.4\alpha^{0.59}$$

α = contrast

up to δ =1000

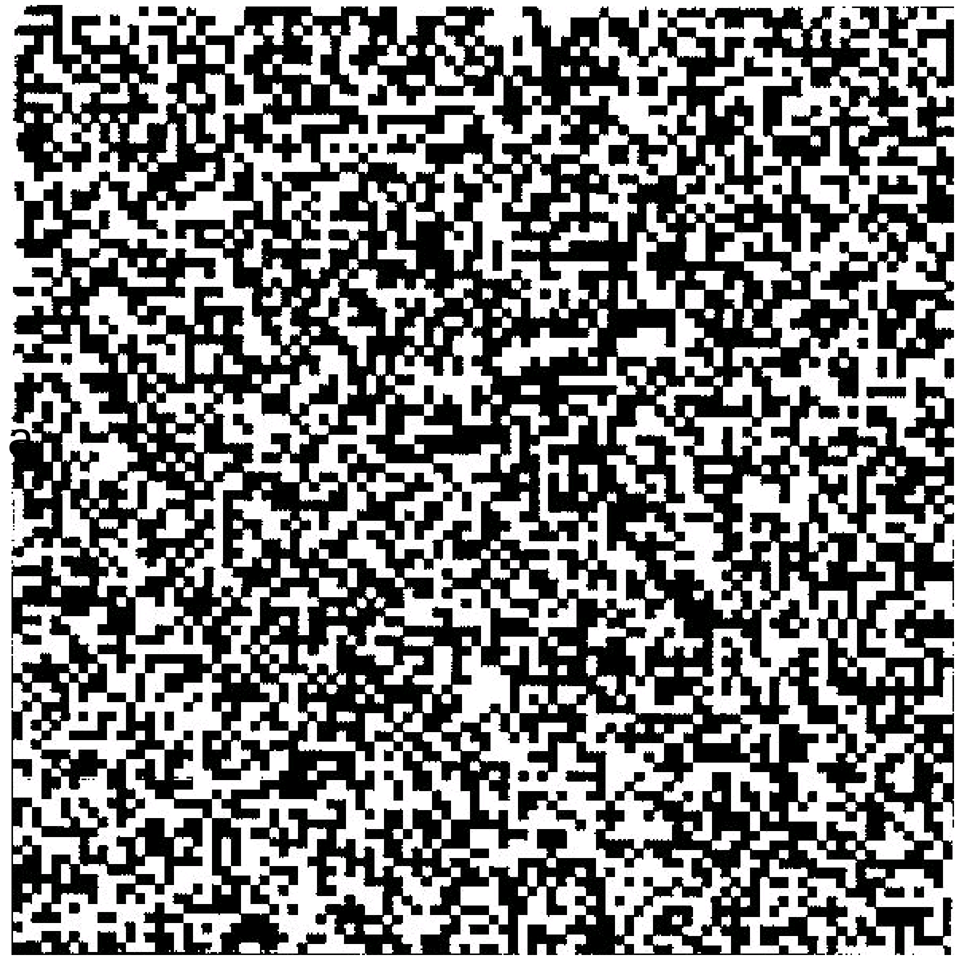

[*Phys. Rev. B*, 1996]

Mesoscale random fields:
as a bridge from micro (nano) to macro scales
as a basis of stochastic finite elements (SFE)

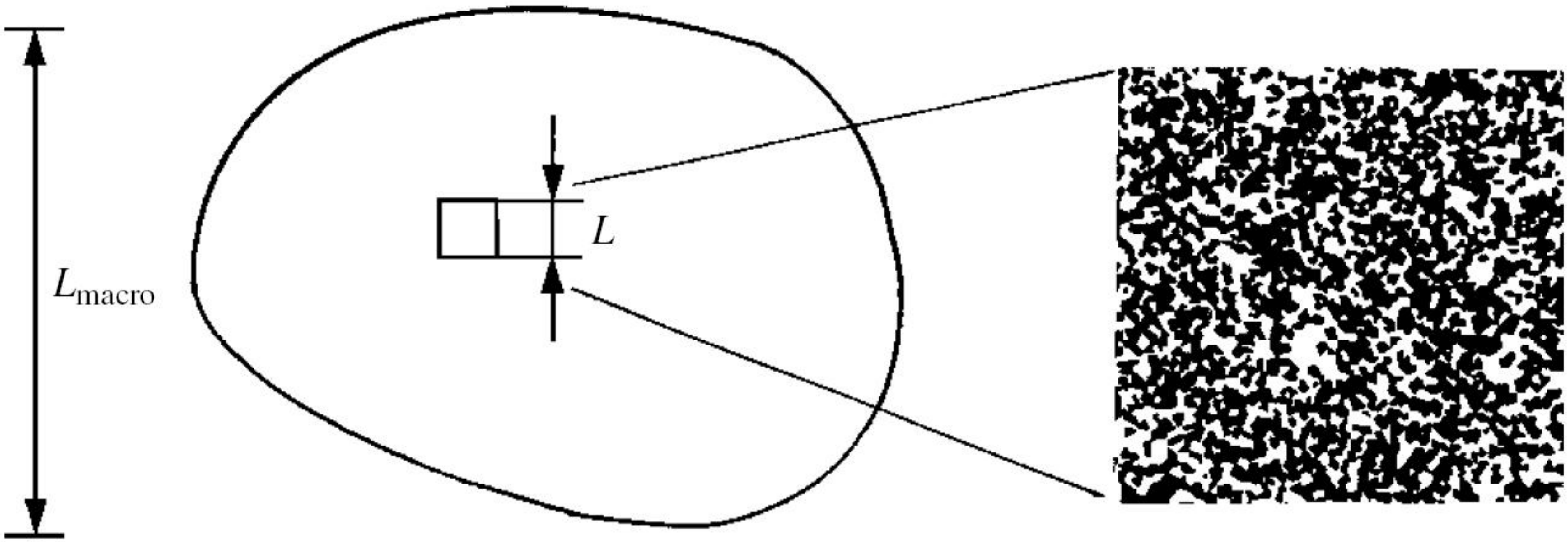

Figure 1. A macroscopic body with a mesoscale window (or finite element) of size L, in which a microstructure of grain size d is shown.

[*CMAME*, 1999; *Proc. Roy Soc. Lond. A*, 1999]

Torsion of a bar of square cross section with bi-percolating microstructure

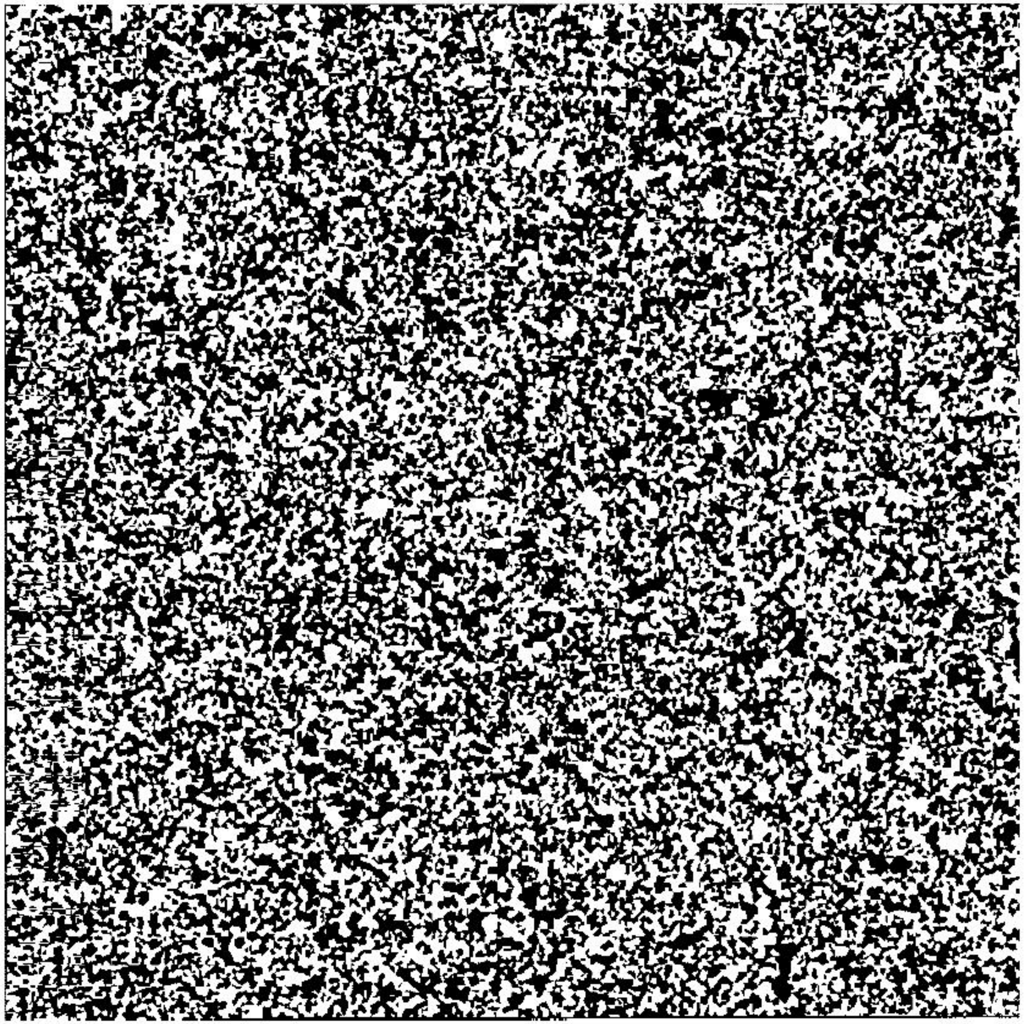

Figure 2. A two-phase material with a Voronoi mosaic microgeometry of a total 104 858 black and white cells, at volume fraction 50% each.

Mesoscale bounds:

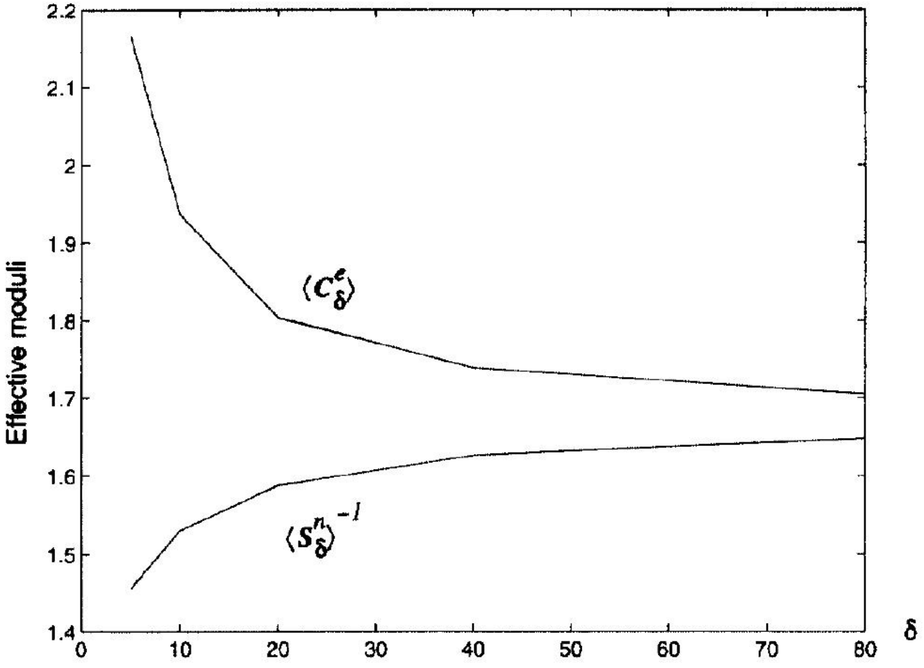

Mesoscale bounds:

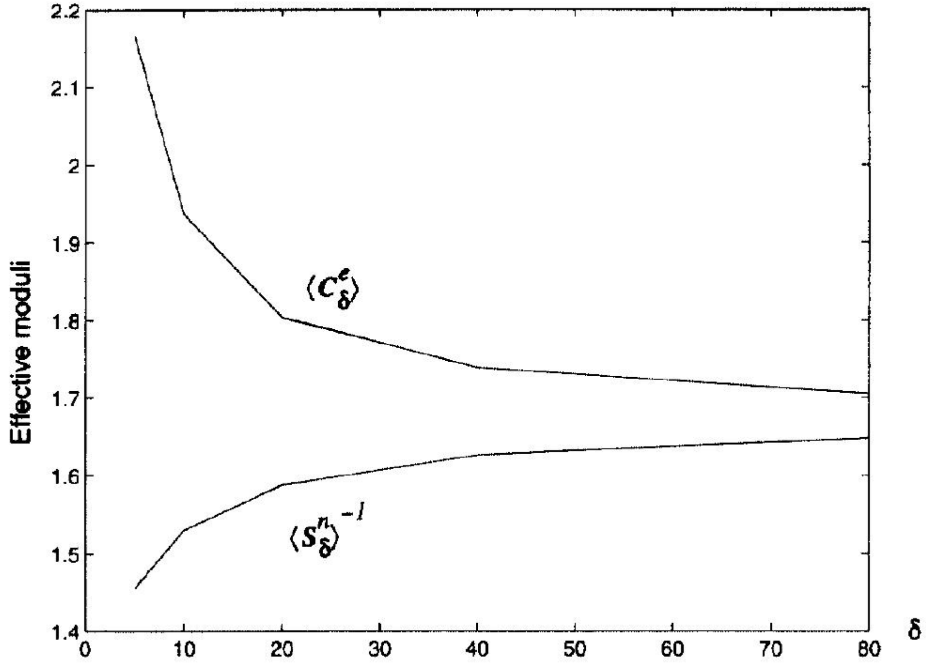

Convergence of torsion solutions for a homogeneous bar:

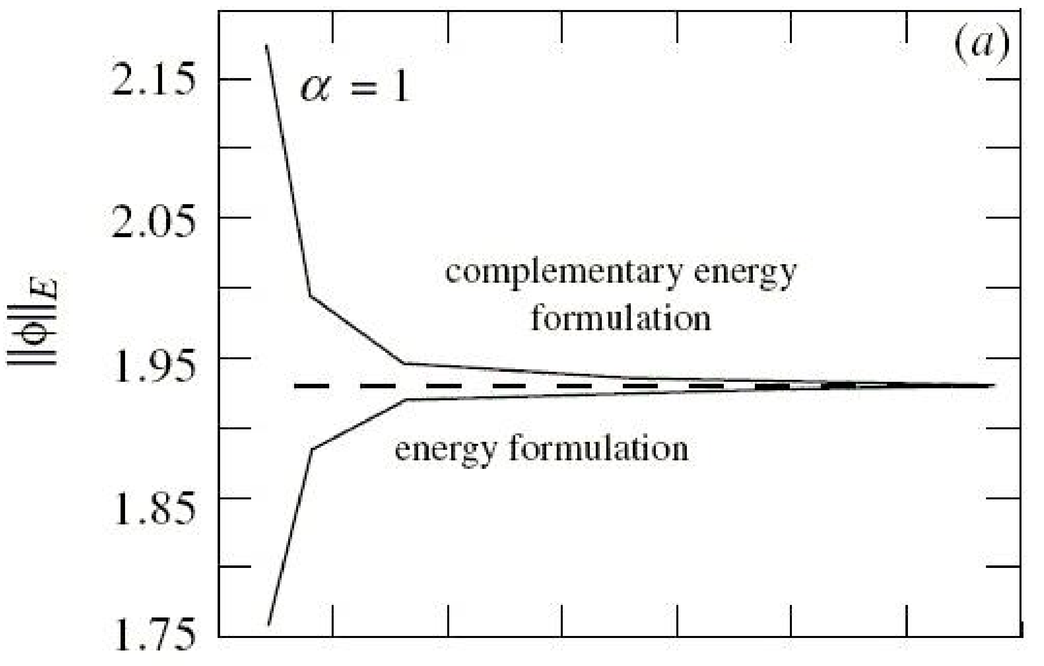

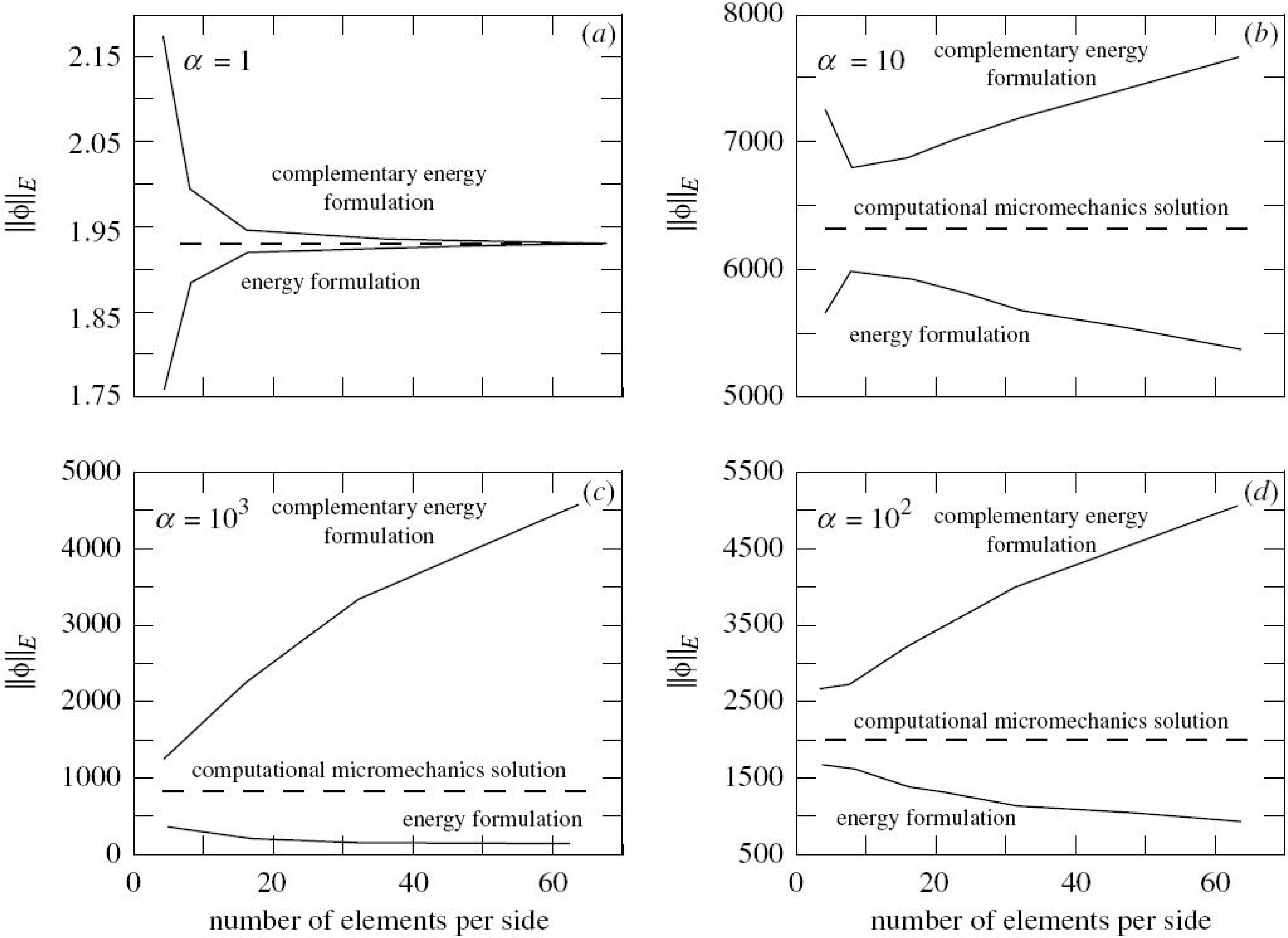

(a)
α = 1
complementary energy formulation
energy formulation
2.15
2.05
1.95
1.85
1.75
||φ||_E
(b)
α = 10
complementary energy formulation
computational micromechanics solution
energy formulation
8000
7000
6000
5000
||φ||_E
(c)
α = 10^3
complementary energy formulation
computational micromechanics solution
energy formulation
5000
4000
3000
2000
1000
0
||φ||_E
0
20
40
60
number of elements per side
(d)
α = 10^2
complementary energy formulation
computational micromechanics solution
energy formulation
5500
4500
3500
2500
1500
500
||φ||_E
0
20
40
60
number of elements per side

Torsion of a bar of square cross section

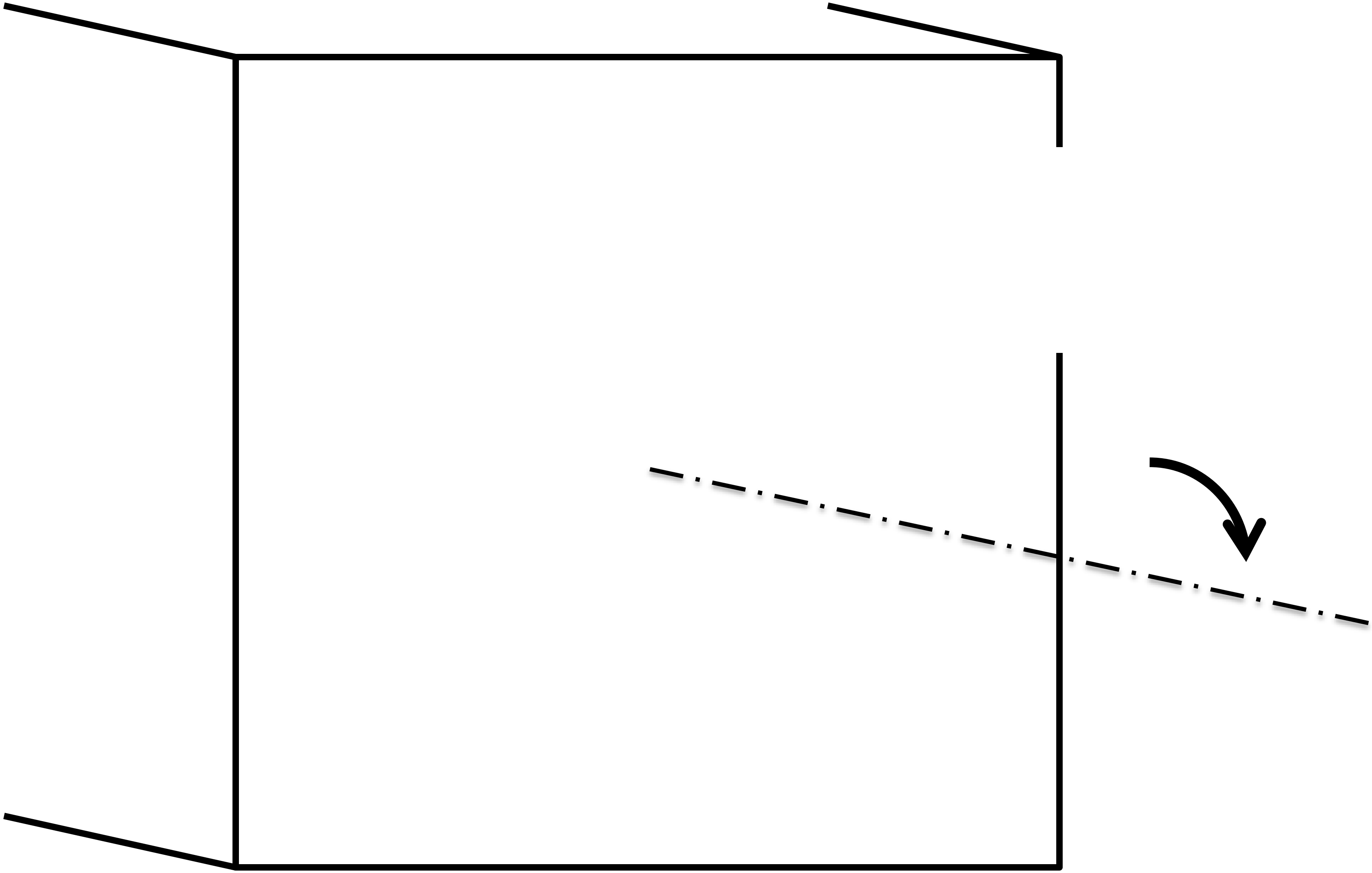

Torsion of a bar
of square cross section

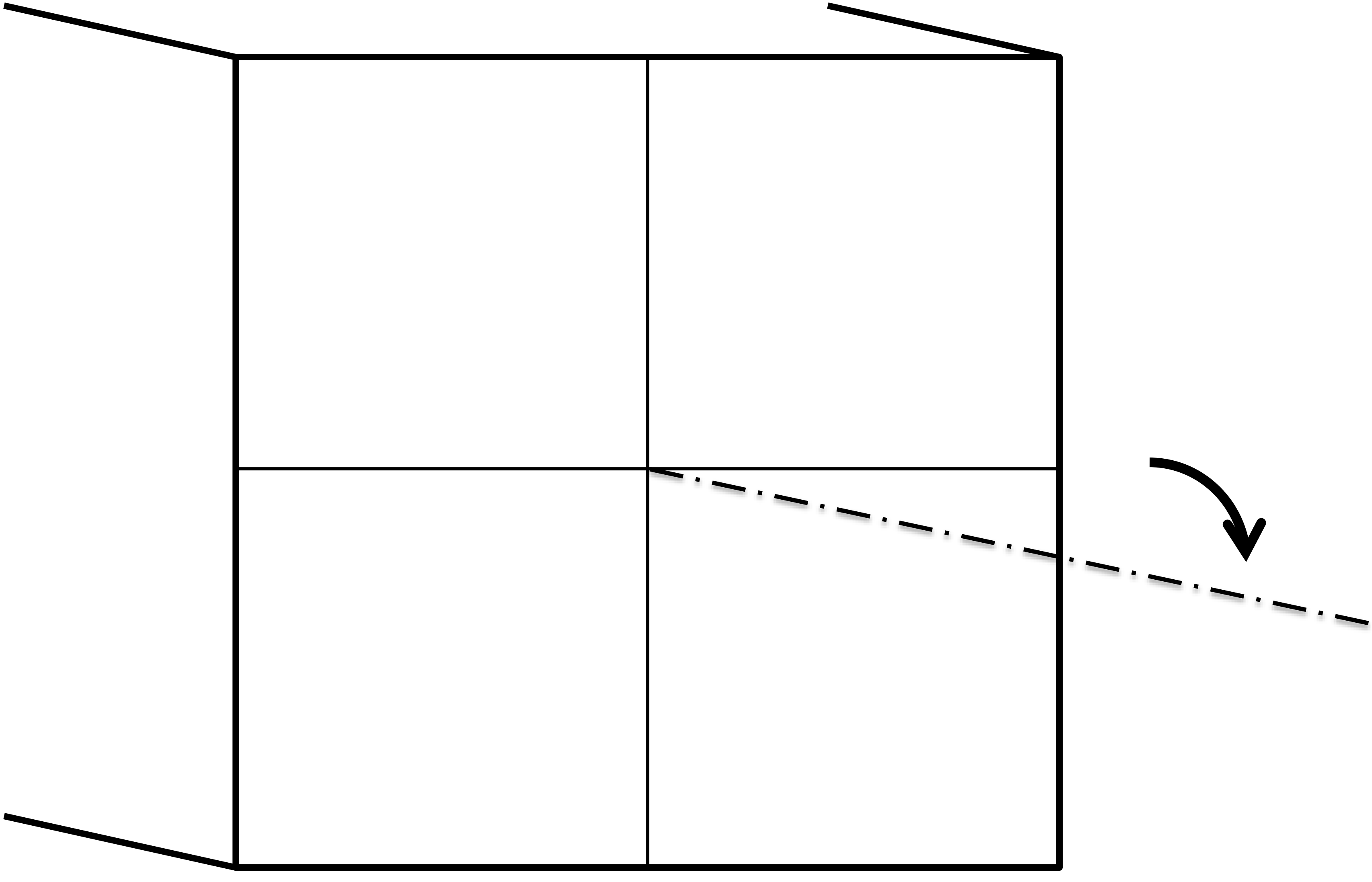

Torsion of a bar
of square cross section

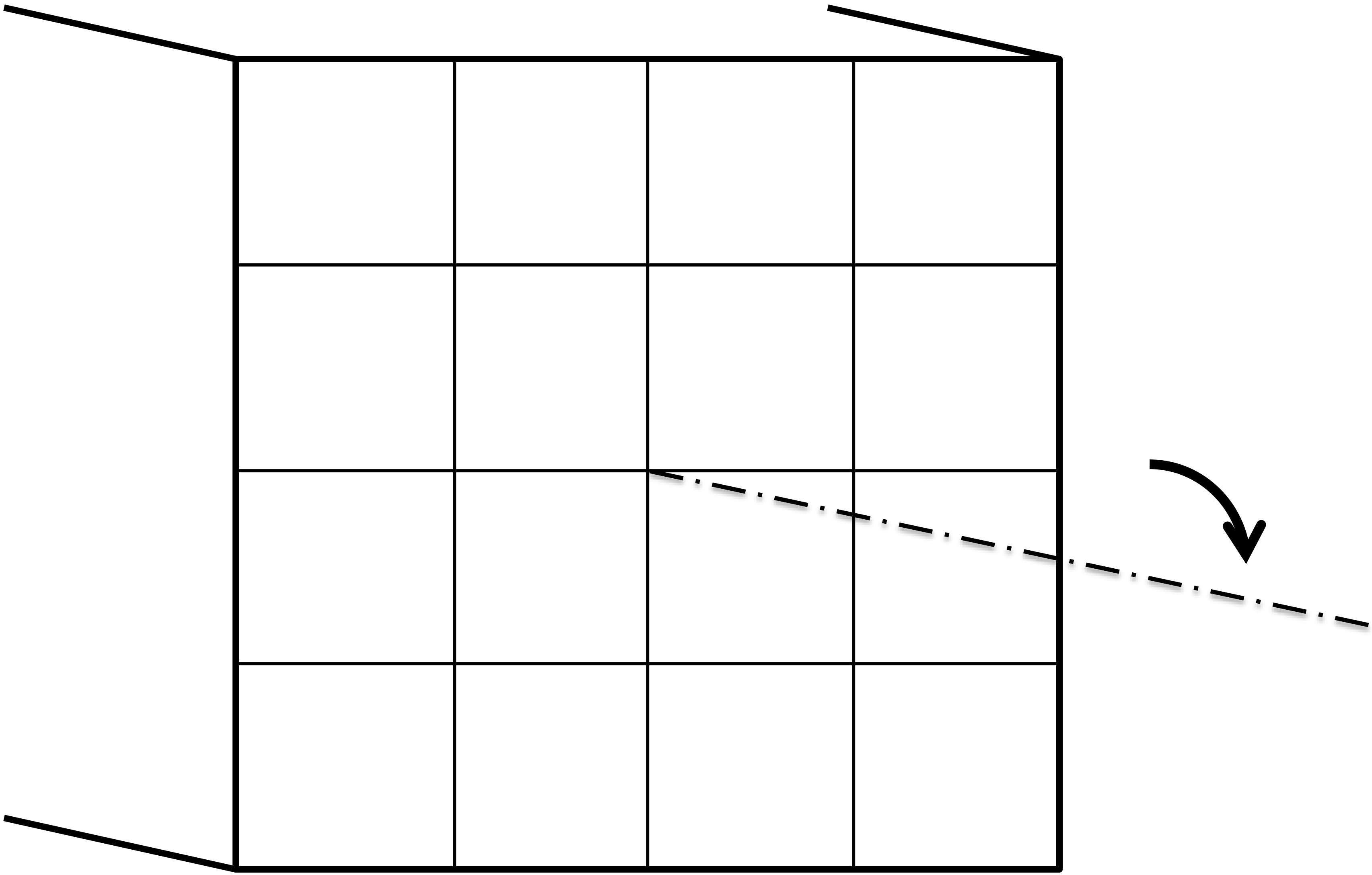

Torsion of a bar of square cross section

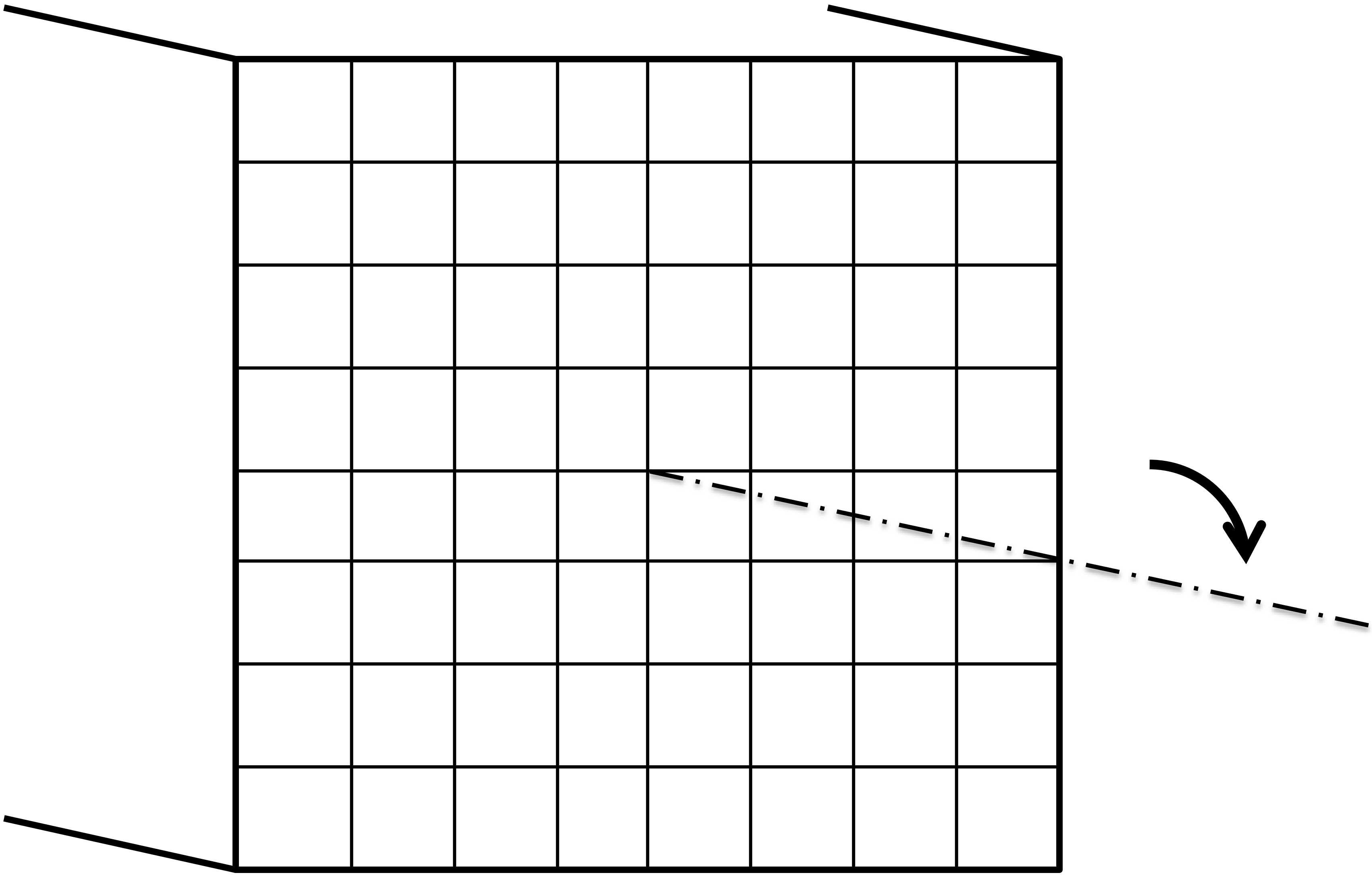

Torsion of a bar
of square cross section

Convergence of torsion solutions for a homogeneous bar:

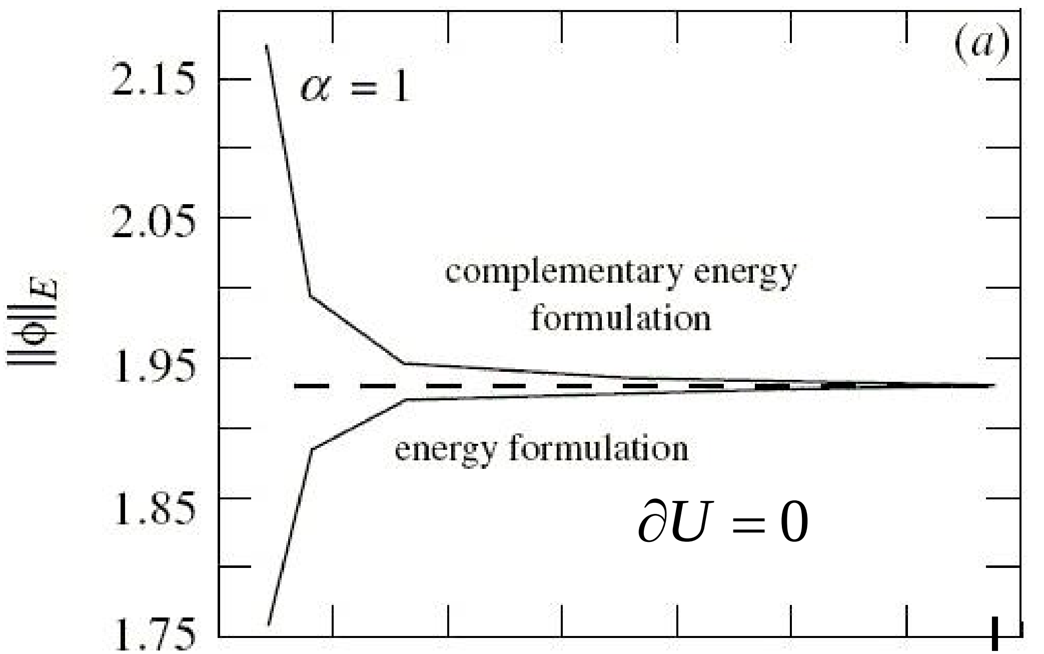

Torsion of a bar of square cross section

$$\mathbf{L}(\omega) = \int_{D_e} \mathbf{B}^T \cdot \mathbf{S} \cdot \mathbf{B} \; dV \quad \Rightarrow$$

Convergence of torsion solutions for a homogeneous bar:

$$\mathbf{K}(\omega) = \int_{D_e} \mathbf{B}^T \cdot \mathbf{C} \cdot \mathbf{B} \; dV \quad \Rightarrow$$

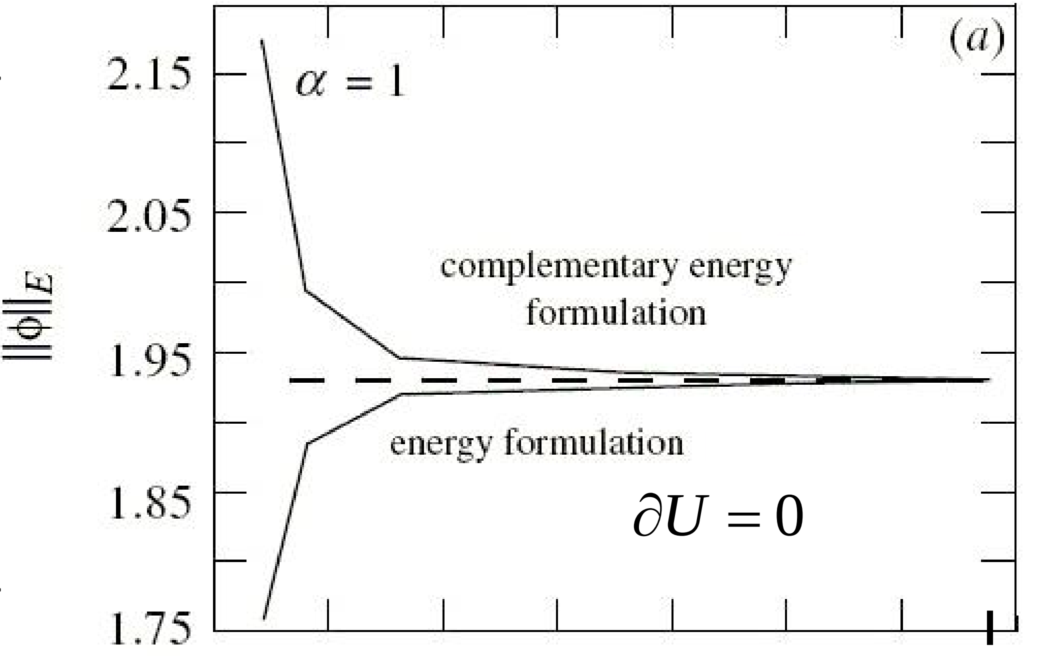

Torsion of a bar of square cross section with bi-percolating microstructure

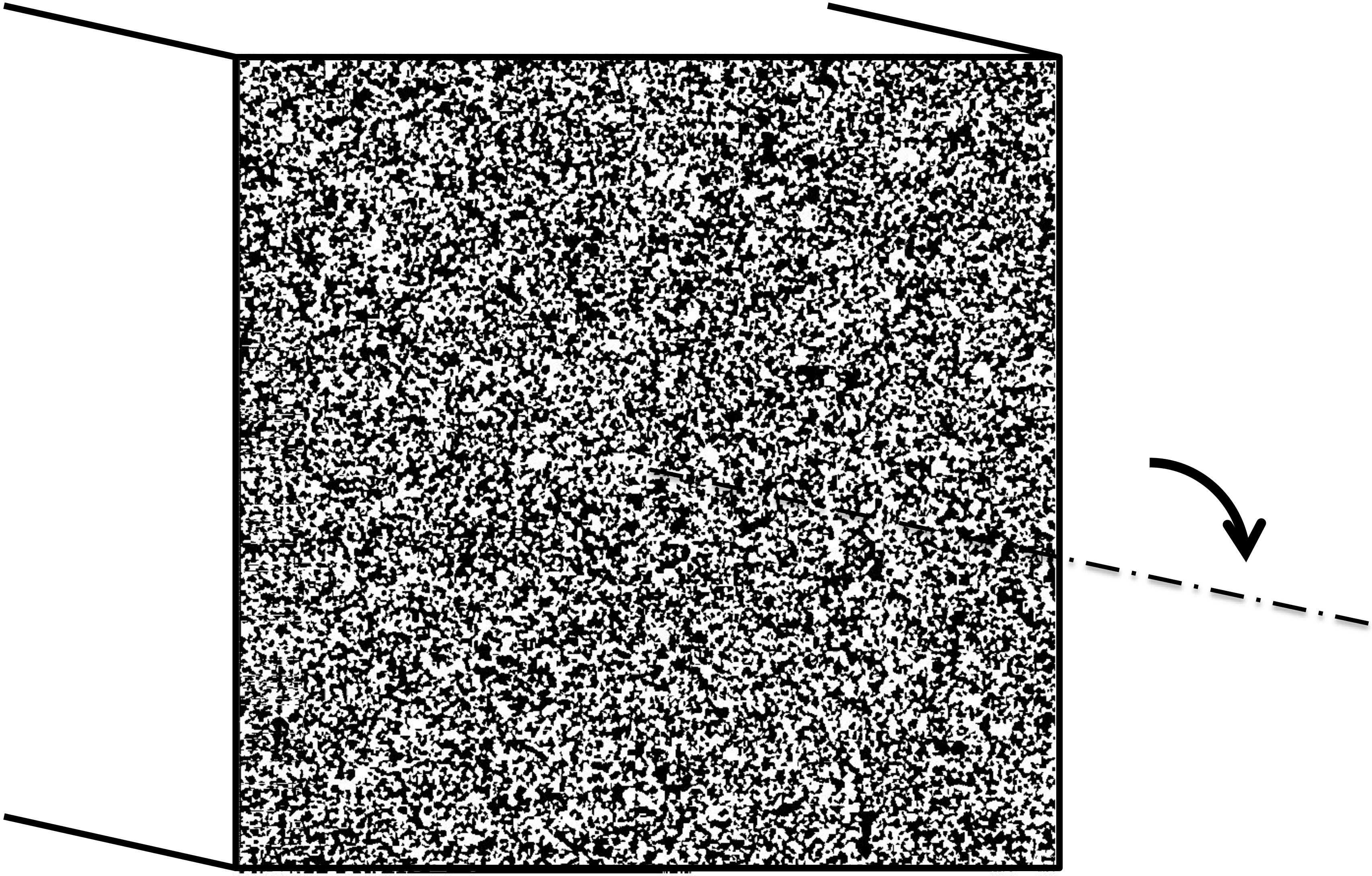

Figure 2. A two-phase material with a Voronoi mosaic microgeometry of a total 104 858 black and white cells, at volume fraction 50% each.

Torsion of a bar of square cross section with bi-percolating microstructure

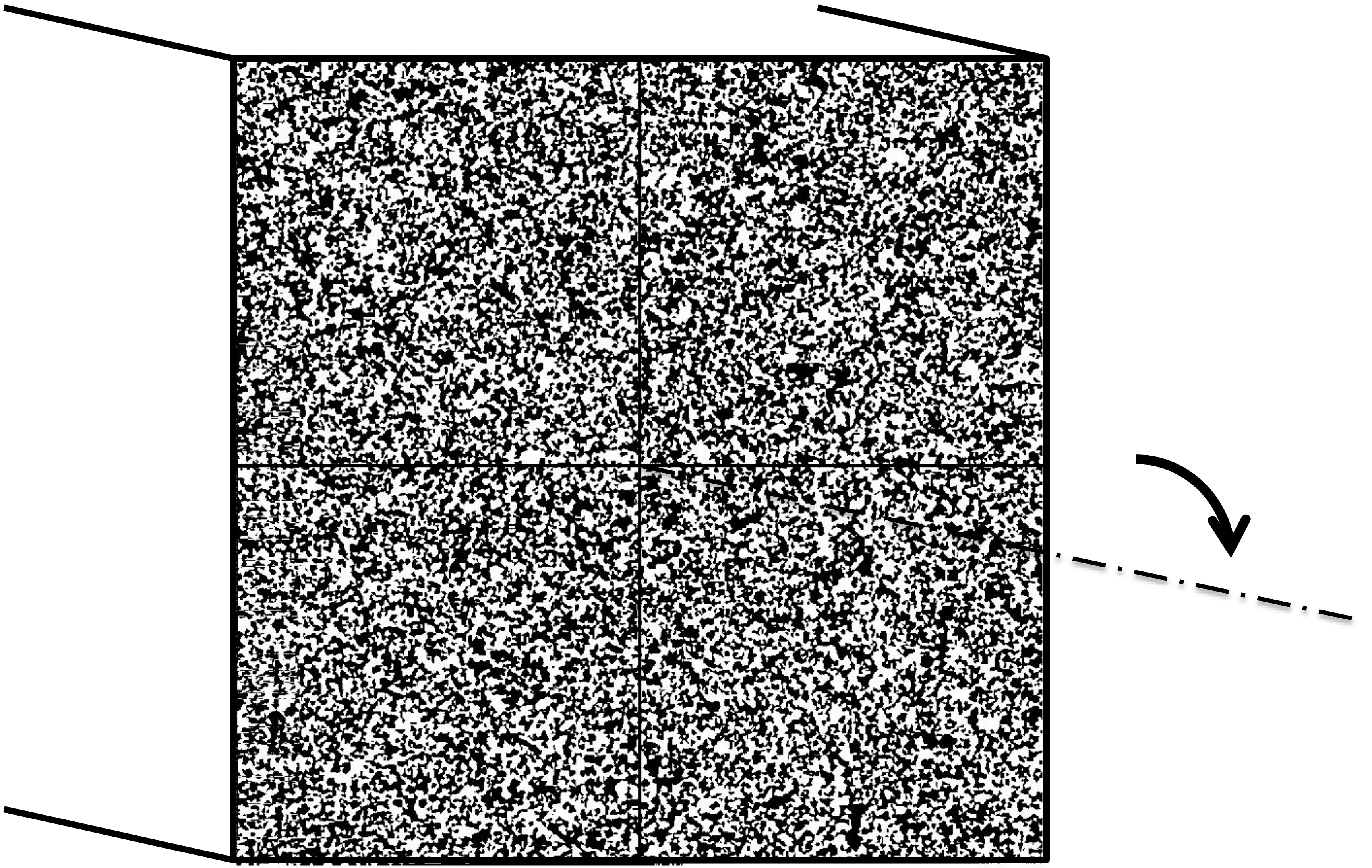

Figure 2. A two-phase material with a Voronoi mosaic microgeometry of a total 104 858 black and white cells, at volume fraction 50% each.

Torsion of a bar of square cross section with bi-percolating microstructure

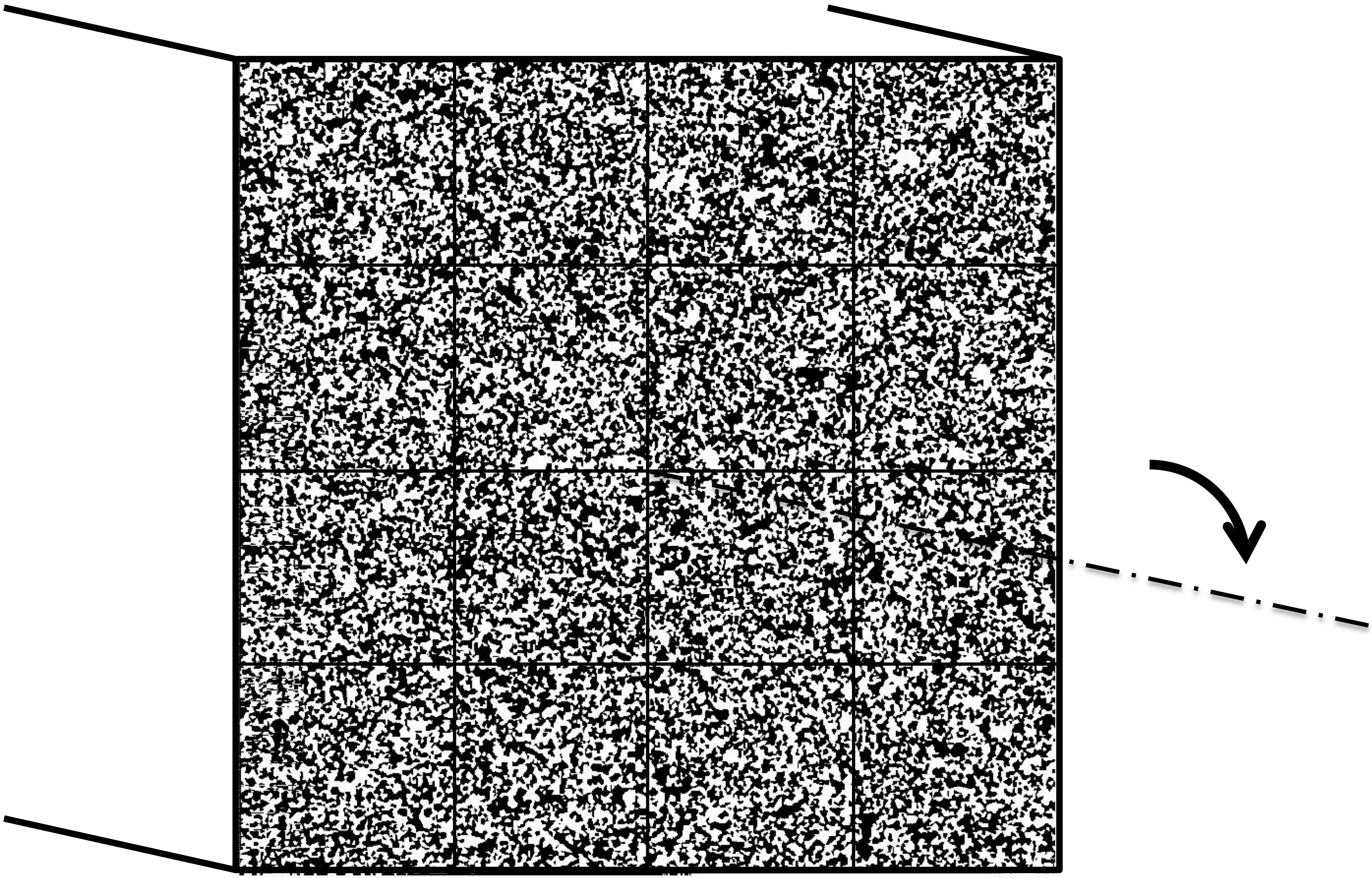

Figure 2. A two-phase material with a Voronoi mosaic microgeometry of a total 104 858 black and white cells, at volume fraction 50% each.

Torsion of a bar of square cross section with bi-percolating microstructure

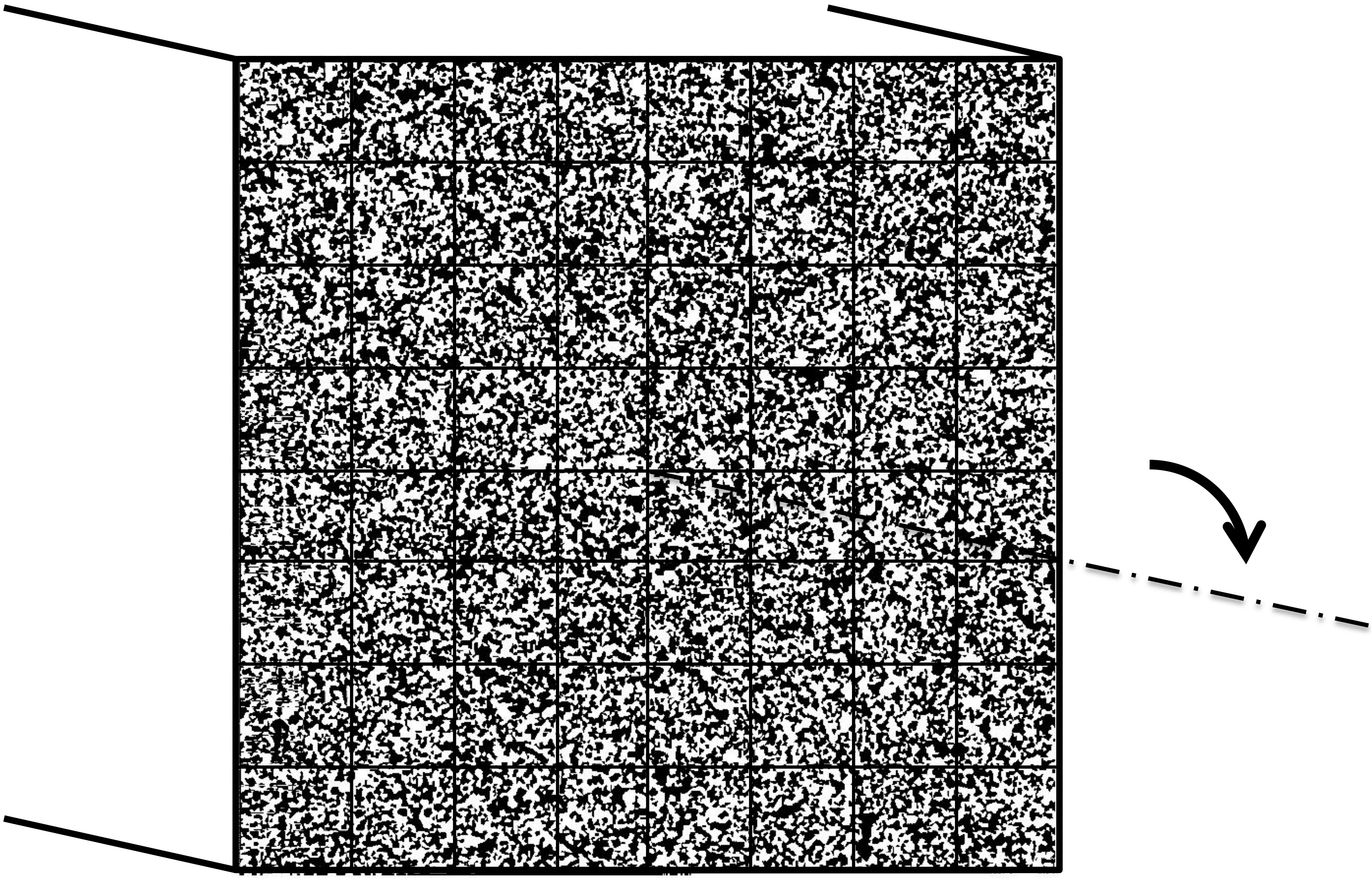

Figure 2. A two-phase material with a Voronoi mosaic microgeometry of a total 104 858 black and white cells, at volume fraction 50% each.

Mesoscale bounds for heterogeneous bar:

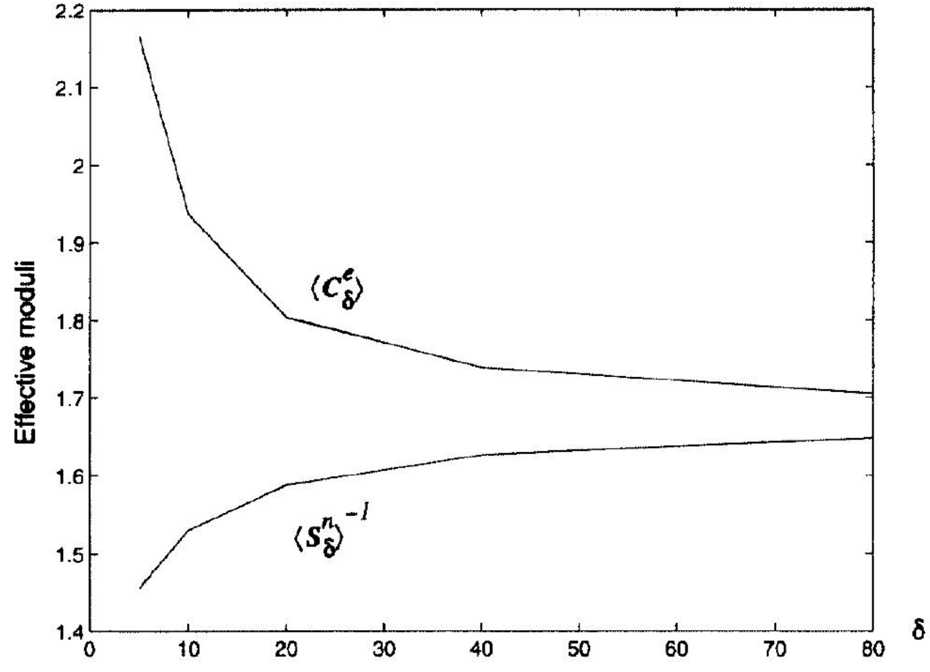

Mesoscale bounds for heterogeneous bar:

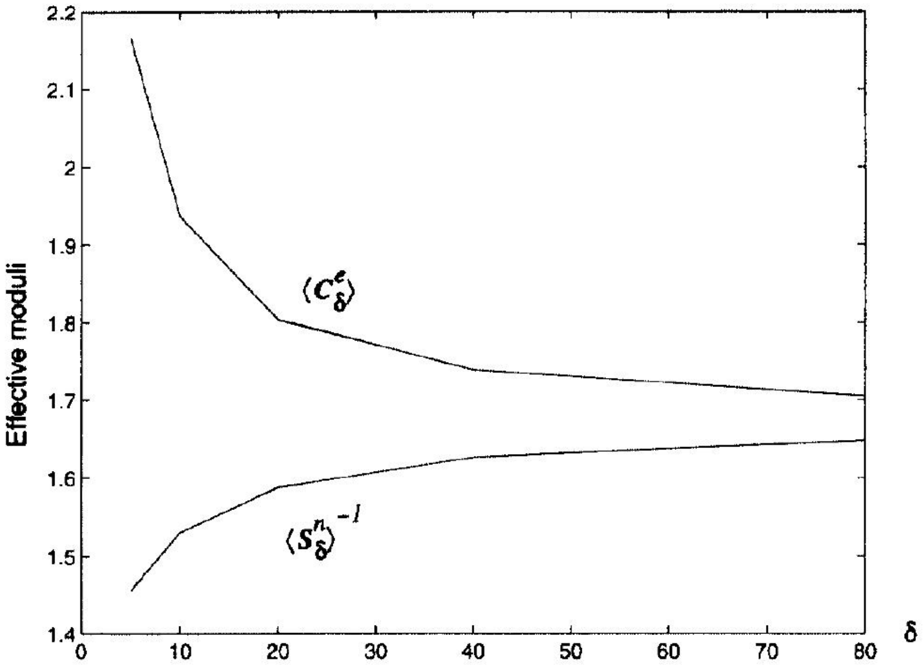

Convergence of torsion solutions for homogeneous bar:

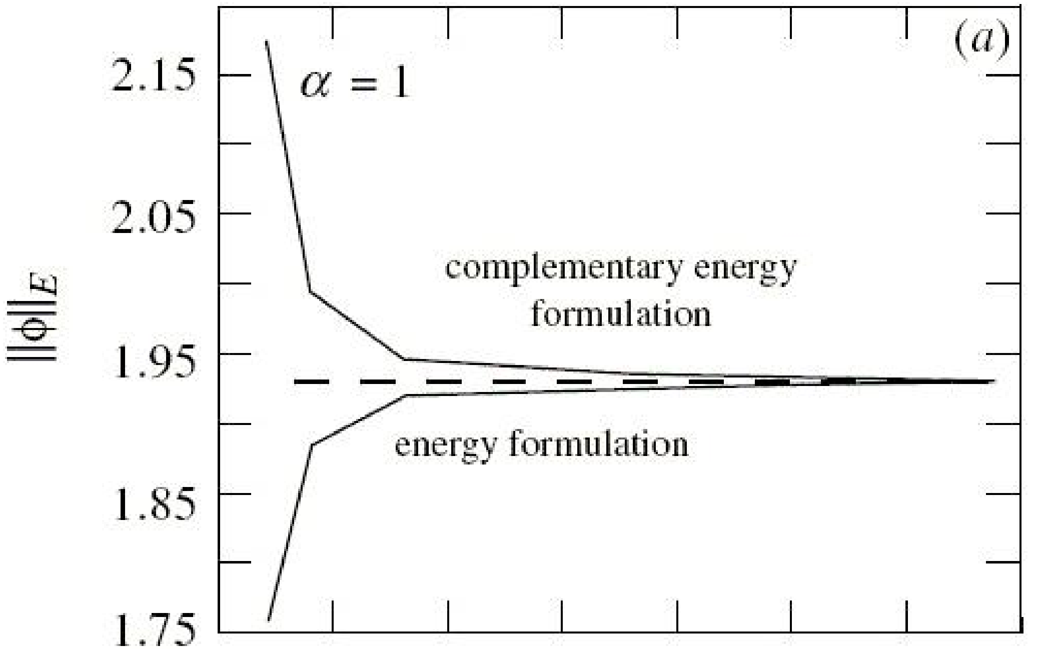

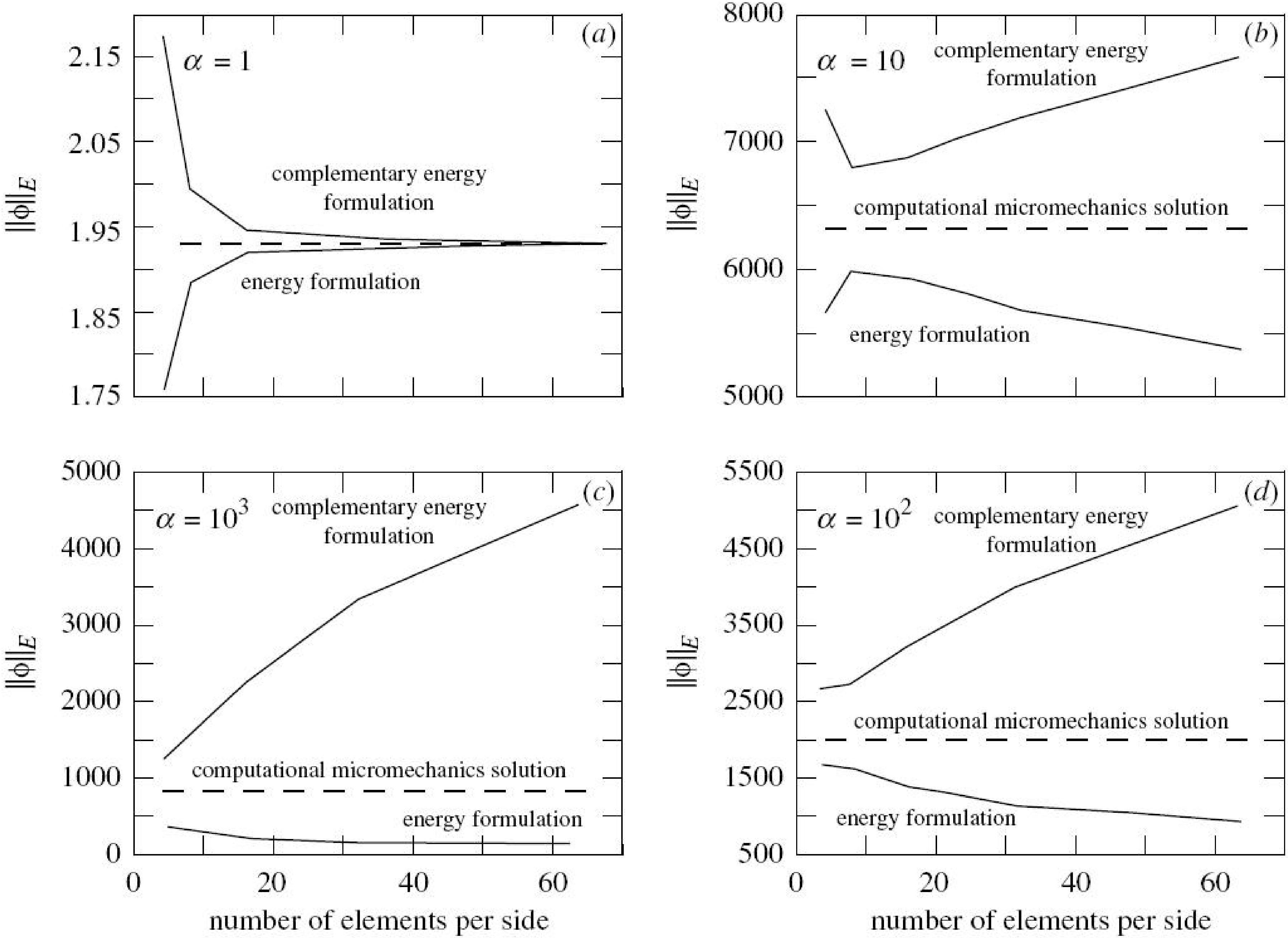

(a)
α = 1
complementary energy formulation
energy formulation
2.15
2.05
1.95
1.85
1.75
‖φ‖E
(b)
α = 10
complementary energy formulation
computational micromechanics solution
energy formulation
8000
7000
6000
5000
‖φ‖E
(c)
α = 10^3
complementary energy formulation
computational micromechanics solution
energy formulation
5000
4000
3000
2000
1000
0
‖φ‖E
0
20
40
60
number of elements per side
(d)
α = 10^2
complementary energy formulation
computational micromechanics solution
energy formulation
5500
4500
3500
2500
1500
500
‖φ‖E
0
20
40
60
number of elements per side

Continuum tensor random field (RF) $\mathbf{C}(\omega,\mathbf{x}) = \overline{\mathbf{C}} + \mathbf{C}'(\omega,\mathbf{x})$

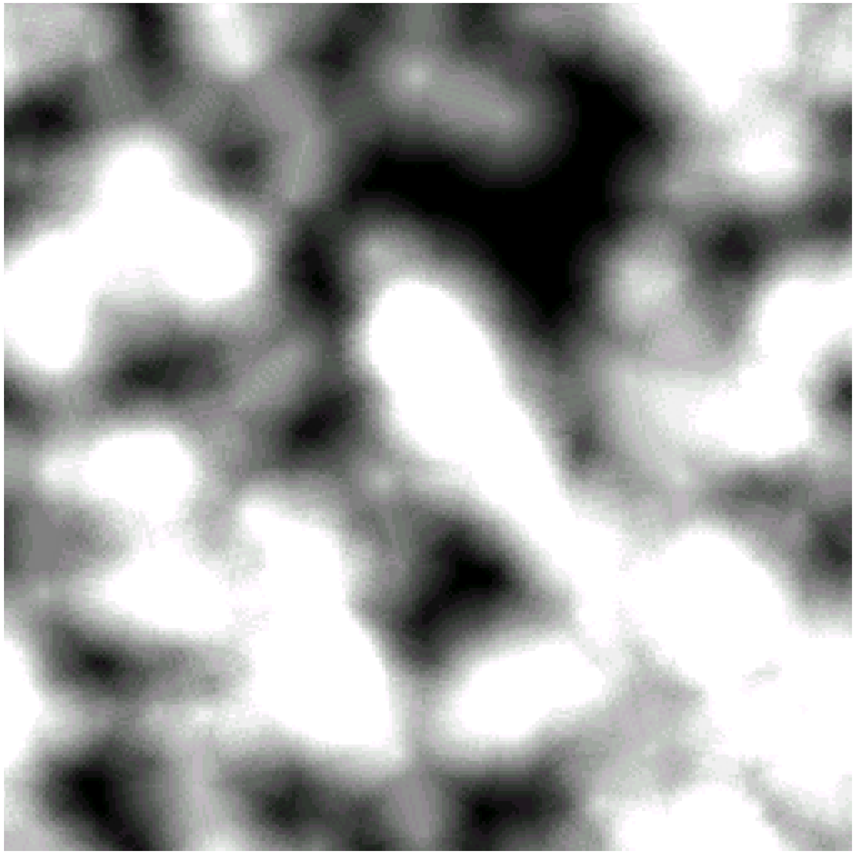

Can it be assumed isotropic (E, ν) and smooth?

Can assume a unique tensor RF with anisotropic realizations?

Can do local averaging of tensor RF for input to stochastic finite elements (SFE)?

Can assume correlation functions of tensor RF w/o reference to micromechanics?

Continuum tensor random field (RF) $\mathbf{C}(\omega, \mathbf{x}) = \overline{\mathbf{C}} + \mathbf{C}'(\omega, \mathbf{x})$

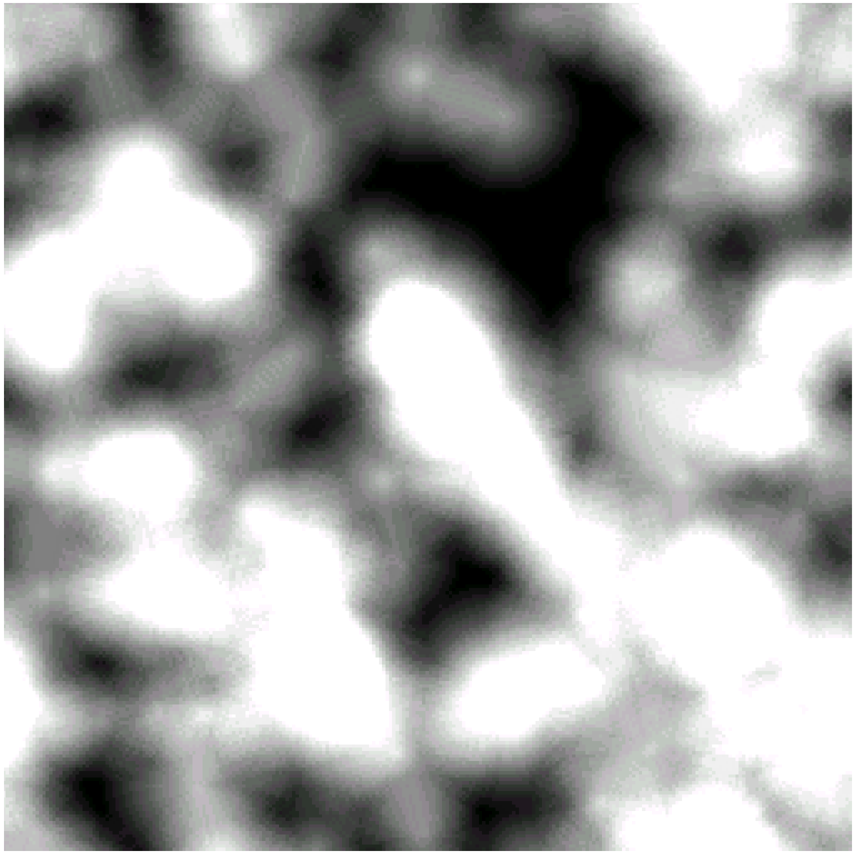

Can it be assumed isotropic (E**,**v) and smooth? **No**

Can assume a unique tensor RF with anisotropic realizations? **No**

Can do local averaging of tensor RF for input to stochastic finite elements (SFE)? **No**

Can assume correlation functions of tensor RF w/o reference to micromechanics? **No**

Continuum tensor random field (RF) $\mathbf{C}(\omega,\mathbf{x}) = \overline{\mathbf{C}} + \mathbf{C}'(\omega,\mathbf{x})$

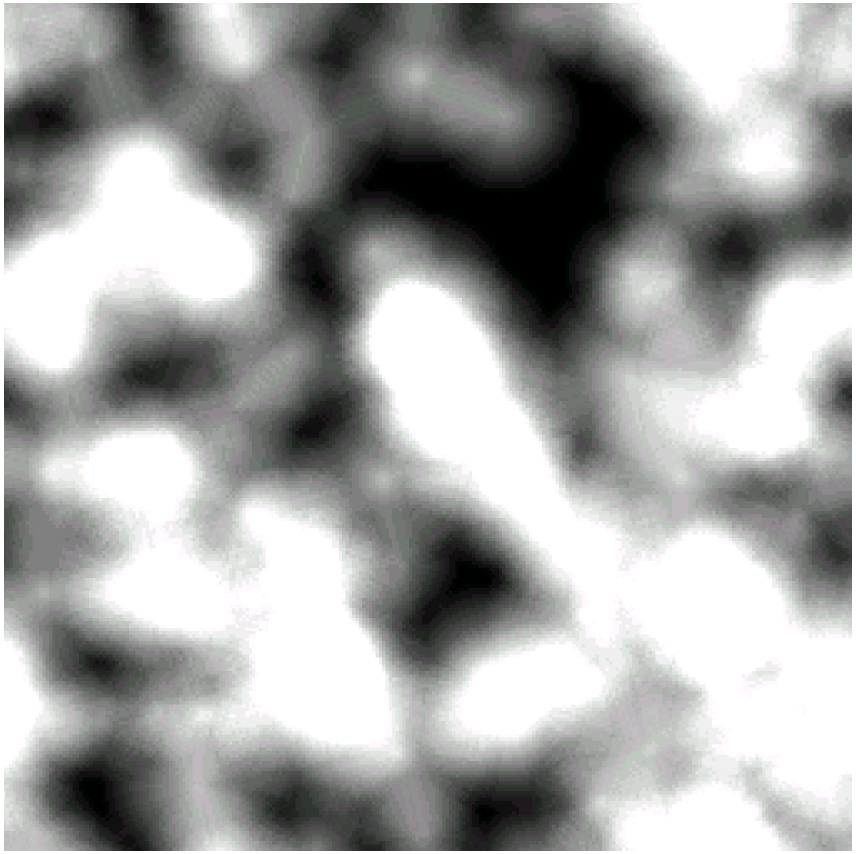

Can it be assumed isotropic (E,v) and smooth? **No**

Can assume a unique tensor RF with anisotropic realizations? **No**

Can do local averaging of tensor RF for input to stochastic finite elements (SFE)? **No**

Can assume correlation functions of tensor RF w/o reference to micromechanics? **No**

Applications:

random field models

uncertainty quantification

waves in random media

FGM …

Fracture mechanics of micro-beams (nano-beams)

Recall strain-energy release rate:

conventionally:

γ = *material constant*

U = *elastic strain energy of a homogeneous materic*

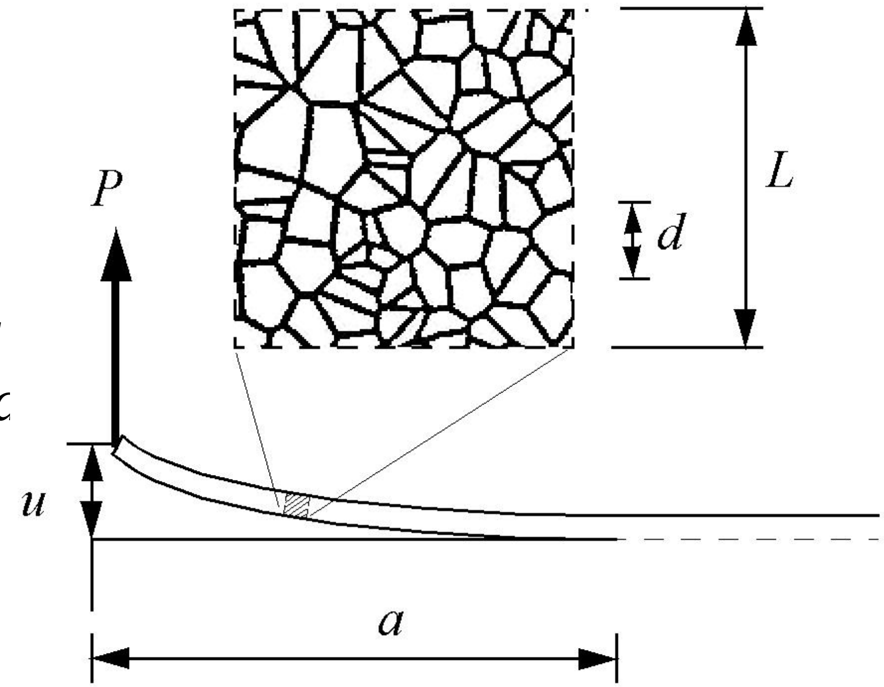

…but, in a **micro-beam**

with a random microstructure:

γ = *random field*

U = *random functional*

$$G = \frac{\partial W}{\partial A} - \frac{\partial U}{\partial A} = 2\gamma$$

Stochastic crack stability:

$$\frac{\partial^2(\Pi+\Gamma)}{\partial A^2} \begin{array}{ll} <0 & \text{unstable equilbrium} \\ =0 & \text{neutral equilbrium} \\ >0 & \text{stable equilbrium} \end{array}$$

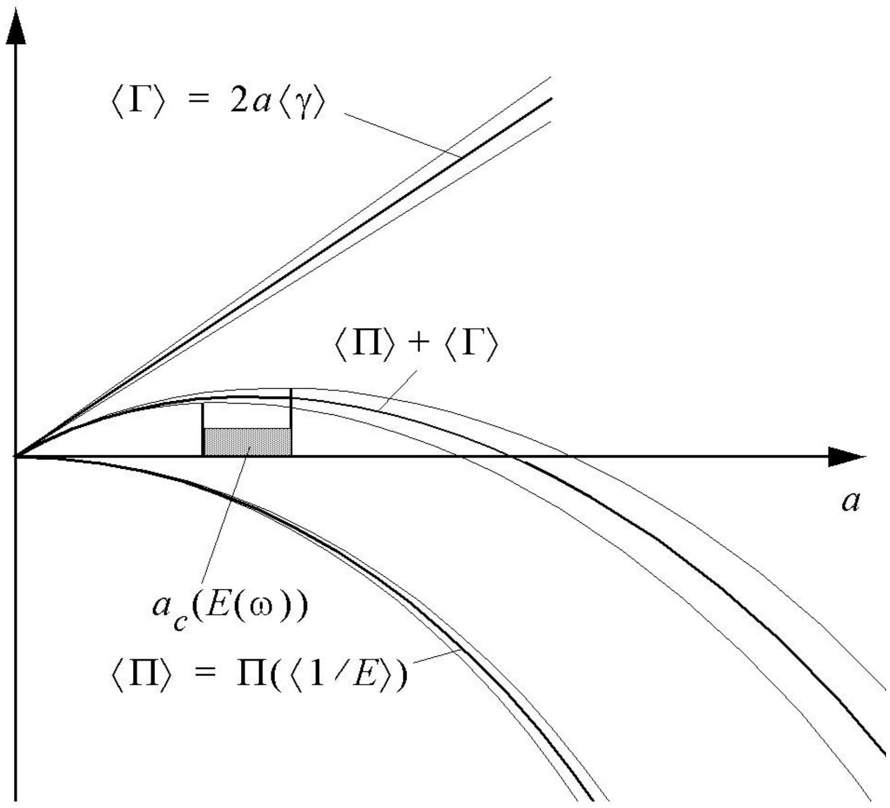

…but, in a micro-beam

with a random microstructure:

γ = random field

U = random functional

[*J. Appl. Mech.*, 2004]

Shape optimization

Optimal truss (Michell, 1904)**:**
a minimum-weight design of a planar truss that transmits a given load to a rigid foundation with axial stresses in all the bars: $-\sigma_0 \leq \sigma \leq \sigma_0$

Solution found by solving a hyperbolic problem

n = # of nodes

$Eff = V/\,V(n)$ ***efficiency***

V = volume of *Michell truss-like continuum*

$V(n)$ = volume of 'finite' truss

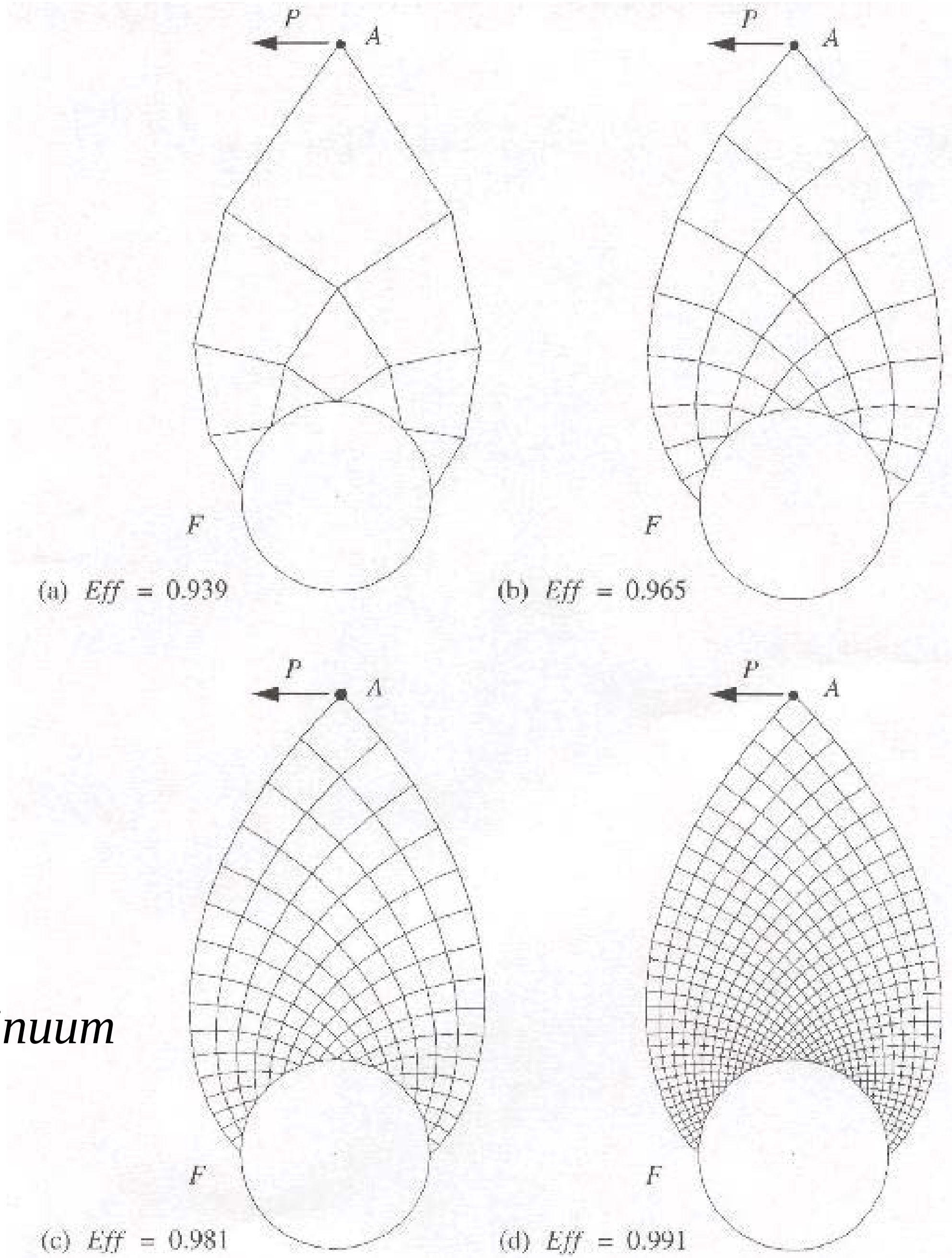

Manufacturing of a truss from a polycrystal

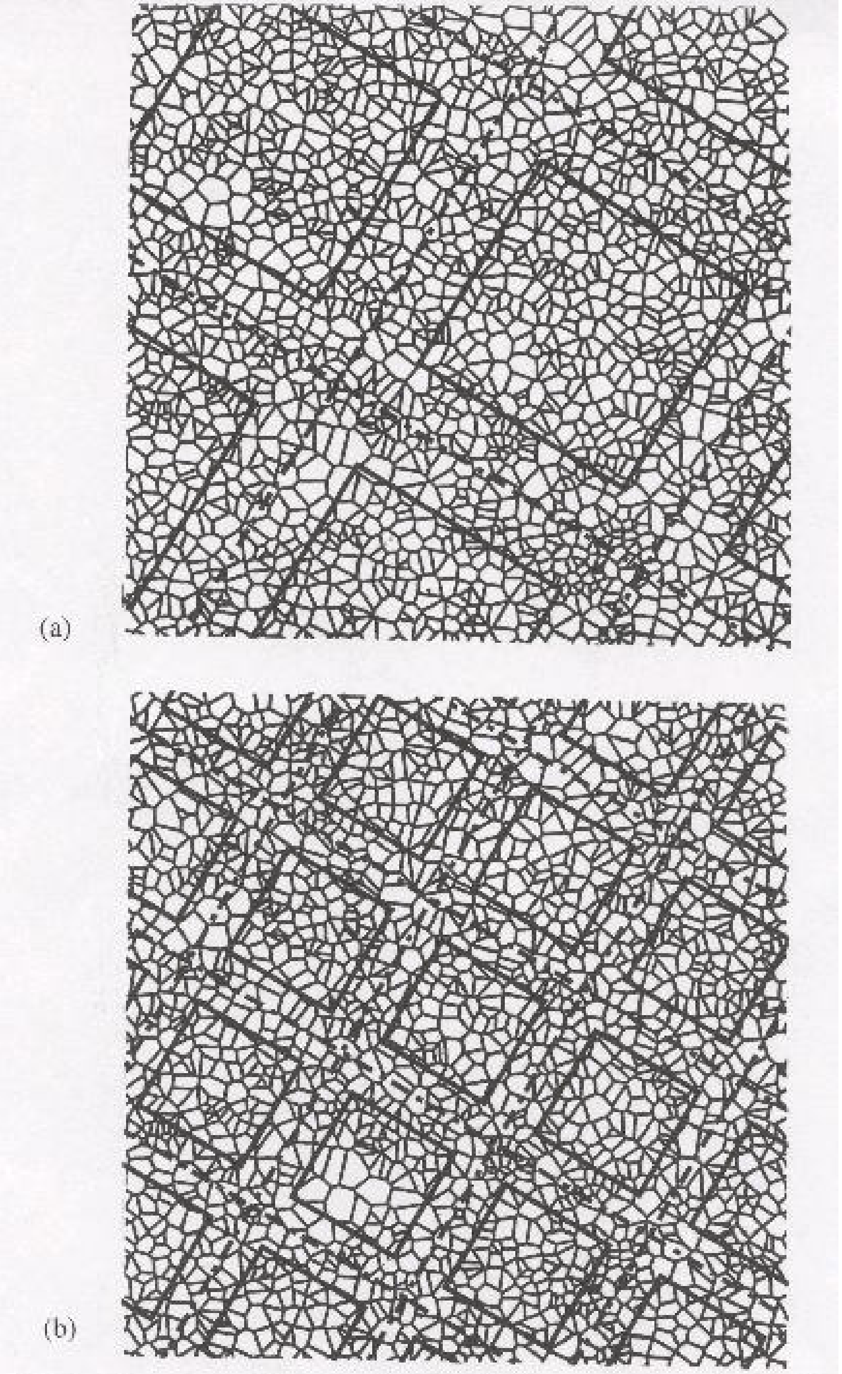

…as the mesh is refined,

random noise in σ_0 grows

Truss made of ‘real’ material:
a minimum-weight design in
the presence of random strengths σ_0

n = # of nodes

$Eff = V/\,V(n)$

V = volume of Michell truss-like continuum

$V(n)$ = volume of ‘finite’ truss

As randomness in σ_0 grows,
characteristics get more scattered

… beyond (d), characteristics intersect!

Material spatial randomness
prevents the attainment of Eff = 1

[*Proc. Roy. Soc. Lond. A*, 2003]

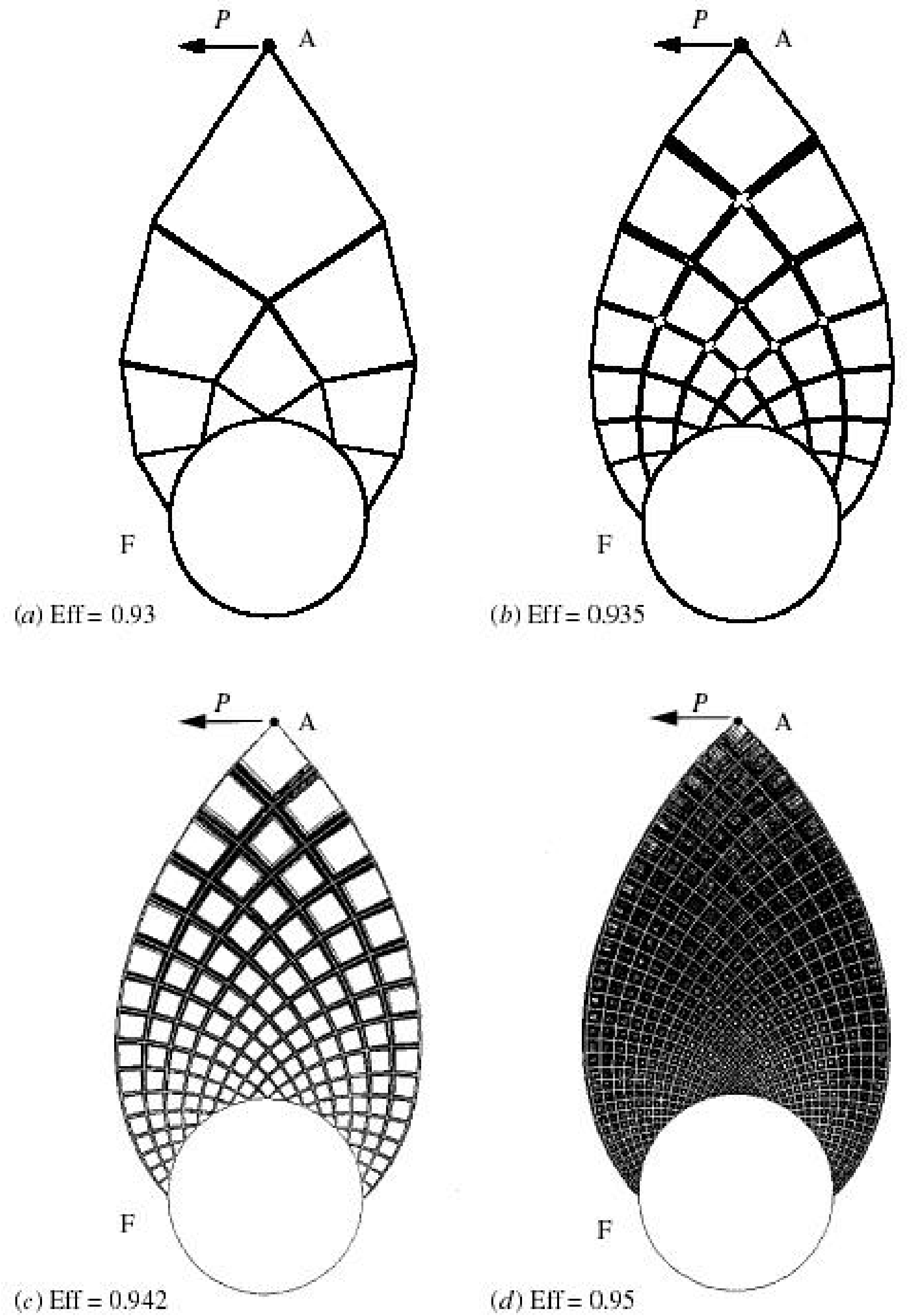

Shape optimization of an elastic structure with minimum compliance, having a prescribed weight

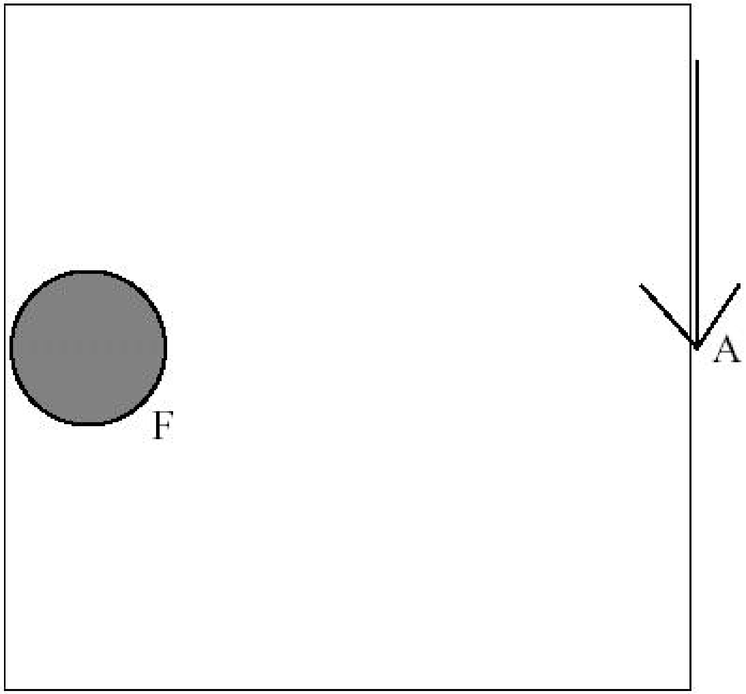

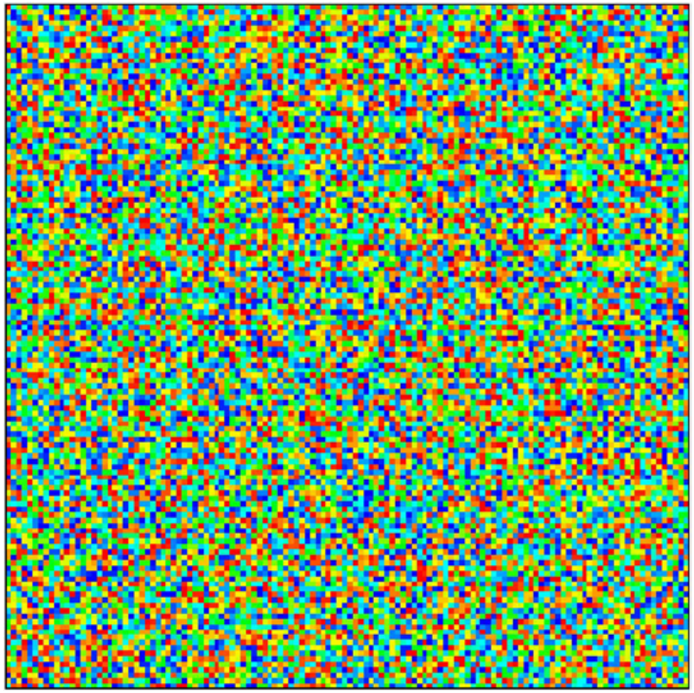

Rigid foundation F
Force applied at A

Material = square mosaic with random stiffnesses:

$$E(\omega) = E + E'(\omega)$$

homogeneous medium case

E = const

increasing randomness in stiffness

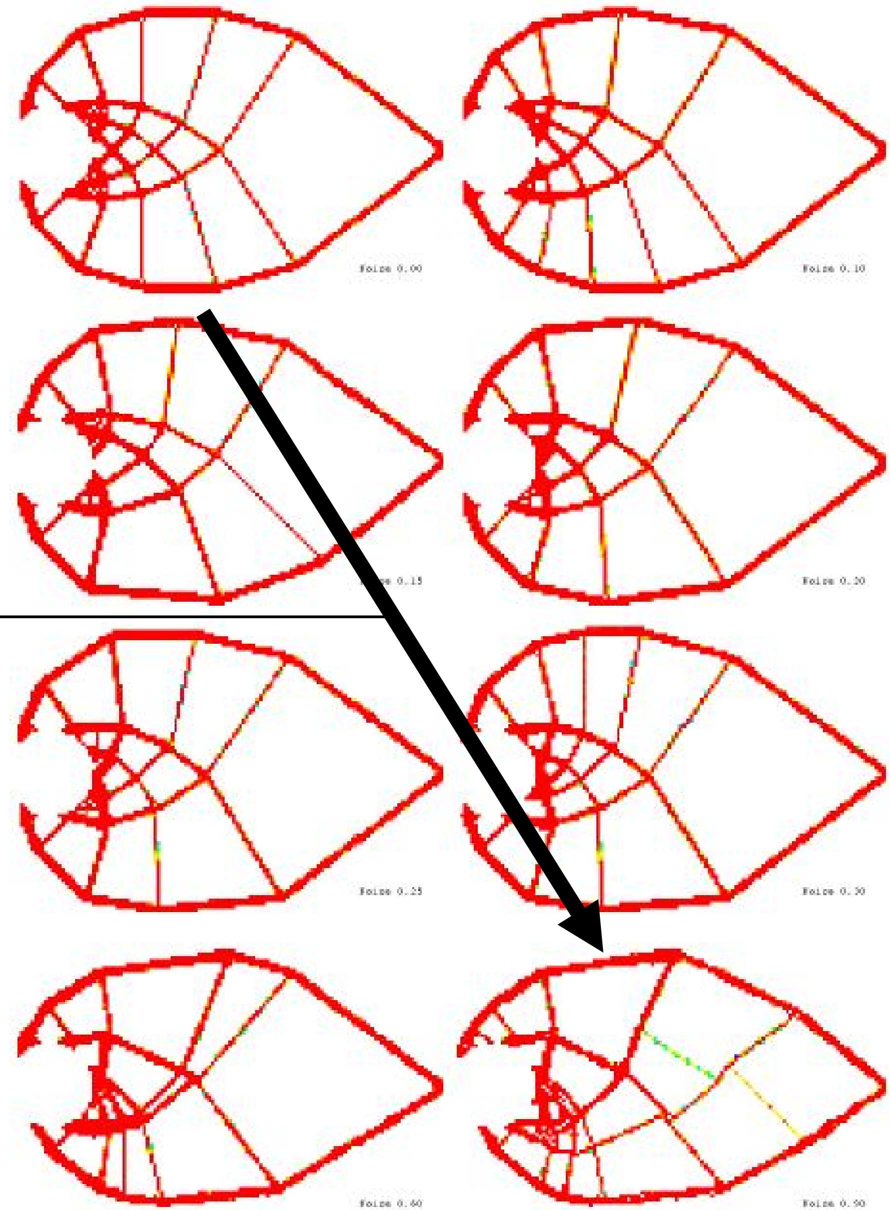

generally, compliance increases

but, for some realizations,

the algorithm may find a lower compliance than in homogeneous medium case

[*Struct. Multidiscipl. Optim.* 2003]

Peeling a beam off a substrate

determine the critical crack length and stability

Strain energy release rate:

$$G = \frac{\partial W}{\partial A} - \frac{\partial U}{\partial A} = 2\gamma$$

γ = *material constant*

U = *elastic strain energy of a homogeneous material*

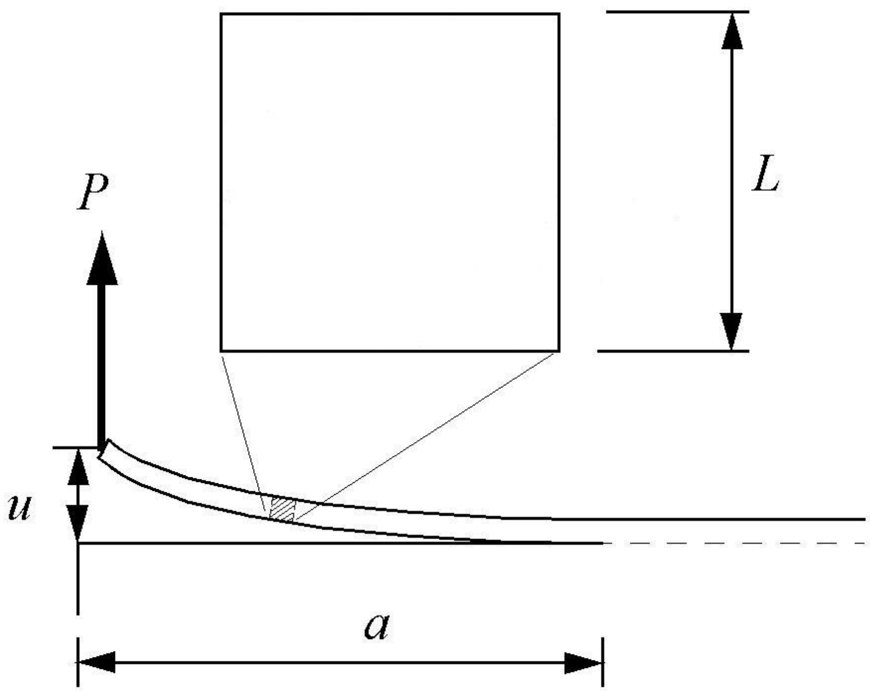

crack stability:

$$\frac{\partial^2(\Pi+\Gamma)}{\partial A^2} \quad \begin{array}{ll} <0 & \text{unstable equilbrium} \\ =0 & \text{neutral equilbrium} \\ >0 & \text{stable equilbrium} \end{array}$$

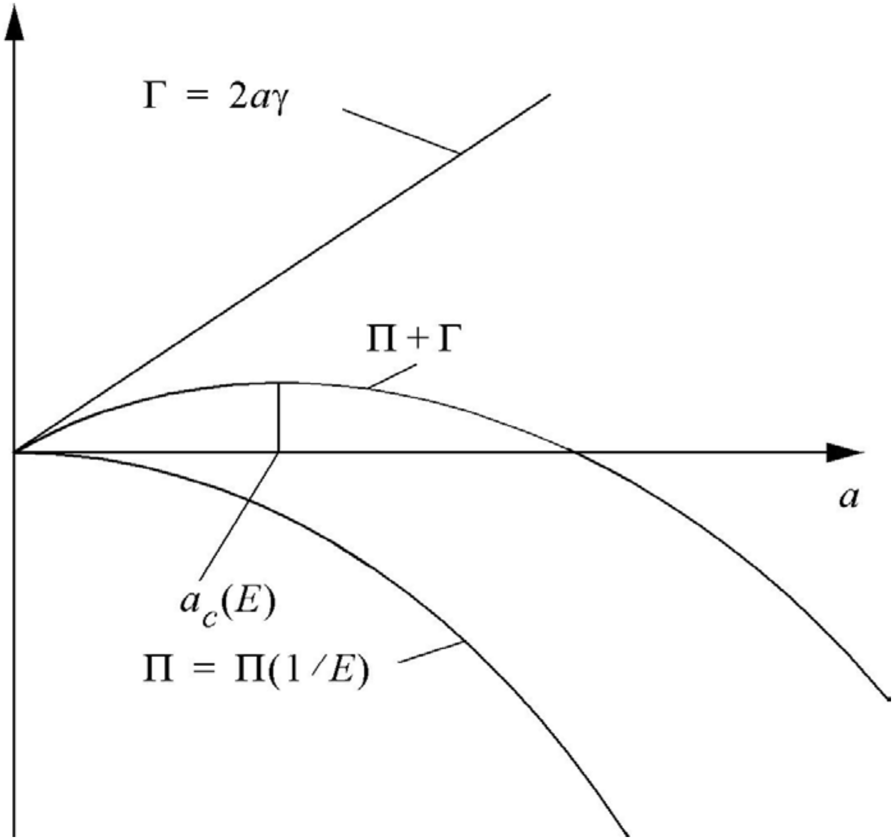

Peeling a random beam off a substrate

Strain energy release rate: $$G = \frac{\partial W}{\partial A} - \frac{\partial U}{\partial A} = 2\gamma$$

γ = *random field* $\{\gamma(\omega, x); \omega \in \Omega, x \in X\}$

U = *random functional*

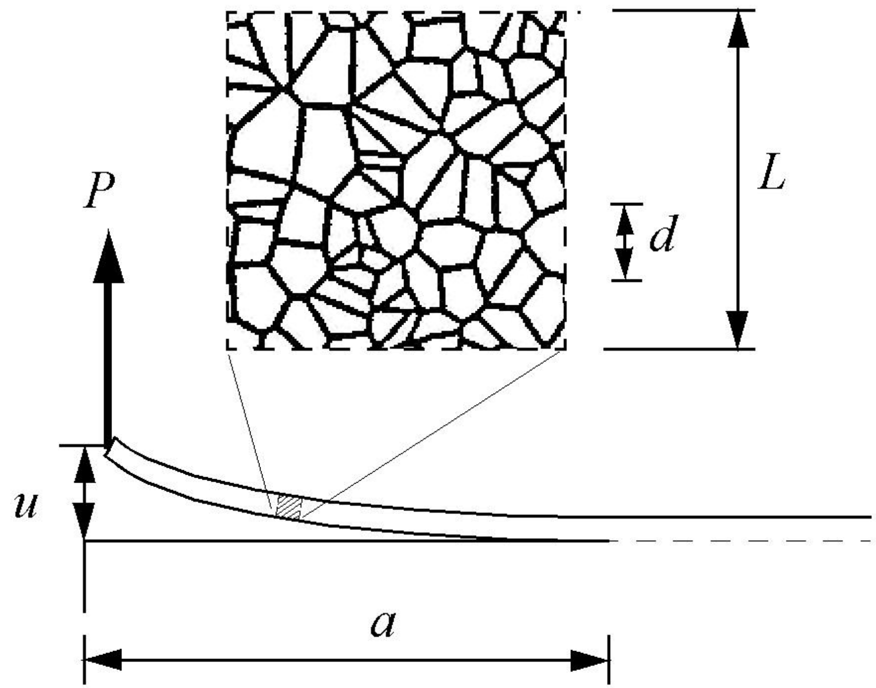

Dead-load conditions (for Euler-Bernoulli beam):

$$U(a) = \int_0^a \frac{M^2}{2IE} dx$$

where $a = A/B$, B = constant beam (crack) width

From Clapeyron's theorem: $$G = \frac{\partial U}{B\partial a}$$

<u>Note</u>: randomness of *E* arises when Representative Volume Element (RVE) of deterministic continuum mechanics cannot be applied to a micro-beam

$\Longrightarrow$ need Statistical Volume Element (SVE)

$\Longrightarrow$ micro-beam is random: $\{E(\omega, x); \omega \in \Omega, x \in [0, a]\}$

(wide-sense stationary)

U is a random integral

$$\forall \omega \in \Omega \qquad U(a, E(\omega)) = \int_0^a \frac{M^2}{2IE(\omega, x)} dx$$

upon ensemble averaging:

$$\langle U(a, E) \rangle = \left\langle \int_0^a \frac{M^2}{2I[E + E'(\omega, x)]} dx \right\rangle$$

In conventional formulation of deterministic fracture mechanics, random heterogeneities $E'(x,\omega)$ are disregarded ($E = \langle E \rangle = const$) $\Longrightarrow$

$$U(a, \langle E \rangle) = \int_0^a \frac{M^2}{2I\langle E \rangle} dx$$

$$\Longrightarrow \qquad \langle U(a, E) \rangle \overset{?}{=} U(a, \langle E \rangle) \qquad \langle G(a, E) \rangle \overset{?}{=} G(a, \langle E \rangle)$$

Note: random field E is positive-valued almost surely

$\Rightarrow$ $$\frac{1}{\langle E \rangle} \le \left\langle \frac{1}{E} \right\rangle$$ by Jensen's inequality

$\Rightarrow$

$$U(a,\langle E\rangle) = \int_0^a \frac{M^2}{2I\langle E\rangle} dx \le \int_0^a \frac{M^2}{2I} \left\langle \frac{1}{E} \right\rangle dx = \left\langle \int_0^a \frac{M^2}{2IE} dx \right\rangle = \langle U(a,E)\rangle$$

Define:

G in hypothetical material: $$G(a,\langle E\rangle) = \frac{\partial U(a,\langle E\rangle)}{B\partial a}$$

G properly averaged in random material: $$\langle G(a,E)\rangle = \frac{\partial \langle U(a,E)\rangle}{B\partial a}$$

with side conditions

$$U(0,\langle E\rangle) = 0 \qquad \langle U(0,E)\rangle = 0$$

$$\Rightarrow \qquad G(a,\langle E\rangle) \le \langle G(a,E)\rangle$$

Define:

G in hypothetical material: $$G(a,\langle E\rangle)=\frac{\partial U(a,\langle E\rangle)}{B\partial a}$$

G properly averaged in random material: $$\langle G(a,E)\rangle=\frac{\partial\langle U(a,E)\rangle}{B\partial a}$$

with side conditions

$$U(0,\langle E\rangle)=0 \qquad \langle U(0,E)\rangle=0$$

$$\Rightarrow \qquad G(a,\langle E\rangle)\leq\langle G(a,E)\rangle$$

G computed by replacing random micro-beam by a homogeneous one ($E(\omega,x)=\langle E\rangle$) is lower than G computed with E taken honestly as a random field:

Define:

stress intensity factor in hypothetical material: $K(a,\langle E\rangle)$

stress intensity factor properly averaged in random material: $\langle K(a,E)\rangle$

$$\Rightarrow \qquad K(a,\langle E\rangle) \le \langle K(a,E)\rangle$$

$$\Rightarrow \qquad J(a,\langle E\rangle) \le \langle J(a,E)\rangle$$

<u>Remark 1</u>: With beam thickness L increasing,

mesoscale L/d grows

$$\Rightarrow E'(\omega, x) \to 0 \qquad \left\langle E^{-1} \right\rangle^{-1} \to \left\langle E \right\rangle$$

$\Rightarrow$ deterministic fracture mechanics is then recovered

<u>Remark 2</u>: Results carry over to Timoshenko beams:

$$G(a, \langle E \rangle, \langle \mu \rangle) \leq \left\langle G(a, E, \mu) \right\rangle = G^{*}(a, \left\langle E^{-1} \right\rangle^{-1}, \left\langle \mu^{-1} \right\rangle^{-1})$$

Fixed-grip conditions:

$$\langle G \rangle = \frac{-u}{2B}\left\langle \frac{\partial P}{\partial a} \right\rangle = \frac{-u}{2B}\frac{\partial \langle P \rangle}{\partial a} = \frac{9u^2 I \langle E \rangle}{2Ba^4}$$

$\Rightarrow$ G can be computed by direct ensemble averaging of E (and μ)

Mixed-loading conditions:

... both load and displacement vary during crack growth

$\Rightarrow$ no explicit relation between the crack driving force and the change in elastic strain energy.

… can get bounds from G under dead-load and G under fixed-grip:

$$G_u \leq G_{mixed} \leq G_P$$

Mixed-loading conditions:

... both load and displacement vary during crack growth

$\Rightarrow$ no explicit relation between the crack driving force and the change in elastic strain energy.

… can get bounds from G under dead-load and G under fixed-grip:

$$G_u \leq G_{mixed} \leq G_P$$

Note: in mechanics of random media, when studying passage from SVE to RVE, energy-type inequalites are ordered in an inverse fashion: kinematic (resp. force) conditions provides upper (resp. lower) bound.

Mixed-loading conditions for Timoshenko beam

... four possibilities:

P and M fixed: G_{P-M}

P and θ fixed: $G_{P-\theta}$

u and M fixed: G_{u-M}

u and θ fixed: $G_{u-\theta}$

$$\Rightarrow \qquad G_{u-\theta} \leq G_{P-\theta} \leq G_{P-M} \qquad G_{u-\theta} \leq G_{u-M} \leq G_{P-M}$$

THANK YOU!

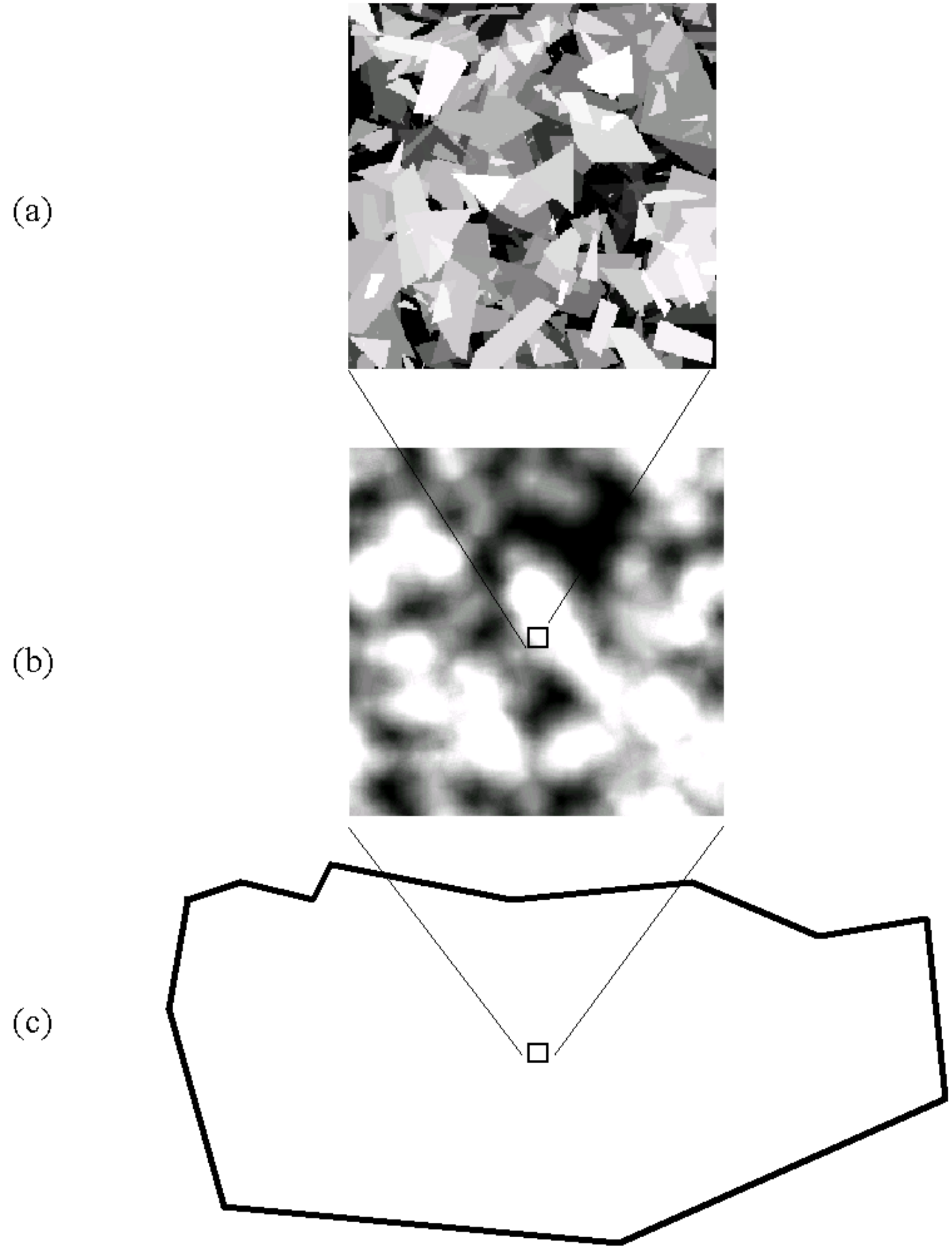

Fractals in Mechanics

Martin Ostoja-Starzewski

Department of Mechanical Science & Engineering,

Institute for Condensed Matter Theory, and Beckman Institute

University of Illinois at Urbana-Champaign

Definition: A **fractal** is "a rough or fragmented geometric shape that can be split into parts, each of which is (at least approximately … statistically) a reduced-size copy of the whole," a property called self-similarity.

H.-O. Peitgen (2010): "*if we talk about impact inside mathematics, and applications in the sciences, Benoît B. Mandelbrot is one of the most important figures of the last 50 years*."

…was often criticized for not being rigorous

Typical features of fractals:

- fine structure at arbitrarily small scales
- too irregular to be easily described by traditional Euclidean geometry
- self-similar (at least approximately or stochastically) (but not R^1)
- has a Hausdorff dimension which is greater than its topological dimension (not space-filling objects in 3d)
- has a simple and recursive definition

Common techniques for generating fractals:

Escape-time fractals – via recurrence relation (Mandelbrot, Julia sets…)

Iterated function systems – via a fixed geometric replacement rule (Cantor set, Sierpiński carpet…)

Random fractals – via stochastic processes (Brownian motion/sheets, Lévy flight…)

Strange attractors – via chaos

Can fractals be generated by mechanics?

e.g. by elasto-inelastic transitions

Can we develop a continuum-type theory of fractal media?

Can we solve initial-boundary-value problems?

Fractal dimension

Fractal = rough or fragmented geometric shape that can be split into parts, each of which is a reduced-size copy of the whole.

- Fractal dimension can be non-integer
- Fractal dimension represents the topological space-filling capacity of a geometric pattern
- Fractal dimension characterizes size scaling: $N_r \propto r^{-D}$

[B. Mandelbrot (1967). "How Long Is the Coast of Britain? Statistical Self-Similarity and Fractional Dimension," *Science*]

– Biological tissues: plants, brains, bones…
– Geological systems: mountains, rivers, rocks…
– Astronomy: Saturn's rings, galaxy star-forming sites…

Example of a *pre-fractal*: a rock at the size of $1m$ and $0.1m$

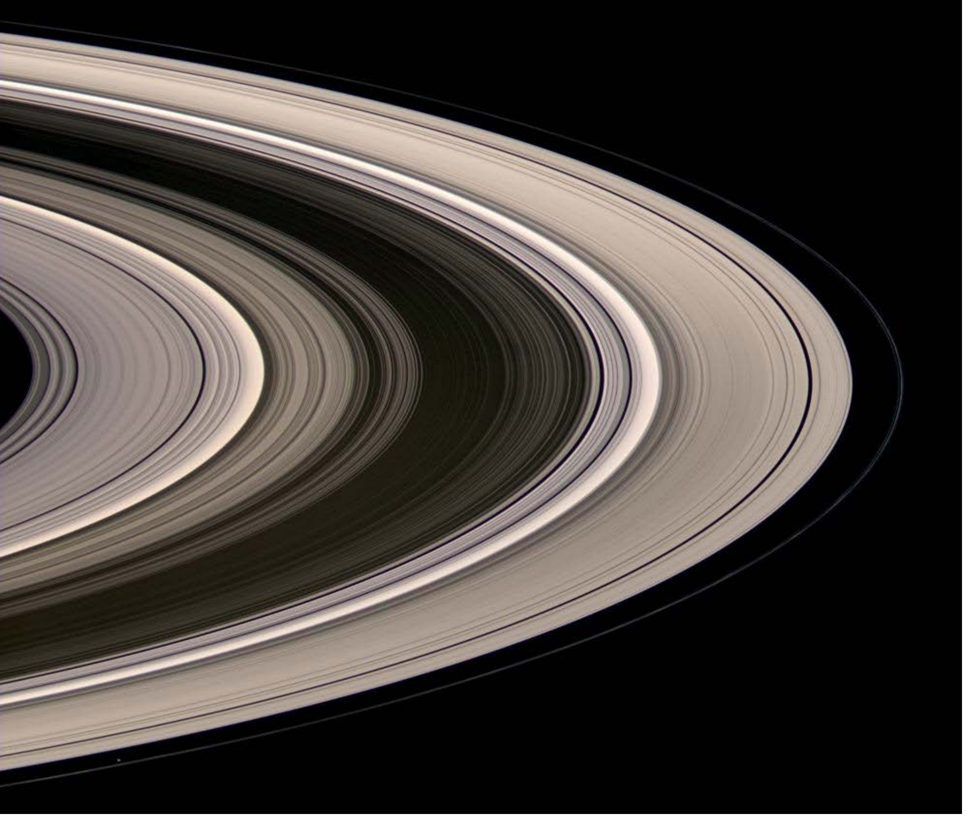 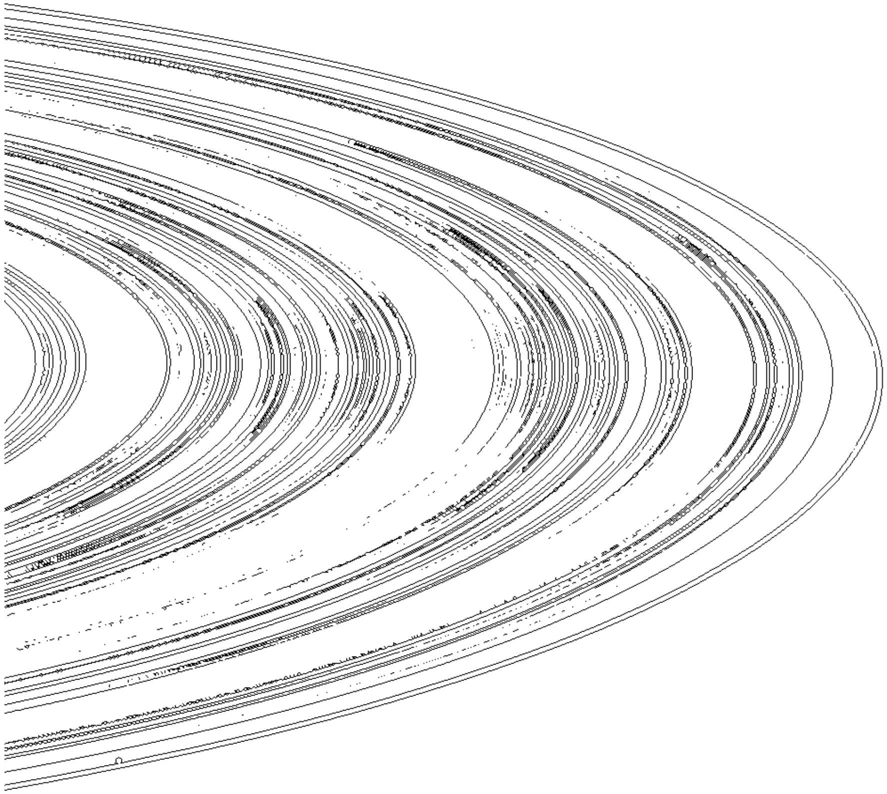

Saturn ring images from Cassini mission
http://saturn.jpl.nasa.gov/photos/halloffame/

processed to capture ring edges

D ~ 1.63 - 1.78

[*arXiv*, 2012; *SpringerPlus*, 2015]

Sierpinski carpet

$$D = \frac{\log(8)}{\log(3)} = 1.89281\ldots$$

$$D_{\text{box counting}} \simeq 1.8927$$

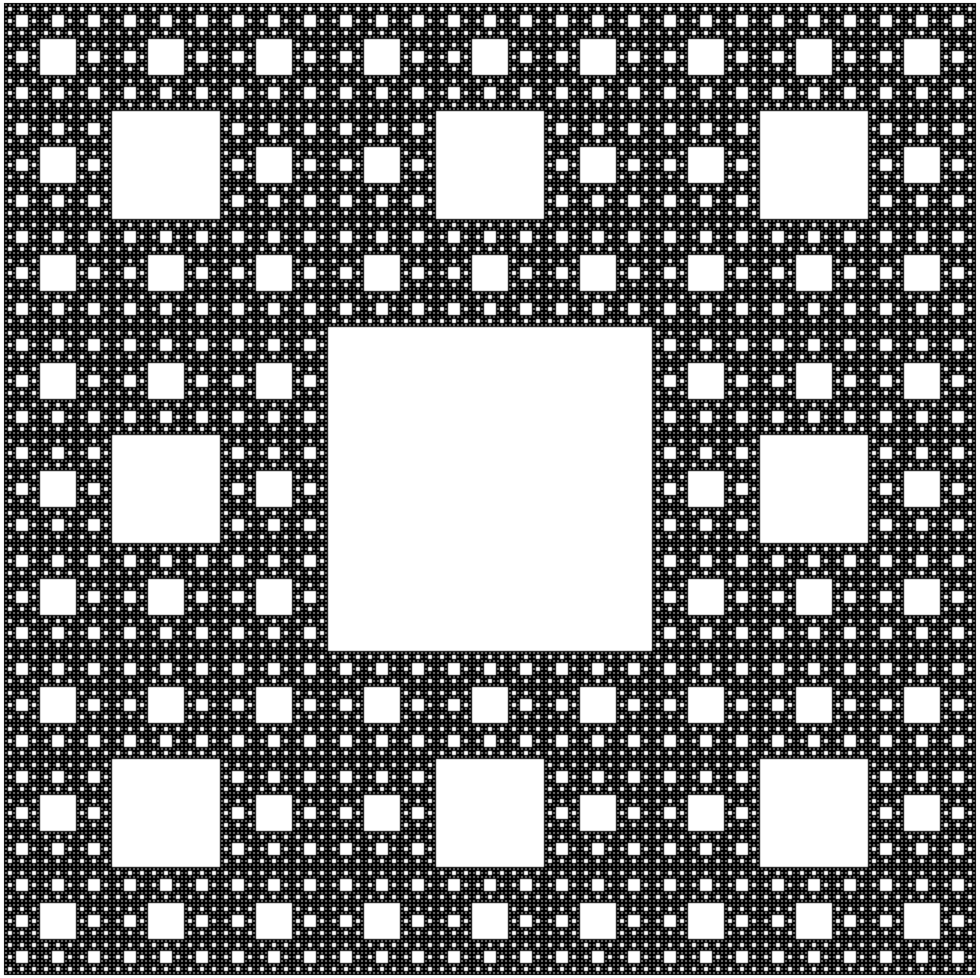

Voyager 2, 1981

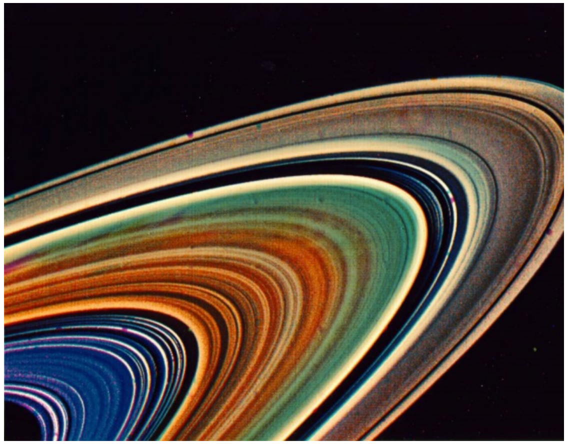

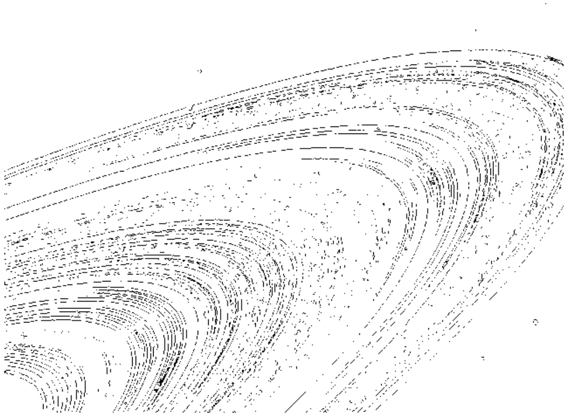

Common techniques for generating fractals:

Escape-time fractals – via recurrence relation (Mandelbrot, Julia sets…)

Iterated function systems – via a fixed geometric replacement rule (Cantor set, Sierpiński carpet…)

Random fractals – via stochastic processes (Brownian motion/sheets, Lévy flight…)

Strange attractors – via chaos

Can fractals be generated by mechanics?

e.g. by elasto-inelastic transitions

Can we develop a continuum-type theory of fractal porous media?

Can we solve initial-boundary-value problems?

Common techniques for generating fractals:

Escape-time fractals – via recurrence relation (Mandelbrot, Julia sets…)

Iterated function systems – via a fixed geometric replacement rule (Cantor set, Sierpiński carpet…)

Random fractals – via stochastic processes (Brownian motion/sheets, Lévy flight…)

Strange attractors – via chaos

Can fractals be generated by mechanics?

e.g. by elasto-inelastic transitions

Can we develop a continuum-type theory of fractal media?

Can we solve initial-boundary-value problems?

Oscillators, rods, beams with random/fractal properties under random/fractal loadings

i.e., random/fractal loadings lacking explicit spectral densities

i.e., having fractal and Hurst effects

Can grasp **fractals** and **Hurst effect**

roughness

heavy-tail behavior of covariance function

A random process Z_x is statistically self-similar if it obeys $Z_x = c^{-H} Z_{cx}$ for some c, where H is *Hurst parameter*

- when stretched by some factor c in x dimension, Z looks the same if stretched by c^{-H} in Z dimension

- most time series Z_t look “flat” if stretched like this

fractals: those enchanting, self-similar things

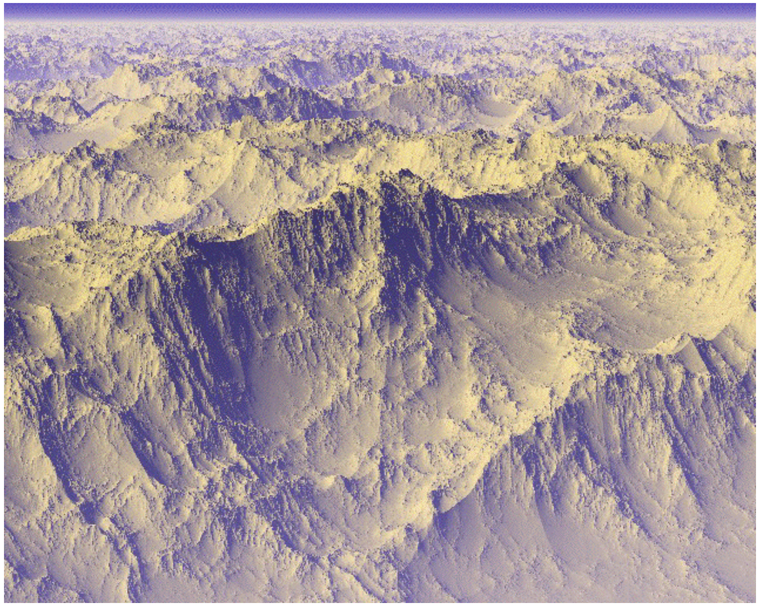

Hurst effect: long-term memory (Joseph effect)

$0 < H < 0.5$: time series with negative autocorrelation (e.g. a decrease between values will likely be followed by an increase)

$0.5 < H < 1$: time series with positive autocorrelation (an increase between values followed by another increase)

$H = 0.5$: true random walk, where there is no preference for a decrease or increase following any particular value.

$F(t)$ is zero-mean, Gaussian random process

covariance:

wide-sense stationary (WSS): $C(t_1, t_2) = C_F(|t_1 - t_2|)$

If for some

then $D = \dim(\text{Graph } F) = \min\left(\dfrac{1}{\alpha/2}, 1 - \alpha/2\right)$

If for some $\beta \in (0,1)$,

then $F(t)$ has long memory, with Hurst coefficient $H = \beta/2$

If , process is *persistent*

If , process is *anti-persistent*

Transient response of a linear system:

$$cX' + kX = c(\beta + \gamma t)U(t)F(t)$$

to a wide-sense stationary random excitation $F(t)$ with

- white noise,
- Ornstein-Uhlenbeck (OU),
- Matérn,
- Cauchy,
- Dagum covariance function

$$X' + aX = F(t) \quad \Rightarrow \quad X(t) = \int_0^t h_a(t-\tau)F(\tau)\mathbf{d}\tau$$

$$E[F(t)] = 0 \quad \Rightarrow$$

[Shen, M. Ostoja-Starzewski & E. Porcu, “Responses of first-order dynamical systems to Matérn, Cauchy, or Dagum excitations,” *Math. Mech. Complex Syst. (MEMOCS)* **3**(1), 27-41, 2015]

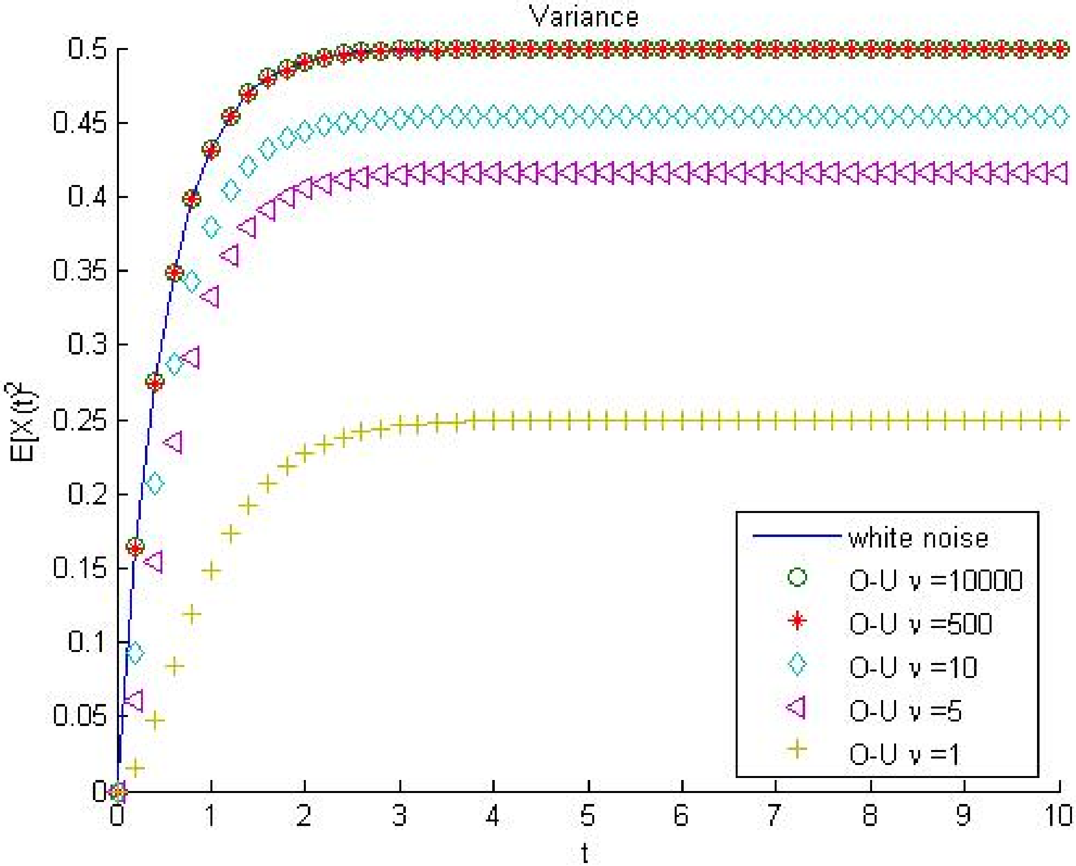

$$C_{\mathbf{WN}}(r) := \delta(r), \quad r \geq 0,$$

$$C_{\mathbf{OU}}(r;\nu) := \frac{\nu}{2}\mathbf{e}^{-\nu r}, \quad r \geq 0,$$

Variances of response *X*(*t*) under white noise and OU forcings.

$F(t)$ is zero-mean, Gaussian random process

covariance:

wide-sense stationary (WSS): $C(t_1, t_2) = C_F(|t_1 - t_2|)$

Gaussian white noise: $$C_{\mathbf{WN}}(r) := \delta(r), \quad r \geq 0,$$

Ornstein-Uhlenbeck: $$C_{\mathbf{OU}}(r;\nu) := \frac{\nu}{2}\mathbf{e}^{-\nu r}, \quad r \geq 0,$$

Matérn: $$C_{\mathbf{M}}(r;\nu) := r^{\nu}\mathbf{K}_{\nu}(r), \quad r \geq 0,$$

Cauchy: $$C_{\mathbf{C}}(r;\theta,\eta) := \left(1 + r^{\theta}\right)^{-\eta/\theta},$$

Dagum: $$C_{\mathbf{D}}(r;\delta,\varepsilon) := 1 - \left(1 + r^{-\delta}\right)^{-\varepsilon/\delta},$$

$$0 < \delta \leq 2$$

Variance of $F(t)$:

Gaussian white noise:

Ornstein-Uhlenbeck:

Matérn:

Cauchy:

Dagum: no explicit formula

$$C_{\mathbf{WN}}(r) := \delta(r), \quad r \ge 0,$$

$$C_{\mathbf{OU}}(r;\nu) := \frac{\nu}{2}\mathbf{e}^{-\nu r}, \quad r \ge 0,$$

$$C_{\mathbf{M}}(r;\nu) := r^{\nu}\mathbf{K}_{\nu}(r), \quad r \ge 0,$$

$$C_{\mathbf{C}}(r;\theta,\eta) := \left(1+r^{\theta}\right)^{-\eta/\theta},$$

$$C_{\mathbf{D}}(r;\delta,\varepsilon) := 1-\left(1+r^{-\delta}\right)^{-\varepsilon/\delta}$$

$$0 < \delta \le 2$$

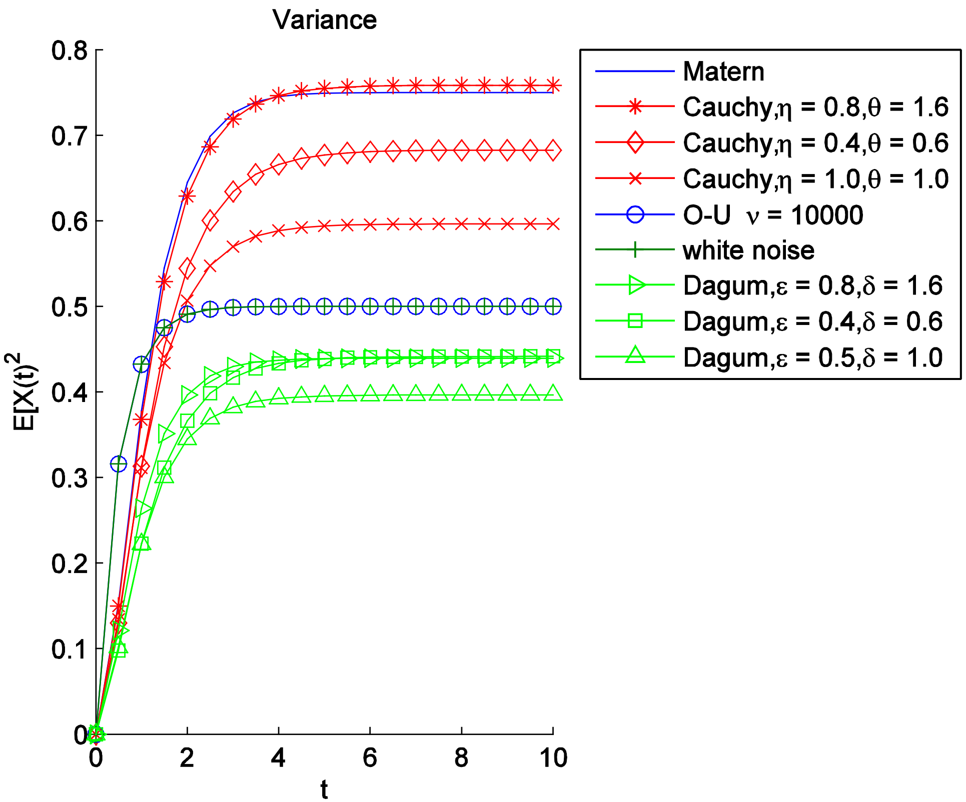

Variances under various forcings: Matérn, Cauchy (η=0.8, θ=1.6; η=0.4,θ=0.6; η=1.0,θ=1.0), Ornstein-Uhlenbeck (*v*=10,000), white noise, and Dagum (ε=0.8,δ=1.6, ε=0.4,δ=0.6, ε=0.5,δ=1.0).

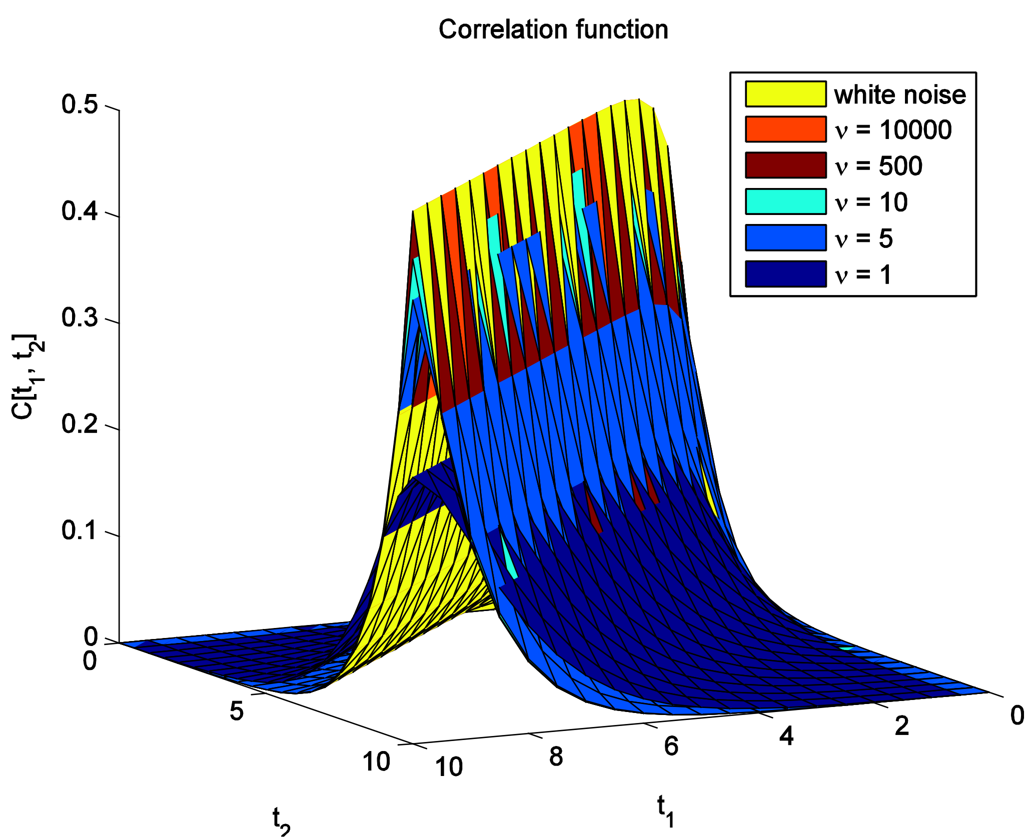

$$C_{\mathbf{OU}}(r;\nu) := \frac{\nu}{2}\mathbf{e}^{-\nu r}, \quad r \geq 0,$$

Correlation function under OU forcings at various ν.

1^{st}-order dynamical system's correlation

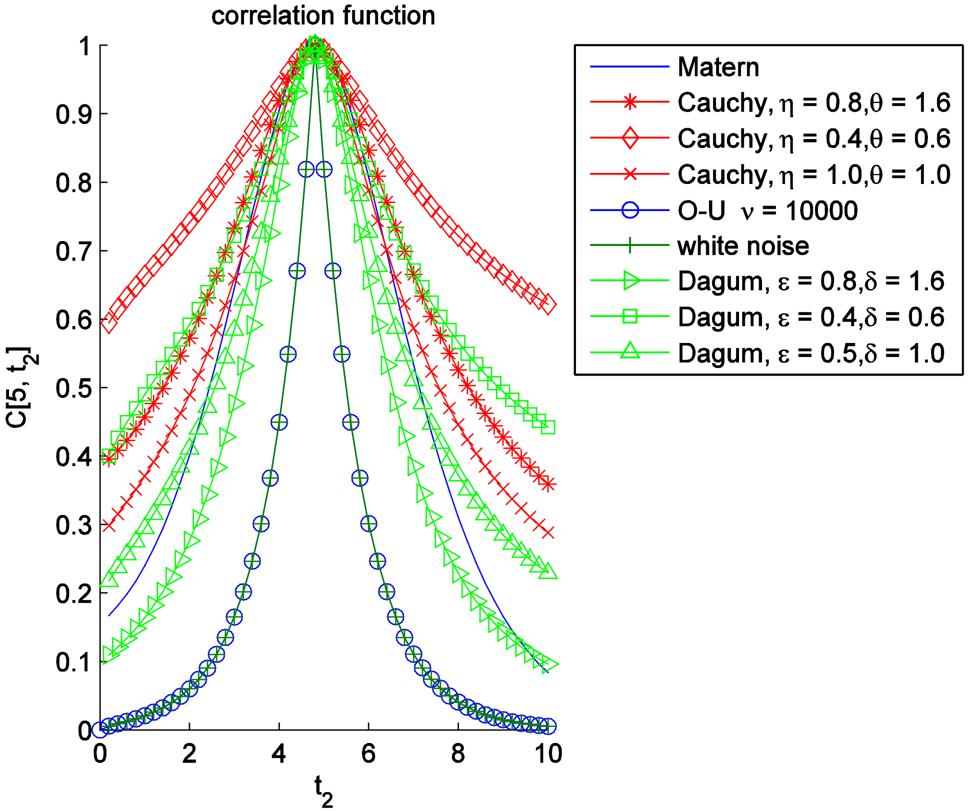

$$C_{\mathbf{WN}}(r) := \delta(r), \quad r \geq 0,$$

$$C_{\mathbf{OU}}(r;\nu) := \frac{\nu}{2}\mathbf{e}^{-\nu r}, \quad r \geq 0,$$

$$C_{\mathbf{M}}(r;\nu) := r^{\nu}\mathbf{K}_{\nu}(r), \quad r \geq 0,$$

$$C_{\mathbf{C}}(r;\theta,\eta) := \left(1+r^{\theta}\right)^{-\eta/\theta},$$

$$C_{\mathbf{D}}(r;\delta,\varepsilon) := 1-\left(1+r^{-\delta}\right)^{-\varepsilon/\delta},$$
$$0 < \delta \leq 2$$

Correlation function of *F*(*t*):

$$
\begin{aligned}
C_X(t_1,t_2) &= E[X(t_1)X(t_2)] \\
&= \int_0^{t_2}\int_0^{t_1}\Psi(\tau_1,\tau_2)C_F(\tau_1,\tau_2)h_a(t_1-\tau_1)h_a(t_2-\tau_2)d\tau_1 d\tau_2
\end{aligned}
$$

Gaussian white noise: explicit formula

Ornstein-Uhlenbeck: explicit formula

Matérn: explicit formula - approximately Matérn

Cauchy: explicit formula – not Cauchy

Dagum: no explicit formula

Transient response of a linear 2nd-order system:

to a wide-sense stationary random excitation $F(t)$ with either

- white noise,
- Ornstein-Uhlenbeck (OU),
- Matérn,
- Cauchy,
- or Dagum covariance function

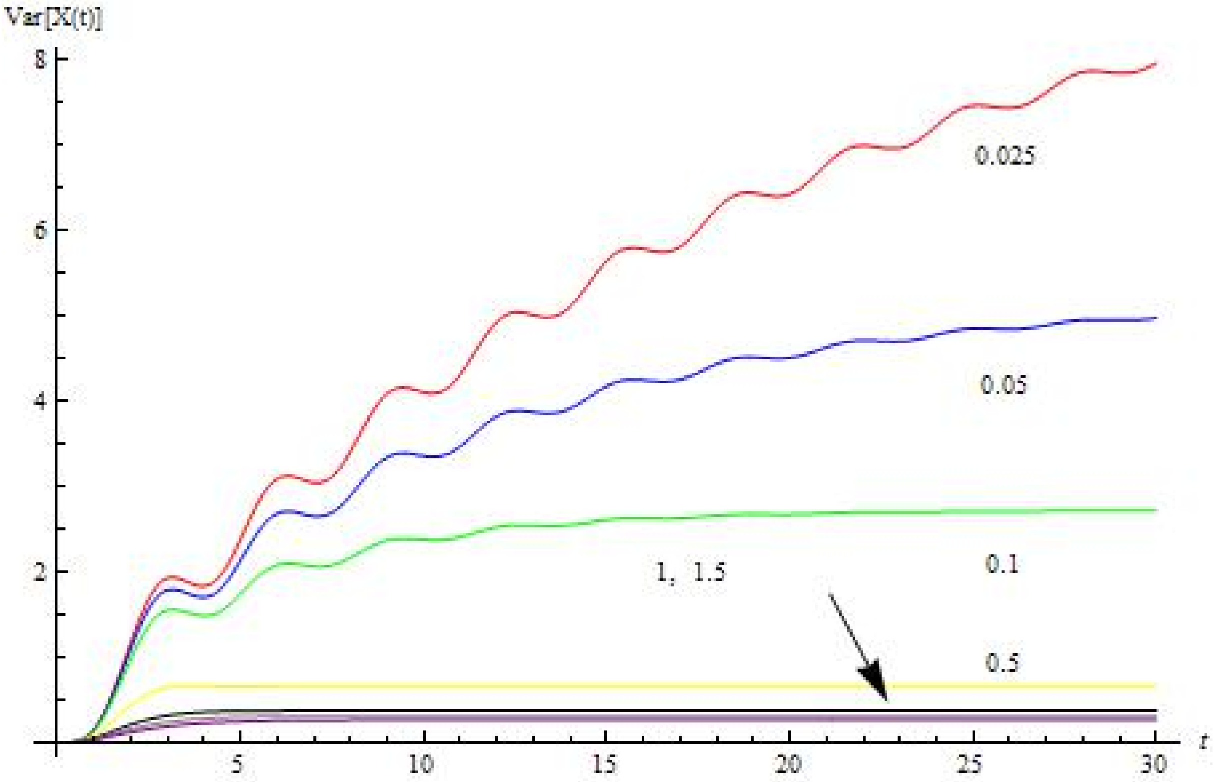

$$C_{\mathbf{WN}}(r) := \delta(r), \quad r \geq 0,$$

$$C_{\mathbf{OU}}(r;\nu) := \frac{\nu}{2}\mathbf{e}^{-\nu r}, \quad r \geq 0,$$

Variances of response $X(t)$ under white noise and OU forcings.

The curve due to white noise overlaps with that due to OU process already for ν=500.

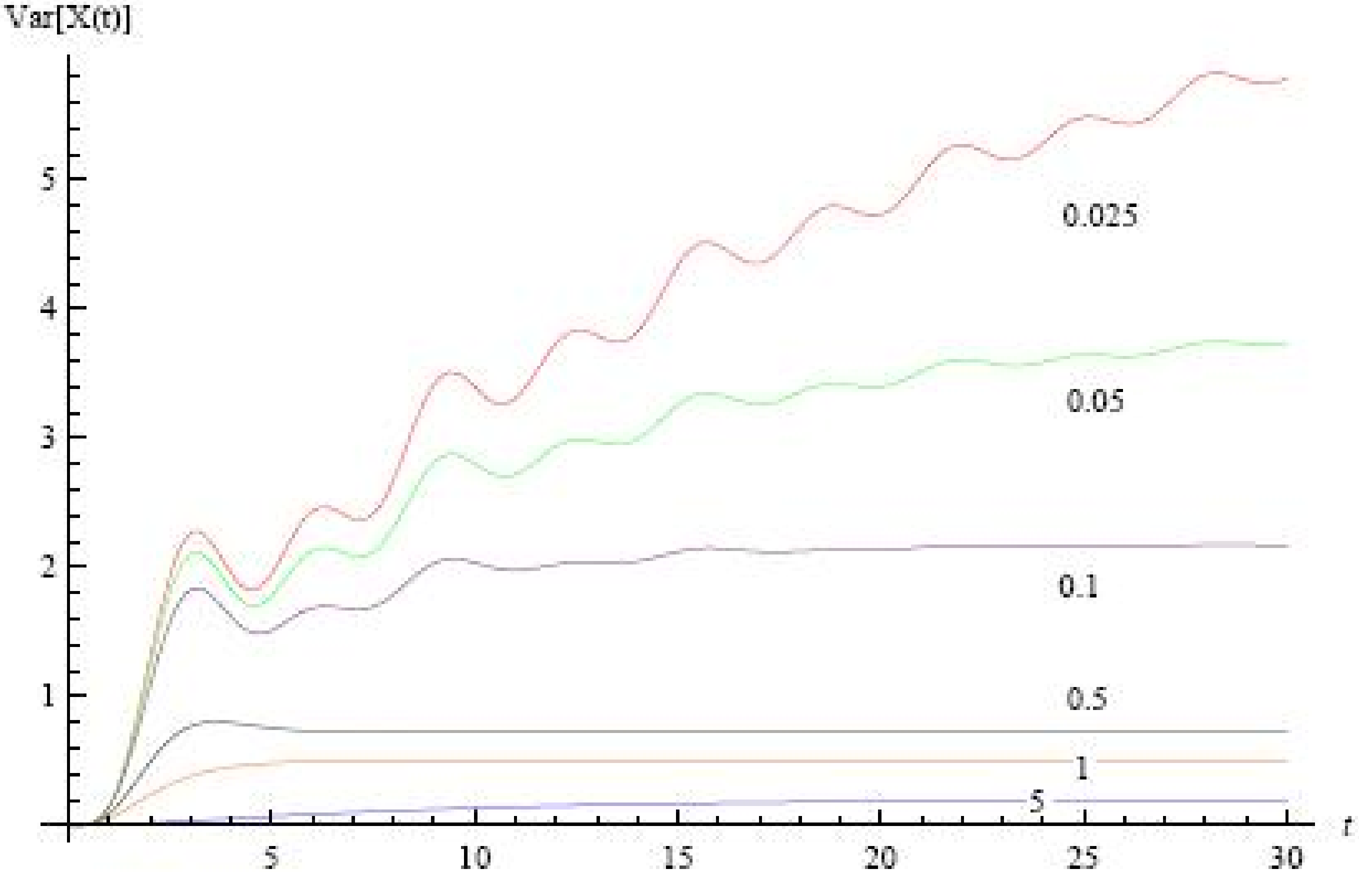

$$C_{\mathbf{M}}(r;\nu) := r^{\nu}\mathbf{K}_{\nu}(r), \quad r \geq 0,$$

Variance of X(t) under forcing by Gaussian process with Matérn covariance, with various ζ (= 0.025, 0.05, 0.1, 0.5, 1,5).

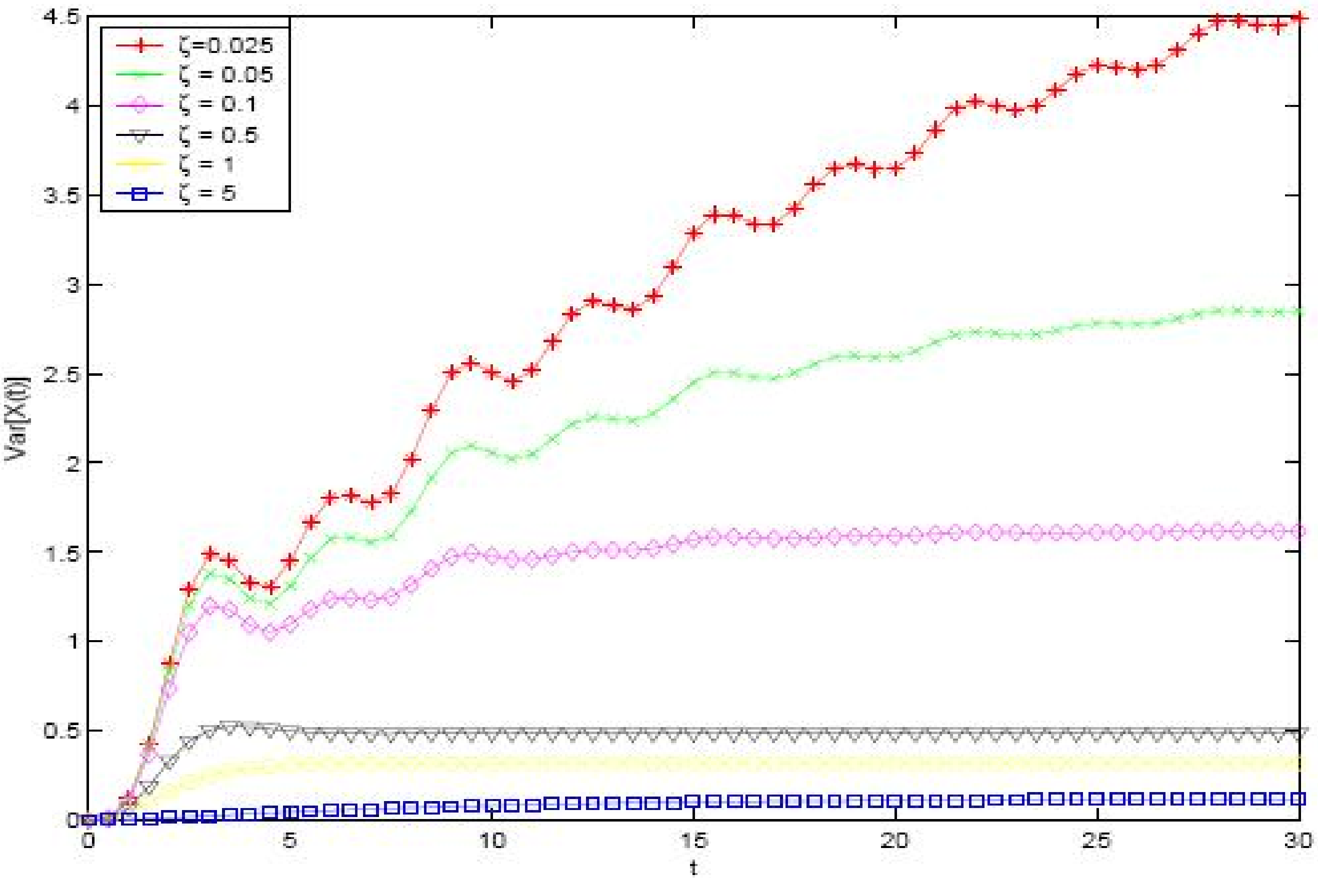

$$C_{\mathbf{C}}(r;\theta,\eta) := \left(1 + r^{\theta}\right)^{-\eta/\theta},$$

Variance of $X(t)$ under the forcing of a Gaussian process with a Cauchy covariance with different values of ζ (0.025, 0.05, 0.1, 0.5, 1,5).

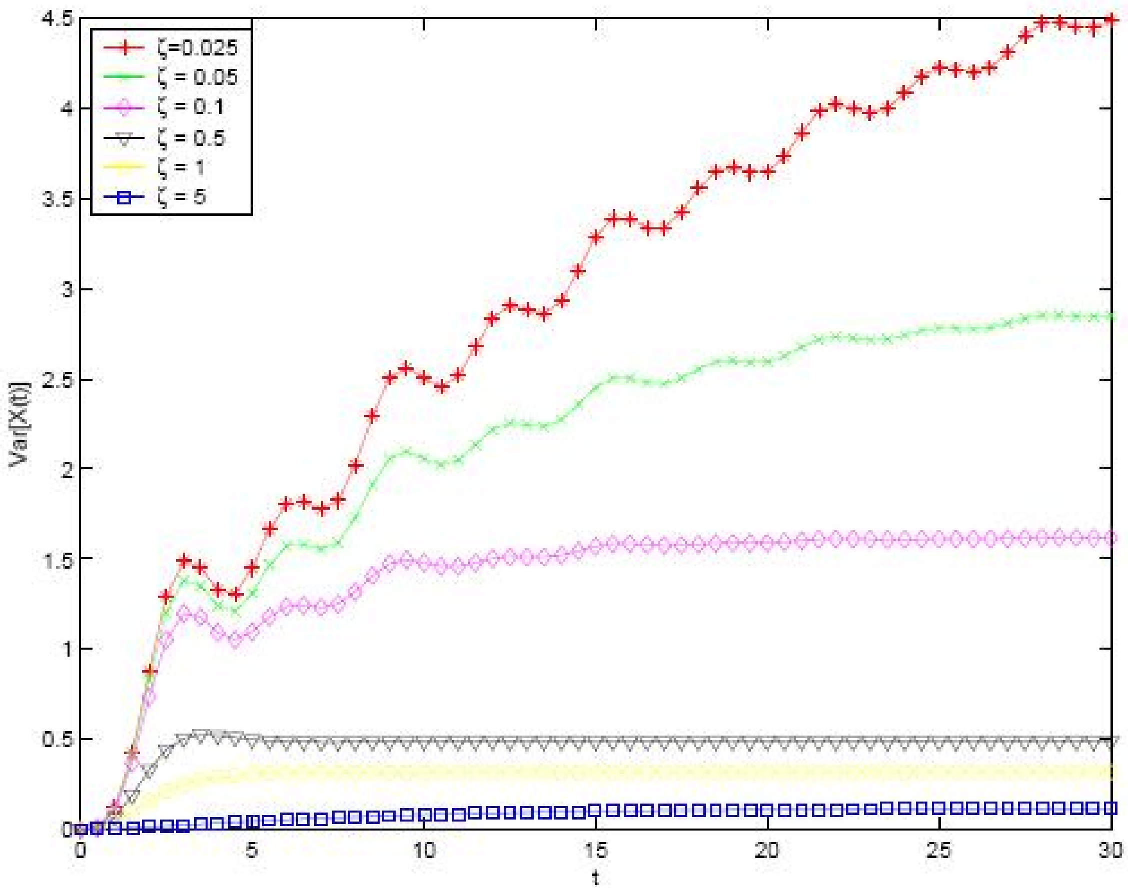

$$C_{\mathbf{D}}(r;\delta,\varepsilon) := 1 - \left(1 + r^{-\delta}\right)^{-\varepsilon/\delta},$$

$$0 < \delta \leq 2$$

Variance of X(t) under Dagum forcing with different value of ζ.

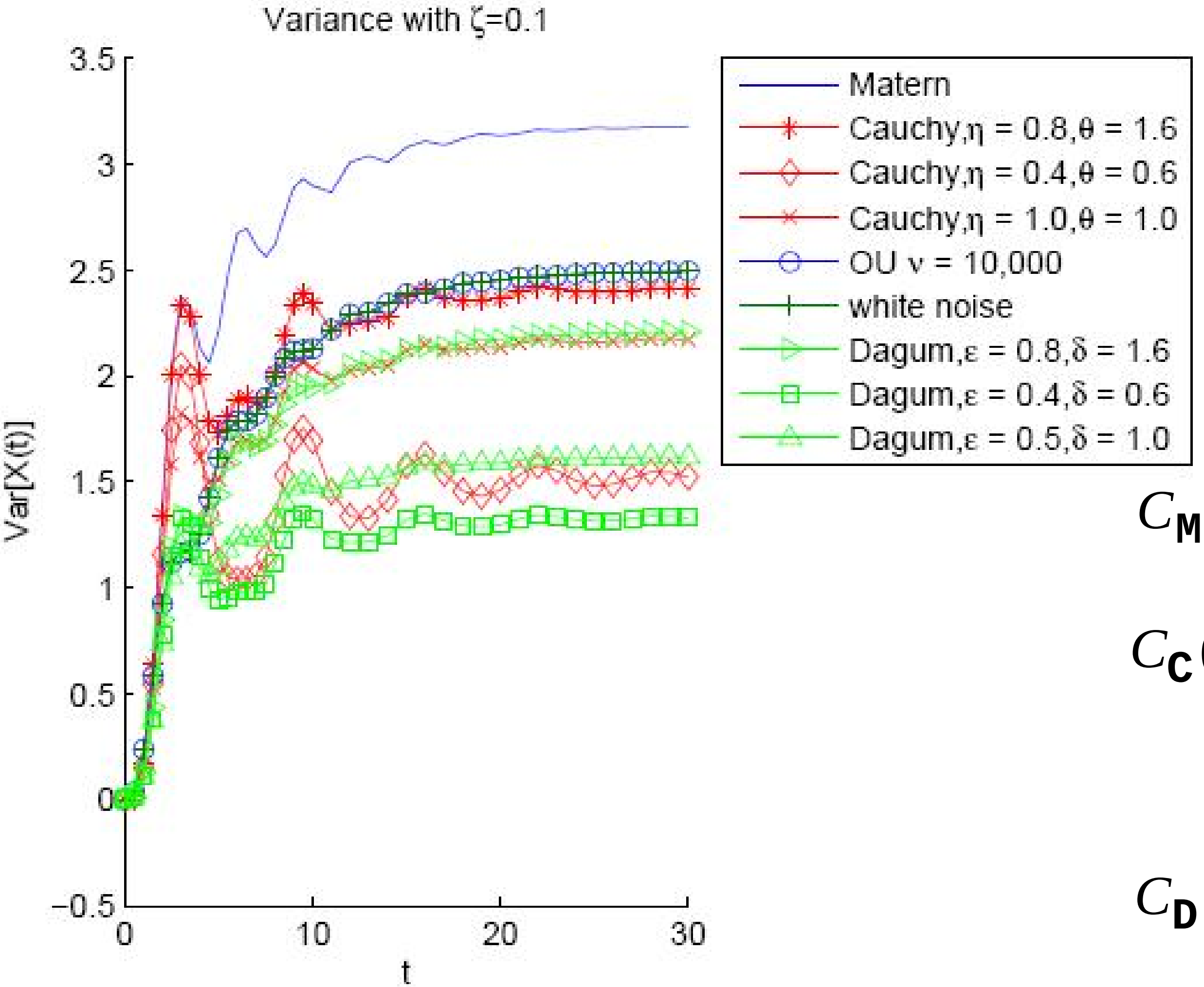

$$C_{\mathbf{WN}}(r) := \delta(r), \quad r \geq 0,$$

$$C_{\mathbf{OU}}(r;\nu) := \frac{\nu}{2}\mathbf{e}^{-\nu r}, \quad r \geq 0,$$

$$C_{\mathbf{M}}(r;\nu) := r^{\nu}\mathbf{K}_{\nu}(r), \quad r \geq 0,$$

$$C_{\mathbf{C}}(r;\theta,\eta) := \left(1 + r^{\theta}\right)^{-\eta/\theta},$$

$$C_{\mathbf{D}}(r;\delta,\varepsilon) := 1 - \left(1 + r^{-\delta}\right)^{-\varepsilon/\delta}, \quad 0 < \delta \leq 2$$

Correlations of $X(t)$ with ζ=0.1 at t_1=15 in underdamped structure under various forcings: Matérn, Cauchy, OU, white noise, and Dagum.

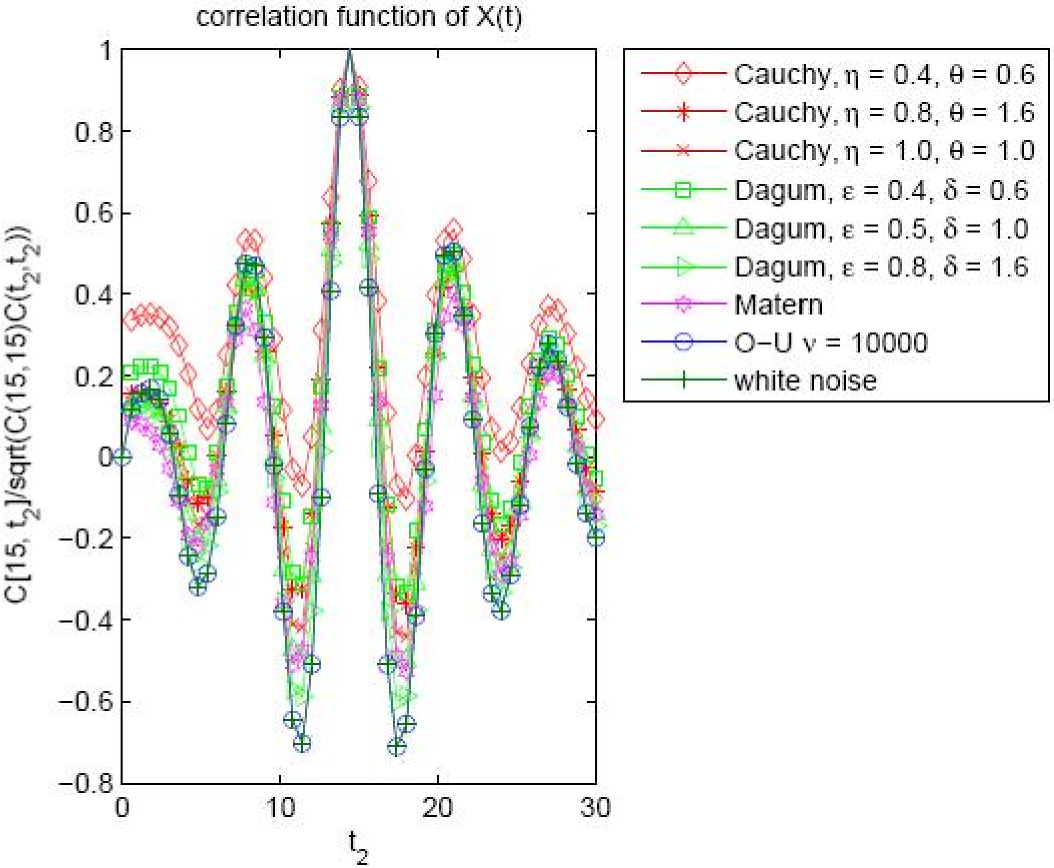

$$C_{\mathbf{WN}}(r) := \delta(r), \quad r \geq 0,$$

$$C_{\mathbf{OU}}(r;\nu) := \frac{\nu}{2}\mathbf{e}^{-\nu r}, \quad r \geq 0$$

$$C_{\mathbf{M}}(r;\nu) := r^{\nu}\mathbf{K}_{\nu}(r), \quad r \geq 0,$$

$$C_{\mathbf{C}}(r;\theta,\eta) := \left(1 + r^{\theta}\right)^{-\eta/\theta},$$

$$C_{\mathbf{D}}(r;\delta,\varepsilon) := 1 - \left(1 + r^{-\delta}\right)^{-\varepsilon/\delta},$$

$$0 < \delta \leq 2$$

Variances of *X*(*t*) with ζ=0.1 in underdamped structure under various forcings: Matérn, Cauchy, OU, white noise, and Dagum.

Randomly inhomogeneous rods and beams under random forcings:

[L. Shen, M. Ostoja-Starzewski and E. Porcu, “Elastic rods and shear beams with random field properties under random field loads: fractal and Hurst effects,” *ASCE J. Eng. Mech.,* 2015.]

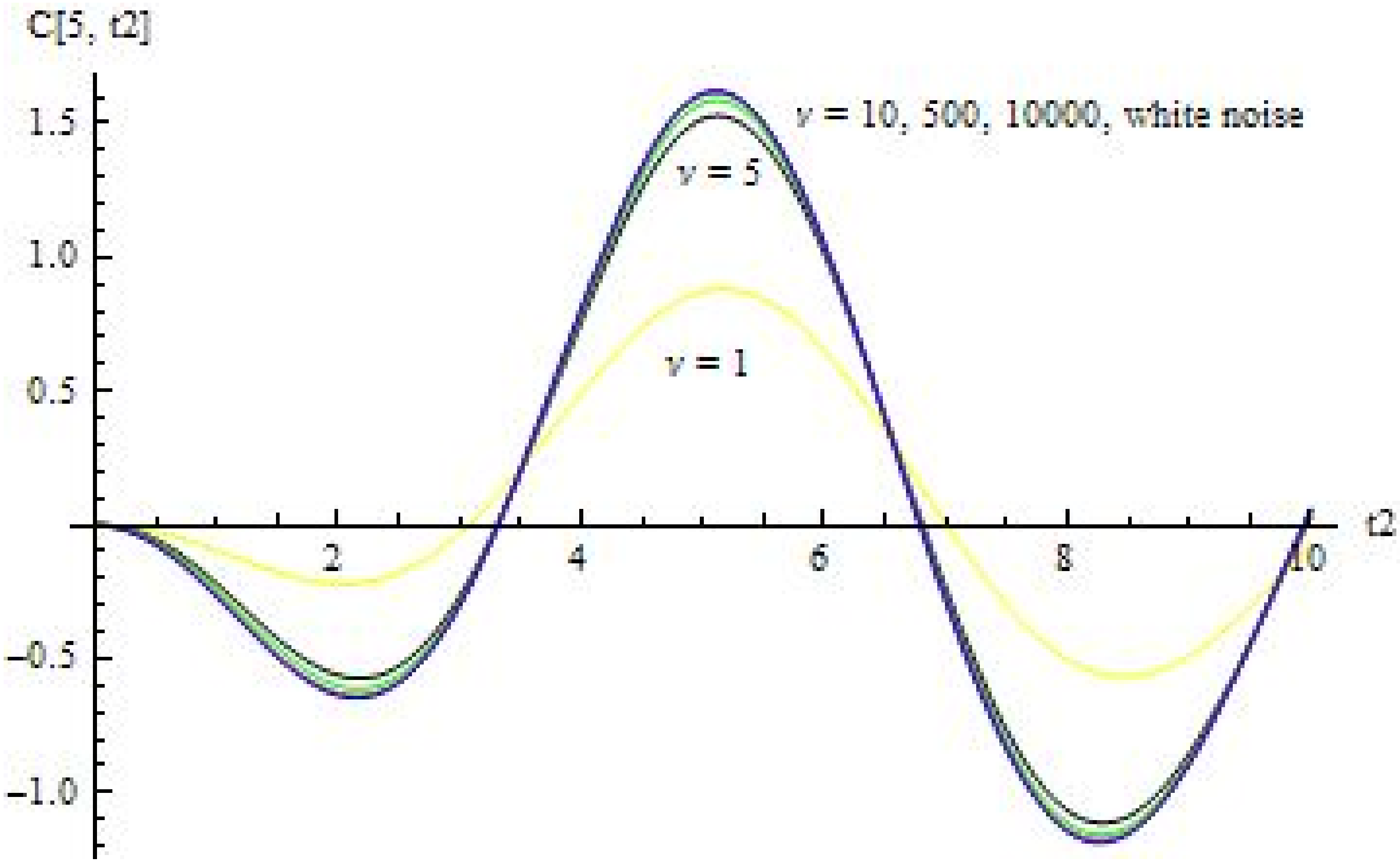

Correlation functions of X(t) at t =5 under white noise and OU (ν=1,5,10,500 and 10,000) forcings.

The curve due to white noise overlaps with those due to OU process for ν=10,000 and already for 500.

OBSERVE

1. Time-stationary random forcings of Cauchy and Dagum types lack explicit parametric spectral densities, yet they allow decoupling of the fractal dimension and Hurst effect.

2. Working directly in time domain, find transient 2^{nd}-order characteristics of response and, for comparison, also examine effects of Gaussian white noise, Ornstein-Uhlenbeck, and Matérn forcings.

3. Given the same variance on input, the variance on output is strongest for Matérn, then Cauchy, then O-U, then white noise, and finally, Dagum forcing.

4. If the excitation correlation function is Matérn, the correlation function of response is approximately Matérn.

- … response due to Cauchy excitation is not Cauchy
- … cannot yet say whether response due to Dagum excitation (with its fractal and Hurst effects) is Dagum or not

A porous rock at R = 1m (a) and R = 0.1m (b); example of a **pre-fractal**.

Many brittle and/or ductile materials display fractal features: fracture surfaces, dislocation patterns, plastic ridges in ice fields, shear bands in rocks, phase transitions…

J.D. Goddard and M. Sahimi, 1986, *Phys. Rev. B* **33**.
M. Zaiser, K. Bay and P. Hahner, 1999, *Acta Mater*, **47**.
M. Ostoja-Starzewski, 1990, *Pure Appl. Geophys*. **133**.
A.N.B. Poliakov, H.J. Herrmann, Y.Y. Podladchikov and S. Roux, 1994, *Fractals* **2**.
D. Sornette, 2004, *Critical Phenomena in Natural Sciences*, Springer.

[“From fractal media to continuum mechanics,” *ZAMM* **93**, 1-29]

Common techniques for generating fractals:

Escape-time fractals – via recurrence relation (Mandelbrot, Julia sets…)

Iterated function systems – via a fixed geometric replacement rule (Cantor set, Sierpiński carpet…)

Random fractals – via stochastic processes (Brownian motion/sheets, Lévy flight…)

Strange attractors – via chaos

Can fractals be generated by mechanics?

e.g. by elasto-plasticity

Can we develop a continuum-type theory of fractal porous media?

Can we solve initial-boundary-value problems?

Mass in a fractal geometric structure W obeys a power law

$$m(L) \propto L^D, \quad D < 3$$

[V.E. Tarasov, *Ann. Phys.*, 2005]

Use a fractional integral to represent mass in a fractal region

$$m(W) = \int_W \rho(\mathbf{R})dV_D = \int_W \rho(\mathbf{R})c_3(D,\mathbf{R})dV_3$$

Mass in a fractal geometric structure W obeys a power law

$$m(L) \propto L^D, \quad D < 3$$

[V.E. Tarasov, *Ann. Phys.*, 2005]

Use a fractional integral to represent mass in a fractal W

$$m(W) = \int_W \rho(\mathbf{R}) dV_D = \int_W \rho(\mathbf{R}) c_3(D, \mathbf{R}) dV_3$$

$in\ W \subset \mathrm{R}^3$

$in\ \mathrm{R}^3$

$\Rightarrow$

integration and differentiation in non-integer-dimensional spaces

$$c_3(D, R) = |\mathbf{R}|^{D-3} \frac{2^{3-D} \Gamma(3/2)}{\Gamma(D/2)}$$

Riesz potential for a locally integrable function on

$\Rightarrow$

integration and differentiation in non-integer-dimensional spaces

Green-Gauss theorem

$$\int_{\partial W} \mathbf{v} \bullet \mathbf{n} dS_d = \int_W c_3^{-1}(D,R) \nabla \bullet \left(c_2(d,R)\mathbf{v}\right) dV_D$$

where

$$dS_d = c_2(d,R)\, dS_2 \qquad dV_D = c_3(D,R)\, dV_3$$

surface fractal dimension of W

mass fractal dimension of W

$\Rightarrow$

integration and differentiation in non-integer-dimensional spaces

$$c_2(D,R) = |\mathbf{R}|^{d-2} \frac{2^{2-D}}{\Gamma(d/2)}$$

Fractal continuity equation for *W*

$$\left(\frac{d}{dt}\right)_D \rho = -\rho \nabla_k^D v_k$$

Fractal linear and angular momentum equations

$$\rho \left(\frac{d}{dt}\right)_D v_k = \rho f_k + \nabla_l^D \sigma_{kl} \qquad \sigma_{kl} = \sigma_{kl}$$

Fractional equation of energy balance

$$\rho \left(\frac{d}{dt}\right)_D u = c\left(D, d, R\right) \sigma_{kl} v_{k,l} - \nabla_k^D q_k$$

Fractional equation of 2nd law of thermodynamics (C-D inequality)

$$0 \le T \rho \left(\frac{d}{dt}\right)_D s^{(i)} = \sigma_{ij}^{(d)} \left[\left(\frac{d}{dt}\right)_D u_{(i}\right]_{,j)} + \beta_{ij}^{(d)} \left(\frac{d}{dt}\right)_D \alpha_{ij} - c\left(D, d, R\right) \frac{T_{,k}\, q_k}{T}$$

Fractal continuity equation for *W*

$$\left(\frac{d}{dt}\right)_D \rho = -\rho \nabla_k^D v_k$$

Fractal linear and angular momentum equations

$$\rho \left(\frac{d}{dt}\right)_D v_k = \rho f_k + \nabla_l^D \sigma_{kl} \qquad \sigma_{kl} = \sigma_{kl}$$

Fractional equation of energy balance

$$\rho \left(\frac{d}{dt}\right)_D u = c(D, d, R)\sigma_{kl} v_{k,l} - \nabla_k^D q_k$$

Fractional equation of 2nd law of thermodynamics (C-D inequality)

$$0 \le T\rho \left(\frac{d}{dt}\right)_D s^{(i)} = \sigma_{ij}^{(d)} \left[\left(\frac{d}{dt}\right)_D u_{(i}\right]_{,j)} + \beta_{ij}^{(d)} \left(\frac{d}{dt}\right)_D \alpha_{ij} - c(D, d, R)\frac{T_{,k}\, q_k}{T}$$

non-fractal medium *(D=3, d=2)* $\Rightarrow$ recover conventional forms

$\Rightarrow$ two generalized operators

$$\nabla_k^D f = c_3(D,R)\frac{\partial}{\partial x_k}\left[c_2(d,R)\, f\right] := c_3(D,R)\nabla_k\left[c_2(d,R)\, f\right]$$

$$\left(\frac{d}{dt}\right)_D f := \frac{\partial f}{\partial t} + c(D,d,R)\, v_k \frac{\partial f}{\partial x_k}$$

where

$$c(D,d,R) = |\mathbf{R}|^{d+1-D}\,\frac{2^{D-d-1}\Gamma(D/2)}{\Gamma(3/2)\Gamma(d/2)}$$

$$c_2(d,R) = |\mathbf{R}|^{d-2}\,\frac{2^{2-d}}{\Gamma(d/2)}$$

$$c_3(D,R) = |\mathbf{R}|^{D-3}\,\frac{2^{3-D}\Gamma(3/2)}{\Gamma(D/2)}$$

$$c(D,d,R) = c_3^{-1}(D,R)\, c_2(d,R)$$

$\Rightarrow$ two generalized operators

$$\nabla_k^D f = c_3(D,R)\frac{\partial}{\partial x_k}\left[c_2(d,R) f\right] := c_3(D,R)\nabla_k\left[c_2(d,R) f\right]$$

$$\left(\frac{d}{dt}\right)_D f := \frac{\partial f}{\partial t} + c(D,d,R) v_k \frac{\partial f}{\partial x_k}$$

where

$$c(D,d,R) = |\mathbf{R}|^{d+1-D} \frac{2^{D-d-1}\Gamma(D/2)}{\Gamma(3/2)\Gamma(d/2)}$$

$$c_2(d,R) = |\mathbf{R}|^{d-2} \frac{2^{2-d}}{\Gamma(d/2)}$$

$$c_3(D,R) = |\mathbf{R}|^{D-3} \frac{2^{3-D}\Gamma(3/2)}{\Gamma(D/2)}$$

$$c(D,d,R) = c_3^{-1}(D,R) c_2(d,R)$$

$\Rightarrow$ $\nabla_k^D fg = f\nabla_k^D g + cg\nabla_k f$

Drawbacks of Tarasov's formulation

1. Usual fractional derivative (Riemann-Liouville) of a constant $\neq 0$

2. The mechanics-type derivation of wave equations yields a different result from the variational-type derivation

3. The 3d wave equation

$$\frac{\partial^2 p}{\partial t^2} = \left(c \frac{2^{D-3}\Gamma\left(D/2\right)}{\Gamma\left(3/2\right)} |R|^{2-D} \right)^2 \left[(3-D)\vec{R}\cdot\vec{\nabla}p + |R|^2 \nabla^2 p \right]$$

does not reduce to the 1d wave equation

$$c_1(D,x)\frac{\partial^2 p}{\partial t^2} = \frac{\partial}{\partial x}\left[v^2 c_1(D,x)\frac{\partial p}{\partial x} \right]$$

[Continuous medium model for fractal media, *Phys. Lett.* **336** (2005)]
[Fractional hydrodynamic equations for fractal media, *Ann. Phys.* **318** (2005)]
[*Fractional Dynamics*, Springer (2010)]

Formulation via product measures…

Mass in an anisotropic fractal: $m(x_1, x_2, x_3) \sim \left(\frac{x_1}{l_{10}}\right)^{\alpha_1} \left(\frac{x_2}{l_{20}}\right)^{\alpha_3} \left(\frac{x_3}{l_{30}}\right)^{\alpha_3}$

l_{k0} characteristic length in

α_k fractal dimension along

In other directions the fractal dimension is not necessarily the sum of projected fractal dimension…

(Falconer, 2003): "*Many fractals encountered in practice are not actually products, but are product-like*."

expect $D = \alpha_1 + \alpha_2 + \alpha_3$

Formulation via product densities…

power law relation w.r.t. each coordinate

$$m(x_1, x_2, x_3) \sim x_1^{\alpha_1} x_2^{\alpha_2} x_3^{\alpha_3}$$

use a fractional integral with *product measure*

$$m(x_1, x_2, x_3) = \iiint \rho(x_1, x_2, x_3) d\mu_1(x_1) d\mu_2(x_2) d\mu_3(x_3)$$

and length measurement in each coordinate

$$d\mu_k\left(x_k\right) = c_1^{(k)}\left(\alpha_k, x_k\right) dx_k, \quad k = 1, 2, 3$$

Vector calculus on anisotropic fractals

fractal derivative (*fractal gradient*) operator

$$\boldsymbol{\nabla}^D \varphi = \mathbf{e}_k \nabla_k^D \varphi \quad \text{or} \quad \nabla_k^D \varphi = \frac{1}{c_1^{(k)}} \frac{\partial \varphi}{\partial x_k} \quad \text{(no sum on } k\text{)}$$

= base vectors

$\Rightarrow$ *fractal divergence* of a vector field

$$\operatorname{div} \mathbf{f} = \boldsymbol{\nabla}^D \cdot \mathbf{f} \quad \text{or} \quad \nabla_k^D f_k = \frac{1}{c_1^{(k)}} \frac{\partial f_k}{\partial x_k}$$

$\Rightarrow$ *fractal curl* operator of a vector field

$$\operatorname{curl} \mathbf{f} = \boldsymbol{\nabla}^D \times \mathbf{f} \quad \text{or} \quad e_{jki} \nabla_k^D f_i = e_{jki} \frac{1}{c_1^{(k)}} \frac{\partial f_i}{\partial x_k}$$

$\Rightarrow$ four fundamental identities of vector calculus divergence of curl of a vector field

$$\mathrm{div}\cdot\mathrm{curl}\,\mathbf{f} = \nabla_j^D \cdot e_{jki}\nabla_k^D f_i = \frac{1}{c_1^{(j)}}\frac{\partial f}{\partial x_j}\left[e_{jki}\frac{1}{c_1^{(k)}}\frac{\partial f_i}{\partial x_k}\right] = e_{jki}\frac{1}{c_1^{(j)}}\frac{1}{c_1^{(k)}}\frac{\partial f_i}{\partial x_j \partial x_k} = 0$$

curl of gradient of a scalar field

$$\mathrm{curl}\times(\mathrm{grad}\,\varphi) = e_{ijk}\nabla_j^D(\nabla_k^D\varphi) = e_{ijk}\frac{1}{c_1^{(j)}}\frac{\partial}{\partial x_j}\left[\frac{1}{c_1^{(k)}}\frac{\partial\varphi}{\partial x_k}\right] = e_{jki}\frac{1}{c_1^{(j)}}\frac{1}{c_1^{(k)}}\frac{\partial f_i}{\partial x_j \partial x_k} = 0$$

divergence of gradient of a vector field fractal *Laplacian*

$$\mathrm{div}\cdot(\mathrm{grad}\,\varphi) = \nabla_j^D \cdot \nabla_k^D\varphi = \frac{1}{c_1^{(j)}}\frac{\partial}{\partial x_j}\left[\frac{1}{c_1^{(j)}}\frac{\partial\varphi}{\partial x_j}\right] = \frac{1}{c_1^{(j)}}\left[\frac{\partial\varphi,_j}{c_1^{(j)}}\right],_j$$

curl of curl operating on a vector field

$$\mathrm{curl}\times(\mathrm{curl}\,\mathbf{f}) = e_{prj}\nabla_r^D(e_{jki}\nabla_r^D f_i) = \nabla_p^D\left(\nabla_r^D f_r\right) - \nabla_r^D\nabla_r^D f_p$$

divergence of curl of a vector field

$$\mathrm{div}\cdot\mathrm{curl}\,\mathbf{f} = \nabla_j^D \cdot e_{jki}\nabla_k^D f_i = \frac{1}{c_1^{(j)}}\frac{\partial f}{\partial x_j}\left[e_{jki}\frac{1}{c_1^{(k)}}\frac{\partial f_i}{\partial x_k}\right] = e_{jki}\frac{1}{c_1^{(j)}}\frac{1}{c_1^{(k)}}\frac{\partial f_i}{\partial x_j \partial x_k} = 0$$

curl of gradient of a scalar field

$$\mathrm{curl}\times(\mathrm{grad}\,\varphi) = e_{ijk}\nabla_j^D(\nabla_k^D\varphi) = e_{ijk}\frac{1}{c_1^{(j)}}\frac{\partial}{\partial x_j}\left[\frac{1}{c_1^{(k)}}\frac{\partial\varphi}{\partial x_k}\right] = e_{jki}\frac{1}{c_1^{(j)}}\frac{1}{c_1^{(k)}}\frac{\partial f_i}{\partial x_j \partial x_k} = 0$$

divergence of gradient of a vector field fractal *Laplacian*

$$\mathrm{div}\cdot(\mathrm{grad}\,\varphi) = \nabla_j^D \cdot \nabla_k^D\varphi = \frac{1}{c_1^{(j)}}\frac{\partial}{\partial x_j}\left[\frac{1}{c_1^{(j)}}\frac{\partial\varphi}{\partial x_j}\right] = \frac{1}{c_1^{(j)}}\left[\frac{\partial\varphi,_j}{c_1^{(j)}}\right],_j$$

curl of curl operating on a vector field

$$\mathrm{curl}\times(\mathrm{curl}\,\mathbf{f}) = e_{prj}\nabla_r^D(e_{jki}\nabla_r^D f_i) = \nabla_p^D\left(\nabla_r^D f_r\right) - \nabla_r^D\nabla_r^D f_p$$

Helmholtz decomposition holds:

with

Stokes theorem

$$\int_{\partial W} (\boldsymbol{\nabla}^D \times \mathbf{f}) \cdot \mathbf{n}\, dS_d \equiv \int_{\partial W} n_k e_{kji} \nabla_j^D f_i\, dS_d \equiv$$

$$= \int_{\partial W} n_k e_{kji} \frac{1}{c_1^{(j)}} f_{i,j}\, dS_d = \int_{\partial W} n_k e_{kji} \frac{1}{c_1^{(j)}} f_{i,j}\, c_2^{(k)}\, dS_2$$

$$= \int_{\partial W} n_k e_{kji} f_{i,j}\, c_1^{(i)}\, dS_2 = \int_{\partial W} n_k e_{kji} \left(f_i c_1^{(i)} \right)_{,j}\, dS_2$$

$$\Rightarrow \quad \int_{S_d} \mathbf{n} \cdot \mathrm{curl}\, \mathbf{f}\, dS_d = \int_l \mathbf{f} \cdot d\mathbf{l}_{\alpha_1}$$

… *volume coefficient* $c_3 = c_1^{(1)} c_1^{(2)} c_1^{(3)} = \prod_{i=1}^{3} c_1^{(i)}$

… *surface coefficient* associated with the surface $S_d^{(k)}$

$$c_2^{(k)} = c_1^{(i)} c_1^{(j)} = \frac{c_3}{c_1^{(k)}}, \quad i \neq j \ \text{and} \ i, j \neq k.$$

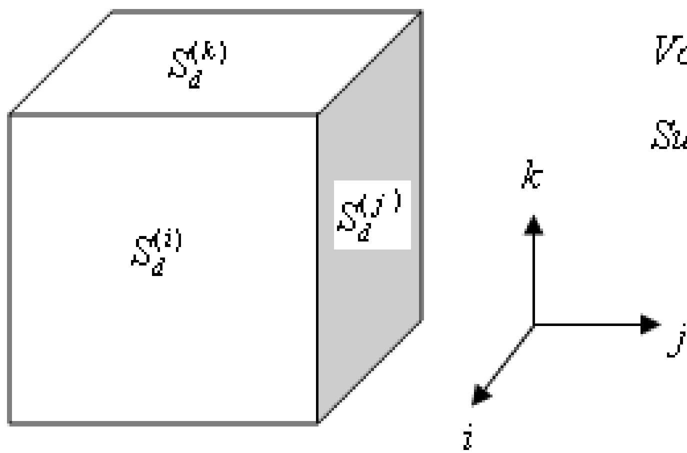

Volume $V_D \rightarrow c_3 = c_1^{(i)} \cdot c_1^{(j)} \cdot c_1^{(k)}$

Surface

$S_d^{(i)} \rightarrow c_2^{(i)} = c_1^{(j)} c_1^{(k)} = \dfrac{c_3}{c_1^{(i)}}$

$S_d^{(j)} \rightarrow c_2^{(j)} = c_1^{(i)} c_1^{(k)} = \dfrac{c_3}{c_1^{(j)}}$

$S_d^{(k)} \rightarrow c_2^{(k)} = c_1^{(i)} c_1^{(j)} = \dfrac{c_3}{c_1^{(k)}}$

$$c_1^{(k)} = \alpha_k (l_k - x_k)^{\alpha_k - 1}, \ k = 1, 2, 3$$

Fractional integral $$\int_{S_d} \bar{f} \cdot \hat{n} dS_d = \int_{S_2} f_k c_2^{(k)} n_k dS_2$$

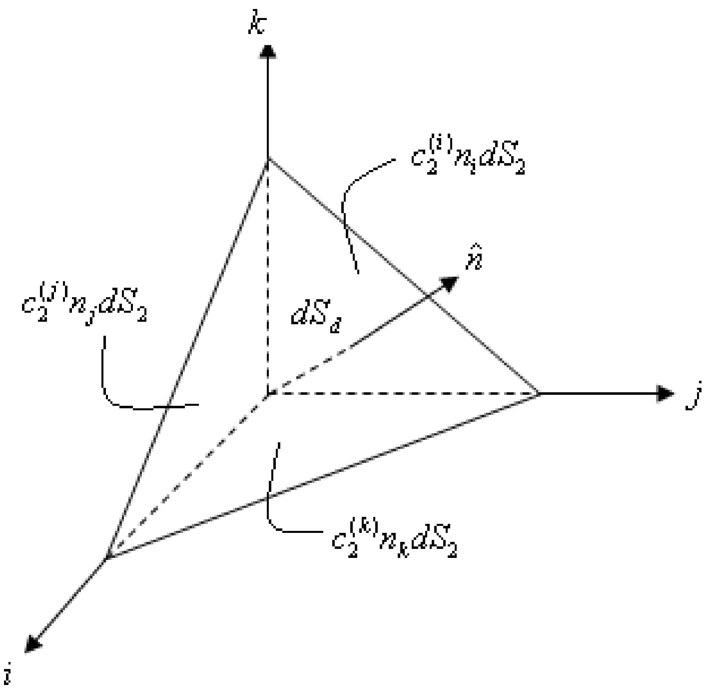

Integral element $\hat{n} dS_d$

$n_i dS_d \to c_2^{(i)} n_i dS_2$

$n_j dS_d \to c_2^{(j)} n_j dS_2$

$n_k dS_d \to c_2^{(k)} n_k dS_2$

$$\int_{\partial W} f_k c_2^{(k)} n_k dS_2 = \int_W \left(f_k c_2^{(k)} \right)_{,k} dV_3$$

$$\int_{\partial W} f_k n_k dS_d = \int_W \left(f_k c_2^{(k)} \right)_{,k} c_3^{-1} dV_D = \int_W f_{k,k} c_2^{(k)} c_3^{-1} dV_D = \int_W \frac{f_{k,k}}{c_1^{(k)}} dV_D \coloneqq \int_W \nabla_k^D f_k dV_D$$

$\Rightarrow$ fractal derivative: $\nabla_k^D \coloneqq \dfrac{1}{c_1^{(k)}} \dfrac{\partial}{\partial x_k} (\cdot)$

[*ZAMP* 2009; *Proc. R. Soc. A*, 2009; *J. Elast*, 2011]

1. ∇^D is the "inverse" operator of fractional integrals:

and $$\nabla_x^D \int f(x) d\mu^D(x) = \frac{1}{c_1(x)} \frac{d}{dx} \int f(x) c_1(x) dx = \frac{1}{c_1(x)} \left[f(x) c_1(x) \right] = f(x)$$

$$\int \nabla_x^D f(x) d\mu^D(x) = \int \left[\frac{1}{c_1(x)} \frac{df(x)}{dx} \right] c_1(x) dx = \int \frac{df(x)}{dx} dx = f(x)$$

2. rule of "term-by-term" differentiation is satisfied:

$$\nabla_k^D(AB) = \frac{1}{c_1^{(k)}} \frac{\partial}{\partial x_k}(AB) = \frac{1}{c_1^{(k)}} \frac{\partial(A)}{\partial x_k} B + \frac{1}{c_1^{(k)}} \frac{\partial(B)}{\partial x_k} A = B\nabla_k^D(A) + A\nabla_k^D(B)$$

3. operation on any constant is zero: $\nabla_k^D(C) = \frac{1}{c_1^{(k)}} \frac{\partial(C)}{\partial x_k} = 0$

Note: usual fractional derivative (Riemann-Liouville) of a constant $\neq 0$

$\Rightarrow$ fractional generalization of Reynolds transport theorem:

$$\frac{d}{dt} \int_{W_t} P dV_D = \int_{W_t} \left(\frac{\partial}{\partial t} P + \left(P v_k \right)_{,k} \right) dV_D.$$

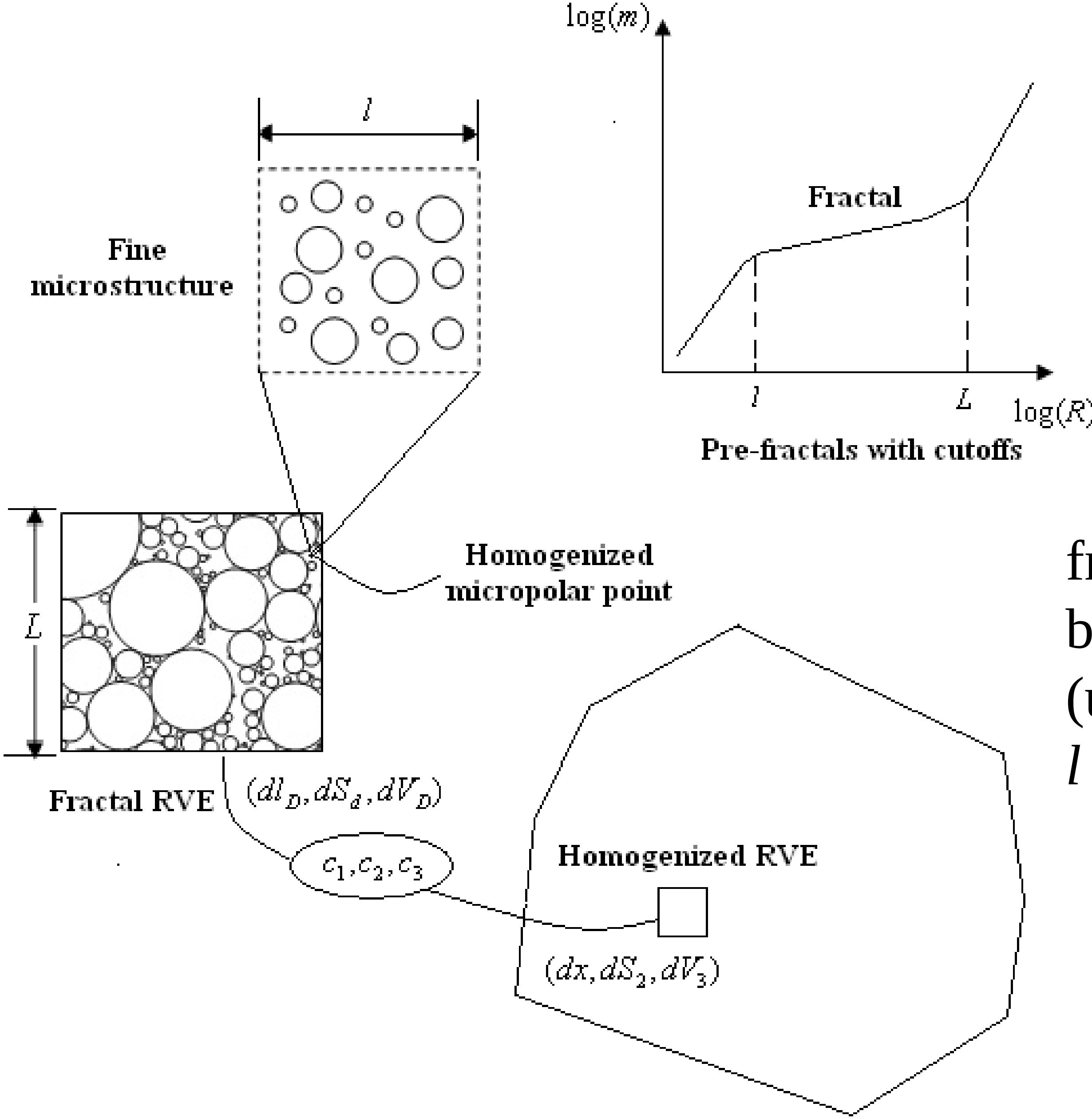

fractal effects are present between the resolutions (upper and lower cut-offs) *l* and *L* in a fractal RVE

random
Apollonian packing

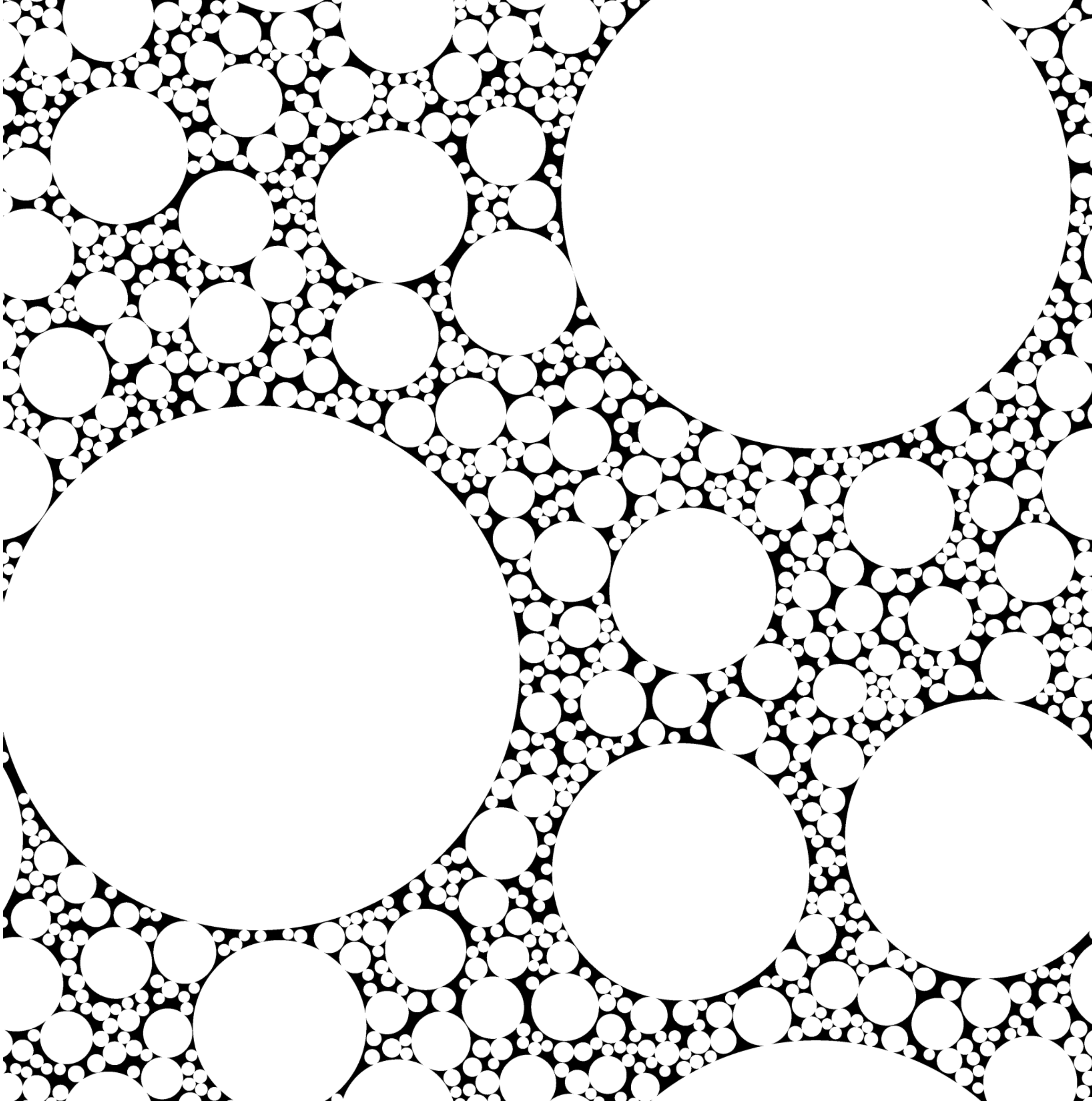

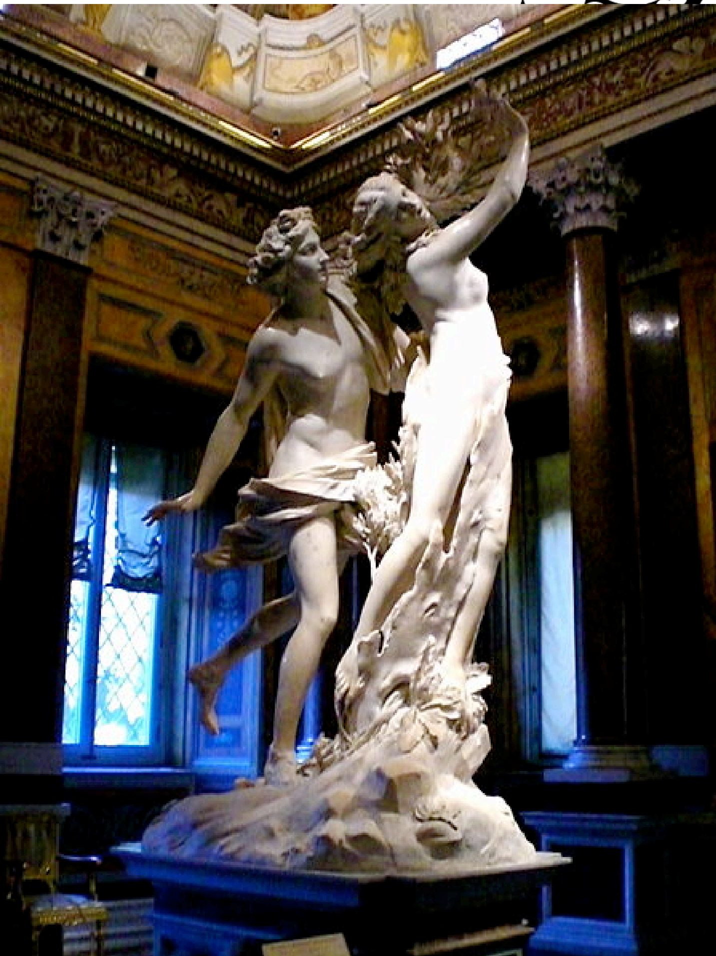

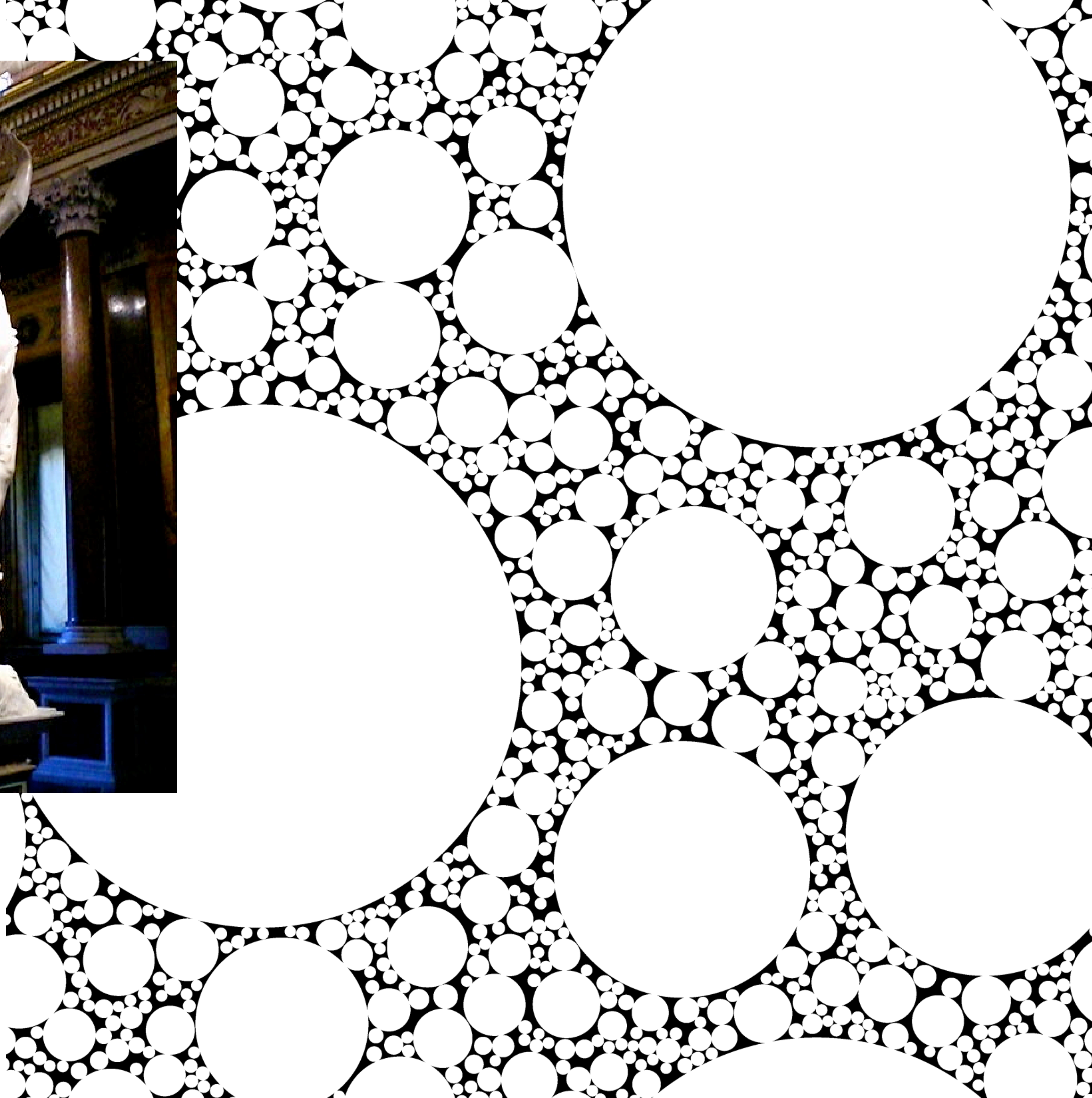

Apollo and Daphne
by Bernini
[Galleria Borghese]

Express Cauchy stress via fractional integral, and strain via fractal derivative

$$F_k^S = \int_S \sigma_{lk} n_l dS_d = \int_S \sigma_{lk} n_l c_2^{(l)} dS_2 \qquad \varepsilon_{ij} = \frac{1}{2}\left(\nabla_j^D u_i + \nabla_i^D u_j\right) = \frac{1}{2}\left(\frac{1}{c_1^{(j)}} u_{i,j} + \frac{1}{c_1^{(i)}} u_{j,i}\right)$$

… balance law of linear momentum in fractal medium

$$\frac{d}{dt}\int_W \rho \mathbf{v} dV_D = \mathbf{F}^B + \mathbf{F}^S \quad \Rightarrow \quad \frac{d}{dt}\int_W \rho v_k dV_D = \int_W X_k dV_D + \int_{\partial W} \sigma_{lk} n_l dS_d$$

$$\Rightarrow$$

e.g. a linear elastic solid: $\sigma_{ij} = \lambda \varepsilon_{kk} \delta_{ij} + 2\mu \varepsilon_{ij}$

Balance of angular momentum in fractal medium

$$\frac{d}{dt}\int_{W}\rho e_{ijk}x_j v_k dV_D = \int_{W} e_{ijk}x_j X_k dV_D + \int_{\partial W} e_{ijk}x_j \sigma_{lk} n_l dS_d$$

… using G-G theorem and Reynold’s transport theorem, localize to: $e_{ijk}\dfrac{\sigma_{jk}}{c_1^{(j)}} = 0$

… but due to general anisotropy of a fractal $\Rightarrow \quad \sigma_{jk} \neq \sigma_{kj}$

$\Rightarrow$ ***micropolar continuum***
not Cauchy continuum!

$\Rightarrow$ must work with stress τ and couple-stress μ tensors

$$\Rightarrow \quad \frac{e_{ijk}}{c_1^{(j)}}\tau_{jk} + \nabla_j^D \mu_{ji} + Y_i = I_{ij}\dot{w}_j$$

$\Rightarrow$ Balance of energy: $\dot{e} = \tau_{ij}\dot{\gamma}_{ij} + \mu_{ij}\dot{\kappa}_{ij}$

[*Int. J. Eng. Sci.*, 2011]

1d wave equation

Mechanical approach: $\rho \ddot{u} = c_1^{-1} \sigma_{,x}$

Hooke's law $\sigma = E\varepsilon \quad \Rightarrow \quad \rho \ddot{u} = E c_1^{-1} \varepsilon_{,x}$

With conventional strain definition $\varepsilon = u_{,x} \quad \Rightarrow \quad \rho \ddot{u} = E c_1^{-1} u_{,xx}$

With our strain definition $\varepsilon = c_1^{-1} u_{,x} \quad \Rightarrow \quad \rho \ddot{u} = E c_1^{-1} \left(c_1^{-1} u_{,x} \right)_{,x}$

$$\Uparrow$$

Variational approach:

$$T = \frac{1}{2} \rho \int \dot{u}^2 dl_D = \frac{1}{2} \rho \int \dot{u}^2 c_1 dx$$

$$U = \frac{1}{2} E \int \varepsilon^2 dl_D = \frac{1}{2} E \int \varepsilon^2 c_1 dx$$

$$\delta \int L dt = \delta \int \left(T - U \right) dt = 0$$

2d anti-plane wave equation

$$\rho c_1^{(1)} c_1^{(2)} \ddot{u}_3 - \mu \left[c_1^{(2)} \left(\frac{u_{3,1}}{c_1^{(1)}} \right)_{,1} + c_1^{(1)} \left(\frac{u_{3,2}}{c_1^{(2)}} \right)_{,2} \right] = 0$$

3d waves

$$\rho \ddot{u}_i = \mu \frac{1}{c_1^{(j)}} \left(\frac{u_{i,j}}{c_1^{(j)}} \right)_{,j} + (\lambda + \mu) \frac{1}{c_1^{(i)}} \left(\frac{u_{j,j}}{c_1^{(j)}} \right)_{,i}$$

Timoshenko beam

$$\rho_0 A \ddot{w} = \nabla_x^D \left[\kappa \mu A \left(\nabla_x^D w - \phi \right) \right]$$

$$\rho_0 I \ddot{\phi} = \nabla_x^D \left(EI \nabla_x^D \phi \right) + \kappa \mu A \left(\nabla_x^D w - \phi \right)$$

$$\Rightarrow \quad \nabla_x^D \nabla_x^D \left(EI \; \nabla_x^D \nabla_x^D \; w \right) = 0$$

$\Rightarrow$ mechanical approach is consistent with the variational approach

[*Proc. R. Soc. A*, 2013]

Electromagnetism on Anisotropic Fractal Media

Charge conservation on anisotropic fractals

$$\int_{\partial W} \mathbf{J} \cdot \mathbf{n} \, dS_d = -\int_W \eta \, dV_D$$

$$\Rightarrow \quad \begin{array}{ll} \text{global form} & \int_W \nabla^D \cdot \mathbf{J} \, dV_D = -\frac{d}{dt} \int_W \eta \, dV_D \\ \text{local form} & \nabla^D \cdot \mathbf{J} = -\frac{\partial}{\partial t} \eta \end{array}$$

All the relations will depend explicitly on three fractal dimensions $(i = 1,2,3)$ in the respective Cartesian direction as well as the spatial resolution.

All the formulas may be evaluated by

$$c_1^{(k)} = \alpha_k \left(\frac{l_k - x_k}{l_{k0}} \right)^{\alpha_k - 1}, \quad k = 1, 2, 3, \quad \text{(no sum)}$$

Electromagnetism on Anisotropic Fractal Media

Charge conservation on anisotropic fractals

$$\int_{\partial W} \mathbf{J} \cdot \mathbf{n} \, dS_d = -\int_W \eta \, dV_D$$

$$\Rightarrow \quad \begin{array}{ll} \text{global form} & \int_W \nabla^D \cdot \mathbf{J} \, dV_D = -\frac{d}{dt} \int_W \eta \, dV_D \\ \text{local form} & \nabla^D \cdot \mathbf{J} = -\frac{\partial}{\partial t} \eta \end{array}$$

Ohm's law for anisotropic fractals: $\mathbf{J} = \boldsymbol{\sigma} \cdot \mathbf{E}$ or $J_i = \sigma_{ij} E_j$

… by analogy to elastic media where Hooke's law is unchanged when going from non-fractal to fractal media

that result ensured the consistency of the Newtonian and Lagrangian-Hamiltonian approaches to the derivation of governing equations

Electromagnetism on Anisotropic Fractal Media

Faraday's law

$$\frac{d}{dt}\int_A \mathbf{B}\cdot\mathbf{n}\,dS_d = -\int_l \mathbf{E}\cdot d\mathbf{l}_{\alpha_i}$$

$$\Rightarrow \quad 0 = \frac{\partial}{\partial t}B_k + e_{kji}\nabla_j^D E_i \equiv \frac{\partial}{\partial t}B_k + e_{kji}\frac{1}{c_1^{(j)}}E_{i,j} \quad \text{or}$$

$$\mathbf{0} = \frac{\partial}{\partial t}\mathbf{B} + \boldsymbol{\nabla}^D \times \mathbf{E}$$

Ohm's law for anisotropic fractals: $\mathbf{J} = \boldsymbol{\sigma}\cdot\mathbf{E}$ or $J_i = \sigma_{ij}E_j$

… by analogy to elastic media where Hooke's law is unchanged when going from non-fractal to fractal media

that result ensured the consistency of the Newtonian and Lagrangian-Hamiltonian approaches to the derivation of governing equations

Electromagnetism on Anisotropic Fractal Media

<u>Ampère's law</u>

$$\int_S \mathbf{C}\cdot\mathbf{n}\,dS_d = \int_l \mathbf{H}\cdot d\mathbf{l}_{\alpha_1} = \int_S \mathbf{n}\cdot(\nabla^D \times \mathbf{H})\,dS_d$$

$$\Rightarrow \qquad \int_S \left(\mathbf{J} + \frac{\partial \mathbf{D}}{\partial t} - \nabla^D \times \mathbf{H} \right) dS_d = 0 \quad \text{or}$$

$$\frac{1}{\varepsilon_0}\mathbf{J} + \frac{\partial \mathbf{E}}{\partial t} - c^2 \nabla^D \times \mathbf{B} = \mathbf{0}$$

where $\quad \mathbf{C} = \mathbf{J} + \dfrac{\partial \mathbf{D}}{\partial t}$

… subject to <u>constraints</u>:

Electromagnetism on Anisotropic Fractal Media

<u>Derivation from variational principle</u>

$$\delta \iint \mathsf{L} \; dV_D dt = 0$$

with

$$\mathsf{L} = \varepsilon_0 \left[\frac{1}{2} c^2 B_i B_i - \frac{1}{2} E_i E_i + A_i \left(\frac{\partial E_i}{\partial t} - c^2 e_{ijk} B_{k,j} + \frac{1}{\varepsilon_0} J_i \right) + \chi E_{i,i} \right]$$

$\Rightarrow$ the same set of equations as before

$$\nabla^D \cdot \mathbf{E} = 0 \qquad \nabla^D \cdot \mathbf{B} = 0$$

$$\frac{1}{c}\frac{\partial}{\partial t}\mathbf{B} + \nabla^D \times \mathbf{E} = \mathbf{0} \qquad \frac{1}{c}\frac{\partial \mathbf{E}}{\partial t} - \nabla^D \times \mathbf{B} + \frac{4\pi}{c}\mathbf{J} = \mathbf{0}$$

[Z*AMP* 2012]

Griffith theory of elastic-brittle porous solids

Energy release rate:

$$G = \frac{\partial W}{\partial A} - \frac{\partial U^e}{\partial A} = 2\gamma$$

$$U^e = \int_W \rho u \; dV_D = \int_W \rho u \; c_3 \; dV_3 \qquad \Rightarrow \qquad U^e = \frac{\pi a^2 c_1^2 \sigma^2}{8\mu}(K+1)c_3$$

Dead-load conditions:

$$G = \frac{\partial U^e}{\partial A} = 2\gamma$$

Fixed-grip conditions:

$$G = -\frac{\partial U^e(a)}{B\partial l_{DF}} = -\frac{\partial U^e(a)}{Bc_1\partial a}$$

$\Rightarrow$ critical stresses get modified

Peeling a layer off a substrate

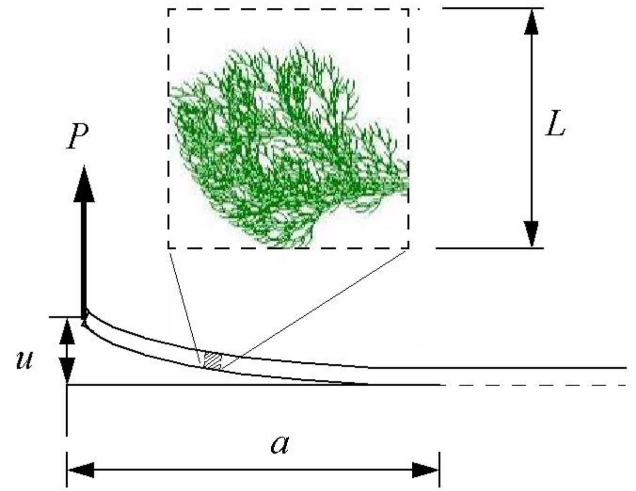

Dead-load conditions:

$$U(a) = \int_0^a \frac{M^2}{2IE}\, dl_D = \int_0^a \frac{M^2}{2IE}\, c_1 dx$$

$$\Rightarrow \quad G = \frac{\partial U}{c_1 B \partial a}$$

If random material $\quad E(\omega, x) = \langle E \rangle + E'(\omega, x) \qquad \omega \in \Omega$

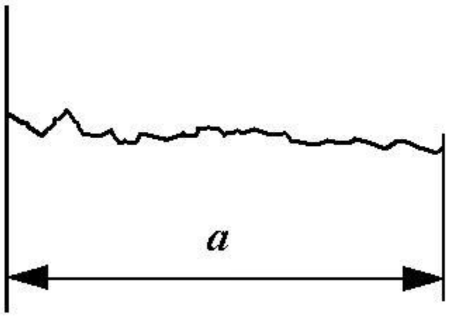

$$\Rightarrow \quad \frac{1}{\langle E \rangle} \le \left\langle \frac{1}{E} \right\rangle \quad \Rightarrow \quad G(a, \langle E \rangle) \le \langle G(a, E) \rangle$$

Fixed-grip conditions:

$$\langle G \rangle = -\frac{u}{2Bc_1}\left\langle \frac{\partial P}{\partial a} \right\rangle = -\frac{u}{2Bc_1}\frac{\partial \langle P \rangle}{\partial a} = \frac{9u^2 I \langle E \rangle}{2B(c_1 a)^4}$$

$\Rightarrow$ G can be computed by direct averaging of E

Peeling a layer off a substrate

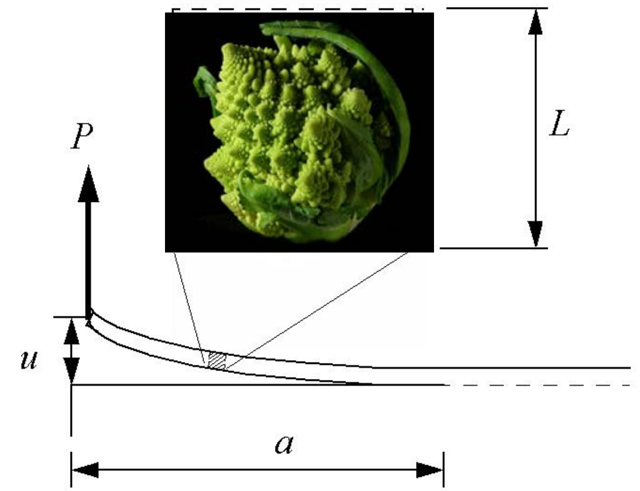

Dead-load conditions:

$$U(a) = \int_0^a \frac{M^2}{2IE}\, dl_D = \int_0^a \frac{M^2}{2IE}\, c_1 dx$$

$$\Rightarrow \quad G = \frac{\partial U}{c_1 B \partial a}$$

If random material $\quad E(\omega, x) = \langle E \rangle + E'(\omega, x) \qquad \omega \in \Omega$

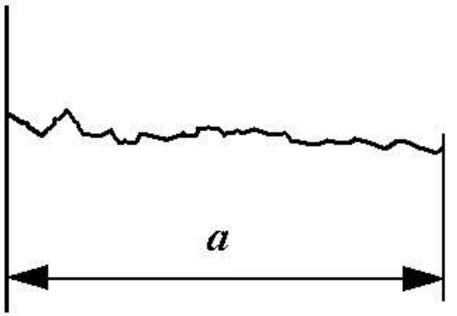

$$\Rightarrow \quad \frac{1}{\langle E \rangle} \le \left\langle \frac{1}{E} \right\rangle \quad \Rightarrow \quad G(a, \langle E \rangle) \le \langle G(a, E) \rangle$$

Fixed-grip conditions:

$$\langle G \rangle = -\frac{u}{2Bc_1} \left\langle \frac{\partial P}{\partial a} \right\rangle = -\frac{u}{2Bc_1} \frac{\partial \langle P \rangle}{\partial a} = \frac{9u^2 I \langle E \rangle}{2B(c_1 a)^4}$$

$\Rightarrow$ G can be computed by direct averaging of E

In fractal porous media:

[*IJES* 2011, Z*AMP* 2012, ZAMM 2013]

- when the surface and volume fractal dimensions (*d* and *D*) become integers (2 and 3, resp.), or when *R* falls outside [*l*, *L*], all the equations revert back to well-known forms of conventional continuum mechanics of non-fractal media
- Beltrami-Michell reciprocity theorem, uniqueness…
- extension to thermomechanics with internal variables
- field/wave equations derived from variational principles are the same as those from mechanical approach
- …

- can extend to finite motions

[*PRE*, 2013]

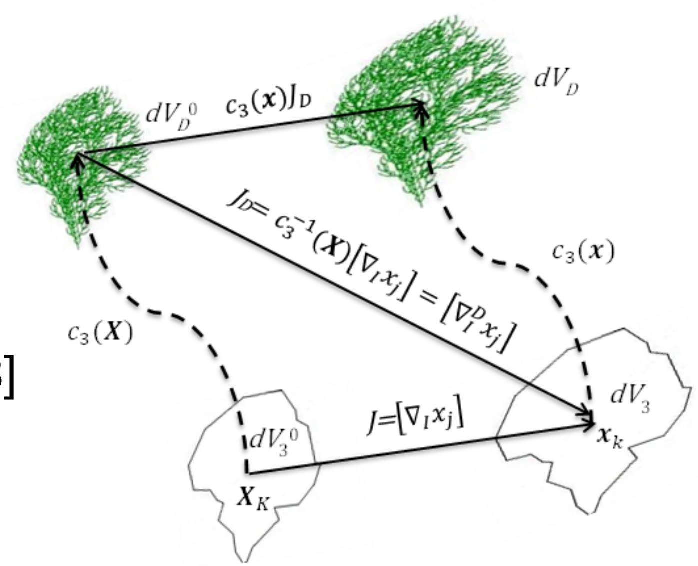

Common techniques for generating fractals:

Escape-time fractals – via recurrence relation (Mandelbrot, Julia sets…)

Iterated function systems – via a fixed geometric replacement rule
(Cantor set, Sierpiński carpet…)

Random fractals – via stochastic processes
(Brownian motion/sheets, Lévy flight…)

Strange attractors – via chaos

Can fractals be generated by mechanics?
e.g. by elasto-inelastic transitions

Can we develop a continuum-type theory of fractal porous media?

Can we solve initial-boundary-value problems? need random fields

random fields

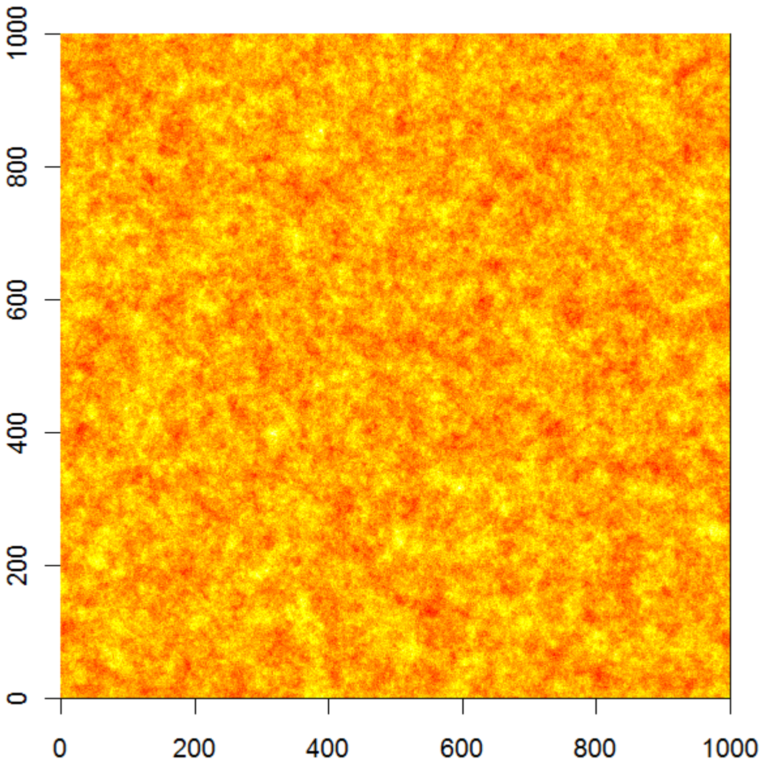

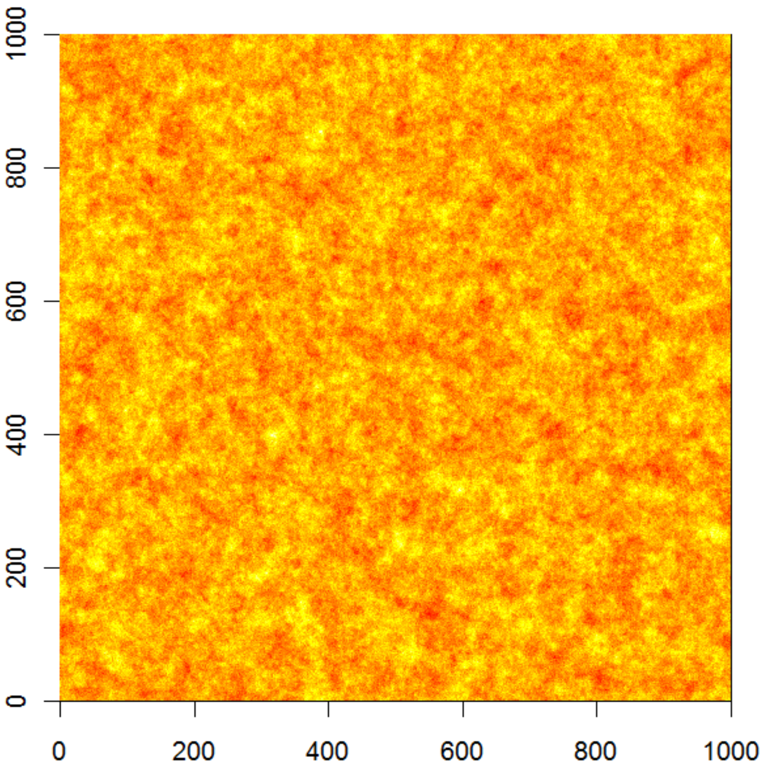

RFs with exponential or Gaussian correlation functions

$$C(x) = \exp[-Ax^{\alpha}], \quad A > 0, \quad 0 < \alpha \leq 2$$

random fields

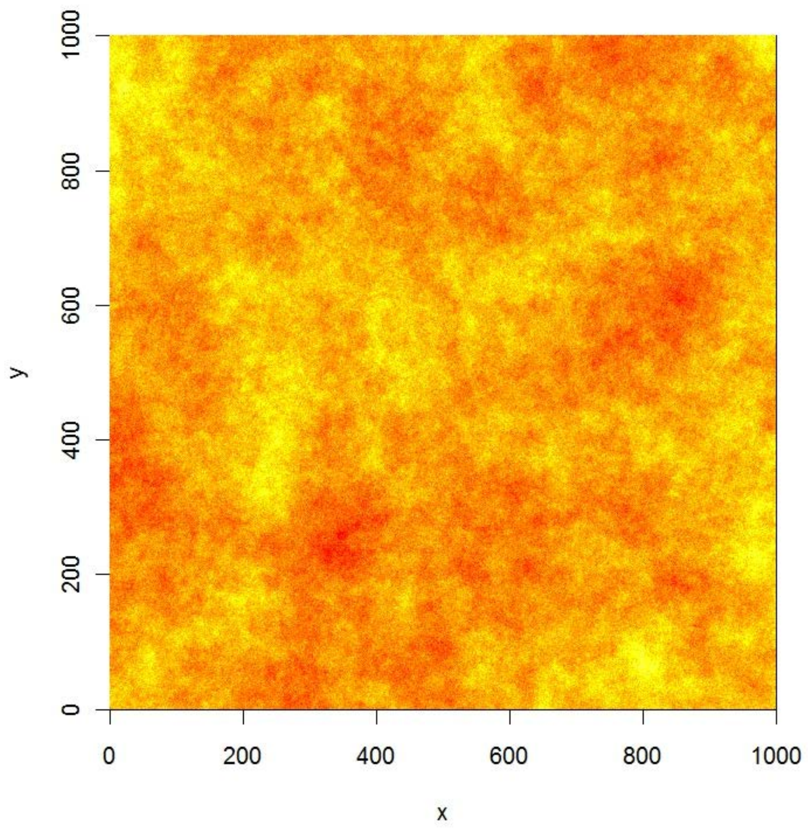

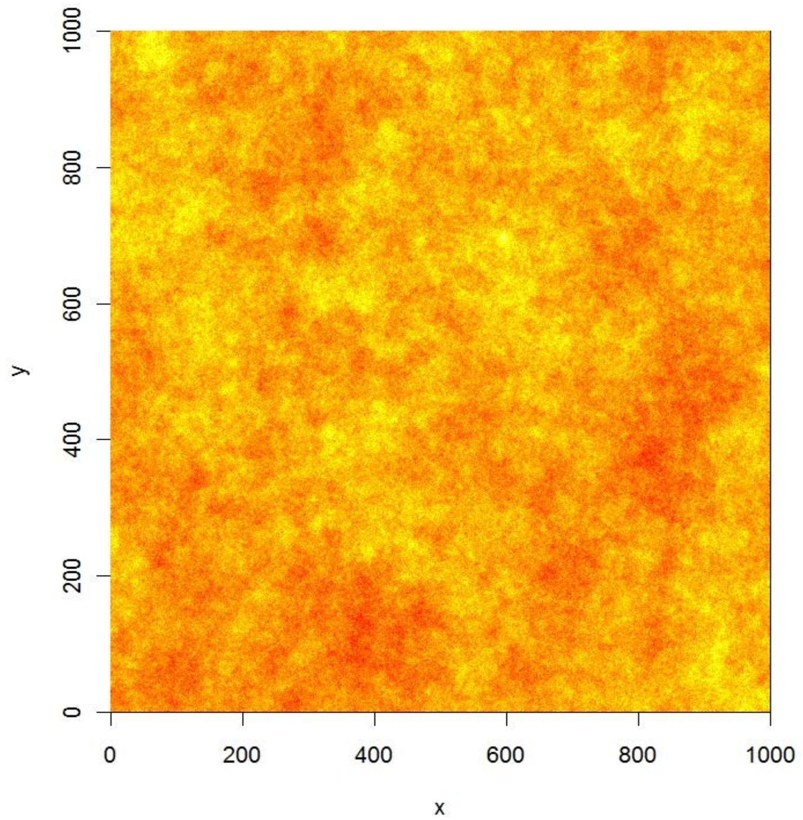

RFs with fractal + Hurst effects

Cauchy

$$C_{\mathbf{C}}(r;\alpha,\beta) := \left(1 + r^{\alpha}\right)^{-\beta/\alpha},$$

$\beta > 0 \qquad 0 < \alpha \le 2$

Dagum

$$C_{\mathbf{D}}(r;\beta,\gamma) := 1 - \left(1 + r^{-\beta}\right)^{-\gamma/\beta},$$

$\gamma < 7\beta \qquad \beta^2 + \beta(5\gamma - 7) + \gamma < 0$

Can grasp **fractals** and **Hurst effect**

roughness

heavy-tail behavior of covariance function

A random process Z_x is statistically self-similar if it obeys $Z_x = c^{-H} Z_{cx}$ for some constant c, where H is known as the *Hurst parameter*

- Crudely: when stretched by some factor c in x dimension, Z looks the same if stretched by c^{-H} in the Z dimension

- Most time series Z_t look "flat" if stretched like this

fractals: those enchanting, self-similar things

Hurst effect: long-term memory, extreme events

$0 < H < 0.5$: time series with negative autocorrelation (a decrease between values will likely be followed by an increase)

$0.5 < H < 1$: time series with positive autocorrelation (an increase between values followed by another increase)

$H = 0.5$: true random walk, w/o preference for a decrease or increase following any particular value

Gaussian white noise: $$C_{\mathbf{WN}}(r) := \delta(r), \quad r \geq 0,$$

Ornstein-Uhlenbeck: $$C_{\mathbf{OU}}(r;\nu) := \frac{\nu}{2}\mathbf{e}^{-\nu r}, \quad r \geq 0,$$

Matérn: $$C_{\mathbf{M}}(r;\nu) := r^{\nu}\mathbf{K}_{\nu}(r), \quad r \geq 0,$$

Cauchy: $$C_{\mathbf{C}}(r;\theta,\eta) := \left(1 + r^{\theta}\right)^{-\eta/\theta},$$

Dagum: $$C_{\mathbf{D}}(r;\delta,\varepsilon) := 1 - \left(1 + r^{-\delta}\right)^{-\varepsilon/\delta},$$
$$0 < \delta \leq 2$$

OBSERVE

1. Time-stationary random forcings of Cauchy and Dagum types lack explicit parametric spectral densities, yet they allow decoupling of the fractal dimension and Hurst effect.

2. Working directly in time domain, find transient 2^{nd}-order characteristics of response and, for comparison, also examine effects of Gaussian white noise, Ornstein-Uhlenbeck, and Matérn forcings.

3. Given the same variance on input, the variance on output is strongest for Matérn, then Cauchy, then O-U, then white noise, and finally, Dagum forcing.

4. If the excitation correlation function is Matérn, the correlation function of response is approximately Matérn.

- … response due to Cauchy excitation is not Cauchy
- … cannot yet say whether response due to Dagum excitation (with its fractal and Hurst effects) is Dagum or not

- Constitutive law

$$\tau_{ij} = C^{(1)}_{ijkl}\gamma_{kl}$$

$$\mu_{ij} = C^{(2)}_{ijkl}\kappa_{kl}$$

$$\tau_{ij} = (\beta+\alpha)\gamma_{ij} + (\beta-\alpha)\gamma_{ji} + \lambda\gamma_{kk}\delta_{ij}$$

$$\mu_{ij} = (\psi+\varepsilon)\kappa_{ij} + (\psi-\varepsilon)\kappa_{ji} + \eta\kappa_{kk}\delta_{ij}$$

$$C^{(1)}_{ijkl} = (\beta-\alpha)\delta_{jk}\delta_{il} + (\beta+\alpha)\delta_{jl}\delta_{ik} + \lambda\delta_{ij}\delta_{kl}$$

$$C^{(2)}_{ijkl} = (\psi-\varepsilon)\delta_{jk}\delta_{il} + (\psi+\varepsilon)\delta_{jl}\delta_{ik} + \eta\delta_{ij}\delta_{kl}$$

β, λ Lamé’s constants

α, ψ, ε, η micropolar constants

$$\gamma_{ij} = \nabla^D_i u_j - e_{kij}\frac{\varphi_k}{g_j}$$

$$\kappa_{ij} = \nabla^D_i \varphi_j$$

$$\nabla^D_i = \frac{1}{g_i}\frac{\partial}{\partial x_i}$$

$$g_i = D_i (L_i - x_i)^{D_i - 1} \quad g^* = \prod_i g_i$$

$$\rho\ddot{u}_i = \nabla^D_j \tau_{ji} + \rho f_i \quad \text{in } \bar{\Omega}\times \mathrm{T}^+$$

$$I\ddot{\varphi}_i = \nabla^D_j \mu_{ji} + e_{ijk}\frac{\tau_{jk}}{g_j} + Im_i \quad \text{in } \bar{\Omega}\times \mathrm{T}^+$$

Governing Equations

$$\rho \ddot{u}_i = (\beta+\alpha)\nabla_j^D \nabla_j^D u_i + (\lambda+\beta-\alpha)\nabla_j^D \nabla_i^D u_j + e_{ijk}\nabla_j^D \left[(\beta+\alpha)\frac{\varphi_k}{g_j} - (\beta-\alpha)\frac{\varphi_k}{g_i} \right] + \rho f_i$$

$$I\ddot{\varphi}_i = e_{ijk}\left[(\beta+\alpha)\frac{\nabla_j^D u_k}{g_j} - (\beta-\alpha)\frac{\nabla_j^D u_k}{g_k} \right] + (\psi+\varepsilon)\nabla_j^D \nabla_j^D \varphi_i + (\psi+\eta-\varepsilon)\nabla_j^D \nabla_i^D \varphi_j$$
$$-\frac{e_{ijk}}{g_j}\left[(\beta+\alpha)\frac{e_{ijk}\varphi_i}{g_j} - (\beta-\alpha)\frac{e_{ijk}\varphi_i}{g_k} \right] + Im_i$$

- Characteristics
  - reproduction of Eringen’s work in absence of fractal effects
  - limitation to box shaped domains that can be contained in Cartesian system
  - fractal dimensions in three directions

Numerical Solution

- Finite element formulation

$$\int_\Omega \rho g_3 \ddot{u}_i w_i d\Omega = \int_\Omega (\lambda+\mu)\left[\left(\frac{g_3 u_{j,i} w_i}{g_i g_j}\right)_{,j} - \frac{g_3 u_{j,i} w_{i,j}}{g_i g_j}\right] d\Omega + \int_\Omega \mu \left[\left(\frac{g_3 u_{i,j} w_i}{g_j g_j}\right)_{,j} - \frac{g_3 u_{i,j} w_{i,j}}{g_j g_j}\right] d\Omega$$

$$\int_\Omega \rho \ddot{u}_i w_i d\Omega + (\lambda+\mu)\int_\Omega \frac{u_{j,i} w_{i,j}}{g_i g_j} d\Omega + \mu \int_\Omega \frac{u_{i,j} w_{i,j}}{g_j g_j} d\Omega = 0$$

second elastic term

inertia term

first elastic term

- Resulting equation

$$\mathbf{M}\cdot\ddot{\mathrm{U}} + (\mathbf{K}+\mathbf{H})\cdot\mathrm{U} = 0$$

Carpinteri column FE mesh

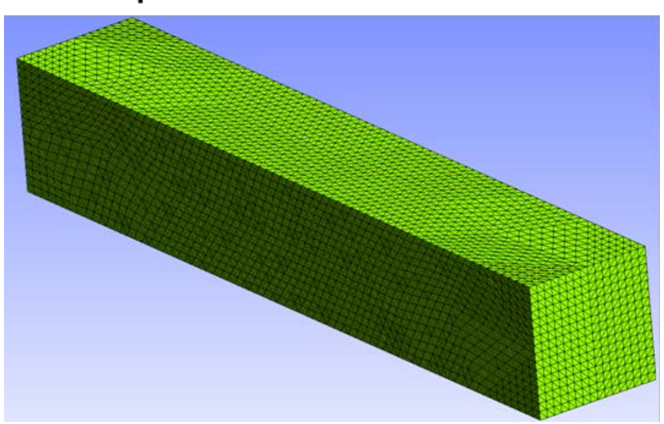

$L_1 = 1$ $\quad D_1 = D_2 = \frac{1}{2}\frac{\ln 8}{\ln 3}$

$L_2 = 1$

$L_3 = 6$ $\quad D_3 = \frac{\ln 2}{\ln 3}$

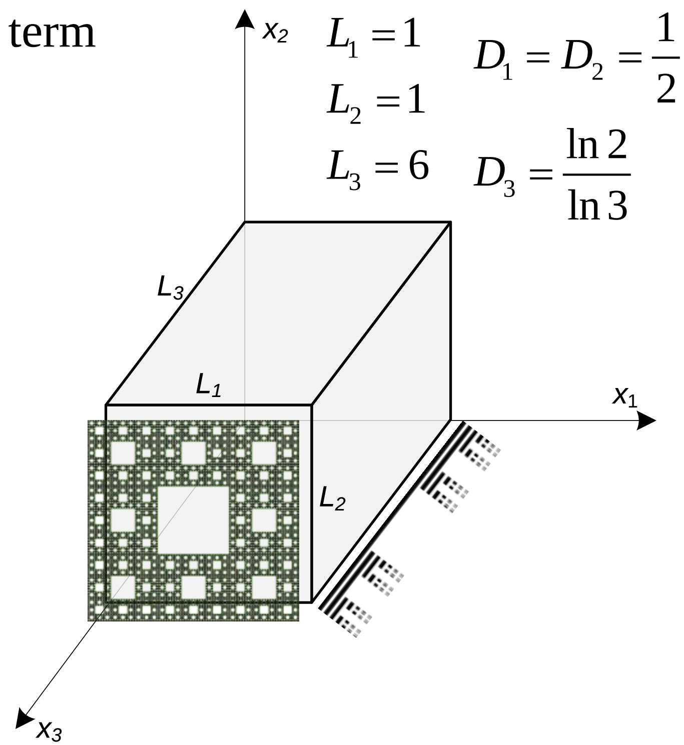

Simulation Results

- Modal shapes

$$D = \frac{1}{2}\frac{\ln 8}{\ln 3} = 0.946$$

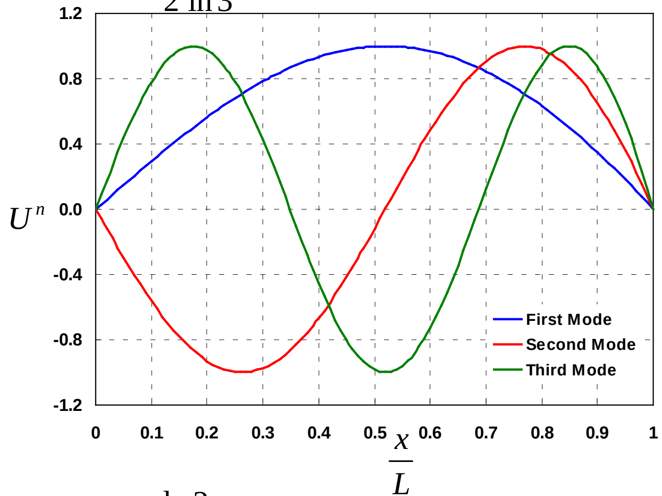

$$D = \frac{\ln 2}{\ln 3} = 0.631$$

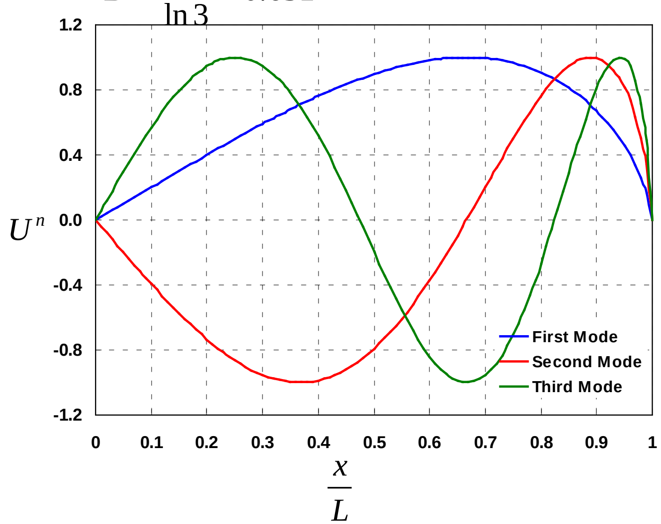

- Modal excitation
- Transient response

first mode excitation in all directions

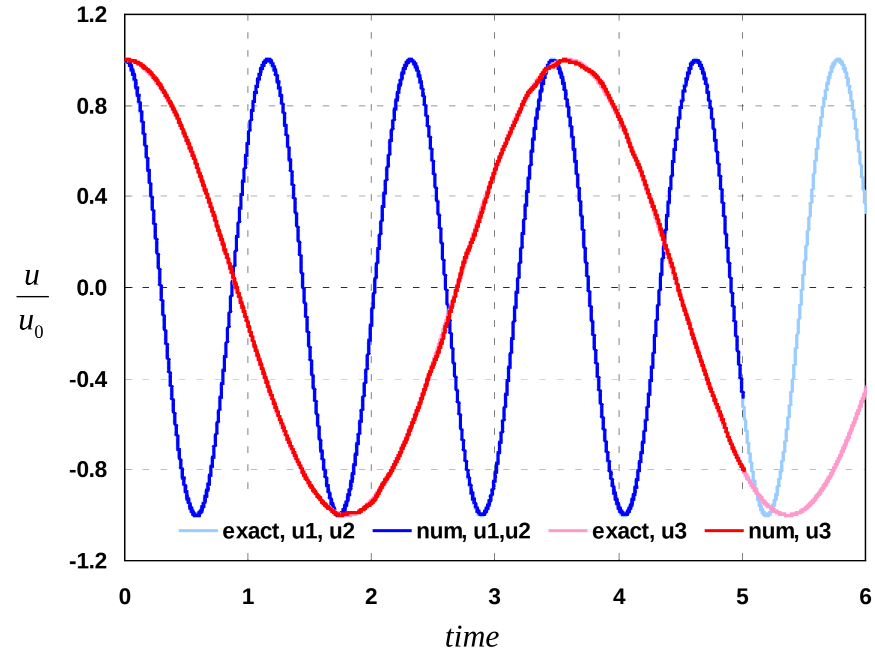

material properties

$l = 1$

$m = 1$

$r = 1$

modal frequencies

$w_1 = w_2 = 5.441$

$w_3 = 1.757$

Analytical solution

- Modal decomposition in a spherical system

$$H'' + m^2 H = 0$$

$$G'' + \frac{G'}{\tan\theta} + G\left[n(n+1) - \frac{m^2}{\sin^2\theta}\right] = 0$$

$$r^2 F'' + (5-D) rF' + k^2\lambda^2 r^{2D-4} F - n(n+1) F = 0$$

fractal radial harmonic functions of 1st and 2nd kind

- Decoupled solution

$$F_\nu^{(2)}(r,k,D) = r^{\frac{D-4}{2}} Y_\nu\left(\frac{k\lambda}{D-2} r^{D-2}\right)$$

$$H(\phi) = h_m e^{\pm im\phi}$$

$$F_\nu^{(1)}(r,k,D) = r^{\frac{D-4}{2}} J_\nu\left(\frac{k\lambda}{D-2} r^{D-2}\right)$$

$$G(\theta) = g_{mn} L_n^m(\cos\theta)$$

$$F(r) = f_1 F_\nu^{(1)}(r) + f_2 F_\nu^{(2)}(r)$$

$$\nu = \frac{\sqrt{4n(n+1) + (D-4)^2}}{2(D-2)} > 0$$

Numerical solution

- Finite element formulation

$$\left(\frac{\lambda}{c}\right)^2 \int_V \frac{\partial^2 p}{\partial t^2}\,\hat{p}\,dV = \int_V (3-D)\,\hat{p}\,|R|^{4-2D}\,\vec{R}\cdot\vec{\nabla}p\,dV + \int_V \hat{p}\,|R|^{6-2D}\,\nabla^2 p\,dV$$

$$\left(\frac{\lambda}{c}\right)^2 \underbrace{\sum_{e=1}^{N_e}\int_{V_e} \frac{\partial^2 p}{\partial t^2}\,\hat{p}\,dV_e}_{\text{inertia term}} + \underbrace{(3-D)\sum_{e=1}^{N_e}\int_{V_e} \hat{p}\,|R|^{4-2D}\,\vec{R}\cdot\vec{\nabla}p\,dV_e}_{\text{fractal elastic term}} + \underbrace{\sum_{e=1}^{N_e}\int_{V_e} |R|^{6-2D}\,\vec{\nabla}\hat{p}\cdot\vec{\nabla}p\,dV_e}_{\text{regular elastic term}} = 0$$

- Elastodynamic approach
  - elemental mass matrix
  - elemental elastic matrices

$$M_e = \left(\frac{\lambda}{c}\right)^2 \int_{V_e} H^T H dV_e$$

$$L_e = (3-D)\int_{V_e} |R|^{4-2D}\,H^T\left(\vec{R}\cdot\vec{\nabla}H\right)dV_e \qquad K_e = \int_{V_e} |R|^{6-2D}\,\vec{\nabla}H^T\cdot\vec{\nabla}H dV_e$$

  - final assembly $\mathbf{M}\ddot{p} + (\mathbf{L}+\mathbf{K})\,p = 0$

Simulation results

- Modal excitations on a spherical shell
- Newmark method (trapezoidal) for time-marching transient solution

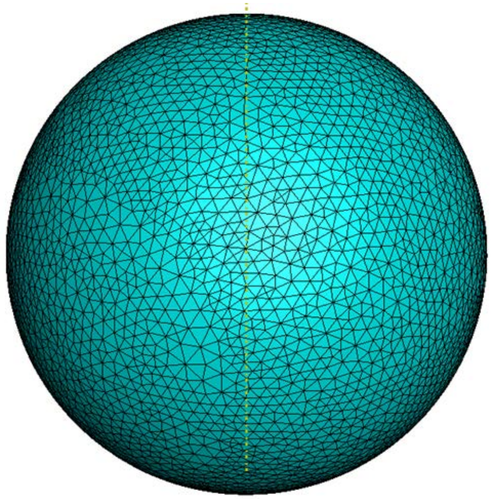

spherical shell meshed with tetrahedral elements

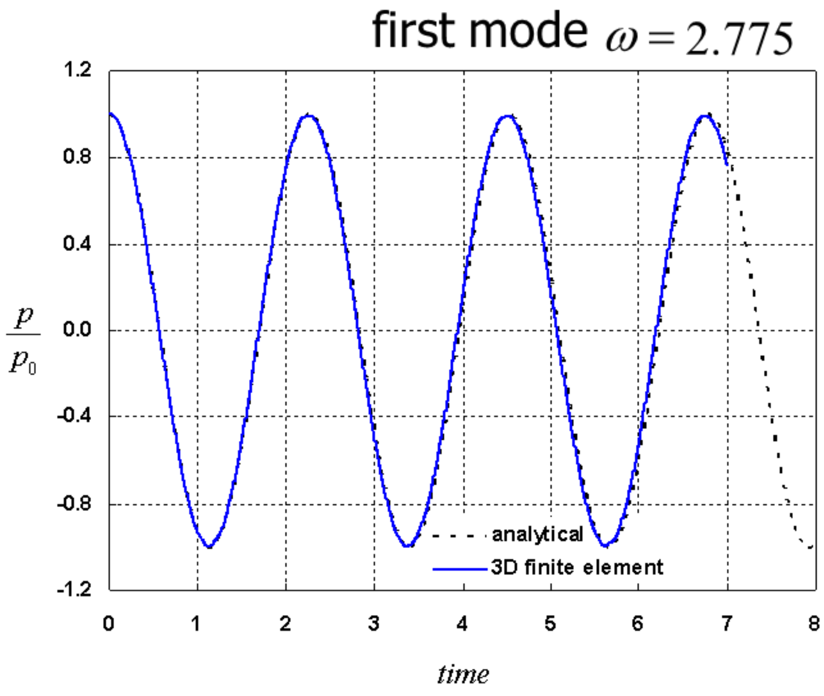

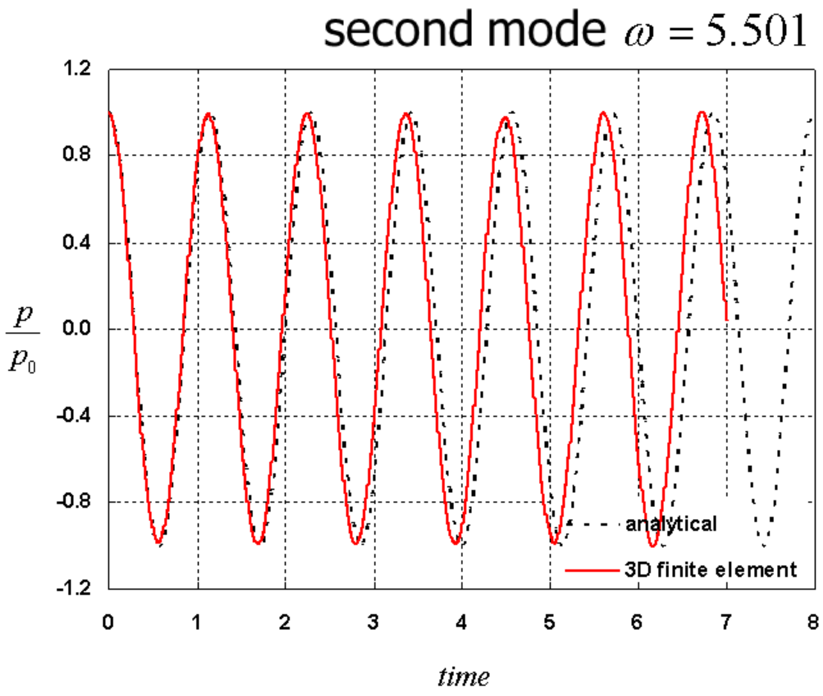

Elastodynamics of fractal solids

- 3d wave equation

$$\rho \ddot{u}_i = \frac{\lambda + \mu}{c_3} \left(\frac{c_3 u_{j,i}}{c_i c_j} \right)_{,j} + \frac{\mu}{c_3} \left(\frac{c_3 u_{i,j}}{c_j c_j} \right)_{,j}$$

- Analytical solution $\quad u_i \equiv u_i \left(x_i, t \right)$
  - limited to special problems
  - modal decomposition in Cartesian system

$$\left(L - x \right)^2 f''\left(x \right) + \left(D - 1 \right) \left(L - x \right) f'\left(x \right) + k^2 D^2 \left(L - x \right)^{2D} f\left(x \right) = 0$$

  - two independent homogeneous solutions (*fractal harmonic functions*)

$$f_1\left(x \right) \equiv \cos\left[k \left(L - x \right)^D \right] \qquad f_2\left(x \right) \equiv \sin\left[k \left(L - x \right)^D \right]$$

Simplified Problems

- Difficulty (if not impossibility) to obtain analytic solutions to general problems)
- Sequential validation of the numerical solver by…
- Special problems constructed by imposed kinematics
  - type I
    - a: $u_i \equiv u_i(x_i) \qquad \varphi_i \equiv 0$
    - b: $u_i \equiv 0 \qquad \varphi_i \equiv \varphi_i(x_i)$

"Carpinteri column" =

Sierpinski carpet in (x_1x_2)

and Cantor set along x_3

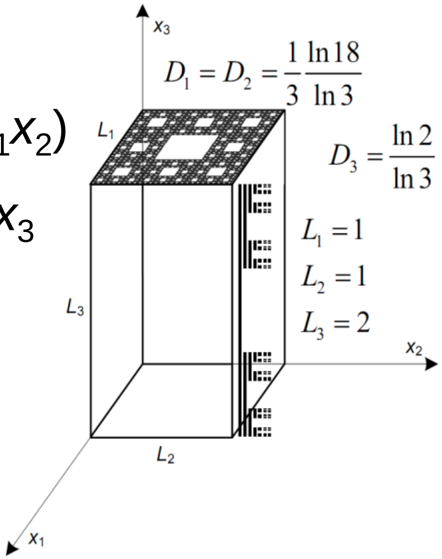

  - type II: in-plane

$$u_1 \equiv u_1(x_1) \quad u_2 \equiv u_2(x_2) \quad u_3 \equiv 0$$
$$\varphi_1 \equiv 0 \quad \varphi_2 \equiv 0 \quad \varphi_3 \equiv \varphi_3(x_1, x_2)$$

  - type III: out-of-plane

$$u_1 \equiv 0 \quad u_2 \equiv 0 \quad u_3 \equiv u_3(x_1, x_2)$$
$$\varphi_1 \equiv \varphi_1(x_1, x_2) \quad \varphi_2 \equiv \varphi_2(x_1, x_2) \quad \varphi_3 \equiv 0$$

Problem I-a, I-b

- Modal decomposition

$$u(x) \equiv f(x)e^{i\omega t}$$

$$v = \sqrt{\frac{\lambda + 2\beta}{\rho}}$$

$$k = \frac{\omega}{v}$$

$$(L-x)^2 f''(x) + (D-1)(L-x) f'(x) + k^2 D^2 (L-x)^{2D} f(x) = 0$$

$$D = \frac{1}{3}\frac{\ln 18}{\ln 3}$$

$$f_1(x,k) \equiv \cos\left[k(L-x)^D\right]$$

$$f_2(x,k) \equiv \sin\left[k(L-x)^D\right]$$

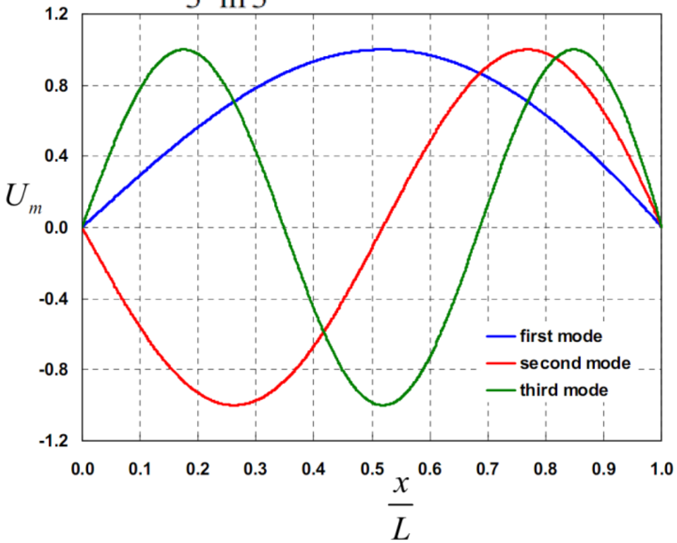

Mode shapes for BVP admitting homogeneous BCs $u(0) = u(L) = 0$.

$$v = \sqrt{\frac{\psi + 2\eta}{I}}$$

Problem II

- Governing equation for φ_3

$$I\ddot{\varphi}_3 = (\psi + \varepsilon)\left[\frac{\varphi_{3,11}}{g_1^2} + \frac{\varphi_{3,22}}{g_2^2} - \frac{\varphi_{3,1}g_{1,1}}{g_1^3} - \frac{\varphi_{3,2}g_{2,2}}{g_2^3}\right] + 2(\beta + \alpha)\frac{\varphi_3}{g_1 g_2} - (\beta - \alpha)\left[\frac{\varphi_3}{g_1^2} + \frac{\varphi_3}{g_2^2}\right]$$

$$\alpha \quad \beta$$

$$\varphi_3(x_1, x_2, t) = P(x_1)Q(x_2)e^{i\omega t}$$

$$P(x_1, k_1) = A_1\ f_1(x_1, k_1) + A_2\ f_2(x_1, k_1) \qquad Q(x_2, k_2) = B_1\ f_1(x_2, k_2) + B_2\ f_2(x_2, k_2)$$

$$v = \sqrt{\frac{\psi + \varepsilon}{I}} \qquad k_1^2 + k_2^2 = \frac{\omega^2}{v^2}$$

$$v = \sqrt{\frac{\lambda}{\rho}}$$

FEM Procedure – Linear Momentum

- Weak formulation
  - multiply by admissible (test) function $w_i \in H_0^1(\Omega)$ and integrate over domain
  - apply Green-Gauss theorem to eliminate surface integrals

$$\int_\Omega \rho \ddot{u}_i w_i d\Omega = (\beta+\alpha)\int_\Omega \frac{u_{i,j} w_{i,j}}{g_j g_j} d\Omega + (\lambda+\beta-\alpha)\int_\Omega \frac{u_{j,i} w_{i,j}}{g_i g_j} d\Omega$$

$$+ e_{ijk}\left[(\beta+\alpha)\int_\Omega \nabla_j^D\left(\frac{\varphi_k}{g_j}\right) w_i d\Omega - (\beta-\alpha)\int_\Omega \nabla_j^D\left(\frac{\varphi_k}{g_i}\right) w_i d\Omega\right]$$

- Mass and stiffness matrices evaluation
  - absence of fractal or micropolar effects in mass matrix
  - loss of SPD feature for stiffness matrices

$$\mathbf{M} = \int_\Omega \rho u_i w_i d\Omega \qquad \mathbf{K}_{u\varphi} = e_{ijk}\left[(\beta+\alpha)\int_\Omega \nabla_j^D\left(\frac{\varphi_k}{g_j}\right) w_i d\Omega - (\beta-\alpha)\int_\Omega \nabla_j^D\left(\frac{\varphi_k}{g_i}\right) w_i d\Omega\right]$$

$$\mathbf{K}_{uu} = (\beta+\alpha)\int_\Omega \frac{u_{i,j} w_{i,j}}{g_j g_j} d\Omega + (\lambda+\beta-\alpha)\int_\Omega \frac{u_{j,i} w_{i,j}}{g_i g_j} d\Omega$$

FEM Procedure – Angular Momentum

- Weak formulation generation ($\sigma_i \in H_0^1(\Omega)$ is the test function)

$$\int_\Omega I\ddot{\varphi}_i\sigma_i d\Omega = (\psi+\varepsilon)\int_\Omega \frac{\varphi_{i,j}\sigma_{i,j}}{g_j g_j} d\Omega + (\eta+\psi-\varepsilon)\int_\Omega \frac{\varphi_{j,i}\sigma_{i,j}}{g_i g_j} d\Omega - 4\alpha\int_\Omega \frac{\varphi_i g_i \sigma_i}{g^*} d\Omega$$

$$+ e_{ijk}\int_\Omega \frac{\sigma_i}{g_j}\left[(\beta+\alpha)\nabla_j^D u_k + (\beta-\alpha)\nabla_k^D u_j\right] d\Omega$$

$$\mathbf{I} = \int_\Omega I\varphi_i\sigma_i d\Omega \qquad \mathbf{K}_{\varphi u} = e_{ijk}\int_\Omega \frac{\sigma_i}{g_j}\left[(\beta+\alpha)\nabla_j^D u_k + (\beta-\alpha)\nabla_k^D u_j\right] d\Omega$$

$$\mathbf{K}_{\varphi\varphi} = (\psi+\varepsilon)\int_\Omega \frac{\varphi_{i,j}\sigma_{i,j}}{g_j g_j} d\Omega + (\eta+\psi-\varepsilon)\int_\Omega \frac{\varphi_{j,i}\sigma_{i,j}}{g_i g_j} d\Omega - 4\alpha\int_\Omega \frac{\varphi_i g_i \sigma_i}{g^*} d\Omega$$

$$\begin{bmatrix} \mathbf{M} & \mathbf{0} \\ \mathbf{0} & \mathbf{I} \end{bmatrix}\begin{Bmatrix} \ddot{\boldsymbol{u}} \\ \ddot{\varphi} \end{Bmatrix} + \begin{bmatrix} \mathbf{K}_{uu} & \mathbf{K}_{u\varphi} \\ \mathbf{K}_{\varphi u} & \mathbf{K}_{\varphi\varphi} \end{bmatrix}\begin{Bmatrix} \boldsymbol{u} \\ \varphi \end{Bmatrix} = \begin{Bmatrix} \boldsymbol{f} \\ \boldsymbol{m} \end{Bmatrix}$$

Integration & Time March

- Application of the 4-node tetrahedral element
  - Integration by Gauss-Legendre quadrature formulas (Rathod, 2005)

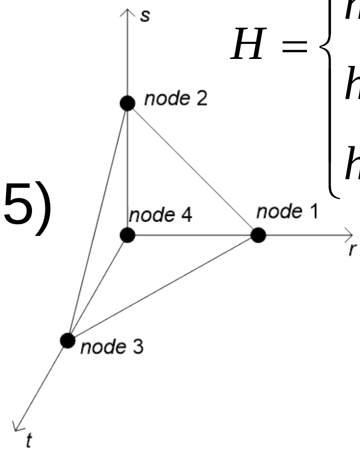

$$H = \begin{cases} h_1(r,s,t) = r \\ h_2(r,s,t) = s \\ h_3(r,s,t) = t \\ h_4(r,s,t) = 1 - r - s - t \end{cases}$$

Δ

First Mode Excitation

- Numerical solution snapshots for normalized displacement along all three directions in the first mode excitation

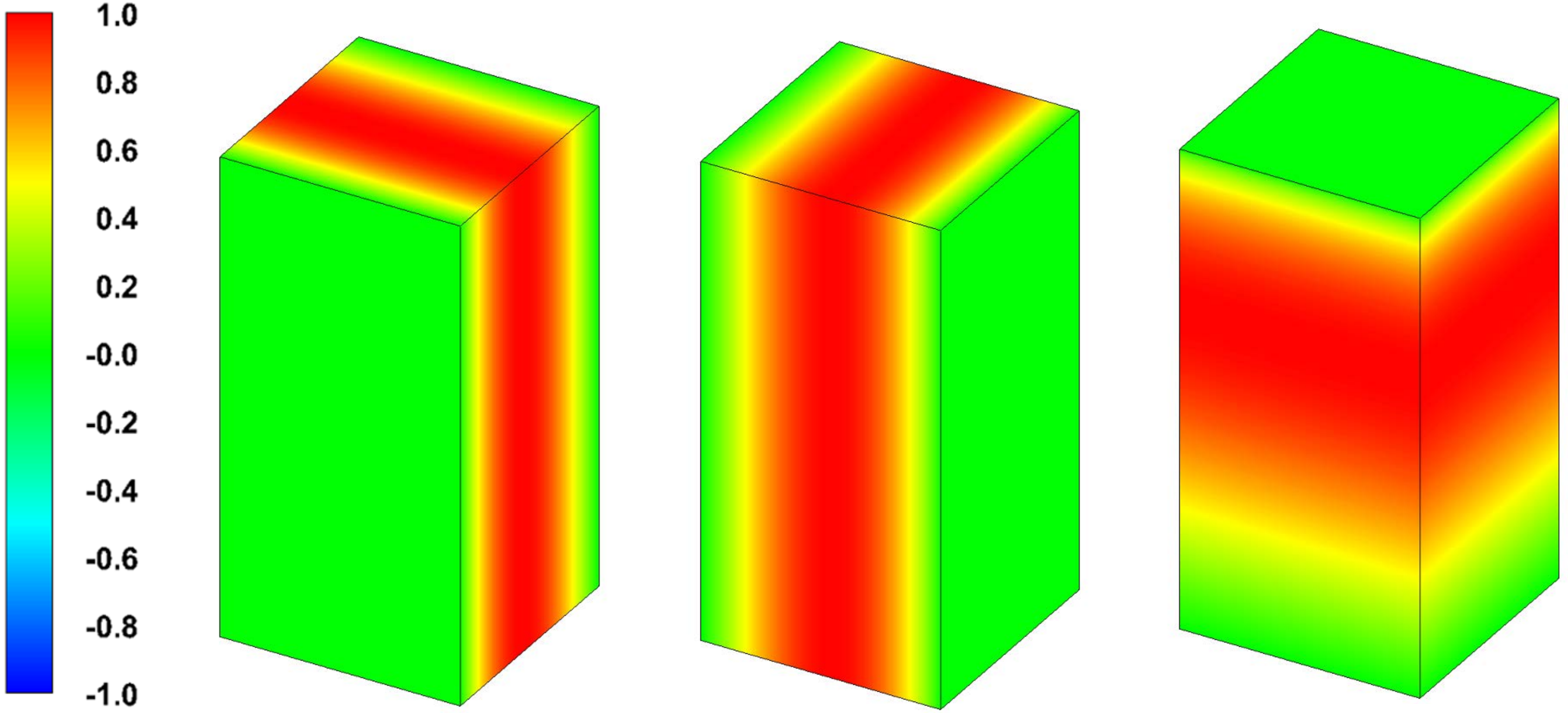

Second Mode Excitation

- Numerical solution snapshots for normalized displacement along all three directions in the second mode excitation

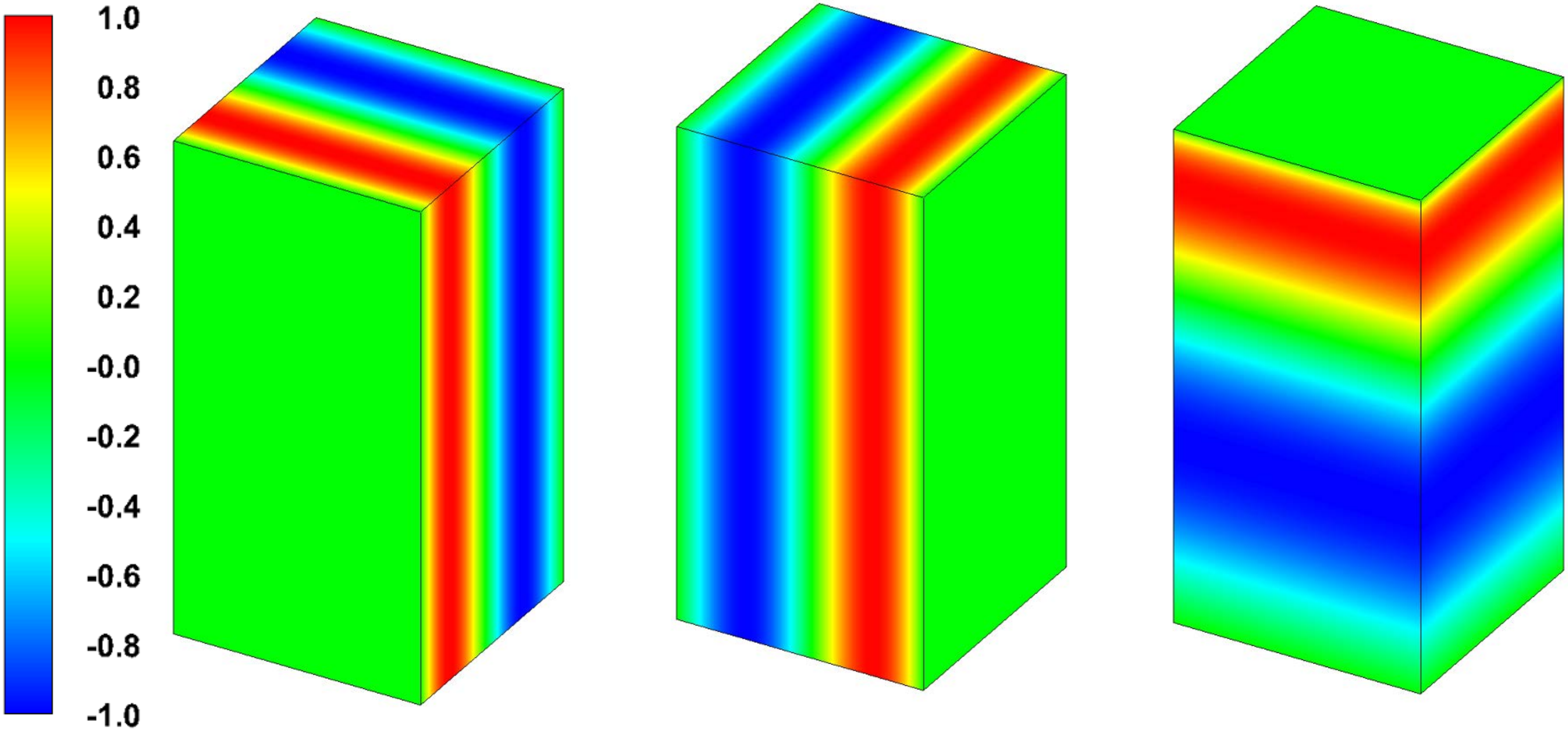

Transient Response - First & Second Mode

ω = 3.514

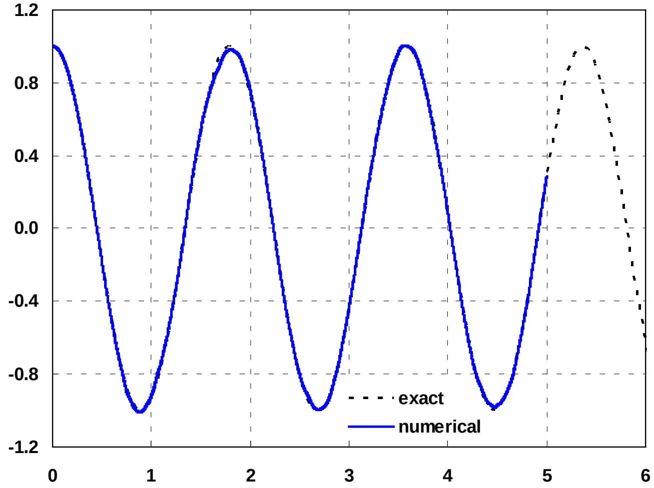

ω = 7.027

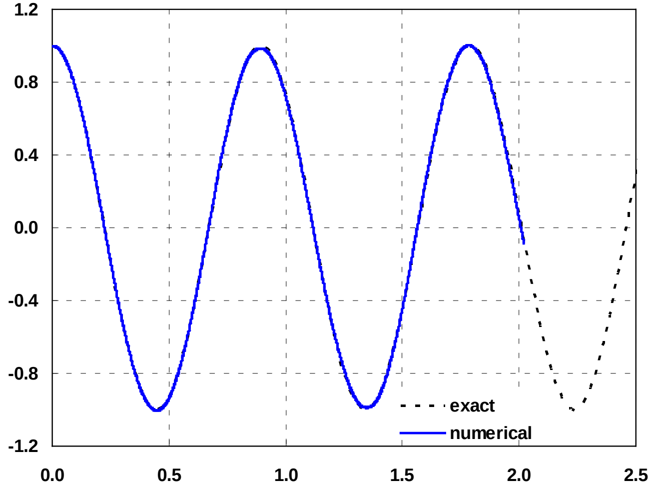

$$D_{1,2} = \frac{1}{3}\frac{\ln 18}{\ln 3}$$

ω = 5.441

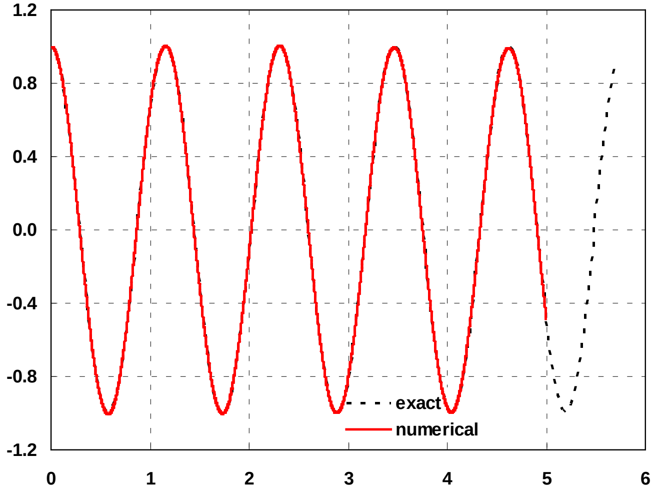

ω = 10.882

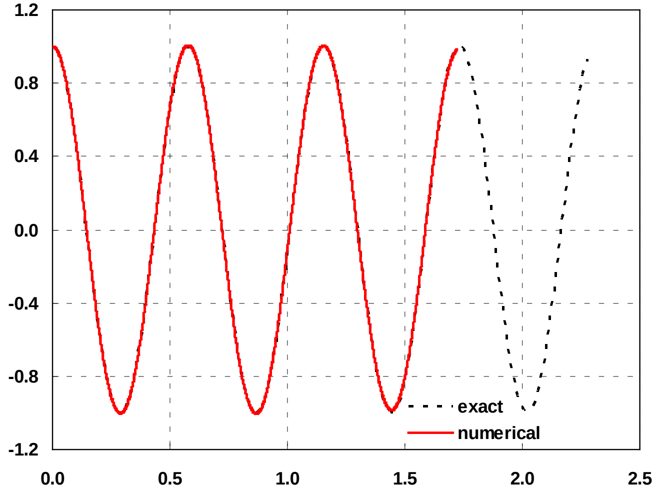

$$D_3 = \frac{\ln 2}{\ln 3}$$

Electromagnetism on Anisotropic Fractal Media

Second order differential equations of electromagnetism

$$\nabla^D \cdot (\nabla^D \mathbf{E}) - \nabla^D (\nabla^D \cdot \mathbf{E}) = \frac{1}{c^2}\frac{\partial^2 \mathbf{E}}{\partial^2 t} + \frac{4\pi}{c^2}\frac{\partial}{\partial t}\mathbf{J} \quad \text{or}$$

$$\frac{1}{c_1^{(p)}}\left[E_{k,p}/c_1^{(p)}\right]_{,p} - \frac{1}{c_1^{(k)}}\left[E_{k,l}/c_1^{(l)}\right]_{,p} = \frac{1}{c^2}\frac{\partial^2 E_k}{\partial t^2} + \frac{4\pi}{c}\frac{\partial J_k}{\partial t}$$

$\Rightarrow$ conductor: $\nabla^D \cdot \nabla^D \mathbf{H} = \frac{\boldsymbol{\sigma}}{c^2} \cdot \frac{\partial \mathbf{H}}{\partial t}$ or $\frac{1}{c_1^{(p)}}\left[H_{k,p}/c_1^{(p)}\right]_{,p} = \frac{\sigma_{km}}{c^2}\frac{\partial H_m}{\partial t}$

$\Rightarrow$ dielectric: $\nabla^D \cdot \nabla^D \mathbf{E} = \frac{\boldsymbol{\sigma}}{c^2} \cdot \frac{\partial^2 \mathbf{E}}{\partial^2 t}$ or $\frac{1}{c_1^{(p)}}\left[E_{k,p}/c_1^{(p)}\right]_{,p} = \frac{\sigma_{km}}{c^2}\frac{\partial^2 E_m}{\partial t^2}$

$\Rightarrow$ Poynting vector has the same form as in non-fractal media but the electric and magnetic force densities change

WAVEFRONTS IN RANDOM MEDIA

Martin Ostoja-Starzewski
Department of Mechanical Science & Engineering
University of Illinois at Urbana-Champaign

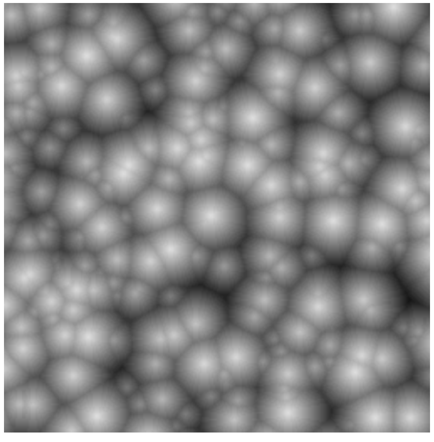
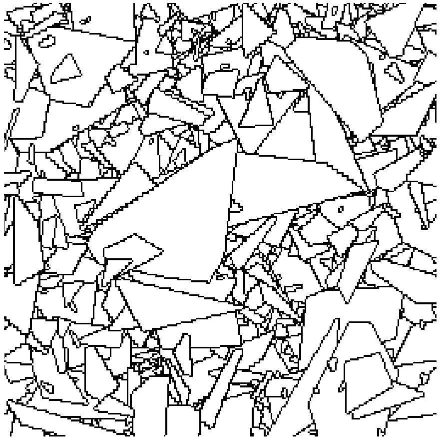
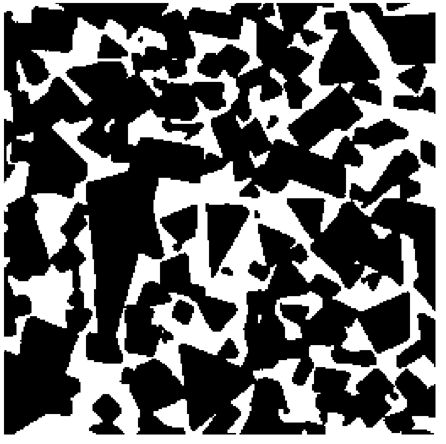

studies of wave phenomena

various classifications possible

linear	nonlinear	
steady-state	transient	
whole space-time	wavefront	
deterministic	random	
analytical	computational	
…		

studies of wave phenomena

various classifications possible

linear	nonlinear	
steady-state	transient	
whole space-time	wavefront	
deterministic	random	
analytical	computational	
…		

Indicatrix envelopes in random media

(a) **locally isotropic**

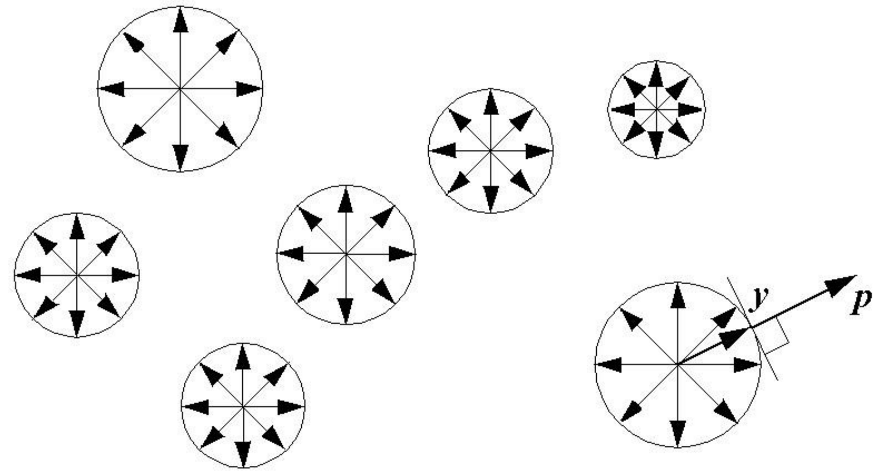

(a)

(b) **locally anisotropic**

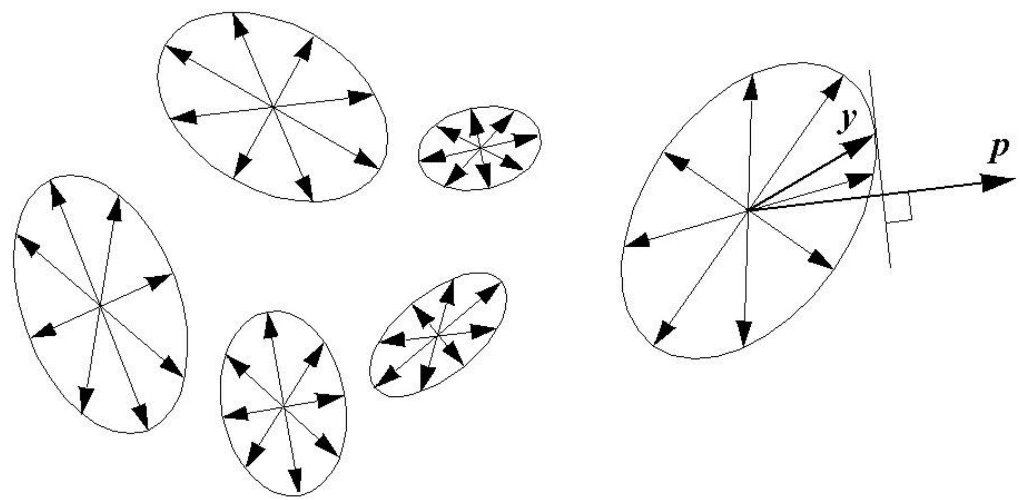

(b)

Basic methods in stochastic linear wave propagation

Long wavelength case

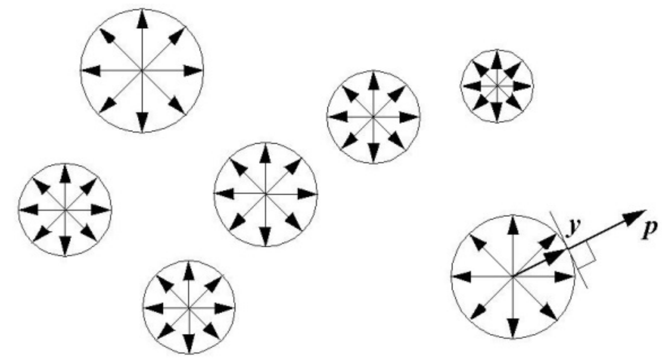

(a)

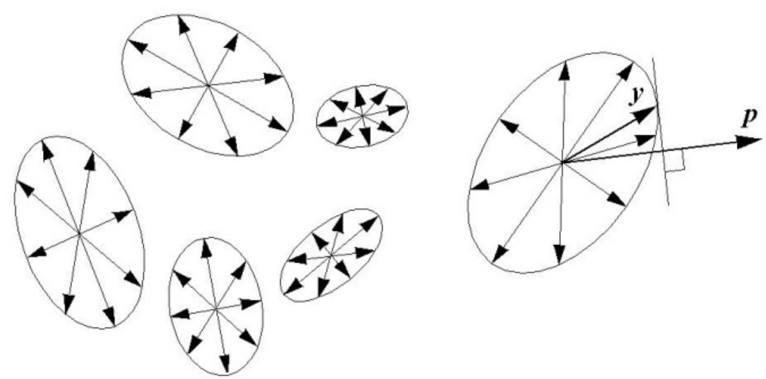

(b)

Basic methods in stochastic linear wave propagation

Long wavelength case

Series expansion

Basic methods in stochastic linear wave propagation

Short wavelength case – ray method

Fermat's principle

Using the Euler-Lagrange equations,
obtain equations of ray dynamics:

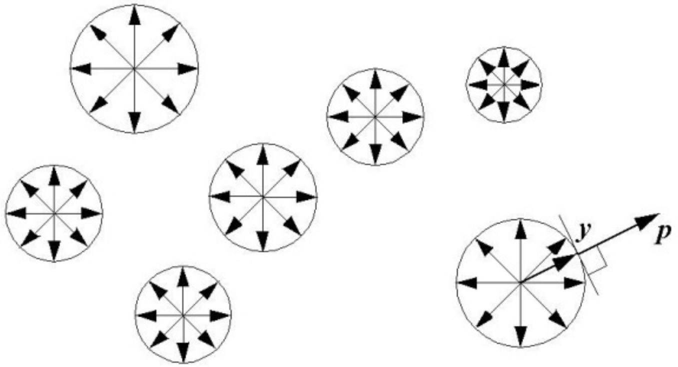

(a)

If want to account for local anisotropy, use

…obtain equations of ray dynamics:

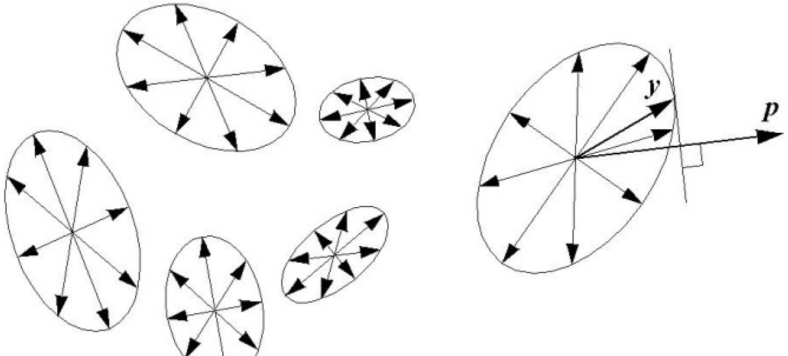

(b)

Dynamic/Impact Models

- Half-Plane subject to load (Lamb's Problem)
  - Normal, triangular-impulse load
  - Solved by cellular automata (CA) or peridynamics (PD)

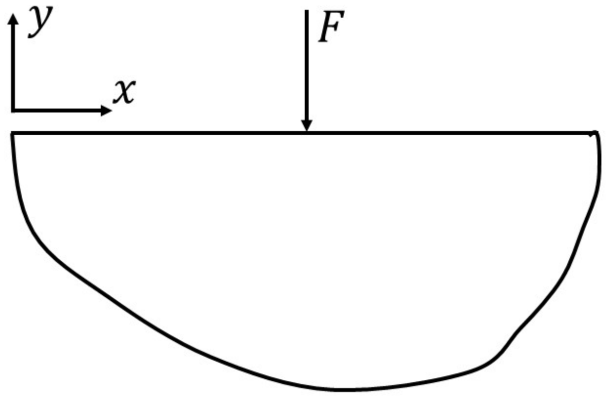

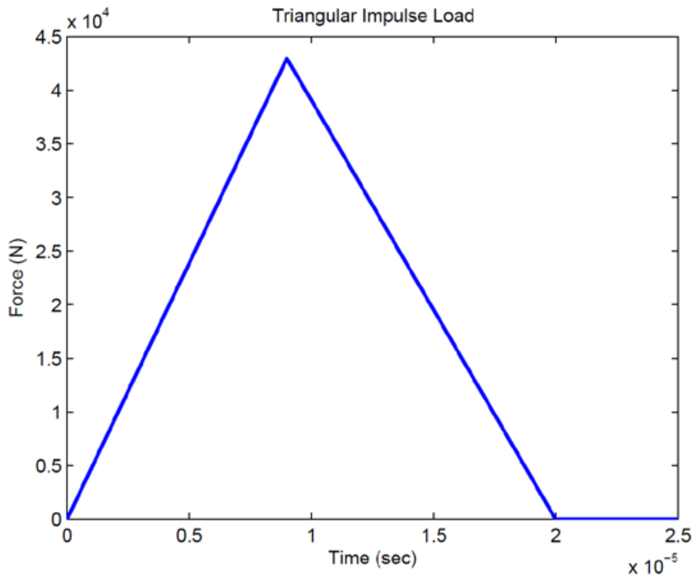

- Motivation:
  - Details of cable-cable impacts
  - Surface structures subject to earthquakes, impact…
  - Terrorist attacks on structures, explosions

Simulation of elastodynamics on a square grid

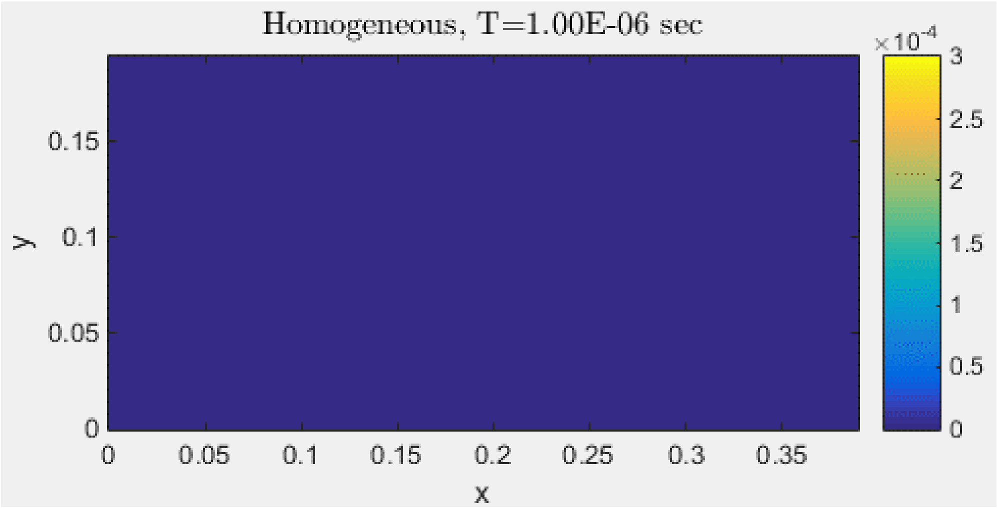

Plots of displacement magnitude

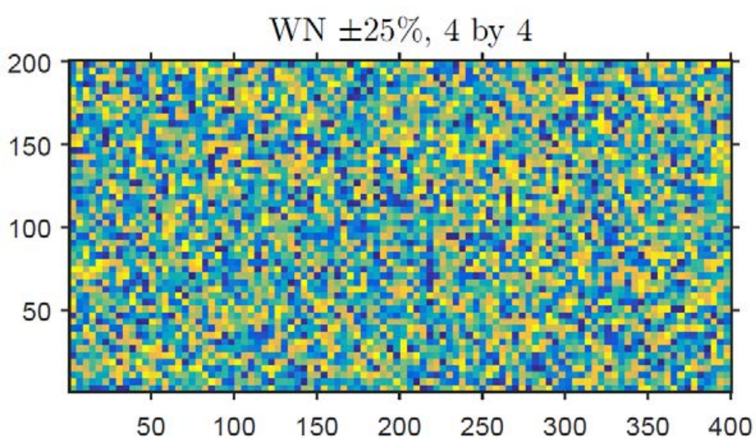

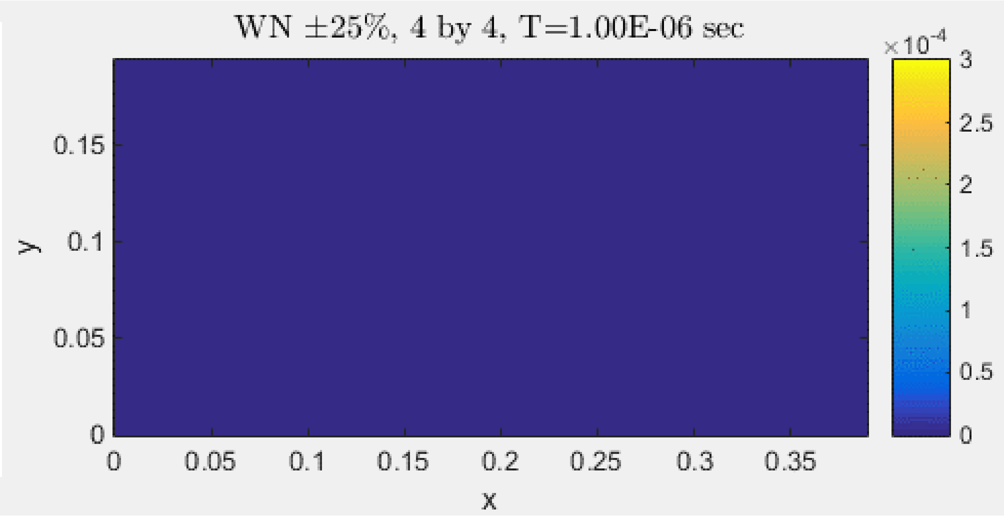

Random mass density on a coarse grid

Comparing CA and PD

$c_R = 0.919c_s$

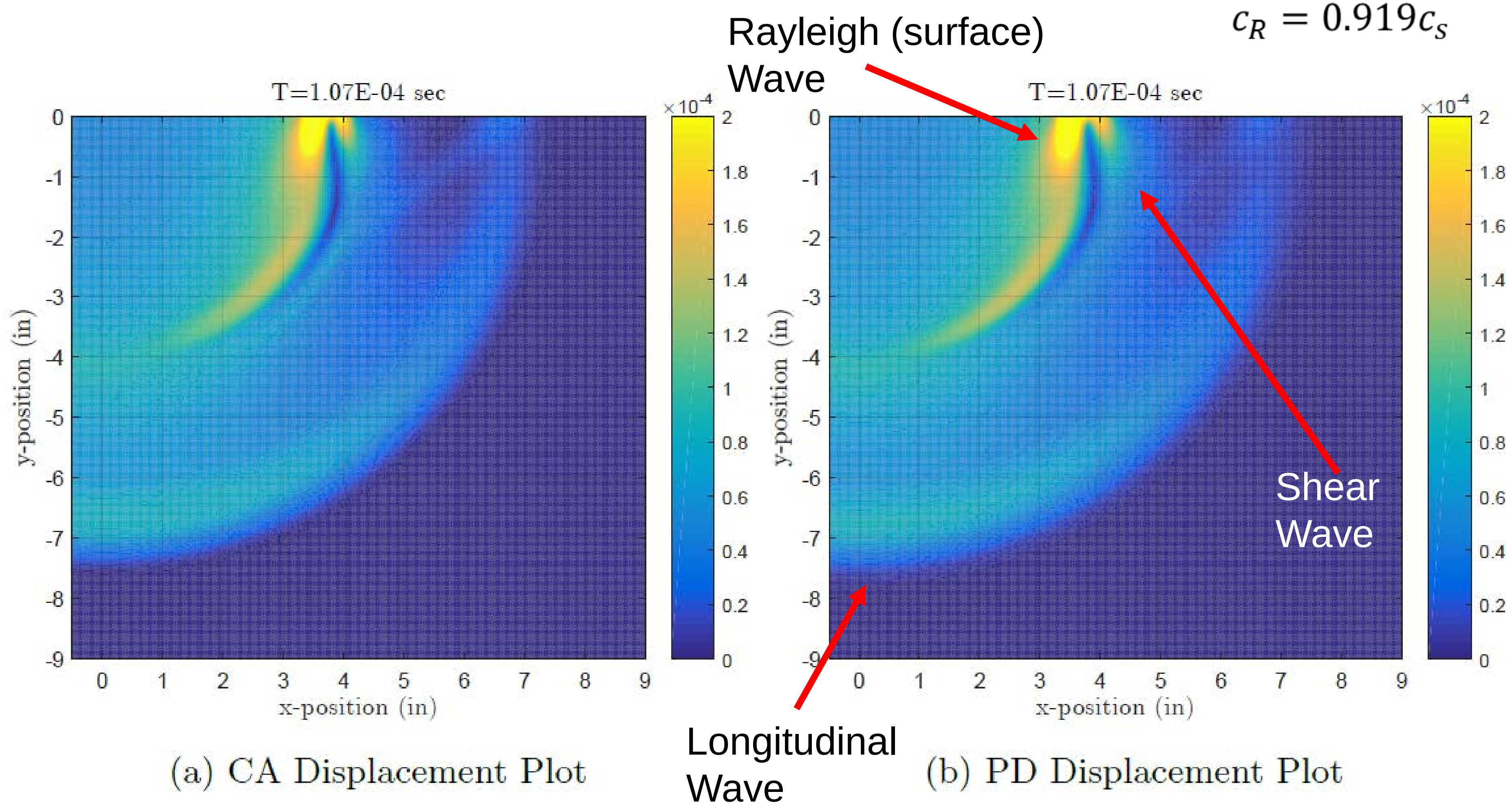

(a) CA Displacement Plot

(b) PD Displacement Plot

Towards spectral finite elements for random media

Spectral finite element for waves in rods

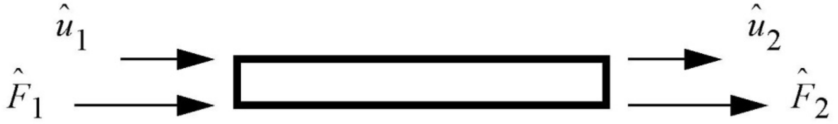

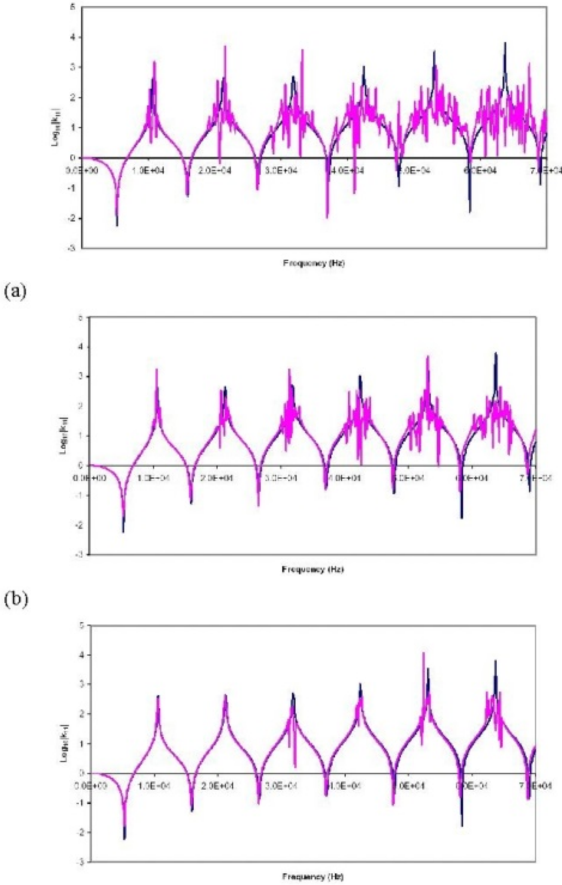

(a)

(b)

(c)

Towards spectral finite elements for random media

Spectral finite element for flexural waves

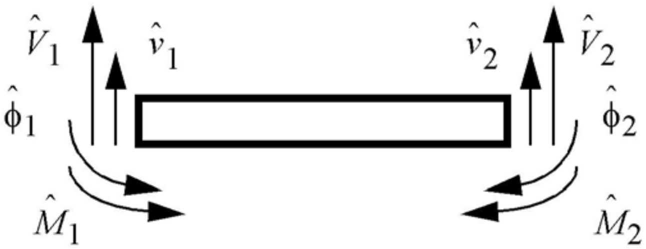

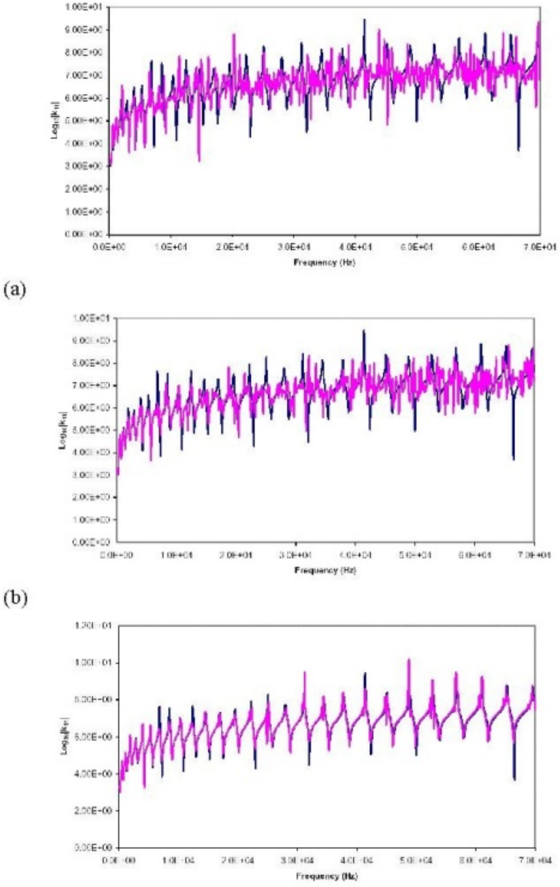

Fig. 5

Transient waves in heterogeneous nonlinear media

A class of models of random media

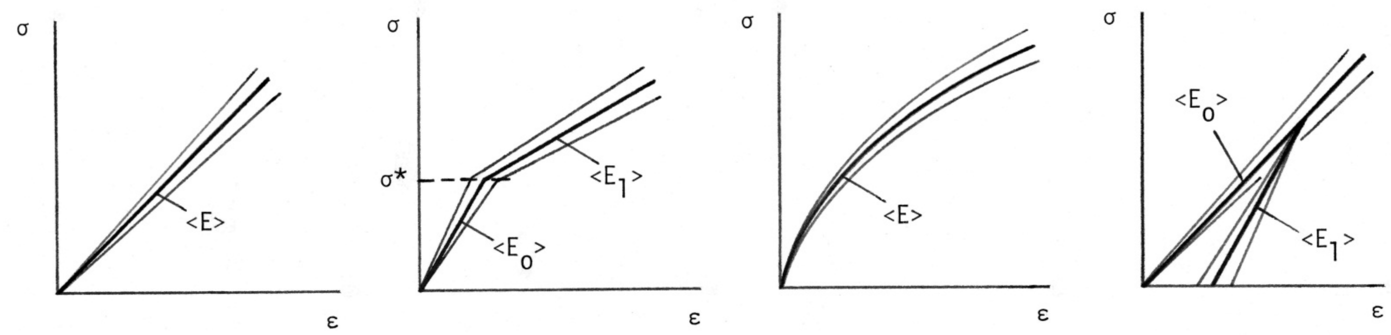

(a) linear elastic;

(b) soft bilinear elastic;

(c) soft non-linear elastic;

(d) linear-hysteretic.

Consider various material parameters as random fields

Stochastic evolution of simple wave

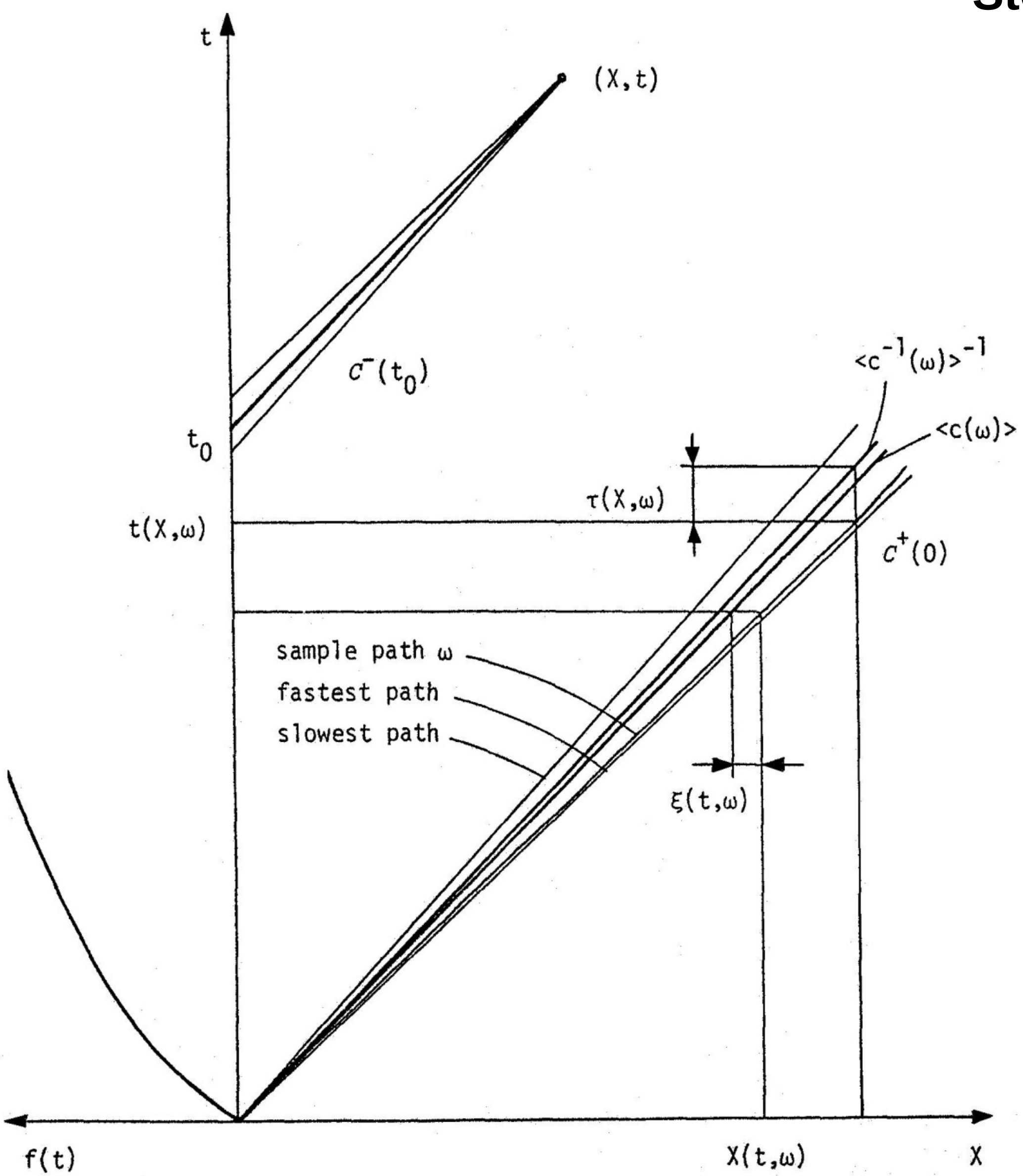

straight characteristics

are replaced

by wedges of random curves

grain-to-grain transmission:

$$\frac{2}{1} \qquad \sqrt{}$$

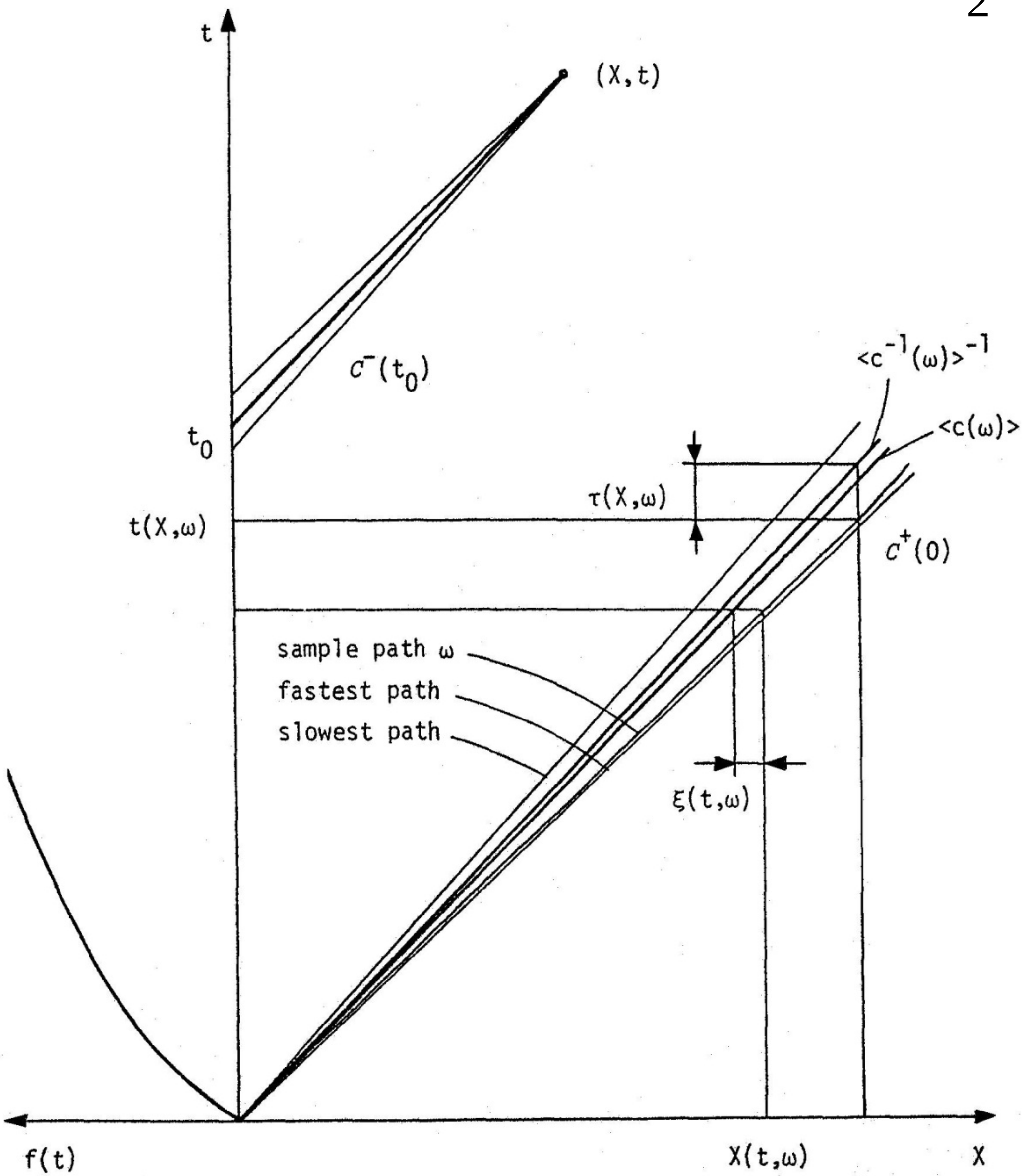

$\frac{1}{2}\frac{\quad^2}{\quad^2}$ $\frac{1}{2}\frac{\quad^2}{\quad^2}$ $\frac{\quad^2}{\quad}$

, 0,

^{2}, ,

Transient waves in random bilinear elastic media

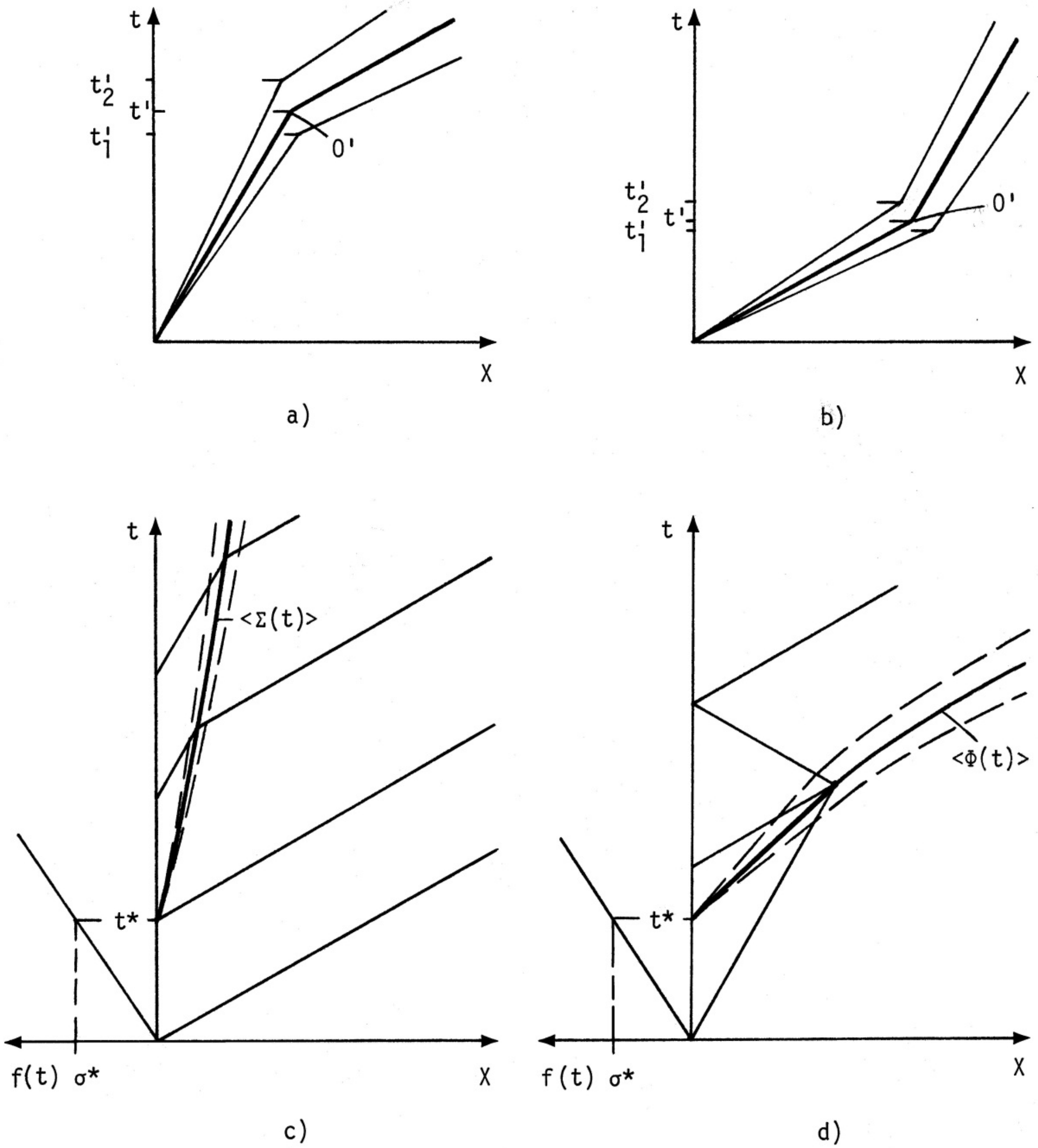

washing-out of a pulse

or

shock diffusion

Transient waves in random nonlinear elastic media

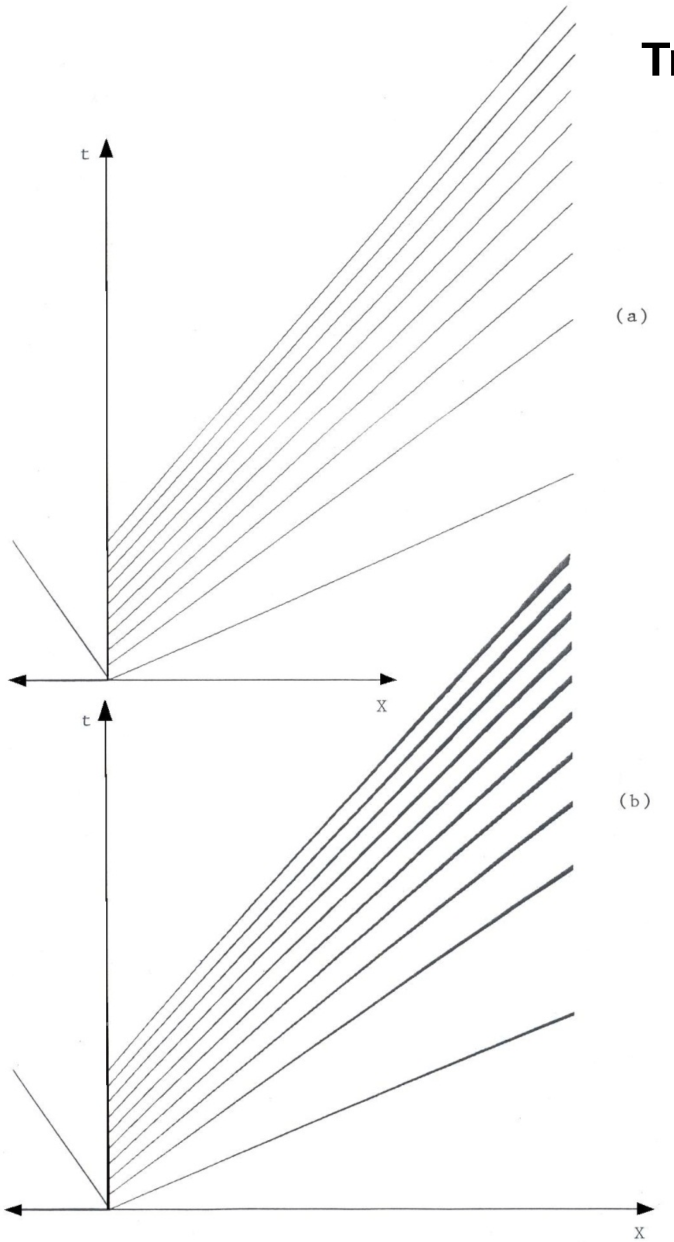

homogeneous medium:
characteristic remain straight

washing-out of pulse

random medium:
characteristic are curving
due to stochastic wave attenuation

washing-out of pulse is amplified

Transient waves in random nonlinear elastic media

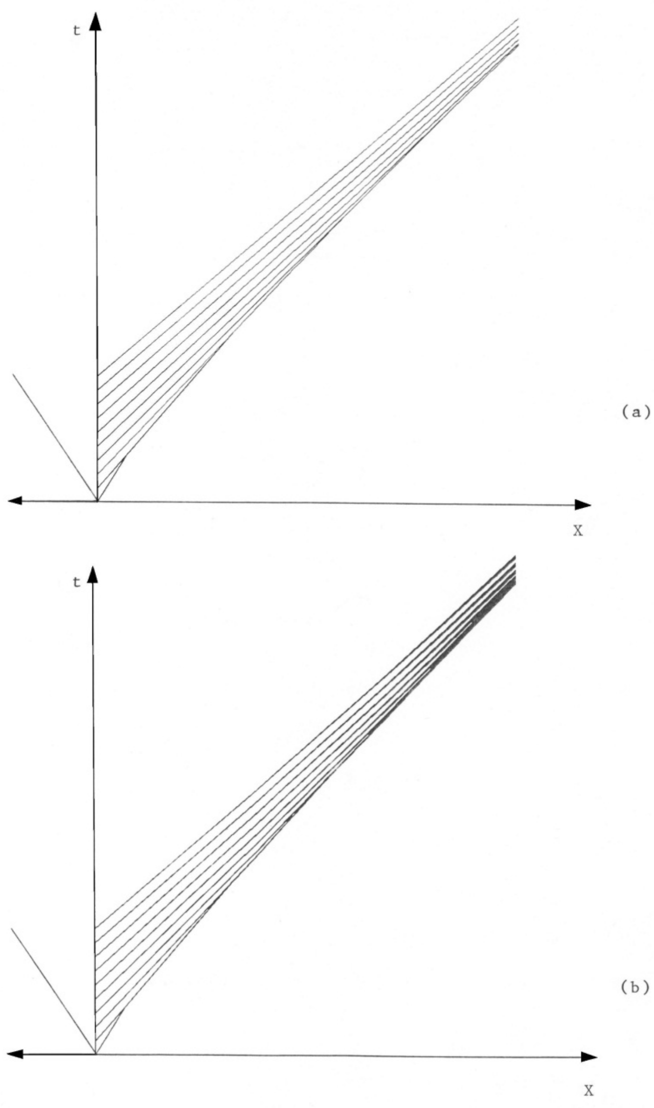

homogeneous medium:
characteristic remain straight

shock formation

random medium:
characteristic are curving
due to stochastic wave attenuation

earlier shock formation, weaker magnitude

Transient waves in random elastic-hysteretic media

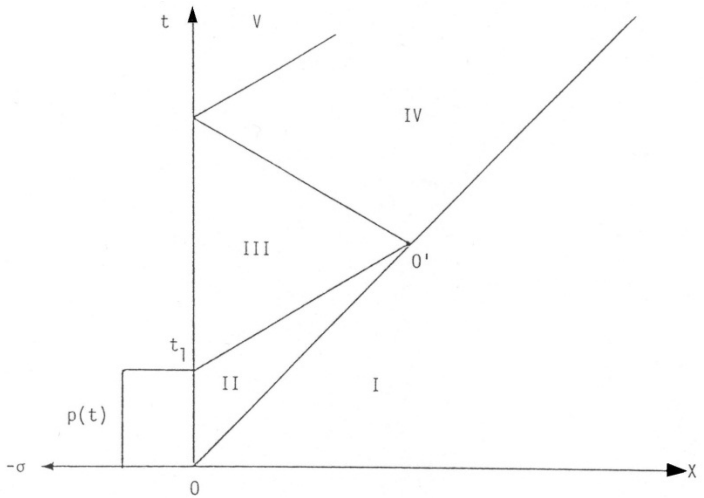

a)

homogeneous medium:
deterministic shock formation

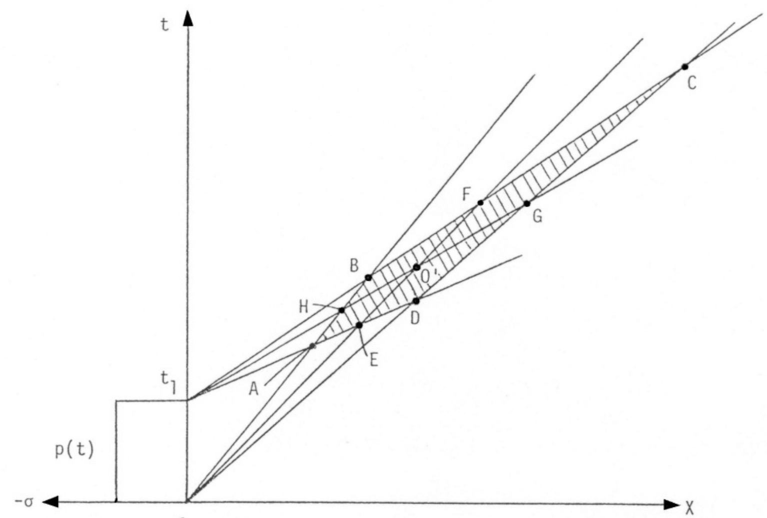

b)

random medium:
strong scatter in shock formation

Wavefront in continuum mechanics
is modeled as a **singular surface**

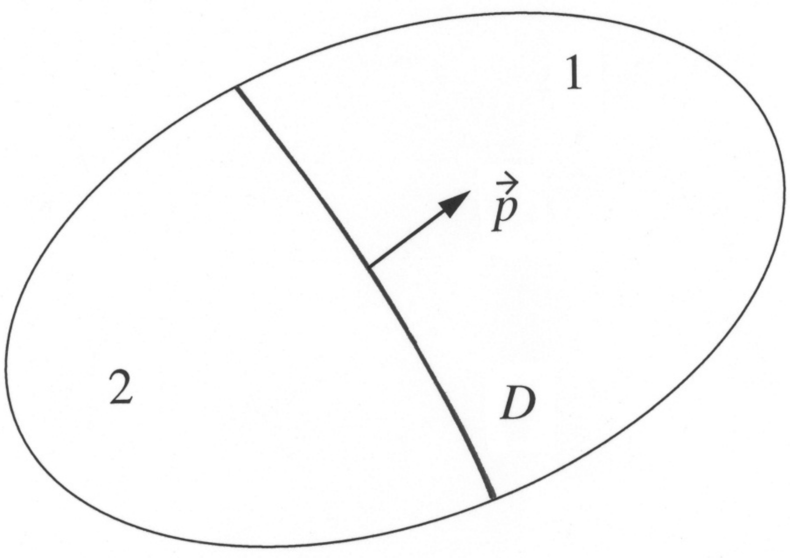

… idealized model:

homogeneous continuum, no microstructure

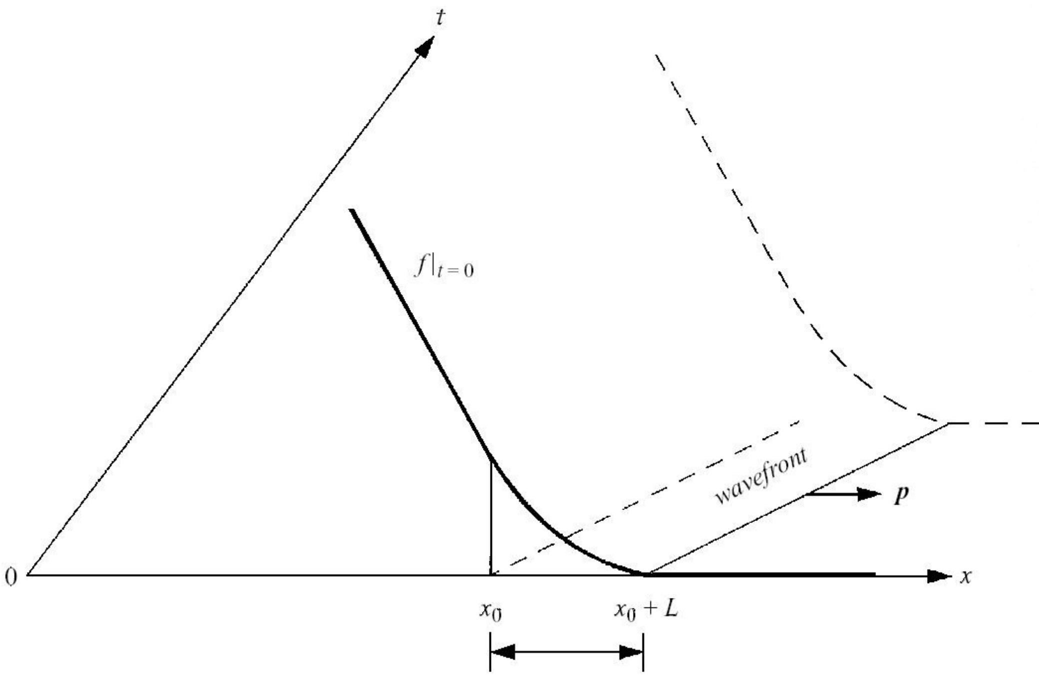

t
$f|_{t=0}$
wavefront
p
0
x
x_0
$x_0 + L$

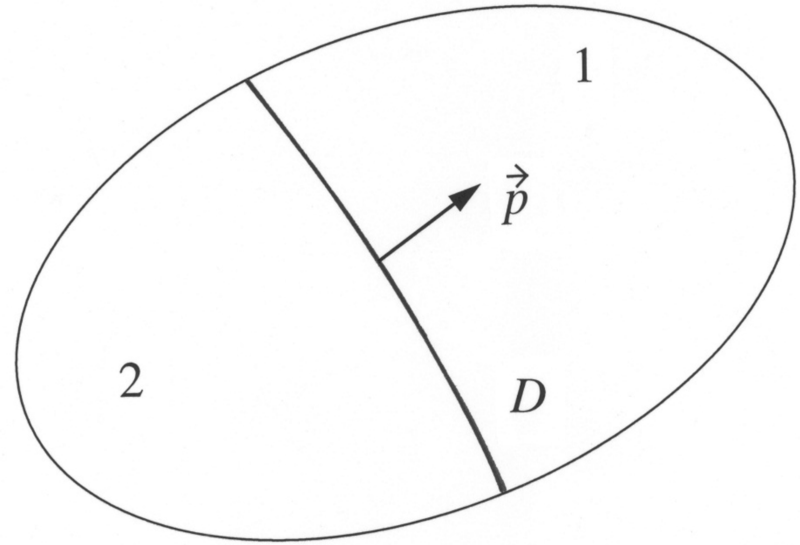

1
$\vec{p}$
2
D

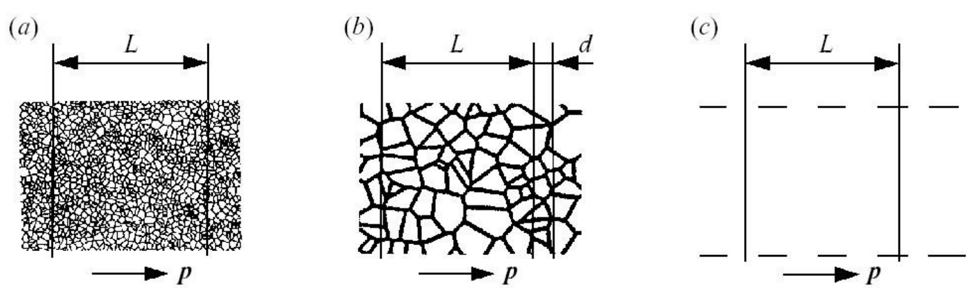

(a)
L
p
(b)
L
d
p
(c)
L
p

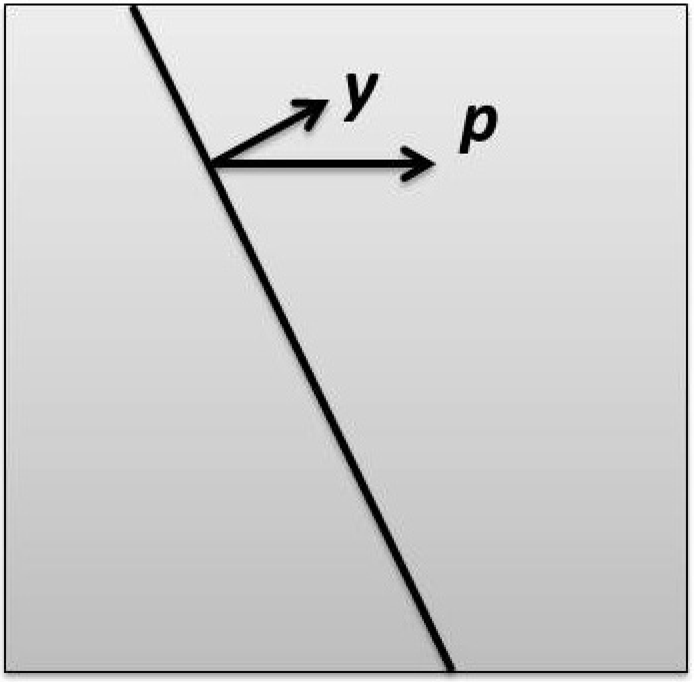

(a)

Wavefront in a homogeneous anisotropic medium, propagating in direction , locally along a ray of direction .

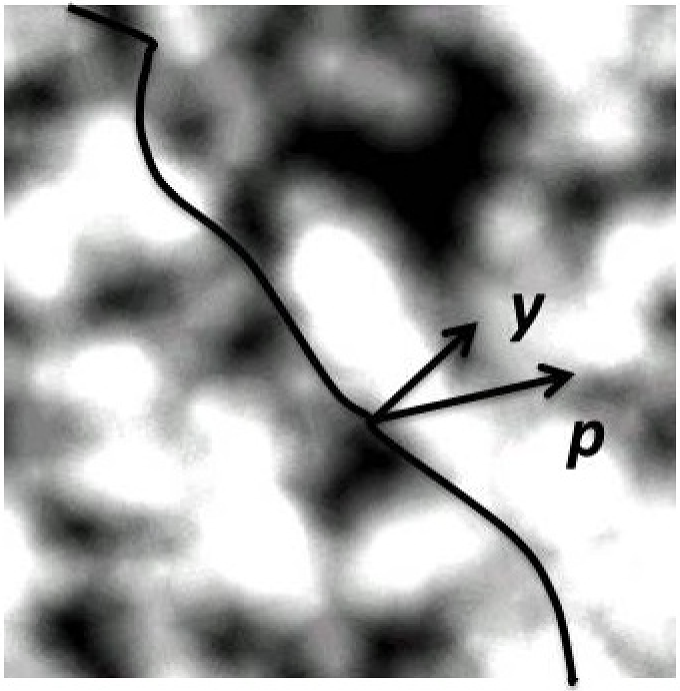

(b)

Wavefront in a realization of a random anisotropic medium.

Indicatrix envelopes in random media

(a) locally isotropic

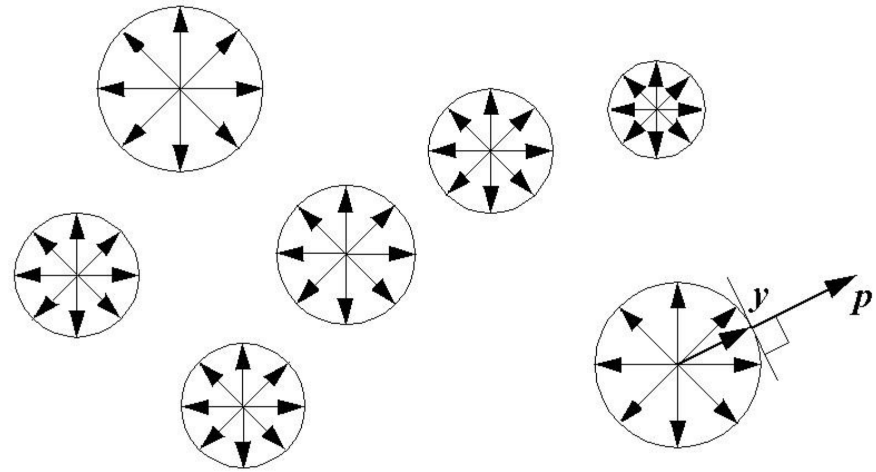

(a)

(b) locally anisotropic.

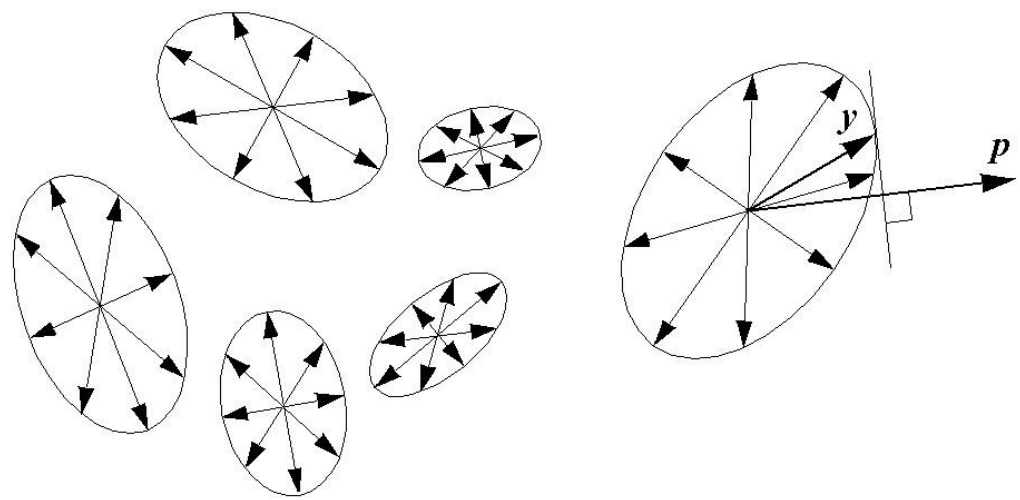

(b)

Acceleration waves in 1D media

$2 \quad 1$

in deterministic media:
[Coleman, Gurtin & Herrera, 1965;
Bland, 1966; Chen, 1971]

Bernoulli equation

$$\frac{\quad}{\quad} \quad {}^{2}$$

dissipation

elastic nonlinearity

competition

$$\frac{\quad}{\quad}$$

$$\frac{1}{\quad}\ln(1 \quad \frac{\quad}{\quad_0})$$

— ^{2} driven by random fields $\{(\ , \ ) ; \ [0, \ )\}$

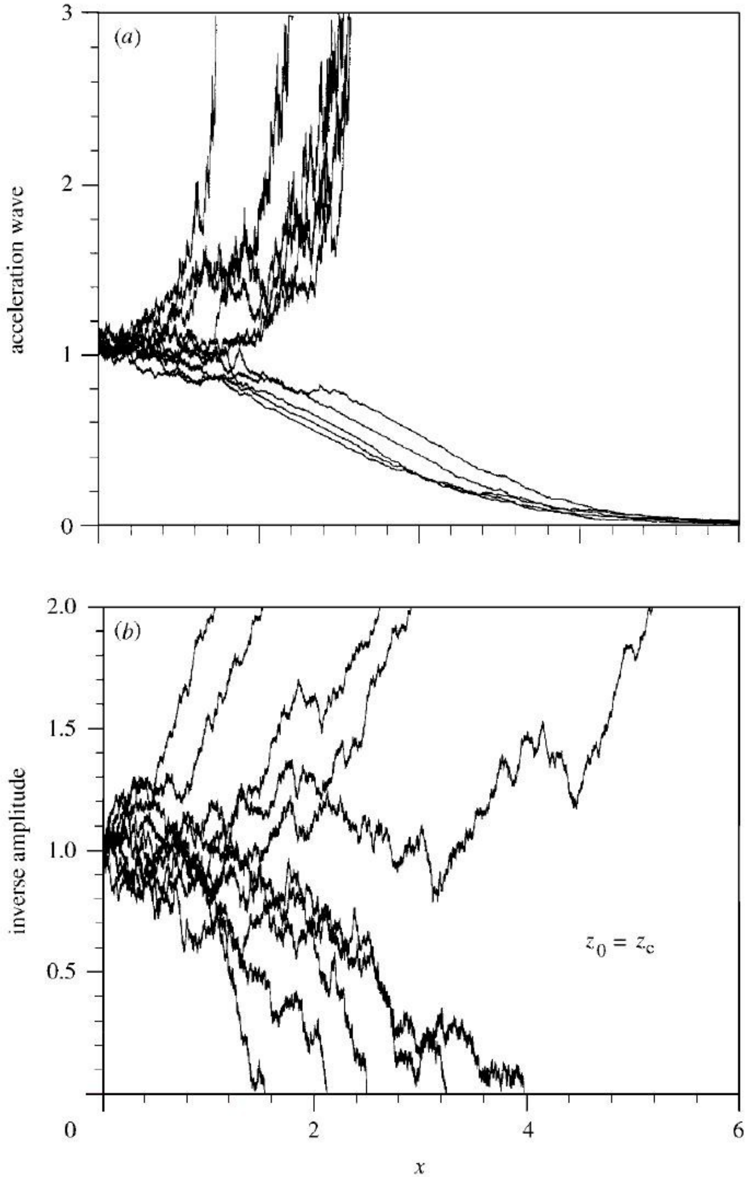

1/

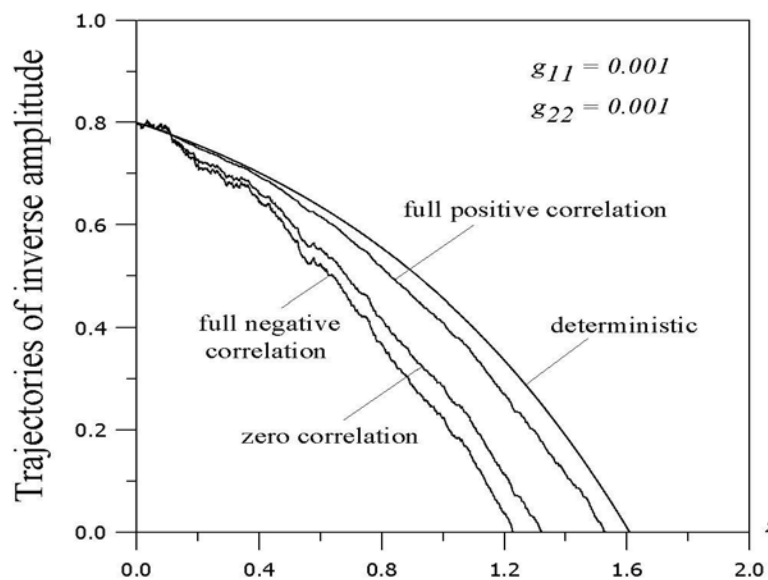

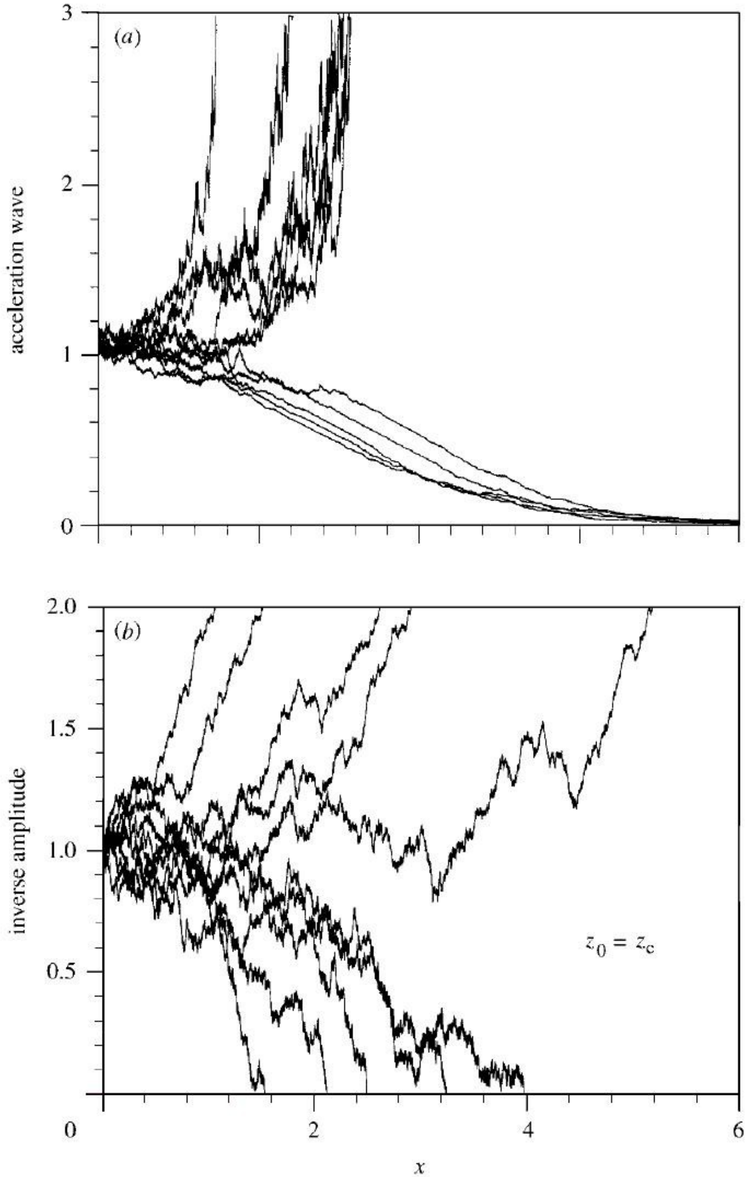

2

$$\frac{0}{2\ 0}, \qquad \frac{0}{2\ 0}, \qquad \sqrt{\frac{0}{}}.$$

$$\frac{0}{2\ 0} \quad \frac{0}{2\ 0}\sqrt{\frac{}{0}}^{2}$$

is driven by driven by
a four-component random field

$_0$, $_0$, ^{0},

Acceleration waves in 1D media

2 1

Bernoulli equation

in random media

2

[1991; . 1999;
. 2003; 2006]

<u>random fields</u>: dissipation elastic nonlinearity

stochastic competition

$$\frac{1}{}\ln(1 \quad \frac{}{})$$

0

Acceleration waves in 1D media

2 1

Bernoulli equation

in random media

[1991; . 1999;
. 2003; 2006]

—— 2

<u>random fields</u>: dissipation elastic nonlinearity

stochastic competition

Model with two or four correlated noises

Noises are white, or Gaussian, Ornstein-Uhlenbeck

Micromechanics-based random fields

Shock waves in 1D media

- First, deterministic, (in)homogeneous

[Valanis, 1965;
Coleman, Gurtin & Herrera, 1965;
Achenbach & Reddy, 1967;
Singh & Gupta, 1986]

- Next, random media

Initial condition

$(\; ,0) \quad , \; (\; ,0) \quad 0, \qquad (0, \;) \qquad {}_0 \; (\;)$

Momentum balance

$, \qquad ,$

Dynamic compatibility

$[[\quad]] \qquad [[\; , \;]] \;\; \text{in} \;\; (\; , \;)$

Kinematic compatibility

$[[\; , \;]] \qquad ,$

Viscoelastic response

$$(\ ) \quad (0) \ (\ ) \quad {}_{0} \ , \ (\quad) \ (\ ) \quad (0)\frac{1}{{}_{1}} \ , \ (\ ) \quad {}_{0} \ , \ (\quad)\frac{1}{{}_{1}} \ , \ (\ ) \quad ,$$

Wave propagation speed

$$\sqrt{\frac{(0)}{\ }}.$$

Evolution equation

$$\frac{}{}[[\quad]] \quad \frac{1}{2}\frac{\ , \ (0)}{(0)}[[\quad]].$$

$$[[\quad]] \qquad {}_{0}\exp \ \frac{1}{2}\frac{\ , \ (0)}{(0)} \quad .$$

$, \ (0) \quad 0, \quad (0) \quad 0$ deterministic attenuation

Viscoelastic response

$$(\;) \quad (0) \; (\;) \quad {}_0 \; , \; (\quad) \; (\;) \quad (0)\frac{1}{}_1 \; , \; (\;) \quad {}_0 \; , \; (\quad)\frac{1}{}_1 \; , \; (\;) \; ,$$

Wave propagation speed

$$\sqrt{\frac{(0)}{}}.$$

In random medium $\;, \; (0), \;\; , (0)$ **are random fields**

Evolution equation **stochastic evolution**

$$\text{—}[[\;\;]] \quad \frac{1}{2}\frac{, (0)}{(0)}[[\;\;]].$$

$$[[\;\;]] \quad {}_0 \exp \; \frac{1}{2}\frac{, (0)}{(0)} \quad .$$

$$, (0) \quad 0, \quad (0) \quad 0$$ deterministic attenuation

Stochastic evolution equation for weakly inhomogeneous media:

$$\frac{\quad}{\quad} \qquad \frac{\quad}{2} \qquad \frac{\quad^{1/2}}{2 \quad^{3/2}}$$

for [[ ]] driven by random field , ,

Wavefront's position: ( )

random speed (,) $\frac{\quad}{\quad}\sqrt{\frac{(\; , \;)}{(\; , \;)}}$ random arrival time (,) $_0 \frac{\quad}{(\; , \;)}$

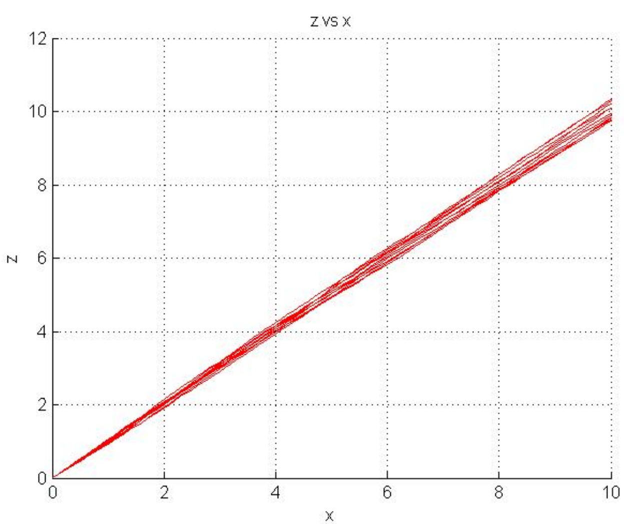

(a) uncoupled model

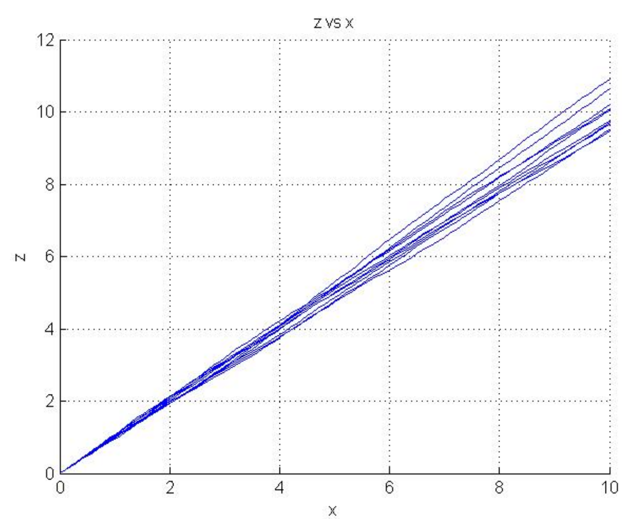

(b) coupled model

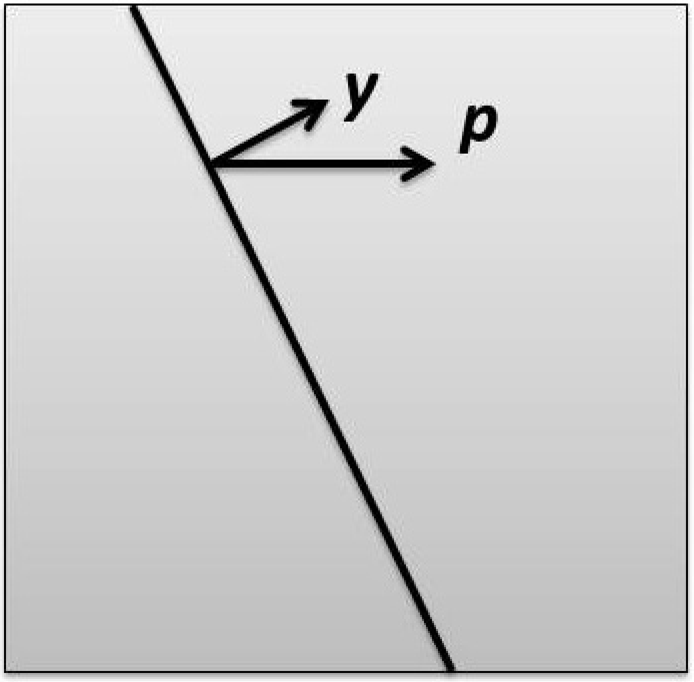

(a)

Wavefront in a homogeneous anisotropic medium, propagating in direction , locally along a ray of direction .

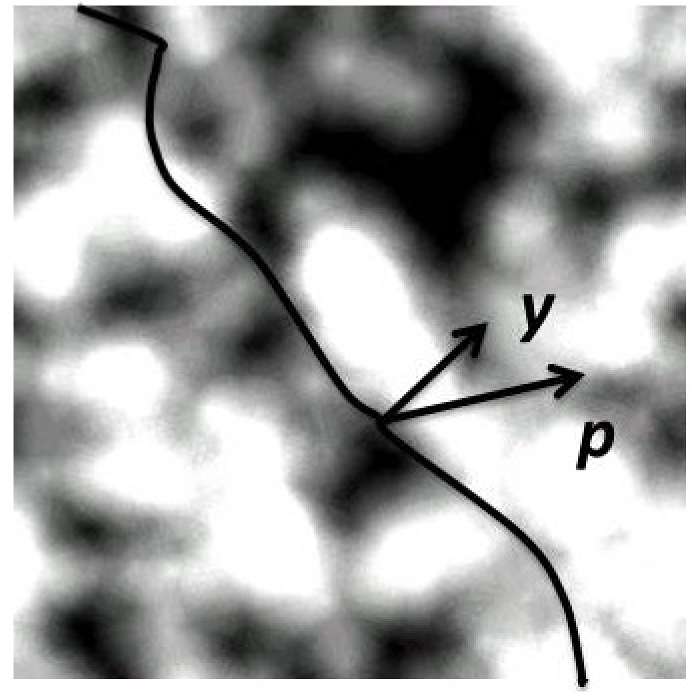

(b)

Wavefront in a realization of a random anisotropic medium.

Random field model $\{ \quad , \quad , \quad ; \quad [0, \quad)\}$ of weakly inhomogeneous media

$$\langle \quad \rangle \qquad {}_{1} \quad {}_{1} \quad , \qquad 0$$

$$\langle \quad \rangle \qquad {}_{2} \quad {}_{2} \quad , \qquad 0$$

$$\langle \quad \rangle \qquad {}_{3} \quad {}_{1} \quad , \qquad 0$$

$$1$$

$$\langle \qquad , \qquad \rangle \quad 0$$

$$1, 2, 3$$

How different is the response of random medium B ;

from that of homogeneous medium $_{\text{hom}}$ **?**

$$[\qquad 0; \qquad 1, 2, 3]$$

An analytically tractable case: white noise randomness in only

stochastic evolution equation = Stratonovich equation:

$$(\ ) \quad (\ ) \quad ^{(\ )}(\ )$$

$$(\ ) \quad \langle \quad \rangle \frac{1/2}{2 \quad 3/2}$$

$$(\ ) \quad 2 \frac{1/2}{2 \quad 3/2}$$

$^{(\ )}(\ )$ Stratonovich-type differential of Wiener process

Itô equation:

$$(\ ) \quad (\ ) \quad (\ )$$

$$(\ ) \quad (\ ) \quad \frac{1}{2} \quad (\ ) \frac{(\ )}{} \quad \langle \quad \rangle \frac{1/2}{2 \quad 3/2} \quad \frac{2}{2} \frac{}{8 \quad 3}$$

$$(\ ) \quad 2 \frac{1/2}{2 \quad 3/2}$$

differential of Wiener process

Itô formula for : $(\quad) - \frac{1}{2} \, {}^{2}(\quad) \frac{^{2}}{_{2}} \quad (\quad) - \quad (\quad)$

$$- \langle \quad \rangle \quad (\quad) \quad \langle \quad \rangle \frac{^{1/2}}{2 \quad ^{3/2}} \quad {}^{2}_{2} \frac{}{8 \quad ^{3}}$$

$$\langle \quad \rangle \quad (0) \exp \quad \langle \quad \rangle \frac{^{1/2}}{2 \quad ^{3/2}} \quad {}^{2}_{2} \frac{}{8 \quad ^{3}}$$

zero-mean white noise in results in attenuation of average amplitude being weaker than that in the homogeneous medium $_{\text{hom}}$

Same result for being an Ornstein-Uhlenbeck noise evolution of second moment: $-\langle {}^{2} \rangle \quad \langle \quad \rangle \frac{{}^{1/2}}{{}^{3/2}} \quad {}^{2}_{2} \frac{}{4 \quad {}^{3}} \langle {}^{2} \rangle$

$$-\langle \quad \rangle \quad (\quad) \quad \langle \quad \rangle \frac{{}^{1/2}}{2 \quad {}^{3/2}} \quad {}^{2}_{2} \frac{}{8 \quad {}^{3}}$$

$$\langle \quad \rangle \quad (0) \exp \quad \langle \quad \rangle \frac{{}^{1/2}}{2 \quad {}^{3/2}} \quad {}^{2}_{2} \frac{}{8 \quad {}^{3}}$$

Again, noise in implies that $\langle {}^{2} \rangle$ attenuates more slowly than in $_{\text{hom}}$

Fokker-Planck equation: $\dfrac{(\ \ ,\ \ )}{\quad}$ $(\ \ ,\ \ ),$ $(\ _0,\ _0)$ $(\qquad _0)$

$$(\ \ ,\ \ )\quad(\ \ )\ (\ \ ,\ \ )\ \frac{1}{2}\frac{}{\quad}[\ (\ \ )\ (\ \ ,\ \ )]$$

$\{ \quad , \quad , \quad ; \quad [0, \quad)\}$ modeled by Ornstein-Uhlenbeck processes $\quad , \quad 1, 2, 3$

Gaussian, Markovian and stationary, all very realistic properties

$$\sqrt{2} \qquad , \quad ,$$

$$^{2} \exp \qquad , \qquad 1, 2, 3 \quad \text{correlation f's}$$

$1/$ = correlation lengths

= standard deviations

Assume shock evolution to be independent of shock front thickness:

$$/ \qquad \frac{\langle \quad \rangle \;\; {}_{2 \;\; 2} \quad , \qquad \langle \quad \rangle \;\; {}_{3 \;\; 3} \quad ,}{2 \langle \quad \rangle \;\; {}_{2 \;\; 2} \quad , \quad {}^{3/2}}^{1/2}$$

$$\mathbf{X} \qquad \mathbf{AX} \qquad \mathbf{B} \;\; \mathbf{W} \quad ,$$

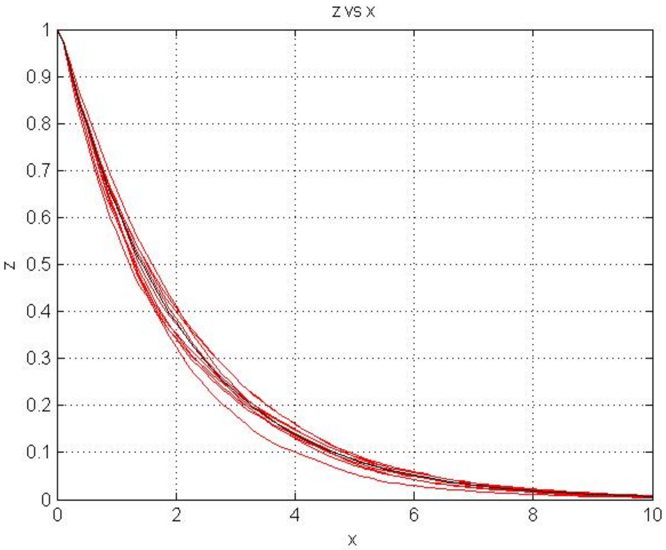

random

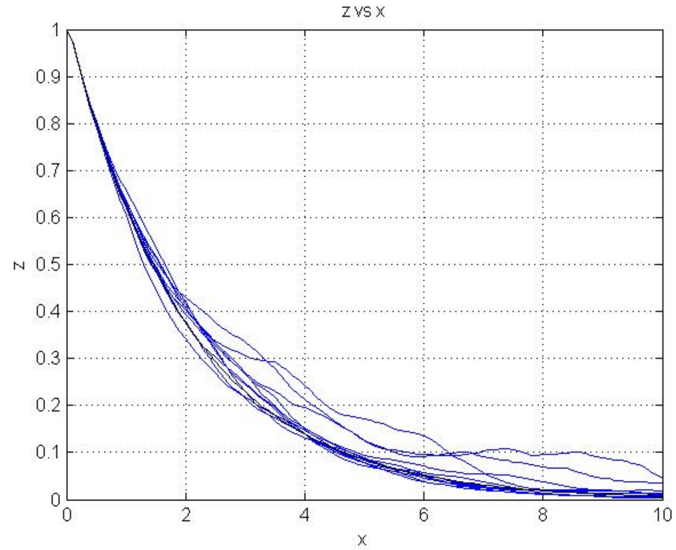

random

correlation lengths = 1

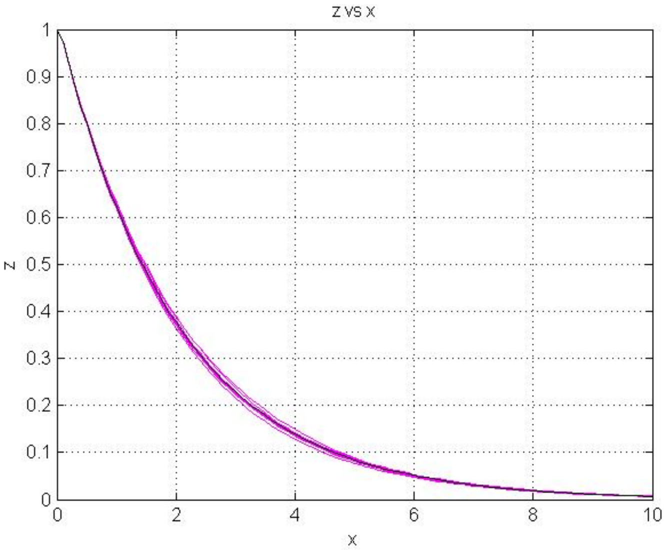

random

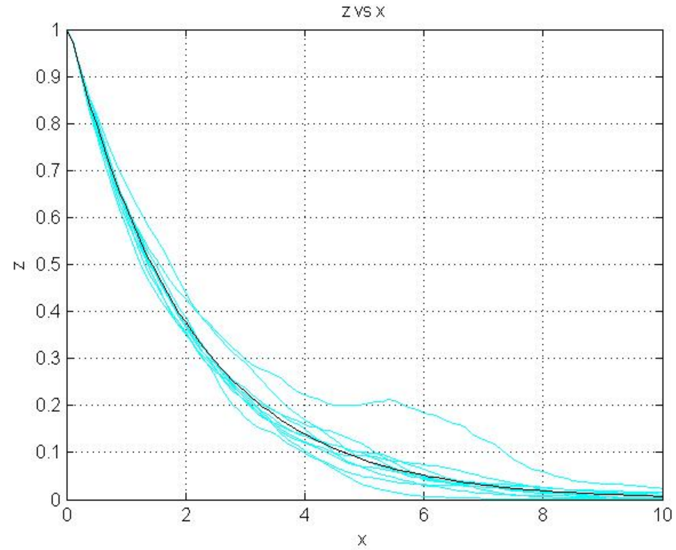

, , uncorrelated

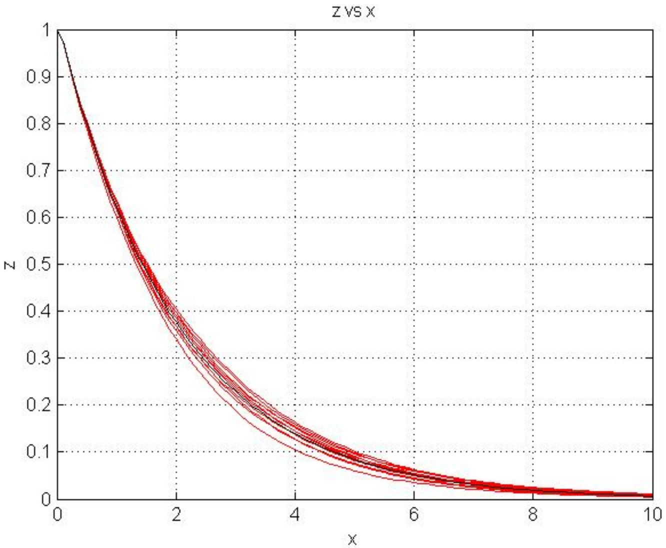

random

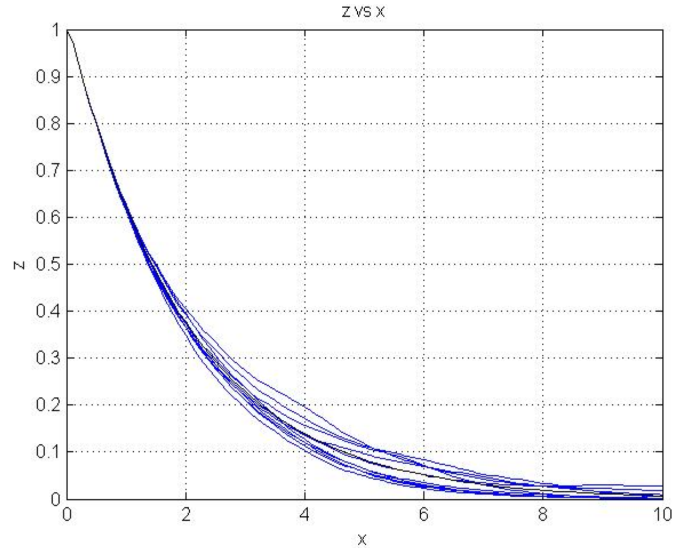

random

correlation lengths = 10

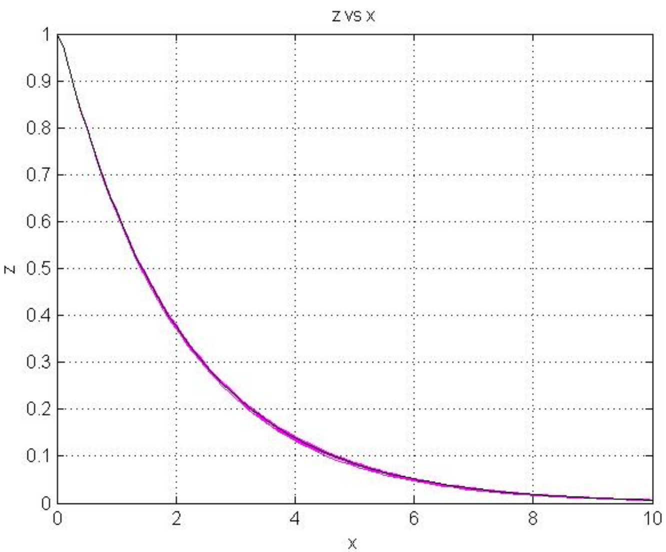

random

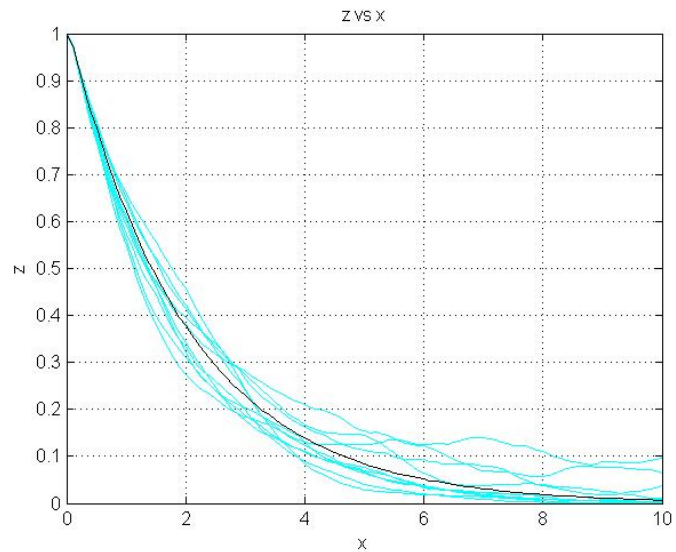

, , uncorrelated

$\{\ ,\ ,\ ;\ [0,\ )\}$ modeled by Ornstein-Uhlenbeck processes $,\ 1,2,3$

Assume shock evolution to be coupled with shock front thickness:

the thinner is the wavefront, the stronger is the randomness in constitutive response

correlation lengths and standard deviations

$$\frac{\langle\ \rangle_{2\ 2}\ ,\ \langle\ \rangle_{3\ 3}\ ,\ ^{1/2}}{2\langle\ \rangle_{2\ 2}\ ,\ ^{3/2}}$$

$$\sqrt{\quad}\ ,$$

w/ initial conditions: $_0\ 1,\ _0\ 1,\ ,\ 0,\ 1,2,3$

10-component stochastic dynamical system

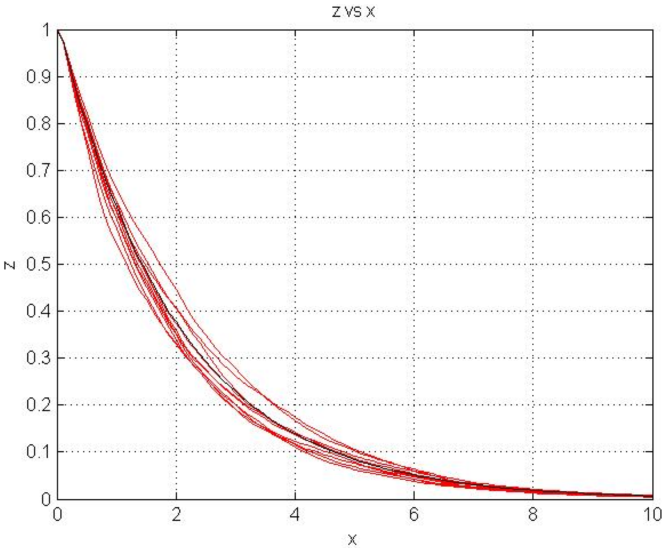

random

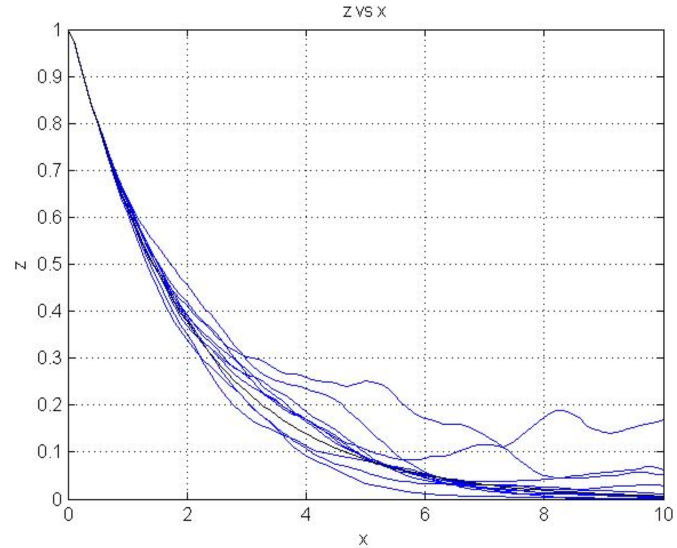

random

correlation lengths = 1

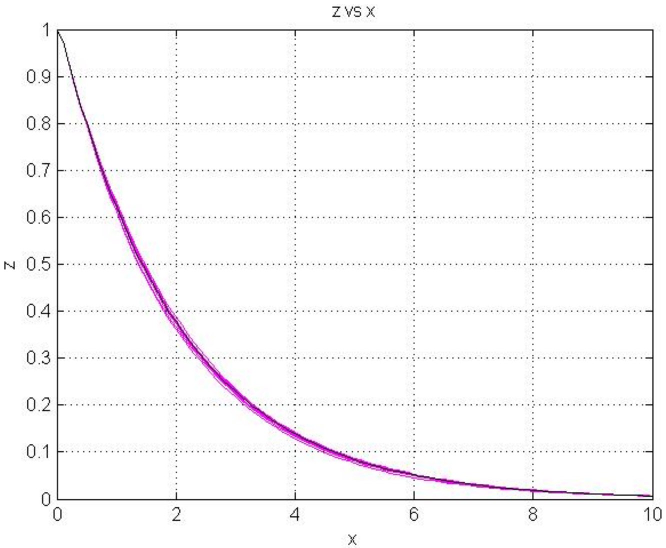

random

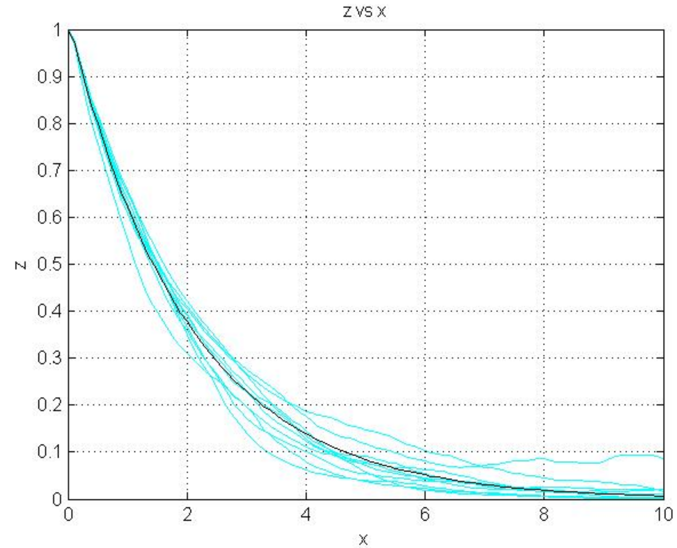

, , uncorrelated